

**Human Perception of Vibrations
due to Synchronised Crowd Loading in Grandstands**

Gillian Gordon Browning

A thesis submitted for the degree of Doctor of Philosophy

University of Bath

Department of Architecture and Civil Engineering

October 2011

COPYRIGHT

Attention is drawn to the fact that copyright of this thesis rests with its author. A copy of this thesis has been supplied on condition that anyone who consults it is understood to recognise that its copyright rests with the author and they must not copy it or use material from it except as permitted by law or with the consent of the author.

This thesis may be made available for consultation within the University Library and may be photocopied or lent to other libraries for the purposes of consultation.

<u>CONTENTS</u>	Page
Contents	i
List of Figures	vii
List of Tables	xvii
Acknowledgements	xix
Abstract	xxi
1 Introduction	1
1.1 Current Design Approach for Structures Subject to Synchronised Crowd Loads	1
1.2 Research Proposal	2
1.3 Key Objectives	3
1.4 Thesis Outline	5
2 Literature Review	7
2.1 Designing for Dynamic Crowd Loading	8
2.1.1 The Introduction of Human Dynamic Loading to British Standards	8
2.1.2 Structural Safety, Stadium Design and the Avoidance of Resonance	12
2.1.3 Additional Codes and Standards	23
2.1.3.1 British Standards	23
2.1.3.2 Summary of Additional British Standards	31
2.1.3.3 International Standards	31
2.1.4 Summary of British and International Standards for Designing for Dynamic Crowd Loading	37
2.2 Dynamic Loading of Grandstands	40
2.2.1 Examples of Stadia with Vibration Issues	40
2.2.2 Measurements from Grandstands	43
2.3 Serviceability Criteria	49
2.3.1 Previously Published Guidelines	49
2.3.2 Summary of Human Acceptance Criteria for Vibrations	58

<u>CONTENTS</u>	Page
2.4 Human Perception – Experimental Precedents	59
2.5 Summary of Findings of Literature Review	63
3 Test Rig Design	65
3.1 Test Rig Design	65
3.1.1 Concept	65
3.1.2 Layout	67
3.1.3 Design Loads	68
3.1.4 Stability	69
3.1.5 Springs	71
3.1.6 Details	71
3.1.7 Natural Frequencies and Mode Shapes	72
3.2 Computational Modelling	73
3.2.1 Computational Modelling - Analysis	73
3.2.2 Computational Modelling - Input	74
3.2.2.1 Structural Model	74
3.2.2.1.1 Two or Three Dimensions?	74
3.2.2.1.2 Representation of Structural Elements	75
3.2.2.1.3 Size of Mesh and Number of Nodes	76
3.2.2.1.4 Connections and Supports	77
3.2.2.1.5 Material Properties	78
3.2.2.1.6 Springs	79
3.2.2.1.7 Applied Loads	80
3.2.2.1.8 Non Structural Elements	81
3.2.2.1.9 Damping	81
3.2.2.1.10 Analysis Time	81
3.2.2.1.11 Appropriate Mode Shapes	82
3.2.2.2 Human Loading	82
3.2.2.2.1 Forcing Functions and Fourier Series	82
3.2.2.2.2 Frequency of Movement and Harmonics to be Considered	87
3.2.2.2.3 Crowd Factors	89

<u>CONTENTS</u>	Page
3.2.2.2.4 Pre-experiment Forcing Functions	91
3.2.2.2.4.1 Magnitude and Form	92
3.2.2.2.4.2 Frequency	98
3.2.2.3 Summary of Computational Modelling Input	99
3.2.3 Computational Modelling - Results	100
3.2.3.1 Results of Modal Analysis	100
3.2.3.2 Results of Time History Analysis	104
3.2.3.2.1 Displacements	107
3.2.3.2.2 Accelerations	110
3.2.3.2.3 Frequency Content	112
3.2.3.2.3.1 Frequency Content of Forcing Functions	112
3.2.3.2.3.2 Model Response and Frequency Content	114
3.2.3.3 Summary of Computational Analysis Results	115
4 Testing	117
4.1 Initial Testing of the Rig	117
4.1.1 Modal Testing	117
4.1.1.1 Frequency	117
4.1.1.2 Damping	120
4.1.2 Instrumentation of the Test Rig	121
4.2 Participant Selection and Testing	123
4.2.1 Participant Selection	123
4.2.2 Human Perception and Emotion Testing	126
4.3 Test Procedure	129
4.3.1 Vibration Generation	129
4.3.2 Jump Frequency	130
4.3.3 Jump Groups	131
4.3.4 Combinations	131
4.3.5 Test Procedure	132
4.3.6 December 2006 Tests	134
4.3.7 October 2007 Tests	134
4.3.8 Monitoring of Rig Movements	135

<u>CONTENTS</u>	Page
4.4	Data Analysis 137
4.4.1	Instrumentation Readings 137
4.4.2	Human Results 139
5	Results 141
5.1	Range of Movements 141
5.2	Human Response 143
5.2.1	Initial Observations – Perception 146
5.2.2	Initial Observations – Emotion 150
5.2.3	Statistical Analysis - Methodology 151
5.2.4	Statistical Analysis - Results 160
5.2.4.1	Single Variable Models 160
5.2.4.2	Range of R^2 Values 160
5.2.4.3	4 Variable / 8 Term Base Models 161
5.2.4.4	Maximum R^2 Models 162
5.2.4.5	Reduced Variable Models 162
5.2.5	Statistical Analysis – Checks 165
5.2.5.1	Combination Models - Checks 165
5.2.5.2	Single Variable Models - Checks 169
5.2.5.3	Model Checks for Perception Rating while Seated 172
5.2.5.4	Model Checks for Emotion Rating while Seated 177
5.2.5.5	Model Checks for Perception Ratings for those Jumping 183
5.2.5.6	Model Checks for Emotion Ratings for those Jumping 191
5.2.5.7	Statistical Analysis - Summary of Check Results 199
5.2.6	Human Response - Summary 200
5.2.7	Human Response - Conclusion 210
5.3	Comparison with other Research 212
5.3.1	Perception Categories 212

CONTENTS

5.3.2	Floor Vibrations	214
5.3.3	Design Standards	219
5.3.4	Summary of Comparison of Perception Tests with other Research	223
6	Acceptability	225
6.1	Statistical Analysis	225
6.1.1	Statistical Analysis - Procedure	225
6.1.2	Statistical Analysis – Results	232
6.1.2.1	Acceptability for Seated Participants	232
6.1.2.2	Acceptability for Jumping Participants	236
6.1.3	Statistical Analysis – Conclusions	239
6.2	Comparison of Acceptability Results with Published Guidelines	246
6.3	Calculation of Predicted Accelerations	250
6.3.1	Modelling using British Guidelines	250
6.3.2	Alternative Models Considered	256
6.4	Proposed Acceptability and Loading Criteria	264
6.4.1	Proposed Acceptability and Loading Criteria - High Energy Concerts	265
6.4.2	Proposed Acceptability and Loading Criteria - Medium Tempo Concerts and High Profile Sporting Events	270
6.4.3	Proposed Acceptability and Loading Criteria - Classical Concerts and Typical Sporting Events	273
6.5	Comparison of Proposed Acceptability Criteria with Published Guidelines	282
6.5.1	Comparison of Proposed Acceptability Criteria - High Energy Concerts	282
6.5.2	Comparison of Proposed Acceptability Criteria - Medium Tempo Concerts and High Profile Sporting Events	283
6.5.3	Comparison of Proposed Acceptability Criteria - Typical Well Attended Sporting Events	286
6.5.4	Comparison of Proposed Acceptability Criteria - Classical Concerts	286
6.5.5	Further Comparisons of Proposed Acceptability Criteria	286
6.6	Comparison of Proposed Acceptability Criteria with Recorded Perception Ratings	306

<u>CONTENTS</u>	Page
6.7 Comparison of Proposed Acceptability Criteria with Published Recorded Vibrations	309
6.8 Acceptability - Conclusion	311
7 Conclusions and Further Research	313
7.1 Conclusions	313
7.1.1 Current Design Limitations and Aims of Research Project	313
7.1.2 Experimental Testing	314
7.1.3 Human Perception and Emotional Response to Crowd Induced Vibrations	315
7.1.4 Acceptability	320
7.2 Further Research	324
Appendix A Photographs of Experimental Work	327
References	339

LIST OF FIGURES**Page**

Figure 1.1	Designing for Dynamic Crowd Loads	2
Figure 2.1	Publication Time Line	8
Figure 2.2	Designing for Dynamic Crowd Loads in the UK pre 2004	9
Figure 2.3	Designing for Dynamic Crowd Loads in the UK post 2004	11
Figure 2.4	Design Procedure for Structures Subject to Synchronised Crowd Loads	39
Figure 2.5	Nausea Threshold for Vibration Frequencies Below 10Hz Based on 3 Minute Exposure	49
Figure 2.6	Kasperski's Acceleration Limits, from S20	50
Figure 2.7	Summary of Acceleration Limit Serviceability Criteria	52
Figure 2.8	Base Curve for Vertical Accelerations to ISO 10137:2007	53
Figure 2.9	Fatigue Limits to ISO2631-2 1989 from Bachmann et al 1994	54
Figure 2.10	Exposure Limits to ISO2631-2 1989 from Bachmann et al 1994	55
Figure 2.11	Reiher Meister Perception Curves for Steady State Vibrations from Lenzen 1966	56
Figure 2.12	Modified Reiher Meister Perception Curves for Transient Vibrations by Lenzen 1966	56
Figure 2.13	McCormick and Mason (1974) Vibration Perceptibility Chart for Transient Vibrations	57
Figure 3.1	Cross Section of the Test Rig	66
Figure 3.2	Rear Elevation of Test Rig	70
Figure 3.3	Stick Diagram of Test Rig Highlighting In-plane Bracing	70
Figure 3.4	Precast Terrace Unit Support Detail	71
Figure 3.5	Flow Diagram of Proposed Design Procedure Highlighting Input Requirements	73
Figure 3.6	Computational Model of the Test Rig	76
Figure 3.7	Computational Model showing the Test Rig Connections	77

<u>LIST OF FIGURES</u>		Page
Figure 3.8	Cracked Section Properties of Precast Terrace Units	79
Figure 3.9	Using a Fourier Series to Define an Half Sine Wave	83
Figure 3.10	Measured and Simulated Load for one person jumping from Ji and Ellis 1994b	85
Figure 3.11	Summary of Collated Impact Factors for Human Dynamic Loading	87
Figure 3.12	Summary of Crowd Factors	90
Figure 3.13	‘Maximum’ Forcing Function	93
Figure 3.14	Aligned Half Sine Waves for ‘Realistic’ Forcing Function	94
Figure 3.15	Proportioned Half Sine Waves for ‘Realistic’ Forcing Function	94
Figure 3.16	‘Realistic’ Forcing Function	95
Figure 3.17	Effect of Ellis and Ji (2002) Crowd Factor on Half Sine Wave Forcing Function	95
Figure 3.18	Proposed and Previously Recorded Forcing Functions	96
Figure 3.19	Simplification of Load Model used for Pre-experiment Analysis	97
Figure 3.20	Fundamental Mode Shape of the Test Rig with no Springs	101
Figure 3.21	Second Mode Shape of the Test Rig with no Springs	101
Figure 3.22	Fundamental Mode Shape of the 2Hz Test Rig with Springs	102
Figure 3.23	Second Mode Shape of the 2Hz Test Rig with Springs	102
Figure 3.24	Third Mode Shape of the 2Hz Test Rig with Springs	103
Figure 3.25	Location of Node 314	104
Figure 3.26	Time History Plots for 6.5Hz Rig using 2.4Hz Forcing Function	105
Figure 3.27	Maximum Peak Vertical Displacements from THA	106
Figure 3.28	Dynamic Amplification for Single Degree of Freedom System	109
Figure 3.29	Peak Vertical Accelerations from THA	111
Figure 3.30	Form of the Forcing Functions used in THA	112
Figure 3.31	Fast Fourier Transforms of Forcing Functions	113

<u>LIST OF FIGURES</u>		Page
Figure 4.1	Sample Decay Trace for 6.5 Hz Rig Impact Test	119
Figure 4.2	Fast Fourier Transform of Decay Trace shown in Figure 10.1	119
Figure 4.3	Fast Fourier Transform used to calculate Modal Damping	119
Figure 4.4	Participant Health Questionnaire	124
Figure 4.5	Participant Questionnaire – Additional Questions	125
Figure 4.6	Participant Response Sheet - December 2006	127
Figure 4.7	Sample Participant Response Sheet - Filled	127
Figure 4.8	Participant Response Sheet - October 2007	128
Figure 4.9	Definition of Unacceptable as Communicated to the Participants	128
Figure 4.10	Typical Stand Layouts showing Location of Jump Groups	131
Figure 4.11	Testing Underway	133
Figure 4.12	Range of Vibration Magnitude	135
Figure 4.13	Location of Monitoring Equipment	136
Figure 4.14	Samples of Instrumentation Graphs	138
Figure 4.14	Location of Key Monitoring Equipment Used to Determine Magnitude of Vibrations Experienced by Participants	140
Figure 5.1	Range of Movements experienced during Tests	142
Figure 5.2	Peak Movements Recorded during the Tests Compared to those Predicted by the ‘Realistic’ THA Computer Model	143
Figure 5.3	Seated Perception Results	144
Figure 5.4	Seated Emotion Results	144
Figure 5.5	Jumping Perception Results	145
Figure 5.6	Jumping Emotion Results	145
Figure 5.7	Perception Results for 6.5Hz Rig	146
Figure 5.8	Perception Results for 4Hz Rig	146

<u>LIST OF FIGURES</u>	<u>Page</u>
Figure 5.9 Perception Results for 2Hz Rig	147
Figure 5.10a All Perception Results for Seated Participants	148
Figure 5.10b All Perception Results for Jumping Participants	148
Figure 5.11 Perception Results for Seated Participants	149
Figure 5.12a All Emotion Results for Seated Participants	150
Figure 5.12b All Emotion Results for Jumping Participants	150
Figure 5.13 Statistical Analysis Procedure	155
Figure 5.14 Sample of Initial Outlier and Model Overview Scatter Plot	165
Figure 5.15 Sample of Scatter Plot to check fit of Model & Deviation of Errors	166
Figure 5.16 Sample Normal Probability Plots	167
Figure 5.17 Sample of Q-Q Plots (Q=Quantile)	169
Figure 5.18 Sample of Single Variable Model Graphs	170
Figure 5.19 Procedure for Model Validation	171
Figure 5.20 Actual and Predicted %P Seat Ratings v Vertical Individual (per Test) Vibration Dose Value	172
Figure 5.21 Residuals from Test Models v Predicted Seated %P Ratings	173
Figure 5.22 Normal Probability Plot for Selected %P Seat Models	174
Figure 5.23 Q-Q Plots for Selected %P Seat Models Cross Validation Checks	176
Figure 5.24 Actual and Predicted %E Seat Ratings v Vertical Individual (per Test) Vibration Dose Value	177
Figure 5.25 Scatter Plot of V RMS d v Residuals for %E Seat Models	178
Figure 5.26 Residuals from Test Models v Predicted Seated %E Ratings	179
Figure 5.27 Normal Probability Plots for Selected %E Seat Models	180
Figure 5.28 Q-Q Plots for Selected %E Seat Models Cross Validation Checks	182

<u>LIST OF FIGURES</u>	Page
Figure 5.29 Actual and Predicted %P Jump Ratings v Vertical RMS Acceleration	184
Figure 5.30 Scatter plot of Vertical Displacement against Residuals	185
Figure 5.31 Scatter plot of Predicted %P Jump against Residuals	186
Figure 5.32 Sample of Scatter Plots of Run Order versus Residuals	186
Figure 5.33 Normal Probability plot for selected %P Jump models	187
Figure 5.34 Distribution of 5/10 Model Residuals	188
Figure 5.35 Identification of Extreme Residuals	188
Figure 5.36 Q-Q Plots for Selected %P Jump Models Cross Validation Checks	190
Figure 5.37 Comparison of Models %P Jump and %E Jump	192
Figure 5.38 Comparison of Scatter Plots %P Jump and %E Jump	193
Figure 5.39 Sample of Scatter Plots of Run Order versus Residuals	194
Figure 5.40 Normal Probability plot for selected %E Jump models	195
Figure 5.41 Distribution of 4/8 Model Residuals	195
Figure 5.42 Scatter Plot Identifying Clustering of Responses along X-Axis	196
Figure 5.43 Q-Q Plots for Selected %E Jump Models Cross Validation Checks	198
Figure 5.44 Normal Probability plot for selected %E Jump models (for data above 4mm VRMSd)	199
Figure 5.45 Selected Models for Seated Perception Ratings	201
Figure 5.46 Selected Models for Seated Emotion Ratings	202
Figure 5.47 Selected Models for Jumping Perception Ratings	205
Figure 5.48 Selected Models for Jumping Emotion Ratings	205
Figure 5.49 Graphs of Selected Perception Models, Seated and Jumping	208
Figure 5.50 Graphs of Selected Emotion Models, Seated and Jumping	209
Figure 5.51 Seated Perception Data showing Questionnaire Categories	213
Figure 5.52 Jumping Perception Data showing Questionnaire Categories	213

<u>LIST OF FIGURES</u>	Page
Figure 5.53 Derivation of 'Barely Perceptible' Trendlines	215
Figure 5.54 Seated Participants' Perception Trendlines	216
Figure 5.55 Jumping Participants' Perception Trendlines	216
Figure 5.56 Reiher Meister Perception Curves for Steady State Vibrations	217
Figure 5.57 Lenzen's Modified Reiher Meister Perception Curves for Transient Vibrations	218
Figure 5.58 McCormick and Mason's Perception Curves for Transient Vibrations	219
Figure 5.59 Vibration limits to ISO 2631-2 1989	220
Figure 5.60 Comfort limits to ISO 2631-1:1997 for Passengers on Public Transport	222
Figure 5.61 IStructE (2008) Recommended Acceleration Limits for Events at Permanent Grandstands	222
Figure 6.1 Flow Chart of Development of Acceptability Model	227
Figure 6.2 Scatter Plot of Recorded %E Rating against log Vertical RMS Acceleration showing Acceptability Results	228
Figure 6.3 Scatter Plot of Recorded %E Ratings against Recorded %P Ratings showing Acceptability Results	228
Figure 6.4 Histograms showing Distribution of Acceptability for Seated Participants	229
Figure 6.5 Logistic Function	230
Figure 6.6 Acceptability for Seated Participants using Emotion Rating as the Predictor	231
Figure 6.7 Acceptability for Seated Participants using Perception Rating as the Predictor	231
Figure 6.8 Acceptability for Seated Participants using the logarithm of Vertical RMS acceleration as the Predictor	231
Figure 6.9 Acceptability for Seated Participants using the logarithm of Vertical RMS displacement as the Predictor	231
Figure 6.10 Acceptability for Jumping Participants using Emotion Rating as the Predictor	234

<u>LIST OF FIGURES</u>	Page
Figure 6.11 Acceptability for Jumping Participants using Perception Rating as the Predictor	234
Figure 6.12 Acceptability for Jumping Participants using the square of Vertical RMS Displacement as the Predictor	234
Figure 6.13 Acceptability for Jumping Participants using Vertical RMS Displacement as the Predictor	234
Figure 6.14 Acceptability for Jumping Participants using the square of Vertical RMS Acceleration as the Predictor	235
Figure 6.15 Acceptability for Jumping Participants using Vertical RMS Acceleration as the Predictor	235
Figure 6.16 Acceptability for Jumping Participants using the square of Vertical RMS Acceleration as the Predictor plotted in terms of Vertical RMS Acceleration	235
Figure 6.17 Acceptability Test Results for Jumping Participants plotted as Recorded Emotion Ratings against Proposed Predictors	238
Figure 6.18 Comparison of Acceptability Curves for Jumping Participants Calculated using Different Banding Methods [Even Bandwidths shown Solid and Equal Bands (4 or 7 data points) shown Dashed]	241
Figure 6.19 Seated Acceptability Data overlaid with estimated %E Rating based on the logarithm of Vertical RMS Acceleration (Chapter 5)	242
Figure 6.20 Seated Acceptability Graph based on Emotion Ratings	243
Figure 6.21 Seated Acceptability Graph based on the Logarithm of Vertical RMS Acceleration (Log Scale)	243
Figure 6.22 Seated Acceptability Graph based on the Logarithm of Vertical RMS Acceleration (Linear Scale)	244
Figure 6.23 Jumping Acceptability Graph based on the Square of Vertical RMS Displacement	244
Figure 6.24a Conversion of Vertical RMS Displacement to Vertical RMS Acceleration using Recorded Rig Movements	246
Figure 6.24b Conversion of Vertical Peak Acceleration to Vertical RMS Acceleration using Recorded Rig Movements	246
Figure 6.25 Seated Acceptability Curves based on the logarithm of Vertical RMS Acceleration	247

<u>LIST OF FIGURES</u>		Page
Figure 6.26	Jumping Acceptability Graph based on the square of Vertical RMS Displacement	248
Figure 6.27	IStructE (2008) Body Unit model	253
Figure 6.28	Results of IStructE (2008) Scenario 3 Model for each Rig Set up	255
Figure 6.29	Alternative Analysis Models Considered	256
Figure 6.30	Equivalent Effectiveness Factors derived from Parkhouse and Ewins (2006)	258
Figure 6.31	Results of 3 DOF Model for each Rig Set-up	262
Figure 6.32	3 Degree-of-Freedom Model Recommended for use with the Author's Proposed Loadings and Acceptability Limits	264
Figure 6.33	Recorded Acceptability Results from Experimental Testing	266
Figure 6.34	Recommended Acceptability Criteria	280
Figure 6.35	Recommended Acceptability Criteria together with Previously Published Guidelines	284
Figure 6.36	Load Models for Calculating Acceptability	287
Figure 6.37	Acceleration Response of a Single Degree-of-freedom System	296
<u>LIST OF FIGURES</u>		Page
Figure 6.38	Acceleration Response of a Single Degree-of-freedom System showing the Effect of the IStructE Scenario 3 Effectiveness Factor	299
Figure 6.39	Graphs showing calculation of Peak Accelerations for a Stand with Mass Ratio $\mu=0.19$ and 2% Damping using IStructE Scenario 3 Loading and Effectiveness Factor and 2 Degree-of-freedom Model (shown in Figure 6.36 b)	303
Figure 6.40	Recorded Experimental Perception Data showing Recommended Acceleration Limits based on 20% Overall Crowd Acceptability	307
Figure 7.1	Recommended Seated Perception and Emotion Models	319
Figure 7.2	Recommended Jumping Perception and Emotion Models	319
Figure 7.3	Acceptability Curves for Seated and Jumping Spectators	321

LIST OF TABLES

	Page
Table 2.1 Summary of Frequency Limits given in the IStructE's (2001) 'Dynamic Performance Requirements for Permanent Grandstands Subject to Crowd Action: Interim Guidance on Assessment and Design'	17
Table 2.2 Summary of Vertical Frequency Limits given in British Standards and Design Guides	21
Table 2.3 Summary of Horizontal Frequency Limits given in British Standards and Design Guides	22
Table 2.4 Summary of Acceleration Ranges given in BS6841:1987 Appendix C Relating to Comfort	25
Table 2.5 Kasperski's (1996) peak acceleration limits as summarised in BRE Digest 426 (2004) (for a frequency range <10Hz)	37
Table 2.6 Summary of Recorded Accelerations from Littler 2000a, 2000b and 2000c	46
Table 2.7 An Indication of Human Perceptibility Thresholds for Vertical Harmonic Vibration (Person Standing), (Bachmann et al 1994)	51
Table 3.1 Ji and Ellis (1994a) Proposed Fourier Coefficients and Phase Lags for Various Activities/Contact Ratios	85
Table 3.2 Summary of Proposed Forcing Functions	97
Table 3.3 Rig and Forcing Function THA Model Combinations	99
Table 3.4 Fourier Coefficients of Forcing Functions	113
Table 4.1 Test Jump Frequencies	130
Table 4.2 Sample Test Schedule	132
Table 5.1 Summary of Predictors used in Models	152
Table 5.2 Summary of Single Variable Models	153
Table 5.3 Summary of 1 st and 2 nd Order Predictors for use in Models	156
Table 5.4 Summary of Terms used in the Initial Combination Models for those Seated	158
Table 5.5 Summary of Terms used in the Initial Combination Models for those Jumping	158

<u>LIST OF TABLES</u>		Page
Table 5.6	Best 4 Variable/8 Term Base Models	161
Table 5.7	Summary of R ² Values for Best Combination Models Identified	164
Table 5.8	Selected Combination Models for Predicting %P Seat	172
Table 5.9	Selected Single Variable Model for Predicting %P Seat	175
Table 5.10	Selected Combination Models for Predicting %E Seat	177
Table 5.11	Selected Single Variable Model for Predicting %E Seat	181
Table 5.12	Selected Combination Models for Predicting %P Jump	183
Table 5.13	Selected Single Variable Model for Predicting %P Jump	189
Table 5.14	Selected Combination Models for Predicting %E Jump	191
Table 5.15	Selected Single Variable Model for Predicting %E Jump	197
Table 5.16	Summary of R ² and Standard Deviation of Residuals for Selected %P Models for those Seated	203
Table 5.17	Summary of R ² and Standard Deviation of Residuals for Selected %E Models for those Seated	204
Table 5.18	Summary of R ² and Standard Deviation of Residuals for Selected %P Models for those Jumping	206
Table 5.19	Summary of R ² and Standard Deviation of Residuals for Selected %E Models for those Jumping	206
Table 5.20	Recommended Perception and Emotion Models	211
Table 6.1	Assessment of Accuracy of Acceptability Models	239
Table 6.2	Summary of IStructE (2008) Dynamic Crowd Loading	252
Table 6.3	Dynamic Load Factors (DLFs) from Parkhouse and Ewins (2006)	259
Table 6.4	Average Dynamic Load Factors (DLFs) from Parkhouse and Ewins (2006)	260
Table 6.5	Proposed Loading and Acceptability Limits for High Energy Concerts	267

LIST OF TABLES**Page**

Table 6.6	Proposed Loading and Acceptability Limits for Medium Tempo Concerts and High Profile Sporting events	271
Table 6.7	Proposed Loading and Acceptability Limits for Classical Concerts and Typical Sporting Events	276
Table 6.8	Summary of Proposed Loading to be used with Recommended Acceptability Limits	279
Table 6.9	Loadings and Acceptability Limits used with the Load Models shown in Figure 6.36	288
Table 6.10	Minimum Vertical Natural Frequency at which Acceleration Limit is met when calculated for a Stand with a Crowd to Mass Ratio of 0.28 and 2% Critical Damping and a Maximum Fundamental Frequency of the Crowd Activity of 3.2Hz	290
Table 6.11	Frequency at which Peak Acceleration Limit is met when calculated for a Stand with a Crowd to Mass Ratio of 0.28 and 2% Critical Damping and a Maximum Fundamental Frequency of the Crowd Activity of 3.2Hz	292
Table 6.12	Frequency at which Peak Acceleration Limit is met when calculated for a Stand with varying Mass Ratio μ and 2% Critical Damping and a Maximum Fundamental Frequency of the Crowd Activity of 3.2Hz	293
Table 6.13	Acceptability Limits based on Peak Accelerations	294
Table 6.14	Acceleration Levels recorded by others during live events	309
Table 7.1	Recommended Perception and Emotion Models	318

Acknowledgements

I would like to thank Antony for pushing me harder than I wanted to go and Ian for convincing me that statistics could be understood. I am grateful to all those in the structures lab at the University of Bath who threw themselves into constructing the outsized section of grandstand and who helped me run all the tests. I am indebted to all those who participated in the experiments and to those who convinced others it would be fun. Thank you to Buro Happold Engineers, Bath, for their financial backing of this project and I hope it delivers all that I promised.

And most of all to Spencer for his continued support throughout.

Abstract

Since the identification, in the UK, of the need for further information on the dynamic loading of grandstands in the early 1990s, a number of research projects have investigated the issues relating to dynamic loading of structures due to groups of people participating in synchronised activities. These studies have, to date, largely focused on producing load models to accurately represent the dynamic crowd load and the human-structure interaction. However, whilst the vibrational response of grandstand structures is becoming better understood, the question arises as to what level of dynamic response is acceptable to the users. Currently there is very little experimental data available regarding human perception of vibrations in such crowd loading situations. As a result those producing design standards and design guides have very little information on which to base serviceability requirements.

To address this, tests have been carried out at the University of Bath using a section of grandstand, whose dynamic properties could be varied, with the aim of developing acceptability criteria. Groups of participants were subjected to a range of vibrations induced by selected members of the group jumping in synchrony. Both those seated and jumping during the tests were asked to rate their perception and emotion of each vibration as well as the acceptability of the vibration in a real grandstand situation. These ratings were then used to statistically model perception and emotion to find the key vibration characteristics influencing the human response of both the seated and jumping participants prior to developing acceptability curves for each group.

It was found that those seated are more sensitive to vibrations than those jumping to create them. The response of the jumpers is relatively simple and can be fairly accurately modelled using just a single variable namely the square of vertical RMS displacement. The seated response is much more complex but can be relatively accurately represented using logarithm of vertical RMS acceleration.

The proposed acceptability criteria and load model generally tie in well with previously published guidelines provided that the serviceability criteria are in the same format as the original research upon which they were based (i.e. peak accelerations).

1 Introduction

In recent years the role of sports grounds has changed considerably. Previously grandstands were used on alternate Saturday afternoons and occasional midweek evenings for viewing sport, during the competition season, and for little else between times. Nowadays stadia are much more multipurpose and function as entertainment hubs, hosting events from sermons to pop concerts as well as a variety of sporting events. As a result the demands on the building and structure may be more onerous, in particular in relation to dynamic loading.

Stadium design has also evolved. Spectators now demand unobstructed views and wish to be closer to the action. This has led to seating tiers cantilevering ever further in an attempt to tighten the seating bowl around the pitch. In parallel the supporting structure has been cut down in size for economy and to increase the number of seats for a given building envelope. This combination of longer more flexible cantilevers with livelier crowd behaviour, such as occurs at pop concerts, has led to several cases of problems with vibration serviceability.

Whilst the importance of the issue of synchronised dynamic crowd loading has been recognised by the relevant authorities and guidance publications issued, there is still insufficient knowledge and understanding of the subject to allow engineers to proceed with confidence when designing a new stadium or appraising an existing one.

1.1 Current Design Approach for Structures Subject to Synchronised Crowd Loads

Current UK guidance follows two distinct approaches when assessing serviceability of vibrations induced by synchronised crowd activity (Figure 1.1). The first is a simplistic method, using frequency limits to reduce the likelihood of an unacceptable resonant response occurring. This approach sets minimum vertical and horizontal frequencies for the empty structure which are greater than, what is deemed to be, the highest relevant harmonic component of the excitation force. The second method proposes a human dynamic loading function to be used in conjunction with a given load model to determine the likely vibrations that will be induced in the structure, for a

given type of crowd loading. These predicted vibrations are then to be compared against human acceptance criteria, mainly in the form of acceleration limits.

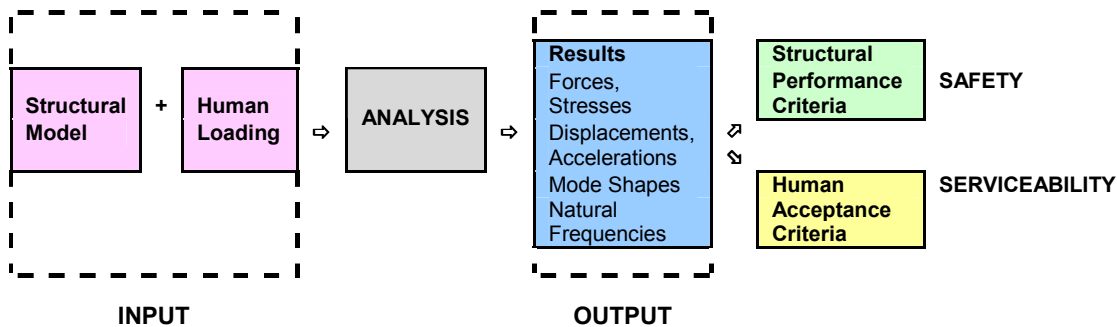


Figure 1.1 Designing for Dynamic Crowd Loads

Recent research has concentrated on refining the load model for this second approach to achieve more accurate vibration predictions, incorporating the complex relationship of human-structure interaction and the synchronisation of large groups of people. Despite this, no detailed investigations have been undertaken, concurrently, to develop human acceptance requirements for serviceability. Because of this published guidelines are based on what little information is currently available on how human's perceive vibration levels in grandstands, namely limited research carried out by Kasperski (1996) and serviceability records of how existing stands have performed under dynamic crowd loading.

1.2 Research Proposal

Therefore the objective of this research is to address this deficiency by developing a better understanding of the key factors influencing human perception of vibrations in grandstands and from this experimentally deriving serviceability criteria for permanent grandstands based on human acceptance levels of crowd induced vibrations in seating tiers. These experimentally determined acceptance criteria will either validate current recommendations or generate an alternative approach and, in so doing, will add significantly to the body of knowledge in this field.

The proposed method of achieving this aim is to construct a section of grandstand in the laboratory and subject it to human dynamic loading, while monitoring the response of the participants to the vibrations encountered. The testing rig is to be designed so that it resembles as far as possible a permanent grandstand, whilst

being engineered such that the natural frequency of the structure can be varied allowing various magnitudes of vibration to be examined, including resonance.

In order to design the test stand a computational model will be built to enable the range of likely experimental vibrations to be estimated. This will use a load model developed from previous research together with a standard finite element computer analysis package to predict the output response of the structure.

Following the testing, statistical analysis will be used to combine the human responses together with the recorded rig movements to develop an understanding of how the participants perceived the motion and what factors influenced their emotional response. Acceptability charts will then be generated using logistic regression, based on the experimental data and compared against previously published guidelines.

The final step is to establish the most appropriate loading model for use in conjunction with the experimentally derived human acceptance criteria in the design procedure briefly outlined in Figure 1.1. In order to do this, the original computer model will be re-examined, together with alternative load models and compared with the actual measurements from the stand to determine the one that gives the best fit.

From this the output of this research will be a design procedure that allows the designer to predict the dynamic response of a grandstand to various event scenarios and estimate the likely level of acceptability to seated and jumping spectators, based on the results of the experimental tests.

1.3 Key objectives

The main research objectives fall into two core categories: human perception and emotional response to vibrations induced by synchronised dynamic crowd loading and; acceptability of such vibrations. The primary objectives of this research are summarised below, divided into these categories.

Human Perception/Emotion Response

- To investigate if there is a difference in perception/emotion response of those experiencing the vibration whilst seated and those jumping to create the vibration
- To find out whether human perception/emotion is linked more closely to displacement, acceleration, vibration dose values (incorporating both RMS acceleration and vibration duration) or frequency of vibration,
- To determine what form the relationship between human perception/emotion and vibration magnitude takes, i.e. is it best described by a linear, logarithmic, exponential, polynomial or power function,
- To establish whether average forms for describing a vibration (RMS, average peak) are more accurate than peak (maximum, minimum, peak to peak) forms when modelling human perception or emotion,
- Crowd induced vibrations in grandstands generally have a dominant vertical component, but do typically much smaller horizontal components have a significant influence on human perception/emotion?,
- To find out how complex a model is required to predict the human response to a vibration, i.e. does including terms describing the displacement of the structure in three dimensions plus the vertical acceleration and vibration duration significantly improve the accuracy of the model or can a much simpler model based on a single variable be just as accurate.

Acceptability

- To establish what is/are the key factors determining the acceptability of vibrations due to synchronised crowd loading in permanent grandstands and whether this is different for those seated and those jumping,

- To investigate the shape of the relationship between these key factors and acceptability and to determine the best model to predict acceptability
- To find out how acceptability relates to the human perception/emotion response,
- To decide how best to define acceptance criteria based on the experimental data and then determine such serviceability criteria (to be used within the design procedure shown in Figure 1.1)
- And finally to compare the proposed acceptability criteria with Kasperski (1996) and current guides/standards for the design of permanent grandstands subject to dynamic crowd loading

1.4 Thesis Outline

Chapter 2 Literature Review

The thesis begins with a literature review to establish the current situation with regard to designing permanent grandstands subject to synchronised crowd loading and specifically human serviceability criteria. This review focuses, in particular, on British publications as the type and intensity of coordinated crowd activity has been shown to be different for different countries. However the review does also look at international guidance to seek insight, comparisons and improvements to the British standards. In addition to grandstand specific publications, a wide variety of design standards are reviewed specifically in relation to how these deal with human perception, vibrations and acceptability criteria. Case studies from real stands and events are presented including ones which have failed to meet the spectators' expectations. Finally precedents of experimental testing of human perception of vibrations are reviewed.

Chapter 3 Test Rig Design

Chapter 3 deals with the design of the section of grandstand used for the experimental testing. The key requirements for this structure, identified by the literature review, are expanded to develop the concept of the rig. Then the computational modelling carried out to predict response of the test rig under dynamic loads is described in terms of the procedure, the input and the output.

Chapter 4 Testing

Initial tests were performed to confirm modal properties and behaviour of the test rig as well as the instrumentation for the main tests. These are described in Chapter 4 together with details of the main testing, including - participant selection, test procedure, vibration generation, recording of results and data analysis.

Chapter 5 Results

Chapter 5 begins with a summary of the recorded movements during tests before moving on to describe the statistical analysis carried out on the human response data. This determined the key factors influencing human perception and emotional response to crowd induced vibrations and the nature of the relationship. For the analysis the results were split into two groups - those jumping to create the vibration and those seated. The findings of the statistical analysis are then compared against published vibration perception research.

Chapter 6 Acceptability

The analysis of the experimentally collected acceptability data is described in Chapter 6 in conjunction with the derivation of the acceptability curves drawn up for the two groups, jumping and seated. From these curves serviceability limits are proposed and together with a recommended three degree-of-freedom human-structure model and loading criteria. These are then compared against previously published guidance.

Chapter 7 Conclusions and Further Research

The findings and conclusions of the research project are summarised in Chapter 7 along with recommendations for further research required, in this field, to strengthen the work carried out here.

Appendix A Photos of Experimental Work

Finally Appendix A contains a series of photographs charting the experimental testing in the laboratory.

2 Literature Review

The following literature review will chronologically explain the development of codes of practice and design guides in the United Kingdom, in relation to dynamic loading, stadium design and acceptability, so that the evolution to the current status quo can be fully understood (Sections 2.1.1 and 2.1.2). The review will then move on to look at additional codes and standards (Section 2.1.3), both British and International, to see how vibrations are assessed in relation to human exposure and perception, in grandstand and non-grandstand situations, with a view to seeing if any of these alternative approaches are worthy of incorporation into the proposed research (Section 2.1.4).

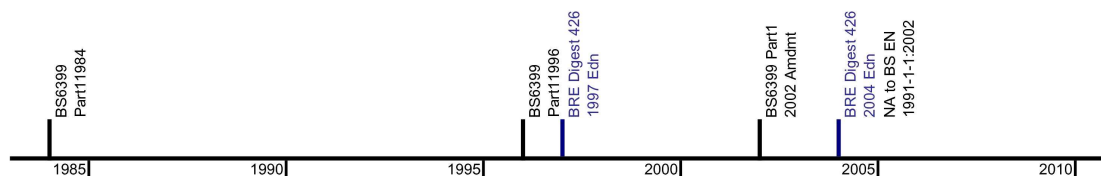
Stadium specific examples of unacceptable vibrations plus supplementary measurements of accelerations recorded during actual events will then be studied (Section 2.2). This will aid the development of the proposed experimental work by giving a better understanding of the magnitude and duration of crowd induced vibrations which occur in real grandstands and the implications of inadequate design.

Penultimately current stadia human acceptance criteria and their derivation will be critically reviewed and compared against serviceability criteria for other building types (Section 2.3). Finally past research projects into human perception of vibrations will be analysed to aid the development of the perception testing aspect of this research project (Section 2.4).

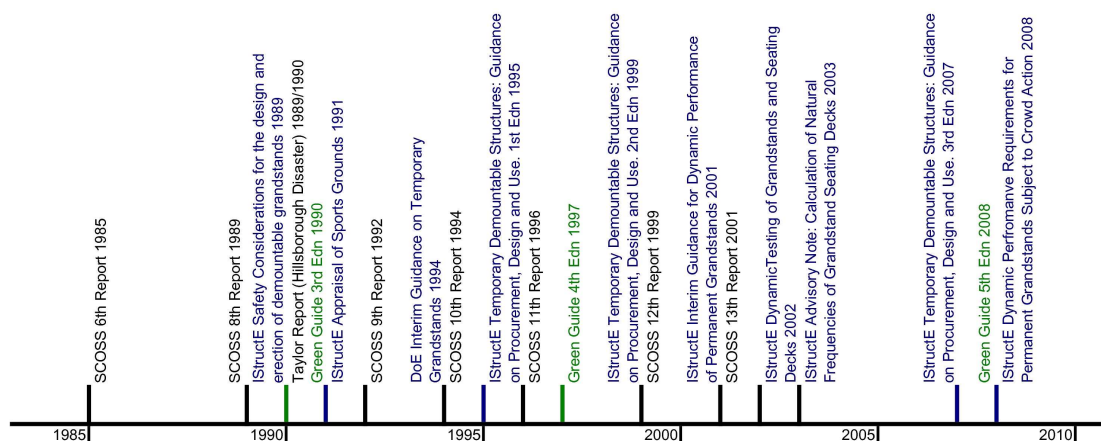
2.1 Designing for Dynamic Crowd Loading

2.1.1 The Introduction of Human Dynamic Loading to British Standards

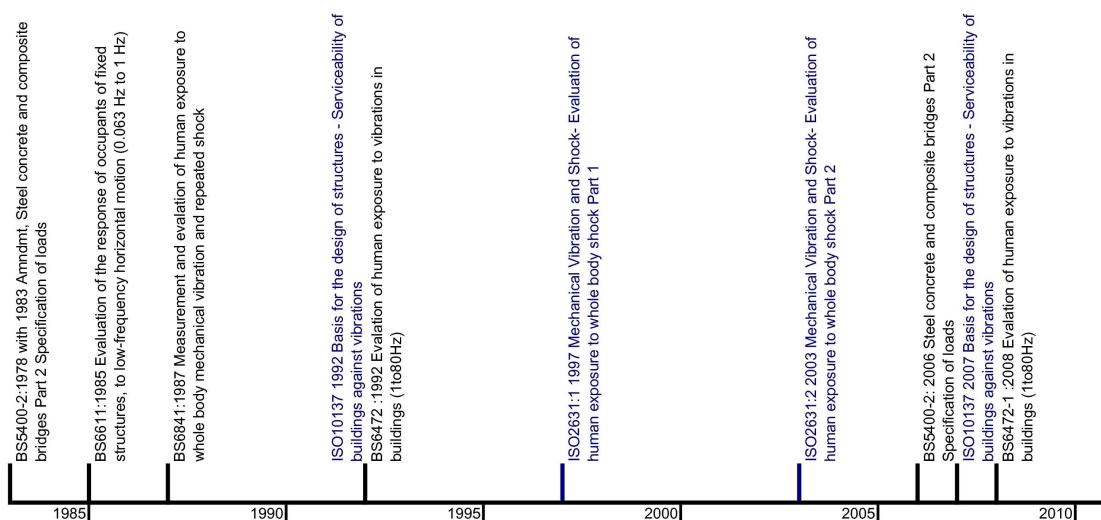
Publication Time Line



British Standards (and Referenced Guidance Documents) for Dynamic Loading



Stadium Specific Guidance



Additional British and ISO Standards for Vibrations

Figure 2.1 Publication Time Line

Dynamic loading due to crowds was first acknowledged in the British Standard for loading in the 1984 Edition of BS6399 Part 1 (Figure 2.1). At that stage no values for the magnitude of the load or guidance on assessing such loads were given, although the use of load factors applied to static loads was cautioned. (Prior to this the British Standard for loading, CP3 Chapter V Part 1 1967, contained a section on dynamic loading, however this just related to loads imposed by machinery and other plant.)

This mention of human dynamic loading was added to BS6399 Part 1 1984 following the Greater London Council's ruling in 1981, that they would not allow pop concerts to be held in London unless the floor could withstand a static live load of 10kN/m^2 i.e. twice the static imposed load given in CP3 Chapter V Part 1 (1967) (New Civil Engineer 1981). The British Standard Institution's (BSI) loading committee were also alerted to the results of load tests carried out in the Playhouse in Edinburgh in 1981 during a concert by The Who (Wade, NCE international 1981). The conclusion of this report was that the equivalent static load required to simulate a 'pogo-ing' crowd, jumping in unison, was between 9kN/m^2 and 12kN/m^2 , depending on the mass of the floor structure. This amplified loading was to ensure the safety of the structure under dynamic loading rather than for acceptability of vibrations to the concert goers (Figure 2.2).

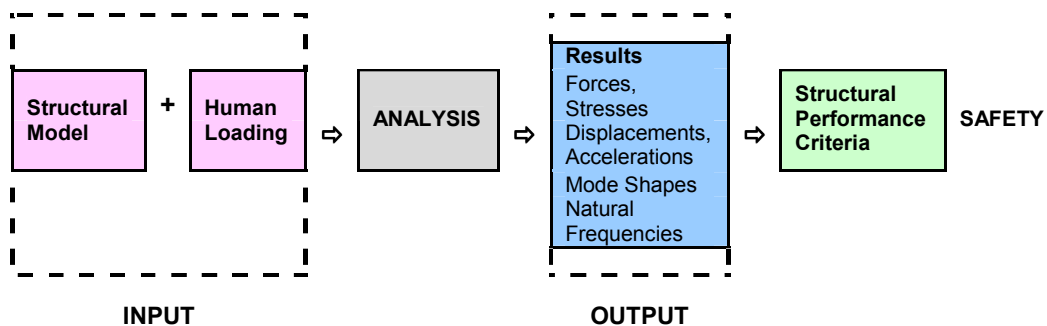


Figure 2.2 Designing for Dynamic Crowd Loads in the UK pre 2004

The subsequent 1996 edition of BS6399 Part 1 was the first time that a specific clause on the assessment of synchronised crowd loading was included, together with an appendix relating explicitly to floors subject to dance type loads. This introduced frequency limits as a means of specifying acceptability to official UK design standards although the concept had been used in the Institution of Structural Engineers (IStructE) / Department of the Environment's (DoE) publication 'Interim Guidance on Temporary Grandstands' in 1994.

The principle of the new clause was that if the fundamental natural frequency of the empty structure was above a given value (for a given direction) then resonance (in that direction) would be avoided and hence any dynamic magnification of the given static load could be ignored. If the frequency was below the given limit, and the structure was likely to be subjected to synchronised crowd loading, then further dynamic analysis was required. Both vertical and horizontal frequency limits were specified. Annex A of the same code gave limited information on calculating dynamic loads in the form of a Fourier series for various types of group activities together with the frequency ranges over which these loads should be considered. A crowd factor of 0.67 was also recommended to allow for lack of synchronisation between members of the crowd. In addition to the vertical dynamic load, calculated as described, a horizontal load of 10% of the vertical load was specified to be resisted. At this stage the acceptability criteria focussed solely on the safety aspects of designing the structure for increased forces due to the dynamic nature of the load (Figure 2.2).

The frequency limits set by BS6399 Part 1 1996 and the IStructE/DOE interim guidance note (1994) were 8.4Hz vertically and 4Hz horizontally. The vertical limit was based on avoiding resonance of the structure due excitation from the first three harmonics of the loading function, while the horizontal limit avoided resonance due to the first harmonic only. (These limits assumed that the maximum frequency at which large groups of people can perform a coordinated activity is 2.8Hz.)

The first edition of BRE Digest 426 'The Response of Structures to Dynamic Crowd Loads', published in 1997, provides background information on the 1996 revisions to BS6399 Part 1 and additional formulae for the calculation of the response of structures to human induced dynamic loading. Similar to the British Standard no additional acceptance criteria were provided for comparing the output response against except for a structural integrity check for the magnified loading (Figure 2.2).

In 2002 an amendment to BS6399 Part 1 was issued. This revision saw a change in the British Standard's approach to dynamic loading. The previous clause on dynamic loading was moved from the main body of the text to the appendices and the status of the information provided changed from 'normative' i.e. prescribed rules, to 'informative' i.e. for guidance. The former Annex A, covering loading advice, was

removed and replaced with references to specialist guidance documentation, namely BRE Digest 426 (1997). The frequency limits were, however, retained. It was stated that the reason for these amendments was that the BSI wished to limit the guidance given in the British Standard and to place the emphasis on specialist advice and publications.

In response to this amendment the BRE published the second edition of their Digest 426 in 2004. This superseded the 1997 edition and included experimentally derived load models for crowds of people jumping (Ellis and Ji 2002). Plus for the first time in British guidance, human acceptability criteria based on Kasperski's (1996) acceleration limits (Figure 2.3) (Refer to Section 2.3 for further information on Kasperski's (1996) acceleration limits). The 2004 BRE Digest 426 focuses on vertical movement only, removing previous references to horizontal components of vertical dynamic loading and horizontal frequency limits. This is presumably because of the upgraded status of this report in relation to the British Standard and the fact that the previous guidance on the horizontal aspects of crowd loading was based on very limited research that had been carried to date on horizontal loading and acceptability due to synchronised vertical dynamic crowd action.

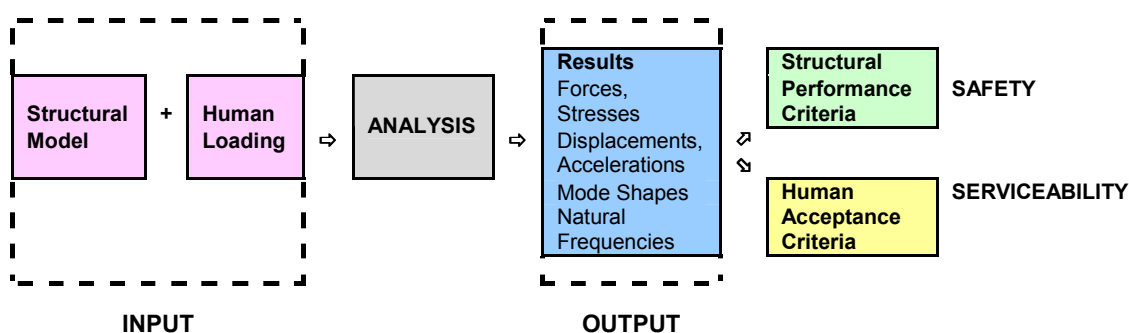


Figure 2.3 Designing for Dynamic Crowd Loads in the UK post 2004

With the UK move to the use of Eurocodes (for structural design) in 2010, BS6399 became superseded. However the approach to designing for synchronised crowd loading used in BS6399 Part 1 1996 (2002 edition) was transferred almost directly to the equivalent Eurocode National Annex (NA to BS EN 1991-1-1:2002 (published 2005)). The one main alteration was the addition of a clause relating to structures providing spectators facilities where 'the relevant certifying body may refer to specific guidance documents that are considered appropriate and sufficient for compliance with their requirements' e.g. stadium specific guidance.

(The frequency limits given in the British Standards, BRE Digest 426 and other British design guides are summarised in Tables 2.2 and 2.3.)

2.1.2 Structural Safety, Stadium Design and the Avoidance of Resonance

The importance of human dynamic loading in relation to the safety of crowds at sports grounds has long been recognised. The Standing Committee on Structural Safety (SCOSS) is a joint working body of the Institution of Structural Engineers (IStructE), the Institution of Civil Engineers (ICE) and the Health and Safety Executive (HSE). SCOSS reports biannually on current matters relating to safety of structures and in particular how better informed design can minimise the risk of accidents occurring. Since their sixth report in 1986 the issue of safety of grandstands has been a recurring topic.

The collapse of a temporary grandstand, in May 1982, during the filming of a BBC television programme, brought the safety of such scaffolding structures to the attention of SCOSS. Furthermore in their sixth report (1986), with reference to a paper published in *The Structural Engineer* by Dickie (1983), they highlighted the main factors which could contribute to the failure of temporary grandstands. This list included 'possible dynamic response leading to overload' and was followed by support of the IStructE's initiative to produce a guidance document on the structural safety and stability of temporary grandstands.

The eighth SCOSS report, published in 1989, followed the Hillsborough disaster in April 1989 where 96 people died as a result of overcrowding due to poor crowd management and stadium design. Unsurprisingly, the report focussed again on safety at sports grounds in particular, the flow of high density crowds. Since the sixth report, in 1986, a draft version of the report 'The Design and Erection of Demountable Grandstands' had been produced by the IStructE and submitted to Lord Justice Taylor to aid in his inquiry into the events which occurred at Hillsborough (cited by SCOSS 1989). The eighth report noted that the final version of this IStructE report would cover synchronised crowd loading of demountable grandstands. The IStructE at this stage was also drafting a report on the 'Appraisal of Sports Grounds' which planned, amongst other items, to address structural condition, crowd density, flow and management.

In May 1989 the IStructE published the final version of 'Safety Considerations for the Design and Erection of Demountable Grandstands'. This guidance report recommended the use of the standard static load given in the British Standard for loading and included a section on dynamic response. The report explains how the dynamic load, due to rhythmic activities, can be calculated. It suggests that stands with fundamental frequencies above 6Hz should give an acceptable response whilst the use of stands with a frequency between 4Hz and 6Hz should be carefully considered and those with a frequency below 4Hz should be analysed further. (The direction of this fundamental frequency is not given but is assumed to be vertical.) The advice provided at this time was similar to that given in the 1985 edition of the National Building Code of Canada (NBCC) (cited IStructE 1989).

By the time the ninth SCOSS report was published in 1992 the findings of the Taylor Report on the Hillsborough disaster had been released. This recommended that the standing terraces at all top division football grounds be converted to all-seater stands (cited SCOSS 1992). SCOSS (1992) identified that if similar numbers were to be accommodated as had been with standing terraces this legislation would necessitate the construction of large span roofs and long cantilevers and that the design of such elements would require specialist technical skills and raise a host of structural safety issues.

Prompted by the tragic collapse of a temporary stand in Bastia, Corsica in 1992 (which killed 17 and injured over 2000) SCOSS, in their ninth report, recommended that all temporary grandstands and stages, plus all retractable and demountable terracing, be subject to an independent structural engineering check prior to being licensed. They also recommended that 'further research should be carried out on crowd loading and that additional technical guidance should be prepared'.

In 1991 the IStructE published 'Appraisal of Sports Grounds' as a complementary guide to HMSO's 1990 3rd Edition of the 'Guide to Safety at Sports Grounds'. The aim of this IStructE publication was to help unify the level of safety provided at all sports grounds independent of their size and nature (as observed by Snelson 1989 and Dickson 1991). The IStructE's recommendations, in relation to loading, were that grandstands should be designed to withstand the static vertical imposed loads given in BS6399 Part 1 (1996) and a horizontal force, in addition to the wind loading,

representing the effect of the crowd surging. This load was to be taken as 156N per person parallel to the row of seats and 200N per person perpendicular to the row of seats (approximately 10% of the vertical imposed loads). In addition to these loads it was advised that to avoid resonant response of the structure, due to dynamic crowd loading, the natural frequency of the stand should be above 4Hz. (Again the direction of this fundamental natural frequency is not specified but is assumed to be vertical)

In August 1994 the Department of the Environment's Interim Guidance on Temporary Grandstands was published in *The Structural Engineer* (IStructE/DOE 1994). This two page article covered safety issues relating to temporary grandstands including a segment on structural design. The recommendations given were that temporary grandstands should be designed for the static loads given in the relevant British Standards including (from BS5973 for scaffold structures) a horizontal load equivalent to 10% of the vertical imposed load in addition to any wind load. For dynamic performance, the guidance was that the stand should be designed either to withstand the likely dynamic load or have a high enough natural frequency that resonance is avoided. The fundamental frequency limits given, to prevent significant dynamic response for load cases such as occur at pop concerts, were 8.4Hz vertically and 4Hz horizontally based on a an empty stand. No advice was provided on estimating the magnitude of the dynamic loading due to crowd movement. This guidance note was issued as a precursor to the definitive report on temporary and demountable structures first published by the IStructE in 1995. The frequency limits and notional horizontal loads, first specified in the publication, were later incorporated into BS6399 Part 1 1996.

The tenth SCOSS report, published in 1994, again raised the topic of the safety of temporary grandstands and acknowledged that the IStructE's guidance notes on demountable (IStructE 1989) and temporary (IStructE/DOE 1994) grandstands 'should help engineers to avoid unacceptable dynamic movements'. The report also mentions that the Department of the Environment had commissioned the Building Research Establishment (BRE) to research the effects of dynamic loading on sensitive stands to clarify uncertainties identified in the preparation of the Interim Guidance Note on Temporary Grandstands (IStructE/DOE 1994).

In 1995 the IStructE published guidance on the design and use of temporary grandstands within 'Temporary Demountable Structures: Guidance on Procurement Design and Use'. This document advised that such structures be designed for the static loads given in the British Standard BS6399 Part 1 but that a notional horizontal load be resisted in addition to any calculated wind load. This notional horizontal load consisted of two components. The first allowed for imperfections in the structure and the second for dynamic lateral loads due to the crowd. The magnitude of this horizontal force varied between 5 and 10% of the vertical imposed load depending on the likelihood of synchronised movement of the spectators. The livelier the crowd were likely to be, the greater the additional horizontal load. For resistance to dynamic loading future amendments to BS6399 Part 1 were referenced and it was advised that to avoid resonant response from rhythmic movement of spectators at events such as pop concerts that the fundamental frequency of the empty stand be above 8Hz vertically and 4Hz horizontally.

The 1996 eleventh SCOSS report yet again highlighted the high risk of loss of safety on temporary grandstands and stages, citing two non fatal collapses in 1994 and 1995. The SCOSS committee stressed the need to implement the recommendations given the IStructE guide to temporary demountable structures to ensure better safety of such structures.

In 1997 the 4th Edition of HMSO's 'Guide to Safety at Sports Grounds' (The Green Guide) was published. This revision included new advice on the effect of dynamic forces and acknowledgement of the wider uses of grandstands for non sporting events. Similar to the British Standard, the principle of designing for or avoiding the problem due to dynamic loading was introduced. Frequency limits of 6Hz vertically and 3Hz horizontally were set, below which further dynamic analysis of the structure was required. Interestingly the Green Guide specifically notes that the mass of the spectators should be given due consideration when carrying out the dynamic analysis. This differs from the British Standard and IStructE publications which advocate the use of natural frequencies based on an empty stand (i.e. with no live load due to people). The Green Guide also highlights that, for venues staging pop concerts or events at which rhythmic activities could occur, the dynamic loading may be greater than for sporting events, although no specific guidance as to these loads is either given or referenced.

The second edition of the IStructE's 'Temporary Demountable Structures: Guidance on Procurement Design and Use' was published in 1999 and contained similar advice to before on the loading of temporary grandstands. The main revision in relation to temporary grandstands was the addition of reference to the dynamic loading clauses in BS6399 Part 1 1996. The frequency limits of BS6399 Part 1, at 8.4Hz vertically and 4Hz horizontally, were recommended and temporary demountable stands with a natural frequency below these limits, which were likely to be subject to synchronised crowd loading, were required to be analysed using the dynamic loads given in BS6399 Part 1 1996. Those above this limit were deemed satisfactory. The additional notional horizontal loads remained as before.

The twelfth SCOSS report in 1999 focussed on structural inspections and safety appraisals of sports grounds in particular large stadia structures.

In January 2000 a Joint Working Group (JWG) was set up by the IStructE, the Department for the Environment, Transport and the Regions (DETR) and the Department for Culture, Media and Sport (DCMS) to make recommendations on what additional guidelines were required in relation to the dynamic performance and design of stadia structures and seating decks. The first step was for the JWG to publish 'Dynamic Performance Requirements for Permanent Grandstands Subject to Crowd Action: Interim Guidance on Assessment and Design' in 2001 (IStructE 2001). This document recognised that the use of sports grounds has changed over the years and grandstands are now much more likely to be used for entertainment events such as pop concerts. Stand design has also changed. Obstructed views are no longer considered acceptable and spectators wish to be as close to the field of play as possible. These factors have led to longer, more flexible cantilevered tiers combined with livelier crowd behaviour, meaning that human dynamic loading has become a serious issue that needs addressing.

The interim guidance gave vertical frequency limits for grandstands used for various types of event, dependent on the likelihood of synchronised crowd movements occurring. These limits (summarised in Table 2.1) are suitable for new and existing stands and are based on observations of existing grandstands and an understanding of dynamic behaviour of structures.

Table 2.1 Summary of Frequency Limits given in the IStructE's (2001) 'Dynamic Performance Requirements for Permanent Grandstands Subject to Crowd Action: Interim Guidance on Assessment and Design'

Proposed Use of Grandstand	Frequency Limit (Vertical)	Harmonics Considered
Viewing Events only – No singing or music played	3.5Hz for new stands 3.0Hz may be satisfactory for existing stands	1 st Harmonic only
Incidental Music – Some music played and crowd singing without musical accompaniment likely	5Hz	1 st and most 2 nd Harmonics
Pop Concerts	6Hz	1 st and 2 nd Harmonics

As for previous publications, these limits are based on the assumption that the maximum frequency that large groups of people can jump vertically in a coordinated fashion is 2.8Hz and are to be compared against the natural frequency of the empty stand. Unlike previous guidance using a 8.4Hz limit where the first three harmonics of the dynamic loading function are considered ($3 \times 2.8\text{Hz} = 8.4\text{Hz}$) the interim guidance deems that even for the most onerous loading during pop concerts only the first two harmonics are critical for avoidance of resonance in permanent grandstands ($2 \times 2.8\text{Hz} = 5.6\text{Hz}$). This could be due to the nature of the seating in such venues restricting the most intense dynamic loading.

As for the IStructE's (1999) 'Temporary Demountable Structures: Guidance on Procurement Design and Use', notional horizontal loads were given to be designed for, in addition to any wind loads given in the British Standard. This supplementary load is equivalent to 7.5% of the design vertical live load in stands where pop concerts are to be held and 5% in all other cases. This is typically less than the equivalent horizontal load specified for temporary grandstands, presumably due to the inherent difference in robustness between permanent and temporary structures. The interim guidance for permanent grandstands proposed that if adequate horizontal stiffness is provided by designing for this notional horizontal load then the Green Guide requirement for detailed dynamic analysis of grandstands with horizontal natural frequencies below 3Hz is fulfilled.

The JWG were satisfied that if grandstands were properly constructed and maintained and designed to the static loads given in BS6399 Part 1, in addition to the notional horizontal load given in the guidance, then provided that the natural frequency of the stand is above the limit for the proposed use then structural collapse due to synchronised dynamic crowd loading is 'extremely unlikely'. Although stating that the guidance focuses on how individuals react to induced motion, the avoidance of panic and the provision of adequate levels of comfort, the publication stresses that frequency limits are a coarse grained approach and highlights that there are existing grandstands with frequencies below the given limits that have performed satisfactorily, even under pop concert use. It recommended that in many cases a more detailed assessment to predict the levels of vibration is preferable and comments that the dynamic loading function given in BS6399 Part 1 1996 (pre 2002 amendment) has been shown to overestimate the dynamic response of the structure when compared to real grandstands. The JWG acknowledged that further research into dynamic crowd loading, the way in which the dynamic response of the structure can be reliably predicted from the loading function and appropriate criteria for levels of vibration that can be tolerated without discomfort or panic, was required. The interim guidance also recommended that a central database on the dynamic performance of existing grandstands was set up in order to help develop the design requirements.

As promised, the IStructE JWG followed up the publication of the Interim Guidance Note with advisory notes on the 'Dynamic Testing of Grandstands and Seating Decks' in 2002 and the 'Calculation of Natural Frequencies of Grandstand Seating Decks' in 2003. The first of these notes, published as a stand alone document by the IStructE, was an aid to specifying and procuring dynamic tests of a grandstand structure and gave details of the various tests that are available with advice on the levels of testing that are required for different situations. The second advisory note, published in *The Structural Engineer*, aimed at clarifying the method that should be used to calculate the natural frequency of the grandstand, highlighting common pitfalls and inaccuracies in approximations. The need for the above guidance was summarised in the thirteenth SCOSS report published in 2001.

The 3rd edition of the IStructE's 'Temporary Demountable Structures: Guidance on Procurement, Design and Use' was published in April 2007. The frequency limits and dynamic vertical loading remain, as before, as defined by BS6399 Part 1. The main change in relation to temporary demountable grandstands is that the minimum notional horizontal force has been increased from 5% to 6% of the vertical imposed load. For demountable stands for concerts and football/rugby matches this notional horizontal force rises to 7.5% or 10% of the vertical imposed load depending on the predicted behaviour of the crowd (as per previous editions of this publication).

In December 2008 the Joint Working Group of the IStructE finally published 'Dynamic Performance Requirements for Permanent Grandstands subject to Crowd Action', the follow-up to the Interim Guidance (IStructE 2001). This design guide proposes two acceptable methods for the design of permanent grandstands subject to synchronised crowd loading. Route 1 is based on frequency limits, similar to the Interim Guidance, while Route 2 aims to estimate the performance of a stand under a particular loading scenario. The frequency limits of Route 1 are a simplification of those used in the Interim Guidance. 3.5Hz is given as the minimum vertical frequency acceptable for the Route 1 method when calculated for an empty stand. This limit rises to 6Hz for stands where any form of synchronised crowd participation, from standing spectators, is likely to occur e.g. pop concerts and high profile sporting events. The Route 2 method uses a two degree-of-freedom system to model the crowd-structure interaction. Loadings are given for various event scenarios along with corresponding root mean square (RMS) acceleration limits which need to be complied with. Although the loading model for this publication has incorporated a significant amount of recent research, the human acceptance criteria are still based on the original thresholds suggested by Kasperski in 1996 (see Section 2.3 for further details). The acceleration limits are a means of assessing the comfort of the spectators located on the stand. A further acceptance criterion is given in the guidance for those seated beneath the structure in question this limits the dynamic displacement of the stand to 7mm RMS (from Kasperski 2001).

Despite all these recent publications, the guidance in relation to the dynamic design of stadia in the United Kingdom (as for structures subject to dancing and jumping to BS6399 Part 1:1996 with 2002 amendment) is based largely on the use of frequency limits (Tables 2.2 and 2.3). Limited advice is available on the design of permanent

grandstands (IStructE 2008) and other structures (BRE Digest 426 2004) for dynamic crowd loads. However, although loading functions are given, the corresponding human acceptance criteria provided are based on extremely limited published research, namely Kasperski 1996.

Table 2.2 Summary of Vertical Frequency Limits given in British Standards and Design Guides

Publication	Vertical Frequency Limit*	Harmonics Avoided
BS6399 Part 1 1984⁺	None	-
IStructE Safety Considerations for the design of Demountable Grandstands 1989	6Hz	1 st and 2 nd
IStructE Appraisal of Sports Grounds 1991	4Hz	1 st only
IStructE/DoE Interim Guidance on Temporary Grandstands 1994	8.4Hz	1 st 2 nd and 3 rd
IStructE Temporary Demountable Structures 1995	8.0Hz	1 st 2 nd and most 3 rd
BS6399 Part 1 1996⁺	8.4Hz	1st 2nd and 3rd
HMSO Green Guide 4 th Edn 1997	6Hz	1 st and 2 nd
BRE Digest 426 1997 Edn	8.4Hz	1 st 2 nd and 3 rd
IStructE Temporary Demountable Structures 1999	8.4Hz	1 st 2 nd and 3 rd
IStructE Interim Guidance for Dynamic Performance of Permanent Grandstands 2001	3.5Hz for viewing only 5Hz for incidental music 6Hz for pop concerts	1 st and some 2 nd for viewing only 1 st and most 2 nd for incidental music 1 st and 2 nd for pop concerts
BS6399 Part 1 1996 with 2002 amendment⁺	8.4Hz	1st 2nd and 3rd
BRE Digest 426 2004 Edn	8.4Hz for jumping on floors 6Hz for pop concerts on grandstands	1 st 2 nd and 3 rd 1 st and 2 nd for pop concerts on grandstands
National Annex to Eurocode 1 NA to BS EN 1991-1-1:2002 ⁺ (pub 2005)	8.4Hz	1 st 2 nd and 3 rd
IStructE Temporary Demountable Structures 2007	8.4Hz	1 st 2 nd and 3 rd
IStructE Dynamic Performance Requirements for Permanent Grandstands 2008	3.5Hz for viewing of typical sporting events and classical concerts 6Hz for pop concerts and high profile sporting events	1 st and some 2 nd 1 st and 2 nd

* Frequency limits given for empty structure

⁺ For structures subject to synchronised crowd loads

Table 2.3 Summary of Horizontal Frequency Limits given in British Standards and Design Guides

Publication	Horizontal Frequency Limit*	Harmonics Avoided	Notional Horizontal Load **
BS6399 Part 1 1984 ⁺	None	-	-
IStructE Safety Considerations for the design of Demountable Grandstands 1989	None	-	-
IStructE Appraisal of Sports Grounds 1991	None	-	156N / person parallel to row of seats plus 200N / person perpendicular to row of seats
IStructE/DoE Interim Guidance on Temporary Grandstands 1994	4Hz	1 st	10% of vertical imposed load
IStructE Temporary Demountable Structures 1995	4Hz	1 st	5%, 7.5% or 10% of the vertical imposed load based on use of grandstand
BS6399 Part 1 1996 ⁺	4Hz	1st	10% of the vertical load
HMSO Green Guide 4 th Edn 1997	3Hz	1 st	-
BRE Digest 426 1997 Edn	4Hz	1 st	7% to 10% of the vertical load
IStructE Temporary Demountable Structures 1999	4Hz	1 st	5%, 7.5% or 10% of the vertical imposed load depending on use of grandstand
IStructE Interim Guidance for Dynamic Performance of Permanent Grandstands 2001	Refers to 3Hz given in Green Guide but no limit set	-	5% or 7.5% of the vertical imposed load depending on use of grandstand
BS6399 Part 1 1996 with 2002 amendment ⁺	4Hz	1st	-
BRE Digest 426 2004 Edn	None	-	-
National Annex to Eurocode 1 NA to BS EN 1991-1-1:2002 ⁺ (pub 2005)	4Hz	1 st	-
IStructE Temporary Demountable Structures 2007	4Hz	1 st	6%, 7.5% or 10% of the vertical imposed load depending on use of grandstand
IStructE Dynamic Performance Requirements for Permanent Grandstands 2008	1.5Hz	-	Typically 5% of the vertical imposed load or 7.5% of the vertical live load if used for pop concerts or other lively events

* Frequency limits given for empty structure

** To be designed for in addition to design wind loading

⁺ For structures subject to synchronised crowd loads

2.1.3 Additional Codes and Standards

2.1.3.1 British Standards

In addition to BS6399 Part 1 there are several other British Standards relating to vibrations. Although these are not directly related to stadium design they are worth reviewing in order to obtain a better understanding of how dynamics and vibrations are dealt with across the board by the British Standards Institution and to see if they provide any further insight into human perception of vibrations and acceptance criteria.

The most general code relating to the exposure of people to vibrations is **BS6841:1987 Guide to Measurement and Evaluation of Human Exposure to Whole-Body Mechanical Vibration and Repeated Shock**. This standard deals with vibrations, due to transport, machinery and industrial activities, which are transmitted to the whole body and gives methods for quantifying vibrations in relation to; perception, discomfort, interference with activities, motion sickness and human health. Vibration limits are not given in the code but methods are provided to enable such limits to be calculated separately. The appendices (which are for information only) provide current information on the possible effects of vibrations on humans.

The introduction to the code lists various factors influencing human response to vibrations. These are split into intrinsic variables such as age, sex, fitness, experience, expectation, motivation, posture etc. and extrinsic variables e.g. vibration magnitude, frequency duration, axis etc.

Methods for measuring vibration in terms of frequency weighted root mean square acceleration (a_{RMS}) are outlined, including the direction of measurement and the preferred measurement locations. The measured accelerations are to be frequency weighted by a factor (≤ 1) dependent on;

- a. the axis of the vibration,
- b. whether the human subject is likely to be standing, seated or lying down,
- c. which category of vibration is being considered (e.g. affecting health, activity, comfort etc) ,
- d. the frequency of the vibration.

The purpose of frequency weighting is to even out the human reaction to vibrations at different frequencies. Humans are more sensitive to certain frequencies of vibrations dependent on the factors a. to c. listed above and so the frequency weighting factor is set as 1 for the most sensitive frequencies and tapers down away from these key frequencies.

Interestingly BS6841:1987 notes that for measuring vibrations on non-rigid surfaces live subjects are to be used, because dummies/representative masses do not normally provide the correct dynamic response. This indicates that when carrying out any experimental work additional mass should not be used to represent humans. It also suggests that when preparing an analytical model of a structure, loaded by humans, the people need to be modelled as more than just an equivalent mass. Modelling the humans as an additional degree of freedom system, similar to the Route 2 method used by IStructE 2008, could possibly be appropriate.

BS6841:1987 divides the effects of whole body vibration (horizontal and vertical) on humans into 4 categories

1. Effects on Health (Clause 4/Appendix A)
2. Effects on Activities (Clause 5/Appendix B)
3. Effects on Comfort and Perception (Clause 6/Appendix C)
4. Motion Sickness (vertical only) (Clause 7/Appendix D)

The clauses provide the information required to calculate the frequency weighted a_{RMS} (for that category) based on recorded root mean square (RMS) accelerations. The informative appendices then give limited guidance on assessing the calculated frequency weighted acceleration.

Appendix A (Effects on Health) covers how to calculate vibration dose values (VDVs) based on a recording of the accelerations throughout the duration of the vibration, where,

$$VDV = \left(\int_0^T a^4(t) dt \right)^{1/4} \quad \text{eq 2.1}$$

With VDV = Vibration dose value in $\text{ms}^{-1.75}$

$a(t)$ = the frequency weighted acceleration

T = the total period of the day (in s) during which the vibration may occur

Alternatively (for certain situations) the VDV value for a day can be estimated (eVDV) using shorter segments of frequency weighted root mean square acceleration a_{RMS} and the duration of the vibration see (eq 2.2).

$$eVDV = [(1.4 \times a_{RMS})^4 \times T]^{0.25} \quad \text{where } T = \text{vibration duration in seconds} \quad \text{eq 2.2}$$

To allow readers to better understand VDV's, a graph is included showing the relationship between exposure time, weighted root mean square accelerations (a_{RMS}) and vibration dose values (VDVs). Appendix A of BS6841:1987 suggests that although 'there is no consensus of opinion on the precise relation between VDV's and the risk of injury, it is known that a VDV in the region of $15\text{ms}^{-1.75}$ will usually cause severe discomfort'. From the graph given, this is equivalent to $a_{RMS} = 10\text{ms}^{-2}$ for 1 second, i.e. 1g for 1s.

Appendix B of BS6841:1987 (Effects on Human Activities) gives guidelines for hand manipulation and control and visual control.

In Appendix C, Relating to Comfort, the following values (Table 2.4) are given as an approximate indication of the likely human reactions to various magnitudes of frequency weighted RMS accelerations: (Note: the same values are given in ISO2631-1 (1997) as vibration levels for passengers on public transport)

Table 2.4 Summary of Acceleration Ranges given in BS6841:1987 Appendix C Relating to Comfort

Frequency Weighted RMS Acceleration Range	BS6841:1987 Description of likely human reaction	Comparable Vibration Limits from Alternative References
< 0.135 ms^{-2}	not uncomfortable	0.005 ms^{-2} vertical perception limit (BS6472:1992)
0.135 to 0.63 ms^{-2}	a little uncomfortable	
0.5 to 1.0 ms^{-2}	fairly uncomfortable	0.55 ms^{-2} disturbing for 1-10Hz (Bachmann et al 1994)
0.8 to 1.6 ms^{-2}	uncomfortable	
1.25 to 2.5 ms^{-2}	very uncomfortable	1.8 ms^{-2} intolerable for 1-10Hz (Bachmann et al 1994)
> 2.5 ms^{-2}	extremely uncomfortable	3.5 ms^{-2} panic limit (Kasperski 1996)

It is stressed that acceptable conditions in one situation may not be acceptable in another. This is presumably due to the numerous factors (listed in BS6841:1987) that affect human response to vibrations and include environment, activity and expectation.

Appendix C also covers perception and states that 50% of fit alert people can just detect a weighted vibration with a peak magnitude of approximately 0.015ms^{-2} . This is slightly greater than the lowest limit of perception of vertical accelerations given in BS6472:1992 as 0.005ms^{-2} . Clause 6.3.5 of BS6841:1987 also adds the interesting point that perception thresholds decrease slightly when the duration of the vibration is increased up to 1 second but very little beyond this point i.e. perception threshold values are fairly constant if the vibration lasts 1 second or more but if the vibration lasts less than 1 second the vibration has to be slightly larger to achieve the same level of perception as a longer vibration. Therefore BS6841:1987 suggests that when determining perception thresholds there is little point in looking at time averaged acceleration values (e.g. a_{RMS}) or any time component. However for comfort/annoyance BS6841:1987 is clear that the duration of the vibration can play an important part and the cumulative effect should be considered using root mean quad acceleration, i.e. VDV.

Appendix D, of BS6841, deals with motion sickness, which occurs between 0.1 and 0.5 Hz. Although it is unlikely that permanent grandstands will vibrate at such a low frequency it is worth bearing in mind especially for horizontal mode shapes which generally occur at lower frequencies than vertical mode shapes.

BS6472:1992 Guide to Evaluation of Human Exposure to Vibration in Buildings 1 to 80Hz (superseded by the 2008 Edition) is probably the most relevant additional British Standard, as this code of practice addresses how vibrations occurring in buildings are perceived by the occupants and provides guidance as to levels of acceptability. Both continuous and impulsive vibrations, due to blasting etc., are considered. Throughout the code the use of frequency weighted accelerations (to BS641:1987) is preferred.

Recommendations are given for the measurement of vibrations in terms of root mean square (RMS) accelerations, which can then be compared against baseline curves,

together with the appropriate magnification factor, for various building occupancies and time periods. Both horizontal and vertical vibrations are considered. The acceptance criteria are provided in two forms, vibrations dose values (VDVs) (as eq 2.1 and 2.2) and root mean square (RMS) accelerations. Both are in such a form as to be time dependent and so the duration of exposure to the vibration is deemed important.

The base curves included in the document represent magnitudes of vibrations in buildings for approximately equal human response with respect to annoyance and/or complaints about interference with activities. The curves are given for vibrations horizontally and vertically, plotting peak velocity or RMS accelerations against frequency of vibration. The level of the curves is set so that with a magnification factor of 1 the values can be used in sensitive situations such as operating theatres and precision labs (human criterion governed) for all time periods. At vibration magnitudes below the base curves 'adverse comments or complaints of vibration are rare'. This implies that the values must be on or below the limit of human perception although the code does state that the curves are not necessarily the same profile as perception curves would be.

From the base curves it can be interpreted that the threshold of perception of vertical vibrations for standing or seated humans is approximately 0.01ms^{-2} (RMS) at 1Hz reducing to a constant value 0.005ms^{-2} (RMS) between 4 and 8Hz before increasing to 0.05ms^{-2} (RMS) at 80Hz. (This suggests that humans are most sensitive to vertical vibrations with frequencies between 4 and 8Hz.) Similar information is provided for horizontal vibrations. The base curve for horizontal vibration is lower than the curve for vertical vibrations at low frequencies as the human body is more sensitive to horizontal motion at low frequencies.

Using Appendix A of BS6472:1992 and the concept of Vibration Dose Values (VDVs), formulae are given to allow the reader to calculate an acceptable RMS acceleration for a given time period and a given building occupancy provided the frequency of the vibration is known. Alternatively if the frequency and duration of the vibration is known, then the RMS acceleration at which varying degrees of adverse comment are likely can be predicted. However this standard is very difficult to use in

the design stage of a structure as the designer needs to be able to predict the loading function of the vibration and advice on this is limited.

Guidance is provided at the end of the standard, in Appendix C, as to how velocity records can be compared against the recommendations given for accelerations, if these are the only form of vibration data available.

The current version of **BS6472-1:2008 Guide to Evaluation of Human Exposure to Vibration in Buildings, Part 1: Vibration Sources other than Blasting** no longer includes the base curves but focuses on the frequency weighting of measured accelerations and the calculation of VDV values (previously Appendix A) for comparison against an acceptance range, dependent on the building use and the time of day/night at which the vibration occurs. This change of emphasis reduces the background information provided to the user on the derivation of the given acceptance criteria and hence its relative influence on this research project.

British Standard BS ISO 4866:2010 Mechanical Vibration and Shock - Vibration of Fixed Structures - Guidelines for the measurement of vibrations and evaluation of their effects on structures supersedes BS7385 Part 1:1990 and provides guidance on monitoring vibrations in buildings in relation to damage likely to be sustained by the building itself. Evaluation of vibration response is covered at the end of the code with normative reference to other ISO and European standards regarding maximum limits for the safety of buildings but no actual figures are quoted. (The German design code DIN 4150-3 is one of the standards referenced in these clauses of BS ISO 4866:2010 and DIN 4150-3 (1999) is reviewed in Section 2.1.3.3 of this thesis.) Information on likely vibration sources and ranges of structural response are given in Annex A while Annex B of BS ISO 4866:2010 provides informative guidance on the classification of buildings in relation to their vibration resistance. Informative Annexes D and E cover respectively, predicting natural frequencies and damping of buildings and, how to assess soil/structure interaction under vibration loading.

Part 2 of BS7385 (**BS7385-2:1993 Evaluation and Measurement for Vibrations in Buildings – Part 2: Guide to damage levels from groundborne vibrations**) gives guidance on the levels of groundborne vibration above which building structures

could be damaged. It provides information on factors which may affect the building's susceptibility to damage and outlines how to measure vibrations in relation to assessing the possibility of vibration induced damage. Both transient and continuous vibrations are considered.

Vibration limits are given for different building types (replicated in BS5228:2 2009 Annex B). These limits are typically given in terms of peak velocities and vary depending on the frequency of the vibration however, below 4Hz the governing factor is displacement. For 'unreinforced or light framed structures, residential or light commercial buildings' a displacement limit of 0.6mm (zero to peak measured at ground level) is given above which cosmetic damage (hairline cracks in plaster/mortar joints) could possibly occur. Magnification factors for minor and major damage are also given. Informative annexes at the rear of the publication describe additional factors to be considered when assessing the affect of groundborne vibrations on buildings.

BS 6611:1985 Guide to Evaluation of the Response of Occupants of Fixed Structures, Especially Buildings and Off-Shore Structures, to Low Frequency Horizontal Motion (0.063Hz to 1Hz) provides guidance on the design of buildings and fixed off-shore structures in relation to their horizontal vibration response to infrequent excitation by external environmental forces (wind/waves).

Standard design curves (RMS acceleration ν freq) and design curves for special cases e.g. where an apparently stationary environment is required (i.e. below threshold of human perception) are provided in the appendices. These design criteria are based on the vibrations being perceived using non-visual cues. (If there are any slight oscillations of rotation about the vertical axis, visual effects exaggerate the sense of motion and accelerations less than those given by the curves are needed to produce a satisfactory response.)

Only one axis is considered by this code and so it applies to all orientations of the human body. Also the frequencies considered are similar to those causing motion sickness in BS 6841:1987 but in the horizontal plane rather than the vertical plane.

BS6611 notes that infrasound generated by the flow of air in ducts can induce the sense of structural vibration in the occupants of the structure. Therefore 'care should be taken when assessing adverse comments of occupants that a combination of motion and infrasound effects, acting simultaneously, have not combined to exaggerate the sensation of motion'.

An interesting point is made in the code that people living in low rise housing are sometimes prepared to accept magnitudes of motion due to frequently occurring events such as large vehicles passing that would concern occasional visitors. Whereas, those living in high-rise buildings do not readily adapt to motions that cause them alarm on the first occurrence. This is presumably due to the height off the ground and the implications of collapse.

The final British Standard considered is **BS 5400-2:2006– Steel, Concrete and Composite Bridges – Part 2: Specification for Loads**. This loading code for bridges deems that for highway bridges the effects of vibration due to traffic do not need to be considered. However for foot and cycle track bridges the vibration serviceability requirements, in summary, are that if the natural frequency of the unloaded bridge is less than or equal to 5Hz vertically then the maximum vertical acceleration should be limited to $0.5\sqrt{f_0} \text{ ms}^{-2}$, where f_0 is the natural frequency (in Hz) of the unloaded bridge. Formulae are provided for calculating the maximum vertical acceleration. A similar limit of 1.5Hz horizontally is given for the fully loaded bridge. This is similar to the frequency limit approach generally taken in the British Standards for the design of structures subject to synchronised crowd loading (see Tables 2.2 and 2.3).

As for other British design guides the vertical natural frequency of the bridge is to be calculated for self weight and applied dead loads only and it is recommended that the short term modulus of concrete is used in calculating this and the vertical acceleration.

Vandal loading (i.e. the deliberate inducing of a resonant response) is mentioned and it is suggested that the bridge and its bearings be suitably robust to resist this. An indication of the likely uplift force due to this loading, for prestressed bridges, is given as '10% of the static live load bending moment'.

2.1.3.2 Summary of Additional British Standards

As mentioned previously none of these additional British Standards relate directly to stadium design however there are several key issues that can be taken forward for consideration during this research project;

1. The various factors given in BS6841:1987 and BS6611:1985 which influence human perception of vibrations,
2. The use of frequency weighted RMS accelerations,
3. The use of Vibration Dose Values (VDVs) to measure human acceptance of vibrations,
4. The outline acceleration ranges of accelerations for human comfort given in BS6841:1987,
5. The avoidance of motion sickness due to low frequency vibrations (<1Hz),
6. The need to design the structure and finishes to allow for the structural movements that can be induced by synchronised crowd loading,
7. The possibility of deliberate vandal loading

As observed in Section 2.1.1 re BS6399 Part 1, there is a general swing of the more recent British Standards away from providing specific guideline values when designing for vibrations, instead alternative publications (including ISO and European Standards and specialist design guides) are being referenced.

2.1.3.3 International Standards

In addition to the British Standards reviewed above there are several International Standards produced by the International Organisation of Standardisation (ISO) regarding human exposure to vibrations and vibrations in buildings which have not yet been adopted as accepted codes of practice in the United Kingdom. Two of these standards, ISO 2631 and ISO 10137 are widely referenced in papers relating to human interpretation of vibration and so it is worth taking into consideration any supplementary information they may contain.

ISO 2631-1:1997 Mechanical Vibration and Shock – Evaluation of Human Exposure to Whole-body Vibration – Part 1: General Requirements. This part of ISO 2631 gives the general requirements for the evaluation of human exposure to

whole-body vibration. As such it explains in great detail how vibrations are to be measured and frequency weighted. (Similar to BS6472:1992 this is not much use for buildings that have yet to be constructed.) It also details how vibrations should be evaluated in terms of accelerations depending on the nature of the vibration, in relation to its effects on health, comfort and perception and motion sickness.

This ISO standard is very similar to BS6841:1987 with main clauses covering the frequency weighting of RMS accelerations and informative annexes providing limited advice on acceptable vibration levels.

For guidance on the effects of vibration on health, two equations are used to calculate vibration exposure using frequency weighted RMS acceleration a_{fw} and exposure period T ($a_{fw} \times T^{0.5}$ and $a_{fw} \times T^{0.25}$). Graphs of caution zones for each of these formulae are given. Above these zones health risks are likely. The caution zones for the two equations overlap for exposure periods between 4 to 8 hours.

The guidance provided on the effects of vibration on perception and comfort is the same as given in BS6841:1987 Annex C, including the guideline values and perception levels. ISO2631-1 does, however, clarify that the range of comfort levels given is for passengers on public transport and is therefore related to the type of activities that the passengers may expect to accomplish. For comfort levels vibrations in buildings ISO2631 Part 2 (1989) is referenced.

Part 2 of ISO 2631, **ISO 2631-2:2003 Mechanical Vibration and Shock – Evaluation of Human Exposure to Whole-body Vibration – Part 2: Vibration in Buildings (1Hz-80Hz)**, relates to human exposure to vibrations in buildings and is similar to BS6472.

This standard has been rewritten since the 1989 edition to bring it in line with ISO 2631-1:1997. The frequency weighting definitions have remained the same as the previous edition but these now form the main part of this code (in Annex A) together with advice on the collection of data concerning human response to building vibration (Annex B), as the guidance values for vibration levels have been omitted.

The only guidance as to acceptable levels of vibration, in relation to perception and comfort (in buildings and elsewhere), is now given in Annex C of ISO 2631-1:1997, which, as described above, only covers comfort levels of vibrations in vehicles. For buildings, ISO2631 Part 1 refers back to ISO 2631-2, which no longer gives guidance levels for vibrations.

The guidance levels for vibrations in buildings previously provided by ISO 2631-2 (1989) were in a similar form to BS6472 and are still part of the current ISO standard ISO10137:2007.

ISO 10137:2007 Bases for Design of Structures – Serviceability of Buildings Against Vibration covers all sources/types of vibrations and looks at effects of vibrations on structures and their contents as well as the human aspects. It also includes footbridges in addition to buildings.

Advice is provided on evaluating vibrations in buildings by calculation/analysis and by measurement. Vibrations are typed and classed as continuous, impulsive or intermittent. Similarly types of human occupancies of buildings are categorised as sensitive, regular, or active, and classes for how the vibrations affect the human occupants are given;

- a. Below human perception threshold (Generally used when criterion governed by requirements for sensitive instruments, see ISO 8569.)
- b. Basic threshold effects
- c. Intrusion, alarm and fear (may be associated with adverse comments)
- d. Interference with activities
- e. Possibility of injury/health risk

In addition to this, a list of the factors which influence human perception of vibrations in buildings is given. This includes direct effects such as frequencies, magnitude, duration, direction, form, variability etc plus indirect effects on the subjective response including; audible noise, visual cues, population type, familiarity with vibration, structural appearance, confidence in a building structure, height above ground, warning of events, activities engaged in, knowledge of the source of the vibration etc.

The informative annexes to ISO 10137 provide information on; the calculation of the applied dynamic loading from human activity and machinery using Fourier series, methods for analysing vibrations, vibration acceptance criteria and methods for isolating vibrations. The loading functions for human activities are taken from various sources and are provided for individuals walking and running and for coordinated group activities. The information provided on acceptance criteria, for various building uses, utilises base curves for vibrations in the x, y and z directions plotting frequency against acceleration (RMS) together with multiplication factors. This information is taken from ISO 2631-2 1989 (now superseded) in a revised format. Additional RMS acceleration limits are provided for the design of stadiums and floors in assembly halls. Two vibration criteria are given for such situations. The first, for the comfort of seated members of the audience, is set as 200 times the base curve. This RMS acceleration is to be measured over a 10s period whilst the second vibration limit, for the avoidance of panic, is to be measured over a 1s period. The vibration levels for the panic limit are twice those given for comfort i.e. 400 times the base curve (see Section 2.3.1).

As well as ISO 2631 and ISO 10137 the German standard DIN 4150 is commonly referenced when evaluating the influence of vibrations on occupants of buildings.

DIN 4150-2 Structural Vibration Part 2: Human Exposure to Vibration in Buildings covers a similar range of frequencies, 1-80Hz, as BS6472 however the procedure for assessing the vibrations is very different. The German standard uses weighted normalised RMS velocities and converts them to a KB(t) signal (using DIN 45669-1). The KB signal is related to the RMS velocity and the ratio of the vibration frequency to a cut-off frequency of 5.6Hz. Similar to BS6472-1:2008 and ISO10137 various acceptance ranges are given for different building occupancies dependent on whether day or night time use is being considered.

Separate guidelines are given for assessing vibrations due to traffic, various types of trains and construction activities.

Part 3 of DIN 4150 **DIN 4150-3 Structural Vibration Part 3: Effects of Vibrations on Structures** covers the effects of both short and long term vibrations on structures. These can either be calculated using empirical formulae or using measurements from

the building. Guidelines in terms of un-weighted velocities are given for vertical vibrations at foundation level and for horizontal vibrations at the upper-most storey depending on the use and construction of the building. Limits are also provided for serviceability of floors and buried pipework.

Of the additional codes of practice discussed, all except ISO 10137, focus on the measurement of vibrations in existing buildings and the effects these may have on the occupants and the building itself. Only ISO 10137 provides guidance on predicting the likely dynamic loading and the vibrational response of the structure. ISO10137 is also the only standard that covers human dynamic loading and, in particular, that due to synchronised crowd movement. In the previous edition of ISO10137:1992 advice on this topic was taken from the National Building Code of Canada which was internationally acknowledged as the leading design standard on human dynamic loading at the time and therefore demands a more detailed examination.

The **National Building Code of Canada 2005** (NBCC 2005) (sentence 4.1.3.6) states that where a structural system, with a natural frequency of $<6\text{Hz}$, supports an assembly occupancy, the effects of resonance shall be investigated by means of a dynamic analysis, as specified in Commentary D (**NBC 2005 Structural Commentaries (Part 4 of Division B) - Commentary D Deflection and Vibration Criteria for Serviceability and Fatigue Limit States**). (This clause also covers footbridges.)

The NBCC also gives minimum horizontal loads that are required to be taken by structural elements that support fixed seats in any building used for assembly occupancies e.g. grandstands, stadia and theatres. These forces are 0.3kN/m length of seats acting parallel to the rows of seating and 0.15kN/m length of seats acting perpendicular to the rows of seating which, are to be assumed to act independently of one another. This is similar to the (7.5% of live load) horizontal load given in the IStructE (2008) guidance on stadia.

As for British design guides (Wyatt 1989 and Hicks and Devine 2004), the formula for calculating the natural frequency of the floor system, in Commentary D, is based on

its total deflection and in this case, unlike the British guidance, the weight of the participants is included.

Formulae are also given, in Commentary D, for calculating the dynamic load for various rhythmic activities and for the dynamic response factor ($\delta_{\text{dyn}}/\delta_{\text{static}}$). Damping ratios are provided for various floor constructions loaded with large or small groups of people. Using this information the structural integrity of the building can be checked to avoid overloading and fatigue. This is the safety criterion; additional serviceability criteria for occupant comfort also have to be satisfied.

A range of acceleration limits are specified for various combinations of activities together with formulae for calculating the peak acceleration based on dynamic load factor, ratio of weight of the participants to the total weight (floor + people) and the ratio of the natural frequency of the floor to the forcing frequency. The peak acceleration limits specified, for human comfort, are 0.4 to 0.7%g (0.04 to 0.07ms⁻²) for offices and residential floors, 1.5 to 2.5%g (0.15 to 0.25ms⁻²) for those occupancies sharing a floor with rhythmic activities i.e. dining and dancing, weightlifting and aerobics. Finally for rhythmic activities only separate limits are given for office/residential buildings 4 to 7%g (0.4 to 0.7ms⁻²) and for stadiums/arenas 10 to 18%g (1.0 to 1.8ms⁻²). As for the other standard and design guides reviewed, the stadium specific acceleration limits are based on the research carried out by Kasperski (see Section 2.3.1).

The Canadian code recommends that to avoid resonance ‘the fundamental natural frequency of the floor structure should be greater than the highest significant harmonic forcing frequency’. For dancing and lively sports events/concerts this is taken as the first two harmonics while for aerobics it is recommended that the first three harmonics are considered. This is similar in principle to the British vertical frequency limits of 8.4Hz for floors subject to dancing and jumping and 6Hz for pop concerts at grandstands, where 2.8Hz is taken as the maximum frequency which large groups of people can jump in unison. However the formula given for calculating the Canadian code frequency limit is more complex incorporating the acceleration limit for the floor occupancy and the ratio of the total floor weight to the weight of the participants. From this, a table of examples for various floor constructions and activities has been calculated. This shows that lightweight floors may require a

natural frequency of 15Hz for aerobics and weight lifting to occur simultaneously while a solid concrete floor with a natural frequency of 6Hz would be suitable for a lively concert. Interestingly the Canadian code does not distinguish between floors and grandstands, therefore a floor where large crowds could jump at a concert has the same frequency limitations as a tiered seating tier.

2.1.4 Summary of British and International Standards for Designing for Dynamic Crowd Loading

For buildings and structures with areas subject to dancing and jumping loads the most recent edition of the British loading code (BS6399 Part 1 1996 with 2002 amendment) and the current National Annex to Eurocode 1 (NA to BS EN 1991-1-1:2002), recommend either designing to avoid resonance using frequency limits or designing for the applied dynamic loads. If one proceeds down the dynamic load route, loading functions in terms of Fourier series are given in BRE Digest 426 (2004) for rhythmic activities and advice is provided on calculating the dynamic response of the structure. While this information and the resulting output can be used for checking the structural safety, the guidance for assessing serviceability and human perception of vibrations is less clear. BRE Digest 426 suggests the use of acceleration levels and cites Kasperski's (EuroDYN 1996) proposed peak acceleration limits. However the authors note, in the same paragraph, that from experience vibration levels below those given by Kasperski as 'disturbing comfort' can still feel uncomfortable, even for those who understand why the vibrations are occurring. Kasperski's threshold limits are summarised in Table 2.5.

Table 2.5 Kasperski's (1996) peak acceleration limits as summarised in BRE Digest 426 (2004) (for a frequency range <10Hz)

Vibration Level (x = peak acceleration)	Reaction
5%g	Reasonable limit for passive persons
5%g < x < 18%g	Disturbing (<i>comfort</i>)
18%g < x < 35%g	Unacceptable
>35%g	Probably causing panic

For stadia design a similar approach is taken i.e. either avoiding resonance or designing for dynamic loading of the structure. The frequency limits given by the current IStructE (2008) British guidance, are 3.5Hz vertically for predominantly seated audiences and 6Hz for more excitable crowds. Under the recommendations all permanent grandstands have to be designed for additional notional horizontal loads, to allow for crowd action, as well as achieving 1.5 Hz as a minimum horizontal natural frequency. For cases where it is difficult to meet the vertical frequency requirement for a specific event a 2 degree-of-freedom load model is given together with maximum acceptable RMS accelerations for human comfort under various design scenarios. Although specified as RMS values these acceleration limits appear to be based primarily on Kasperski's 1996 peak acceleration thresholds.

In Canada, the section of the building code (NBCC 2005) relating to dynamic loading similarly covers the response of structures to coordinated rhythmic activities at lively sports events and concerts. The National Building Code of Canada supplements its basic frequency limit of 6Hz vertically with guidance on calculating the likely load that will be experienced by the structure together with accelerations that this loading will induce. Peak acceleration limits are then provided for human comfort, as a serviceability check.

ISO10137:2007 does not use frequency limits but instead gives information on a possible Fourier series loading function for coordinated rhythmic activities. Suggested acceptance criteria for stadiums are then given for the comfort of seated spectators and for the avoidance of panic.

Both the Canadian (NBCC 2005) and British (IStructE 2008) stadium specific design guides for synchronised crowd loads use the same key research paper published by Kasperski in 1996 (Table 2.5) as the basis for their serviceability limits for human acceptability. It is unclear what references were used to determine the stadium acceptance criteria given in ISO10137:2007 but it is likely that Kasperski's threshold values were used. The reason Kasperski (1996) is so heavily referenced is largely down to the fact that little other stadium specific acceptability research has been carried out. This is possibly due to the cross discipline nature of the subject (psychology/engineering) and the difficulty testing in-situ

From reviewing current British and International standards, and UK design guides for stadium design, two distinct methods of achieving serviceability under synchronised crowd loading are fairly universally adopted. The first of these is very simplistic; avoiding resonant vibrations by designing the fundamental natural frequency of the structure to be greater than a frequency that can be excited by the key harmonic frequencies of an active crowd. This approach is deemed to be somewhat conservative as existing structures with natural frequencies below the set minimum frequencies have been shown to perform adequately in service. Therefore the second, more economic, approach is to calculate the predicted response of the structure to a synchronised crowd load and compare the calculated vibration against both structural safety criteria and human acceptance criteria (Figure 2.4). Although different methods have been proposed for calculating predicted vibrations due to coordinated crowd loading, the human acceptance criteria given in all the publications are based primarily on one research paper, namely Kasperski 1996. Because of the extremely limited knowledge base upon which all these guidelines are based, it is on the human acceptance criteria for synchronised crowd loads in grandstands that this research focuses.

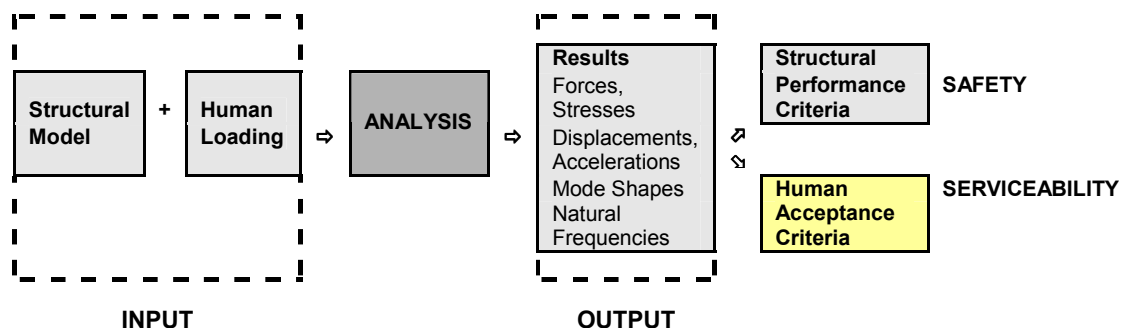


Figure 2.4 Design Procedure for Structures Subject to Synchronised Crowd Loads

The codes of practice and design guides reviewed have highlighted several factors that must be considered as part of this project and include;

1. The need for the research to be situation specific ,
2. Deciding what form to describe the vibration (displacement, velocity or acceleration),
3. Assessing whether peak or averaged values (RMS) should be used,
4. Investigating time and frequency dependency on acceptability.

2.2 Dynamic Loading of Grandstands

In order to obtain a better understanding of the magnitude and nature of vibrations which occur in real grandstands, a study has been carried out of past dynamic testing of grandstands focussing specifically on results obtained during real events (Sections 2.2.1 and 2.2.2). This review also highlighted the potentially serious implications of inadequate serviceability criteria (Section 2.2.1).

2.2.1 Examples of Stadia with Vibration Issues

Maracanã Stadium in Rio de Janeiro was built in the late 1940s to house 150,000 spectators and is still one of the largest stadia in the world. It has a reinforced concrete frame with two tiers and a 30m cantilevered roof. The 21m long cantilevered upper tier is supported by means of triangular concrete shear walls up to 3 storeys high and has a natural frequency of 4.6Hz (Batista and Magluta 1993).

In the 1990s problems due to human-induced vibrations raised concerns for the administrators of the stadium. As a result experimental measurements and Finite Element analysis of the stadium was carried out in order to arrive at a solution to the problem.

From laboratory tests the first 3 Fourier coefficients for jumping, bouncing and dancing and hard rock dance were determined (Batista and Magluta 1993). The highest recorded value of impact factor K_p (dynamic load/weight of participants) was 3.0. The authors stress that Brazilians, in particular, jump and bounce at football matches in an uninhibited fashion resulting in particularly high dynamic loads, even greater than those recorded for concert type loading.

Using the derived Fourier coefficients the authors predicted accelerations and displacements for the upper tier using a finite element model. The predicted accelerations varied from $20\text{--}30\text{ms}^{-2}$ with an accompanying displacement of 6.5mm for jumping football fans to $3\text{--}4.6\text{ms}^{-2}$ with 1mm displacement for a crowd at a rock concert. These values were compared against serviceability criteria. The limit set by the authors was $5\text{--}6.5\text{ms}^{-2}$ for short term exposure to vibrations of 1 to 5 minutes at a football match, based on ISO 2631-1 1985. For longer term vibrations such as those

at pop concerts the authors suggested a guideline upper bound limit of 20%g (2ms^{-2}). Clearly the calculated response far exceeded these serviceability requirements and so remedial works were proposed.

While Batista and Magluta preferred a solution using tuned mass dampers, due to time constraints, the administrators opted for a temporary solution of steel columns to prop the cantilever and barriers to stop spectators from jumping on the tip of the cantilever. These columns had an installed pre-compression which had to be maintained in order to avoid bolt fatigue and damage to the main concrete frame. In 2006 there was a wish to remove these columns to improve sightlines along with concerns over cracking to the cantilever beams and so Batista et al (2008) returned to carry out some further testing. Monitoring during several football matches recorded peak accelerations of 2.6ms^{-2} at 2.26Hz (combined with a peak displacement of 6mm) from short 15-30s bursts of highly coordinated jumping following a goal. Clearly this was less than previously predicted and so the loading model was correlated with the collected data (Batista et al 2008) and a solution using multiple synchronised dynamic attenuators designed and installed effectively reducing the vibrations by 50%.

Another football stadium with vibration issues is Feyenoord in Rotterdam. As with Maracanã there is a single cantilevered upper tier and cantilevered roof, but in this case the structure is a steel frame supporting concrete floor slabs and has a fundamental natural frequency of 5.8Hz vertically. Since the stadium was constructed in 1936 perceptible vibrations of 2-3mm in magnitude have occurred following goal events but these quickly die away and so were not deemed to be a problem (Van Staalduinen and Courage 1994).

Then in the 1980s the stadium started to be used as a venue for pop concerts. However this did not last long as after the second concert the vibrations were so strong that members of the audience were frightened and an immediate investigation was ordered. The concerns over large dynamic displacements and stress amplitudes meant that the authorities had to withdraw the stadium's permit to hold pop concerts only allowing limited permits for a few concerts, to allow measurements to be taken.

During the monitoring of one quarter of the upper tier dynamic, vertical displacements of 3mm were recorded on top of a static deflection of around 10mm. This was accompanied by a peak acceleration of 1.3m/s^2 .

As modifications to the structure proved too costly to allow concerts to be held a permanent monitoring system of the upper tier was installed. During an event if the magnitude of the vibrations reaches 4mm (above static) the sound level is reduced. Then if the vibrations continue to increase to 6mm the sound level is turned off. At an early stage the video screens go blank. This has been shown to effectively stop the rhythmic crowd movements and so far only on one occasion has the music nearly been switched off (Van Staalduinen and Courage 1994).

Problems with grandstand vibrations have also occurred at three of the premier ship clubs in the UK (Rogers 2000). At Manchester United's ground, Old Trafford, perceptible movement of the third tier of the North Stand was encountered during a pop concert in 1996. Since then the club have 'fixed' this and the tier is now only used for football matches. Rivals, Arsenal took a different approach and fitted tuned mass dampers to the top deck of the North Bank stand at Highbury, in 1998, after 'more movement than usual was detected during a game with Everton'.

In 2000 the new upper terrace at Liverpool's Anfield Road stand experienced clearly noticeable vibrations during one of the opening matches. Additional columns were then installed to raise the natural frequency of the structure before the first premier ship game was held (Rogers 2000). A similar situation occurred at the Millennium Stadium in Cardiff where steel props are now added to stiffen the cantilevered club tier before pop concerts are held.

Clearly even with modern guidelines, stadia are being built that do not meet the serviceability requirements set by the end users, the spectators. If their perception of the movement of the stand is such that they are disturbed then, the management has to take actions to remedy the situation. The reason for remedial works being required at all is largely due to the very limited information that has been published to date on human perception of vibrations due to synchronised crowd loading. As mentioned earlier this is the topic that this research aims to address. The following

section (Section 2.2.2) will look at measurements that have been taken on actual stands in terms of both input and output.

2.2.2 Measurements from Grandstands

In March 1992 a BRE research programme (funded by DETR) was initiated to look at the dynamic response of permanent, retractable and demountable seating (Littler 2000a, 2000b and 2000c). The dynamic characteristics of 50 empty demountable stands (Littler 2000a), 11 permanent cantilevered grandstands (Littler 2000c) and 6 retractable stands (Littler 2000b) were tested and then approximately half were monitored during subsequent pop concerts or sporting events. These showed the critical case to be rhythmic loading of the structure. Results from these tests (Table 2.6) were incorporated into subsequent guidance notes on the design of demountable stands and resulted in the inclusion of the dynamic load case in the 1996 edition of BS6399 Part 1.

The natural frequency of the empty stands was determined using various techniques; ambient vibration tests using wind excitation, single impact tests and steady state forced vibration tests. The natural frequency of the stands was calculated using Fast Fourier Transforms (FFT) of the recorded response. Forced vibration tests also allow the mode shapes and damping values to be established. Natural frequency of the stand when full was calculated using wind excitation therefore no values are available if there was no wind at the time of recording.

For the 11 permanent cantilevered grandstands (Littler 2000c) the vertical natural frequency of the empty stands varied from 2.65Hz to 6.79Hz with a median value of 4.69Hz. All those used for concerts were above 4.65Hz. The author is keen to point out that few of the tested stands were built after the publication of BS6399 part 1 1996 or the 4th Edition of the HMSO's Green Guide in 1997, when frequency limits were introduced.

In addition to the detailed tests the BRE also determined the natural frequencies of permanent stands at 18 major English football grounds and found that all had possible vertical modes less than 6Hz. 45% of these stands had vertical frequencies between 2.0 and 2.8Hz although none of these are used for concerts (Littler 2000c).

For the retractable (Littler 2000b) and demountable (Littler 2000a) stands the key issue was their horizontal frequency due to the difficulties in bracing such stands. The horizontal frequencies varied from 1.8 to 6Hz with the retractable stands being stiffer in the sway direction (side to side) and the demountable stands stiffer front to back. In the vertical direction all but two of the stands had frequencies above 9Hz. These two were 7.6Hz and 7.9Hz.

Mode shapes were recorded for the stands where steady state forced vibrations were carried out. The test results showed that while some stands acted as a single body, on other stands parts of the structure acted independently.

Generally the author noted a reduction in the frequency of the stands as they filled with people together with an increase in the level of damping although this too varied depending on crowd size and whether the crowd was standing or seated. Some of the reductions in natural frequency were accompanied by a change in mode shape.

The testing of the stands, carried out during events, was based on the assumption that human perception of vibrations is through accelerations. Therefore accelerometers were located on all the stands during monitoring while only a few were fitted with displacement transducers.

The results were highly dependent on the liveliness of the audience. For fairly sedentary events such as horse racing, golf, tennis and some concerts the peak accelerations were recorded when the crowd were moving on and off the stand. For other sporting events, football, rugby etc. the peak values coincided with the crowd reacting to an event on the pitch. At pop concerts the maximum accelerations occurred when people were jumping up and down in time to the music or stamping their feet for an encore.

The vibrations recorded at sports events were short lived and cause no apparent concern in the crowd. For the pop concerts the vibrations were perceptible in the majority of the stands however audience discernment appeared to be directly related to the exuberance of the crowd i.e. more active = more movement = more comments/complaints.

Interestingly, for sporting events, the maximum accelerations did not occur at the natural frequency of the stand. For the permanent cantilevered grandstands the peak acceleration for sporting events ranged from 0.25ms^{-2} to 5.13ms^{-2} and contained a large portion of high frequency vibrations. When the time history recording was passed through a 10Hz low pass filter the peak acceleration of 5.13ms^{-2} reduced to 0.237ms^{-2} .

The response of the same stand during a pop concert was quite different. Tests showed that one person jumping slightly off the resonant frequency of the stand could produce 4% of the response magnitude as thousands of people at a sports event.

The accelerations recorded during concerts were all at either the beat frequency of the music or at one of its harmonics. For concerts the peak accelerations ranged from 0.30ms^{-2} to 1.62ms^{-2} , which when passed through a 10Hz low pass filter reduced the maximum to 0.80ms^{-2} .

All the results were low pass filtered at 10 Hz to remove the higher frequency element. This is because human perception of vibrations is better below 10Hz than it is above 50Hz (BS6472:1992). However, using BS6472:1992, perception of vibrations between 10 and 15Hz is roughly the same as those below 4Hz, plus several of the stands monitored had vertical natural frequencies of over 10Hz. Therefore it may have been more appropriate to filter at a slightly higher frequency so that vibrations between 10 and 15Hz were not excluded. Alternatively frequency weighting could have been used.

The tests showed that the suggested 0.5ms^{-2} acceleration level (Kasperski 1996) at which vibrations disturb comfort is possibly slightly conservative as most of the recorded responses exceeded this limit for both sport and concert use. Even if a higher acceptability criterion was adopted the results show that high accelerations can occur locally and so a stand could pass in one area and fail in another. The author suggests a vibration dose measurement, which includes both frequency weighting and duration of each acceleration level, might be a better approach. See Section 2.3.1 for Littler's development of this proposal.

Table 2.6 Summary of Recorded Accelerations from Littler 2000a, 2000b and 2000c

Stand Type	Natural Frequency Hz		Event	Recorded Acceleration ms ⁻² Low pass filtered at 10Hz	
	Vertical	Horizontal		Vertical	Horizontal
Demountable	>9.0	>2.0	Pop Concert	2.1	12.7
	>9.0	>2.0	Pop Concert	0.9	1.5
	>9.0	>2.0	Pop Concert	1.5	0.7
	>9.0	>1.8	Football	4.1	0.6
	>9.0	>1.8	Football	2.8	1.3
	>9.0	>1.8	Football	0.7	0.2
	>9.0	>1.8	Football	0.7	0.4
	>7.9	>1.8	Motor racing	0.4	0.3
	>7.9	>1.8	Motor racing	2.2	0.6
	>7.9	>1.8	Motor racing	0.3	0.2
	>7.9	>1.8	Motor racing	0.1	0.1
	>7.9	>1.8	Motor racing	0.2	0.2
	>7.9	>1.8	Horse racing	0.4	0.1
	>7.9	>1.8	Golf	0.7	0.1
	>7.9	>1.8	Golf	0.3	0.8
	>7.9	>1.8	Golf	0.2	>0.05
	>7.9	>1.8	Tennis	0.3	0.1
	>7.9	>1.8	Drama Festival	0.1	0.1
Retractable	>9.5	~2.5	Pop Concert	3.7	3.2
	>9.5	~3.0	Pop Concert	1.2	1.2
Permanent	5.70		Pop Concert	0.255	
	5.70		Pop Concert	0.2	
	4.93		Pop Concert	0.76	
	4.93		Pop Concert	0.474	
	4.69		Pop Concert	0.804	
	4.69		Pop Concert	0.555	
	4.76		Pop Concert	0.53	
	6.36		Pop Concert	0.307	
	6.79		Pop Concert	0.378	
	2.66		Sport	0.716	
	2.66		Sport	0.536	
	2.66		Sport	0.949	
	3.55		Sport	0.237	
	6.60		Pop Concert	0.206	
	6.60		Pop Concert	0.176	

A similar study was carried out in Canada by Pernica (1983) who recorded the vibrations of 18.8m span precast concrete terracing units, at an arena, during a 3 hour rock concert. The audience stayed seated for most of the concert even when foot stamping and clapping occurred. For over a quarter of the songs the synchronised crowd movement induced accelerations in excess of 0.01ms^{-2} for more than 30 seconds. The peak acceleration recorded on the terrace units, which had a natural frequency of less than 3Hz, was $0.30g$ (3.0ms^{-2}) vertically and $0.17g$ (1.7ms^{-2}) horizontally with maximum peak to peak deflections of over 12mm for the one song that clearly resulted in a resonant response. Pernica calculated that this movement was equivalent to a dynamic live load of 1.5kN/m^2 in addition to the 1.5kN/m^2 static weight of the crowd i.e. a maximum dynamic load factor of 2.

More recently various institutions have carried out monitoring of grandstands during pop concerts as part of wider based research projects. Researchers from the Politecnico di Milano and the University of Sheffield (Caprioli et al 2007) compared the response of two different stadiums (the G. Meazza stadium in Milan and the City of Manchester Stadium in Manchester) during the hosting of same Red Hot Chilli Peppers concert in 2004. The Manchester stadium had a natural frequency between 4 and 5Hz and during the concert peak accelerations of up to 1ms^{-2} were fairly consistently reached with some peaks reaching over 1.25ms^{-2} . The same concert in the Meazza stadium gave much lower peak accelerations (approximately 0.3ms^{-2}) for a similar stand frequency. This lower response was probably purely down to the excitement of the crowd, as at a concert of an Italian artist held at the same stadium peak accelerations similar to those recorded in Manchester were achieved during the most popular songs.

Another major UK stadium was monitored by University of Sheffield (Reynolds and Pavic 2005 and Pavic and Reynolds 2008) during a high profile music concert. The cantilevered tier had a vertical natural frequency of around 4.3Hz which reduced to 3.8Hz with the additional mass of the crowd when fully loaded. The maximum peak acceleration recorded during the event was close to 1ms^{-2} with a corresponding RMS acceleration of 0.6ms^{-2} calculated over the period of 5 minutes when the greatest vibrations were experienced.

In the United States of America it is common at American football events for a section of high energy popular music to be played directly following a scoring event on the pitch. In order to understand the magnification of dynamic loading for these increased periods of synchronised crowd activity researchers from Pennsylvania State University recorded the vibrations of a cantilevered tier during a football match where in addition to music being played the word 'bounce' was simultaneously flashed on the large scoreboards encouraging the crowd to participate (Salyards and Hansen 2007). During four episodes where the music was played, consistent peak accelerations of close to 0.5ms^{-2} were recorded for a duration of 30s. After the biggest 'play' of the game much larger accelerations of around 0.8ms^{-2} were recorded for around 12s followed by 42s of peak accelerations about 0.4ms^{-2} . The frequency of the accelerations was similar to that of the song being played at 2.3Hz. The natural frequency of the stand was 2.7Hz.

These measurements of real events confirm that the highest accelerations in grandstands generally occur during pop concerts when dynamic crowd loading in the form of jumping, bouncing, stamping and clapping is coordinated by a musical beat. This synchronised crowd loading results in a periodic loading at multiples of the beat frequency with peak accelerations typically in the region of 1ms^{-2} (for stands with a fundamental vertical natural frequency greater than 4Hz) with periods of intense activity lasting roughly 30s. The vibrations recorded during sports events were non-periodic and much shorter in duration.

2.3 Serviceability Criteria

2.3.1 Previously Published Guidelines

As mentioned previously, in this field of research there have been very few papers published on the subject of serviceability of grandstands from a human acceptability point of view. One of the few researchers who has written on this topic is Kasperski.

In the early 1990s Kasperski and Niemann (1993) carried out full scale tests on one bay of a permanent cantilevered stand of a football ground using 50 policemen, from which they developed a load model.

In their paper Kasperski and Niemann acknowledge that humans are sensitive to vibrations being able to detect accelerations from $0.005g$ ($0.05ms^{-2}$) upwards. The authors used a formula from ISO2631:1980 to determine the vibration level at which nausea could be expected and include a graph of allowable accelerations based on a 3 minute duration for frequencies between 1 and 10 Hz, reproduced in Figure 2.5. The recommended levels range from $0.35g$ to $0.75g$ depending on the frequency of the vibration.

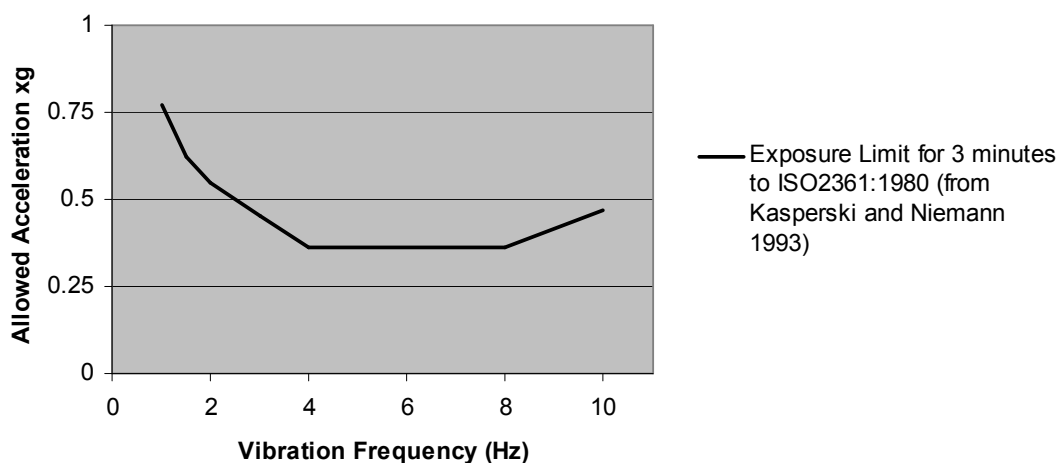


Figure 2.5 Nausea Threshold (to ISO 2631:1980) for Vibration Frequencies Below 10Hz Based on 3 Minute Exposure

As with his later articles Kasperski then looks at the acceleration levels which might induce panic in the audience. Avoidance of panic is key, for the design of large capacity structures, as historically it has been panic induced incidents that have

resulted in the greatest number of fatalities at sports stadiums. From the tests undertaken by Kasperski (1996), the first time that the participants experienced considerable vibration accelerations (0.35g) they stopped jumping although they quickly got used to the larger vibrations and several times exceeded 0.5g without inducing a second panic attack.

The most commonly cited paper by Kasperski is the one he presented at the Eurodyn Conference in 1996. The purpose of this paper was to compare the static live loads given in Eurocode 1 with the likely dynamic loads to be experienced by a grandstand. As part of this, Kasperski included a short section on 'psycho-dynamics' where he proposed serviceability criteria based acceleration levels due to crowd-induced vibrations. It is for this section of the paper which he has become well known.

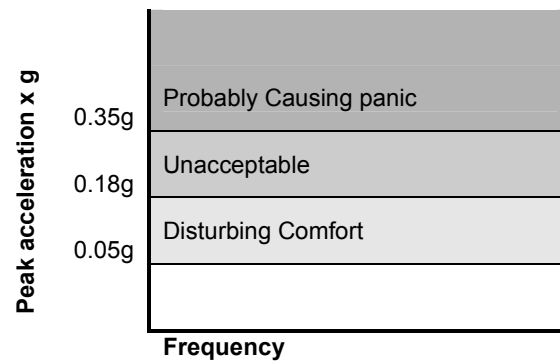


Figure 2.6 Kasperski's 1996 Acceleration Limits

The lower limit of vibrations, above which they disturb the comfort of passive persons, was judged by Kasperski to be 0.05g as a peak acceleration (Figure 2.6). The level at which these vibrations become unacceptable he took as 0.18g from CEB Bulletin d'Information No 209 (reproduced by Bachmann et al 1994 and in Table 2.7 below).

Finally the limit for panic of 0.35g was taken from Kasperski's own research backed up with reference to ISO 2631:1980 as a similar acceleration to that causing nausea and dizziness (Figure 2.5). All the acceleration limits given by Kasperski (1996) are peak values and are independent of the frequency of the vibration.

Kasperski does make the point that while the unacceptable and disturbing levels are more relevant to the passive crowd, not participating in the activity causing the

vibration, the active persons will be governed by the panic threshold. It is worth noting that for most stands the areas with the highest accelerations will be those where the majority of the crowd are active with the magnitude of the acceleration quickly dropping off away from these areas.

Table 2.7 An Indication of Human Perceptibility Thresholds for Vertical Harmonic Vibration (Person Standing), (Bachmann et al 1994)

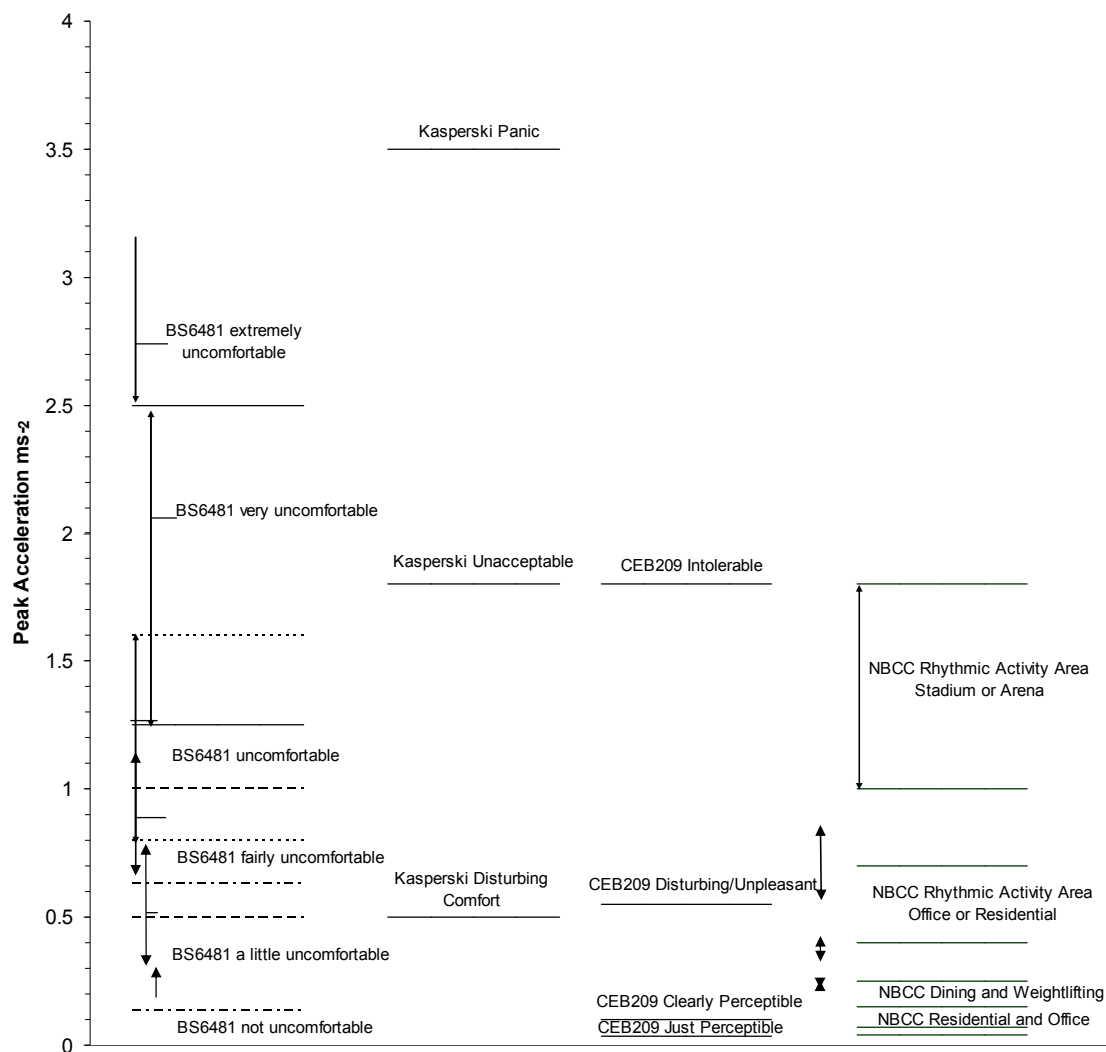
Description	Frequency Range 1-10Hz Peak Acceleration (mm/s ²)	Frequency Range 10-100Hz Peak Velocity (mm/s)
Just perceptible	34	0.5
Clearly perceptible	100	1.3
Disturbing/unpleasant	550	6.8
Intolerable	1800	13.8

Note: Data combined from various authorities. There is a scatter by a factor of up to about 2 on the values given. (No references provided)

In subsequent papers Kasperski (2001 and 2002) adds an additional serviceability criterion – that for those situated below the vibrating tier. He states that if sufficient reference points are available, people beneath the vibrating stand can feel distinctly uneasy when the amplitude of the vibration is in the order of 10mm and that this becomes the driving factor for cantilevered tiers with natural frequencies below 3Hz.

The National Building Code of Canada (NBCC 2005) takes a more simplistic approach and provides acceleration limits for vibrations due to rhythmic activities depending on the occupancy affected by the vibration. For areas where the rhythmic activity is occurring in conjunction with more sensitive occupancies, e.g. in a residential or office building, this limit is set at 0.04g to 0.07g based on the more sensitive occupants. For stadiums and arenas where there are no sensitive occupancies the limit rises to 0.10g to 0.18g based on testing and feedback from experience.

A summary of the peak acceleration limits given by Kasperski (1996), CEB 209 (from Bachmann et al 1994) and NBCC (2005) is given in Figure 2.7 together with the RMS values presented previously from BS 6841:1987 for railway passengers (in Section 2.1.3.1). These four publications use acceleration levels, as serviceability criteria, which are independent of the frequency of the vibration and highlight the differences in opinion on the use of acceleration levels as a serviceability criterion for vibrations.



Note Limits are given in terms of peak acceleration except for BS6481 which uses RMS values

Figure 2.7 Summary of Acceleration Limit Serviceability Criteria

As discussed in Section 2.1, several of the British and International Standards use base line curves for determining acceptance criteria. These give varying acceleration (or displacement) limits based on the frequency of the vibration. Of these only ISO 10137:2007 provides limits relevant to grandstand situations. This standard recommends that the base curve given for vertical head to foot accelerations (Figure 2.8) be multiplied by 200 as a comfort limit for seated members of the audience not participating in the crowd activity. For the avoidance of panic induced by large vibrations it is suggested that a limit of 400 times the base curve is not exceeded. These acceleration limits seem to fit reasonably with Kasperski (1996) although they are in terms of RMS rather than peak accelerations. For the comfort criterion ISO

10137 suggests the RMS acceleration is calculated over a period of 10s while for the panic criterion a 1s RMS value is recommended. This means that the panic RMS acceleration value is likely to be closer to the peak acceleration than the comfort limit RMS acceleration and raises the question over what is the relevant duration for calculating RMS accelerations in order to determine human acceptability.

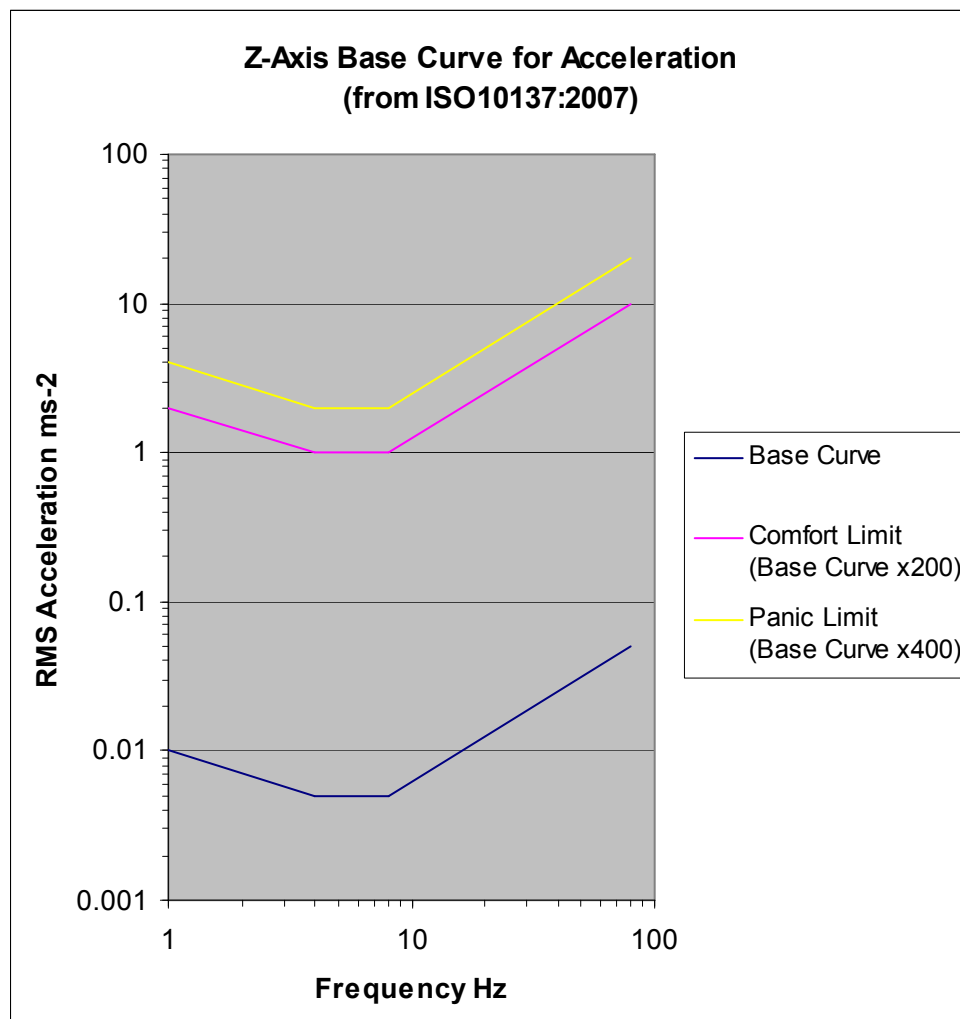


Figure 2.8 Base Curve for Vertical Accelerations to ISO 10137:2007

ISO 2631-2:1989 (now superseded) gave curves which could be used to assess the level of discomfort likely to be induced by a certain magnitude of vibration at a certain frequency for a given period of time. Different classes of limit were defined in ISO2631-1 1985. These were (from Bachmann et al 1994)

- The 'reduced comfort boundary' at which activities such as eating, reading or writing are disturbed.

- The 'fatigue decreased proficiency boundary' at which the level of recurring vibrations cause fatigue to working personnel with a resulting loss of proficiency. This occurs at around 3 times the reduced comfort boundary.
- The 'exposure limit' which defines the maximum tolerable vibration with respect to health and safety and is set at about 6 times the reduced comfort boundary.

The fatigue and exposure limit curves are reproduced in Figures 2.9 and 2.10 below.

A direct comparison with Kasperski's (1996) peak acceleration thresholds is difficult given the ISO2631-2:1989 limits are in terms of RMS accelerations. However if compared to Kasperski's peak acceleration unacceptable threshold of 1.8ms^{-2} , the graphs show that vibrations of the order of 1.4ms^{-2} (just below Kasperski's) if maintained for a 2.5 hour concert is within the tolerable limit for health and safety issues (Figure 2.10) and, that much higher levels of acceleration are tolerable for short periods of time.

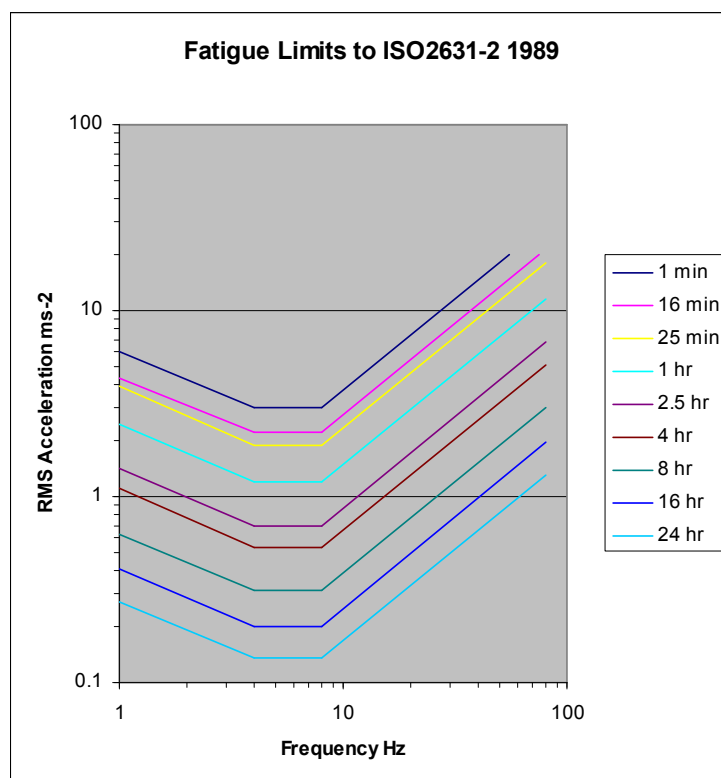


Figure 2.9 Fatigue Limits to ISO2631-2 1989 from Bachmann et al 1994

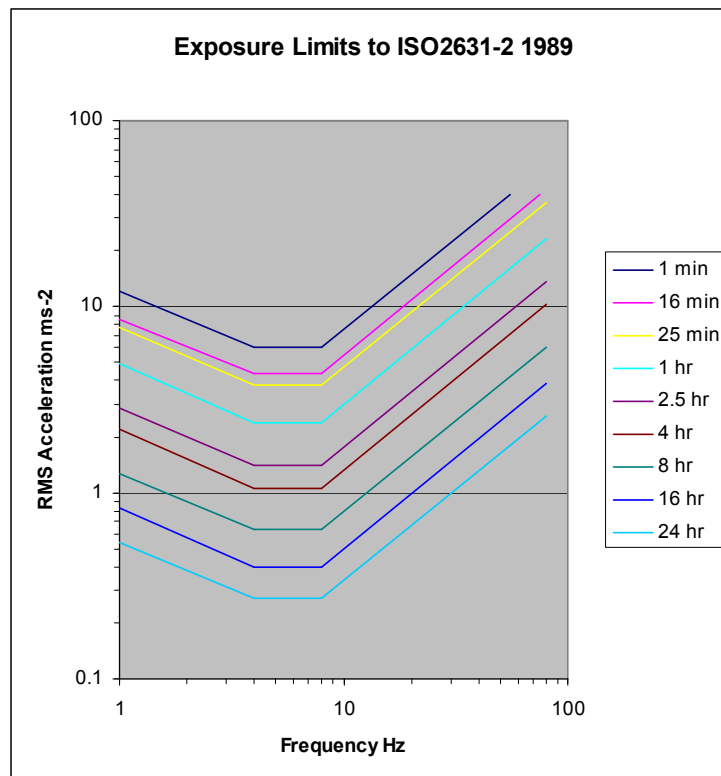


Figure 2.10 Exposure Limits to ISO2631-2 1989 from Bachmann et al 1994

CEB 209 (Table 2.7) only uses acceleration limits for frequencies between 1 and 10Hz, above 10Hz the authors promote the use of velocity as the serviceability criteria in gauging human perception of vibrations. Few other sources except for the German DIN Standards (Section 2.1.3.3) use velocity levels as acceptance criteria. Other references do however use displacements to measure human perception of vibrations.

The first to do this were Reiher and Meister in 1931 when they subjected 10 individuals to a range of steady state vibrations of varying magnitude and frequency and asked them to rate the vibration from not perceptible to very disturbing. These perception curves are reproduced in Figure 2.11 in terms of displacement and frequency of vibration.

In 1966 Lenzen proposed that these curves be multiplied by a factor of 10 so that they could be used to assess transient vibrations. These modified curves are shown in Figure 2.12.

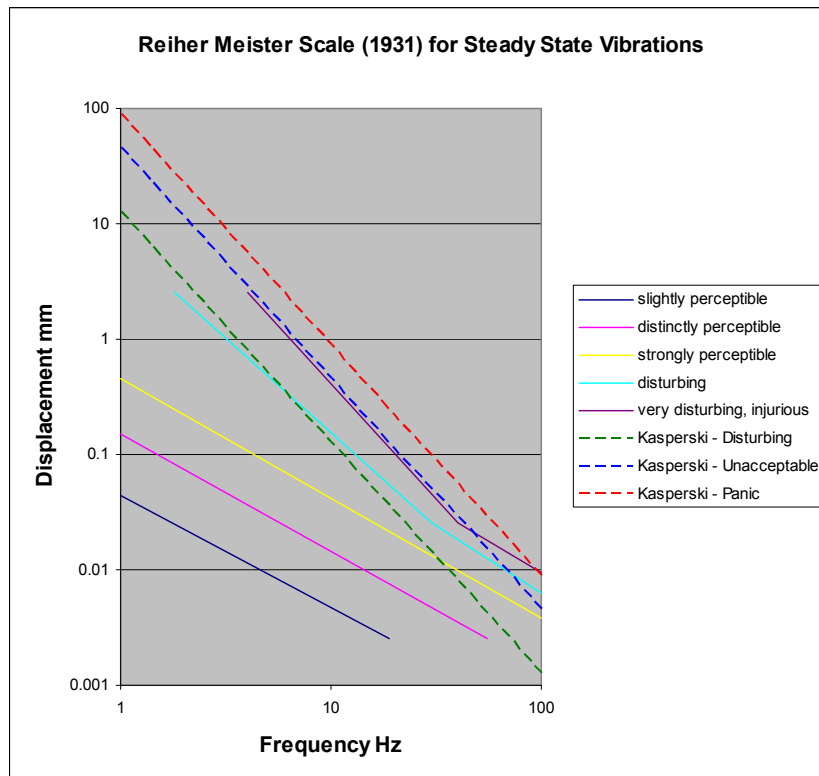


Figure 2.11 Reiher Meister Perception Curves for Steady State Vibrations from Lenzen 1966

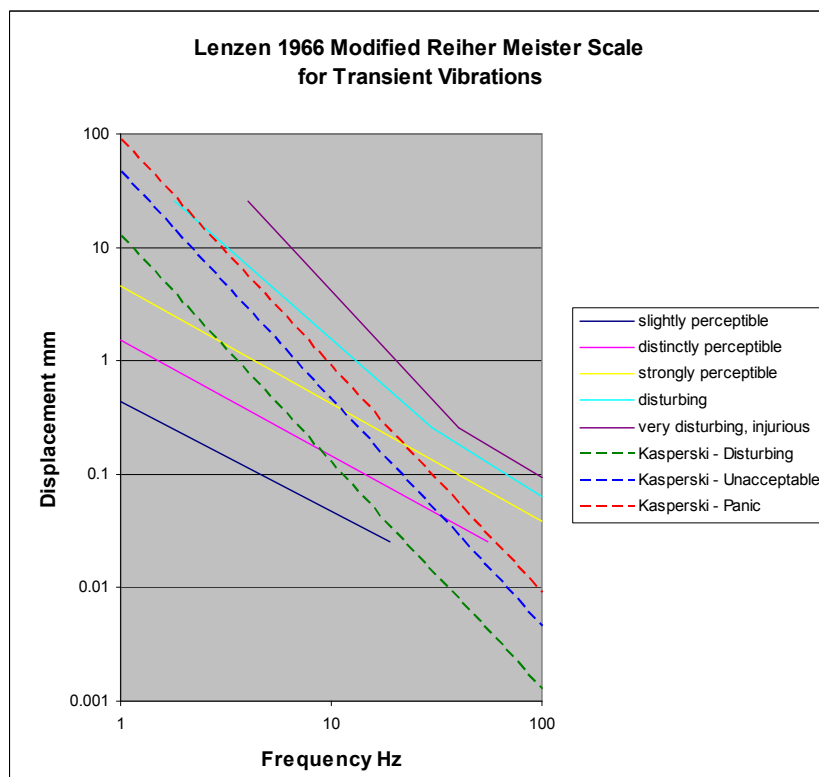


Figure 2.12 Modified Reiher Meister Perception Curves for Transient Vibrations by Lenzen 1966

A similar approach was taken by McCormick and Mason in 1974 when assessing office floor vibrations. They modified, another author, Dieckmann's perception curves for steady state vibrations by a factor of 10 to account for transient vibrations and used these values together with Lenzen's curves to determine their acceptance criteria. The McCormick and Mason's modified Dieckmann curves are typically slightly higher than the corresponding Lenzen curves particularly for frequencies below 5Hz, Figure 2.13.

Figures 2.11 to 2.13 show how as the frequency of the vibration increases the magnitude of the displacement required for humans to detect the vibration decreases. To give some context to these curves Kasperski's (1996) acceleration limits have been converted to displacements by dividing by $(2\pi f)^2$ and added to Figures 2.11 and 2.12. This shows that Kasperki's grandstand limits lie somewhere between the limits for transient and steady state vibrations for floors set by Lenzen and Reiher Meister which seems reasonable.

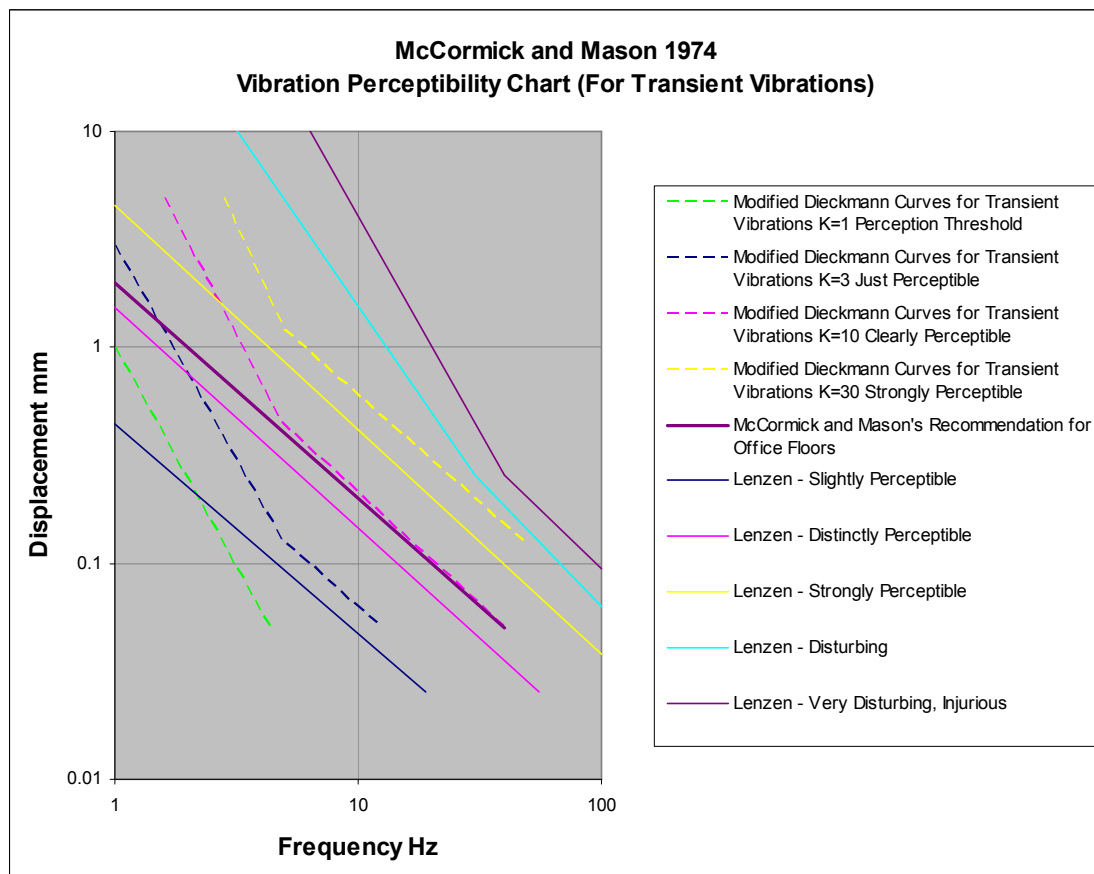


Figure 2.13 McCormick and Mason (1974) Vibration Perceptibility Chart for Transient Vibrations

Another approach to determine acceptability criteria is to use a vibration dose method as suggested by Littler (2000a, 2000b and 2000c), where (as Section 2.1.3.1) from BS6472 and BS6841;

$$VDV = (\int_0^T a^4(t)dt)^{1/4} \quad \text{eq 2.1}$$

With VDV = Vibration dose value in $\text{ms}^{-1.75}$

$a(t)$ = the frequency weighted acceleration

T = the total period of the day (in s) during which the vibration may occur

In their paper published in the ICE Proceedings in August 2004 Ellis and Littler (2004a) attempt to use the vibration dose values (VDV) to measure the acceptability of vibrations previously recorded on grandstands at a number of different types of events. Unfortunately the authors fail to fully utilize the time variable in the VDV formula and as a result end up with $VDV = \text{constant} \times \text{acceleration}$ which negates the point of using a vibration dose approach. This could be a very powerful tool for assessing the affect of varying vibrations on spectators over the duration of an event and possibly as a gauge of acceptability. As such the use of VDV's will be looked into in more detail in the analysis stage of this research.

2.3.2 Summary of Human Acceptance Criteria for Vibrations

What this review has highlighted is that the derivation of most human acceptance serviceability criteria is either not referenced (in the case of the standards BS6481:1987, ISO 10137:2007 and ISO 2631-2:1989) or based on very limited experimental research (Kasperski 1996, Reiher and Meister 1931). The Canadian Code (NBCC 2005) cites many references but of these only Kasperski (1996) and Braun et al (2002) (see below) provide any experimental testing of human acceptability of vibrations.

In the field of grandstand acceptance criteria even the most commonly cited paper Kasperski (1996) relies largely on values suggested by others in publications which do not reference their sources (Pretlove and Rainer 1991 (reproduced by Bachmann et al 1994) and ISO 2631:1980). The only experimentally derived value provided by Kasperski (1996) is the panic threshold which was based on observations during field tests, not on rigorous perception tests. Braun et al, referenced in the Canadian Code 2005 (NBCC 2005), made a similar reference to undefined testing of acceptability in

grandstand seating. Their 2002 paper described the synchronised crowd load testing of some bespoke stadia terracing and commented that all vibrations measured during the laboratory tests were considered acceptable to the participants although peak accelerations of 0.10g to 0.13g were recorded. These values are below Kasperski's (1996) unacceptable threshold of 0.18g (peak acceleration).

These findings again strengthen the need for further specific research into human perception of vibrations in grandstands to aid or confirm the definition of acceptance criteria for such situations.

2.4 Human Perception – Experimental Precedents

The following section reviews previous research carried out in the field of human perception of vibrations in buildings. None of these projects relates specifically to either grandstands or dynamic crowd loading. However, it is hoped that the methods and findings of other researchers will give an idea of the key issues that need to be addressed in this type of human psychology testing

As mentioned in Section 2.3.1 Reiher and Meister (1931) carried out a series of experiments, on 10 individuals, in order to determine human sensitivity to steady-state vibrations. Using a shaking platform they subjected each participant to a particular vibration for approximately 5 minutes before asking them to rate their feeling of the vibration using one of the following categories;

0	Not perceptible
Ia	Weakly perceptible
Ib	Distinctly perceptible
Ic	Strongly perceptible, annoying
IIa	Unpleasant and with longer duration harmful
IIb	Very unpleasant and already with short duration causing harm

Categories Ia to Ic were classed as bearable without causing health trouble while categories IIa and IIb were deemed dangerous to health.

The tests were carried out for the participant standing and lying and for both vertical and horizontal vibrations. The frequency range of the tests was 3 to 70Hz and the

amplitude ranged from 0.001mm to 1mm. Acceleration levels varied from 0.03ms^{-2} to 10ms^{-2} although the results in terms of acceleration are only given for vertical vibrations for lying individuals.

In 1972 Wiss and Parmalee undertook similar tests to investigate human perception of transient vibrations. To do this they constructed a test room, within the laboratory, with a raised floor whose vibration could be controlled by a hydraulic shaker located underneath. Forty standing participants were subjected individually to a range of sinusoidal transient vibrations. Each vibration had the same form; building up to a determined maximum before the shaker was turned off and the vibration decayed with time due to the damping of the structural system. The duration of the vibration varied from 0.3 to 5 seconds, the frequency from 2.5 to 25 Hz and the amplitude from 0.0025 to 2.5 mm. The damping of the floor structure was also varied.

As for Reiher and Meister's experiments the participants were asked to class the vibrations using provided categories:

- 1 Imperceptible
- 2 Barely perceptible
- 3 Distinctly perceptible
- 4 Strongly perceptible
- 5 Severe

Wiss and Parmalee found that for the case where there was no damping, i.e. the vibration was close to steady state, there was good correlation with Reiher and Meister's results even though the duration of the vibration was 5 seconds not 5 minutes.

It is worth noting that, when analysing the results, Reiher and Meister used the lowest readings to set the boundaries between the perception classes while, Wiss and Parmalee used the mean.

Around the same time as Wiss and Parmalee (1974), experimental studies were carried out by Kahn and Parmalee (1971), and Chen and Robertson (1972) to assess human perception of horizontal motion in relation to wind excitation of tall buildings. Both sets of researchers subjected individual participants to a range of movements

and asked them to rate their perception using the similar categories to those described above. For the tests Kahn and Parmalee investigated human perception of horizontal accelerations using a rotating display table while, Chen and Robertson looked at sinusoidal motion using a wheeled windowless test room. Kahn and Parmalee looked purely at acceleration levels and the effect of different body postures, whereas Chen and Robertson suggested measuring maximum values of displacement, velocity, acceleration and jerk (rate of change of acceleration) and the influence on perception of various factors; period of oscillation, body orientation and posture, expectancy of movement, visual clues etc.

Kahn and Parmalee found that the position of the test subject had less influence on the variation in perception of accelerations than the differences in perception thresholds between individuals.

Chen and Robertson concluded that for horizontal sinusoidal motion

- a. Perception thresholds increase as the period of the oscillation increases i.e. as the frequency reduces
- b. Perception thresholds of walking subjects are generally higher than those standing
- c. Perception thresholds are smaller when the subject anticipates the motion
- d. Perception thresholds while seated are higher than those while standing

This final finding conflicts with research by Parson and Griffin (1988) who carried out tests to determine human perception thresholds for both horizontal and vertical vibrations at varying frequencies (2Hz to 100Hz) for various postures (sitting, standing, supine), at the University of Southampton. Their experiments were conducted on individuals whose perception was gauged either by confirming if they felt a vibration during the signal period or by allowing the test subject to vary the intensity of the vibration using an adjustable dial until the vibration was at the level that they could just feel it. Generally the results showed that the experimental threshold for perception to be above that given in BS6472 except when the frequency of the vibration exceeded around 50Hz.

Horizontal vibrations were shown, by Parsons and Griffin (1988), to be more perceptible when seated rather than standing, whereas the perception levels for

vertical accelerations were similar for seated or standing positions. Overall the test subjects were most sensitive to vibrations when lying down.

In addition, Parsons and Griffin investigated the effect of the number of cycles of a sinusoidal vibration on perception levels and found that if the vibration lasted longer than 0.25s the number of cycles did not appear to affect the perception threshold. Visual and acoustic stimuli were also found not to affect perception thresholds determined in the laboratory.

Before carrying out the tests Parsons and Griffin asked each of the test subjects to complete a questionnaire. This included medical questions confirming the person's suitability to participate in the proposed experiment and also a personality test based on an Eysenck Personality Inventory to determine whether their ability to perceive vibrations was linked to how extrovert/introvert/neurotic they were. No link was confirmed.

Although this research provides useful background information none is grandstand specific and there are key differences between the perception tests, carried out by others, and those required in order to determine human perception in a grandstand situation. All the previous studies used mechanical means to simulate the vibration which were generally hidden from the view of the test subject. In the case of grandstands the primary source of vibrations, being considered, is synchronised crowd loading therefore it is important that any perception testing uses humans to generate the vibration and that the test subjects see the source of the vibration as they would in an actual stand. The other important difference is that past research has focussed on individuals. Because perception is situation dependent, it is critical to simulate as many aspects of the real situation as possible during the tests. Therefore perception tests for grandstands need to be carried out on groups of subjects as it is the response in a crowd that is likely to be most representative. Also for this reason the test setup has to simulate as far as possible a real permanent grandstand, replicating amongst other things the raked seating, the elevation and the feeling of solidity.

2.5 Summary of Findings of Literature Review

The literature review has confirmed the observation that the design of permanent grandstands for dynamic crowd loads is generally based on avoiding resonance through the use of frequency limits. This method has been shown to be simplistic with existing structures with fundamental natural frequencies below the given limits performing satisfactorily in service. Alternative methods, based on calculating the vibrations that are likely to be experienced during a specific event, have been also been published. If engineered correctly this method could provide more efficient solutions compared to the coarse-grained frequency based approach. However, whilst detailed research has been carried out into the definition of the dynamic loading function and the representation of human-structure interaction, to be used in the design procedure, the human serviceability criteria are largely based on very limited research by Kasperski (1996). This means that, although vibration magnitudes can be predicted using detailed methods, the acceptance criteria against which they are compared are much less well defined. Therefore the purpose of this research project is to experimentally determine the factors affecting human perception of vibrations in grandstands (due to synchronised crowd loading). This is to be done with a view to deriving acceptance criteria which will either confirm current guidelines or propose an alternative.

A study of design guides/standards and past research in this (and similar) fields has highlighted key issues that need to be considered as part of this research, including;

- The various intrinsic factors which influence human response to vibrations e.g. age, sex, fitness, experience, expectation, body posture, activity,
- The various extrinsic variables which influence human response to vibrations e.g. vibration magnitude, frequency, axis, duration, location,
- The need for the research to be situation specific i.e. relating to synchronised crowd loading of tiered permanent grandstands,
- The range of vibration magnitudes to be tested,
- The nature of the vibrations typically experienced at sporting and non-sporting events in grandstands including pop concerts,
- The localisation of areas of high accelerations,
- The issue of deliberate dynamic vandal loading,
- The possibility of motion sickness due to low frequency horizontal vibrations

- The differentiation between vibrations which can be tolerated by a spectator and those which cause cosmetic or structural damage to the building

3 Test Rig Design

3.1 Test Rig Design

The purpose of this research project is to experimentally determine the key factors influencing human perception and acceptability of vibrations in permanent grandstands, induced by synchronised crowd loading. The proposed method of achieving this aim is to subject a section of permanent grandstand to synchronised crowd loading from groups of participants whilst monitoring the vibrations and the response of the participants. Ideally this would be an actual grandstand during a real event, however, this is very difficult to organise logistically and also to guarantee the required range of vibrations. Therefore it was decided to construct a section of permanent grandstand in the laboratory designed specifically so that the fundamental vertical natural frequency could be changed thus providing a means of varying the magnitude of the vibrations experienced by the participants.

3.1.1 Concept

A key part of the project was the design and construction of the test section of grandstand. The literature review has shown that human perception of vibrations is highly situation dependant. Therefore the test rig had to be as representative as possible of a permanent grandstand in order for the experimental results to replicate, as far as possible, those that would be experienced on a real stand.

Because vibrations in grandstands are generated, and experienced, by groups of people, the scale of the stand needed to be such that a fairly large group could be accommodated comfortably allowing a crowd atmosphere to be generated. The structure also had to have sufficient elevation and rake to give the feeling of a cantilevered tier rather than a shallower tier close to the ground. The idea here was to recreate the awareness regarding safety and means of escape as a real upper tier of a stadium. Finally the rig had to be sufficiently robust to give the impression of solidity rather than a temporary structure. These criteria were achieved using three standard stadium precast concrete terrace units, each 5.6m long, supported on a raking steel frame, 3.5m high, with seating for a maximum of 30 people. See Figure 3.1.

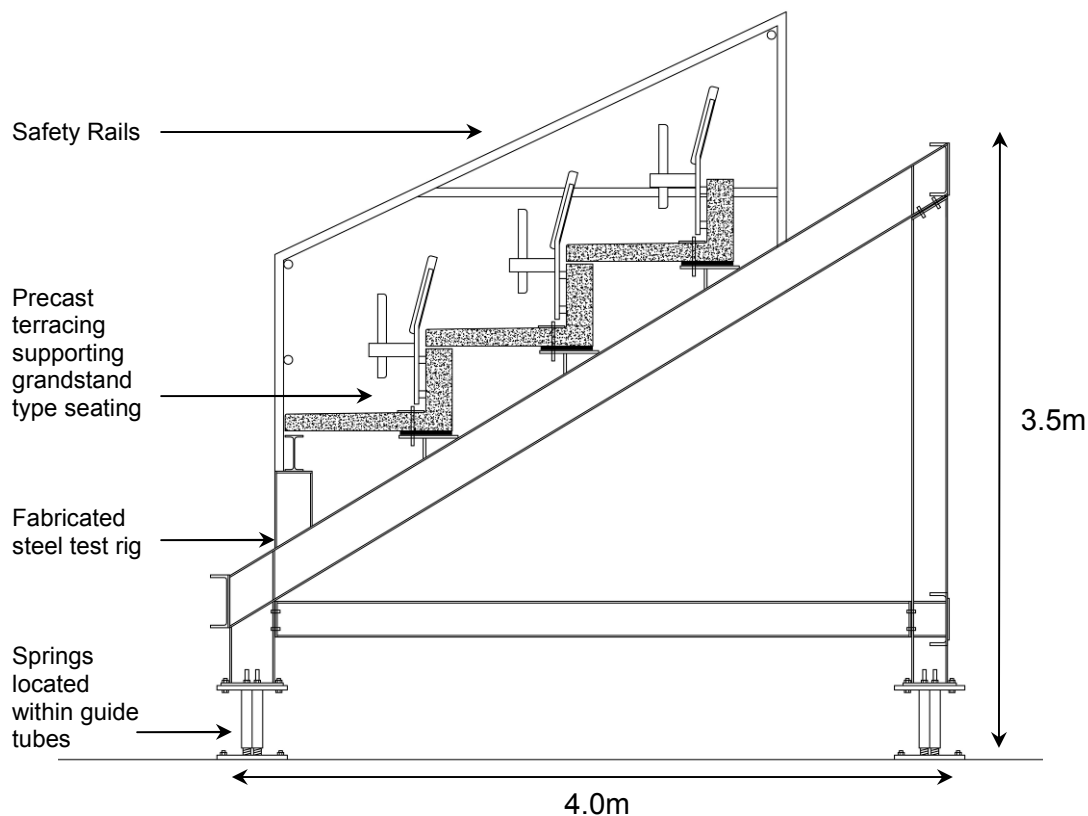


Figure 3.1 Cross Section of the Test Rig

The feet of the steel frame were designed such that various combinations of springs could be placed beneath them to alter the natural frequency of the rig. Thus, by employing different excitation frequencies combined with the various spring set-ups a full spectrum of vibration amplitudes could be achieved. The vibrations were stimulated purely by members of the group of participants jumping, in a coordinated fashion, in time with a given beat.

The whole seating tier was enclosed by safety barriers to offer a sense of security. In addition the front parapet handrail was sheathed in fabric to attempt to limit the participants' ability to gauge the movement of the rig relative to stationary objects in the laboratory. Standard folding stadium seats were provided for comfort of the participants and also to ensure that the crowd were located, relative to the structure, as they would be in a real grandstand.

3.1.2 Layout

The structural design of the test rig was carried out in conjunction with the development of the computational model. (See Section 3.2 Computational Modelling.)

The starting point for the test rig design was several terrace units surplus from the recent construction of a premiership football stadium. These precast concrete 'L' shaped units formed the basis of the stand and also governed its size. Originally the units had been designed to span 7.6m between supports. This was, however, too long a span and too heavy a unit to easily be accommodated in the laboratory. Therefore, the units had to be cut down in length. The amount that could be cut off the units was limited by the positioning of the cast-in lifting eyes and the need to ensure that these remained securely anchored while retaining the balance of load between the lifting points. This gave a final unit length of 5.6m which tied in well with the 5m lengths of stock steel in the laboratory and gave the opportunity to have a maximum of 10 participants per row. The reduced span also made the precast units stiffer (relative to their original design scenario) meaning that the deflection along the length of each unit was fairly uniform. This was beneficial as it meant that the vibration of each precast unit was relatively constant along its length, when subjected to synchronised crowd loading.

The total number of precast units that could be used was governed by the headroom in the laboratory. The rig design needed to allow for the uppermost unit to be installed by the crane while allowing those participants stood on this top unit to be able to jump freely without fear of hitting their heads. This limited the total number of units to three. See Figure 3.1.

The steel frame beneath the precast units was designed to represent, as far as possible, a typical grandstand structure, with inclined steel raker beams supported on steel columns. The rakers were positioned approximately 5.2m apart with 200mm of the precast unit protruding beyond the centre of the support. This was done, as mentioned previously, in order to achieve the required reinforcement anchorage on the cut ends of the precast units and to allow the use of the laboratory's 5m long stock steel sections as transverse members.

The precast units were located with the upstand beam portion of the middle unit central to the span of the steel rakers. This was done to keep the vibrations experienced by the participants as similar as possible while pushing the centre of the load slightly towards the front of the rig to produce a movement akin to a cantilevered tier i.e. primarily vertical with a small front-to-back horizontal component.

The structural action of the precast terrace units was such that the rear upstand beam section spans between the steel rakers while the slab spans front to back between the beam portion of the unit and the beam of the precast unit below. Therefore an additional steel beam was required to pick up the front edge of the lowest terrace unit, see Figure 3.1. This beam was designed and located so that its static and dynamic behaviour, replicated as far as possible the support provided by the precast beam to the other units.

Three terrace units 5.6m long can accommodate a maximum of 36 spectators on 450mm wide seats. This layout does not, however, allow the terrace units to be used for access and a separate stair system would have been required. Reducing the numbers down to 11 people per row would allow access at one end but would have resulted in asymmetric loading of the rig. Therefore, it was decided to install 10 seats per row, central to the stand, with 550mm wide access-ways at either end. Although 30 seats were installed, the maximum number of participants was restricted to 24 (as three centralised rows of 8). This was done because it was felt that the proximity of the end seats to the edge of the rig would negatively affect the responses of participants in those locations. This limit of 24 participants was estimated to be sufficient for the purposes of the experimentation to gauge human perception of crowd induced vibrations.

3.1.3 Design Loads

In accordance with the British Standard for loading, BS6399:1996 (with 2002 amendment), the design live load for assembly areas with fixed seating is 4kN/m^2 as a uniformly distributed load. In this instance it was decided to increase this static live load to 5kN/m^2 to allow for dynamic magnification. See Section 3.2.2.2.

The steelwork support structure to the test rig was designed to BS5950 Part 1 (2000), using the 5kN/m^2 live load plus the self weight of the precast units, plastic seats, handrails and the steelwork itself.

The precast terrace units were originally designed, using BS8110 Part 1 (1997), to take a live load of 5kN/m^2 when spanning 7.6m. Therefore there was sufficient tension reinforcement for the units to carry the same load when the units reduced in length by 2m. What did have to be checked was the anchorage of these bars as the original U bar to anchor the main steel was removed when the units were cut down. The anchorage required was calculated based on the 5kN/m^2 live load and the self weight of the unit and the plastic seating for the 5.2m span and was found to require an additional amount of steel past the support, hence the 200mm overhang described in Section 3.1.2.

In addition to the vertical loading the rig was designed to withstand the recommended horizontal live load for a grandstand intended for pop concert use, as set out in the IStructE's 'Dynamic performance requirements for permanent grandstands subject to crowd action' (2001 and 2008). This lateral load is specified as 7.5% of the design vertical live load and is to be combined with any wind loading using partial safety factors given in the relevant codes of practice for the structural materials involved.

3.1.4 Stability

Due to the triangular shape of the rig (Figure 3.1) no additional bracing was required in the front to back direction for stability. Bracing was required longitudinally to minimise any side-to-side horizontal motion of the rig. This was initially only provided to the rear of the rig as shown in Figure 3.2.

It was initially assumed that there would be sufficient plate action from the precast concrete units to avoid the need for lateral bracing of the rakers. However the computer model showed that there was a clear side-to-side sway mode which could easily be excited by vertical dynamic loading. This proved to be the case when the rig was built, so diagonal bracing was installed beneath the units connecting the centres of the two rakers and tying them back to the steel columns as highlighted in Figure 3.3. This proved effective in reducing the unwanted sway mode.

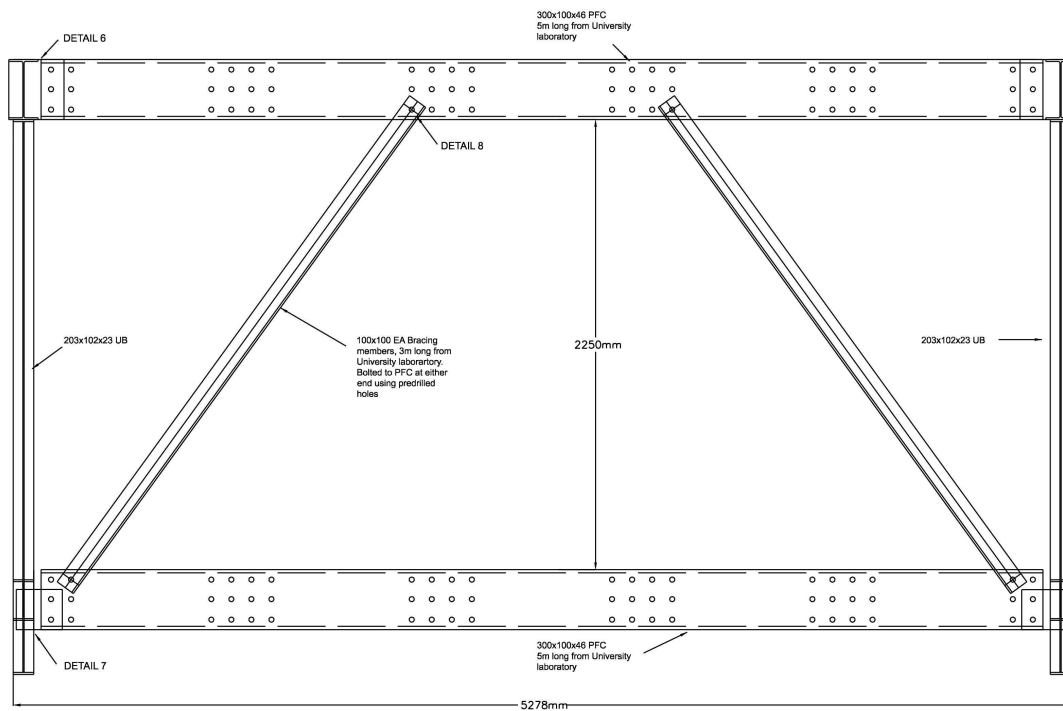


Figure 3.2 Rear Elevation of Test Rig

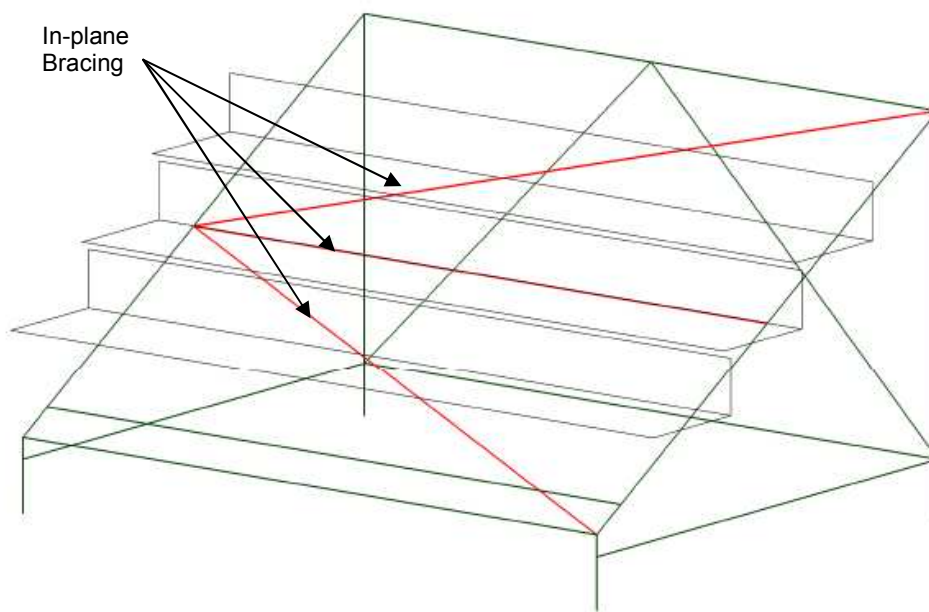


Figure 3.3 Stick Diagram of Test Rig Highlighting In-plane Bracing

3.1.5 Springs

In order to vary the frequency and the magnitude of the induced vibrations during the experiments, the rig was designed to be supported either directly off the floor or via a series of springs. As described in Section 3.1.7 the basic rig, without springs, was engineered to have a fundamental vertical frequency of around 6.5Hz. Two combinations of springs were then designed to be placed under the basic rig to achieve stands with fundamental vertical frequencies of around 2Hz and 4Hz respectively. The spring stiffnesses required for each combination were determined using the computational model (Section 3.2).

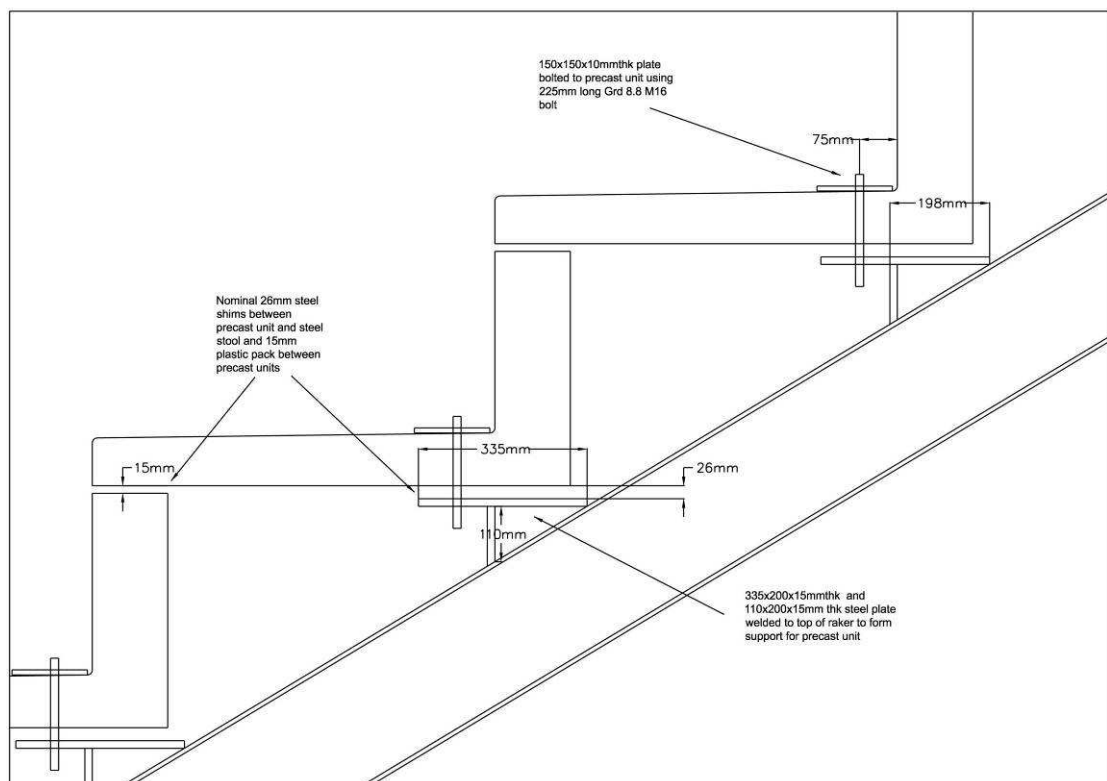


Figure 3.4 Precast Terrace Unit Support Detail

3.1.6 Details

So that the test rig behaved as far as possible like a section of permanent grandstand the precast units were supported using details similar to those used in stadia, see Figure 3.4. The remainder of the connections were designed as simple bolted fixings for ease of erection and dismantling. In addition the steel connections

were designed such that none of the bolted joints carrying primarily shear were subjected to dynamic loading during the tests, to reduce the risk of bolt fatigue.

For safety reasons the sprung supports were located on a series of steel dowels and housed in a cluster of well greased steel tubes (Figure 3.1). This system restrained the springs and the length of the tubes was set to avoid overloading the springs during the more extreme tests. Photographs of the sprung supports and other details of the rig design and construction are included in Appendix A.

3.1.7 Natural Frequencies and Mode Shapes

Once the steel support structure had been sized, based on the ultimate loads, the properties of the members were fed into the computational model to determine the natural frequencies and the mode shapes (Section 3.2).

The primary objective was to ensure that the fundamental mode of the test rig (without sprung supports) was a vertical mode greater than the recommended 6Hz for permanent grandstands (IStructE 2001 and 2008).

3.2 Computational Modelling

The purpose of creating a computational model was twofold;

- Firstly to aid the design of the test rig and to allow some degree of prediction of the magnitude of vibrations likely to be experienced by the participants.
- Secondly to post-analyse the rig data from the experimental work to examine the validity of the assumptions commonly made when analysing structures subjected to synchronised crowd loading.

The computational model constitutes the input, the analysis and the output of the proposed design procedure, outlined previously (Figure 3.5). The input portion of the computational model consists of two parts; the structural model and, the representation of the human loading (described in Sections 3.2.2 and 3.2.3 respectively). The output of the analysis of computational model will then be discussed in Section 3.2.4. Firstly, however, the type of analysis required will be described below (in Section 3.2.1) so that better understanding can be gained of the required input and the expected output, prior to them being explained in greater detail.

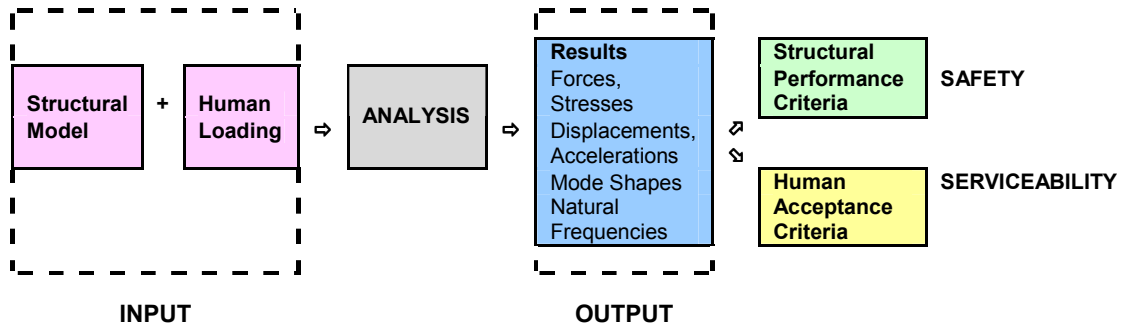


Figure 3.5 Flow Diagram of Proposed Design Procedure Highlighting Input Requirements

3.2.1 Computational Modelling - Analysis

To understand the dynamic behaviour of the structure two types of analyses need be carried out on the computer model. The first is a modal analysis to understand the general behaviour of the structure under dynamic loads by determining the natural frequencies and mode shapes of the structure (mentioned briefly in Section 3.1.7). The second is a time history analysis which predicts the likely dynamic response of the stand under a specific load case and requires a time dependent forcing function

(representing the synchronised crowd loading) to be input into the model. The output of the time history analysis (THA) is the variation of displacements, velocities and accelerations with time and gives an indication of the likely response of the structure under dynamic crowd loading.

3.2.2 Computational Modelling - Input

3.2.2.1 Structural Model

The structural model is a computer representation of the structure to be analysed which, in this case was the test rig.

Various factors need to be considered when constructing the computational structural model. These are discussed in turn below together with the reasoning for the chosen solution.

3.2.2.1.1 Two or Three Dimensions?

Building a two-dimensional model is obviously more straightforward and less time consuming than creating one in three dimensions. However the flexibility of the structure in the third dimension has a significant influence on the natural frequency and mode shapes of the structure as a whole.

For a simple structure, with primary beams, e.g. the rakers, supporting secondary beams, e.g. the precast concrete terrace units, an approximation can be made that the natural frequency of the system varies as shown in equation 3.1 (Steel Designers' Manual 1994).

$$\frac{1}{(f_{\text{Total}})^2} \propto \frac{1}{(f_{\text{Primary}})^2} + \frac{1}{(f_{\text{Secondary}})^2} \quad \text{eq 3.1}$$

Therefore it is important that the structure is modelled in three dimensions.

It is also critical, especially for more complicated structures, that the whole construction is modelled including the foundation flexibility (IStructE 2003 and 2008) or in this case the sprung supports.

3.2.2.1.2 Representation of Structural Elements

Steel elements are typically represented as bars in computational models as the properties of standard steel sections can easily be assigned to those bars. Most analysis packages also let the user define the section properties, allowing fabricated steel box girders and tapered sections to be modelled. While this is an adequate system it has been found that when looking at deep tapered steel raker beams, such as those typically used to support cantilevered steel tiers, that a stiffer model can be produced if these rakers are modelled using a number of finite element plates rather than just plain bars. This is largely because the support and load conditions can be modelled more accurately.

A similar situation occurs with concrete elements and while it is usually relatively straightforward to decide which members to model as bars and which as finite element plates, there are situations where this is not the case. For example the precast L shaped terrace units to the testing rig could be modelled relatively accurately as bars, however, the interaction between the units (in particular the fact that the front edge of each unit bears onto the beam portion of the one in front) can only be modelled if the units are made up of rectangular finite element plates. Here this interaction is important as the model is being constructed to determine the vibrations along the length of the precast units as this is what the participants will experience. It should be noted that this level of detail is likely to be too great when modelling entire grandstands as local modes will dominate the results making it difficult to view and understand the behaviour of the stand as a whole.

An image of the three-dimensional computational model of the test rig is included below (Figure 3.6) showing the precast terrace units constructed as rectangular finite element plates and the steel support structure as simple bars. Bars were chosen to represent the steel beams of the testing rig as the sections were relatively shallow.

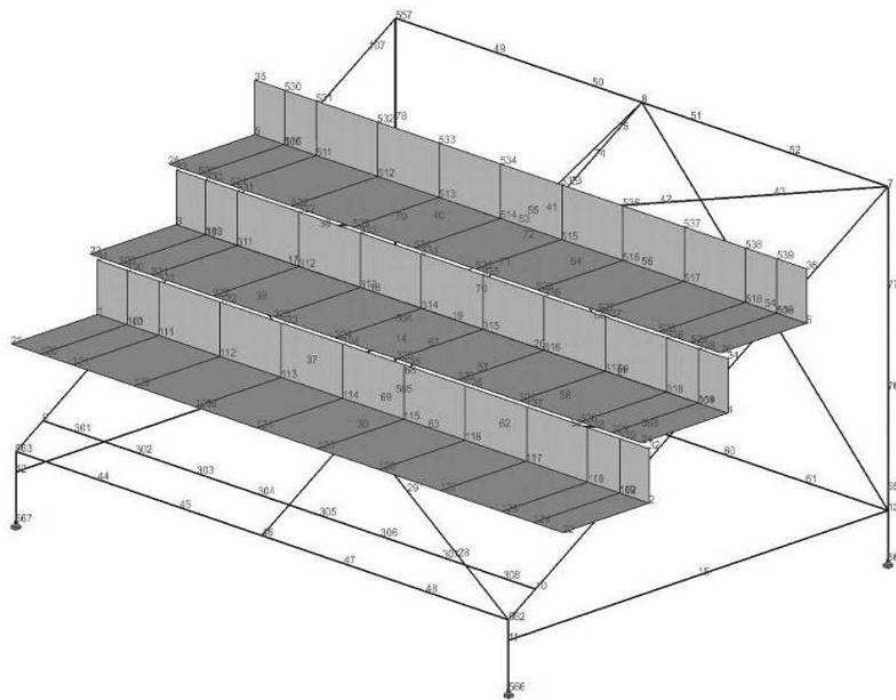


Figure 3.6 Computational Model of the Test Rig

3.2.2.1.3 Size of Mesh and Number of Nodes

The critical output of the computer model in the first instance is the modal analysis, to determine the natural frequencies and mode shapes of the stand. For this it is important that the number of nodes along each member is sufficient to accurately model the dynamic properties of that element. This is because analysis software generally only assigns mass to nodes. If just the ends of a member are defined by nodes then the flexibility of that member is likely to be ignored in the analysis. However if too many nodes are given and the finite element mesh is too fine then the run time of the analysis will be excessively long and the memory capacity of the computer may be exceeded.

For the test rig model intermediate nodes were introduced along the length of each of the bars representing steel members as shown in Figure 3.6. A relatively coarse mesh was chosen for the finite elements to the precast units as, in this case, it is not the local stresses in the finite elements we are interested in but the behaviour of the unit as a whole. The coarser mesh also keeps the model relatively simple while

allowing sufficient nodes to model the connection details correctly. The meshing of the precast concrete terrace units in the rig model is shown in Figure 3.6. (A finer mesh was investigated but took longer to compute the THA results and was shown not to significantly affect the output of the model. Therefore, the coarser mesh was deemed satisfactory.)

3.2.2.1.4 Connections and Supports

As the fixity/interaction between members greatly influences the frequencies and mode shapes of the structure it is important that the member connections and supports are modelled as accurately as possible. This often requires detailed knowledge of the connection design and the construction sequence.

The bolted steel to steel connections, of the test rig model, were modelled as pinned while the supports of the precast units, both precast to precast and precast to raker, were modelled using rigid links (Figure 3.7). Rigid links allow two non-coincident points in the model to be connected together so that if one point is forced to move then the other point moves with it. This tool enabled the modelled precast units to be joined at specific discrete points thus allowing the three terrace units behave as individual L shaped sections rather than a stiffer continuous folded plate. This modelling technique provided a good representation of the structural action exhibited by the actual test rig.

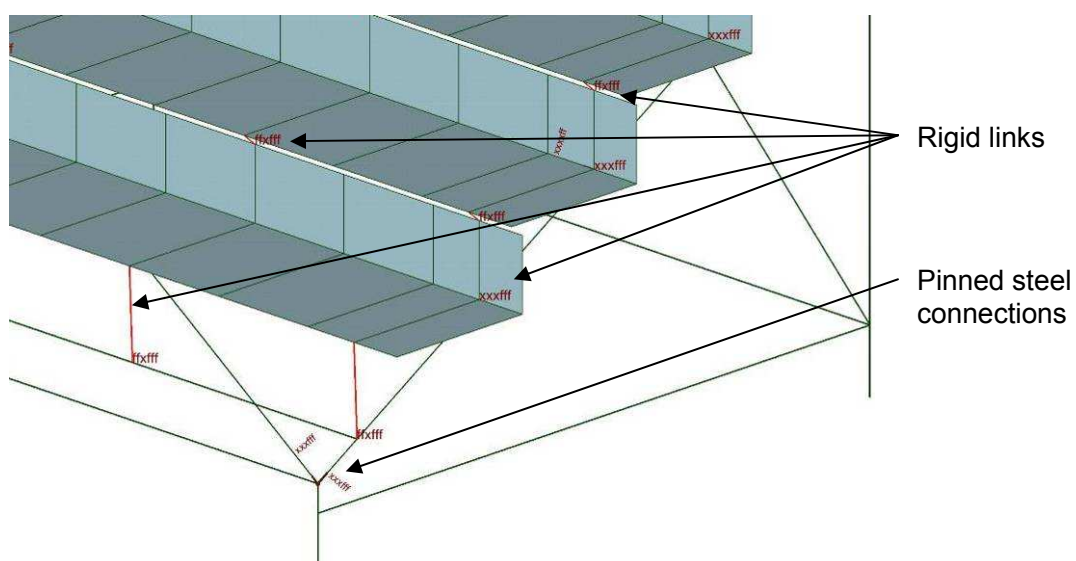


Figure 3.7 Computational Model showing the Test Rig Connections

3.2.2.1.5 Material Properties

The properties of concrete vary with a large number of factors. For dynamic analysis the key properties are Young's modulus E and the second moment of area I . With reinforced concrete, E is dependent on the mix design strength, the amount of reinforcement, the age of the concrete and the duration of the loading. For dynamic loading it is recommended that the short term modulus of elasticity be used for calculations (Wyatt 1989). This can be determined using BS8110 Part 2 1989

$$\text{28 day Young's Modulus} \quad E_{c,28} = K_0 + 0.2f_{cu,28} \quad \text{eq 3.2}$$

where $K_0 = \text{constant} = 20$ and $f_{cu,28} = \text{characteristic cube strength at 28 days}$

$$\text{Dynamic modulus of elasticity} \quad E_{cq} = 0.8(E_{c,28} + 19) \quad \text{eq 3.3}$$

As the precast terrace units used in the test rig were cast using grade 50 standard weight concrete a dynamic modulus of elasticity of 39 kN/mm^2 , calculated using the above formulae, was used in the analysis.

When determining the second moment of area of concrete elements it is important to consider whether the concrete section is cracked or uncracked. This is dependent on knowing the actual reinforcement and the applied serviceability moment as well as the concrete properties of the element. The cracked section properties can then be calculated and an assessment made as to what proportion of the span is cracked.

For the precast terracing used in the test rig the section properties of the concrete L shaped units were estimated assuming that the units were partially cracked along their length. This was done by calculating the applied moment at which the concrete section would crack based on the upstand beam portion of the unit only. This moment, M_{cr} , was then compared to the applied serviceability bending moment diagram which included self weight, applied dead and actual static live loads. By calculating where these two lines intersected the portion of the beam that was theoretically cracked was determined (Figure 3.8).

The section of the unit between the two crack points was taken as cracked and the rest of the unit as uncracked. Using this assumption and the second moment of area for the cracked and uncracked portions the average second moment of area over the

length of the unit was calculated. This average value was found to be 72% of the uncracked value. For ease of modelling this average value was used in the computational model for the whole precast unit rather than having separate cracked and uncracked regions.

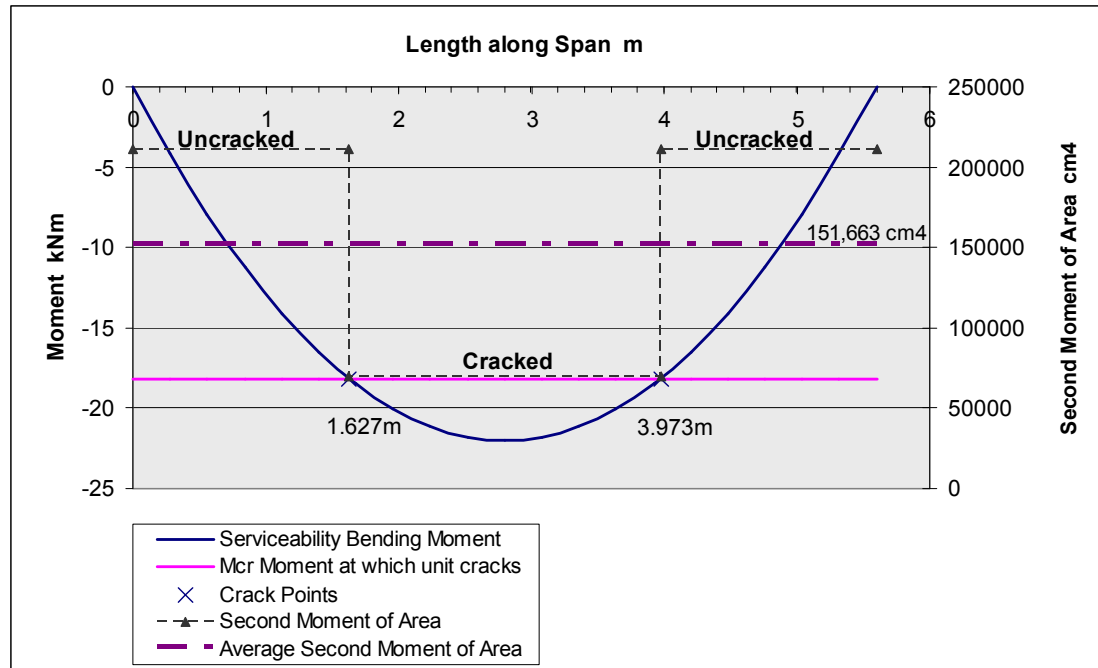


Figure 3.8 Cracked Section Properties of Precast Terrace Units

When modelling structural sections as finite elements it is difficult to change the second moment of area (I) of an element without changing its size. So, it was decided that the value of the Young's modulus (E) be altered instead as the two are used as a product (EI) in the analysis. Thus a value of 72% of $E_{cq} = (0.72 \times 39) = 28$ kN/mm² was used in the analysis to represent the partially cracked dynamic response of the precast terrace units, together with the gross I for the section.

The actual standard UK steel section sizes and the grade of steel (S275) were input into the test rig model for the various steel elements.

3.2.2.1.6 Springs

As part of the experimental procedure the natural frequency of the test rig was varied by changing the support conditions of the four feet. The basic rig was designed so

that when it was supported directly off the laboratory floor the fundamental frequency was slightly greater than 6Hz with a clear vertical mode shape. Two sets of sprung bases were then engineered to sit beneath the feet of the basic rig to lower the natural frequency to around 2Hz with one set of springs and around 4Hz with the other. (See Section 3.1 for further details).

One of the primary functions of the computational model was to confirm the required spring stiffnesses prior to the construction of the test rig.

To model the springs a simple single degree of freedom system model was used to hand calculate the required spring stiffness. This initial value was then input into the computer analysis package, using the spring support function, and adjusted to obtain the target rig frequencies.

For the rig set up with no springs the bases of the four supports were taken as pinned.

3.2.2.1.7 Applied Loads

Natural frequency calculations use mass not force and, as discussed previously, the consensus in the United Kingdom is that natural frequencies should be determined for an empty grandstand without any human live load (IStructE 2008, BS6399-1:1996 with 2002 amendments and NA to BS EN 1991-1-1:2002). Generally the masses that should be included are the structural self weight and any other permanent loads e.g. partitions, fixtures and fittings, plant etc. Therefore the loads used for the modal analysis, to determine the test rig's natural frequencies, were the self weight of the structure and the permanent applied loads of the plastic seats and the safety rail.

For the design of the structure the ultimate loads in the members had to be determined. For this an applied uniformly distributed live load of 5kN/m^2 was used in addition to the self weight and applied dead loads, as explained in Section 3.1.

For serviceability calculations an 'actual' weight of the participants was used. This was assumed to be 2kN/m^2 or 80kg per person with 8 people per row. As this load case was also used as the dynamic mass of the forcing functions for the time history

analysis (Section 3.2.2.2.4.1), it was applied as a series of point loads to simulate as realistic a loading as possible.

3.2.2.1.8 Non Structural Elements

When modelling the dynamic behaviour of permanent grandstands non-structural elements such as vomitory walls, partitions and glazing need to be considered (IStructE 2003 and 2008). As well as adding dead weight, these elements can also add stiffness and damping. Although not relevant in the test rig model this additional stiffness should be considered when calculating the natural frequencies and mode shapes of a structure.

3.2.2.1.9 Damping

While the level of inherent damping of the structure will not significantly affect its natural frequency, it will affect how it responds to dynamic loads. This is important when a time-history analysis of the model is to be carried out to predict the response of the structure to dynamic crowd loading. From previous testing by others (Willford 2005, Kasperski and Niemann 1993, Bastista and Magluta 1993 and Kasperski 2001) damping ratios for empty grandstands tend to vary from 1-2% for steel framed structures to 4% for concrete frames. This value is significantly increased by the presence of people e.g. by a factor of 3-4 for a well populated permanent grandstand (Kasperski 2001, IStructE 2008 and NBCC 2005).

Given the relatively small size of the test rig and the proportion of steel to concrete it was decided to use a damping ratio of 2% of critical as a starting point, for the pre-experimental modelling. The actual damping value of the test rig was then calculated during the preliminary testing of the empty stand (Chapter 4).

3.2.2.1.10 Analysis Time

The time taken to analyse the computer model depends on; the size of the structure under consideration, the level of detail of the model and the processing speed of the computer. While the modal analysis stage of the calculations is relatively quick it is

the time history phase that is likely to determine the maximum size of model that a particular computer can deal within a reasonable period of time. So when building an analysis model one must balance complexity and accuracy with the time available and the number of analysis runs that may be necessary to fully understand the dynamic response of the structure.

3.2.2.1.11 Appropriate Mode Shapes

Once the modal analysis has been carried out to determine the first 15 or so natural frequencies and mode shapes of the structure, each of these must be looked at in turn to establish which are relevant and likely to be excited by the applied dynamic loading. Often parts of the structure which are not directly connected to the seating tiers, e.g. the roof, have lower frequencies than the grandstand. If this is the case then a judgement has to be made as to whether this mode shape is likely to be excited by synchronised crowd behaviour on the tiers and therefore is a probable mode. The lowest frequency probable modes with principal movement in the vertical, sway and front-to-back directions are then selected as the fundamental natural frequencies in those directions.

3.2.2.2 Human Loading

3.2.2.2.1 Forcing Functions and Fourier Series

In order to carry out the time history analysis (THA), to predict the dynamic response of the structure to synchronised crowd loading, a forcing function has to be input into the model representing the movement of the people. Various such functions have been proposed by others (including Allen et al 1985, Pernica 1990, Allen 1990a, Allan 1990b, Kasperski and Niemann 1993, Ji and Eills 1994a, Ji and Eills 1994b, Bachmann et al 1994, NBCC 1995, BS6399-1:1996, Yao et al 2003 and BRE Digest 426 (2004)) based on half sine waves and defined by Fourier series.

The use of Fourier series to model human dynamic loading was introduced to the United Kingdom by Ji and Ellis in their 1994 papers, in *The Structural Engineer*, entitled 'Floor vibration induced by dance type loads: theory (1994a) and verification (1994b)'. These papers draw heavily on previous research undertaken in Canada,

in the preparation of the 1985 National Building Code, by Allen, Rainer, Pernica, Pretlove et al.

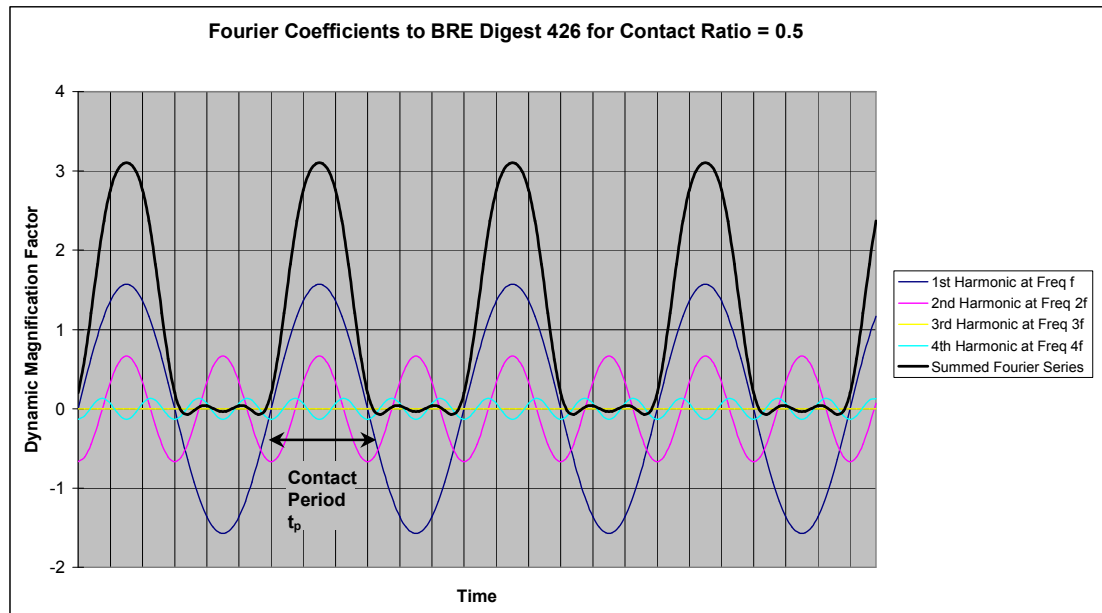


Figure 3.9 Using a Fourier Series to Define an Half Sine Wave

The theory, described by Ji and Ellis, is that the periodic load due to a person/people jumping, known as the forcing function, can be represented by superimposing a series of sine waves with different phase lags to create a half sine wave, see Figure 3.9.

Each component sine wave of this Fourier series is called a harmonic with the frequency of the n^{th} harmonic being n times the frequency f of the forcing function i.e. the frequency of the 2^{nd} harmonic is $2f$ (twice the forcing frequency f) and the frequency of the 3^{rd} harmonic $3f$ (three times the forcing frequency f). Typically the magnitude of the harmonics reduces as n increases. The number of harmonics that need to be considered depends on the type of dynamic load and the ratio of the forcing frequency to the natural frequency of the structure, as will be explained later.

The dynamic load due to people jumping in time to a beat, in terms of a Fourier series, is given as:

$$F(t) = \text{Static Component} + \text{Dynamic Component}$$

$$= G_s \left[1.0 + \sum_{n=1}^{\infty} r_n \sin\left(\frac{2n\pi t}{T_p} + \phi_n\right) \right] \quad \text{eq 3.4}$$

where G_s = static weight of the participants

r_n = Fourier coefficient (or dynamic load factor) of n^{th} term/harmonic

t = time

T_p = period of the jumping or $1/f$ where f is the frequency of the jumping

ϕ_n = phase lag of the n^{th} term/harmonic

In their analysis Ji and Ellis (1994a and 1994b), with reference to previous research by others, make several assumptions. The first is that the mean value of the time history of the dynamic load $F(t)$ is always equal to the weight of the participants G_s . From this it can be shown that the impact factor K_p ($= F_{\text{max}}/G_s$) is inversely proportional to the amount of time the jumpers are in contact with the ground.

$$K_p = \pi/2\alpha \quad \text{eq 3.5}$$

The contact ratio α is defined as the ratio of the time which the participant/s is/are in contact with the ground to the period of the jumping.

$$\alpha = t_p/T_p \quad \text{eq 3.6}$$

where t_p = contact duration (Figure 3.9) & T_p = period of the jumping

Using this assumption for the impact factor K_p , Fourier coefficients and phase lags can then be calculated mathematically for a range of contact ratios.

In their 'verification' paper the authors (Ji and Ellis 1994b) compared the load time history of a single jumper on a simply supported beam with the load function described above and concluded that there is close correlation (Figure 3.10). They also compared the mathematically derived Fourier coefficients with the dynamic load factors obtained experimentally by the Canadian researchers. These generally compared favourably.

Although Ji and Ellis were not the first to use of Fourier series to model human dynamic loading, their approach was different in that they derived the coefficients theoretically and then confirmed them experimentally. The Canadian researchers, Allen, Rainer, Pernica, Pretlove et al, typically measured the dynamic load factors either in a laboratory or on case study floors using groups of people.

The mean values of the impact factors K_p of the various forcing functions, derived by the Canadian researchers, in papers Allen et al 1985, Pernica 1990, Allen 1990a, Allan 1990b, Ji and Ellis 1994a, Ji and Ellis 1994b and Bachmann et al 1994 are summarised in Figure 3.11. Also included in these mean values are the impact factors calculated from the dynamic load factors given the National Building Code of Canada (1995 and 2005) and those from other references (Pernica 1983, Ebrahimpour and Sack 1992, Kasperski and Niemann 1993, Batista and Magluta 1993, Kasperski and Niemann 1993, Van Staalduinen and Courage 1994, Kasperski 1996, BS6399-1:1996, Willford 2001, Ellis and Ji 2002, Ellis and Littler 2004b and BRE Digest 426 (2004)) generally in relation to synchronised crowd movements at stadia. Figure 3.11 shows the impact factors divided into categories of dynamic loading, using the authors' definitions, and compared against the Ji and Ellis (BRE Digest 426 (2004)) impact factors.

As is to be expected there is some overlap between the categories but generally the impact factors reflect the amount of effort required for each activity with dancing having the lowest value and high jumping the greatest. If one focuses on the results for viewing concerts and sporting events, it can be seen that the mean impact factor for this type of loading is two-thirds of that for low impact aerobics to BS6399 Part 1. Even the mean plus standard deviation value for pop concerts and sporting events is lower than the BS6399 Part 1 low impact aerobics impact factor.

For the other categories, when compared against the equivalent British guidance impact factors, the mean values are approximately 6-7% greater for low and high impact aerobics and up to 20% lower for normal and high jumping.

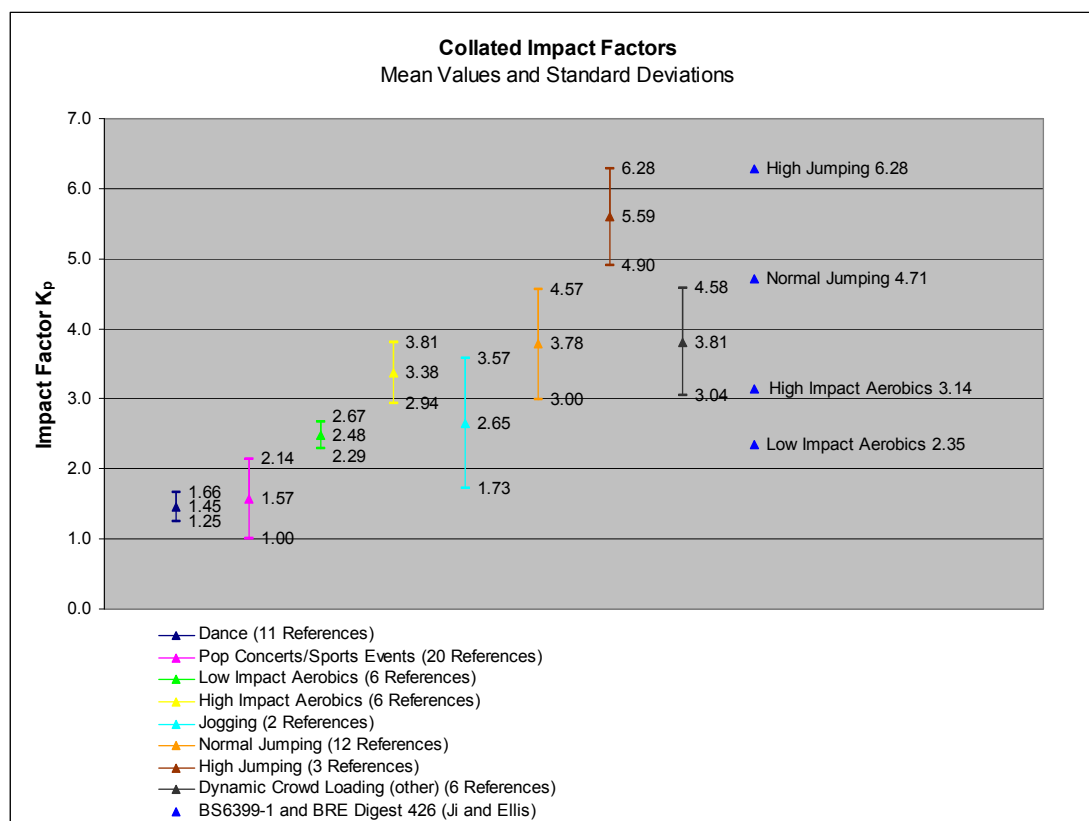


Figure 3.11 Summary of Collated Impact Factors for Human Dynamic Loading

3.2.2.2.2 Frequency of Movement and Harmonics to be Considered

In June 1993 at the European Conference on structural dynamics (Eurodyn'93) it was generally agreed that the range of frequencies that a large group of people could jump and stay synchronised was 1.5 to 2.8Hz (Littler 2003). Subsequent tests carried out by the BRE on dynamically sensitive structures indicate that 2.8Hz may not be the upper bound limit that people can jump in synchronisation (Littler 2003). From tests carried out in a laboratory and from results taken from a nightclub dance floor it was shown that reasonably large groups of people, 100 plus, can jump co-ordinately up to 3.0-3.5Hz. Further testing is required to see whether larger groups on grandstand terracing can achieve the same level of coordination at higher frequencies, although it would seem unlikely.

Secondly it was established at Eurodyn'93, in line with other international codes and guidance, that the first three Fourier components should be used in an assessment of the safety of any structure subject to such synchronised crowd loading (Littler

2003). Thus the 8.4Hz (3x2.8Hz) limit set in the subsequent 1996 edition of BS6399: Part 1. The Canadian Code (NBCC 1995 and Allen 1990b) and the IStructE guidance notes on stadium dynamics (2001 and 2008) however use only the first two harmonics when assessing grandstands, hence the 6Hz frequency limit.

In their 1994 papers on floor vibrations due to dance type loads Ji and Ellis (1994a and 1994b) expand on this and recommend that in order to ensure that all possible resonance conditions are considered, the number of harmonics of the loading function, that need to be included when assessing a floor structure, is the whole integer greater than the ratio of the natural frequency of the floor f_o to the frequency of the forcing function f_p i.e. $n = \text{whole integer} > (f_o/f_p)$. For example the forcing function for people jumping at 2.8Hz on a floor with a fundamental vertical frequency of 6Hz should include the first 3 harmonics as $6\text{Hz}/2.8\text{Hz} = 2.14$ (which is then rounded up to 3).

The reason for this is that although structures with a natural frequency over three times the forcing frequency may not have any structural safety problems due to human dynamic loading, they can still be subject to serviceability problems. This is because higher frequency responses have a larger relative importance in terms of accelerations, assuming that acceleration is the governing serviceability criteria. For displacements the lower harmonics have greater influence while for accelerations it is the harmonics that are closest to the natural frequency of the structure that are critical. Ji and Ellis (1994a) showed experimentally that resonant accelerations can be set up in a stiff floor structure (14Hz) excited by the 6th harmonic while the corresponding displacements are largely due to the first and second harmonics.

This theory can also be proved mathematically as shown below:

$$\text{From before } F(t) = G_s [1.0 + \sum_{n=1}^{\infty} r_n \sin[(2n\pi f_p t) + \phi_n]] \quad \text{eq 3.7}$$

Since deflection is a function of mass and stiffness then if stiffness remains constant

$$\begin{aligned} \text{Deflection } \delta &= A \times G_s [1.0 + \sum_{n=1}^{\infty} r_n \sin[(2n\pi f_p t) + \phi_n]] \quad \text{eq 3.8} \\ \delta &= AG_s [1.0 + r_1 \sin[(2\pi f_p t) + \phi_1] + r_2 \sin[(4\pi f_p t) + \phi_2] + r_3 \sin[(6\pi f_p t) + \phi_3] \\ &\quad + \dots] \end{aligned}$$

$$\text{Velocity} \quad \frac{d\delta}{dt} = v = AG_s \sum_{n=1}^{\infty} (2n\pi f_p) \times r_n \cos[(2n\pi f_p t) + \phi_n] \quad \text{eq 3.9}$$

$$\text{Acceleration} \quad \frac{d^2\delta}{dt^2} = a = -AG_s \sum_{n=1}^{\infty} (2n\pi f_p)^2 \times r_n \sin[(2n\pi f_p t) + \phi_n] \quad \text{eq 3.10}$$

$$\begin{aligned} \frac{d^2\delta}{dt^2} = & -AG_s \{ [(2\pi f_p t)^2 \times r_1 \sin[(2\pi f_p t) + \phi_1]] + [(4\pi f_p t)^2 \times r_2 \sin[(4\pi f_p t) + \phi_2]] \\ & + [(6\pi f_p t)^2 \times r_3 \sin[(6\pi f_p t) + \phi_3]] + \dots \} \end{aligned}$$

$$\begin{aligned} \frac{d^2\delta}{dt^2} = & -AG_s \{ [4\pi^2 f_p^2 t^2 r_1 \sin[(2\pi f_p t) + \phi_1]] + [16\pi^2 f_p^2 t^2 r_2 \sin[(4\pi f_p t) + \phi_2]] \\ & + [36\pi^2 f_p^2 t^2 r_3 \sin[(6\pi f_p t) + \phi_3]] + \dots \} \end{aligned}$$

where A = deflection due to the static load G_s

Therefore for Fourier series forcing functions the contribution of the higher harmonics to the resultant acceleration is $(2n\pi f_p)^2$ times greater than the same harmonics contribution to the displacement. Thus for higher frequency structures the key consideration may not be resonant deflections but resonant accelerations induced when higher harmonics of the forcing function coincide with the fundamental vertical natural frequency of the structure.

It should be noted that, due to the nature of Fourier series, forcing functions with shorter contact ratios, i.e. more active jumping, have a greater proportion of higher harmonics than forcing functions with longer contact ratios.

3.2.2.2.3 Crowd Factors

The loading functions and impact factors described above are generally assumed to be relevant to the size group likely to be participating in the activity. However some of the forcing functions provided by the authors are for specific numbers of people while others recommend the use of a crowd factor when a group exceeds a certain size (Pernica 1983, Ebrahimpour and Sack 1992, Kasperski and Niemann 1993, Van Staaldunin and Courage 1994, Willford 2001 and Ellis and Ji 2002).

A basic crowd factor of 0.67, for 'large groups', was suggested in the 1996 revision of BS6399 Part 1. The idea was that the whole loading function

$$F(t) = G_s [1.0 + \sum_{n=1}^{\infty} r_n \sin[(2n\pi f_p t) + \phi_n]]$$

be multiplied by this crowd factor to allow for the lack of coordination between members of the group performing the activity. No indication was given as to the definition of a 'large group'. However, it would be logical to assume that if you start with just a single person and gradually increase the number in the group then the crowd factor would also gradually increase up to a certain point and then plateau. It could be at this plateau that a 'large group' has been reached.

From the references above, several explicitly define crowd factors to be used with the forcing functions. Interestingly the crowd factors are generally only given for two of the six categories of forcing function; normal jumping and pop concerts/sports events.

The crowd factors are given in one of two forms; either as a single value multiplier as BS6399 Part 1 1996 or as revised Fourier coefficients for larger groups. To allow comparison the Fourier coefficients have been converted to a single value and plotted together with the single value crowd factors against crowd size. See Figure 3.12.

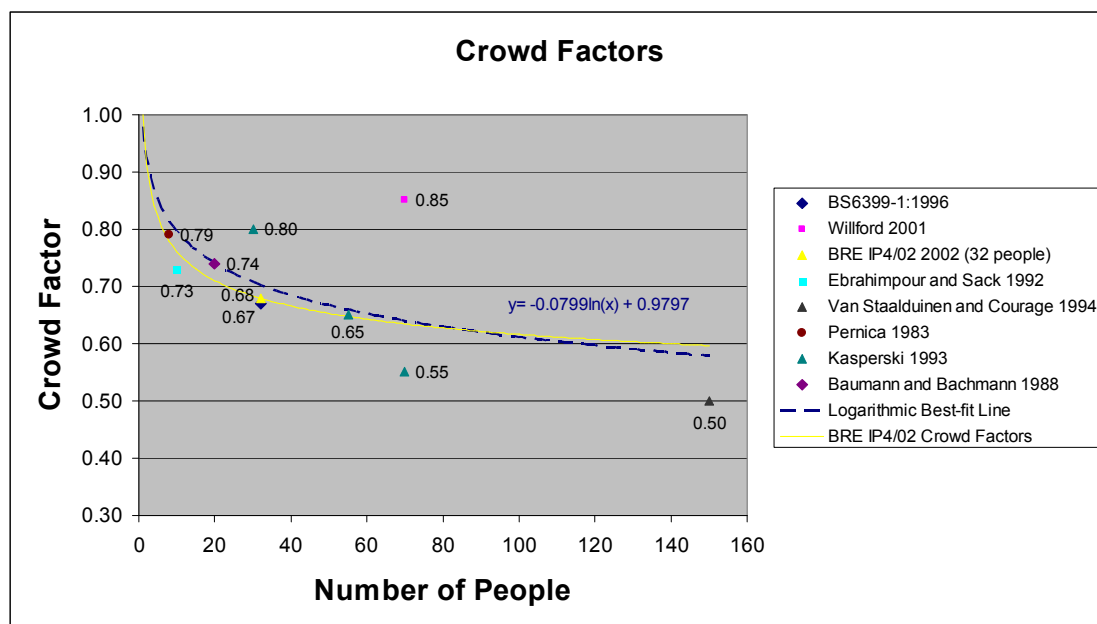


Figure 3.12 Summary of Crowd Factors

From this graph it can be seen that for groups of less than 40 people there is close correlation between the values, with a mean value of 0.73 (+/- 0.06). For larger groups there is a lower consensus in the values, especially Willford (2001) who recommends a crowd factor of 0.85 for large groups over 70 people.

BRE paper IP4/02 2002, by Ellis and Ji, defined experimentally the Fourier coefficients for groups of people jumping in terms of the numbers in the crowd (v) as given below

$$F(v,t) = G_s \{ 1.0 + [1.61v^{-0.082} \sin[(2\pi f_p t) + \frac{\pi}{6}]] + [0.94v^{-0.24} \sin[(4\pi f_p t) - \frac{\pi}{6}]] + [0.44v^{0.31} \sin[(6\pi f_p t) - \frac{\pi}{2}]] + [0.12v^{-0.5} \sin[(8\pi f_p t) - \frac{5\pi}{6}]] \} \quad \text{eq 3.11}$$

If this is plotted onto Figure 3.12 in terms of crowd factor i.e. $F(v,t)/F(1,t)$ it is very close to the logarithmic best fit curve, as shown above. Ellis and Ji's (2002) experimentally derived crowd loading function was incorporated into the British guidance document BRE Digest 426 in 2004.

3.2.2.2.4 Pre-experiment Forcing Functions

For the initial pre-experiment computer modelling (carried out prior to the publication of the current IStructE (2008) permanent grandstand guidance), loading functions based on those proposed by the then current British standard BS6399-1:1996 (with 2002 amendment)/BRE Digest 426 (2004) were used. This loading was used with the understanding that the dynamic loads given in BS6399 Part 1 and BRE Digest 426 tend to be conservative when applied to grandstands and that further research was being carried out into the definition of more accurate human dynamic loading for crowds on grandstands (IStructE 2001).

The purpose of the pre-experiment time-history analysis, was to predict the range of movements that would be induced in the test rig by the crowd during the experiments. As such it was important to be able to assess the maximum and minimum displacements and accelerations that were likely to occur and feed back this information into the design of the test rig.

3.2.2.2.4.1 Magnitude and Form

The first calculation to be carried out was to determine the maximum percentage of the participants that could be jumping at any one time without overloading the test rig. This calculation took into account the following factors; the maximum number of participants on the rig being limited to 24 (see Section 3.1.2), the remaining travel on the springs once the static loads had been accounted for, the BRE Digest 426 (2004) forcing function for low impact aerobics (described in more detail below) and an allowance for a resonant response. This estimated that only 30% of the 24 participants could jump simultaneously before the springs reached their maximum compression.

Because seated inactive spectators are likely to be more sensitive to vibrations than those participating in creating the vibration it was as important, if not more important, to gauge the reaction of those seated as well as those jumping during the experimental work. Therefore it was not a concern that less than 50% of the maximum crowd would be able to participate in creating the stand movement.

The next step, in order to determine the likely maximum and minimum movements of the rig, was to define two different forcing functions to represent the following load cases, in the THA.

- | | |
|--------------------|-----------------------------------------------------------------------------------------------|
| 1 Maximum | based on 30% of the crowd jumping in the same manner perfectly coordinated |
| 2 Realistic | based on 30% of the crowd jumping but not perfectly coordinated or jumping in the same manner |

The 'maximum' dynamic load case was taken directly as the BRE Digest 426 (2004) 'The Response of Structures to Dynamic Crowd Loading' forcing function for low impact aerobics with a contact ratio=0.67 (Figure 3.13). It was assumed for this idealised 'maximum' load case that all of the participants were jumping in unison with exactly the same contact ratio, i.e. no crowd factor was applied.

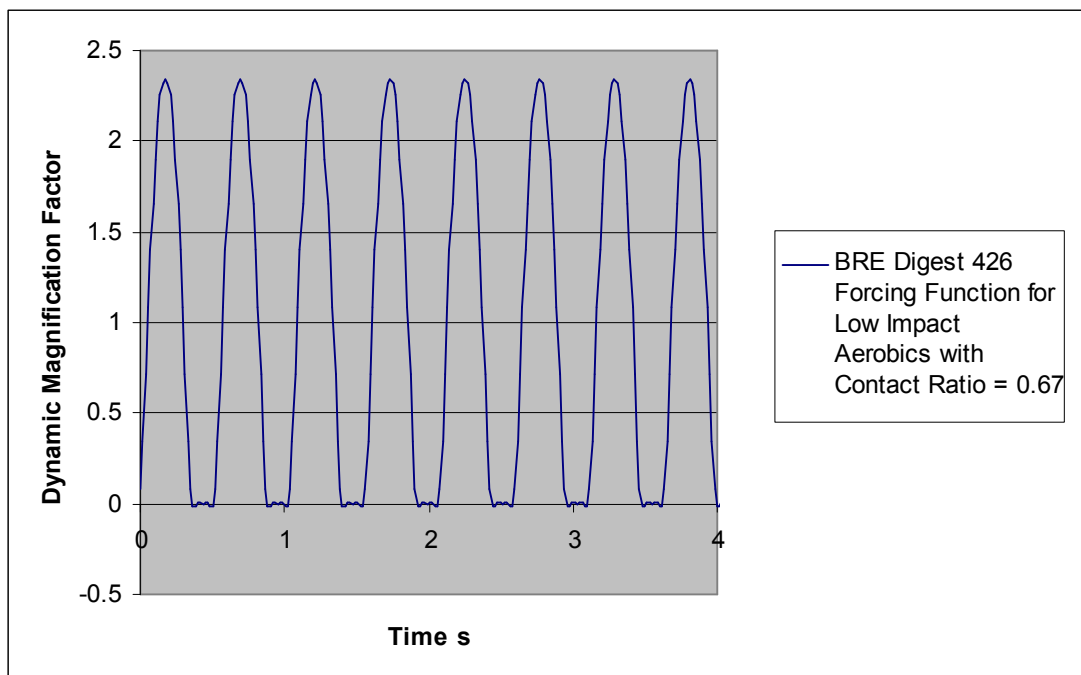


Figure 3.13 'Maximum' Forcing Function

It is very unlikely that a group of untrained individuals will jump with equal contact ratios, as some people will jump higher and more enthusiastically than others. Their actions will also not be totally coordinated. Therefore a separate forcing function was developed in an attempt to predict a more realistic dynamic crowd load.

As for the 'realistic' loading function it was decided, for continuity, to use the normalised half sine waves proposed in BRE Digest 426 as the basis for this 'realistic' loading function. The least intense loading given in this publication is for 'low impact aerobics' which is likely to be more forceful than non-trained individuals could jump on a tiered grandstand with seating. Therefore an additional forcing function, with a contact ratio α of 1.0, representing bobbing up and down on the spot was used to balance out the higher energy BRE Digest forcing functions. An estimate was made of the breakdown of how energetically a crowd could jump on a grandstand based on the mean plus standard deviation impact factor K_p of 2.14 from Figure 3.11. This was taken as 20% jumping with a contact ratio of 0.5 (high impact aerobics), 30% at the equivalent of low impact aerobics (contact ratio=0.67) and the remaining 50% are bobbing up and down on the spot with a contact ratio of 1.0 resulting in an overall impact factor of 2.12.

To create the 'realistic' forcing function the separate half sine waves for each contact ratio were first aligned so that the peaks in the loading corresponded (Figure 3.14). This was done to represent all the participants landing at the same time despite the variation in the type of jumping. These aligned half sine waves were then added together in the correct proportions to create a combined forcing function (Figure 3.15).

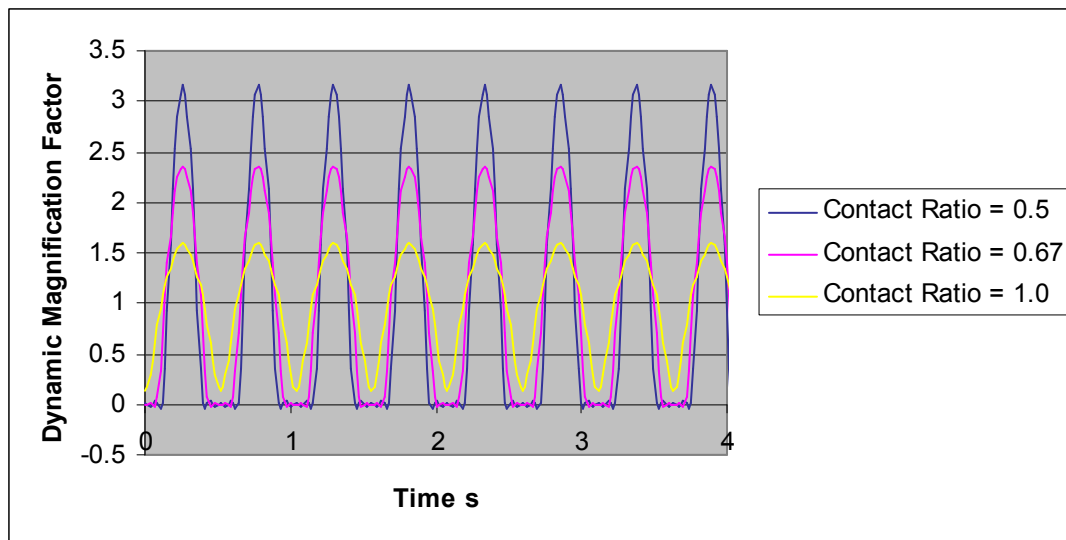


Figure 3.14 Aligned Half Sine Waves for 'Realistic' Forcing Function

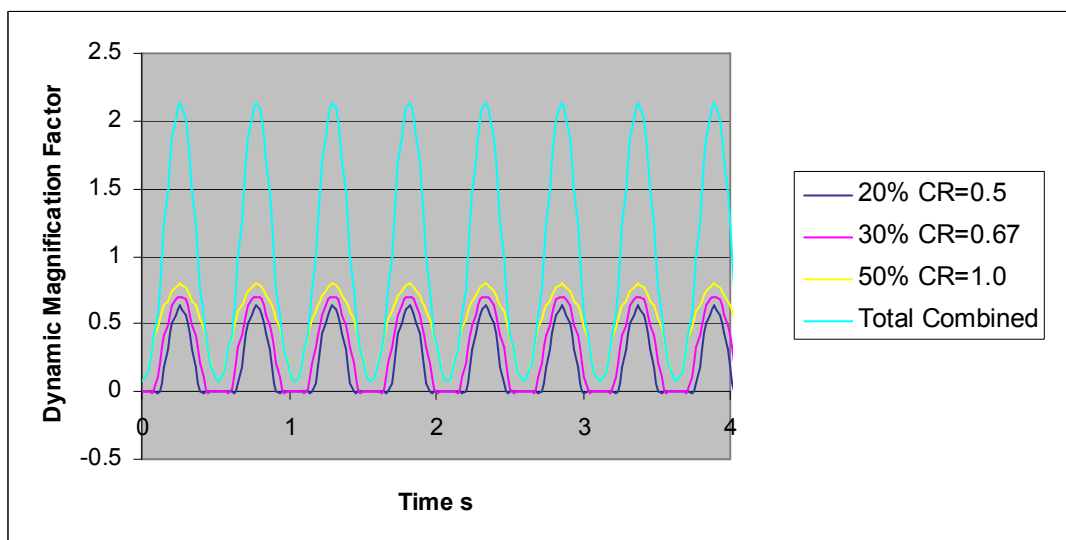


Figure 3.15 Proportioned Half Sine Waves for 'Realistic' Forcing Function

To allow for lack of synchronisation a crowd factor of 0.67 was selected, taken from BS6399 Part 1 pre October 2002 amendment. Rather than just multiplying the forcing function by the crowd factor, which reduces both the peak and mean value, a slightly

different method was used. The peak value of the combined forcing function was reduced to 67% of its former value while maintaining a mean value of 1.0 (Ji and Ellis 1994a and 1994b) (Figure 3.16). Although this seems a rather simplified method of specifying a crowd factor it has a similar effect of reducing the peak dynamic load factor and smoothing the forcing function as the more complex formulae proposed by Ellis and Ji (2002) (and reproduced in BRE Digest 426 (2004)), see Figure 3.17.

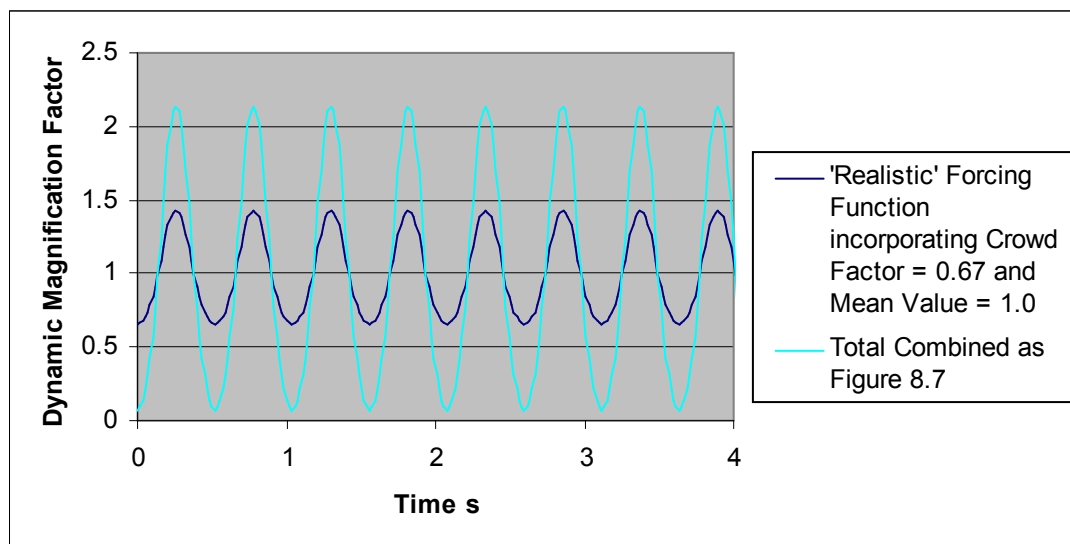


Figure 3.16 'Realistic' Forcing Function

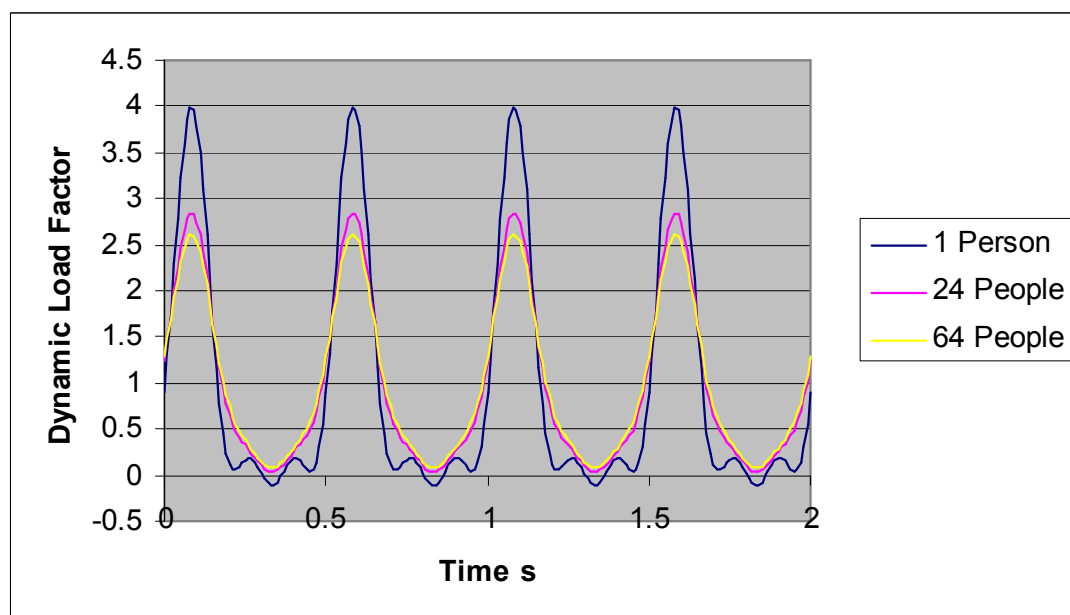


Figure 3.17 Effect of Ellis and Ji (2002) Crowd Factor on Half Sine Wave Forcing Function

Interestingly the resulting 'realistic' forcing function has a very similar form and peak dynamic load factor both to that recorded by the BRE for concert audiences (BRE Digest 426 (2004) and Ellis and Littler 2004b) and that of the Scenario 4 forcing function from the 2008 IStructE guidelines as can be seen in Figure 3.18. (The IStructE 2008 guidelines were published subsequent to this computational analysis and so the methods recommended in this publication were not used but have been reviewed in Chapter 6 in relation to the recorded test data.)

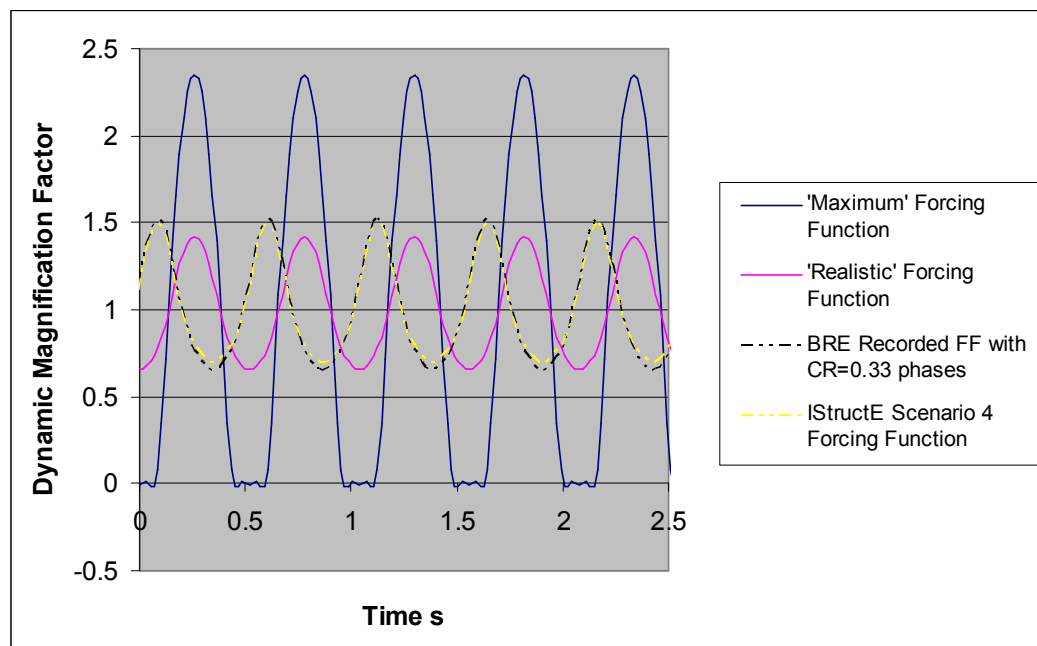


Figure 3.18 Proposed and Previously Recorded Forcing Functions

Recently a lot of research has been carried out in the field of human structure interaction (Ellis and Ji (1996 and 1997), Sasche (2002 and 2003), Ji (2003a and 2003b), Sasche et al (2003a and 2003b), Reynolds et al (2004), Dougill et al (2006), IStructE (2008)) and the effects a large crowd can have on the modal properties and damping of a structure. However at the time of the pre-experiment modelling, there was no agreed method of how human-structure interaction should be incorporated into the dynamic modelling of grandstands. Therefore for the computational model the standard method of analysis, of the time (BRE Digest 426 (2004) and NBCC 2005), which treated the crowd as a lumped mass on the structure was used (Figure 3.19).

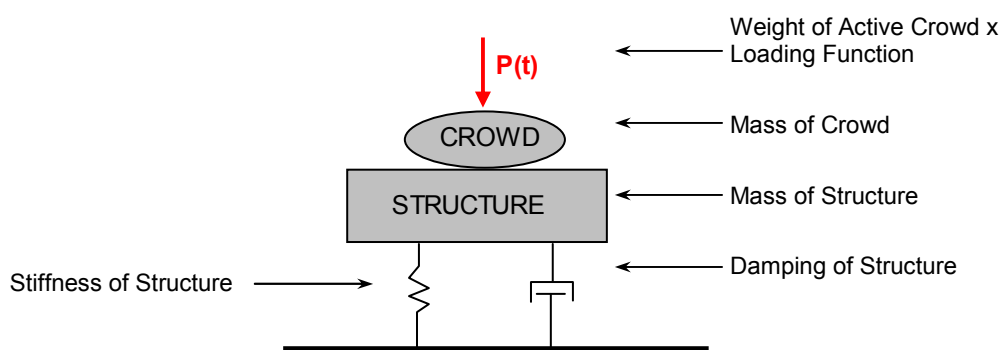


Figure 3.19 Simplification of Load Model used for Pre-experiment Analysis

As the chosen forcing functions were specified in their normalised format they were multiplied by the actual weight of those jumping before being input into the time history analysis (THA). Rather than specifying exactly where the jumpers were to be located, this load was taken as 30% of 24 people weighing 80kg each spread over the entire stand. The load was applied as a series of point loads to more accurately represent the locations of the participants. The remaining 70% of the mass of the participants was applied to the model of the test rig as nodal masses, to be combined with the self weight of the rig and its fixtures, for determination of the rig's response under the time history analysis (THA).

From the data given in Table 3.2 it can be calculated that the resulting maximum peak vertical dynamic load for the THA is 2.82kN/m^2 (30% of $2.36 \times 2\text{kN/m}^2$ plus 70% of 2kN/m^2) i.e. well below the static load of 5kN/m^2 for which the stand was designed.

Table 3.2 Summary of Proposed Forcing Functions

Load Case		Contact Ratio	Participation	Crowd Factor	Dynamic Magnification Factor	Wave Type
1	Maximum	0.67	30%	None	2.36	Half Sine
2	Realistic	20% at 0.5 30% at 0.67 50% at 1.0	30%	0.67	1.42	Modified Sine

3.2.2.2.4.2 Frequency

It is widely accepted that the maximum frequency at which large groups of people can jump in unison, for any length of time, is 2.8Hz due to difficulties of coordination at higher frequencies, and this value might even be lower for very large groups such as those in a grandstand (Ginty et al 2001, IStructE 2001, Littler 2003 and BRE Digest 426 (2004)).

Therefore, in order to determine the maximum response for each of the forcing functions described above, the frequency of the forcing function was set such that it was equal to the lowest achievable harmonic of the natural frequency of the stand. For example, for a stand with a natural frequency of 6.5Hz, the key forcing frequency would be 2.17Hz ($6.5\text{Hz}/3$) as 3.25Hz ($6.5\text{Hz}/2$) is greater than the limiting jump frequency of 2.8Hz. This frequency was chosen as being the one that would excite the natural vibration of the structure to produce maximum resonance and thus the peak response.

The response of the rig to forcing functions of different multiples of the stand frequency was also investigated. So for example the 6.5Hz rig model was run with forcing functions at the stand frequency divided by 3 (as described above) and 4. All the models were also run with two forcing frequencies (1.7Hz and 2.4Hz) at which no resonance should occur. The purpose of this was to compare excitation of the rig due to the various harmonics of the forcing function and also resonant and non-resonant responses. All of the frequency combinations shown in Table 3.3 were run for both the 'maximum' and the 'realistic' forcing function

As the chosen forcing functions assumed that only 30% of the spectators were participating in the dynamic loading, the mass of the stationary crowd (70% of the total) was added to that already in the model, i.e. selfweight and applied dead load. This total mass was used to calculate a revised natural frequency for each of the rig set-ups and the frequency of the forcing functions based on these revised frequencies. For these calculations the actual mass of the spectators was taken as 80kg per person.

Table 3.3 Rig and Forcing Function THA Model Combinations

	<u>Rig Frequency</u>		
Rig Model Frequency (empty)	(2.06 Hz)	(3.94 Hz)	(6.48 Hz)
with 70% max crowd as mass	1.91 Hz	3.65 Hz	5.94 Hz
<u>Forcing Frequency</u>			
0.96 Hz	✓ 2nd	-	-
1.22 Hz	-	✓ 3rd	-
1.49 Hz	-	-	✓ 4th
1.70 Hz	x	x	x
1.83 Hz	-	✓ 2nd	-
1.91 Hz	✓ 1st	-	-
1.98 Hz	-	-	✓ 3rd
2.40 Hz	x	x	x
✓ = Resonance due to given harmonic of forcing function x = No resonance - = Not analysed			

3.2.2.3 Summary of Computational Modelling Input

A computational model was developed in order to aid the design of the test rig. This helped confirm the likely forces in the elements as well as the fundamental natural frequencies and mode shapes of the likely response to dynamic loading. It was also used to estimate the range of movements and accelerations likely to be generated by the participants during the testing, using time history analysis (THA).

The model produced was fairly detailed (for the size of structure being considered) and represented as closely as possible the actual rig. This was done to increase the accuracy of the output results.

The forcing functions employed in the THA drew on experimentally derived and actual recorded impact factors and crowd coordination factors. Two forcing functions were used in the analysis. The first being a simple half sine wave, representing the maximum dynamic crowd loading that it was anticipated could be produced by a group of participants jumping on the test rig. The second was a more complex form,

closer in appearance to a modified sine wave, generated to give a more realistic interpretation of the force likely to be imparted by groups of jumping participants during the testing. The jump frequencies for the forcing functions were selected to match those proposed for the testing (Chapter 4) and also tailored to induce the maximum resonant response for each rig set up.

The results of the computational analysis are summarised in Section 3.2.3.

3.2.3 Computational Modelling - Results

As described in Sections 3.2.1 and 3.2.2, a computer model of the test rig was generated in order to predict the likely movements that would be experienced during the experimental stage of the work. The analysis programme Robot Millennium v19.0, produced by RoboBAT, was used to carry out the pre-experimental modelling. This software was chosen as it is readily available, is enabled for 3D analysis including Finite Element Modelling (FEM) and has the dynamic capability for both modal and time history analysis (THA).

3.2.3.1 Results of Modal Analysis

Modal analysis confirmed that the principal mode was the rakers deflecting in unison in conjunction with the precast units, as shown on Figure 3.20. The computer model calculated the natural frequency of this mode to be around 6.5Hz. The second mode shape predicted was the side-to-side sway of the whole rig at approximately 8Hz (Figure 3.21), followed by three modes of localised minor axis bending of various members. The sixth mode was the next predominantly vertical mode with the rakers vibrating in anti-phase at over 11Hz.

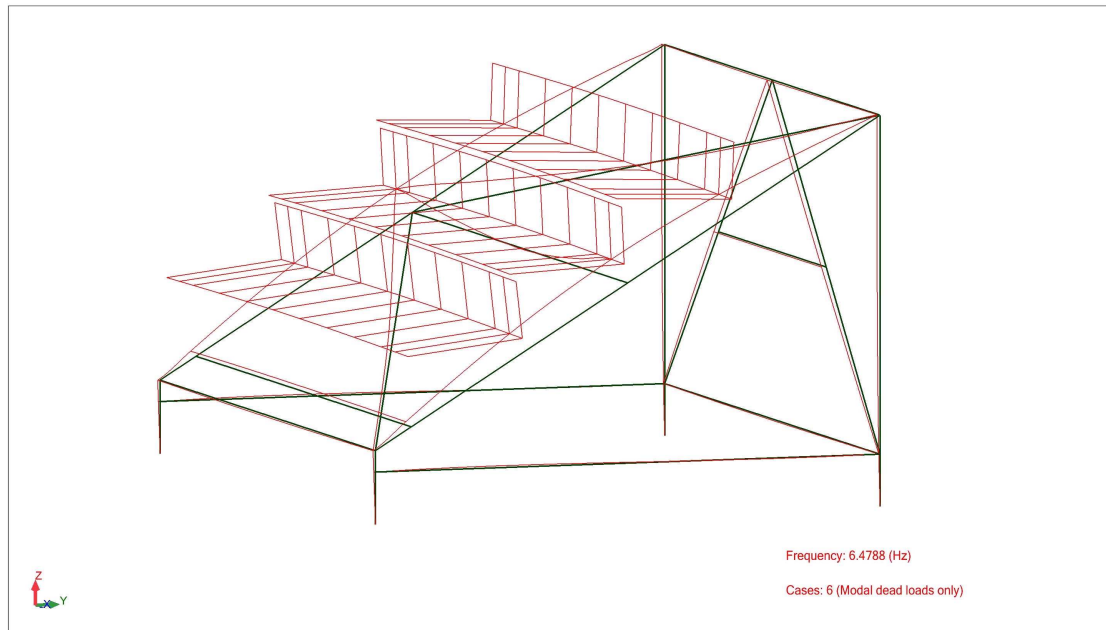


Figure 3.20 Fundamental Mode Shape of the Test Rig with no Springs

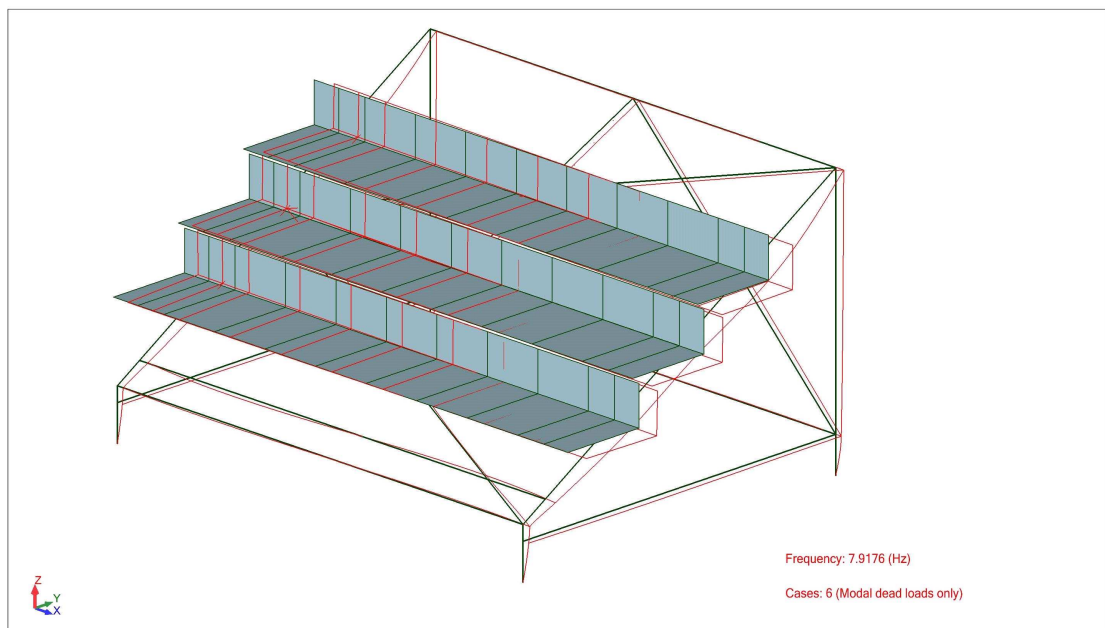


Figure 3.21 Second Mode Shape of the Test Rig with no Springs

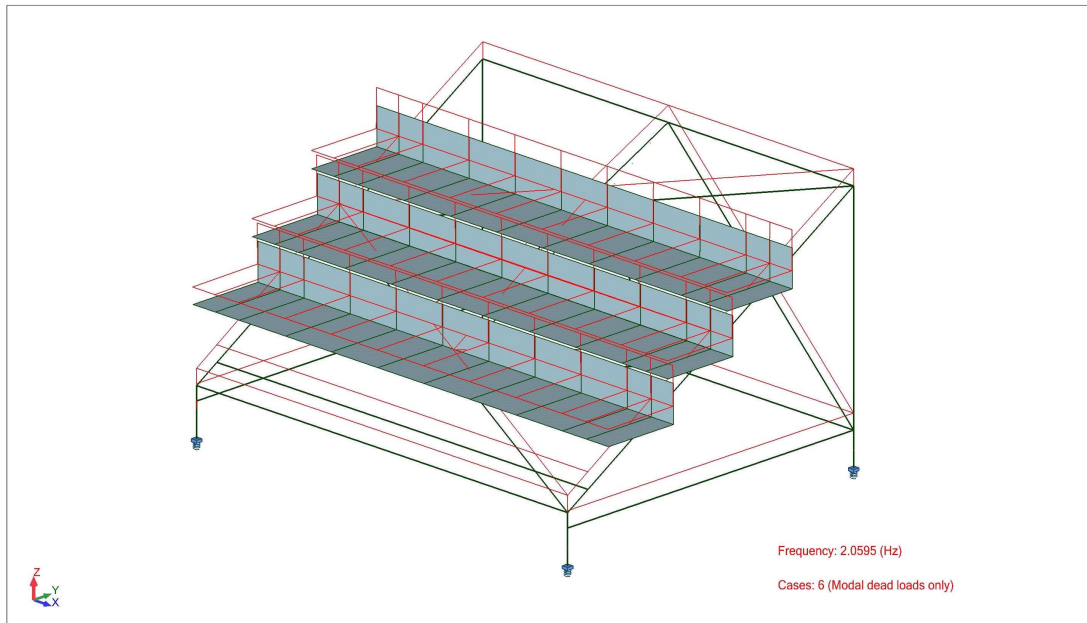


Figure 3.22 Fundamental Mode Shape of the 2Hz Test Rig with Springs

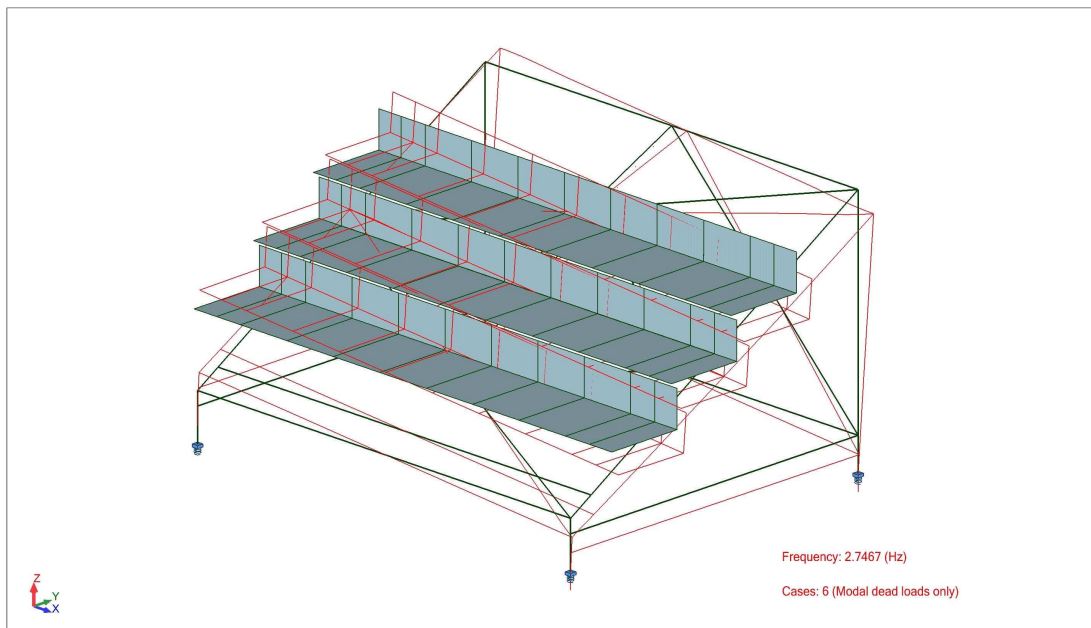


Figure 3.23 Second Mode Shape of the 2Hz Test Rig with Springs

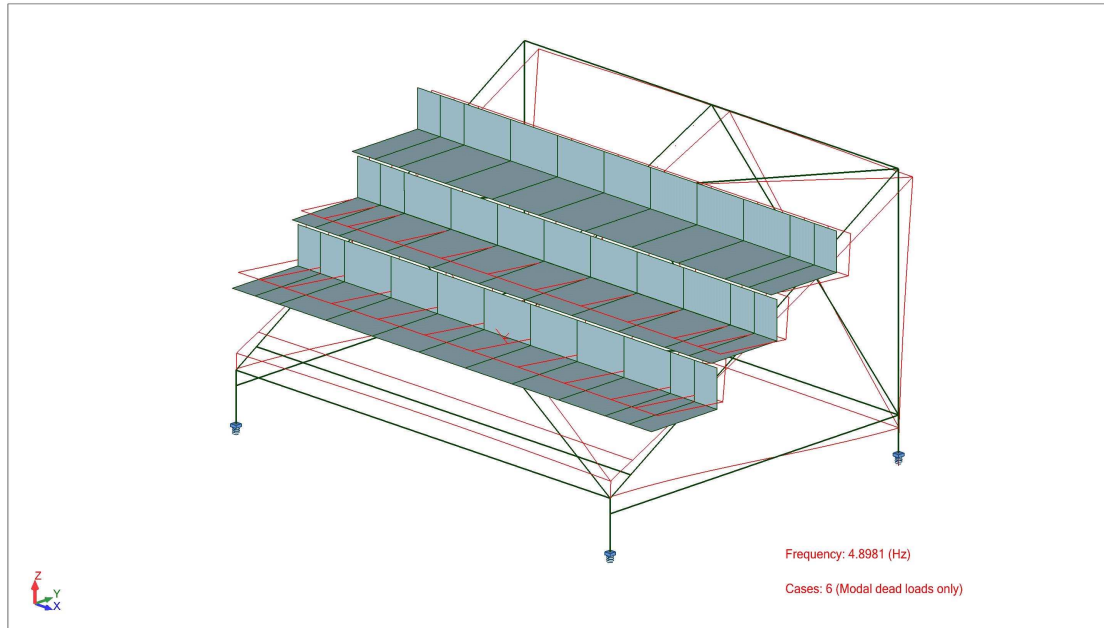


Figure 3.24 Third Mode Shape of the 2Hz Test Rig with Springs

The computational model was rerun with both the 2Hz and the 4Hz spring set-ups. This confirmed that with the addition of the springs the fundamental mode of the rig was still vertical with all the springs moving in unison (Figure 3.22) with frequencies of about 2Hz and 4Hz respectively. The second mode shape of the sprung models was a rotational mode with the left and right hand springs moving out of phase (see Figure 3.23). The frequencies of these second modes were fairly close to the fundamental frequencies of the rigs, 2.7Hz for the 2Hz rig and 4.6Hz for the 4Hz rig. Therefore it was important to take measures to avoid this second mode shape dominating the response of the sprung rigs during the experimental testing of the actual rig. Consequently care was taken to distribute the crowd evenly over the rig and the locations of the jumping participants were specified so as to load the left and right sides of the rig in a similar manner during each of the tests.

The third mode shape of the 2Hz and 4Hz sprung rigs was another rotational mode, this time with the front and back springs moving out of phase (Figure 3.24). As the frequencies for these mode shapes were considerably greater than the fundamental rig frequencies, 4.9Hz and 6.2Hz respectively, there was less concern over these mode shapes being activated during the testing.

3.2.3.2 Results of Time History Analysis

The results from the time history analysis (THA), using the modal decomposition method, for one key location are summarised in the following sections. The point chosen was Node 314 (Figure 3.25), located in the centre of the rig on the central precast terrace unit, as this point consistently gave the maximum vertical response.

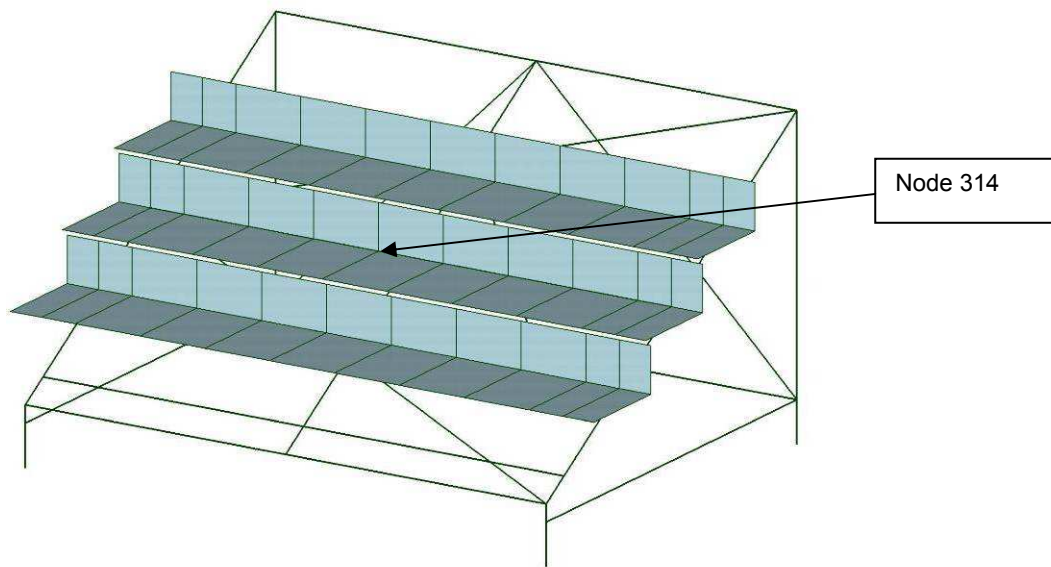


Figure 3.25 Location of Node 314

In order to establish the predicted movement of the rig, the output of the THA (in the form of time history plots) was analysed. Typical time history plots are shown in Figure 3.26. The segment of the output used to determine the predicted displacements and accelerations of the vibrations was that showing a steady-state response to the periodic forcing function. This occurs several seconds into the THA as shown in Figure 3.26. The reason for ignoring the first few seconds of the time history plot is that this section of the trace tends to be erratic as the structure is driven by the forcing function in to the steady-state response. Larger vibrations can be predicted in this period than would happen in reality. This is because actual periodic crowd loads gradually build in strength rather than reaching peak magnitude from the offset as assumed by the constant peak amplitude of the forcing function used in the THA (Figure 3.26). With a gradually increasing forcing function the response of the structure also gradually increases meaning that the peak vibrations happen once the forcing function has reached its peak i.e. the steady-state response.

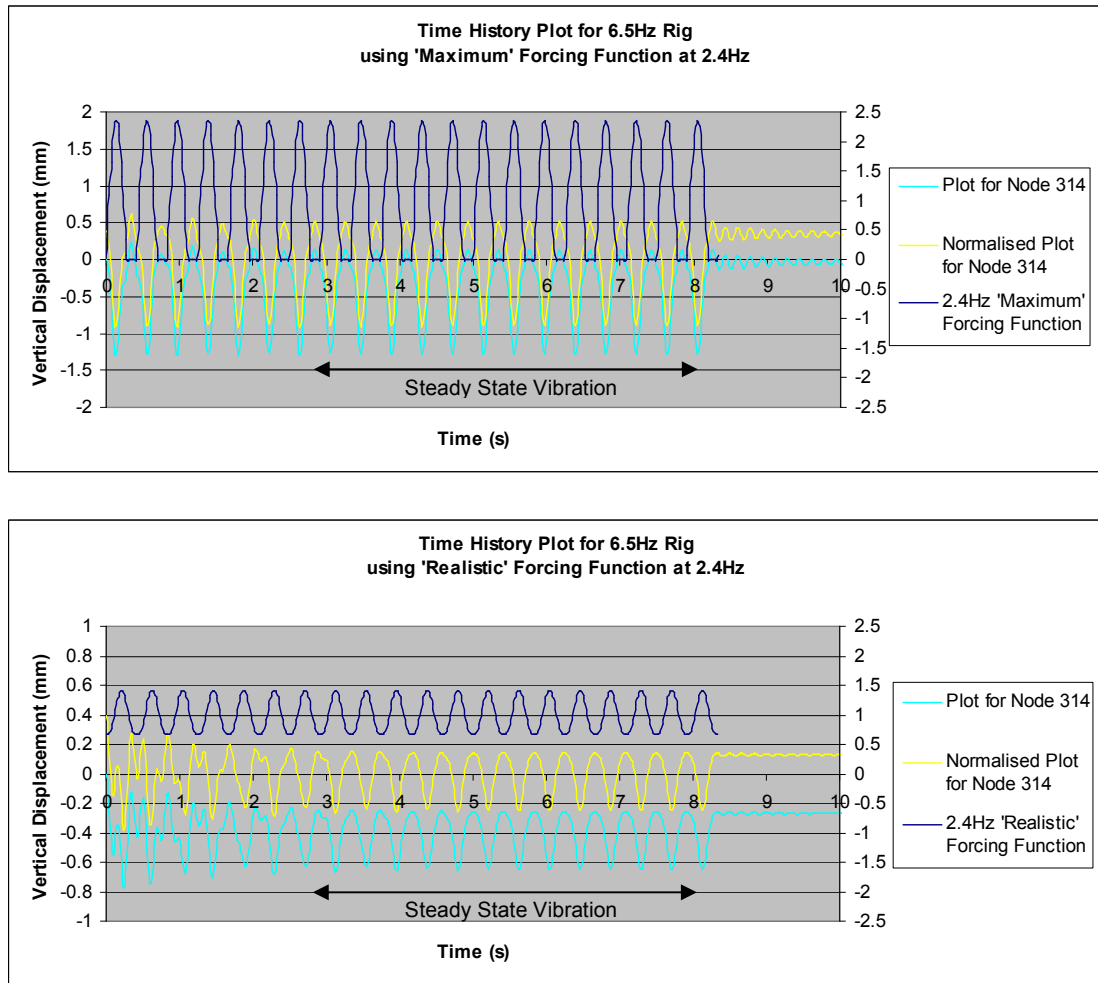


Figure 3.26 Time History Plots for 6.5Hz Rig using 2.4Hz Forcing Function

Once the steady-state response was identified the displacement plots were normalised by removing the static component so that only the dynamic displacement was shown (Figure 3.26) and it is these normalised values that are reported in Section 3.2.3.2.1.

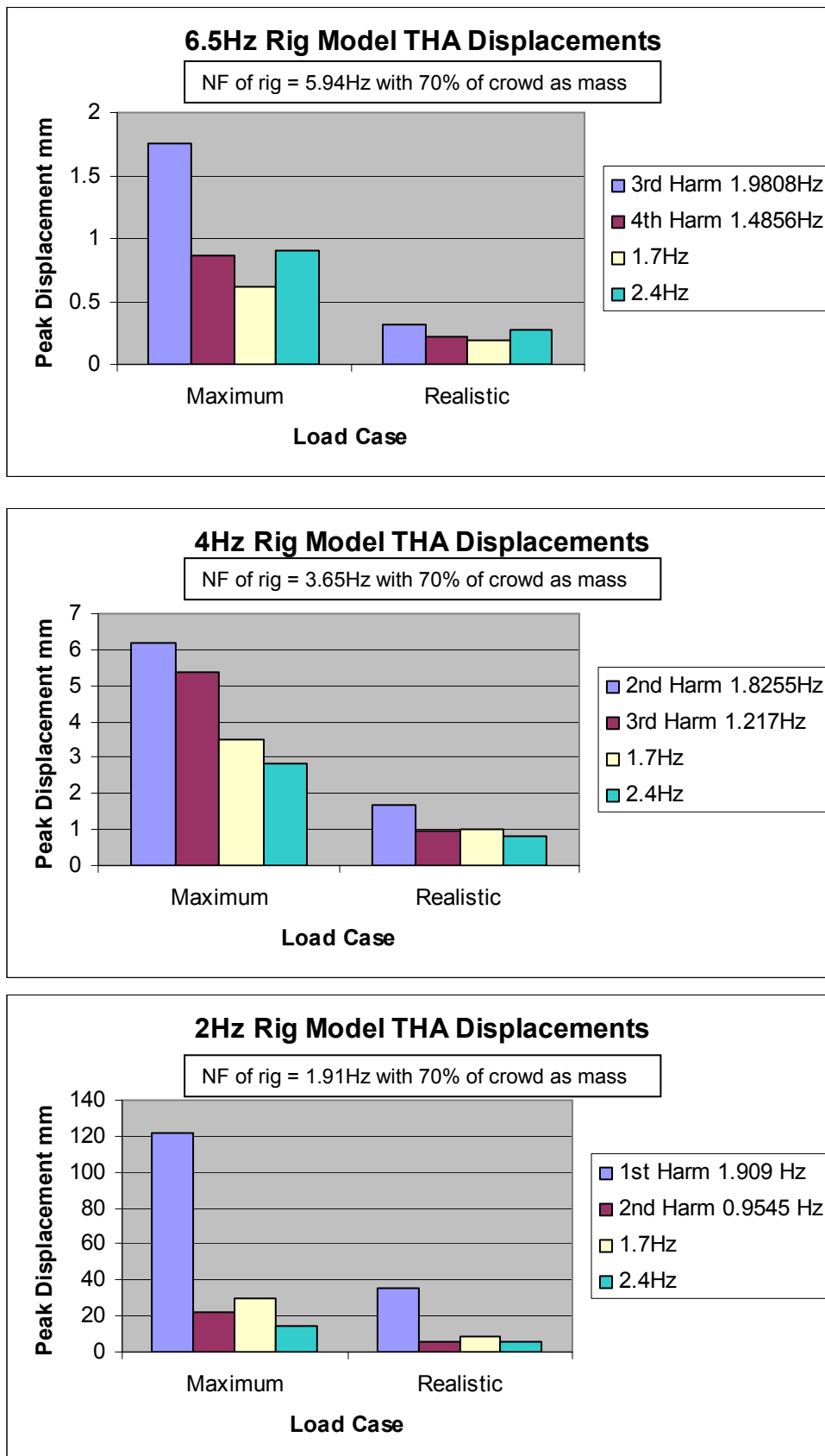


Figure 3.27 Maximum Peak Vertical Dynamic Displacements from THA

3.2.3.2.1 Displacements

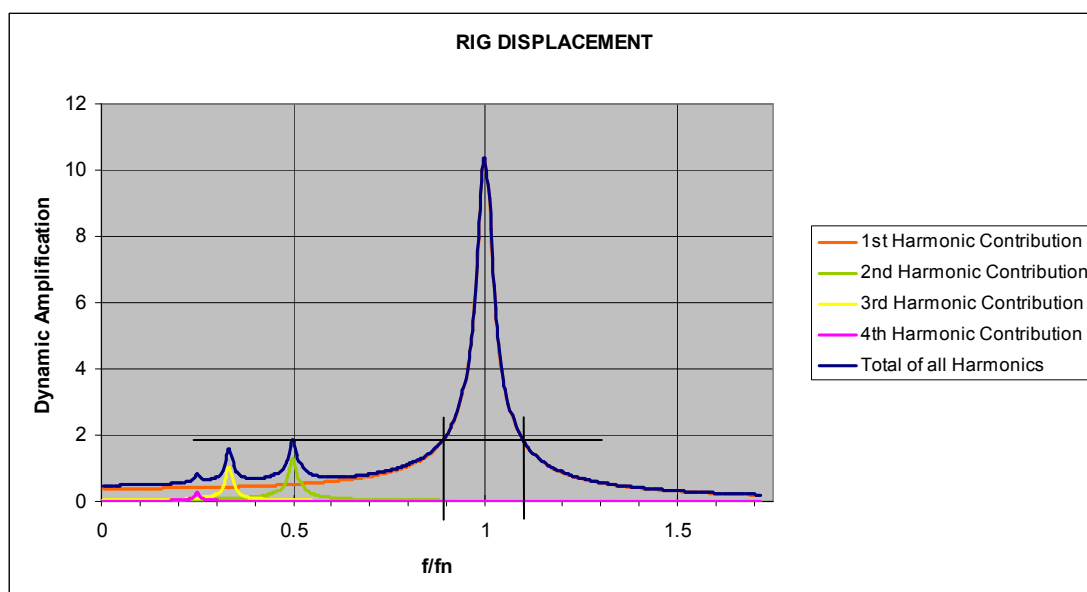
The maximum peak vertical dynamic displacement results from the three different rig set-up models are shown in Figure 3.27. Critically these show that for the proposed range of rig frequencies the peak dynamic displacements, that could be experienced by the participants, cover a range from less than 1mm (6.5Hz rig) to over 30mm (2Hz rig). This compares to a static live load range of 1.4mm to 14mm.

As the main structure of the rig remains constant in all three set-ups the change in frequency and stiffness is purely down to the different spring combinations. The 4Hz rig's springs are 4.5 times stiffer than those of the 2Hz rig while the 6.5Hz rig is supported directly off the laboratory strong floor. For this reason, the predicted dynamic displacements for the 2Hz rig are approximately 3 times greater than those for the 4Hz rig which, in turn are roughly 3 times greater than those for the 6.5Hz rig (comparing similar harmonic excitation). For the extreme case of 1st harmonic excitation under the 'Maximum' forcing function, for the 2Hz rig, the peak dynamic displacement exceeds 120mm. Even if the rig was designed to allow such a magnitude of movement, it is of course unlikely that the crowd would continue to jump if the rig were moving $\pm 100\text{mm}$ beneath them and so these calculated displacements are to be used as a guide only.

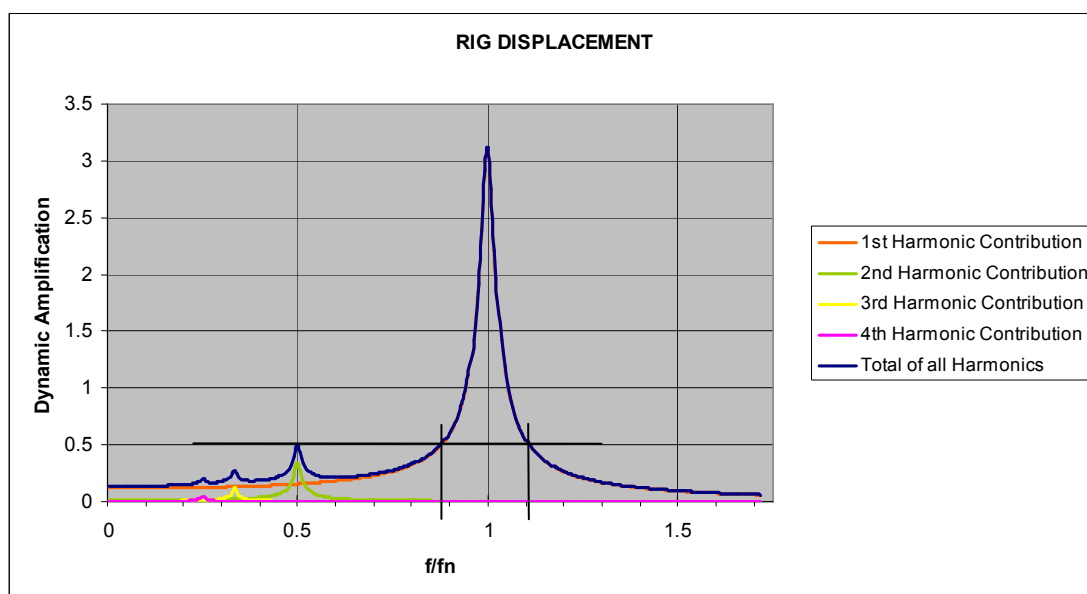
The lower the natural frequency of the rig the greater the likelihood of the crowd being able to induce a significant resonant response. This can be explained by examining the Fourier coefficients defining the forcing functions. As explained in Section 3.2.2.2, the forcing function, applied at a frequency f , can be broken down into its sine wave constituents (harmonics) at frequencies $2f$ (2nd harmonic), $3f$ (3rd harmonic), $4f$ (4th harmonic) etc. Due to the form of the forcing function used to describe human dynamic loading the magnitude of the harmonics typically reduces as the frequency increases i.e. the 1st harmonic (at frequency f) is greater than the 2nd harmonic (at frequency $2f$) which in turn is greater than the 3rd harmonic (at frequency $3f$) etc. When the frequency of one of the harmonics of the forcing function equals the natural frequency of the structure resonance, due to that harmonic, occurs. The greater the magnitude of the harmonic the larger the resonant response. Hence the lower the number of the harmonic of the forcing function corresponding to the natural frequency the rig the greater the excitation of the rig due to resonance.

This is highlighted particularly by the marked difference in the response of the 2Hz rig to the forcing function that corresponds directly with the natural frequency of the rig (1st harmonic) and the forcing function that is at half the natural frequency (2nd harmonic) (Figure 3.27). Figure 3.27 also shows up the differences in the magnitudes of the individual harmonics. The Fourier coefficients for the 'Maximum' forcing function are greater than those for the 'Realistic' forcing function hence result in larger predicted displacements. The ratios of the Fourier coefficients between 1st and 2nd harmonic components are similar for both forcing functions (Figure 3.28 and Table 3.4) and hence the ratios of the displacements of 1st and 2nd harmonic excitation shown on the 2Hz rig are similar for the two loadings considered.

In addition to the forcing frequencies aimed at inducing resonance, the 1.7Hz and 2.4Hz forcing functions were chosen as frequencies that do not correspond to any of the harmonics of the test rig frequencies. Thus the response of the models to these forcing frequencies was expected to be less than that for the forcing functions chosen to induce resonance. However this only proved to be the case for the 'maximum' loading function with the 4Hz model. For all other cases one of the non-resonant frequencies produced a response of very similar magnitude to the lower frequency resonant response. This can be explained by examining the dynamic amplification factor for each forcing function calculated using a simple single degree of freedom system model and shown graphically in Figure 3.28. This shows that the 1st harmonic peak is relatively wide at its base and excitation frequencies of 0.9 and 1.1 times the structural natural frequency can induce vibrations of a magnitude equal to exciting the structure at half its natural frequency (2nd harmonic excitation). Figure 3.28 also shows that, particularly for the 'Realistic' forcing function, the 3rd and 4th harmonic peaks are relatively small and excitation between 0.2 and 0.7 times the structural natural frequency will induce similar sized vibrations with a slight peak at 0.5 equating to 2nd harmonic excitation.



Maximum Forcing Function



Realistic Forcing Function

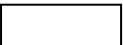




Figure 3.28 Dynamic Amplification for Single Degree of Freedom System

3.2.3.2.2 Accelerations

As for the displacements, the key purpose of the modelling was to confirm that a suitable range of accelerations could be achieved with the proposed rig set-ups and range of jump frequencies. The results of the computer THA for the various load cases/frequency combinations are summarised in Figure 3.29. This shows the estimated magnitude of the peak accelerations and also classifies, by means of a colour key, the accelerations according to Kasperski's (1996) proposed acceptability limits.

The diagrams highlight that as the rig frequency reduces, the likely accelerations increase. Whilst accelerations on the 6.5Hz rig are likely to stay below Kasperski's 1.8ms^{-2} unacceptable threshold, those on the 2Hz rig are likely to exceed his 3.5ms^{-2} panic limit, if a 1st harmonic resonant response is achieved (see Realistic forcing function Figure 3.29). However, as for the coincident vertical dynamic displacements, it is unlikely that the severe accelerations predicted by the 'maximum' forcing function will be attained as the participants are likely to stop jumping/lose coordination if the vibrations become this extreme.

Acceleration Limits to Kasperski (1996)

	Acceptable?	Below 0.5ms^{-2}
	Disturbing Comfort	$0.5\text{--}1.8\text{ms}^{-2}$
	Unacceptable	$1.8\text{--}3.5\text{ms}^{-2}$
	Panic	$3.5\text{--}10\text{ms}^{-2}$
	Severe Panic?	$> 10\text{ms}^{-2}$

Key to Figure 3.29

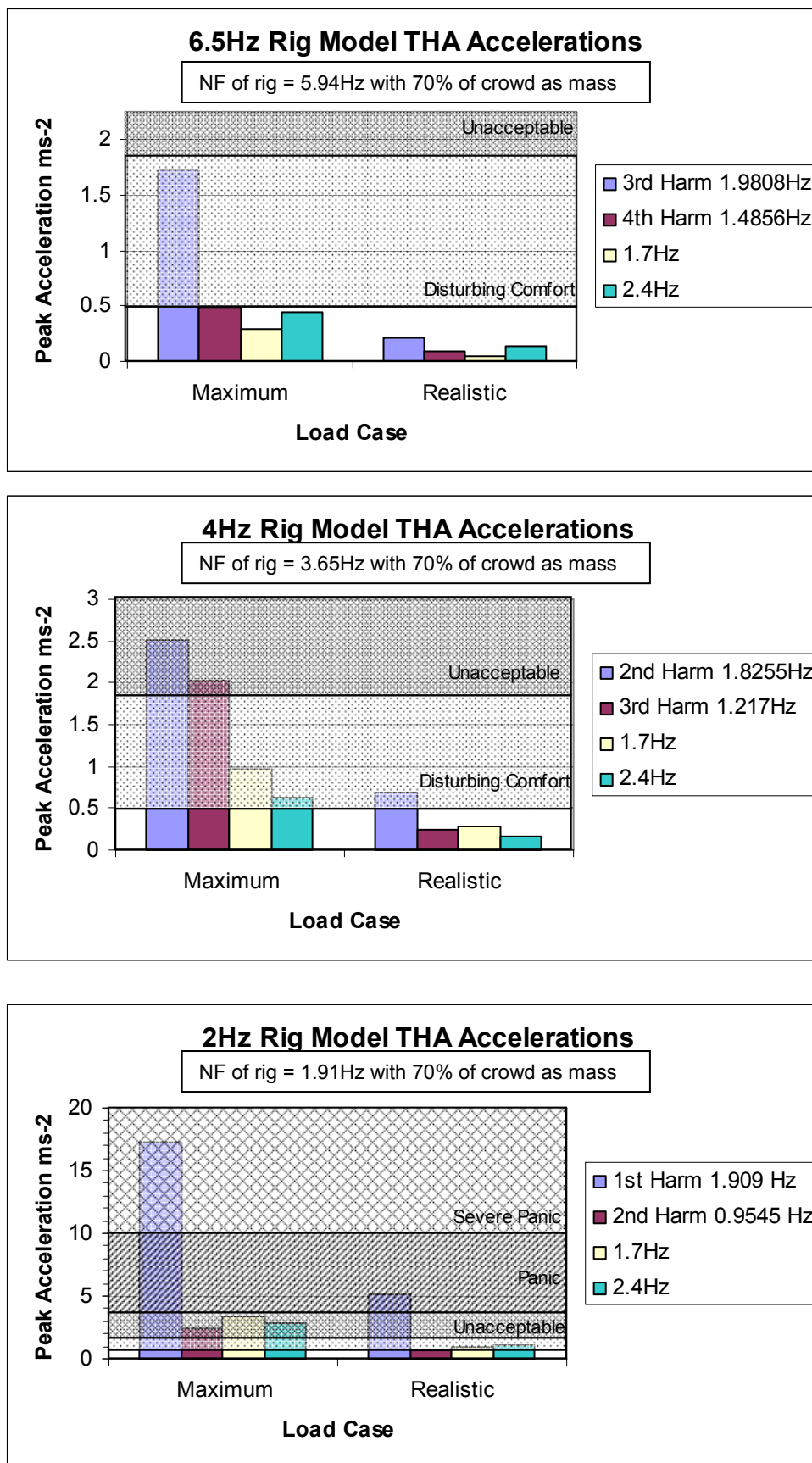


Figure 3.29 Peak Vertical Accelerations from THA

3.2.3.2.3 Frequency Content

Another significant factor to consider is the frequency content of the response. In order to understand the response of the model to the THA input it is important to identify the nature of the forcing function.

3.2.3.2.3.1 Frequency Content of Forcing Functions

The two forcing functions used in the time history analysis could be classed as different forms. The 'maximum' load case is a half sine wave while the 'realistic' case is a modified sine wave as can be seen in Figure 3.30 below. (A description of the derivation of the forcing functions is given in Section 3.2.2.2.4.1)

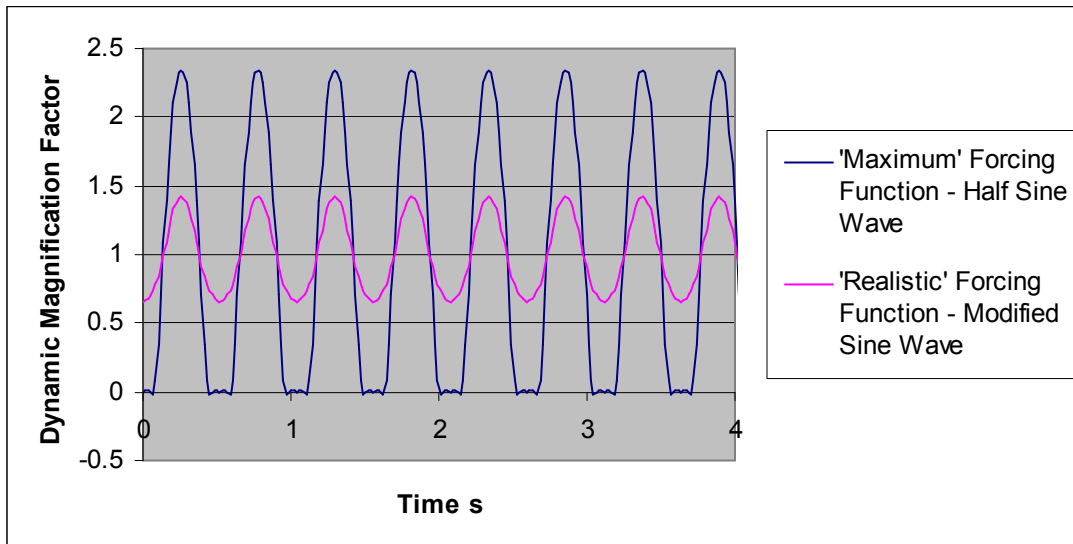


Figure 3.30 Form of the Forcing Functions used in THA

Although the two waves have the same mean value, the range and peak magnitude of the half sine wave is considerably greater than that of the modified sine wave. The frequency content of the functions is also different. This can be seen by examining either the Fast Fourier Transforms (FFT) of the two functions (Figure 3.31) or from the Fourier coefficients used to generate the wave forms (Table 3.4 and Section 3.2.2.2.4.1). Although the relative magnitudes of the first and second harmonics are similar for both forcing functions, the third and fourth harmonic components of the 'realistic' (modified sine wave) forcing function are proportionally much less than for the 'maximum' (half sine wave) load case.

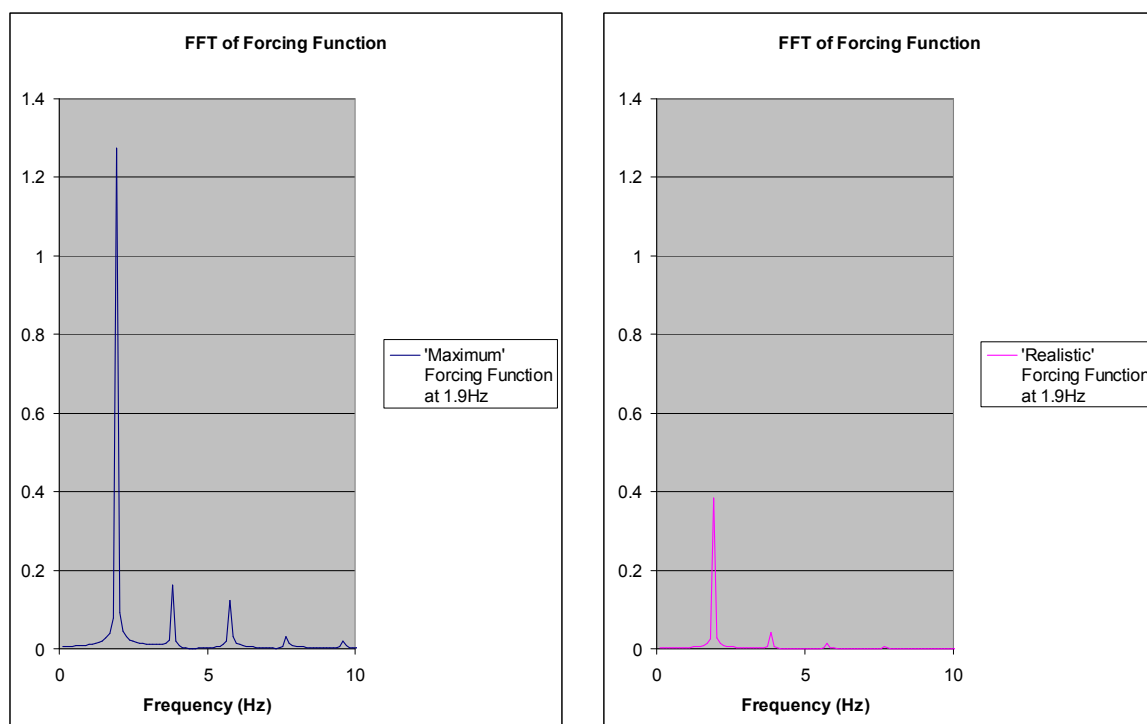


Figure 3.31 Fast Fourier Transforms of Forcing Functions

Table 3.4 Fourier Coefficients of Forcing Functions

		'Maximum' Forcing Function			
Harmonic	n	1	2	3	4
Fourier Coefficient	FC	1.2857	0.1636	0.1333	0.0364
Phase	ϕ	-0.5236	-2.61799	-1.5708	-0.5236
FC as % of 1st Harmonic			12.73	10.37	2.83
FC as % of Total		76.8%*	9.8%*	8.0%*	2.2%*
* remaining 3.2% in 5&6 Harmonics					
FC with ϕ as % of Total		95.7%*	12.2%*	-9.9%*	2.7%*
* remaining -0.7% in 5&6 Harmonics					
		'Realistic' Forcing Function			
Harmonic	n	1	2	3	4
Fourier Coefficient	FC	0.387453	0.043409	0.015	0.005901
Phase	ϕ	-1.5708	-4.71239	-4.71239	-1.5708
FC as % of 1st Harmonic			11.20	3.87	1.52
FC as % of Total		85.8%	9.6%	3.3%	1.3%
FC with ϕ as % of Total		94.5%	10.6%	-3.7%	-1.4%

3.2.3.2.3.2 Model Response and Frequency Content

Once the composition of the forcing functions has been understood a more meaningful interpretation of the THA results can be made.

For both loading functions, the resonant response of the rig model, where the forcing frequency equals the rig frequency, gives a displacement magnitude over three times greater than any other forcing frequency tested. This is due to the dominant nature of the 1st harmonic component in the forcing functions and the effect of pure resonance. For the 2Hz rig the 1.7Hz forcing frequency gave the next largest response due to the proximity to the resonant frequency of 1.91Hz. Where the forcing frequency was set at half the natural frequency of the rig (0.95Hz) the response was similar in magnitude to that of the 2.4Hz forcing frequency even with resonance due to the second harmonic component of the forcing function. This highlights that it is not always straightforward to predict the forcing frequency that will induce the maximum response in a structure.

For the 4Hz rig the maximum response, for both forcing functions, was produced by resonant excitation of the model due to the second harmonic component of the 1.83Hz forcing frequency. As the 3rd harmonic component of the 'Maximum' forcing function is a considerably greater percentage of the total than for the 'Realistic' forcing function, the response for this frequency is greater than the non-resonant response for the 'Maximum' load case but similar in magnitude to the non-resonant responses for the 'Realistic' load case. This observation is consistent for both the 4Hz and 6.5Hz rigs. The 'maximum' forcing function has a small 4th harmonic component while the 'realistic' forcing function has a very small 4th harmonic component. Therefore the 6.5Hz rig model shows a slight increase in the response due to resonance under the 'Maximum' forcing function at 1.49Hz while the 'Realistic' forcing function at the same frequency actually records the lowest reading.

The 2.4Hz forcing frequency was chosen as a 'non-resonant' case as it is not an integer divisor of any of the rig frequencies. However for the 4Hz rig every second peak of the 2.4Hz forcing function ties up with every third peak of the rig natural frequency and similarly with every fifth peak of the 6.5Hz rig natural frequency. This means that every alternate loading instance corresponds to the rigs natural vibration

downwards while the others correspond with the rig moving upwards. For the half sine form of the 'maximum' load case partial resonance occurs as the zero load portion of the forcing function allows for free vibration of the rig during that period. This results in the peak response for the 2.4Hz 'Maximum' forcing function being greater than the true non- resonant 1.7Hz response for both the 4Hz and 6.5Hz rigs. For the 'Realistic' load case the modified sine form forces the rig to move with the forcing function and therefore although the response has larger peaks/troughs every second cycle the magnitude is similar to the non-resonant 1.7Hz case.

Although the above discussion relates to the displacement results of the THA (Figure 3.27) the relative magnitudes of the different frequency/rig combinations are very similar for the THA acceleration results given in Figure 3.29.

3.2.3.3 Summary of Computational Analysis Results

The modal analysis carried out on the computational representation of the test rig (described in Sections 3.2.1 and 3.2.2) showed that, for the empty un-sprung rig, the principal mode of vibration was the fundamental vertical mode with a frequency of approximately 6.5Hz. The second mode shape was the first horizontal mode with the rig swaying side to side at a frequency of around 8Hz. This confirmed that the design of the basic rig met the condition of having a fundamental vertical natural frequency, for the empty structure, of greater than 6Hz as required for permanent grandstands at which high energy concerts are to be staged (IStructE 2001 and 2008). The modal analysis also showed that it was a vertical mode rather than a horizontal mode that had the lowest natural frequency. This was a prerequisite of the design in order that horizontal modes did not complicate the dynamic response of the rig when excited by the test crowd jumping vertically. When the springs were added to the computational model the principal mode remained vertical. However, the analysis showed that the second mode shape, for both of the sprung rig set-ups, was the left and right hand springs bouncing out of phase at a frequency approximately 0.6Hz higher than the principal mode. This highlighted the importance of ensuring that, during the tests, the mass of the jumping portion of the crowd was spread evenly over the rig and that those jumping remained fairly synchronised.

The time history analysis (THA) of the computational model confirmed that, with 30% of a total crowd of 24 people on the rig jumping, peak accelerations could be achieved ranging from below Kasperski's (1996) disturbing comfort threshold of $0.05g$ to above Kasperski's (1996) panic threshold of $0.35g$ by just varying the frequency of jumping on the three proposed test rig set-ups. The THA also showed that the balance of the harmonic components of the forcing function (used to represent the jumping portion of the crowd) had a notable impact on the predicted output response.

4 Testing

4.1 Initial Testing of the Rig

Prior to the main experimental work being carried out, preliminary tests were conducted to confirm the fundamental natural frequency, mode shape and damping for each of the rig set-ups as well as to give an idea of the actual magnitude of movement likely to be achieved during the main tests. In addition, the optimal location for the instrumentation to monitor the rig's movement during the main tests was assessed at this stage.

4.1.1 Modal Testing

4.1.1.1 Frequency

Once the rig structure had been constructed, as described in Section 3.1, each of the three set-ups was subjected to dynamic load (impact) tests. This involved a single participant standing in the centre of the rig and jumping, either once or 20 times, then stopping. The movement of the rig was recorded throughout and the analysis of the modal properties calculated by examining the decay section of the trace once the participant had stopped jumping, i.e. under free vibration. This is the section of the graph shown between the vertical lines in Figure 4.1.

A Fast Fourier Transform (FFT) of this portion of the graph was carried out, using Excel, to determine the natural frequency of the rig. The time period chosen was 2.54 seconds (or 128 readings at the sampling frequency of 50Hz). Although a longer portion of the trace, 256 points, could have been used for the 6.5Hz and, possibly, the 4Hz rig tests, the inherent damping of the 2Hz rig meant that the vibration had totally decayed well before the end of the 256 points resulting in a less accurate FFT when taken over a longer period. The FFT plot for the trace shown in Figure 4.1 is given in Figure 4.2 overleaf.

The graphs shown are for transducer [8] which recorded the vertical displacement of the midpoint of the central precast unit during the impact tests (Figure 4.13). This was chosen as the critical location as the excitation load was applied directly above

this point and it is situated at the position of maximum displacement predicted by the computer model. FFTs for the vertical transducers on the other terrace units and rakers were also calculated to confirm the results from transducer [8].

The FFTs of the initial impact tests provided consistent plots for the 6.5Hz rig indicating the fundamental frequency to be in the region of 6.6Hz. The shape of the 4Hz rig FFT plots was less regular but the fundamental frequency was fairly constant at 3.5Hz. It should be noted that because the FFT used was based on 128 points from transducers sampling at 50Hz the output frequencies are in increments of 0.391Hz ($50\text{Hz} \div 128$) and hence are only a rough guideline of the actual natural frequency of the rig.

Fast Fourier Transforms of the decay trace of the 2Hz rig struggled to produce a dependable result, even when looking at FFT plots for the rakers and sprung supports alongside those for the terrace units. This is probably due to the very high friction damping of free vibrations in this rig set-up – see Section 4.1.1.2. Reducing the period over which the FFT was calculated to 64 points, did little to clarify the natural frequency of the rig.

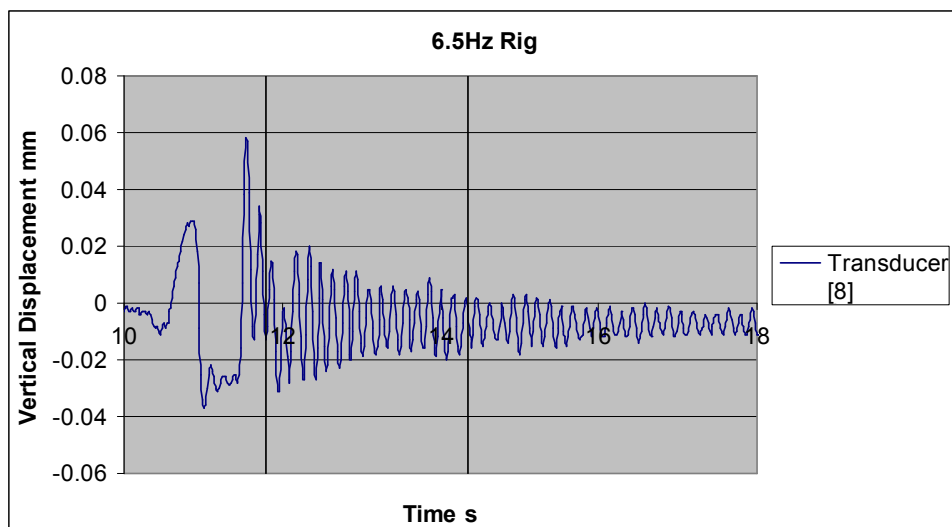


Figure 4.1 Sample Decay Trace for 6.5 Hz Rig Impact Test

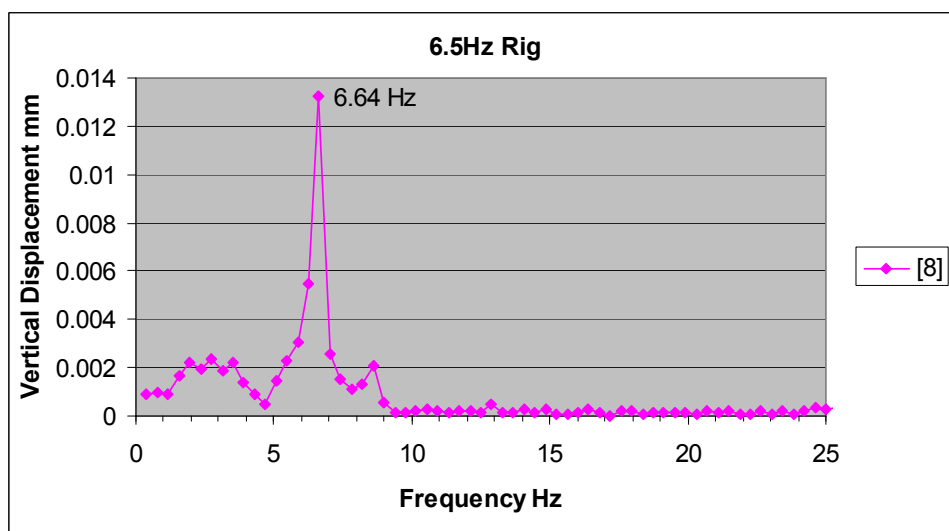


Figure 4.2 Fast Fourier Transform of Decay Trace shown in Figure 4.1

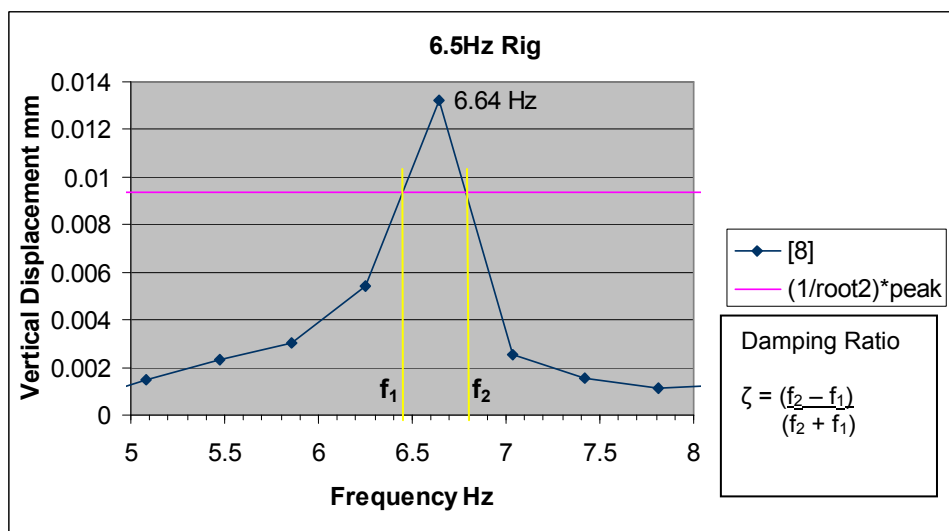


Figure 4.3 Fast Fourier Transform used to calculate Modal Damping

4.1.1.2 Damping

The FFT plots were additionally used to estimate the approximate inherent modal damping of the rig structure. This was done by examining the width of the fundamental peak of the FFT plot at a height equal to the peak value divided by root two, Figure 4.3. The difference between the two frequencies divided by the sum of the two frequencies then gives the percentage damping (Ewins 2000). The values thus calculated are only an approximation as, the resolution of the FFT plot is very coarse (Figure 4.3) and, the damping ratio includes for the person used to create the vibration trace.

The damping ratio, for the 6.5Hz rig, calculated using this method was in the region of 2-2.5%. As described previously the 4Hz and 2Hz rigs were created by adding sprung bases to the 6.5Hz rig. For the rig set ups with springs the friction between the springs and their housings affected the damping calculation using the free vibration of the rig. For the 4Hz rig, which had relatively short springs (76mm), the effect was fairly small and the damping was calculated at around 7%. However with the longer springs (305mm) and support mountings used to create the 2Hz rig the free vibration decay was very rapid due to the high friction in the spring system (even though they were well greased). This made it impossible to calculate the damping using the method used for the other rigs. In spite of this, the transducer recordings, of the preliminary tests, showed that the forced vibration of a single person jumping on the 2Hz rig can overcome the stick-slip nature of friction damping in the spring mountings and the energy dissipation can be approximated by viscous damping. However under free vibration the friction in the 2Hz spring system kicks in relatively quickly and dominates the energy dissipation in a non-linear way making it impossible to calculate an equivalent viscous damping. Because the key portion of the structural response for the main experimental work is the forced vibration under synchronised crowd loading the high friction damping of the free vibration was not deemed to be an issue. The lack of confirmation of the fundamental frequency and damping of the 2Hz rig was also not considered problematic as the initial tests had confirmed the fundamental mode shape and that the vibration amplitudes were greater than those produced by a similar forcing function on the other two rigs.

4.1.2 Instrumentation of the Test Rig

Prior to the main tests it was important to trial the proposed layout of the rig instrumentation and recording facility to ensure;

- sufficient points were monitored to gauge the whole-body movement of the rig and to allow some degree of interpolation should there be any technical issues with the equipment during the main tests
- Location suitability i.e. the instruments could be adequately fixed and would stay in contact with the rig when it moved, especially for the larger movements of the 2Hz rig
- The orientation of the instrumentation, particularly on the inclined rakers, suited the movement path of the rig
- The instruments remained within range during the tests
- The instruments and their fixings could cope with the change over between rig set-ups
- The sample rate was adequate
- There was ample storage for recording an hour of test data and that the procedure was such that this data was backed up so that it would not be lost if the recording computer malfunctioned
- The data logger could cope with the number of instruments attached and would detect faults if, for example, a transducer became unplugged or knocked out of position so it no longer touched the rig.

The first stage of trialling the instrumentation was to see whether the required readings could be made using the equipment available in the university laboratory. The most critical measurements to be taken were those of the three precast units on which the participants would be sat/jumping as it would be these readings that would be related directly to their judgement of perception. To this end, tests were carried out using a series of monitoring positions along each precast unit to determine whether multiple measuring points along the units were required or whether the units were stiff enough only to necessitate a sole midspan monitoring point per unit. This was particularly critical for the accelerometers as only three were readily available. The tests showed minimal variation in the readings along the length of the units and therefore a single central monitoring point on each unit was deemed adequate,

particularly when combined with a measuring point in the midspan of each raking support beam.

While accelerometers were used to record vertical accelerations only, displacement transducers were positioned so that horizontal movements in both sway (side-to-side) and front-to-back directions of the rig were measured in addition to vertical displacements (see Figure 4.13). The displacement transducers available had a range of travel of either 50 or 100mm and so, in order to work within their range, the larger ones were used to monitor the vertical movement and the smaller ones the horizontal movement.

In all, two Vishay Measurements Group System 5000 data loggers were connected to 18 strain-gauge based linear displacement transducers and three Endevco Microtron variable capacitance accelerometers. The maximum sampling rate of 50Hz available on the System 5000 loggers proved, in the initial tests, to be adequate for the purposes required although a higher rate would have given more accurate FFT results. (Aliasing was not considered an issue as the frequency of the vibrations under consideration were below the Nyquist frequency of 25Hz).

The 'Strainsmart' software on the data loggers was found to slow down considerably if too much data was stored locally and so a procedure was set up to download and back up the data files to reduce this issue and to provide a safeguard against losing critical information due to computer glitches. The software coped well with the number of instruments it was recording and provided warnings if any became disconnected. However a more manual approach had to be adopted to check between tests that the transducers had not been knocked out of alignment by the movement of the rig.

As the rig was located on the Structural Engineering laboratory's strong floor and adjacent to the strong wall, the transducers were attached to these fixed elements using steel support stands where required. The accelerometers were glued to the underside of the precast terrace units. Where the initial tests showed the instrumentation to have a tendency to move off its monitoring position on the rig, the layout and fixing was amended appropriately so that the chances of this recurring during the main tests was reduced.

The initial tests also included changeovers between rig support springs. This gave the opportunity to see which of the monitoring equipment could be left insitu during this procedure and which needed to be removed and reattached following the changeover.

4.2 Participant Selection and Testing

4.2.1 Participant Selection

For the testing the ideal participants would cover a wide range of ages, sexes, weights, jumping ability and occupations, in order to sample a representative cross section of the population. However it was difficult to recruit such a spectrum of people for the experiments so the aim was to achieve as much variety as possible. The participants were generally made up of volunteers from the university, including staff, under-graduate and post-graduate students as well as employees from local engineering practices. The resulting group were typically; male, under 30 years old and from an engineering background. This was not deemed to be a major issue as those attending grandstand events are generally young men and although many of the participants had engineering experience none were vibration specialists.

Prior to participating in the experiments the volunteers were asked to complete a health questionnaire confirming their suitability to undertake the tests. This included general enquiries relating to their age, sex, height, weight and occupation as well as specific health queries aimed at identifying individual's suitability to participate in the tests, see Figure 4.4. Additional questions regarding the participants' fitness, coordination and jumping skills, and relevant phobias were also completed (Figure 4.5).

Each volunteer was then allocated a unique reference number so that their position on the rig for each of the tests could be logged.

Stadium Dynamics**REFERENCE****Pre-testing Questionnaire****GENERAL**

Name

Age years

Sex M / F

Occupation

Heightcm orft.....inches

Weight (measured on the day)kg

Contact email

HEALTH**Do you suffer from any of the following conditions**High blood pressure ☐ *Tick as appropriate*Heart problems ☐Haemophilia ☐Epilepsy ☐Ear disorders ☐Asthma ☐Or are you pregnant ☐Or have recently had surgery/fractures ☐Or have any other medical reason preventing you from jumping ☐**How is your current health?**Do you currently have any aches or pains? ☐ DetailsDo you have a cold or flu? ☐Have you a blocked nose/ blocked sinuses? ☐**Figure 4.4 Participant Health Questionnaire**

HEALTH continued

For the following questions mark a line where your answer lies on the scale as shown



How fit do you class your self

**OTHER**

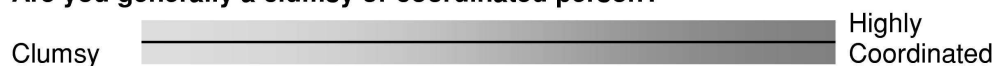
Do you have a musical sense of beat?



Do you have any musical training?



Are you generally a clumsy or coordinated person?



Do you have a natural rhythm/ability to dance



Have you had any dance training?



Do you suffer from

Vertigo – Fear of heights



Claustrophobia – Fear of enclosed spaces



Agoraphobia – Fear of crowds



Figure 4.5 Participant Questionnaire – Additional Questions

4.2.2 Human Perception and Emotion Testing

Two methods were considered for the participants to rate their perception of the magnitude of the vibrations. The first, used a similar scale to that used by Reiher and Meister (1931), with participants asked to categorise the vibration experienced during each test as

1. Imperceptible
2. Barely perceptible
3. Distinctly perceptible
4. Strongly perceptible
5. Large Vibration
6. Extreme Vibration

The alternative method would have been to subject the volunteers to a vibration likely to be similar in size to the mean value during the tests. They would then have been told that this vibration was equal to 50% and then be asked to gauge each subsequent vibration on a scale of 1-100% relative to the initial mean vibration. For this method to work the mean vibration would have needed to be repeated at regular periods throughout the testing and the extremes of 1% and 100% clearly described to the participants. Because of this and the implications of generating the mean vibration the first, simpler, option was adopted.

The system to record the participants' response had to be as foolproof as possible due to the time constraints of redoing the testing. The chosen method was to give each person a pro-forma (Figure 4.6) to be completed directly after each jump test. In this they recorded whether or not they had participated in the jumping and their perception of the magnitude of the vibration during the jumping. This was done using a sliding scale to allow readings between the six categories described above. (See Figure 4.7 for example of filled response sheet.) The volunteers were clearly instructed that the vibration they were to rate was the one experienced while the selected group was jumping, as opposed to that during the free vibration decay.

In addition to asking the participants to gauge the size of the vibration they were asked to rate how they felt about the vibration, i.e. an emotional response. This was done on a more open sliding scale ranging from 'Does not bother me at all' at the lower end to 'Very disturbing' at the other extreme. Finally a section for additional

comments was included for each test which the volunteers were actively encouraged to fill in (Figures 4.6 & 4.7).

NAME SEAT GROUP

TEST			Vibration Perception Rating						Vibration Emotional Rating		Comments
	Jumping J	Seated S	Imperceptible 0	Barely Perceptible 1	Distinctly Perceptible 2	Strongly Perceptible 3	Large Vibration 4	Extreme Vibration 5	Does not bother me at all	Very Disturbing	
1		During Jumping									
2		During Jumping									
3		During Jumping									
4		During Jumping									
5		During Jumping									
6		During Jumping									

Figure 4.6 Participant Response Sheet - December 2006

NAME ..*Bob Smith...* SEAT ...*17*..... GROUP ...*A*.....

TEST			Vibration Perception Rating						Vibration Emotional Rating		Comments
	Jumping J	Seated S	Imperceptible 0	Barely Perceptible 1	Distinctly Perceptible 2	Strongly Perceptible 3	Large Vibration 4	Extreme Vibration 5	Does not bother me at all	Very Disturbing	
1	J	During Jumping									<i>Has it started yet?</i>
2	S	During Jumping									<i>Beginning to get annoying at end</i>
3	S	During Jumping									<i>Jumpers not together!</i>
4		During									

Figure 4.7 Sample Participant Response Sheet - Filled

Following the first set of testing (December 2006) an additional column was added to the response pro-forma for the second suite of tests (October 2007) (Figure 4.8). This was to allow the participants to record whether they thought the vibration they had just experienced was unacceptable and, if not, how long the vibration would

have had to persist for before it became unacceptable. For this section of the form 'unacceptable' was clearly defined as 'a vibration which, if experienced in a real stand, would cause the participant to; leave immediately or complain to the management or think twice about returning to that venue' (Figure 4.9).

4.3 Test Procedure

4.3.1 Vibration Generation

Because human perception of vibrations is situation dependent it was important that the vibrations experienced by the participants during the experiments be as similar as possible to those likely to be experienced in a permanent grandstand. Therefore it was decided that the vibrations should be entirely generated by the participants themselves. This meant that unlike previous human perception tests (Reiher and Meister 1931, Kahn and Parmalee 1971, Chen and Robertson 1972, Wiss and Parmalee 1974 and Parsons and Griffin 1988, see Section 2.4) all those participating in the experiment could see the *cause* of the rig movement.

To vary the magnitude of the vibrations several methods were employed;

1. Modifying the natural frequency of the stand
2. Changing the jump frequency of the crowd
3. Varying the group of people jumping

As described previously, three rig set-ups, each with a different fundamental natural frequency, were chosen to provide a wide spectrum of movements when excited by people jumping on the rig (<1mm to >50mm peak to peak displacement). These rig frequencies were in the region of 2Hz, 4Hz and 6.5Hz respectively and by varying the frequency at which those in the crowd jumped the aim was to achieve resonant and non-resonant responses of the stand. Because of the range of the rig frequencies, resonant responses of the stand due to the 1st through to the 6th harmonic of the jump frequency were possible, thus allowing a wide range of movements.

The final option for modifying the movement of the rig was to have different groups of people jumping. Initially the plan was to have varying sizes of groups jumping but, with the flexibility provided by options 1 and 2, above, and the time constraints on the overall test duration this was found to be unnecessary. Instead the group jumping was rotated so, although there was always the same number of people jumping, they were positioned differently on the rig and had different levels of coordination. This solution also achieved a good balance between the responses of those seated and

those jumping and allowed a comparison of how an individual's perception changes between being seated and when jumping.

4.3.2 Jump Frequency

As far as possible the same jump frequencies were used for each of the three rig set-ups. These ranged from 1.1Hz to 2.4Hz based on previous research (Littler 2003) indicating that groups of people find it difficult to jump together at frequencies either less than 1Hz or greater than 2.8Hz. The jump frequencies were selected to explore resonant responses due to the first four harmonic components of the jumping force. Because the reduction in the natural frequency of the rig due to the mass of the non-jumping participants was unknown the 'resonant' jump frequencies were based on multiples of the empty rig frequencies measured as part of the initial modal testing (Section 4.1.1), see Table 4.1. The 'non-resonant' jump frequencies were kept relatively close to the 'resonant' ones to give a better chance of achieving a true resonant response once the mass of the crowd was factored into the equation.

Table 4.1 Test Jump Frequencies

	Rig Frequency		
Jumping Frequency (Hz)	2Hz (assumed)*	4Hz (assumed)*	6.5Hz (assumed)*
1.1	✓ 2 nd ?	✓ 3 rd	✓ 6 th
1.7	x	✓ 2 nd	✓ 4 th
1.9	✓ 1 st ?	x	x
2.2	✓ 1 st ?	x	✓ 3 rd
2.4	x	x	x
✓ = Resonance due to given harmonic of dynamic crowd load based on actual measured values* of the empty rig natural fundamental vertical frequencies x = No Resonance * See Chapter 4.1.1 for modal testing of rig set-ups			

4.3.3 Jump Groups

The volunteers were split into jumping groups on arrival and each participant was allocated a seat, on a random basis, which they retained for the duration of the tests. Overall the 'crowd' was located centrally on the rig and the jump groups positioned to give an even spread across the rig. Typical layouts based on 24 participants are shown in Figure 4.10.

	x	x	x	A	x	A	x	x	
	A	x	x	A	x	x	x	A	
	x	A	x	x	x	x	A	x	

70% Seated (x), 30% Jumping (A)

	x	B	x	x	x	x	x	B	
	x	x	B	x	x	B	x	x	
	x	x	x	B	B	B	x	x	

70% Seated (x), 30% Jumping (B)

Figure 4.10 Typical Stand Layouts showing Location of Jump Groups

4.3.4 Combinations

It was important to introduce a degree of randomness to the testing in order that the participants were not able to predict the magnitude of the next vibration. However because it took roughly 30 minutes to change over the springs it was necessary to carry out all the tests on one rig set-up before moving on to the next. Therefore in order to vary the size of the vibrations the jump frequencies and the jump groups were alternated in a predetermined random order. This also ensured that each group jumped each frequency at least once.

In addition to the continuous jump tests, single jump tests, simulating the crowd response to a goal event, were scattered throughout the test schedule (Table 4.2).

Table 4.2 Sample Test Schedule

Test	Freq	Jump Group for		
		2 Groups	3 Groups	4 Groups
1	1.7	A	A	A
2	1.9	B	B	B
3	2.4	A	C	C
4	Single J	B	C	D
5	1.2	A	A	A
6	2.2	A	C	C
7	1.2	B	B	B
8	Single J	A	A	C
9	1.7	B	C	D
10	2.4	B	B	B
11	1.9	A	A	A
12	2.2	B	B	D
13	1.2	A	C	C
14	2.2	B	A	B
15	2.4	A	A	D
16	1.7	B	B	B
17	Single J	B	B	A
18	1.9	A	C	C

4.3.5 Test Procedure

In order to coordinate the crowd movement an electronic metronome, set at the required jumping frequency, was played at high volume through loudspeakers to allow the participants to hear the jump prompt over the other noises of the test.

At the start of each test the allocated jump group was asked to stand while everyone else remained seated and the instrumentation was zeroed. The jump frequency was then played through the speakers for several seconds before commencing the test. The jumpers were counted in (3,2,1, go) and then aimed to jump together (in a natural vertical manner) in time with the metronome (Figure 4.11). On completion of 25 jumps (20 for the October 2007 tests) the jump group were instructed to stop and, once they had all done so and the residual vibration decayed they were asked to sit

down. At this point everyone filled in their perception/emotion questionnaire for that test rating the vibration that had been experienced during the jumping phase of the test.



Figure 4.11 Testing Underway

The duration of the dynamic crowd loading had to be long enough for the vibration to build up to a maximum level and remain there for a sufficient length of time for the participants to gauge its magnitude. But as the vibrations were to be induced by groups of the volunteers jumping, the duration had to be set so as not to tire out the participants before all the required tests had been completed. Two options were therefore available, either a time limit of, say, 15-20 seconds or secondly a specified number of jumps. The time limit option was rejected primarily because of the difficulty in coordinating the end of the test and the large variation in the number of jumps between the highest and lowest jump frequencies. The specified number of jumps gave the jump group a good idea of when they had to stop so when the signal was given they generally terminated together resulting in a smooth decay of the vibration. The concern was that if the jumpers did not stop together the resulting vibration and disarray would influence the seated participants' view of the test vibration.

For the single jump goal event tests the participants all started seated, the instrumentation zeroed and then on a count of 3 the selected jump group leapt to their feet simultaneously. Again the participants filled in their perception/emotion ratings following the tests.

4.3.6 December 2006 Tests

The first set of main tests was carried out in one afternoon in December 2006. All three rig setups were tested sequentially, in ascending frequency order, with the same group of 18-20 participants. Two people had other commitments which meant that they missed the final rig set up (6.5Hz). The afternoon was split into three sessions of testing, each lasting approximately 30 to 60min with a 30 minute break between sessions to allow the springs to be changed over.

For the December 2006 tests the participants were divided into 3 groups, A, B and C. Groups A and B jumped for their allocated tests while group C were constantly seated. Groups A and B consisted of 6 people for the 2Hz and 4Hz rigs and 5 people for 6.5Hz rig. For the 2Hz rig both of the jump groups performed the 5 jump frequencies (Table 4.1) plus the single jump test two times i.e. a total of 24 tests. For the 4Hz rig set-up 18 tests were carried out, three of each frequency, shared between jump groups A and B. For the final set of tests, on the 6.5Hz rig, due to time constraints each of the jump frequencies was performed only once by each jump group, giving a total of 12 tests.

4.3.7 October 2007 Tests

A series of follow-on tests were completed in October 2007. These were carried out in four lunchtime sessions spread over a two week period. By this stage some preliminary analysis had been done on the data obtained from the December 2006 tests and so the follow-on tests were tailored to expand on the upper end of the vibration spectrum where perceptions start to change and unacceptability becomes a possible issue, Figure 4.12.

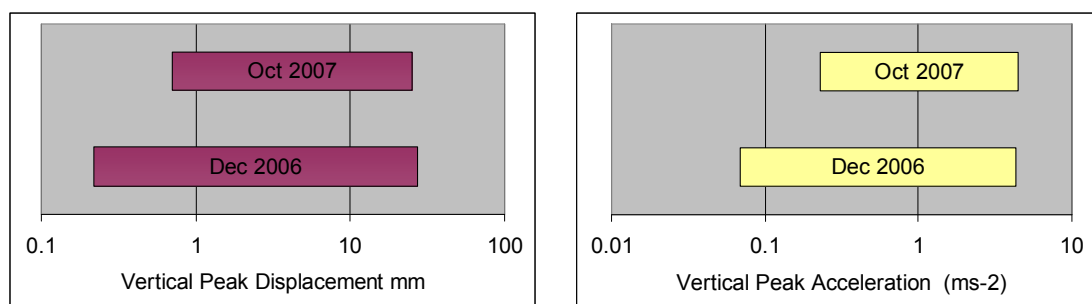


Figure 4.12 Range of Vibration Magnitude

In October 2007 the first two sets of tests were performed using the 2Hz rig with a much smaller group of 8 participants. The volunteers were divided into two groups of 4 and each group carried out half of the 18 tests (3 of each jump frequency plus the single jump tests). A larger group, of 15 participants, were available for the third set of tests and so the 4Hz rig set-up was selected. This group were split into four, two jump groups of 4 and one jump group of 5. The remaining two participants, who were unable to jump for medical reasons, formed the final group. The same 18 tests were carried out as before with the three jump groups performing each of the jump frequencies once. For the final set of experiments 21 people volunteered and were tested on the 2Hz rig. As this was the largest crowd used a maximum jump group of 5 individuals was selected to avoid 'bottoming out' the springs. Thus, the participants were divided into four jump groups of 5 people with a single participant seated for the duration of the tests. Again 18 tests, 3 of each frequency, were performed, shared amongst the jump groups.

4.3.8 Monitoring of Rig Movements

Displacement and acceleration time histories were recorded during the tests using displacement transducers and accelerometers attached to the underside of the precast seating units as described in Section 4.1.2. Monitoring commenced several seconds before the jumping started and continued for a short period afterwards to allow the build up and decay of each vibration to be recorded. This was done to ensure the entire duration of the forced vibration was captured and to enable post experimental analysis to be carried out on the free vibration decay if necessary.

The vertical movement of the centre of each of the three precast terrace units was recorded on transducers [7], [8] & [10] and on accelerometers [16], [17] & [18] respectively (Figure 4.13). The readings from these six instruments together with the

horizontal displacement readings from front-to-back transducer [9] and sway transducer [21] were linked directly to the participants' perception ratings during the post experimental analysis (Section 4.4).

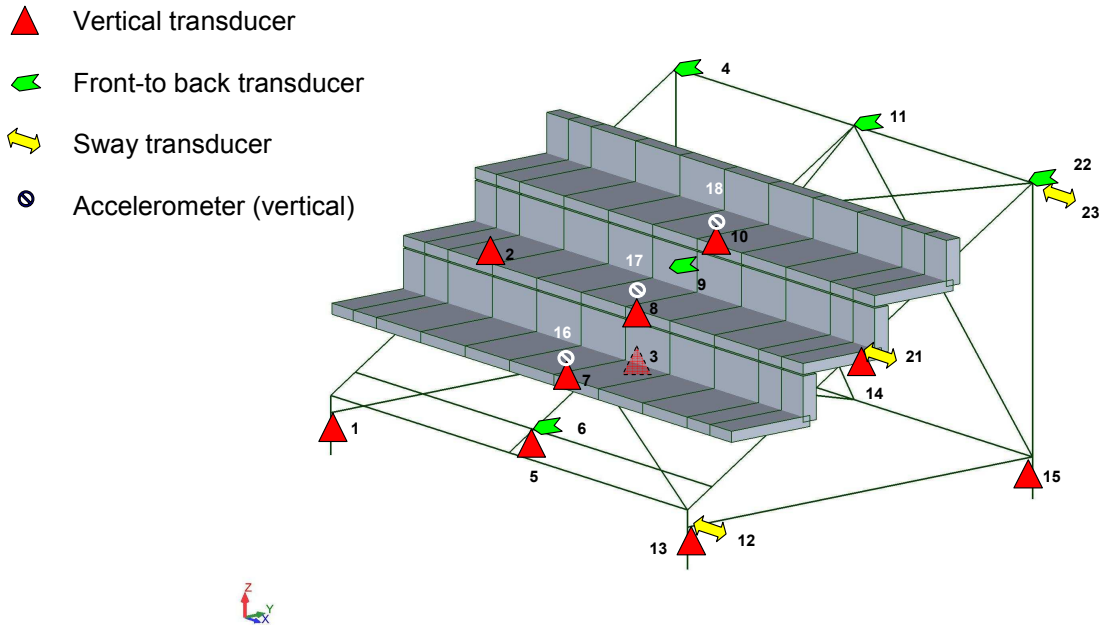


Figure 4.13 Location of Monitoring Equipment

To allow a better understanding of the overall movement of the rig during the tests vertical transducers [1], [3], [13] & [15] monitored the movement of the springs for the 2Hz and 4Hz rigs while horizontal transducers [4], [6], [9], [11] & [22] measured the front-to-back motion. Any side-to-side sway movement was picked up on transducers [12], [21] & [23]. The vertical and horizontal movement of the longitudinal steel beam supporting the leading edge of the lowest precast unit was recorded using transducers [5] and [6] respectively. Finally the displacement of the inclined steel rakers supporting the precast terrace units was captured by transducers [2] & [14] which were positioned perpendicular to the steel beams allowing both the vertical and front-to-back movement to be calculated. Photographs of the transducers and accelerometers, as installed on the test rig, are included in Appendix A.

In addition to monitoring the behaviour of the rig the experiments were also videoed to allow play back to confirm the type of crowd movement, coordination of jumping and location of seated participants.

4.4 Data Analysis

4.4.1 Instrumentation Readings

For each test, graphs of the measured displacements and accelerations were plotted for the key portion of each test, starting 1 second prior to the jumping and ending 1s after the jumping. For the single jump tests the critical period of the test was taken from 1 second before to 4 seconds after the jump commenced.

To allow side-by-side assessment, the graphs of the instruments' readings were grouped as follows;

- Vertical displacement
 - Rakers – Transducers [2] and [14], plus [8] for comparison
 - Precast Terrace Units – Transducers [5], [7], [8] and [10]
 - Supports – Transducers [1], [3], [13] and [15]
- Horizontal Displacement
 - Front-to-back – Transducers [4], [6], [9], [11] and [22]
 - Sway – Transducers [12], [21] and [23]
- Vertical Acceleration
 - Precast Terrace Units – Accelerometers [16], [17] and [18]
- (see Figure 4.13 for location of instrumentation)

These overlaid graphs were used as a means of checking the output, in particular, looking for any permanent offset (instrument not returning to zero following the test) and ensuring realistic readings i.e. comparable with adjacent instruments. See Figure 4.14 for examples.

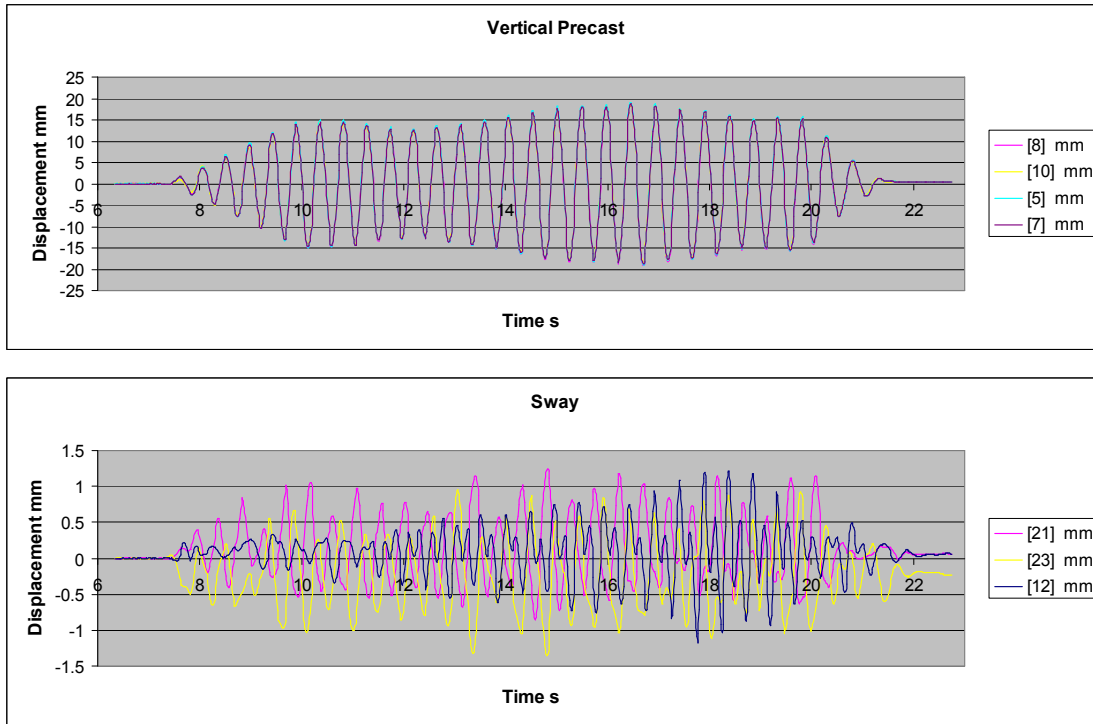


Figure 4.14 Samples of Instrumentation Graphs (Test 6214)

An Excel spreadsheet was set up to determine the maximum and minimum values recorded for each instrument during the key section of each test. The calculated offset (taken as the average of the initial reading and the final reading) was then subtracted from these values to obtain the rectified maximum and minimum peak values for each test. In addition the rectified root mean square (RMS) value and the average peak value (Av Peak) were calculated for the period of activity (i.e. excluding the 1s before and after) , where

$$Y_{RMS} = \sqrt{\frac{\sum_{i=1}^n y_i^2}{n}} \quad \text{where } y_i = \text{every recorded value} \quad \text{eq 4.1}$$

and n = number of recorded values

$$Y_{Average_peak} = \sqrt{\frac{\sum_{j=1}^n y_j^2}{p}} \quad \text{where } y_j = \text{every peak values both +ve and -ve} \quad \text{eq 4.2}$$

and p = number of peak values

The test duration ranged from 10 to 20 seconds, over which the intensity of the vibration varied dependant on the coordination of the jumpers (Figure 14.4). Therefore it was deemed more appropriate to calculate the RMS values and average

values over the entire active duration of each test rather than select a 10 second period as suggested by the IStructE (2008).

Vibration dose values (VDVs) for all the tests were estimated using; the formula contained in BS 6472:1992 Appendix B (eq 4.3 below), the RMS accelerations from each of the three accelerometers and the duration of each test. Estimated VDVs were used as it was felt that generally these are easier, for engineers using the design procedure, to calculate particularly if the overall RMS acceleration is available but not the entire record of the vibration. Cumulative VDVs were also calculated for each test by adding the individual eVDV values for each preceding test, in that session, plus the test just completed (eq 4.4).

$$eVDV_i = 1.4 \times a_{RMS} \times t^{0.25} \quad \text{where } eVDV = \text{Estimated Vibration Dose Value} \quad \text{eq 4.3}$$

and a_{RMS} = RMS acceleration for test in ms^{-2}
and t = duration of the test in seconds
and i = test number

$$CumVDV_i = \sum_{j=0}^i eVDV_j \quad \text{where } CumVDV = \text{Cumulative Vibration Dose Value} \quad \text{eq 4.4}$$

and i = test number

Finally the frequency of the vertical vibration response of the rig was determined using the Fast Fourier Transform (FFT) function in Excel for both displacement transducer [8] and accelerometer [17] located mid-span on the central precast terrace unit. For the continuous jump tests the FFT was based on 512 data points starting 1 second after the jumping. For the single jump tests 128 data points were used in the FFT beginning at the start of the jump.

4.4.2 Human Results

Spreadsheets were set up to record the results of the human perception questionnaires. For each participant the sliding scales for perception and emotional response were converted to data readings by measuring the distance of the response along the sliding scale and converting it to a percentage of the total length. Test by test these values were linked to the accelerometer and displacement transducer readings for the row on which the specific person was located. As one of the key aims of the research project is to determine what measure of movement is

most appropriate for gauging human perception of structural vibrations in grandstand situations the various determinant values described in 4.4.1 were included i.e. minimum peak, maximum peak, average peak and RMS values for vertical displacement and acceleration as well as sway and front-to back horizontal displacement. Vibration dose values to BS6472:1992 (eq 4.3 above) and vibration frequency were also used. The critical instrument readings used for these values were displacement transducers [7], [8] & [10] and accelerometers [16], [17] & [18] for the vertical movement of the front, central and rear precast units respectively. For the horizontal displacements the transducers on the central precast unit were used, transducer [9] for the front-to-back displacement values and transducer [21] for the sway displacement values, Figure 4.15.

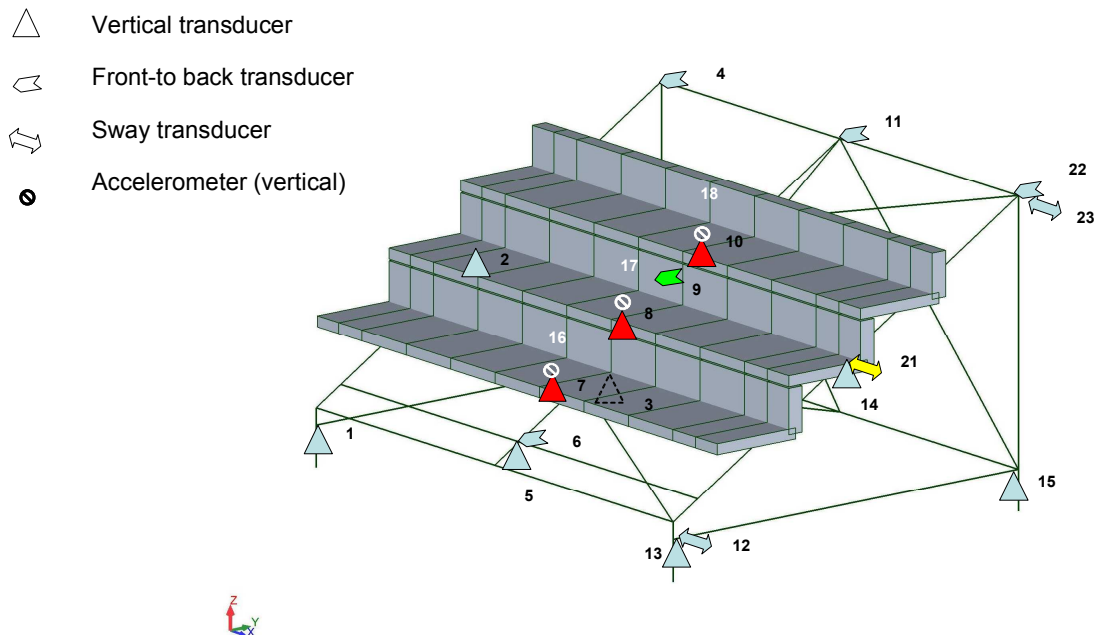


Figure 4.15 Location of Key Monitoring Equipment Used to Determine Magnitude of Vibrations Experienced by Participants

This data together with the individual's seat number, the test number, the rig set-up, the jump frequency, whether the participant was seated or jumping, their comments and unacceptability score was added to the spreadsheet.

5 Results

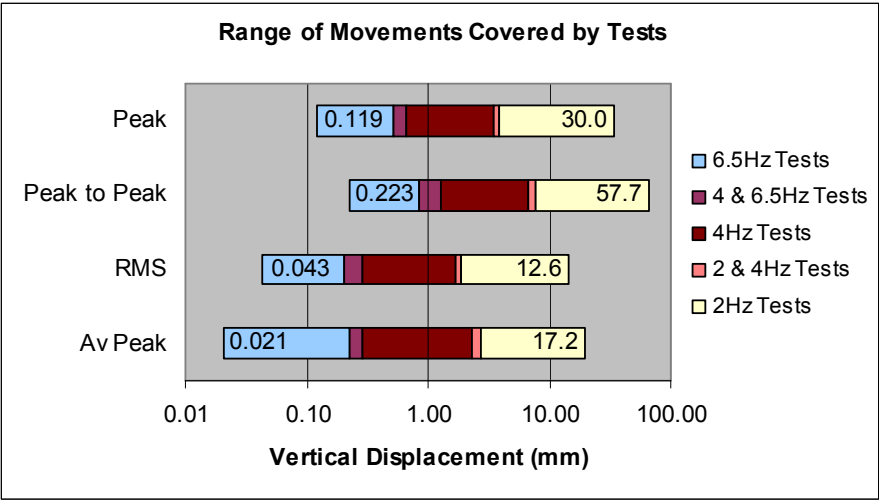
The results from the experimental work fall into two distinct categories; those covering the movement of the test rig and those from the human response. A summary of the movements experienced during the testing is covered in Section 5.1, below, to give an idea of the range of the vibrations that were produced experimentally and how these compare to previous research. The human results form the cornerstone of this research project and Section 5.2 explains how the collected data was analysed and manipulated to produce models for predicting human response to crowd induced grandstand vibrations.

5.1 Range of Movements

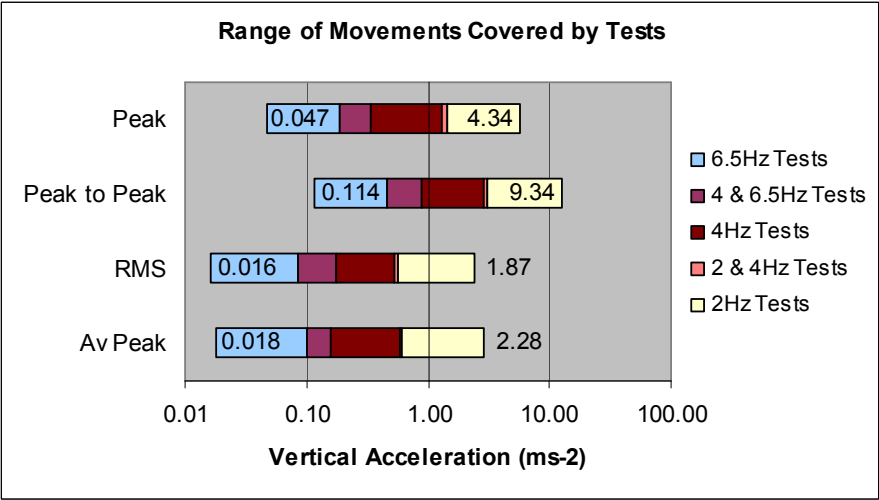
The peak vertical displacements during the tests ranged from a minimum of 0.119mm on the 6.5Hz rig to a maximum of 30mm on the 2Hz rig (Figure 5.1). The corresponding range of the recorded peak vertical accelerations was 0.05ms^{-2} to 4.34ms^{-2} ($0.005g$ to $0.44g$) encompassing vibrations ten times smaller than Kasperski's 1996 disturbing comfort threshold ($0.05g$) and some up to 25% greater than his panic limit ($0.35g$). Because of the way the vibrations built up and decayed during each test the calculated RMS value for each vibration was approximately 0.42 times the recorded maximum peak value. This compares to $\frac{1}{\sqrt{2}}$ (0.707) for a constant magnitude sine wave. This meant that although Kasperski's panic limit was reached during the tests the IStructE's 2008 'Dynamic Performance Requirements for Permanent Grandstands subject to Crowd Action' limit for high energy concerts, $0.2g$ RMS acceleration, was not attained even in the most energetic 2Hz rig tests. (Refer to Chapter 6 for discussion regarding IStructE's 2008 specification of RMS acceleration limits.)

The peak values of vertical displacement and acceleration obtained during the tests were similar to those predicted by the 'Realistic' forcing function time history analysis model in Chapter 3 (Section 3.2.3.2). The notable difference was in the 4Hz rig results where the recorded values were greater than those predicted (Figure 5.2). This could be due to the actual rig potentially having a lower fundamental natural frequency ($\sim 3.5\text{Hz}$ – see Chapter 4) than the 4Hz computational model. Also the

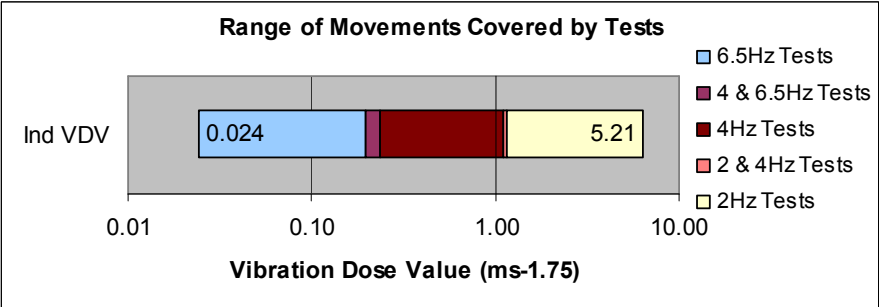
maximum values predicted by the 'Realistic' 2Hz model were slightly larger than those recorded (Figure 5.2). This is likely to be due to the participants reducing the force of their jumping when the vibrations very large because of an element of fear and difficulty in jumping on a very mobile structure.



Displacement



Acceleration



Vibration Dose Value

Figure 5.1 Range of Movements experienced during Tests

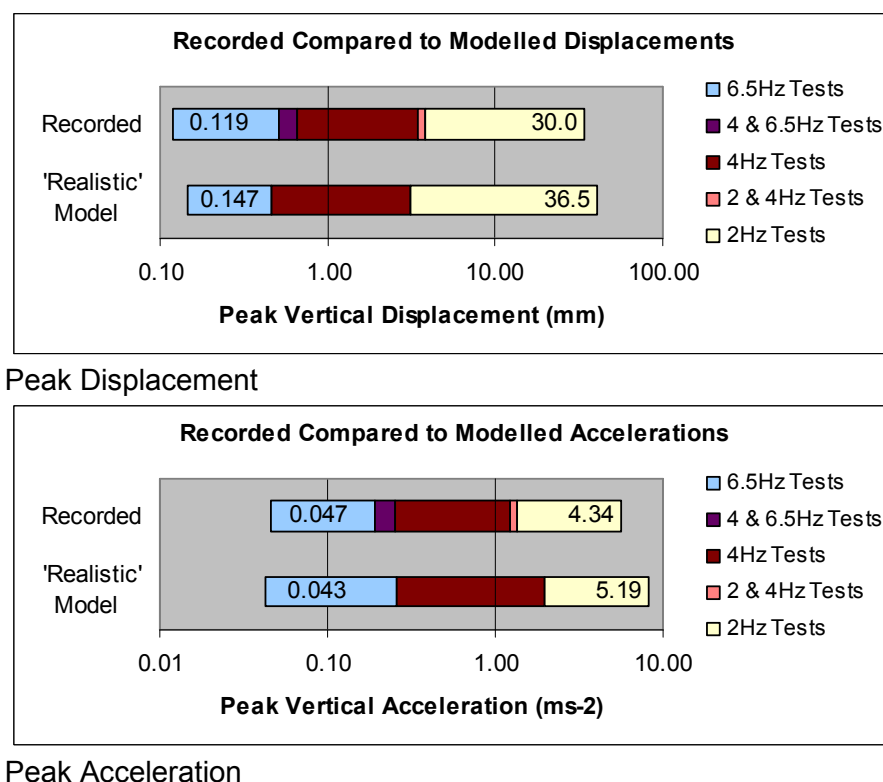
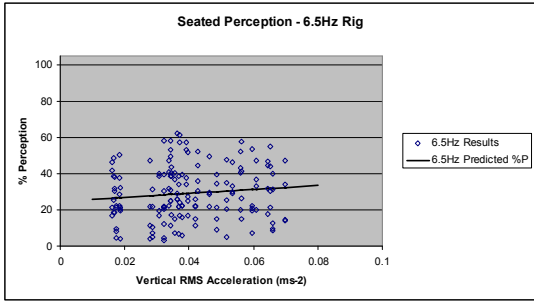


Figure 5.2 Peak Movements Recorded during the Tests Compared to those Predicted by the 'Realistic' THA Computer Model

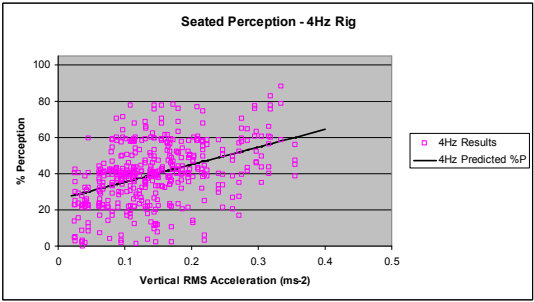
5.2 Human Response

The aim of this research project is to investigate how humans perceive vibrations in a grandstand situation with a view to determining a method to forecast how spectators might respond to similar vibrations in a real grandstand. Therefore the first step is to view the collected data graphically in order to obtain an overview of potential relationships. To do this the participants' results are split, test by test, into 2 groups depending on whether they had been jumping or seated during that test. Then each individual's percentage perception or emotion rating was plotted against the experienced vertical displacement or acceleration for each test. The graphs generated are shown below in Figures 5.3 to 5.6. A linear trendline has been fitted to each of the sets of data. The linear relationship intimated is not necessarily the most accurate form of trendline (i.e. a logarithmic curve may be better) but it gives an initial visual indication of the trend of the data. In addition to the results for each rig being plotted separately, graphs showing all three rigs are included to allow for comparison. To enable the spread of the data to be visible a logarithmic scale was used for these combined graphs while linear scales were used for the individual rig plots.

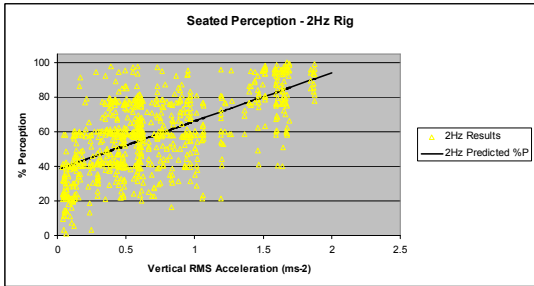
SEATED



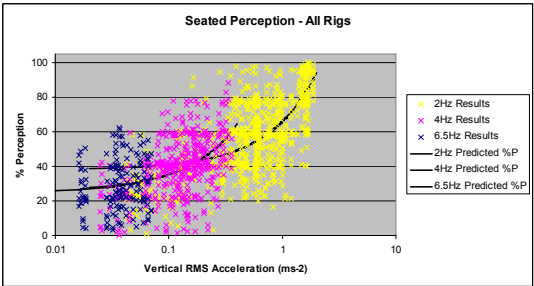
6.5Hz Tests



4Hz Tests



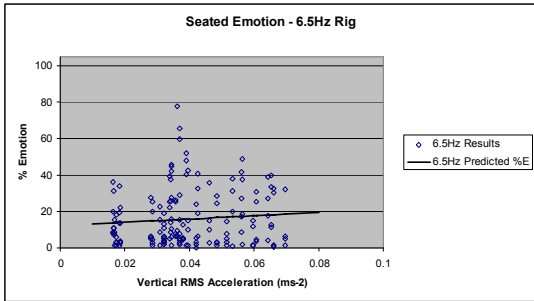
2Hz Tests



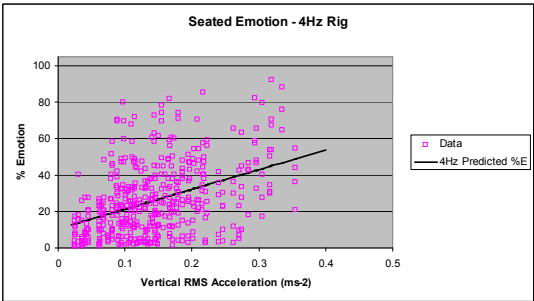
All Tests- Note log scale to x-axis but with same linear trendlines as individual tests

Figure 5.3 Seated Perception Results

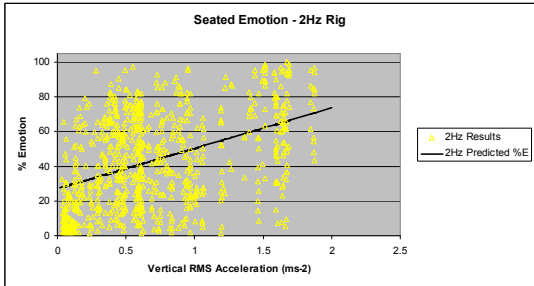
SEATED



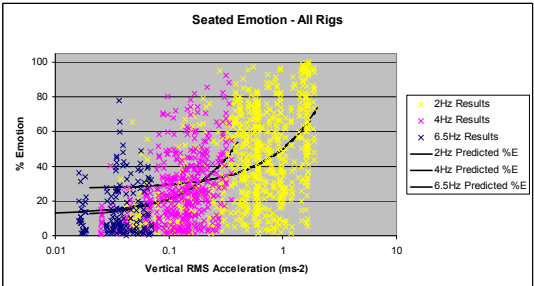
6.5Hz Tests



4Hz Tests



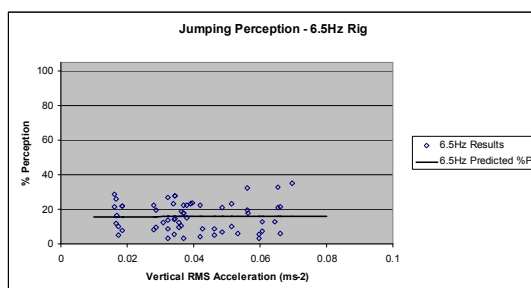
2Hz Tests



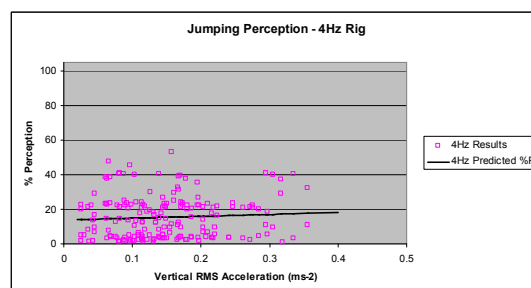
All Tests- Note log scale to x-axis but with same linear trendlines as individual tests

Figure 5.4 Seated Emotion Results

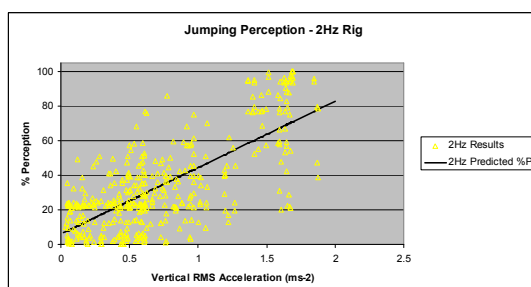
JUMPING



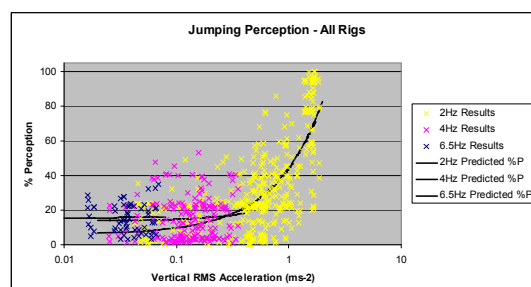
6.5Hz Tests



4Hz Tests



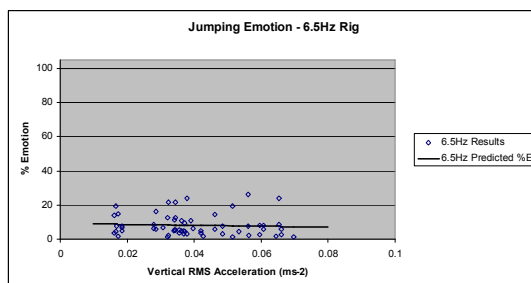
2Hz Tests



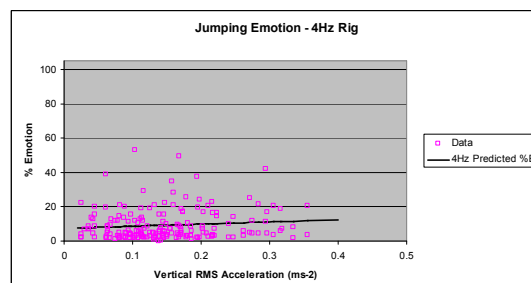
All Tests- Note log scale to x-axis but with same linear trendlines as individual tests

Figure 5.5 Jumping Perception Results

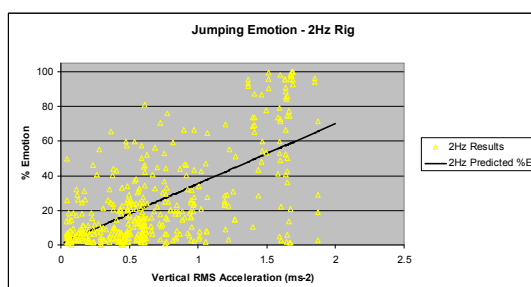
JUMPING



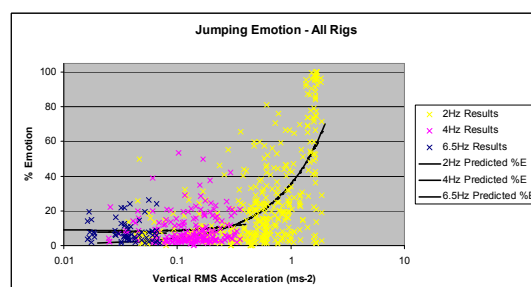
6.5Hz Tests



4Hz Tests



2Hz Tests



All Tests- Note log scale to x-axis but with same linear trendlines as individual tests

Figure 5.6 Jumping Emotion Results

5.2.1 Initial Observations – Perception

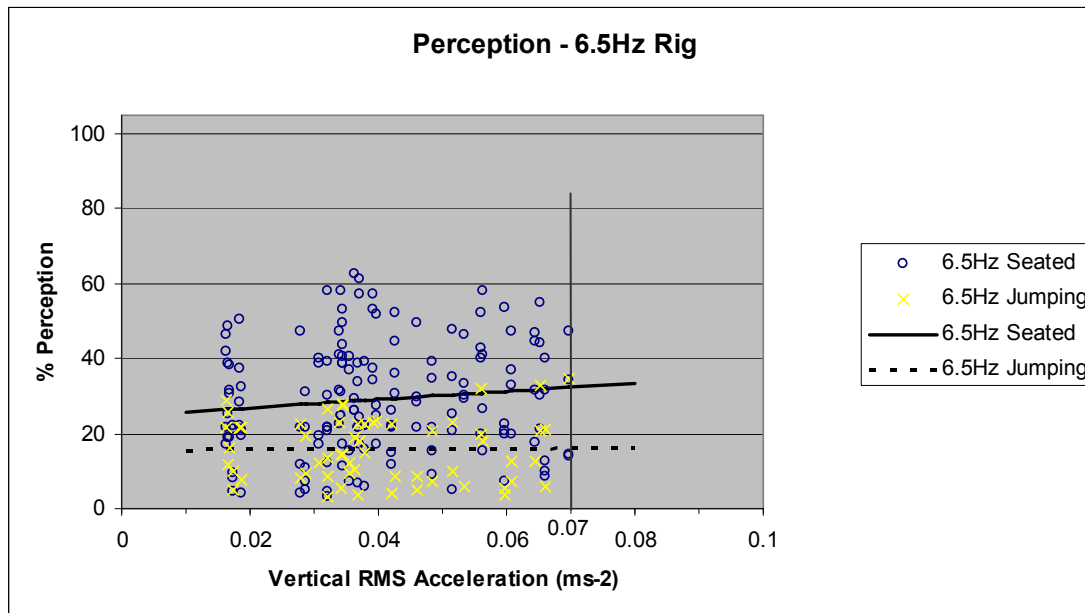


Figure 5.7 Perception Results for 6.5Hz Rig

When the vibrations are very small, below 0.07ms⁻² vertical RMS acceleration (0.25mm vertical RMS displacement), all the participants struggle to judge the relative magnitude of the movements as can be seen by the near horizontal slopes of both jumping and seated linear trendlines from the 6.5Hz rig tests (Figure 5.7). For the 6.5Hz tests the range of the participants' responses for those seated is almost double that for those jumping.

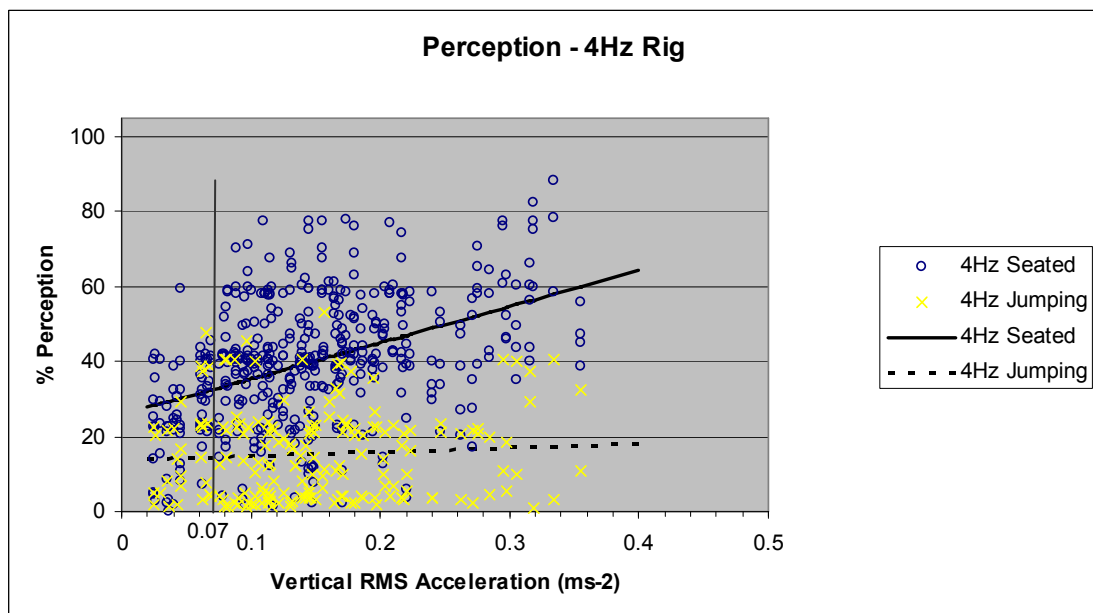


Figure 5.8 Perception Results for 4Hz Rig

As the vibrations increase above approximately 0.07ms^{-2} vertical RMS acceleration (Figure 5.8), those that are seated start to be able to determine the relative size of the movement. Those that are jumping still struggle to perceive the difference in magnitude of the vibrations until they increase still further. This is shown by the almost horizontal trendline for those jumping compared to the notable slope of the trendline for those that are seated in the 4Hz rig graphs (Figure 5.8). As for the 6.5Hz rig the range of responses is notably less for those jumping.

Once the vibrations become significant, i.e. greater than approximately 0.3ms^{-2} RMS acceleration ($\sim 1.5\text{mm}$ vertical RMS displacement), all the participants including those jumping can discern the difference in magnitude (see 2Hz rig graph in Figure 5.9). Additionally as the vibration size increases the agreement in the responses of those seated improves as the top end of the scale is reached. It is likely that a similar trend would be shown for those jumping if the magnitude of the vibrations had been increased still further during the tests. Generally for the 2Hz tests the spread of the results is still slightly less for those jumping than those seated.

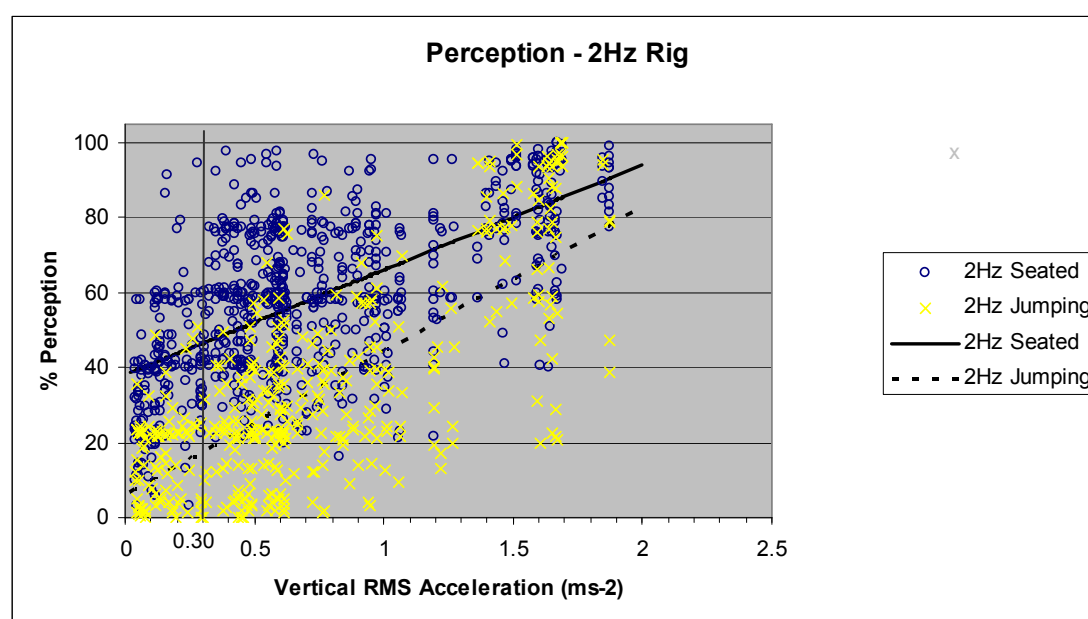


Figure 5.9 Perception Results for 2Hz Rig

The graphs also highlight the differences in the reaction to the vibration between those actively creating it (the jumpers) and those purely subjected to it (those seated) (Figures 5.7 to 5.9). In the vast majority of the tests, the average perception rating

for the group that were jumping is lower than the corresponding rating for those that were seated.

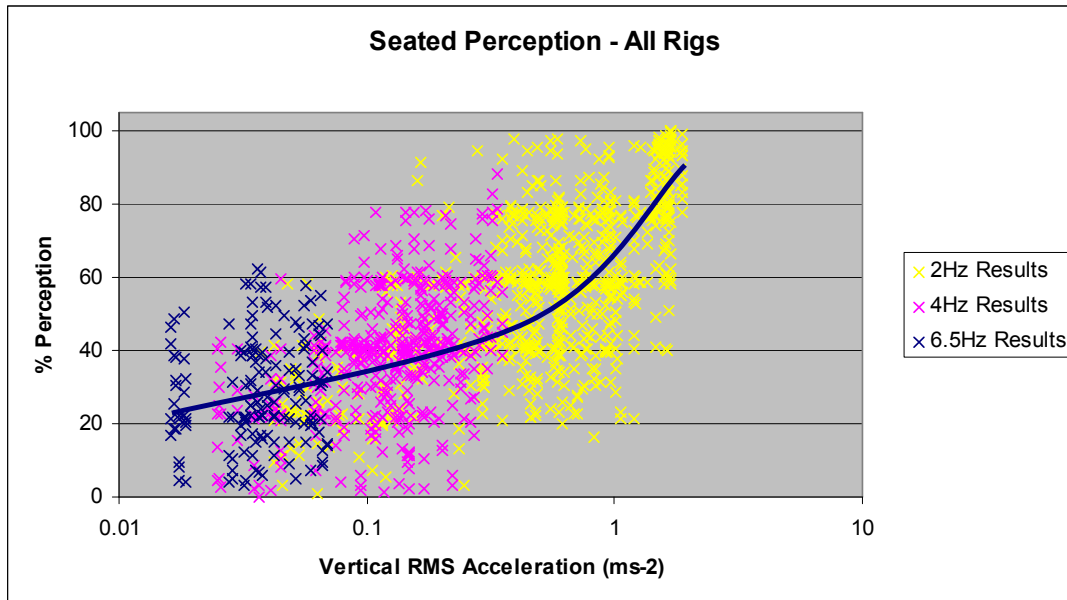


Figure 5.10a All Perception Results for Seated Participants

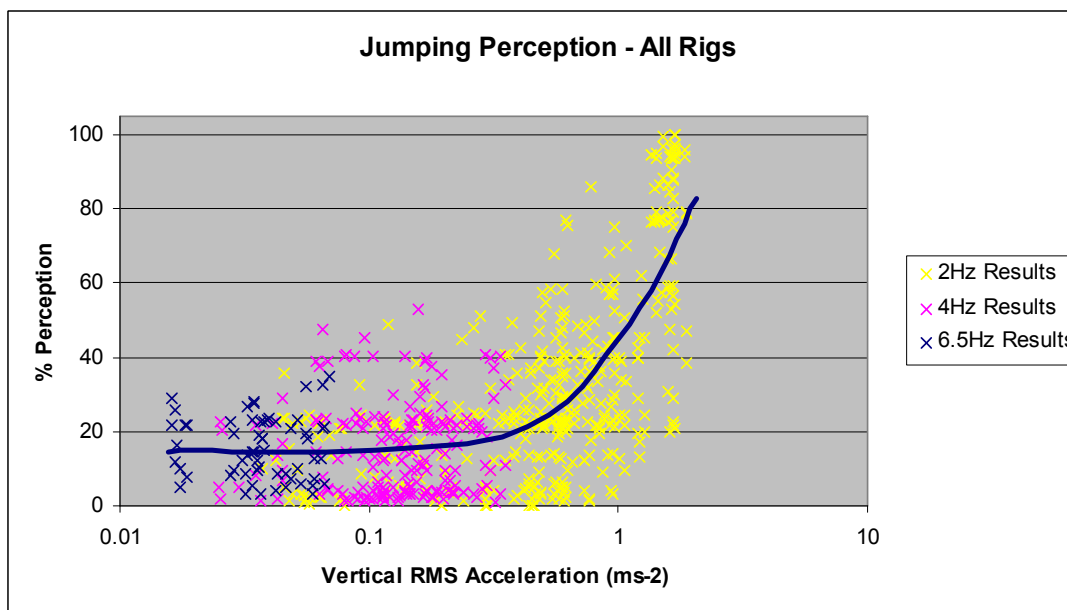


Figure 5.10b All Perception Results for Jumping Participants

From looking at the graphs, where the results from all the rigs have been combined, the overall trend of the data can be approximated as shown in Figures 5.10a and 5.10b. This shows that those seated are actually very sensitive to small vibrations, allocating the same change in rating to small changes in small vibrations (25%

increase in average % Perception rating from 0.02mm to 0.3mm) as to larger changes in larger vibrations (similar 25% increase in average % Perception rating from 0.3mm to 1.3mm). This is shown by the near linear portion of the lower two-thirds of the graph in Figure 5.10a, plotted on a logarithmic scale.

The corresponding graph for those jumping confirms the trend identified in Figures 5.7 and 5.8 that until a vibration reaches a certain magnitude the jumpers cannot accurately gauge its magnitude, indicated by the horizontal portion of the graph in Figure 5.10b. Above this magnitude the jumpers are as able to discern the relative magnitude of the vibration as those seated. Interestingly this key vibration magnitude where the slopes of the trendlines change is roughly the same for those jumping as for those seated.

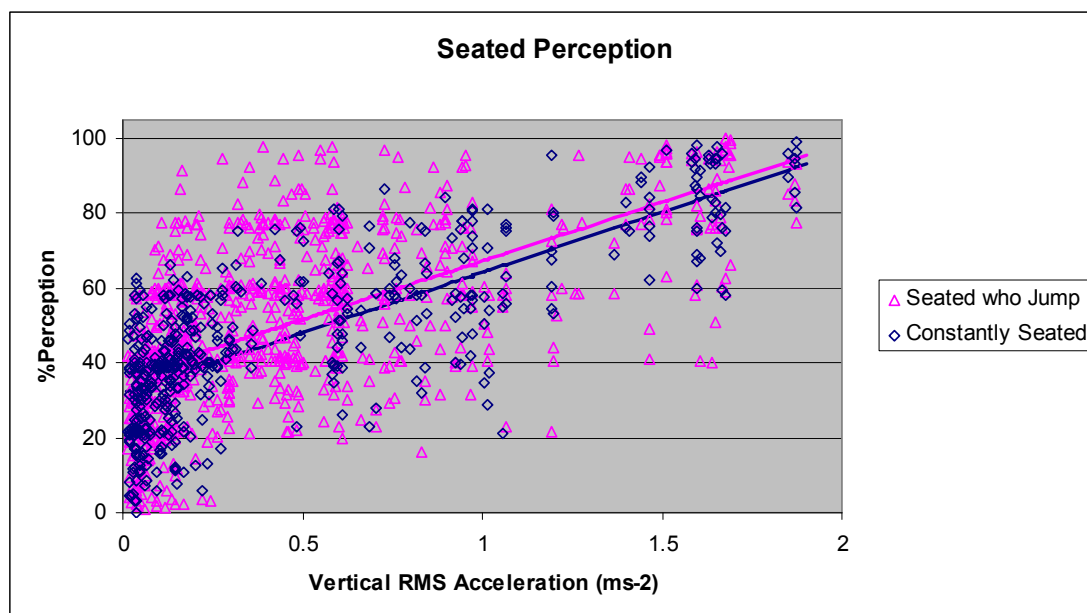


Figure 5.11 Perception Results for Seated Participants

The difference in seated perception readings between those participants that were constantly seated and those that were alternating between sitting and jumping were compared. From Figure 5.11 it can be seen that the scatter of the ratings for those constantly seated was less than those who both sat and jumped. The trendlines for both groups are very similar and although those constantly seated generally rate their perception slightly lower than those jumping and seated, the difference is very small (in the order of 3% Perception). This indicates that a single seated category is likely to be sufficient to cover the response of all seated participants.

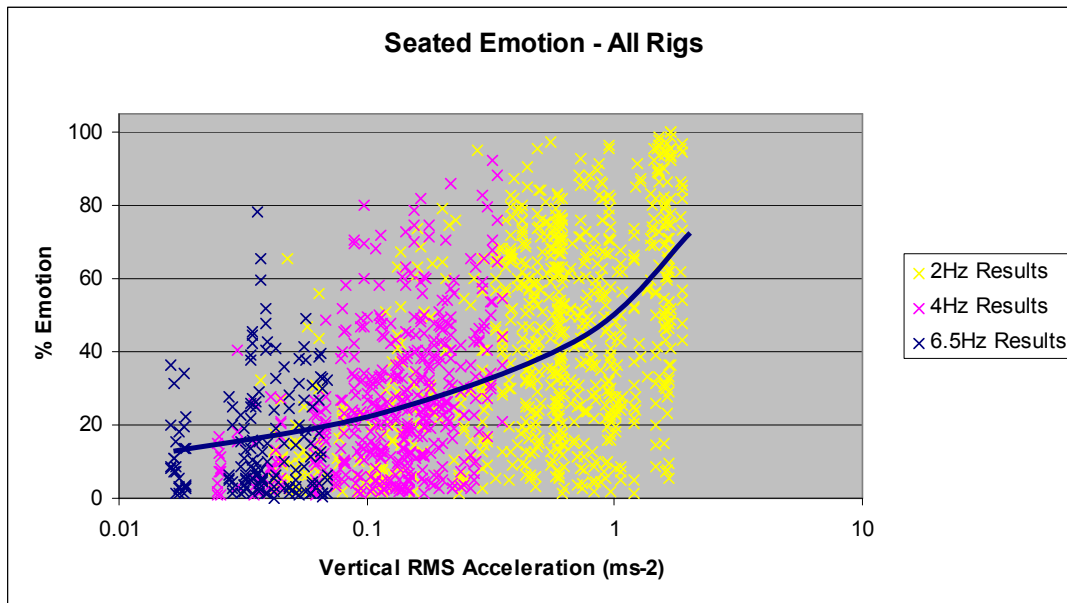


Figure 5.12a All Emotion Results for Seated Participants

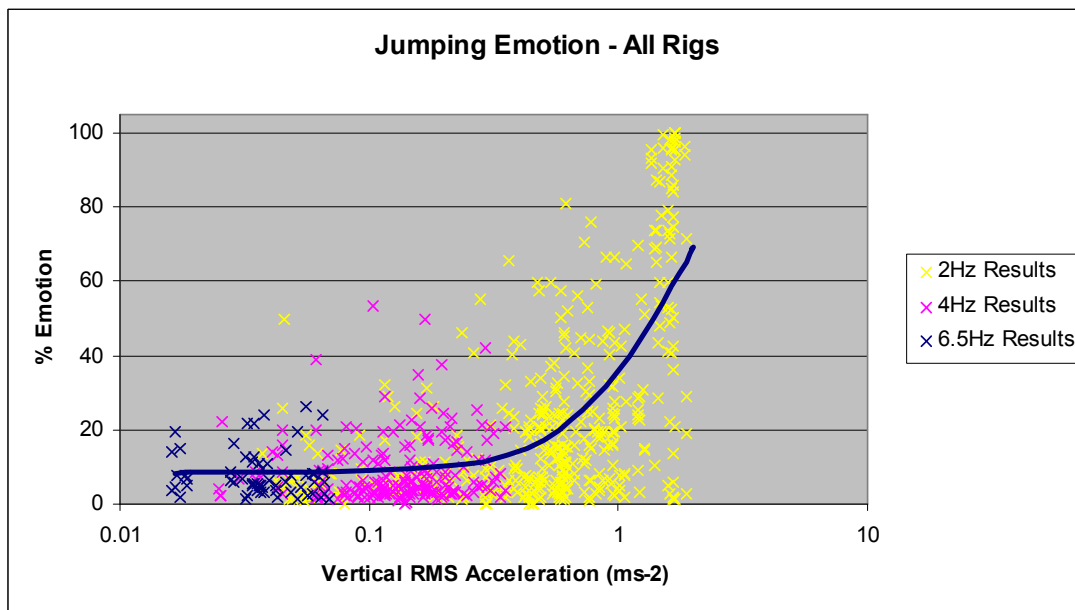


Figure 5.12b All Emotion Results for Jumping Participants

5.2.2 Initial Observations – Emotion

The emotion ratings for those seated follow a similar trend to the perception ratings although the values are typically lower and the range of the responses is greater above approximately 0.25ms^{-2} RMS acceleration (Figure 5.12a). For the jumping participants the emotion ratings are again typically lower than the equivalent perception ratings but the spread of the responses is very similar until the vibrations

reach 1ms^{-2} vertical RMS acceleration (Figure 5.12b). Above this the range of the jumping emotion responses exceed that of the jumping perception ratings.

As for perception the spread of the ratings for those seated is greater than for those jumping for all but the largest observed vibrations. However the difference between the ranges jumping to seated is greater for the emotion ratings than for the perception ratings.

5.2.3 Statistical Analysis - Methodology

The natural progression from the linear graphs of Figures 5.3 to 5.9 is to explore whether the relationship between the magnitude of the vibration and the recorded percentage perception rating (%P) or percentage emotion rating (%E) is best described using a linear, logarithmic, exponential, polynomial or power function.

In order to simplify the handling of the many variables considered, two groups of predictors were created. The first of these, Group 1, consisted of those variables taken directly from the instrumentation of the test rig. Thus the five forms (maximum, minimum, peak to peak, RMS and average peak) of vertical, sway and front-to-back displacement, and vertical acceleration are classed as the twenty Group 1 predictors (Table 5.1). The second group of predictors, Group 2, consisted of the variables which had to be calculated. Therefore individual VDV (calculated per test), cumulative VDV (sum of the individual V DVs), jump frequency, frequency of displacement response and frequency of acceleration response form the five Group 2 predictors (Table 5.1).

Firstly, for all 25 independent variables, the strength of the relationship between the predictor and the %P ratings for the seated group was calculated for the models shown in Table 5.2. This wide range of potential models was used so as not to prejudge relationships and also so as not to eliminate any possible links. It must be noted that all the models created are only truly valid over the range of vibrations obtained during the testing and while it may be possible to extrapolate some of the models, the viability of any of the polynomial models beyond the tested range is questionable due to the nature of these functions.

Table 5.1 Summary of Predictors used in Models

Group 1 Predictors			Notation
Displacement	Vertical	Maximum	V Max d
		Minimum	V Min d
		Peak to Peak	V PtoP d
		Root Mean Square (RMS)	V RMS d
		Average Peak	V AvP d
	Sway	Maximum	Sw Max d
		Minimum	Sw Min d
		Peak to Peak	Sw PtoP d
		Root Mean Square (RMS)	Sw RMS d
		Average Peak	Sw AvP d
	Front to Back	Maximum	FtB Max d
		Minimum	FtB Min d
		Peak to Peak	FtB PtoP d
		Root Mean Square (RMS)	FtB RMS d
		Average Peak	FtB AvP d
Acceleration	Vertical	Maximum	V Max a
		Minimum	V Min a
		Peak to Peak	V PtoP a
		Root Mean Square (RMS)	V RMS a
		Average Peak	V AvP a

Group 2 Predictors			Notation
Vibration Dose Value	Vertical	Individual	V Ind VDV
	Vertical	Cumulative	V Cum VDV
Frequency	Vertical	Jumping	Jump Freq
	Vertical	Displacement Response	V Freq d
	Vertical	Acceleration Response	V Freq a

Table 5.2 Summary of Single Variable Models

Model	Relationship (y = %P or %E)	No of Terms
linear.model	$y \sim x$	1
squared.model	$y \sim x^2$	1
log.model	$y \sim \ln(x)$	1
exp.model	$y \sim \exp(x)$	1
power.model	$y \sim x^b$	1
quadratic.model	$y \sim x + x^2$	2
xplus.log.model	$y \sim x + \ln(x)$	2
xplus.exp.model	$y \sim x + \exp(x)$	2
x*log(x).model	$y \sim x + \ln(x) + x \ln(x)$	2
x*exp(x).model	$y \sim x + \exp(x) + x \exp(x)$	2
cubic.model	$y \sim x + x^2 + x^3$	3
quartic.model	$y \sim x + x^2 + x^3 + x^4$	4

The modelling was carried out in Excel using the least squares method with the strength of the correlation measured using R^2 values (see below). The modelling procedure was repeated for the %P ratings for those jumping and again for both groups for the corresponding %E ratings. (This is illustrated in Figure 5.13 with the further steps that were taken in developing the models for predicting %P and %E).

The method of least squares is a method of fitting a model to data whereby the sum of the squares of the residuals is minimised. A residual is defined as the difference between the observed value and that predicted by the model. The coefficient of determination R^2 is the square of the correlation between the values predicted by the model and those recorded. A R^2 value of 1.0 indicates perfect correlation whereas $R^2=0.0$ indicates no correlation. R^2 can alternatively be written as

$$R^2 = 1 - \frac{SS_{Error}}{SS_{Total}} \quad \text{eq 5.1}$$

where $SS_{Error} = \sum_i (y_i - \hat{y})^2$ where $y_i = \text{recorded value}$ and $\hat{y} = \text{predicted value}$

and $SS_{Total} = \sum_i (y_i - \bar{y})^2$ with mean $\bar{y} = \frac{1}{n} \sum_i y_i$ and $n = \text{number of observations}$

To allow models with different numbers of terms to be compared (such as the combination models) R^2 can be modified (adjusted R^2) to account for the sample size and the number of terms in the model.

$$\text{Adjusted } R^2 = 1 - \frac{(1 - R^2)(n - 1)}{(n - p - 1)} \quad \text{eq 5.2}$$

where n =sample size and p =number of terms in the model (excluding the constant)

From Cohen 1992, for the analysis of psychology testing of this nature, a R^2 value of 0.02 (small effect size) represents a real effect, but one, which requires careful studies of a large number of samples to determine. Cohen defines a medium sized effect as one that is likely to be visible to the naked eye of a careful observer and relates this to a R^2 value of 0.13. Finally he classifies a large effect size as having a R^2 value of 0.26 or greater. To put this in context, the hypothesis that men are taller than women has an effect size of $R^2 = 0.33$ i.e. although there are some small men and some tall women, one only needs a fairly small sample of the population to confirm by eye the hypothesis. Effect size and R^2 values can also be viewed as the amount that the model predicts the variable. Using the height difference example, 33% of our height can be explained by gender alone with the other 67% down to other factors (not currently in the model).

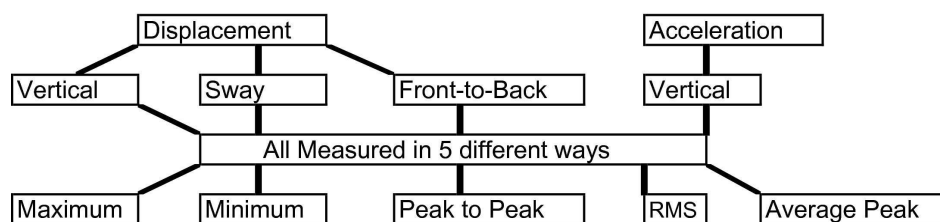
DATA DIVISION

Dependent Variables (DV) - those being Predicted

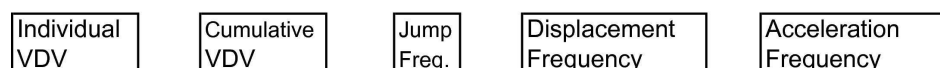


Independent Variables (IV) - Predictors

GROUP 1 (20 Independent Variables)



GROUP 2 (5 Independent Variables)



MODEL DEVELOPMENT

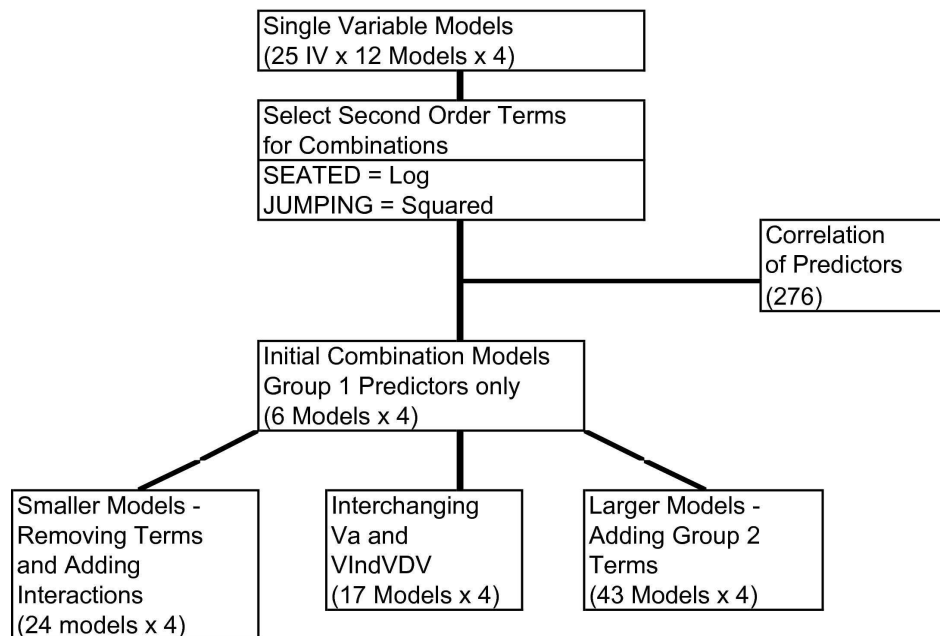


Figure 5.13 Statistical Analysis Procedure

The next step (Figure 5.13 - Model Development) was to combine the predictors in such a way that the human response (%P or %E) could be most accurately estimated using the fewest number of terms and predictors in the equation. As a starting point the squared, log, exp or power model, for each predictor which gave the highest R^2 value was selected to be used as a 'second order' predictor together with the basic variable (first order predictors) in the combinations (Table 5.3).

Table 5.3 Summary of 1st and 2nd Order Predictors for use in Models

Group 1 Predictors	1st Order Predictors	Selected 2nd Order Predictors	
		Seated %P & %E	Jumping %P & %E
Displacement	V Max d	ln V Max d	sqd V Max d
	V Min d	exp V Min d	sqd V Min d
	V PtoP d	ln V PtoP d	sqd V PtoP d
	V RMS d	ln V RMS d	sqd V RMS d
	V AvP d	ln V AvP d	sqd V AvP d
	Sw Max d	ln Sw Max d	sqd Sw Max d
	Sw Min d	exp Sw Min d	sqd Sw Min d
	Sw PtoP d	ln Sw PtoP d	sqd Sw PtoP d
	Sw RMS d	ln Sw RMS d	sqd Sw RMS d
	Sw AvP d	ln Sw AvP d	sqd Sw AvP d
	FtB Max d	ln FtB Max d	sqd FtB Max d
	FtB Min d	exp FtB Min d	sqd FtB Min d
	FtB PtoP d	ln FtB PtoP d	sqd FtB PtoP d
	FtB RMS d	ln FtB RMS d	sqd FtB RMS d
	FtB AvP d	ln FtB AvP d	sqd FtB AvP d
Acceleration	V Max a	ln V Max a	sqd V Max a
	V Min a	exp V Min a	sqd V Min a
	V PtoP a	ln V PtoP a	sqd V PtoP a
	V RMS a	ln V RMS a	sqd V RMS a
	V AvP a	ln V AvP a	sqd V AvP a
Group 2 Predictors	1st Order Predictors	Selected 2nd Order Predictors	
		Seated %P & %E	Jumping %P & %E
Vibration Dose Value	V Ind VDV	ln V Ind VDV	sqd V Ind VDV
	V Cum VDV	ln V Cum VDV	sqd V Cum VDV
Frequency	Jump Freq	exp Jump Freq	sqd Jump Freq
	V Freq d	exp V Freq d	sqd V Freq d
	V Freq a	exp V Freq a	sqd V Freq a

Then, in order to get an understanding of which grouping of predictors would be likely to give the most comprehensive representation of the rig's movement, a correlation analysis was carried out on the 25 first order predictors. This highlighted where there was multicollinearity (i.e. considerable overlap between certain predictors), namely those describing vertical acceleration, vertical displacement and individual VDV. To a lesser extent a correlation was identified between the vertical movement of the rig and the sway component. This gave an insight later on, when it came to reducing the number of predictors, as to which ones could possibly be removed without significantly reducing the accuracy of the model.

Six initial combination models were set up using the Group 1 predictors. The purpose of these was twofold; firstly to estimate the highest achievable R^2 value using the 'saturated model' and secondly to provide a baseline model ('base model') which could be expanded/contracted in order to obtain the best balance of accuracy and number of variables.

The 'saturated model' was a linear combination model using 16 of the 20 Group 1 (first order) predictors with the aim of obtaining a near maximum value of R^2 (Tables 5.4 and 5.5). The four of the 20 Group 1 (first order) predictors that were omitted were the minimum format of each variable as the information is covered by the maximum and peak to peak measures.

The other five initial combinations ('base models') used the same format of the 4 displacement and acceleration measures (e.g. RMS vertical d, RMS sway d, RMS front-to-back d and RMS vertical a) together with the 'second order' format of that predictor (e.g. $\ln(\text{RMS vertical d})$, $\ln(\text{RMS sway d})$, $\ln(\text{RMS front-to-back d})$ and $\ln(\text{RMS vertical a})$) (Tables 5.4 and 5.5). It was decided not to mix the forms of the predictors in the models e.g. using RMS values for the vertical displacement and peak values for the horizontal displacement. This was done to limit the, already large, number of combinations being considered to a sensible level.

All six initial models were analysed using linear regression in Excel and the R^2 values compared.

Table 5.4 Summary of Terms used in the Initial Combination Models for those Seated

<u>Model</u>	<u>Relationship</u> (y = %P or %E)	<u>No of Variables/ Terms</u>
Saturated model	$y \sim V_{Maxd} + V_{PtoPd} + V_{RMSd} + V_{AvPd}$ $+ S_{wMaxd} + S_{wPtoPd} + S_{wRMSd} + S_{wAvPd}$ $+ F_{tBMaxd} + F_{tBPtoPd} + F_{tBRMSd} + F_{tBAvPd}$ $+ V_{Maxa} + V_{PtoPa} + V_{RMSa} + V_{AvPa}$	16/16
Max Base Model	$y \sim V_{Maxd} + S_{wMaxd} + F_{tBMaxd} + V_{Maxa}$ $+ \ln(V_{Maxd}) + \ln(S_{wMaxd}) + \ln(F_{tBMaxd}) + \ln(V_{Maxa})$	4/8
Min Base Model	$y \sim V_{Mind} + S_{wMind} + F_{tBMind} + V_{Mina}$ $+ \exp(V_{Mind}) + \exp(S_{wMind}) + \exp(F_{tBMind}) + \exp(V_{Mina})$	4/8
PtoP Base Model	$y \sim V_{PtoPd} + S_{wPtoPd} + F_{tBPtoPd} + V_{PtoPa}$ $+ \ln(V_{PtoPd}) + \ln(S_{wPtoPd}) + \ln(F_{tBPtoPd}) + \ln(V_{PtoPa})$	4/8
RMS Base Model	$y \sim V_{RMSd} + S_{wRMSd} + F_{tBRMSd} + V_{RMSa}$ $+ \ln(V_{RMSd}) + \ln(S_{wRMSd}) + \ln(F_{tBRMSd}) + \ln(V_{RMSa})$	4/8
AvP Base Model	$y \sim V_{AvPd} + S_{wAvPd} + F_{tBAvPd} + V_{AvPa}$ $+ \ln(V_{AvPd}) + \ln(S_{wAvPd}) + \ln(F_{tBAvPd}) + \ln(V_{AvPa})$	4/8

Table 5.5 Summary of Terms used in the Initial Combination Models for those Jumping

<u>Model</u>	<u>Relationship</u> (y = %P or %E)	<u>No of Variables/ Terms</u>
Saturated model	$y \sim V_{Maxd} + V_{PtoPd} + V_{RMSd} + V_{AvPd}$ $+ S_{wMaxd} + S_{wPtoPd} + S_{wRMSd} + S_{wAvPd}$ $+ F_{tBMaxd} + F_{tBPtoPd} + F_{tBRMSd} + F_{tBAvPd}$ $+ V_{Maxa} + V_{PtoPa} + V_{RMSa} + V_{AvPa}$	16/16
Max Base Model	$y \sim V_{Maxd} + S_{wMaxd} + F_{tBMaxd} + V_{Maxa}$ $+ (V_{Maxd})^2 + (S_{wMaxd})^2 + (F_{tBMaxd})^2 + (V_{Maxa})^2$	4/8
Min Base Model	$y \sim V_{Mind} + S_{wMind} + F_{tBMind} + V_{Mina}$ $+ (V_{Mind})^2 + (S_{wMind})^2 + (F_{tBMind})^2 + (V_{Mina})^2$	4/8
PtoP Base Model	$y \sim V_{PtoPd} + S_{wPtoPd} + F_{tBPtoPd} + V_{PtoPa}$ $+ (V_{PtoPd})^2 + (S_{wPtoPd})^2 + (F_{tBPtoPd})^2 + (V_{PtoPa})^2$	4/8
RMS Base Model	$y \sim V_{RMSd} + S_{wRMSd} + F_{tBRMSd} + V_{RMSa}$ $+ (V_{RMSd})^2 + (S_{wRMSd})^2 + (F_{tBRMSd})^2 + (V_{RMSa})^2$	4/8
AvP Base Model	$y \sim V_{AvPd} + S_{wAvPd} + F_{tBAvPd} + V_{AvPa}$ $+ (V_{AvPd})^2 + (S_{wAvPd})^2 + (F_{tBAvPd})^2 + (V_{AvPa})^2$	4/8

(A variable in this context is taken as one of the measured predictors i.e. $y \sim V_{Maxd} + Sw_{Maxd}$ has 2 variables while $y \sim V_{Maxd} + \ln(Maxd)$ has only 1. Terms are defined as the number of terms in the equation used to define %P or %E excluding the constant i.e. $y \sim V_{Maxd} + Sw_{Maxd}$ and $y \sim V_{Maxd} + \ln(Maxd)$ both have 2 terms.)

The five base models each used 4 independent variables in 8 terms (notated 4/8). The base model that gave the highest R^2 value was then modified by removing one term at a time to explore the impact the change had on the 'goodness of fit' of the model. Interaction terms (e.g. $V_{Maxd} \times \ln(V_{Maxd})$) were added to the smaller models to check if combined predictors were more powerful (in modelling terms) than additional predictors. In parallel with this the same best-fit base was enlarged by the addition of the Group 2 predictors (and their second order terms) with the aim of finding the maximum R^2 value achievable for the collected data. Additionally the Individual VDV values (which incorporate the vertical RMS acceleration and a time component) were interchanged with vertical RMS acceleration variables in the models to test if the accuracy was improved.

5.2.4 Statistical Analysis - Results

5.2.4.1 Single Variable Models

For those seated the logarithmic model typically proved the best single term model for predicting the participants' %P and %E ratings, when using R^2 as a gauge. As identified by the initial graphs, those jumping found it hard to perceive the relative magnitude of the movement until the vibrations exceeded a certain size. Because of this, the graphical link between %P and %E and the rig's movement starts off almost horizontal until it nears the value at which the jumpers start to sense the vibration and then the slope quickly increases to merge with that of those seated. This means that, for those jumping (within the range of vibrations covered by the tests) the quadratic model generally appears to give the most accurate prediction of %P and %E using 2 terms. Therefore for the combination models, $\ln(x)$ and x^2 were taken as the 'second order' predictors for those seated and those jumping respectively (Table 5.3).

5.2.4.2 Range of R^2 Values

A summary of the R^2 values for the best model combinations are shown in Table 5.7. The adjusted R^2 values obtained ranged, for seated %P, from a maximum of 0.560 to 0.481 for the best single term model. Due to the wider scatter of the recorded ratings the corresponding values for the seated participants' %E models were much lower at 0.425 and 0.326 respectively. As the recorded ratings for those jumping were generally lower and less spread out than for the seated participants, the reduction in R^2 values between the %P and %E models for those jumping was much less. The actual R^2 values were also notably greater. For the jumping models the maximum value of adjusted R^2 achieved was 0.661 for %P and 0.595 for %E. The best single term models for those jumping produced R^2 values of 0.626 (%P) and 0.550 (%E), surprisingly close to the maximum R^2 values obtained.

The seated models were based on 1400 data points compared to 653 data points for the jumping models therefore the R^2 values cannot be compared like-for-like. By observing the data collected it can be seen that for a given vibration, as well as the actual values being less, the range of the %P and %E ratings are generally less for those jumping than for those seated. This could explain why the R^2 values for the jumping models are considerably greater than those for the seated models. Another

observation that can be made is that the single variable jumping models produce much higher R^2 values (relative to the maximum R^2 obtained) than the seated models. This indicates that the human response to a vibration whilst seated is more complex than that when jumping to create the vibration.

5.2.4.3 4 Variable/8 Term Base Models

For all four cases (Seated %P, Seated %E, Jumping %P and Jumping %E) the 4 variable/8 term (4/8) base model that gave the highest R^2 value used the RMS format of the variables. These models incorporated variables describing the 3 dimensions of displacement as well as the vertical acceleration (Table 5.6).

Table 5.6 Best 4 Variable / 8 Term Base Models

<u>Dependent Variable</u>	<u>Model</u>	<u>Relationship</u> (y = %P or %E)	<u>Adjusted R^2</u>
Seated %P	RMS Base Model	$y \sim \text{VRMSd} + \text{SwRMSd} + \text{FtBRMSd} + \text{VRMSa} + \ln(\text{VRMSd}) + \ln(\text{SwRMSd}) + \ln(\text{FtBRMSd}) + \ln(\text{VRMSa})$	0.549
Seated %E	"	"	0.416
Jumping %P	RMS Base Model	$y \sim \text{VRMSd} + \text{SwRMSd} + \text{FtBRMSd} + \text{VRMSa} + (\text{VRMSd})^2 + (\text{SwRMSd})^2 + (\text{FtBRMSd})^2 + (\text{VRMSa})^2$	0.650
Jumping %E	"	"	0.566

It was found that for those seated the use of the VDV rating for the individual test (IndVDV) in place of the vertical acceleration increased the R^2 values by an extremely small amount (~ 0.005). From an initial look at the R^2 values only, these 4/8 models seem to fit the data relatively well for a restricted number of terms except in the case of %E, for those jumping, where a higher R^2 value can be obtained using just 1 variable/3 terms $y \sim \text{VRMSd} + \ln(\text{VRMSd}) + [\text{VRMSd} \times \ln(\text{VRMSd})]$.

When variables and terms were added to the four RMS base models (Table 5.6) the best additional variable seemed to be one providing information regarding the duration of the vibration i.e. VDV. This was typically in the form of the cumulative VDV (CumVDV) i.e. the sum of the V DVs up to and including that test (eq 4.4). The exception was the %P models where, for those jumping, where IndVDV (i.e. eVDV value for that test (eq 4.3)) increased R^2 more than CumVDV. However the increase

in R^2 from 4/8 to 5/10 (variables/terms) was tiny, at approximately 0.007. (Note both seated 4/8 base models were taken as using IndVDV in place of V RMS as it gave a slightly higher R^2 value.)

5.2.4.4 Maximum R^2 Models

The highest R^2 values were obtained from RMS models with 15 or 16 terms. However these proved not to be the initial 'saturated' models using 16 of the Group 1 predictors (Tables 5.4 and 5.5). For those seated the maximum R^2 values were from 8/16 models containing four Group 1 and four Group 2 predictors together with their logarithms. A 4/15 model proved best for those jumping using the squared format of the four Group 1 predictors and their 11 interactions (for both %P and %E) i.e. $y \sim a + b + c + d + ab + ac + ad + bc + bd + cd + abc + abd + acd + bcd + abcd$. In most cases the highest R^2 scores were around 0.011 higher than the four 4/8 base models except for the model for %E of those jumping where the increase was higher (0.029). (It has already been noted that the 4/8 %E model for the jumpers gave a relatively poor R^2 score.) Again the increases in R^2 are small (<0.03) indicating that adding complexity to the models does little to improve their accuracy.

5.2.4.5 Reduced Variable Models

For those jumping reducing the number of variables from 4 down to 2 did little to affect the R^2 values (maximum of 0.005 reduction). The two key variables for predicting %P and %E of those jumping are typically the squared RMS form of vertical displacement and acceleration. Both the jumping %P and %E 2/15 models, containing the same terms as the 2/4 models but with the inclusion of all the interactions, produce R^2 values close to the maximum 4/15 models.

For the seated models both the best %P and %E 2/4 models used the linear and logarithmic form of IndVDV and RMS front-to-back displacement but the differences from the 4/8 model were a reduction of 0.024 for %P and 0.046 for %E. Both of the R^2 values for these 2/4 seated models increased by around 0.015 when the interactions were included (2/15 models). For the 2/15 models Va terms rather than IndVDV gave slightly better R^2 values.

All the single predictor models with the highest R^2 values typically used vertical acceleration (Va) or IndVDV (which incorporates Va) except for the %P jump models and the 1/3 %E jump model where vertical displacement produced higher R^2 values. However there is generally not much to choose between vertical displacement, acceleration and IndVDV models for all cases when using just one variable. For the %P models of those seated, vertical acceleration (Va) gave slightly higher R^2 values than vertical displacement (Vd) and, front-to-back (FtBd) and sway (Swd) displacement gave similar but lower again R^2 values. The relative positioning of the R^2 values was similar for the seated %E models but the Swd values were noticeably lower than those for FtBd. The Vd and Va R^2 values for the %P jump models were similar except, strangely, the averaged forms RMS and average peak (AvP) scored significantly lower R^2 values for Va than other predictors. The Swd %P jump models produced R^2 values close to those of RMS and AvP Va followed by FtBd. As for the seated models the relationships between the R^2 values were similar for single term models for %P and %E jump.

Table 5.7 Summary of R² Values for Best Combination Models Identified

	Group 1 Predictors		FTbD	Swd	Group 2 Predictors		Jump Freq	V Freq d	V Freq a	No. of Variables	In/exp/ sqd	Inter- actions	No. Terms	Variables /Terms	R ² (eq 5.1)	Adjusted R ² (eq 5.2)
	Vd	Va			VIndVDV	VCumVDV										
<u>SEAT %P</u>		✓ AvP								1	only In		1	1/1	0.481	0.481
					✓					1	✓ In		2	1/2	0.499	0.499
					✓					1	quartic		4	1/4	0.515	0.513
		✓ RMS	✓ RMS	✓ RMS	✓					2	✓ In	✓	4	2/4	0.527	0.525
			✓ RMS	✓ RMS						2	✓ In	✓	15	2/15	0.546	0.541
<u>JUMP %P</u>	✓ RMS		✓ RMS	✓ RMS	✓					4	✓ In		8	4/8	0.552	0.549
	✓ RMS		✓ RMS	✓ RMS	✓	✓				5	✓ In		10	5/10	0.559	0.556
	✓ RMS	✓ RMS	✓ RMS	✓ RMS	✓		✓			8	✓ In		16	8/16	0.565	0.560
	✓ PtoP									1	only sqd		1	1/1	0.626	0.626
	✓ Min									1	✓ sqd		2	1/2	0.637	0.636
<u>SEAT %E</u>	✓ RMS									1	✓ exp	✓	3	1/3	0.647	0.646
	✓ RMS	✓ RMS								2	only sq's	✓	3	2/3	0.652	0.650
	✓ RMS	✓ RMS								2	✓ sqd	✓	4	2/4	0.647	0.645
	✓ RMS	✓ RMS								2	✓ sqd	✓	15	2/15	0.662	0.654
	✓ RMS	✓ RMS	✓ RMS	✓ RMS	✓					4	✓ sqd		8	4/8	0.655	0.650
<u>JUMP %E</u>	✓ RMS	✓ RMS	✓ RMS	✓ RMS	✓					5	✓ sqd		10	5/10	0.660	0.654
	✓ RMS	✓ RMS	✓ RMS	✓ RMS	✓		✓			6	✓ sqd		12	6/12	0.664	0.658
	✓ RMS	✓ RMS	✓ RMS	✓ RMS						4	only sq's	✓	15	4/15	0.669	0.661
	✓ AvP									1	In only		1	1/1	0.326	0.326
	✓ AvP									1	✓ In		2	1/2	0.329	0.328
<u>JUMP %E</u>					✓					1	quartic		4	1/4	0.353	0.352
		✓ RMS	✓ RMS	✓ RMS	✓					2	✓ In		4	2/4	0.372	0.370
		✓ RMS	✓ RMS	✓ RMS						2	✓ In	✓	15	2/15	0.392	0.385
	✓ RMS		✓ RMS	✓ RMS	✓					4	✓ In		8	4/8	0.419	0.416
	✓ RMS		✓ RMS	✓ RMS	✓	✓				5	✓ In		10	5/10	0.427	0.423
<u>JUMP %E</u>	✓ RMS	✓ RMS	✓ RMS	✓ RMS	✓		✓		✓	8	✓ In		16	8/16	0.431	0.425
	✓ PtoP									1	only sqd		1	1/1	0.550	0.550
	✓ PtoP									1	✓ sqd	✓	2	1/2	0.554	0.552
	✓ RMS									1	✓ exp	✓	3	1/3	0.588	0.586
	✓ RMS	✓ RMS		✓ RMS						2	only sq's	✓	3	2/3	0.566	0.564
<u>JUMP %E</u>	✓ RMS	✓ RMS		✓ RMS						2	✓ sqd	✓	4	2/4	0.567	0.564
	✓ RMS	✓ RMS		✓ RMS						2	✓ sqd	✓	15	2/15	0.602	0.593
	✓ RMS	✓ RMS	✓ RMS	✓ RMS						4	✓ sqd		8	4/8	0.572	0.566
	✓ RMS	✓ RMS	✓ RMS	✓ RMS	✓		✓			5	✓ sqd		10	5/10	0.578	0.572
	✓ RMS	✓ RMS	✓ RMS	✓ RMS						4	only sq's	✓	15	4/15	0.604	0.595

Note: Models using VIndVDV in place of a Va term are highlighted in yellow

5.2.5 Statistical Analysis – Checks

In order to determine further the accuracy of the models and to decide which models best define human perception and emotion when seated or jumping on a grandstand, checks were carried out on the most promising models. For each of the four dependent variable categories (%P Seated, %P Jumping, %E Seated, %E Jumping) (Figure 5.13) the combination models which produced the highest R^2 values using 4/8, 5/10 and 2/4 (or 2/3) variables/terms together with the best single variable model were checked graphically to assess their 'goodness of fit'. (A summary of the procedure used for model validation is shown in Figure 5.19.)

5.2.5.1 Combination Models - Checks

Firstly, for the combination models, scatter plots were produced of the explanatory variables (predictors) against the actual recorded %P or %E ratings (Figure 5.14).

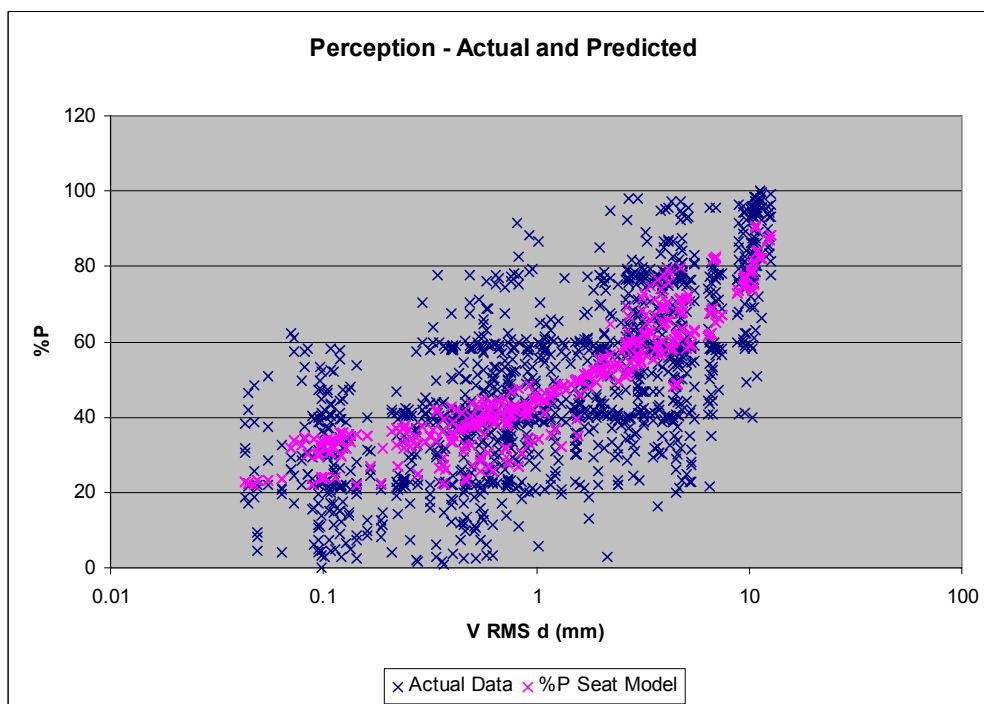


Figure 5.14 Sample of Initial Outlier and Model Overview Scatter Plot

These graphs were used to identify any outliers prior to being overlaid with the predicted %P or %E ratings for each of the three models. A visual inspection of

these overlays gave an overview of where the predicted values for each model sat relative to the actual values for each of the predictors. Because the models being assessed are based on several predictors, the plots of the modelled variable (%P or %E) against a single one of the predictors is not a distinct line but shows the scatter created by the other variables (Figure 5.14).

Each model consists of two parts; the first being the deterministic section (or fit) of the model and the second being the 'random' error component e.g. $y = \alpha x + \beta z + \phi + \text{error}$. In order to check the sufficiency of the functional (fit) part of the model a scatter plot was drawn up of each of the predictor variables versus the residuals for every model, see Figure 5.15 for a sample plot.

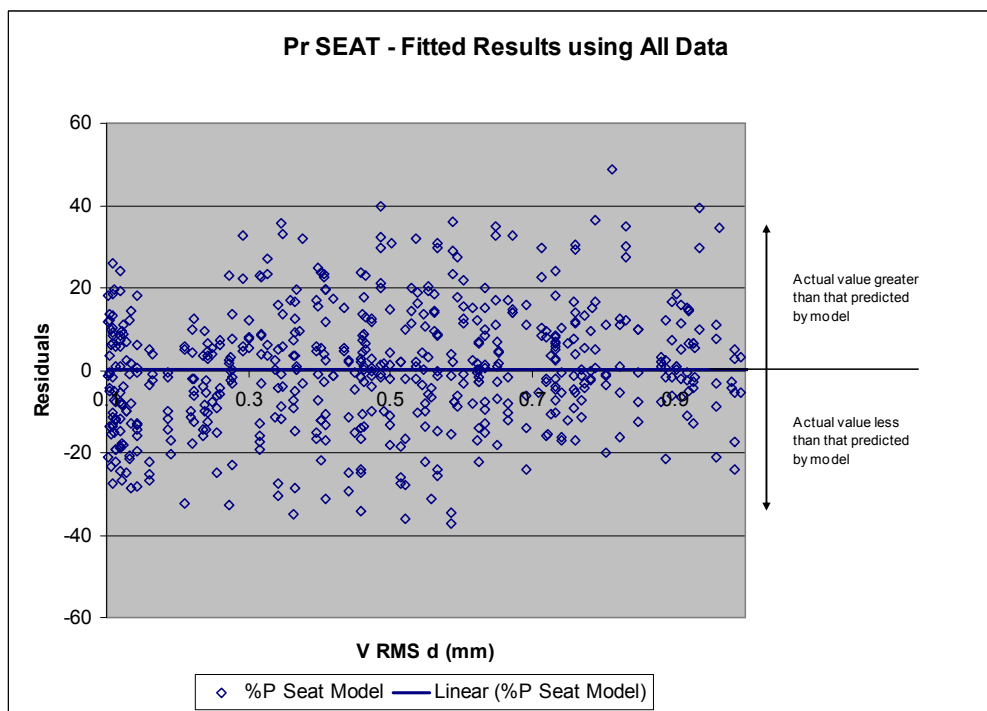
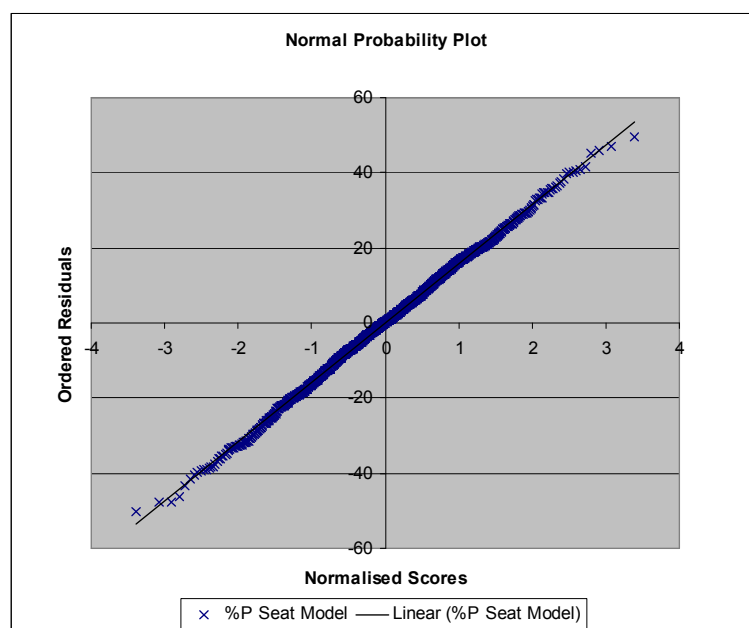


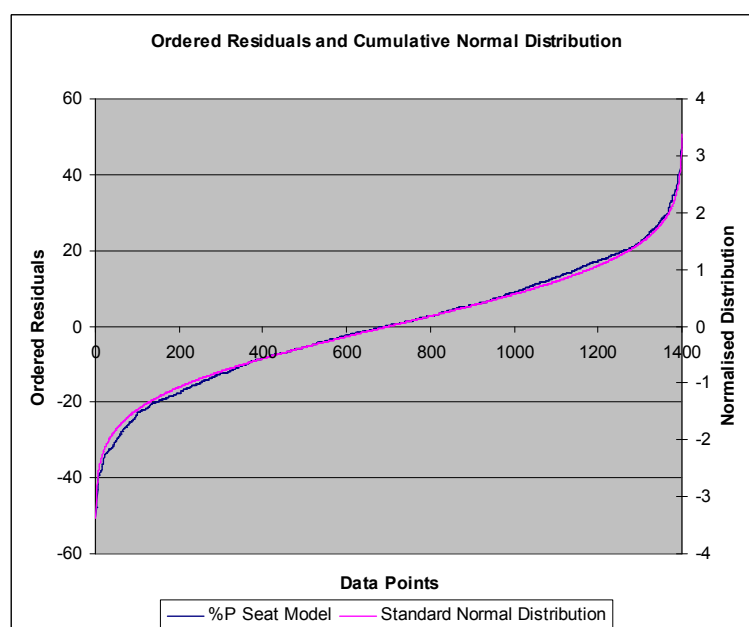
Figure 5.15 Sample of Scatter Plot to check fit of Model & Deviation of Errors

The residuals were calculated by subtracting the predicted rating (calculated using the model) from the relevant recorded %P or %E rating. The distribution of the residuals along the range of each predictor was then assessed to confirm that there was no apparent link between the residuals (for each model) and the predictor, indicating that the model could be improved. If no relationship was visually apparent the same scatter plots were checked to see if there was a constant standard deviation of the 'random' errors. This was done by checking the spread of the

residuals above and below the x-axis across the width of each graph. A constant spread of the residuals for all values of each predictor suggests that the standard deviation of the random errors is the same across the levels of that predictor variable, and is an indicator of a good model. Plots of predicted ratings against residuals were also checked in this manner.



a



b

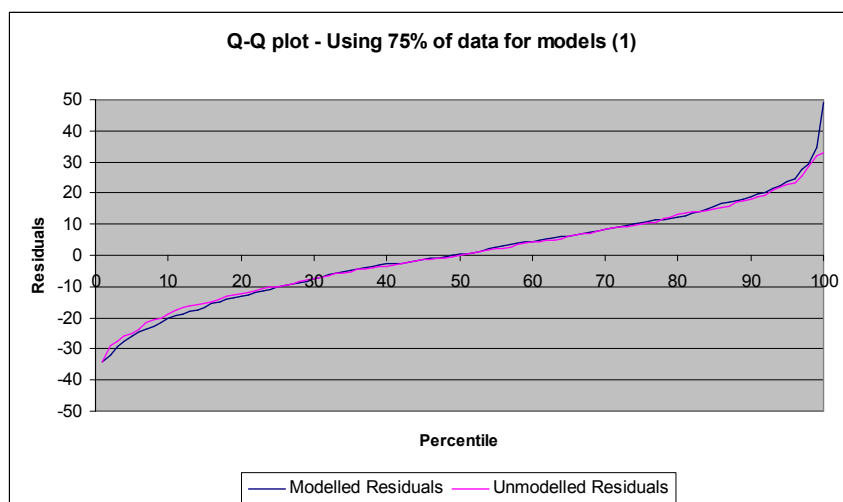
Figure 5.16 Sample Normal Probability Plots

Similar plots of run order versus residuals were used to see if any difference in the residuals could be observed over the course of each set of tests/rigs.

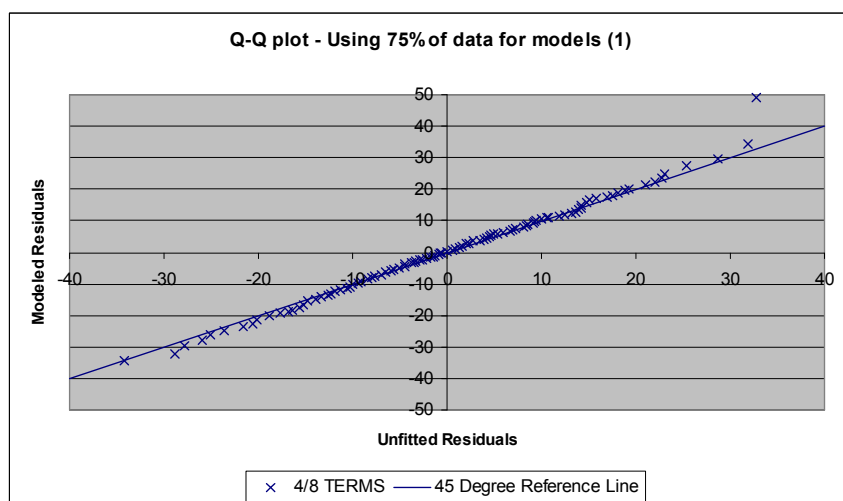
Because we are trying to model a human reaction to a physical situation it is expected that the 'random' errors in the model should conform to a normal distribution. To verify this assumption normal probability plots were produced, for each model, of the ordered residuals against the associated theoretical values from a standard normal cumulative distribution (Figure 5.16 a). The departure of the points on these graphs, from a straight line provides information regarding the distribution of the errors and their deviation from a normal distribution. The reason for plotting the ordered residual against the standard normal cumulative distribution is that it is easier for the human eye to detect variation from a straight line than to detect differences between two similar curves. Figure 5.16 b shows the ordered residuals and the standard normal cumulative distribution (for one model) plotted separately illustrating the difficulty in differentiating between the two lines.

A final cross validation check of the combination models was carried out by splitting the data into quarters and recalculating the components of the best 4/8, 5/10 and 2/4 (or 2/3) models based on three-quarters of test results. The residuals were then calculated for the modelled 75% set of data and also for the remaining quarter of the data i.e. the 25% un-modelled set. In order to compare how well the models created from three quarters of the data fitted the un-modelled quarter of the data, both sets of ordered residuals were converted into percentiles (Figure 5.17 a). This allows unequally sized data sets to be compared. The ordered percentiles for the modelled and unmodelled data sets were plotted against each other to create a Quantile-Quantile (Q-Q) plot (Figure 5.17 b).

The Q-Q plot was then compared to a $y=x$ (45 degree) reference line and the differences in the distribution of the 'random' errors assessed. This process was repeated four times for each model rotating the four quarters as the un-modelled data set.



a



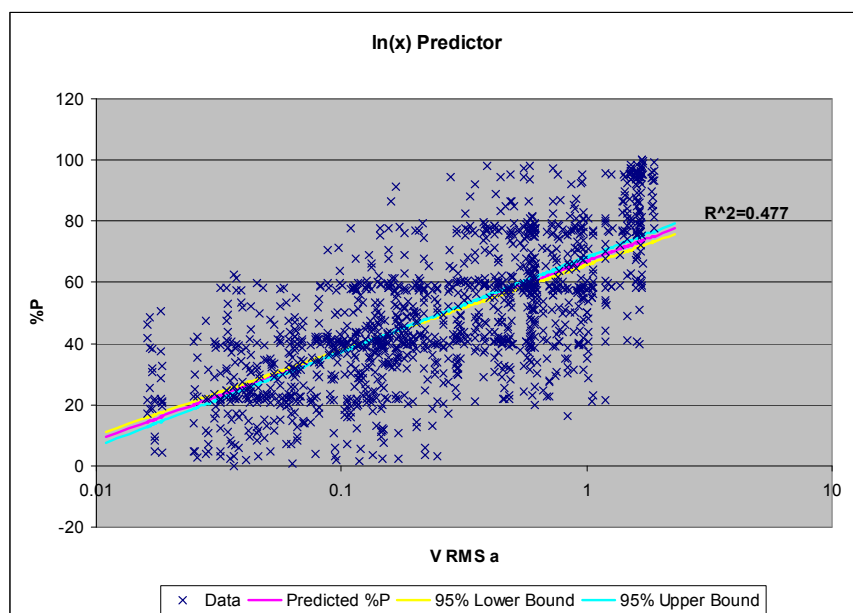
b

Figure 5.17 Sample of Q-Q Plots (Q=Quantile)

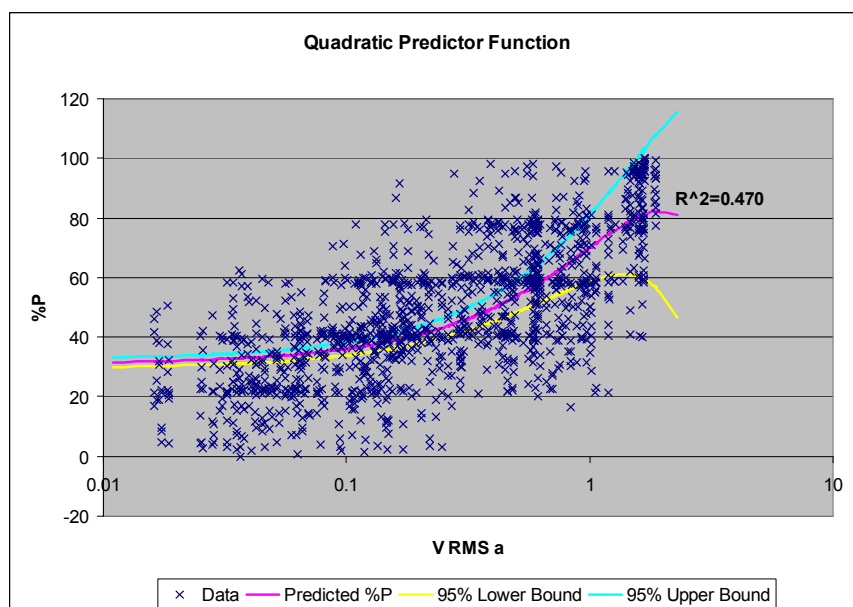
5.2.5.2 Single Variable Models - Checks

The single variable models were validated using slightly different methods. Firstly the best single variable models were selected for each of the four dependent variables (%P Seated, %P Jumping, %E Seated, %E Jumping) using the R^2 results from the initial stages of the combined model development. The fit of each of the models was then checked graphically using the 95% confidence intervals (Figure 5.18) before one single variable model was chosen for each dependent variable. Particular attention was paid to the performance of each model at the extremes of the tested range of vibrations where peculiarities tend to occur and models with high R^2

values can become unrealistic (see downward turn of quadratic model in Figure 5.18 b below). The selected models were not necessarily the ones that produced the highest R^2 values but the ones that gave the best balance of accuracy and simplicity for the vibration range covered in the tests. The four chosen models were then assessed using the normal probability plot and cross validation methods used for the combination models.

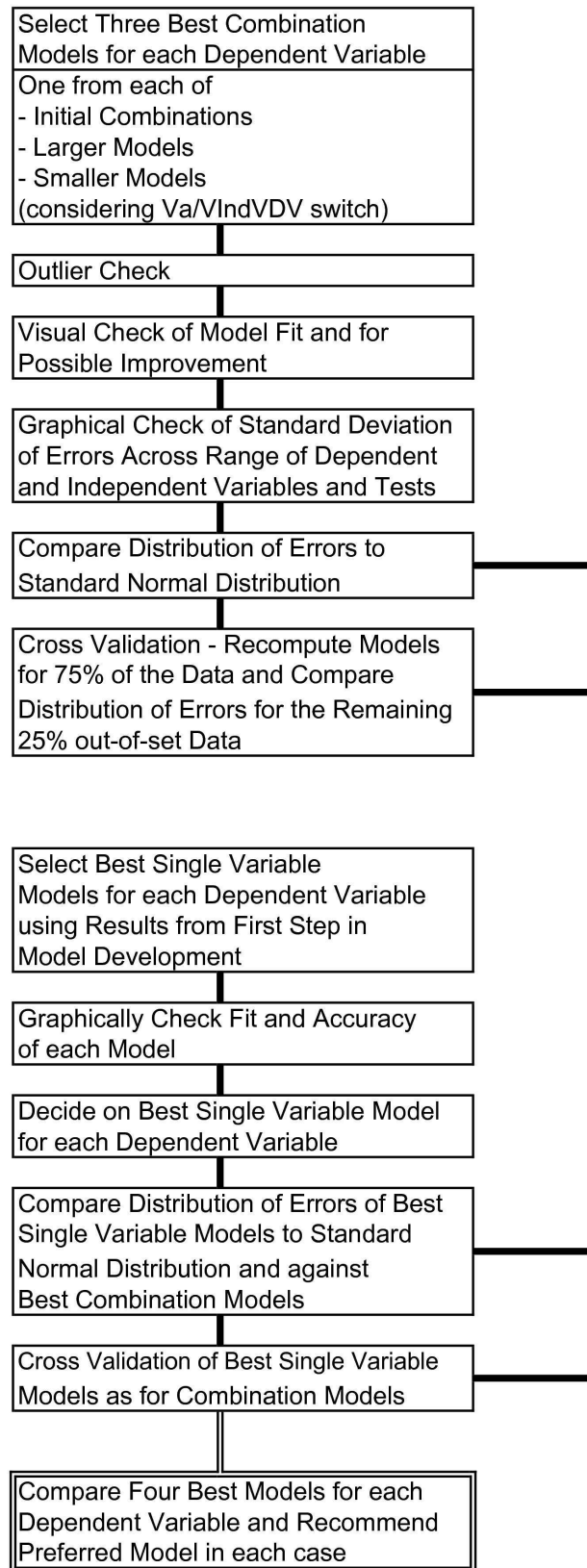


a



b

Figure 5.18 Sample of Single Variable Model Graphs

MODEL VALIDATION**Figure 5.19 Procedure for Model Validation**

5.2.5.3 Model Checks for Perception Rating while Seated

The three combination models listed in Table 5.8 were assessed for goodness of fit as described in Section 5.2.5.1 above.

Table 5.8 Selected Combination Models for Predicting %P Seat

Components

Var./ Terms	V d	FtB d	Sw d	V Ind VDV	V Cum VDV	No. Var.	ln/exp/ sqd	No. Terms	Adjusted R ²
2/4		✓RMS		✓		2	✓ln	4	0.525
4/8	✓RMS	✓RMS	✓RMS	✓		4	✓ln	8	0.549
5/10	✓RMS	✓RMS	✓RMS	✓	✓	5	✓ln	10	0.556

Formulae

Var./ Terms	
2/4	$\%P_{SEAT} = \alpha FtoB RMSd + \beta VIndVDV + \phi$
4/8	$\%P_{SEAT} = \alpha VRMSd + \beta FtoBRMSd + \chi SwRMSd + \delta VIndVDV + \varepsilon \ln(VRMSd) + \phi \ln(FtoBRMSd) + \gamma \ln(SwRMSd) + \eta \ln(VIndVDV) + \phi$
5/10	$\%P_{SEAT} = \alpha VRMSd + \beta FtoBRMSd + \chi SwRMSd + \delta VIndVDV + \varepsilon VCumVDV + \phi \ln(VRMSd) + \gamma \ln(FtoBRMSd) + \eta \ln(SwRMSd) + \iota \ln(VIndVDV) + \kappa \ln(VCumVDV) + \phi$

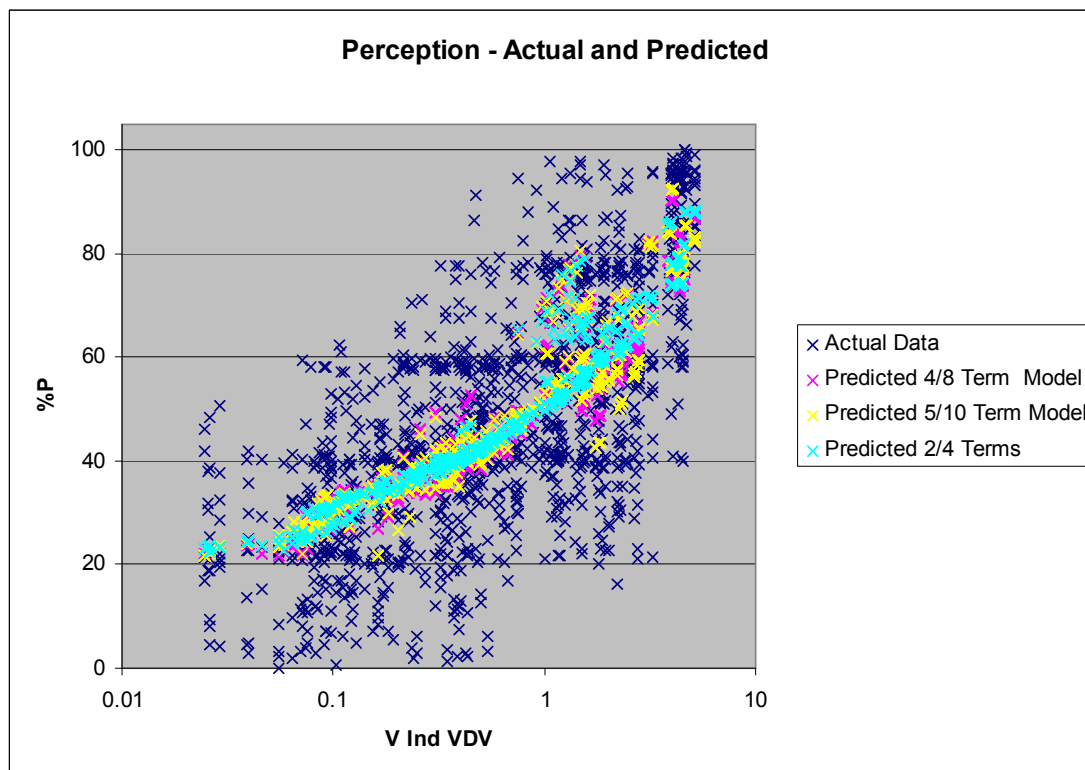


Figure 5.20 Actual and Predicted %P Seat Ratings v Vertical Individual (per Test) Vibration Dose Value

The graphs of the recorded data show some %P ratings on the outer edges of the scatter plot but no outlying points (Figure 5.20). The overlays of the proposed models show that the predicted %P values sit fairly centrally to the actual data. It can be identified that at the very top of the range of the predictors, the models may possibly slightly under-predict the %P rating due to the lack of information beyond the recorded range.

The scatter plots of the residuals against the predictors, to confirm the fit of the models, show that there is no obvious further link between the models and the predictors except for those previously identified. For example, the 2/4 model could be improved by the addition of Swd and Cum VDV terms. These plots also show that the 'random' errors are fairly evenly distributed across all the predictors but with a slight bellying in the centre of the range. This is confirmation that there is more agreement in the %P ratings at the upper and lower end of the scale as can be seen in the scatter plots of the recorded %P ratings (Figure 5.20).

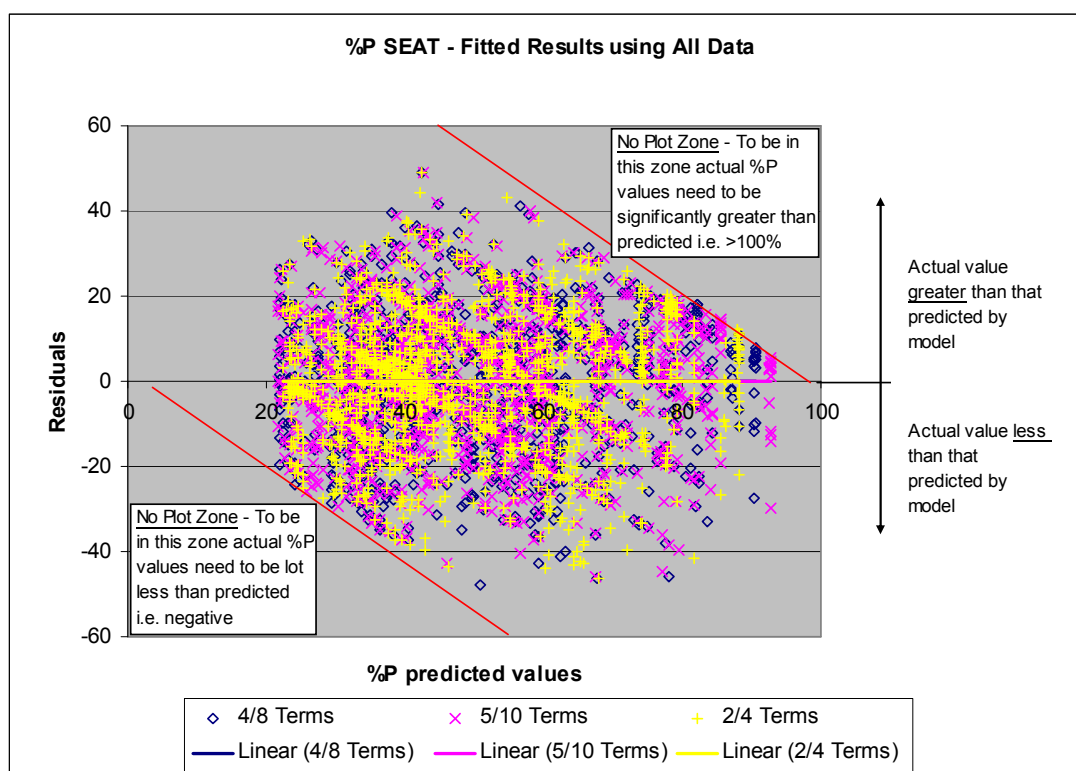


Figure 5.21 Residuals from Test Models v Predicted Seated %P Ratings

The plot of predicted %P ratings against residuals (Figure 5.21) highlights that, for the range of the predictors used in the tests, the lowest predicted %P value from the

chosen models is above 20%. This plot also clearly shows that there are zones of the graph in the bottom left and top right corners that cannot be plotted within as this would require the actual %P ratings to be below zero and above 100% respectively. Although the trendlines in Figure 5.21 are horizontal indicating an equal balance of the predictors either side of the x-axis, it is worth noting that at the top end of the predicted %P ratings there are clusters of points just above the x-axis balancing far fewer points further below it. The distribution of the residuals has a similar central bellying to the predictor plots described above.

For the chosen models predicting %P ratings for those seated, the range of the residuals seems fairly constant across all the tests, independent of which rig was used.

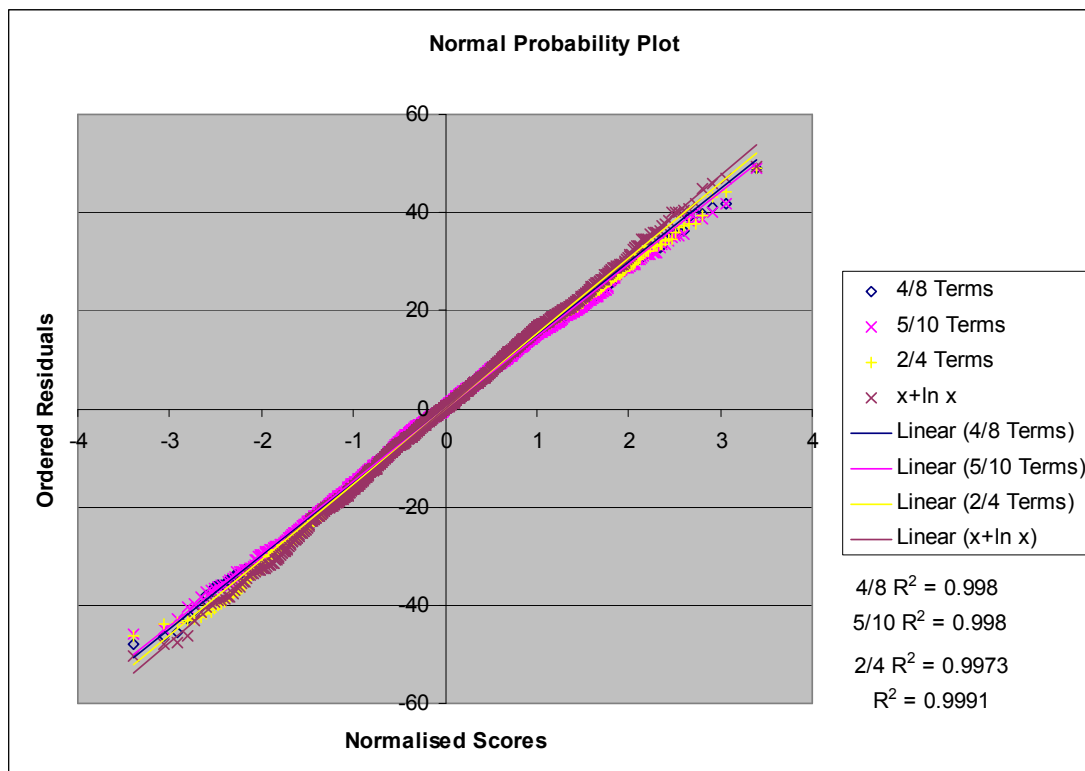


Figure 5.22 Normal Probability Plot for Selected %P Seat Models

The normal probability plot (Figure 5.22) for the selected %P Seat models shows that the residuals from the models conform well to the assumption that the errors are normally distributed. There are a few outliers at the ends of each plot which is to be expected. The 2/4 model has a very slightly greater deviation from a straight line, representing a normal distribution, than the other two combined test models.

From the single variable regression models for predicting seated perception ratings, those using Individual VDV gave the highest R^2 values but the vertical RMS accelerations models produced similar results and are truly single variable. (Vibration Dose Values incorporate a time component as well as RMS acceleration.) Therefore the single variable models considered were the logarithmic and polynomial combinations of $VRMSa$ in Table 5.2. The cubic and quartic models both proved complex with wide confidence intervals at the top end. The quadratic model also had wide confidence intervals and possibly underestimated the higher %P values as did the basic log model. The model that was selected as providing the best estimate of %P ratings was the $x + \ln(x)$ model $[\%P_{SEAT} = \alpha VRMSa + \beta \ln(VRMSa) + \phi]$ (Table 5.9) as it achieved a higher R^2 value than the linear model with only slightly more complexity. As described in Section 5.2.5.2 the residuals for the chosen $x + \ln(x)$ model were plotted alongside the combination models on the Normal Probability Plot (Figure 5.22) and performed as well as the 4/8 and 5/10 models.

Table 5.9 Selected Single Variable Model for Predicting %P Seat

Components

Var./ Terms	V a	No. Var.	ln/exp/ sqd	No. Terms	Adjust- ed R^2
1/2	✓RMS	1	✓ln	2	0.495

Formula

Var./ Terms	
1/2	$\%P_{SEAT} = \alpha VRMSa + \beta \ln(VRMSa) + \phi$

The results from the cross validation checks for all four selected models are shown in Figure 5.23 and show that models based on 75% of the data can accurately represent the remaining unfitted 25%. This implies that the models based on the full data set can be extrapolated to a wider population.

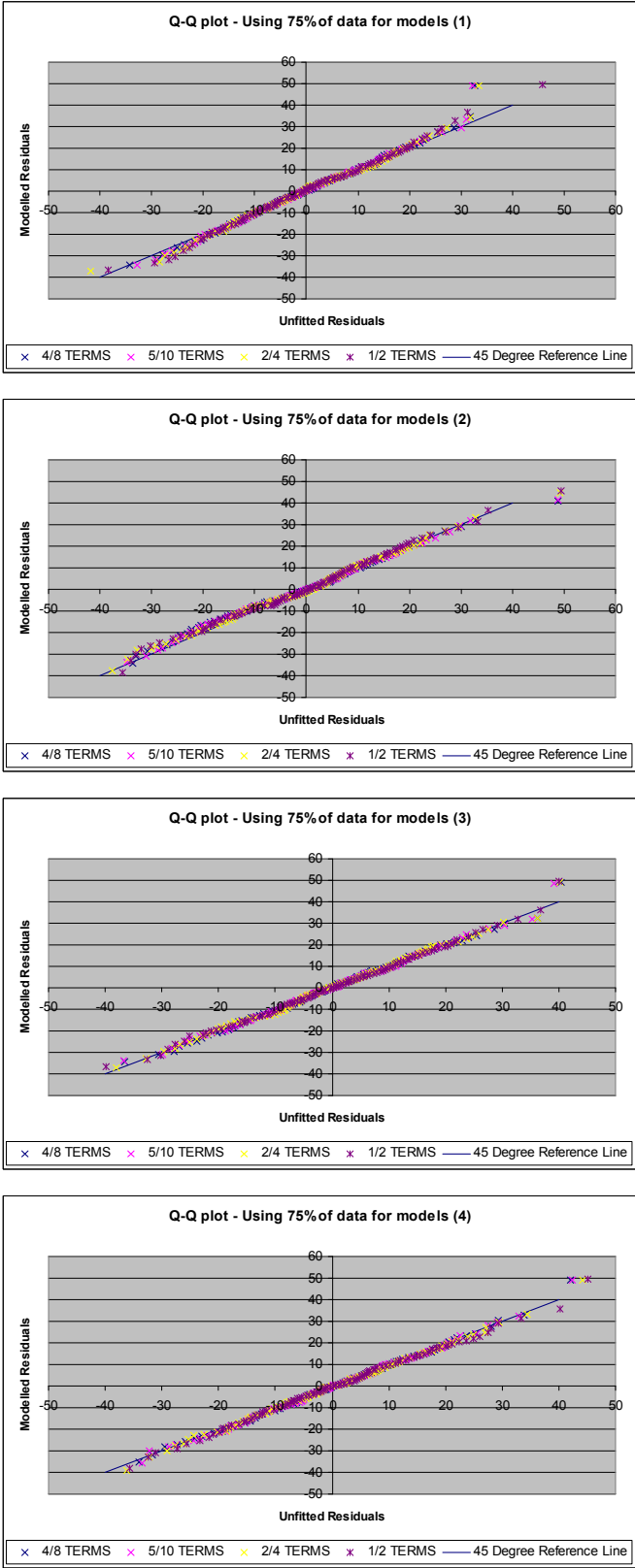


Figure 5.23 Q-Q Plots for Selected %P Seat Models Cross Validation Checks

5.2.5.4 Model Checks for Emotion Rating while Seated

The models selected to predict the %E rating for those seated (Table 5.10) used the same terms and variables as the equivalent models for predicting the perception rating (Table 5.8) and were checked using the same methods.

Table 5.10 Selected Combination Models for Predicting %E Seat

Components

Var./ Terms	V d	FtB d	Sw d	V Ind VDV	V Cum VDV	No. Var.	ln/exp/ sqd	No. Terms	Adjusted R ²
2/4		✓RMS		✓		2	✓ln	4	0.370
4/8	✓RMS	✓RMS	✓RMS	✓		4	✓ln	8	0.416
5/10	✓RMS	✓RMS	✓RMS	✓	✓	5	✓ln	10	0.423

Formulae

Var./ Terms	
2/4	$\%E_{SEAT} = \alpha FtoB \text{ RMSd} + \beta VIndVDV + \phi$
4/8	$\%E_{SEAT} = \alpha VRMSd + \beta FtoBRMSd + \chi SwRMSd + \delta VIndVDV + \epsilon \ln(VRMSd) + \phi \ln(FtoBRMSd) + \gamma \ln(SwRMSd) + \eta \ln(VIndVDV) + \phi$
5/10	$\%E_{SEAT} = \alpha VRMSd + \beta FtoBRMSd + \chi SwRMSd + \delta VIndVDV + \epsilon VCumVDV + \phi \ln(VRMSd) + \gamma \ln(FtoBRMSd) + \eta \ln(SwRMSd) + \iota \ln(VIndVDV) + \kappa \ln(VCumVDV) + \phi$

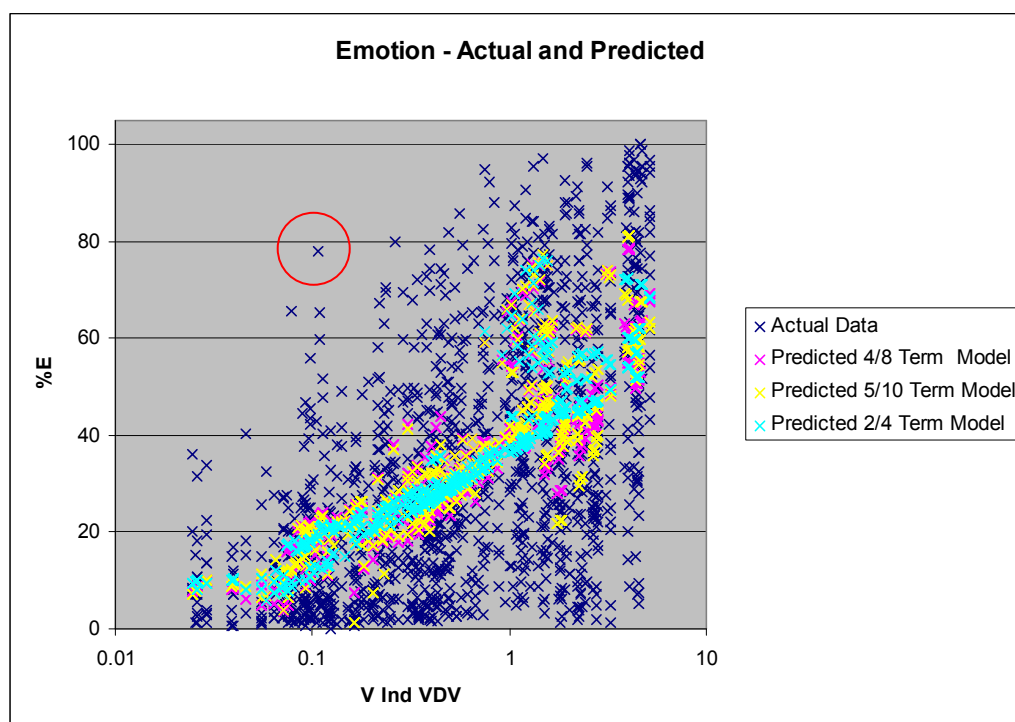


Figure 5.24 Actual and Predicted %E Seat Ratings v Vertical Individual (per Test) Vibration Dose Value

The scatter plots of the actual ratings identified a single point slightly further out from the standard range (Figure 5.24) but it was not deemed sufficiently outlying to be investigated. The modelled %E values sit well with the actual values and appear similar to the equivalent %P models. However compared to the %P models the %E models provide a wider scatter of points to represent the wider range of recorded %E ratings.

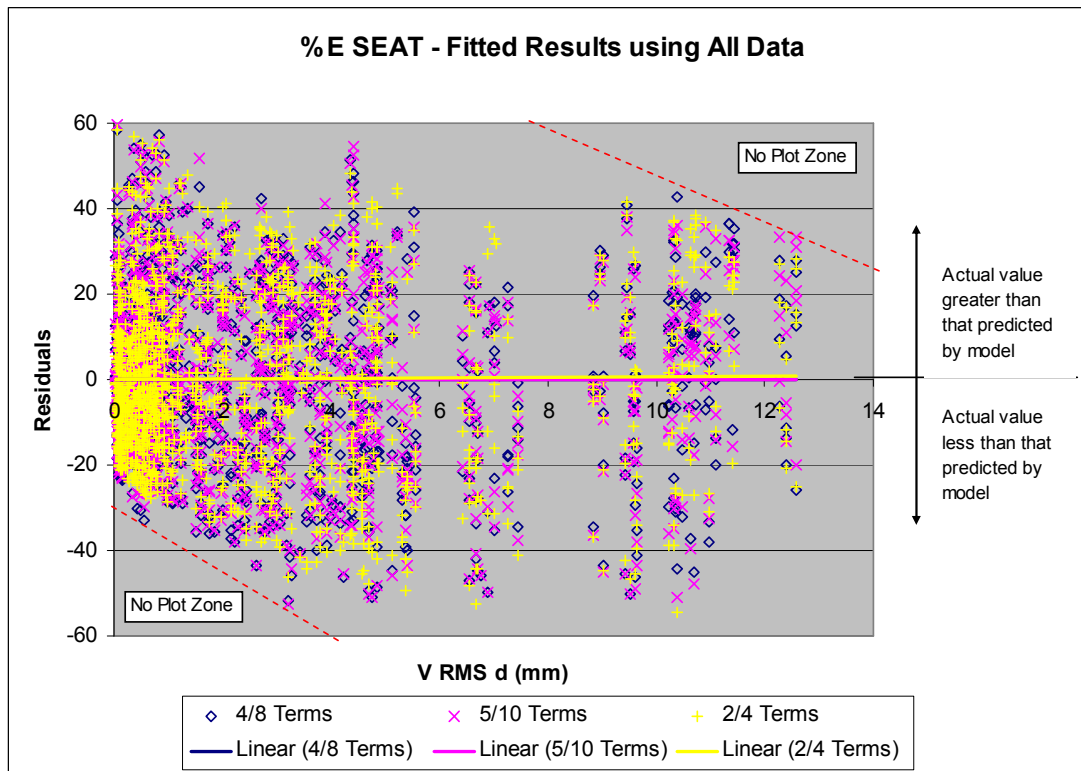


Figure 5.25 Scatter Plot of V RMS d v Residuals for %E Seat Models

As when checking the %P models, for those seated, the scatter plots of each predictor against the residuals do not identify any improvement to the %E models that had not already been previously identified. These plots show that although there is generally an even spread of the residuals across the range of the predictors the no-plot zones identified and explained in Figure 5.21 are becoming evident in these plots, Figure 5.25. This floor effect is particularly noticeable in the bottom left corner due to the low predicted %E ratings for low values of the predictors.

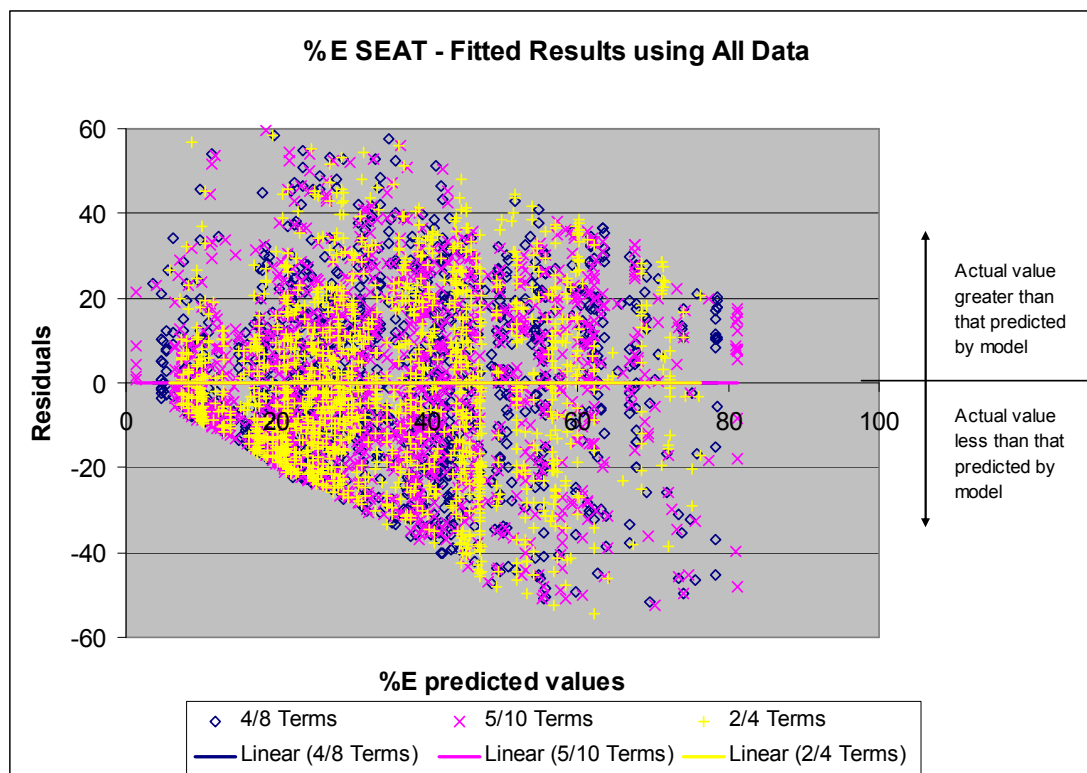


Figure 5.26 Residuals from Test Models v Predicted Seated %E Ratings

The lowest predicted %E value for those seated is 1.2% compared to a minimum prediction of 21.7% for %P seated. As a result the no-plot zones on the predicted %E versus residuals graph are clearly visible (Figure 5.26). Apart from at the lowest end of this plot the difference between the highest and lowest residual at each value of %E is reasonably constant across the predicted %E range.

When the residuals from the selected %E models are plotted against the run order of the tests, the range is slightly less for the 4Hz and 6.5Hz tests carried out in December 2006 compared to the rest of the tests.

As for the perception ratings the errors from the predicted emotion 4/8 and 5/10 model fit well to a normal distribution although the normal probability plots (Figure 5.27) are slightly less straight and with a little more deviation at the extremes than for %P. The distribution of the errors of the selected 2/4 %E model is slightly stepped resulting in a slightly more curved normal probability plot. However the distribution of the 2/4 model errors can still be considered normal as it closely tracks the linear trendline.

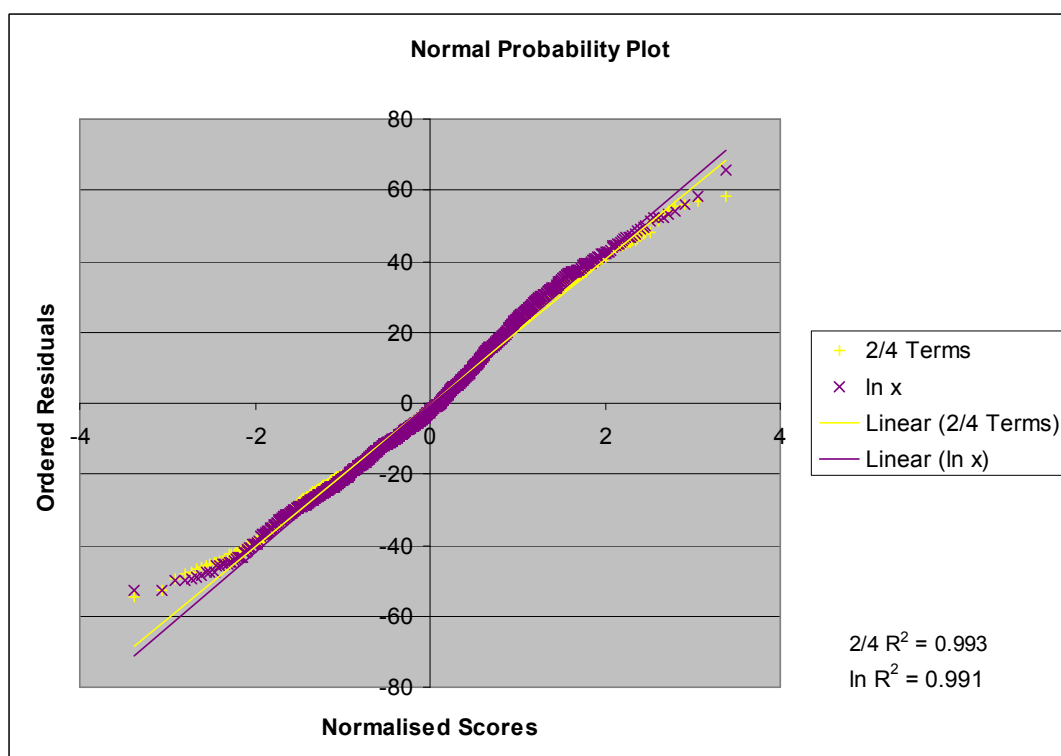
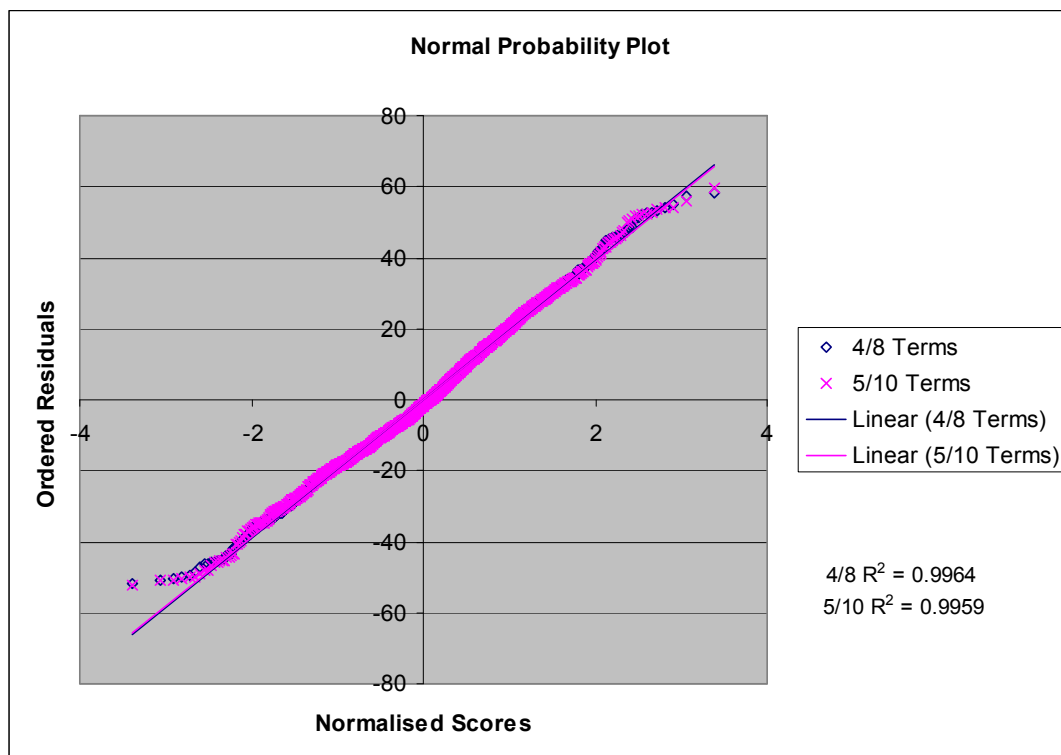


Figure 5.27 Normal Probability Plots for Selected %E Seat Models

As for the combination models, the single variable seated models considered contain the same terms for emotion ratings as for perception ratings. Once again they are based on vertical RMS acceleration ($VRMSa$) but the emotion ratings are harder to predict using a single variable given the wide scatter of the recorded results. This is shown by the R^2 for the %E single variable models being proportionally smaller relative to the maximum R^2 achieved for the %E models than the same comparison for the %P models. The differences between the %E single variable models are similar to those between the perception models but in this case the basic log model was selected (Table 5.11) over the linear and $x + \ln(x)$ as it gave the tightest confidence intervals and only a marginal reduction in R^2 compared to the $x + \ln(x)$ model. The Normal Probability Plot for the selected log model $[\%E_{SEAT} = \alpha \ln(VRMSa) + \phi]$ is very similar to that from the more complex 2/4 combination model, Figure 5.27.

Table 5.11 Selected Single Variable Model for Predicting %E Seat

Components

Var./ Terms	V a	No. Var.	ln/exp/ sqd	No. Terms	Adjust- ed R^2
1/1	✓RMS	1	✓ln only	1	0.318

Formula

Var./ Terms	
1/1	$\%E_{SEAT} = \alpha \ln(VRMSa) + \phi$

Figure 5.28 shows the results from the cross validation checks using out of set data. These show that all four selected models perform well predicting the unfitted data set indicating their potential to be used for a wider population.

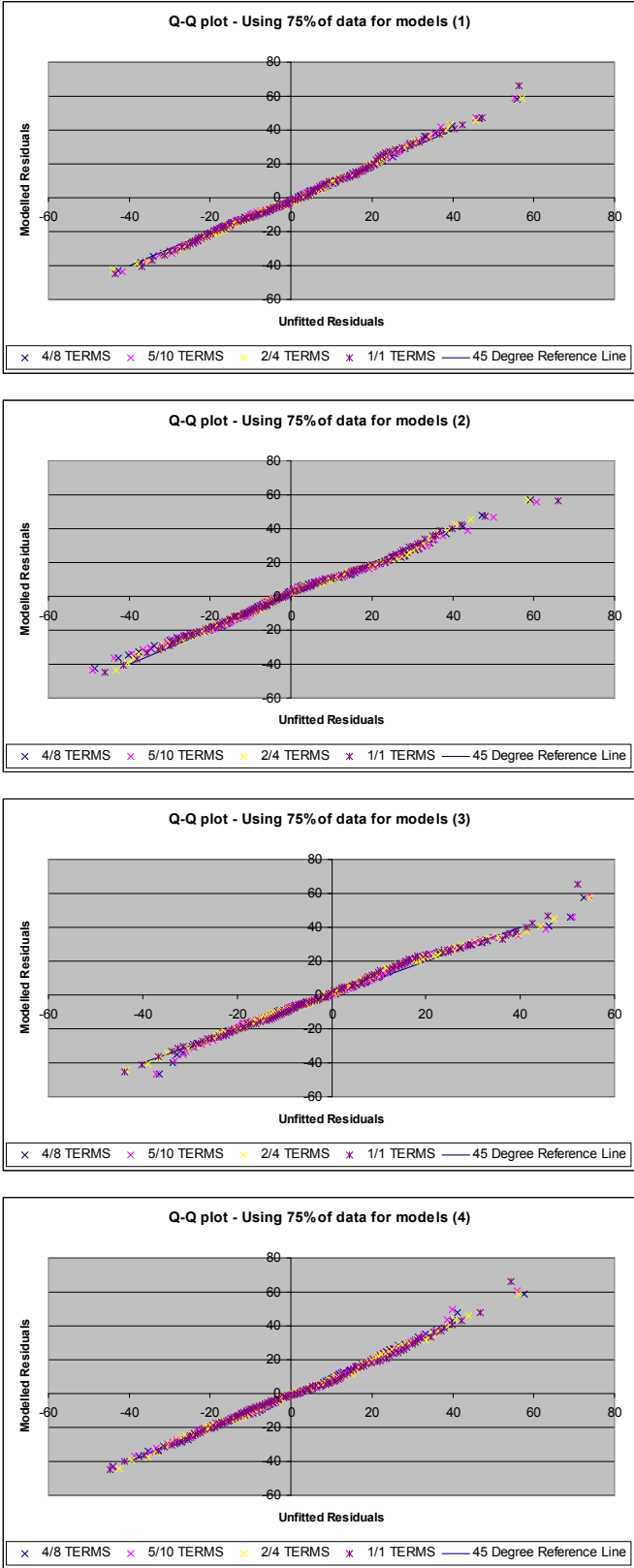


Figure 5.28 Q-Q Plots for Selected %E Seat Models Cross Validation Checks

5.2.5.5 Model Checks for Perception Ratings for those Jumping

Unlike the models for predicting %P and %E for those seated, the selected models for %P for those jumping typically are not improved by the addition of a time component in the form of V IndVDV in place of vertical RMS acceleration (Table 5.12). Interestingly the selected model with 2 variables is based on vertical RMS displacement and acceleration, two predictors which were shown to be very highly interrelated in the correlation analysis. Therefore the accuracy of this model over the best single variable model needs to be critically assessed.

Table 5.12 Selected Combination Models for Predicting %P Jump

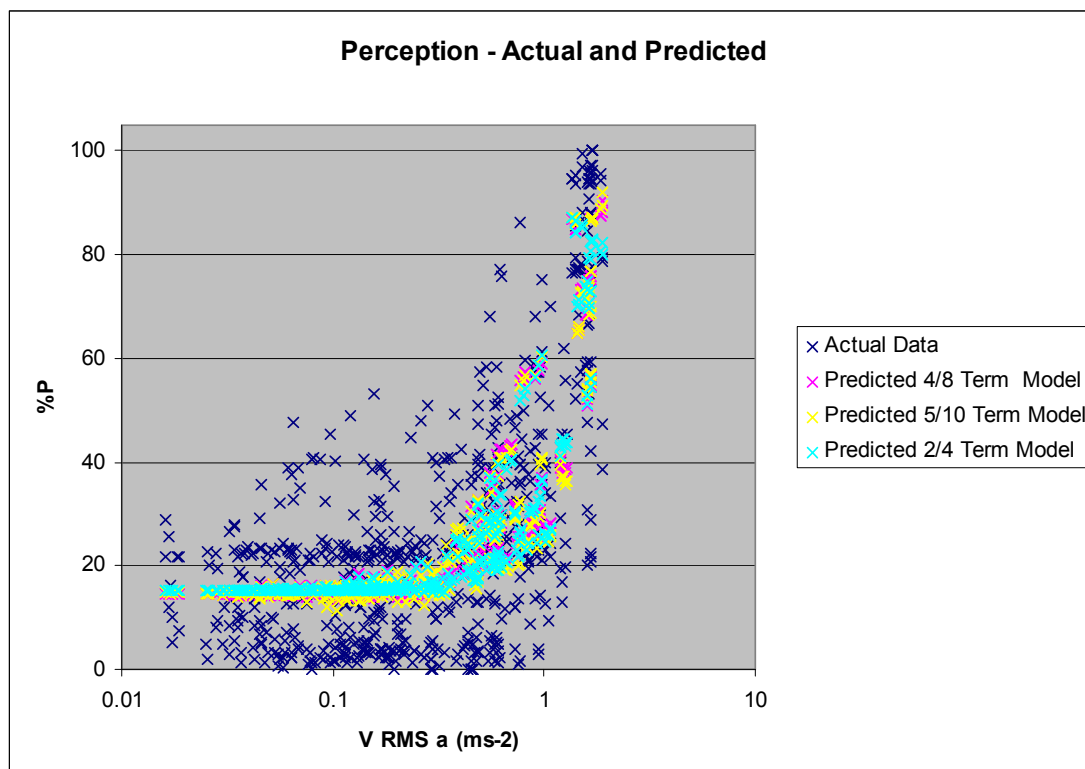
Components

Var./ Terms	V d	V a	FtB d	Sw d	V Ind VDV	No. Var.	In/exp/ sqd	No. Terms	Adjusted R ²
2/3	✓RMS	✓RMS				2	✓ sqd only	3 (with Interaction)	0.650
4/8	✓RMS	✓RMS	✓RMS	✓RMS		4	✓ sqd	8	0.650
5/10	✓RMS	✓RMS	✓RMS	✓RMS	✓	5	✓ sqd	10	0.654

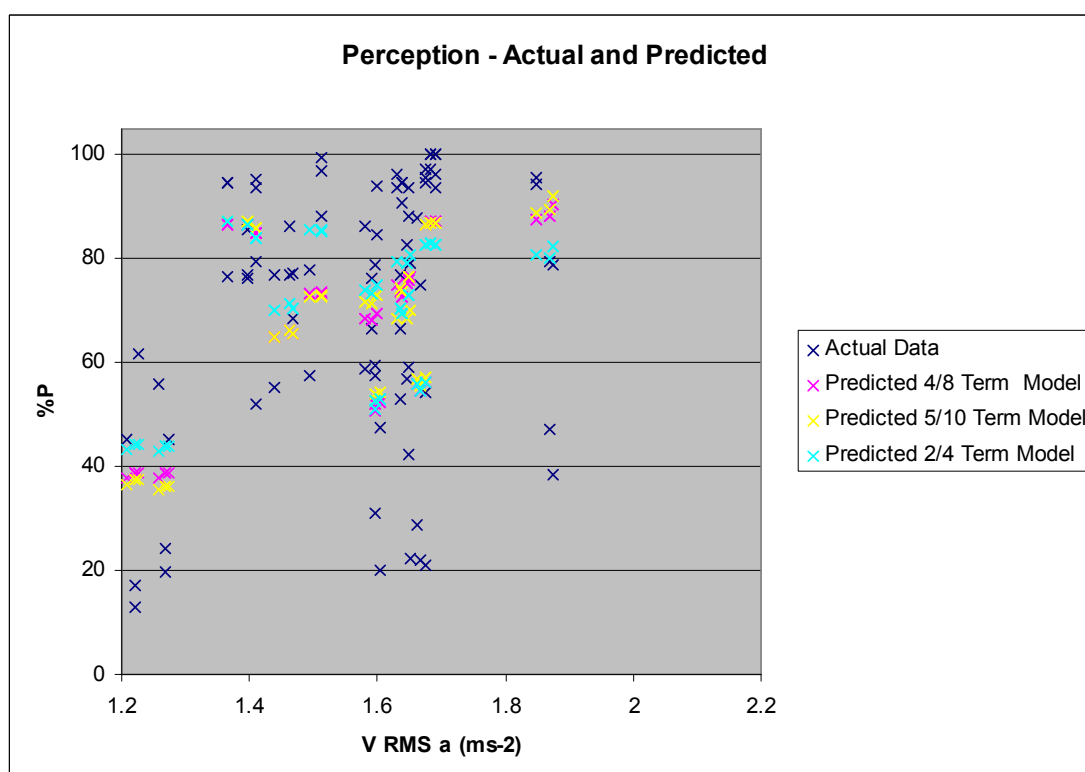
Formulae

Var./ Terms	
2/4	$\%P_{JUMP} = \alpha(VRMSd)^2 + \beta(VRMSa)^2 + \chi((VRMSd)^2 \times (VRMSa)^2) + \phi$
4/8	$\%P_{JUMP} = \alpha VRMSd + \beta VRMSa + \chi FtoBRMSd + \delta SwRMSd + \varepsilon (VRMSd)^2 + \varphi (VRMSa)^2 + \varphi (FtoBRMSd)^2 + \gamma (SwRMSd)^2 + \phi$
5/10	$\%P_{JUMP} = \alpha VRMSd + \beta VRMSa + \chi FtoBRMSd + \delta SwRMSd + \eta VIndVDV + \varepsilon (VRMSd)^2 + \varphi (VRMSa)^2 + \varphi (FtoBRMSd)^2 + \gamma (SwRMSd)^2 + \kappa (VIndVDV)^2 + \phi$

From the initial scatter plots against the predictors, the actual %P ratings show no obvious outliers and the models seem to represent the mean values well for the main body of the results (Figure 5.29a). It is evident from these graphs that the models replicate the initial finding that those jumping have difficulty in perceiving the relative magnitude of small vibrations but once the movement exceeds a certain size the perception ratings rapidly increase. For very small vibrations the models follow an almost constant %P rating. Then once the critical value is reached the predicted ratings increase exponentially and start to show some variation representing the scatter of the actual data.



a) Full Range of Vibrations Tested



b) Upper Bound of Range of Vibrations Tested

Figure 5.29 Actual and Predicted %P Jump Ratings v Vertical RMS Acceleration

At the higher extremes of these plots it can be observed, on close inspection (Figure 5.29 b), that the test which typically produced the maximum predictor values did not record the highest %P ratings. The results from this single test could potentially skew the accuracy of the models at the higher ratings and so the model checks were carried out both including and excluding the results from this test. It was found that omitting the test had very little impact on the outcome except to reduce slightly the number of extreme negative residuals. (This singularity is more apparent for the ratings of those jumping than of those seated).

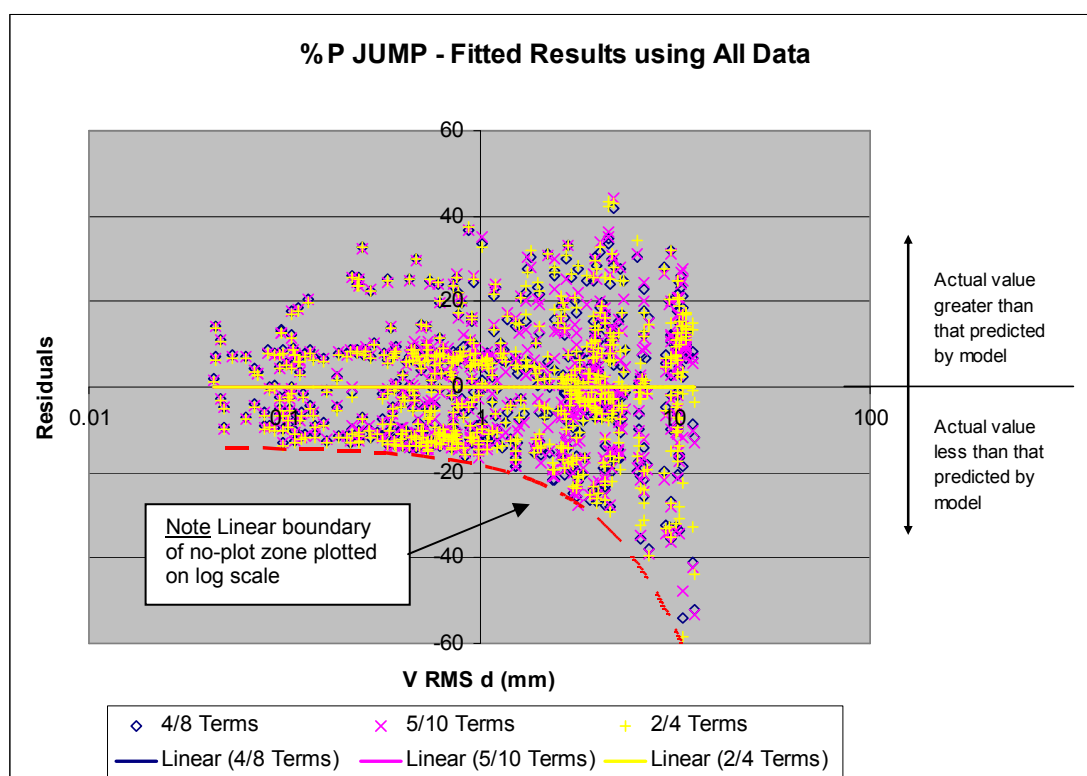


Figure 5.30 Scatter plot of Vertical Displacement against Residuals

The deterministic portion of the %P seat models fit the data well with the only modifications identified being the addition of terms already covered in the model selection process. Because of the jumpers not being able to perceive the vibrations until they reach a critical level the residuals below this level have a relatively constant range but once the vibrations can be perceived the spread of the residuals rises with the vibration size (Figure 5.30). As for %E seat the no-plot zone is very clear below the x-axis for the scatter plots of the predictors against the residuals (Figure 5.30). The upper no-plot zone is harder to see in these graphs but is most evident in the plot with predicted %P (Figure 5.31). Similar to the equivalent plot for predicted %P

for those seated, at the upper end of the range of the predicted values small groups of residuals above the x-axis are balanced by more scattered points further below the x-axis.

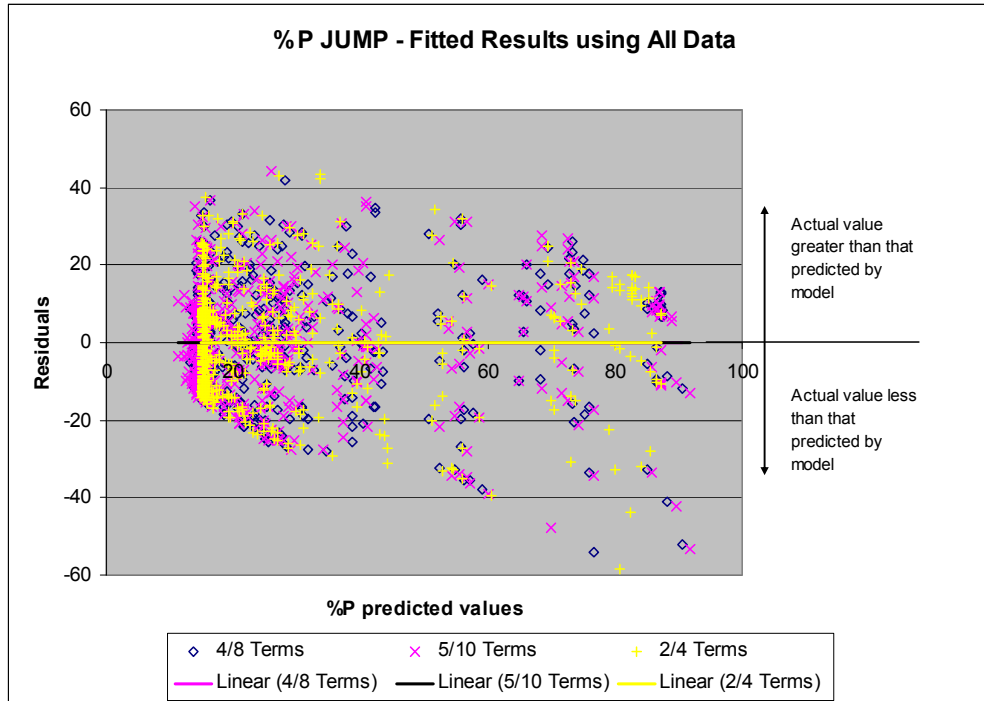
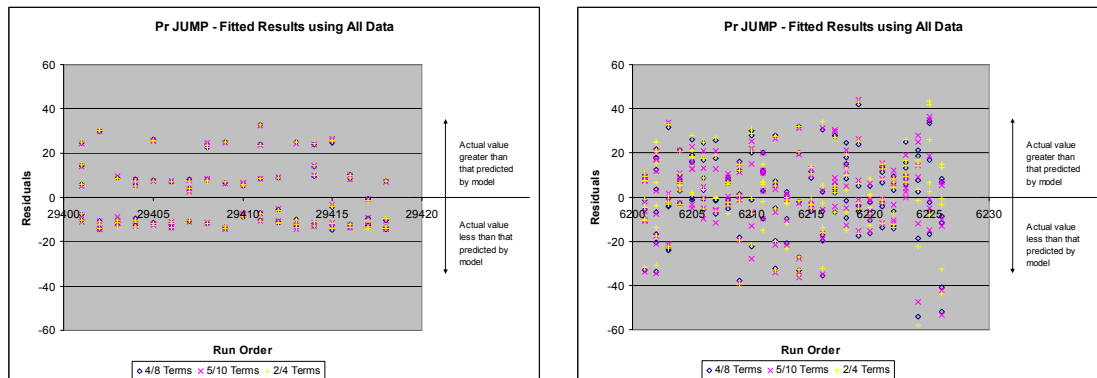


Figure 5.31 Scatter plot of Predicted %P Jump against Residuals



a) 4Hz Rig – October 2007 Tests

b) 2Hz Rig - December 2006 Tests

Figure 5.32 Sample of Scatter Plots of Run Order versus Residuals

From the run order plots the residuals from the three combination models for the tests on the 4Hz and 6.5Hz rigs for %P jump are almost the same (Figure 5.32 a). The differences between the model residuals are greatest on the 2Hz rig in the December 2006 tests (Figure 5.32 b) where the largest vibrations were measured.

The largest range in the residuals for a single test is also recorded on the 2Hz rig in the December 2006 tests. These observations reiterate the finding, from the actual versus predicted ratings scatter plots, that for smaller vibrations the selected models all predict a single value but once past the critical magnitude the models show some spread in the predicted ratings.

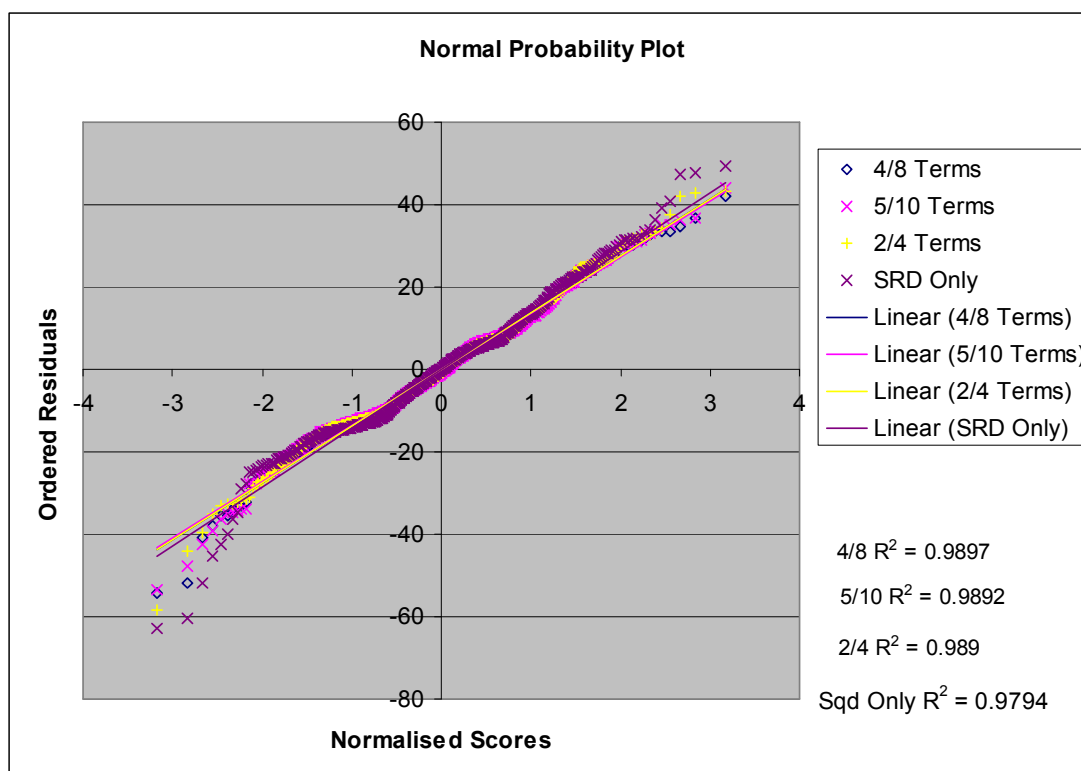


Figure 5.33 Normal Probability plot for selected %P Jump models

As for the seated models the normal probability plots for the residuals follow a straight line but this time the plots clearly cross back and forth along the line (Figure 5.33). This is because although the distribution of the residuals roughly follows a standard normal curve there is evidence of bimodal distribution i.e. two clear secondary peaks (and therefore troughs). This is illustrated in Figure 5.34 where the distribution of the residuals from the 5/10 model is overlaid with the corresponding standard normal distribution curve (based on the mean and standard deviation of the residuals). The reason for these secondary peaks can be found on closer inspection of the recorded ratings. Two clusters of points can be identified either side of the predicted values at the lower end of the graph below (Figure 5.35). These points correspond to the bands on the participant questionnaire for 'imperceptible' and 'barely perceptible' and also to the secondary peaks either side of the mean in Figure 5.34.

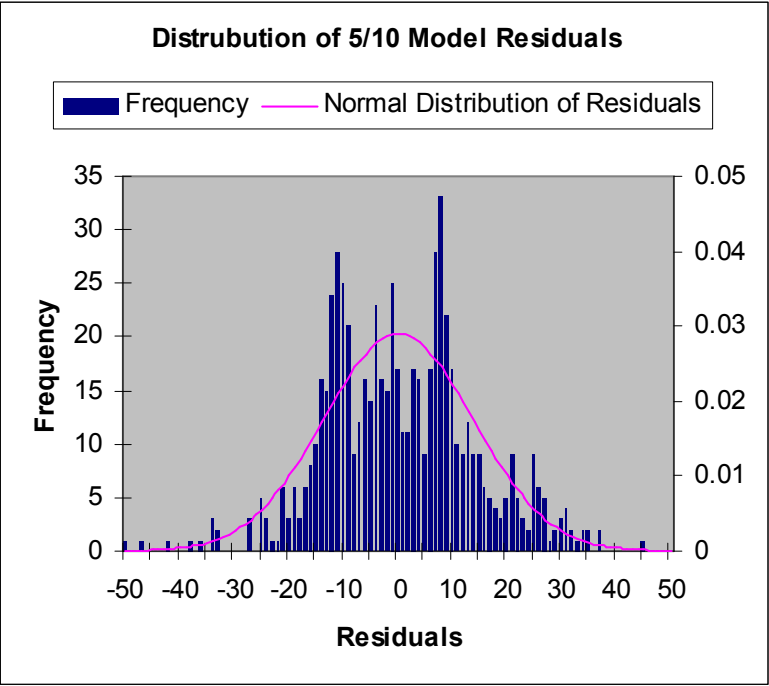


Figure 5.34 Distribution of 5/10 Model Residuals

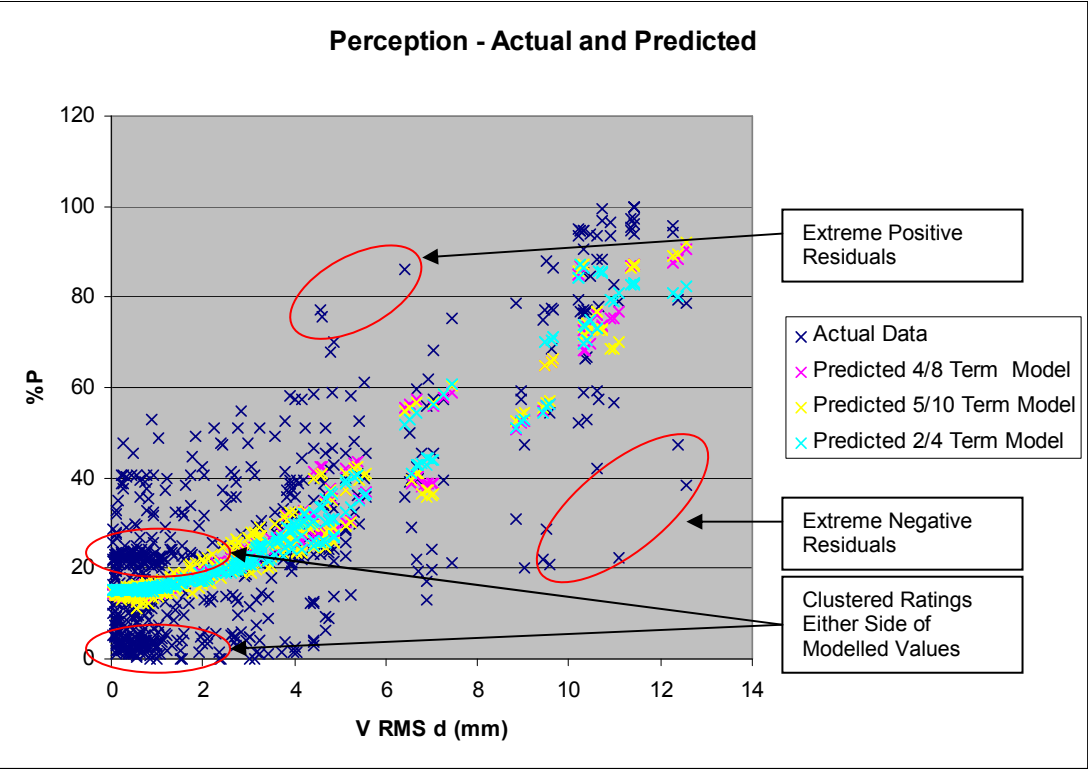


Figure 5.35 Identification of Extreme Residuals

Also in comparison to the seated models the deviation of the points at either end of the normal probability plot is greater. This is particularly noticeable at the lower end of the graph. This can be explained by the extreme recorded responses highlighted in Figure 5.35 and the fact that there are more of these furthest points beneath the modelled ratings than above.

As for the combination models, the key predictor for the single variable models is vertical RMS displacement. For predicting perception ratings for those jumping the polynomial models give the most accurate results for a single predictor. The cubic and quartic models have very wide confidence intervals at the higher end of the ratings. The linear model has tight confidence intervals but fails to sufficiently model the observation that those jumping fail to perceive the relative size of low magnitude vibrations. The model using the square of V RMS d [$\%P_{JUMP} = \alpha(VRMSd)^2 + \phi$] (Table 5.13) was selected over the quadratic model as the confidence intervals were tighter. This simple model performs well against the combination models and gives similar results in both the Normal Probability Plot and the cross validation checks.

Table 5.13 Selected Single Variable Model for Predicting %P Jump

Components

Var./ Terms	V d	No. Var.	In/exp/ sqd	No. Terms	Adjust- ed R ²
1/1	✓RMS	1	✓sqd only	1	0.624

Formula

Var./ Terms	
1/1	$\%P_{JUMP} = \alpha(VRMSd)^2 + \phi$

The cross validation checks for perception models of those jumping are less good than the equivalent models for those seated but still fit reasonably well, Figure 5.36. The outlying points on the Q-Q plots tie in with the extreme residuals identified in Figure 5.35 above.

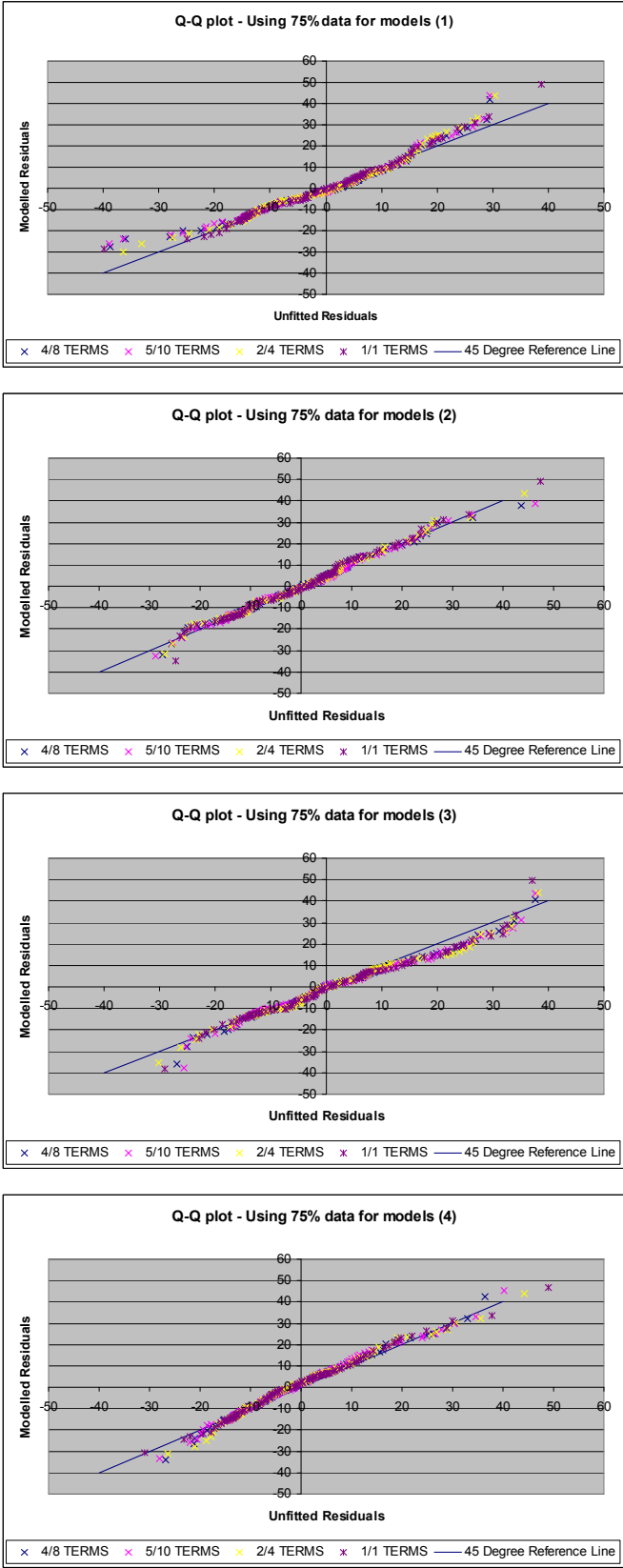


Figure 5.36 Q-Q Plots for Selected %P Jump Models Cross Validation Checks

5.2.5.6 Model Checks for Emotion Ratings for those Jumping

The models chosen to predict %E for those jumping are similar to those used to predict the %P ratings for the same group except the 2/4 model uses vertical displacement with sway displacement in place of vertical acceleration and the 5/10 model uses cumulative VDV rather than individual VDV (Table 5.14).

Table 5.14 Selected Combination Models for Predicting %E Jump

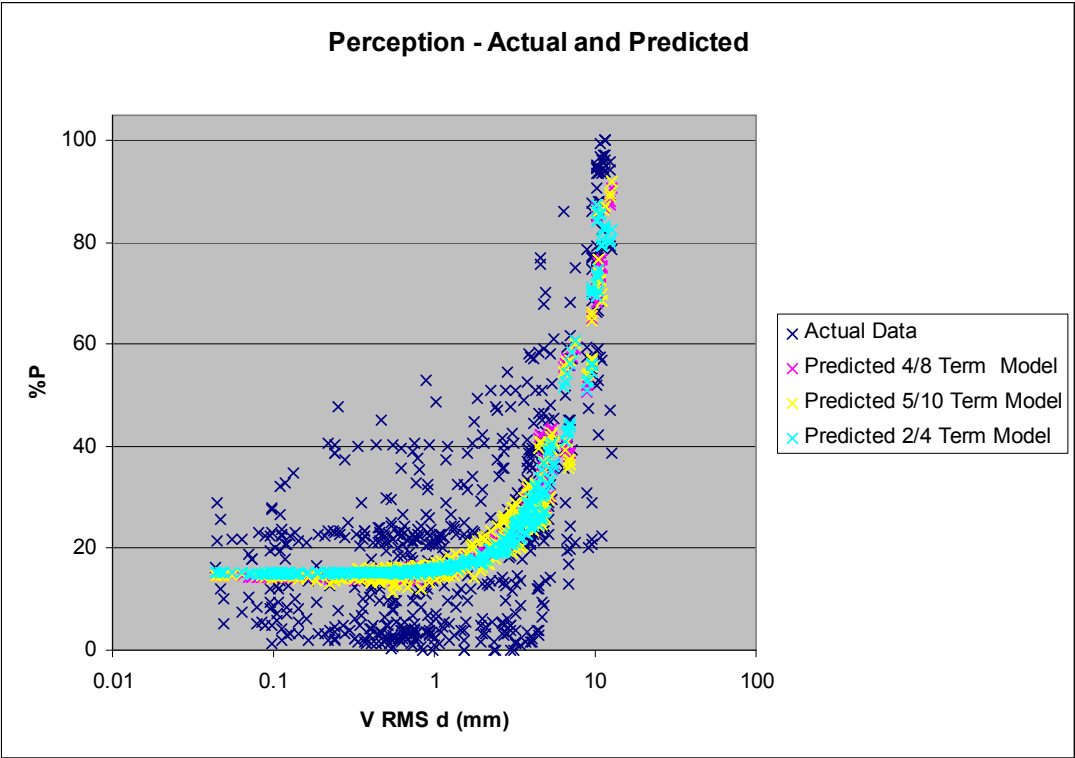
Components

Var./ Terms	V d	V a	FtB d	Sw d	V Cum VDV	No. Var.	In/exp/ sqd	No. Terms	Adjust ed R ²
2/4	✓RMS	✓RMS				2	✓ sqd	4	0.564
4/8	✓RMS	✓RMS	✓RMS	✓RMS		4	✓ sqd	8	0.566
5/10	✓RMS	✓RMS	✓RMS	✓RMS	✓	5	✓ sqd	10	0.572

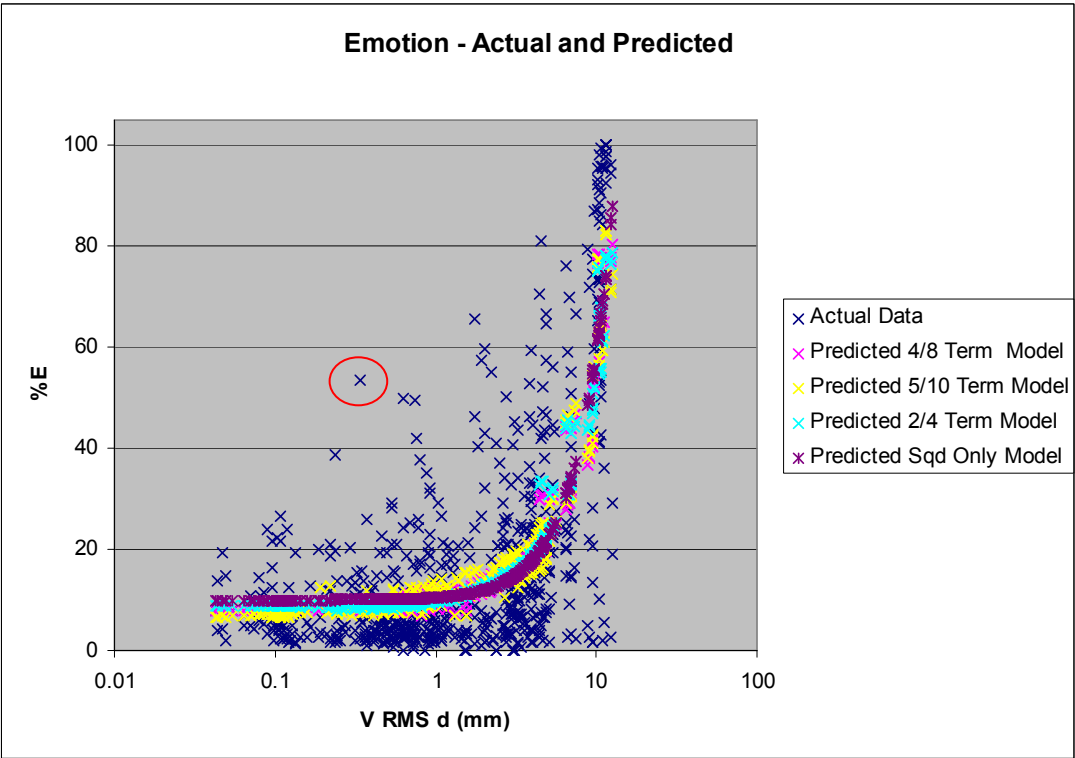
Formulae

Var./ Terms	
2/4	$\%E_{JUMP} = \alpha VRMSd + \beta SwRMSd + \chi (VRMSd)^2 + \delta (SwRMSd)^2 + \phi$
4/8	$\%E_{JUMP} = \alpha VRMSd + \beta VRMSa + \chi FtoBRMSd + \delta SwRMSd + \varepsilon (VRMSd)^2 + \varphi (VRMSa)^2 + \phi (FtoBRMSd)^2 + \gamma (SwRMSd)^2 + \phi$
5/10	$\%E_{JUMP} = \alpha VRMSd + \beta VRMSa + \chi FtoBRMSd + \delta SwRMSd + \eta VCumVDV + \varepsilon (VRMSd)^2 + \varphi (VRMSa)^2 + \phi (FtoBRMSd)^2 + \gamma (SwRMSd)^2 + \kappa (VCumVDV)^2 + \phi$

Again the scatter plots of the actual %E ratings do not identify any significant outliers although there is a single point noticeably just outside the standard variation of the ratings (Figure 5.37 b). As identified for the perception ratings the final 2Hz test from December 2006 produced the highest predictor values but not the corresponding highest perception and emotion ratings. This is more noticeable in the emotion scatter plots as some very low emotion ratings were allocated to this test as well as the expected higher ones. As discussed previously, this single test has the potential to skew the final model but when the model checks were rerun omitting this test the results remained very similar.

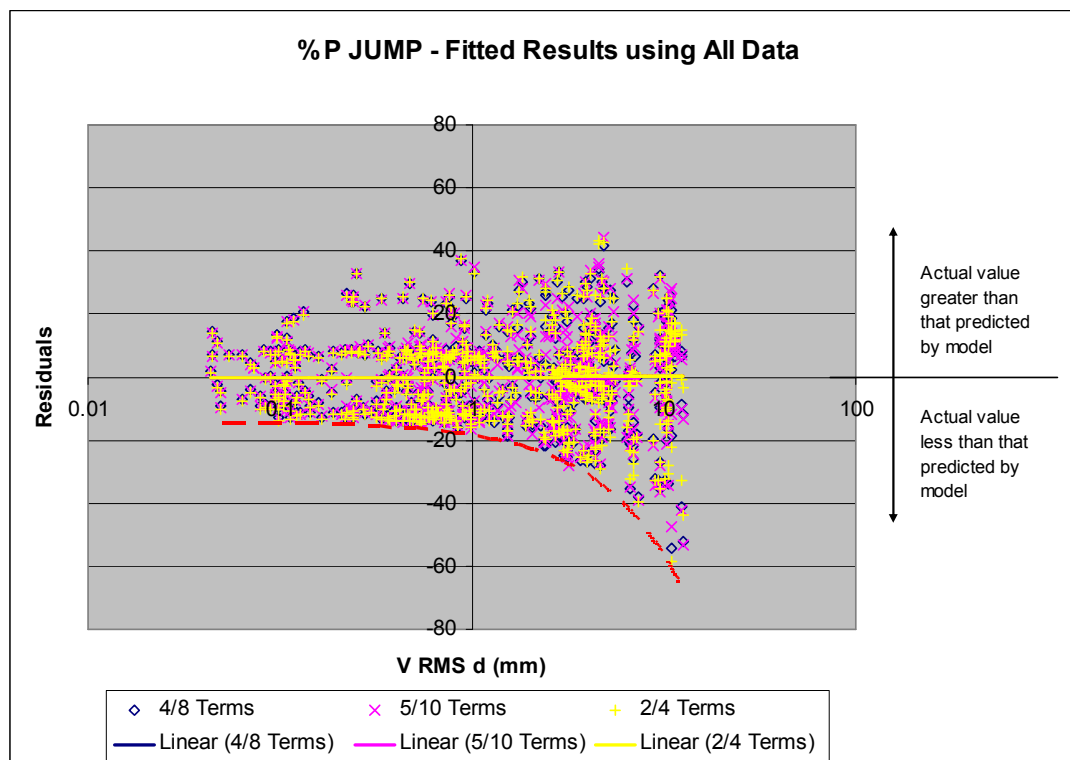


a) %P Jump - Actual and Predicted Ratings

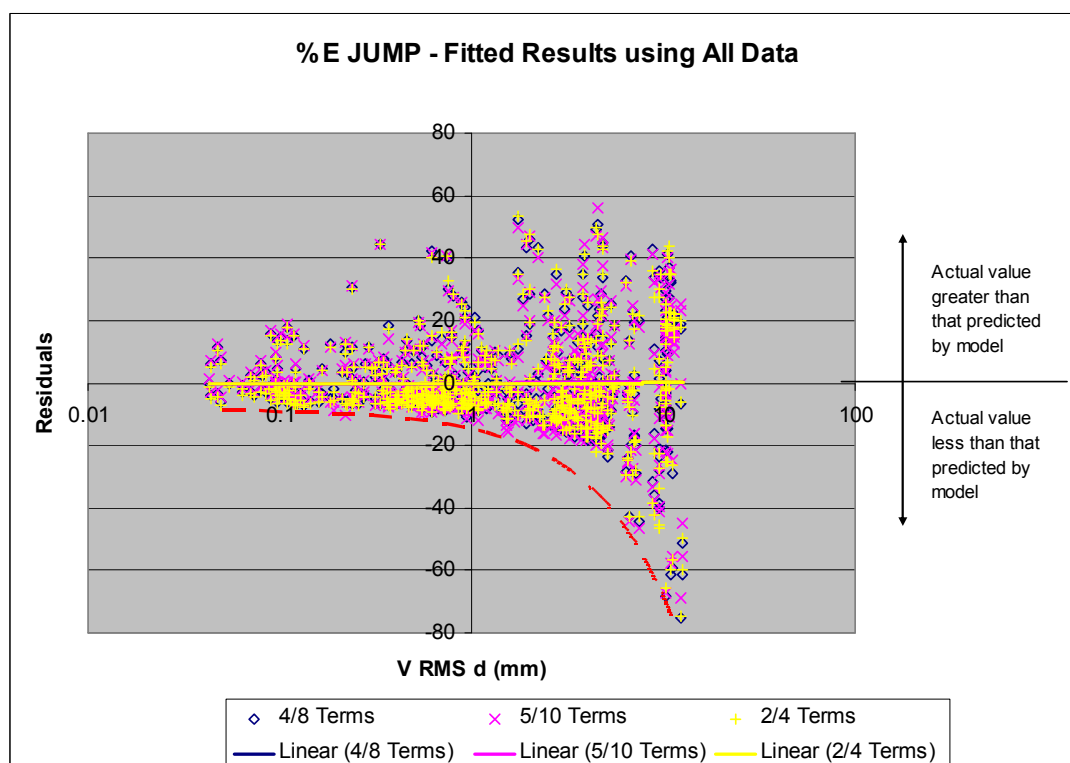


b) %E Jump - Actual and Predicted Ratings

Figure 5.37 Comparison of Models %P Jump and %E Jump



c) %P Jump – Residuals v VRMSd

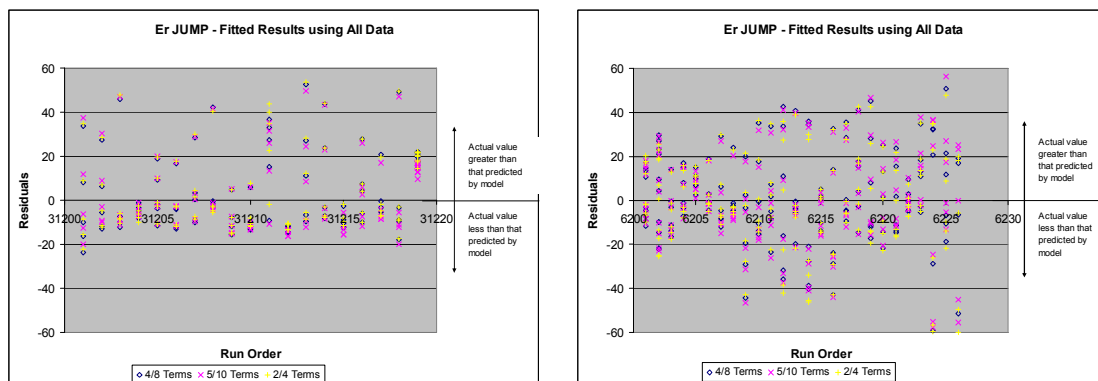


d) %E Jump - Residuals v VRMSd

Figure 5.38 Comparison of Scatter Plots %P Jump and %E Jump

The scatter plots to check the fit of the models did not uncover any additional improvements to the models which had not already been considered. As the emotion ratings lag behind the perception ratings (Figure 5.37 a & b) the plot of predictor versus residuals shows an even steeper drop off in the values beneath the x-axis (Figure 5.38 a & b) corresponding to the steeper rise of the models (Figure 5.38 a & b). Again the lower no-plot zone is clear to the left of the plotted points (Figure 5.38 b) and the upper no-plot zone becomes apparent on the plot of predicted %E values against residuals. The spread of the residuals across the range of the predictors seems fairly even despite the downward trend. Clusters of points below the x-axis balance the more spaced out points above at the lower values of x while the opposite occurs at higher x values. The spread of the %E residuals is greater than for %P mirroring the greater spread of the actual values of %E.

When the residuals are plotted test by test the main difference in the models is clearly how they model the ratings for the 2Hz rig tests from December 2006. For the majority of the other tests the residuals for all three models lie almost on top of one another (Figure 5.39 a) while the residuals for each model are different for the December 2006 test on the 2Hz rig (Figure 5.39 b). Another interesting point is that, except for the 2Hz rig tests from December 2006, the under-predictions are much less than the over-predictions (Figure 5.39 a) possibly related to the fact that the predicted %E remains low for a large section of the range of the predictors.



a) 2Hz Rig – October 2007 Tests

b) 2Hz Rig – December Tests

Figure 5.39 Sample of Scatter Plots of Run Order versus Residuals

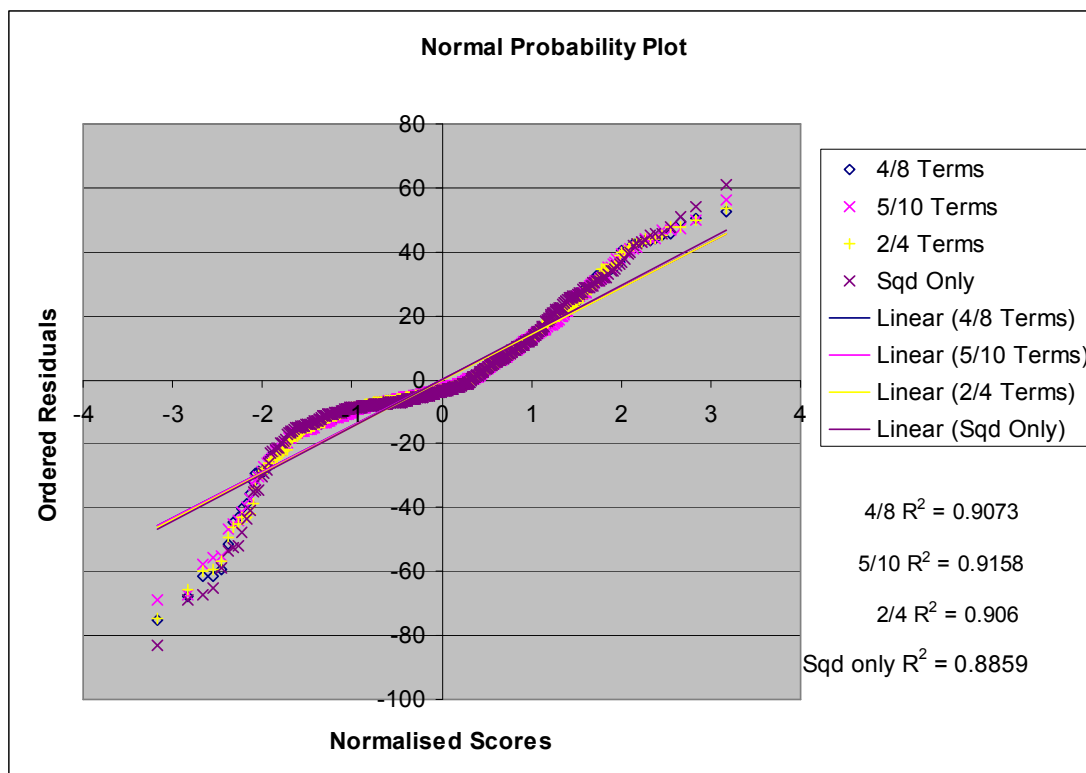


Figure 5.40 Normal Probability plot for selected %E Jump models

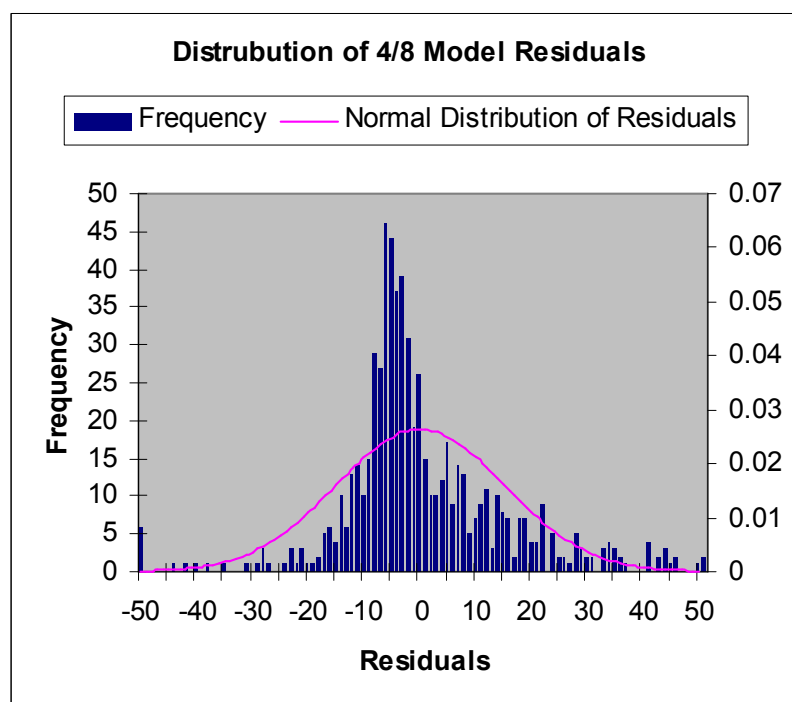


Figure 5.41 Distribution of 4/8 Model Residuals

The probability plot for the %E jump model residuals is S-shaped with significant deviation at either end (Figure 5.40). From an assessment of the histograms of the residuals it appears that the error distribution has much narrower central peak than a standard normal distribution (based on the mean and standard deviation of the residuals), Figure 5.41. The reason for this deviation from a normal distribution appears to be largely due to the floor effect (or no-plot zones) identified earlier. Because the ratings for %E for smaller vibrations are very low and remain low until the jumpers can perceive the vibration there is a clustering of recorded responses between 0 and 10%, Figure 5.42. Then as the model predicts a near constant value through this zone there is a concentration of residuals with similar values below the model resulting in the tall narrow peak in the distribution, Figure 5.41. If the actual values were more evenly scattered about the model at the lower end of the range then a normal distribution of errors would be achieved. The extreme residuals at either end of the Normal Probability Plot (Figure 5.40) are due to the wide spread of the recorded emotion ratings particularly for the larger vibrations.

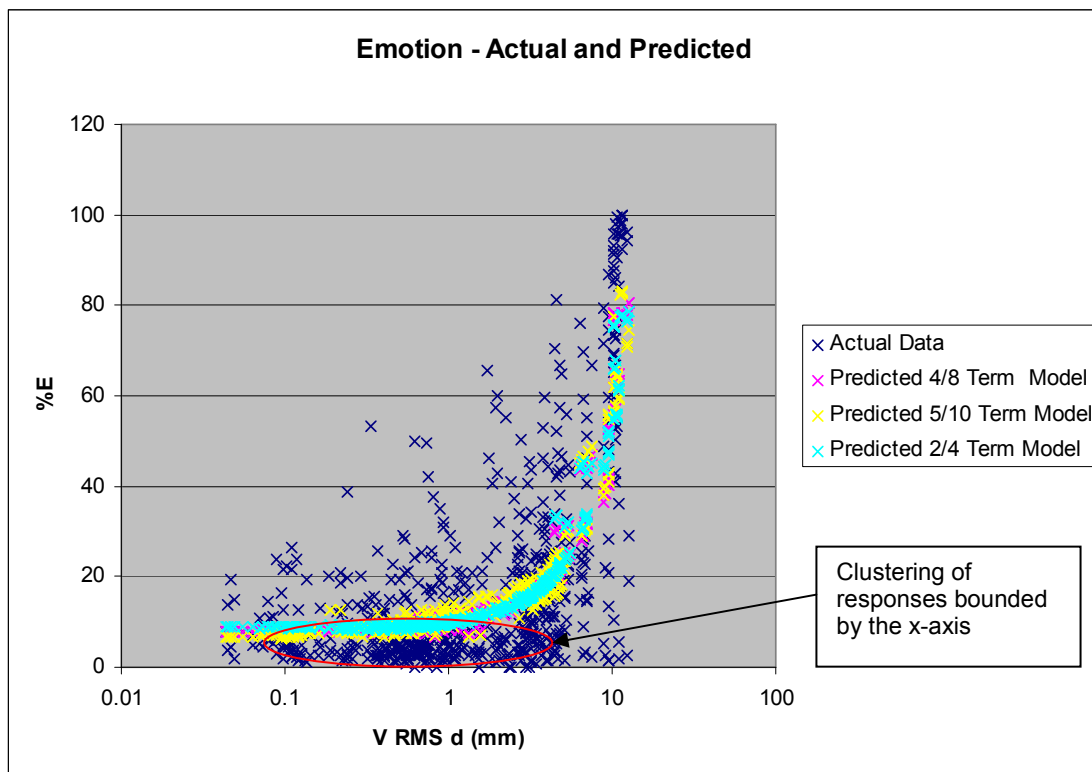


Figure 5.42 Scatter Plot Identifying Clustering of Responses along X-Axis

As for those seated the best single variable jumping models for emotion are similar in form to those for perception. Similar to %P jumping the squared only model using VRMSd provides the best balance of accuracy and simplicity for modelling emotion ratings of those jumping (Table 5.15) and produces a similar response to the more complex models on the Normal Probability Plot, Figure 5.40.

Table 5.15 Selected Single Variable Model for Predicting %E Jump Components

Var./ Terms	V d	No. Var.	In/exp/ sqd	No. Terms	Adjust- ed R ²
1/1	✓RMS	1	✓sqd only	1	0.544

Formula

Var./ Terms	
1/1	$\%E_{JUMP} = \alpha(VRMSd)^2 + \phi$

Again the cross validation checks prove that the four selected models can fairly accurately predict for out of set data, Figure 5.43, albeit with some outlying residuals due to the wide spread of the recorded responses .

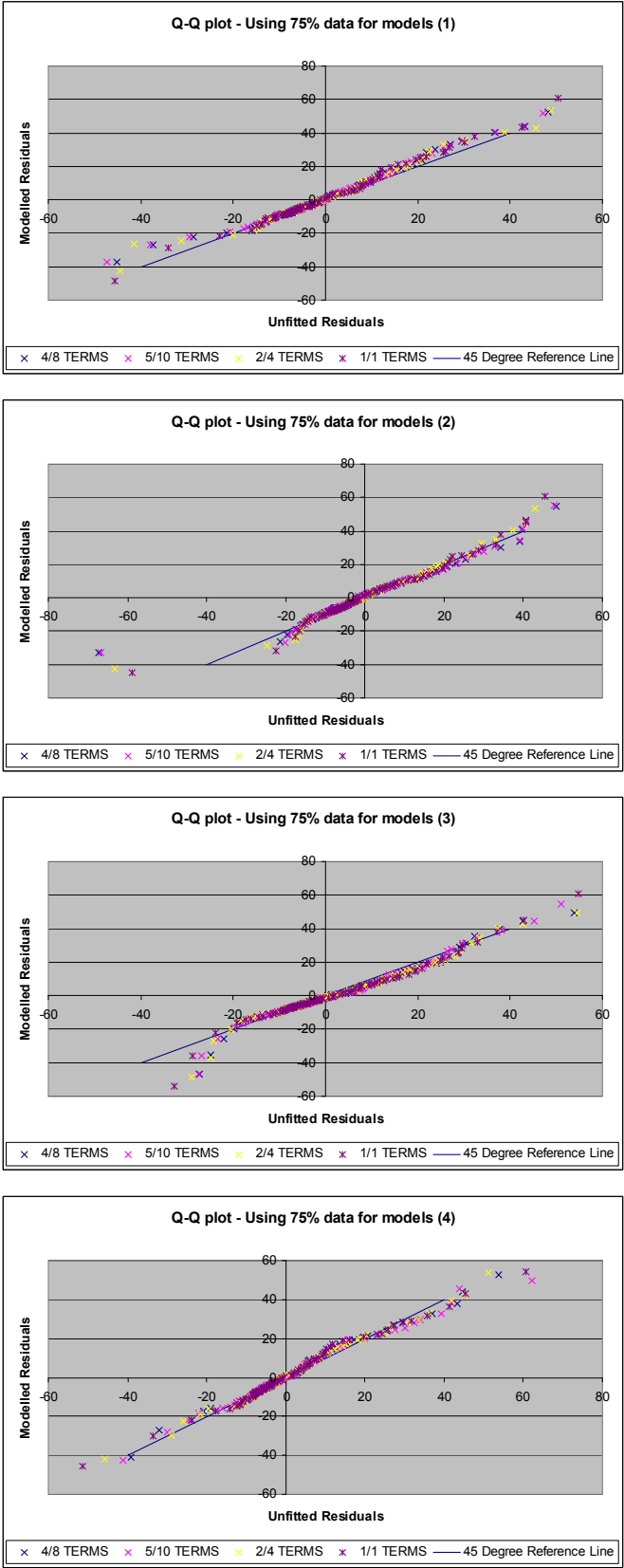


Figure 5.43 Q-Q Plots for Selected %E Jump Models Cross Validation Checks

5.2.5.7 Statistical Analysis - Summary of Check Results

From the checks carried out, all the selected models (Tables 5.8 to 5.15) perform adequately in defining the human response based on the collected data within the vibration range of the tests. For each of the four dependent variables (%P Seat, %E Seat, %P Jump and %E Jump) there is little to choose between the models except for their complexity and accuracy (in the form of R^2). Despite achieving higher R^2 values, than for those seated, the %P and %E models for those jumping performed less well in the validation process. This is, however, largely to do with the floor effect of the collected data being concentrated at the lower end of the ratings scale for small vibrations rather than there being an error with the models. Re-running the checks for the %E Jump models for the data beyond the values clustered on the x-axis (above 4mm VRMSd) produces a much straighter normal probability plot (Figure 5.44).

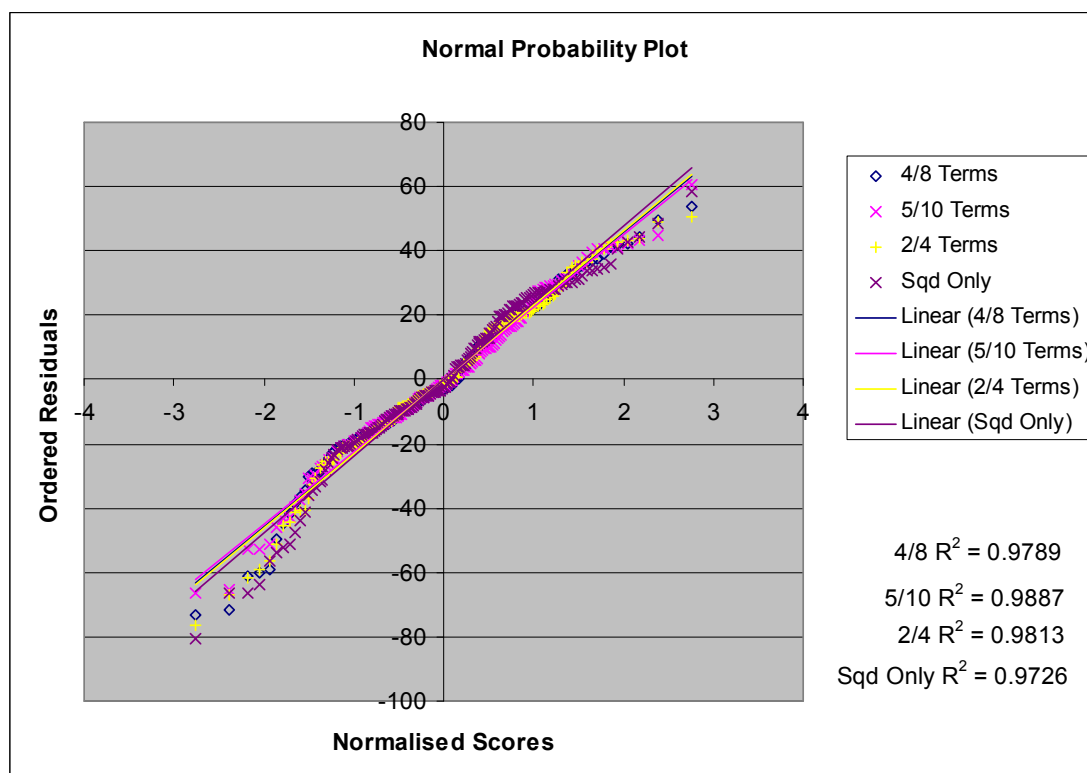


Figure 5.44 Normal Probability plot for selected %E Jump models (for data above 4mm VRMSd)

5.2.6 Human Response - Summary

Those that are seated perceive all but the smallest vibrations and there are many factors which influence their perception. When trying to model this complex relationship the best predictors were found to be those that described the average magnitude of the vibration, in particular the RMS values. Of the models developed the most accurate ones included terms describing the motion of the rig in three dimensions with displacement, acceleration and time components. For those seated, the perception model that gives the best balance of accuracy and simplicity is the selected 2/4 model (Figure 5.45). This takes the form

$$\%P_{SEAT} = \alpha x + \beta \ln x + \chi z + \delta \ln z + \phi \quad \text{where } x = VindVDV \text{ \& } z = FtoB \text{ RMSd}$$

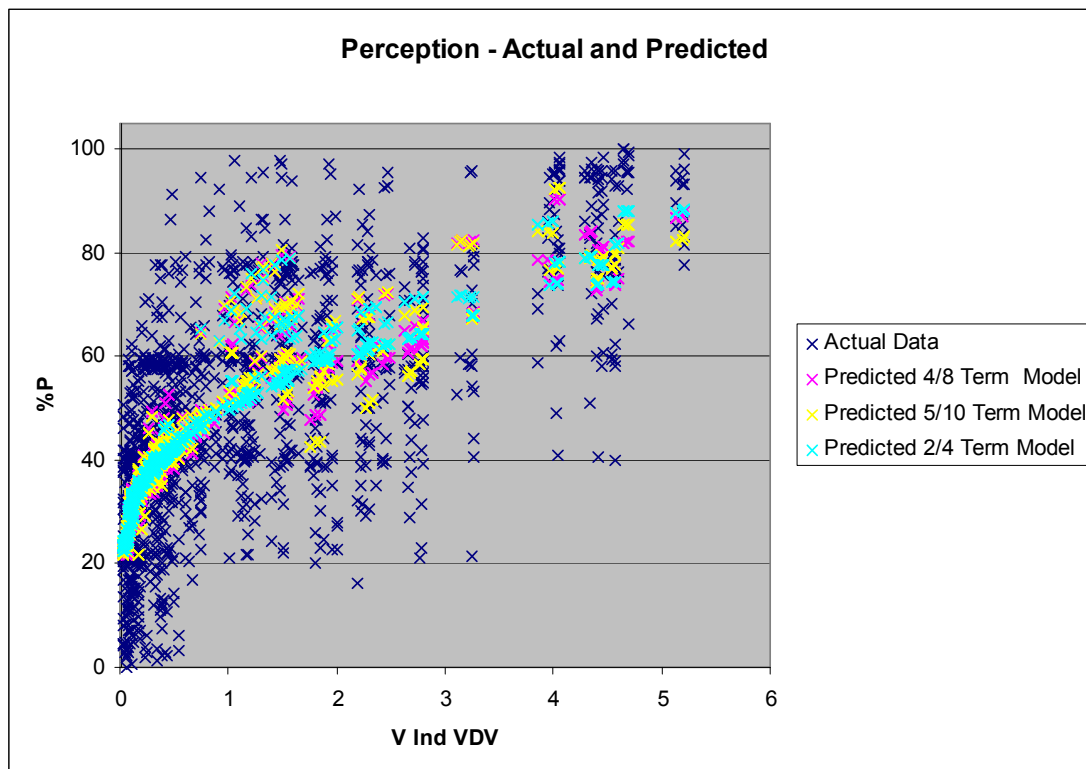
i.e. the seated participants' perception rating is predicted using the RMS vertical acceleration, the duration of the vibration and the RMS front-to-back displacement. The adjusted R^2 value for this model is 0.525, 94% of the value of the model which achieves the highest R^2 for seated %P (using 8 variables and 16 terms) (Table 5.7). However it should be noted that if the time component is excluded from this model (i.e. using VRMSa in place of VindVDV) the difference is insignificant (adjusted R^2 = 0.524). Vibration dose value (VDV) terms were included in the three larger seated perception models selected for checking as they gave marginally better R^2 values although the use of VDV's requires an additional variable to be measured (time) thus adding complexity for very little additional accuracy.

The test rig was designed so that the response would be primarily vertical but similar to a permanent cantilevered grandstand there was an element of front-to-back motion due to the incline of the tier and minimal sway. For a small proportion of the tests the front-to-back component was significantly greater. This occurred for some of the 2Hz rig set-ups where the crowd group was small and located towards front of rig and excited a near resonant response of the rig when jumping at 1.7 and 1.9Hz. Interestingly this larger front-to-back motion affects those seated (making it a significant component of the seated perception and emotion models) but not those jumping.

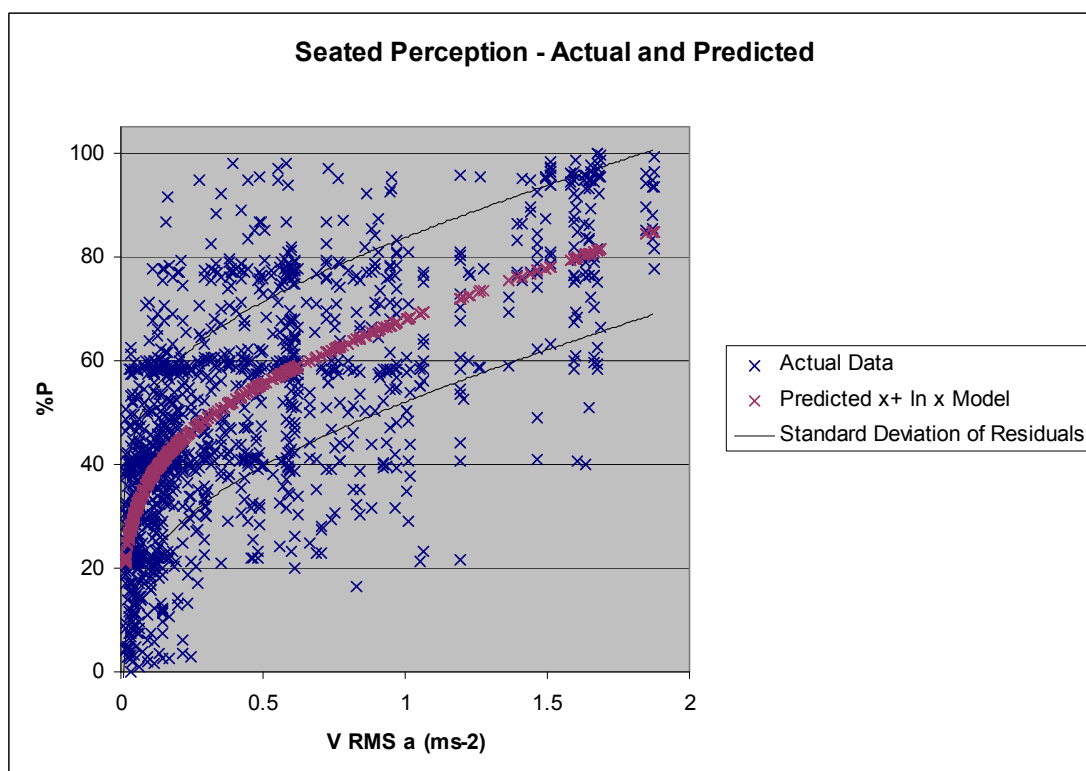
By comparison, the best single variable model (Figure 5.45) is based on

$$\%P_{SEAT} = \alpha x + \beta \ln x + \phi \quad \text{with } x = VRMSa$$

and obtains an adjusted R^2 of 0.496, 89% of the maximum 8/16 %P seated model.

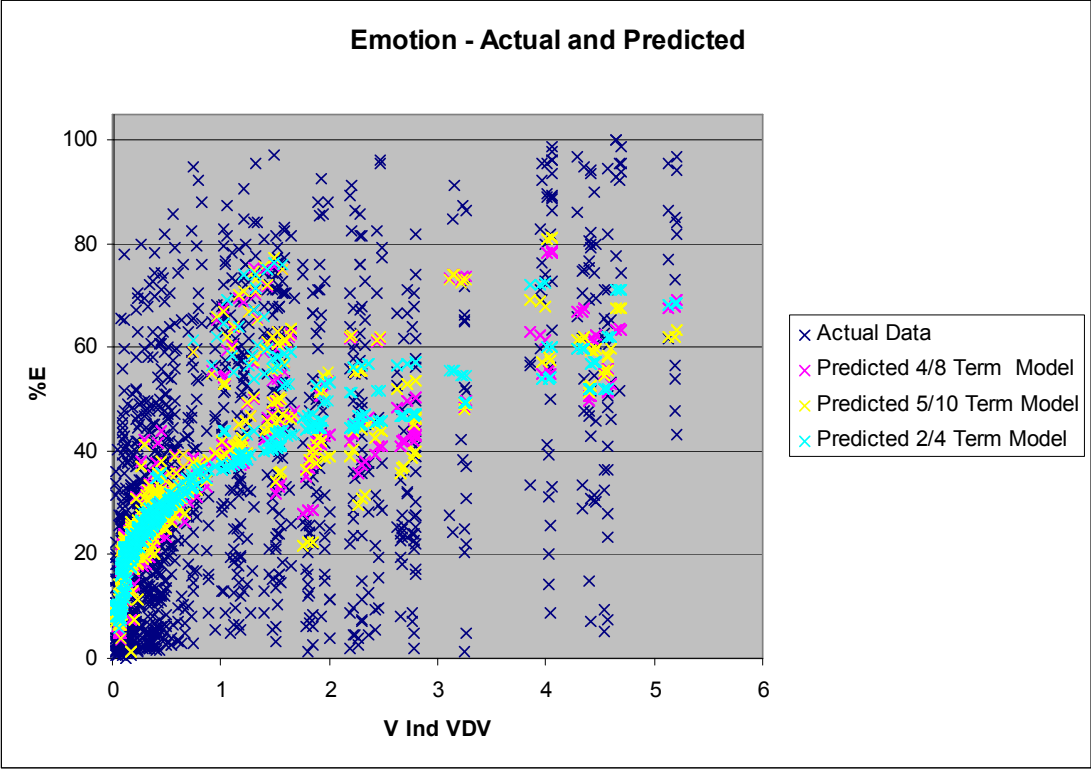


For details of Combination Models see Table 5.8

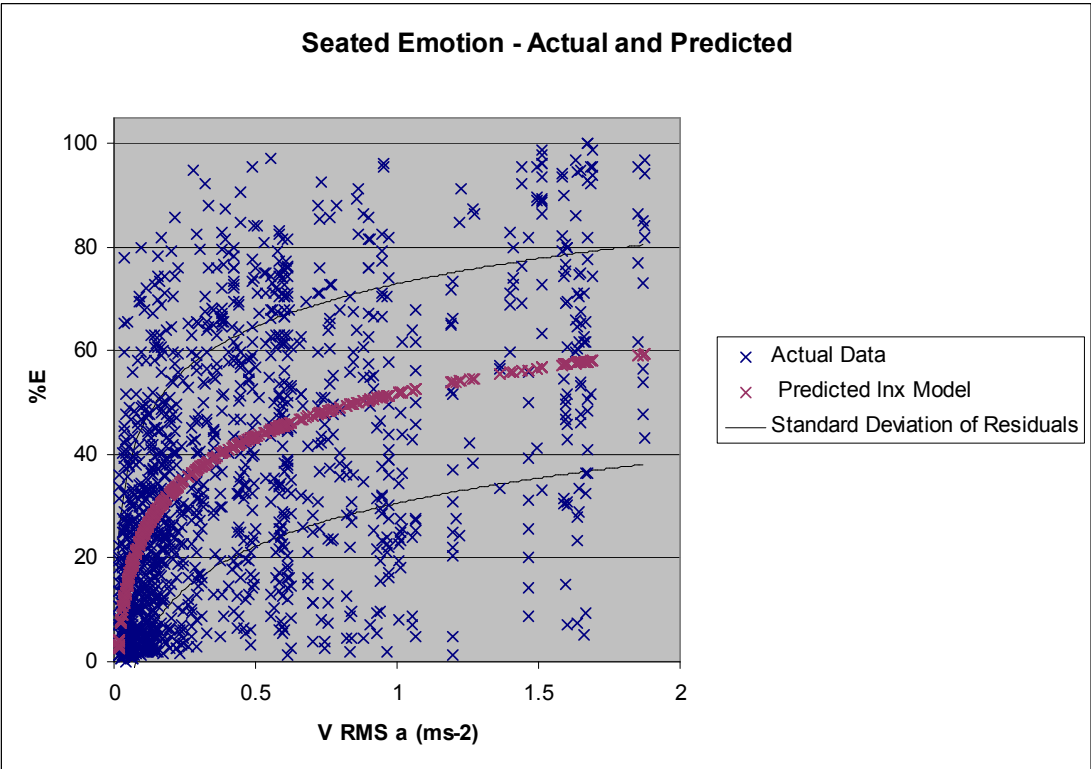


For details of Single Variable Model see Table 5.9

Figure 5.45 Selected Models for Seated Perception Ratings



For details of Combination Models see Table 5.10



For details of Single Variable Model see Table 5.11

Figure 5.46 Selected Models for Seated Emotion Ratings

The changing slope of the logarithmic shape of these models suggests that those seated are very sensitive to small changes in the magnitude of the vibrations when they are below approximately 0.15ms^{-2} vertical RMS acceleration (1mm vertical RMS displacement) but as the vibrations increase in size become less perceptible. The models generated typically reflect the mean values of the recorded responses and give an indication of the relationship between the measured predictors and the recorded perception ratings. What the models fail to show is the spread of the actual values around the mean. This is given by the R^2 value and the standard deviation of the residuals (Table 5.16 and Figure 5.45). For the recorded %P ratings the spread of the values is fairly constant (at 80%) through the majority of the measured vibration range. This spread starts to reduce towards the top of the range as the participants' views on the size of the vibrations begin to converge. A similar observation can be made at the very bottom of the recorded vibration range where the range of actual perception ratings reduces to around 60%.

Table 5.16 Summary of R^2 and Standard Deviation of Residuals for Selected %P Models for those Seated

%P_{SEAT} Models	Adjusted R^2	St Dev of Residuals
Single Variable 1/2	0.496	15.851
Combination 2/4	0.525	15.375
4/8	0.549	14.967
5/10	0.556	14.836

The recorded emotion ratings for the same group of seated participants follow a similar trend to the corresponding perception ratings. The main difference is that the values are generally lower and the spread of the ratings across the range of the measured vibrations is much greater (above 90% for the majority of the tests). The spread of the results is also highlighted in the lower R^2 values and higher standard deviation of the model residuals (Table 5.17 and Figure 5.46). The most accurate models developed for predicting the emotion ratings for those seated use the same terms as those for seated perception ratings but achieve lower R^2 values due to the wider scatter of the results (Figure 5.46). Again the best balance of accuracy and simplicity is the 2/4 model

$$\%E_{SEAT} = \alpha x + \beta \ln x + \gamma z + \delta \ln z + \phi \quad \text{where } x = V \ln dVDV \text{ \& } z = FtoB \text{ RMSd}$$

achieving an adjusted R^2 value of 0.370, 87% of the maximum adjusted R^2 value obtained for the best seated %E model using 8 variables and 16 terms. As for the

perception model replacing the VIndVDV term for the simpler VRMSa has minimal effect on the accuracy of the model.

For the emotion ratings the single variable seated model

$$\%E_{SEAT} = \alpha \ln x + \phi \quad \text{with } x = VRMSa$$

proves the most accurate and has an adjusted R^2 value of 0.318, 75% of the maximum 8/16 seated %E model.

Table 5.17 Summary of R^2 and Standard Deviation of Residuals for Selected %E Models for those Seated

%E _{SEAT} Models	Adjusted R^2	St Dev of Residuals
Single Variable 1/1	0.318	21.194
Combination 2/4	0.370	20.359
4/8	0.416	19.578
5/10	0.423	19.435

Those jumping perceive the vibrations differently from those seated. When the vibrations are small those creating them have difficulty in determining their magnitude but once the movement exceeds approximately 0.3ms^{-2} RMS acceleration ($\sim 1.5\text{mm}$ vertical RMS displacement) the jumpers begin to be able to discern the relative sizes of the vibrations (Figure 5.47). This results in a parabolic trend line when the jumping perception ratings are plotted against the rig movement. As for those seated it is generally the models based on the RMS format of the displacement and acceleration that perform the best. For those jumping the time component seems less important with the most accurate models being based on the three dimensions of displacement of the rig and acceleration. Unlike the seated participants it appears that the jumpers' perception can be modeled fairly accurately using a simple single variable model based on the vertical displacement of the rig (not vertical acceleration as for those seated). The best single variable model takes the form

$$\%P_{JUMP} = \alpha x^2 + \phi \quad \text{where } x = VRMSd$$

and has an adjusted R^2 value of 0.624, 94% of the maximum adjusted R^2 value achieved by the developed jumping perception models (4 variables/15 terms) (Table 5.7). (The slightly more complex 2/3 model achieves an R^2 value of 0.650 98% of the maximum adjusted R^2 value achieved.)

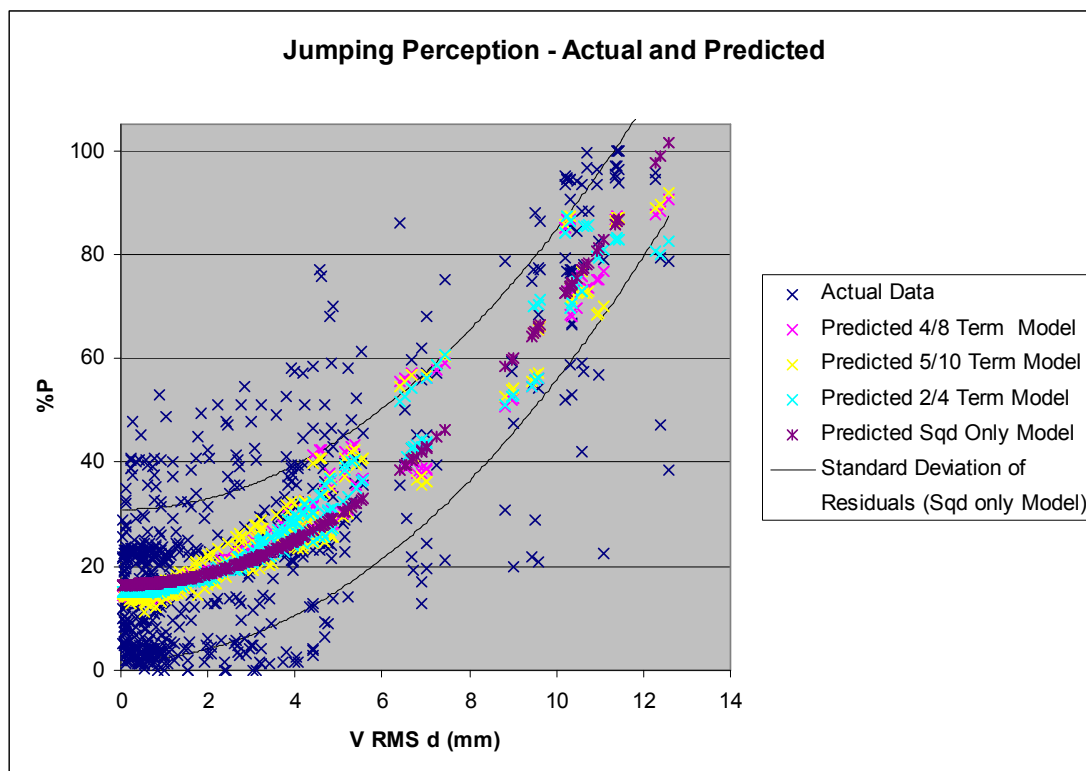


Figure 5.47 Selected Models for Jumping Perception Ratings

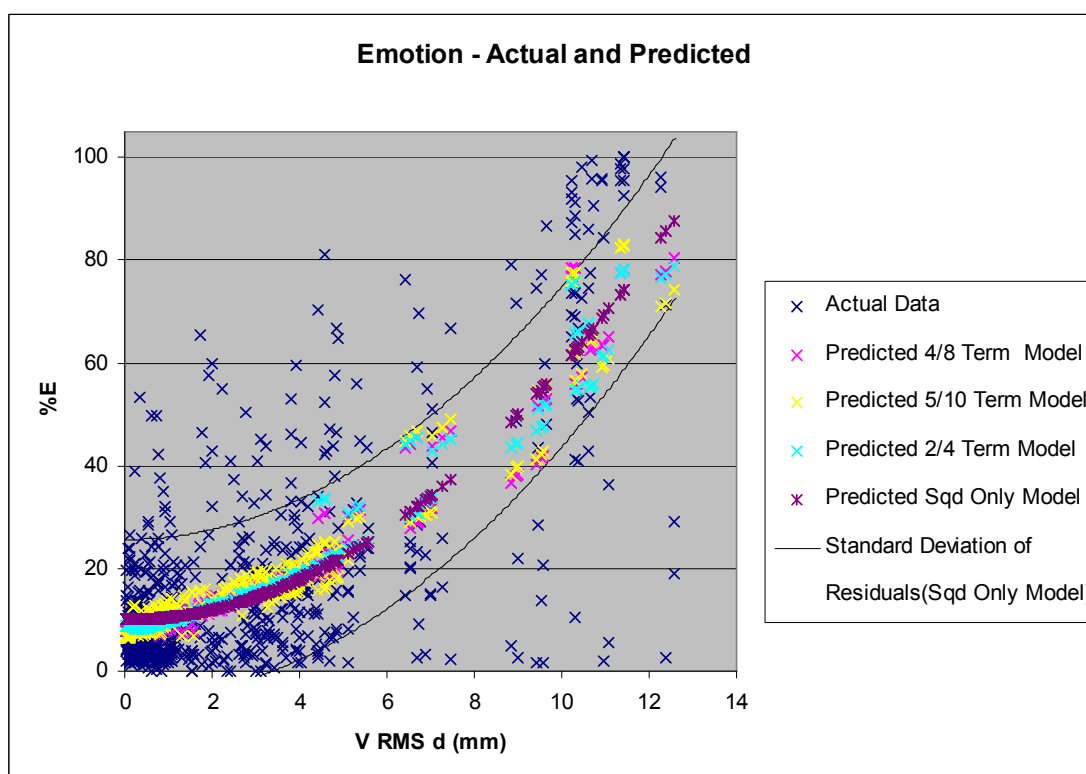


Figure 5.48 Selected Models for Jumping Emotion Ratings

Part of the reason that the single variable model is so effective is that the scatter of the recorded perception ratings for those jumping is much less (typically around 60%) (Figure 5.46 and Table 5.18) than for those seated (~80%) (Figure 5.45 and Table 5.16). This reduced spread of the ratings also explains the R^2 values for the jumping models being greater than those for the seated models.

Table 5.18 Summary of R^2 and Standard Deviation of Residuals for Selected %P Models for those Jumping

%P_{JUMP} Models	Adjusted R^2	St Dev of Residuals
Single Variable 1/1	0.624	14.459
Combination 2/3	0.650	13.912
4/8	0.650	13.860
5/10	0.654	13.760

The relationship between the perception and emotion ratings is similar for both groups of participants (Figure 5.45 - 5.48). The emotion ratings are typically smaller and have a greater spread than the corresponding perception ratings but the form of the correlation between the perception/emotion ratings and the predictors is the same. As for perception the best single variable model (Figure 5.48) in the form

$$\%E_{JUMP} = \alpha x^2 + \phi \quad \text{with } x = VRMSd$$

performs well at predicting the emotion ratings and achieves an adjusted R^2 of 0.544, 91% of the maximum achieved by the 4variable/15 term model. (The 2/4 model gives a R^2 value of 0.566, 95% of the maximum achieved.)

As for those seated, the spread of the recorded %E ratings for those jumping is greater than the spread of the %P ratings for the same group. This is confirmed by the reduced R^2 values and increased standard deviation of the residuals (compared to the equivalent %P_{JUMP} models, as shown in Table 5.19.

Table 5.19 Summary of R^2 and Standard Deviation of Residuals for Selected %E Models for those Jumping

%E_{JUMP} Models	Adjusted R^2	St Dev of Residuals
Single Variable 1/1	0.544	15.609
Combination 2/4	0.566	15.217
4/8	0.566	15.135
5/10	0.572	15.016

For a given vibration, the ratings (perception and emotion) given by the jumpers are generally lower than those seated and this is clearly shown by the shape and positioning of the selected models shown in Figure 5.49 and 5.50. These graphs confirm the shape of original estimation of the trend of the data (Figures 5.10 and 5.12) and also that the ratings converge at the upper end of the recorded vibration scale.

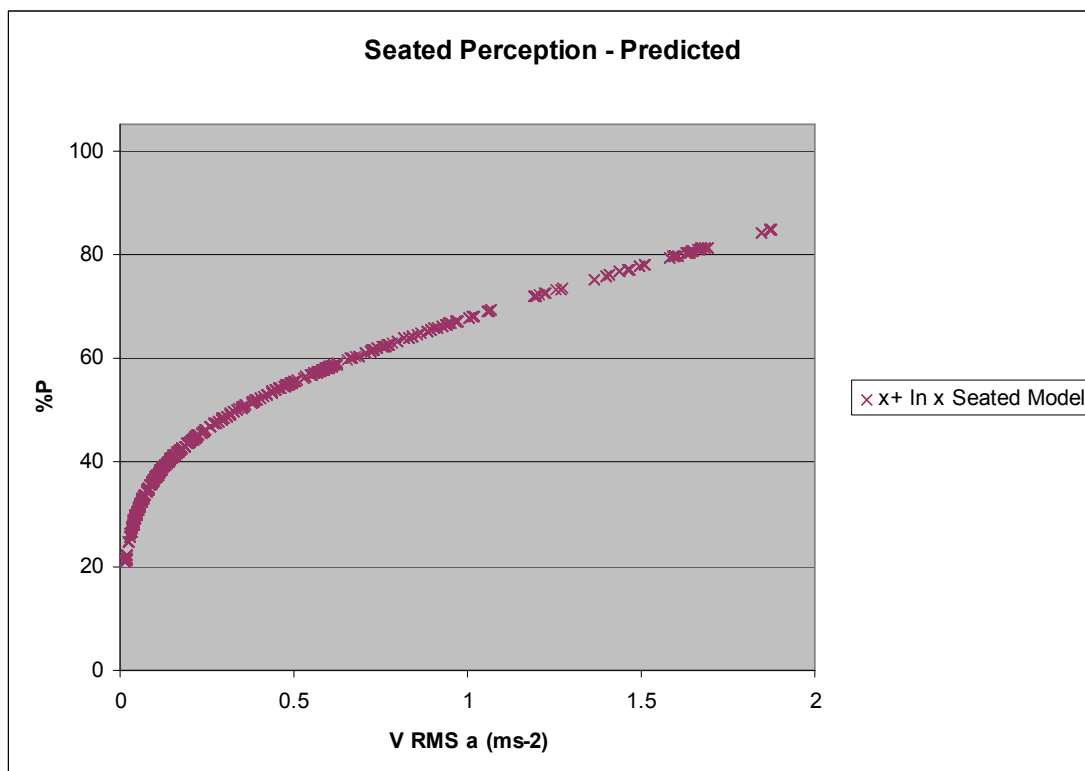
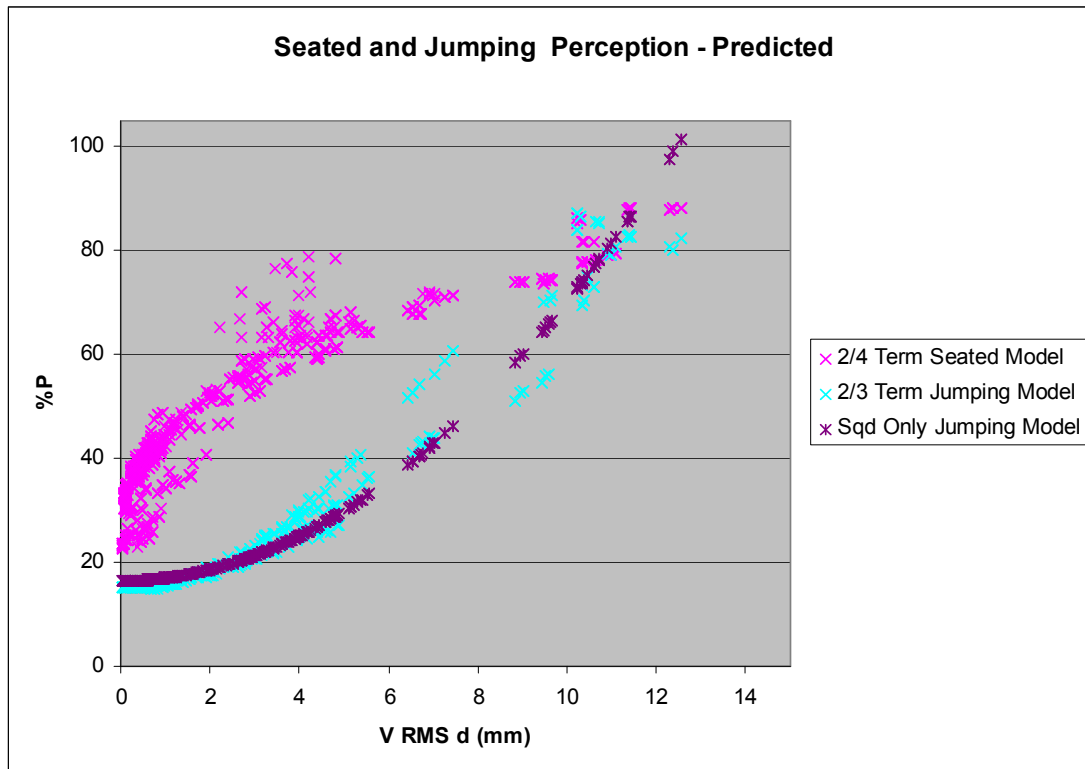


Figure 5.49 Graphs of Selected Perception Models, Seated and Jumping

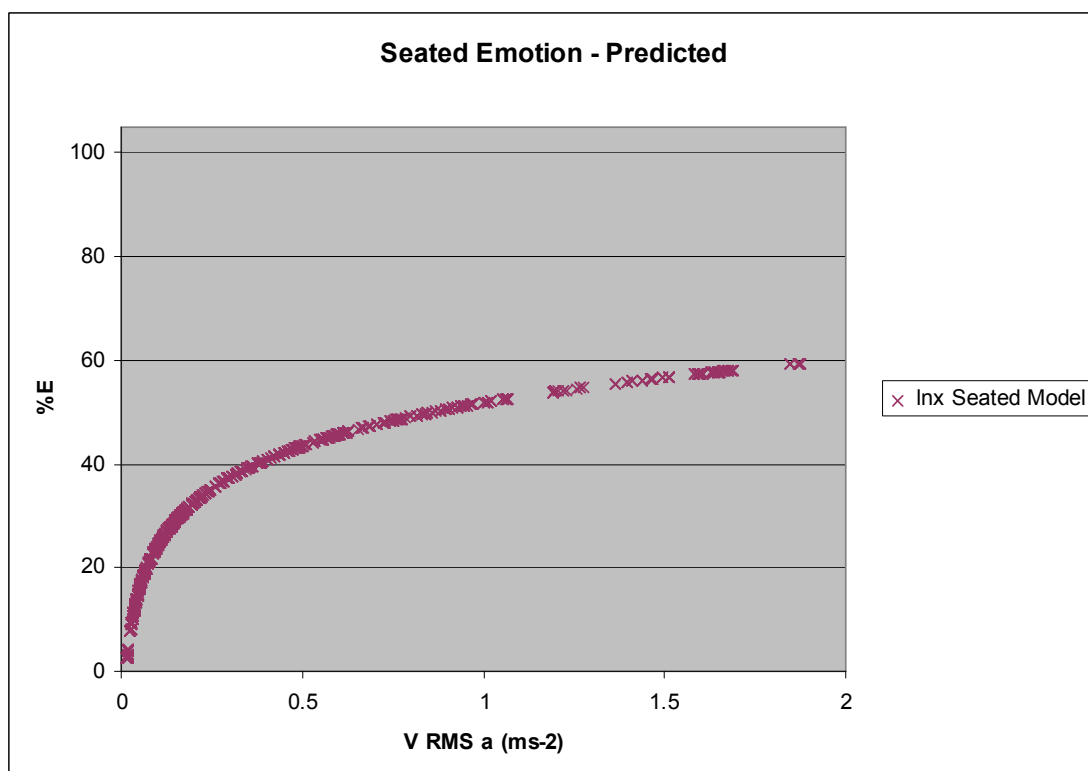
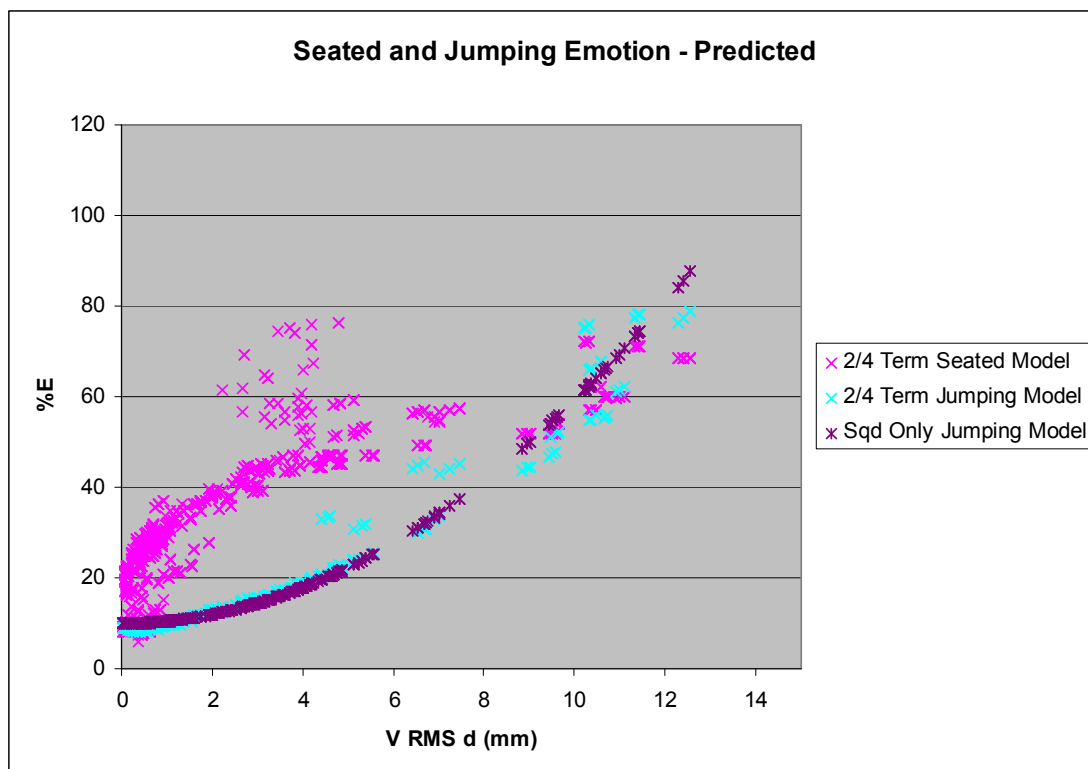


Figure 5.50 Graphs of Selected Emotion Models, Seated and Jumping

5.2.7 Human Response - Conclusion

In summary, the manner in which seated participants perceive vibrations is complex and requires several predictors in order to model the relationship accurately. The key predictor for those seated is the vertical acceleration. For the jumping participants the link between their perception of the vibration and its actual magnitude seems to be much simpler and governed by the vertical displacement. Those seated appear to be more sensitive to changes in the magnitude of small vibrations than to large vibrations and as a result the relationship between perception and vibration size is best described using a logarithmic function. On the other hand, those jumping have difficulty in perceiving the smaller vibrations and so a quadratic function proved the most accurate at predicting the perception ratings within the vibration range of the tests. For all participants the emotion ratings are closely related to the corresponding perception rating and the best emotion models generally take the same form as the best perception models. Typically the emotion ratings are lower than the equivalent perception ratings and the ratings of those jumping (both perception and emotion) are less than those seated except for the largest vibrations experienced during the testing where all participants recorded similar values.

For those jumping the difference in R^2 values between the model using a single variable (VRMSd) and that using two variables (VRMSd and VRMSa) is less than or equal to 0.025. Also the actual R^2 values achieved by the single variable jumping models are 95% and 91% of the maximum achieved for %P and %E respectively. Therefore it makes sense to use the simpler single variable models to predict the perception and emotional response of those jumping on grandstands.

For those seated the difference in performance of the single and two variable perception models is similar to that described for the equivalent jumping model. The reduction in R^2 values between the two variable model (based on VRMSd and FtoB RMSd) and the single variable model (using VRMSd) is 0.029. The single variable seated perception model achieves an R^2 value of 89% of the maximum calculated only 5% less than that for the more complex two variable model. So, as for those jumping, it is recommended that the single variable perception model is used for those seated. The emotional response of those seated is the hardest to model,

shown by the lowest of all the calculated R^2 values and the largest differences in R^2 values between the best single variable model and the maximum R^2 model.

However although it is tempting to use the four variable model which obtains an R^2 value of 98% of the maximum this is a complex model which does not perform significantly better in the checks than the simpler single and two variable models. Although the two variable seated emotion model achieves an R^2 value of 87% of the maximum and the single variable model 75% the actual difference in R^2 values is small (0.052). Therefore using Occam's law of parsimony as a guide (i.e. 'Plurality must never be posited without necessity'; 'It is futile to do with more things that which can be done with fewer') it is suggested that the single variable model is used to predict seated spectators' emotional response to crowd induced vibrations. This also avoids over-fitting the model (where a statistical model describes a random error rather than an underlying relationship), which may not exist in real situations.

In summary it is recommended, in all cases, that although a more complicated model may give a better R^2 value that the best single variable models be used to determine the human response to crowd induced vibrations in grandstands (Table 5.20).

Table 5.20 Recommended Perception and Emotion Models

Perception	Variable and Constants	R^2 value
$\%P_{SEAT} = \alpha x + \beta \ln x + \phi$	$x = VRMSa$ $\alpha = 13.46, \beta = 8.15, \phi = 54.35$	0.496
$\%P_{JUMP} = \alpha x^2 + \phi$	$x = VRMSd$ $\alpha = 0.54, \phi = 16.44$	0.625
Emotion	Variable and Constants	R^2 value
$\%E_{SEAT} = \alpha \ln x + \phi$	$x = VRMSa$ $\alpha = 6.51, \beta = 9.75, \phi = 45.72$	0.318
$\%E_{JUMP} = \alpha x^2 + \phi$	$x = VRMSd$ $\alpha = 0.49, \phi = 9.98$	0.544

From Table 5.20 it is clear that the response of those seated is governed by the vertical acceleration of the structure whilst those jumping base their reaction on the vertical displacement. This could be because the seated spectators are in constant contact with the stand and, because they are not participating in the dynamic activity,

have more awareness of the vibration. Thus it is likely to be the response of those seated that ultimately determines the acceptability of a grandstand.

Those jumping to create the vibration have minimal contact with the structure and their focus is on their activity. Therefore, the magnitude of the vibration has to be larger before those jumping can even perceive it and it is the movement of the structure in the contact period interfering with their jumping (i.e. the displacement) which they perceive. Although the models given for those jumping could be written in terms of vertical RMS acceleration the accuracy (R^2 value) reduces by approximately 10%.

5.3 Comparison with other Research

5.3.1 Perception Categories

To allow the recorded perception data to be compared with previously published research, the perception readings for both the seated and jumping participants were divided into bands relating to the six perception categories given on the questionnaire (0-Imperceptible to 5-Extreme Vibration) (Section 4.2.2). These were overlaid on the perception ratings as shown in Figures 5.51 and 5.52. In this case peak vertical accelerations were used as the abscissae and the perception models in the selected format of Section 5.2.7 (Table 5.20) ($x + \ln x$ for those seated and x^2 for those jumping) were reproduced for this predictor. This allowed Kasperski's 1996 suggested thresholds for comfort disturbing and unacceptable levels of vibration, together with his limit for the probable onset of panic, to be easily overlaid on the graphs (Figures 5.51 and 5.52). These overlays enable the peak acceleration levels used to define the majority of grandstand acceptability limits to be compared against 'laymen's' categories for describing the magnitude of vibrations.

Thus, using the $x + \ln x$ perception model shown in Figure 5.51, all barely perceptible and most distinctly perceptible vibrations, as classed by those seated, fall below Kasperski's comfort disturbing limit (0.5ms^{-2}), while his unacceptable threshold (of 1.8ms^{-2}) is approximately mid way across the range of strongly perceptible vibrations for seated participants. Above Kasperski's peak acceleration panic limit of 3.5ms^{-2} almost all the seated crowd members classified the vibrations as large or extreme. Interestingly, for those seated, it is the strongly perceptible category that is closest to

the National Building Code of Canada's (NBCC 2005) recommended acceleration limits for stadia and arena of 10-18%g (1.0-1.8ms⁻²).

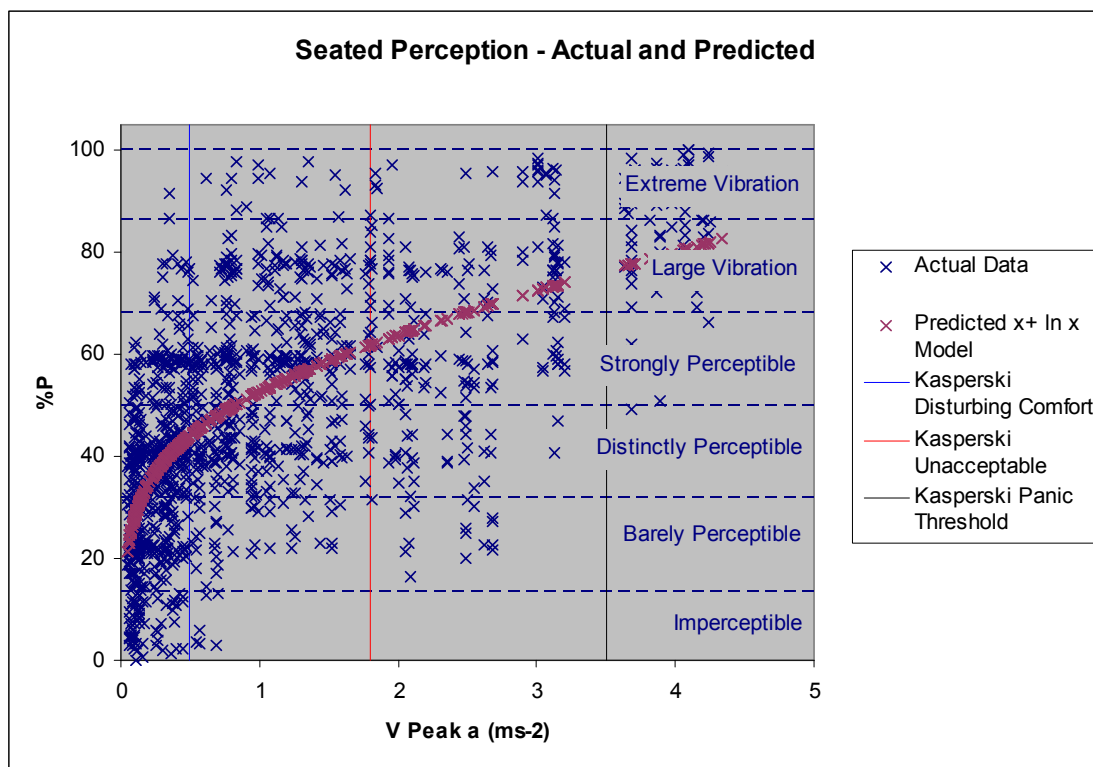


Figure 5.51 Seated Perception Data showing Questionnaire Categories

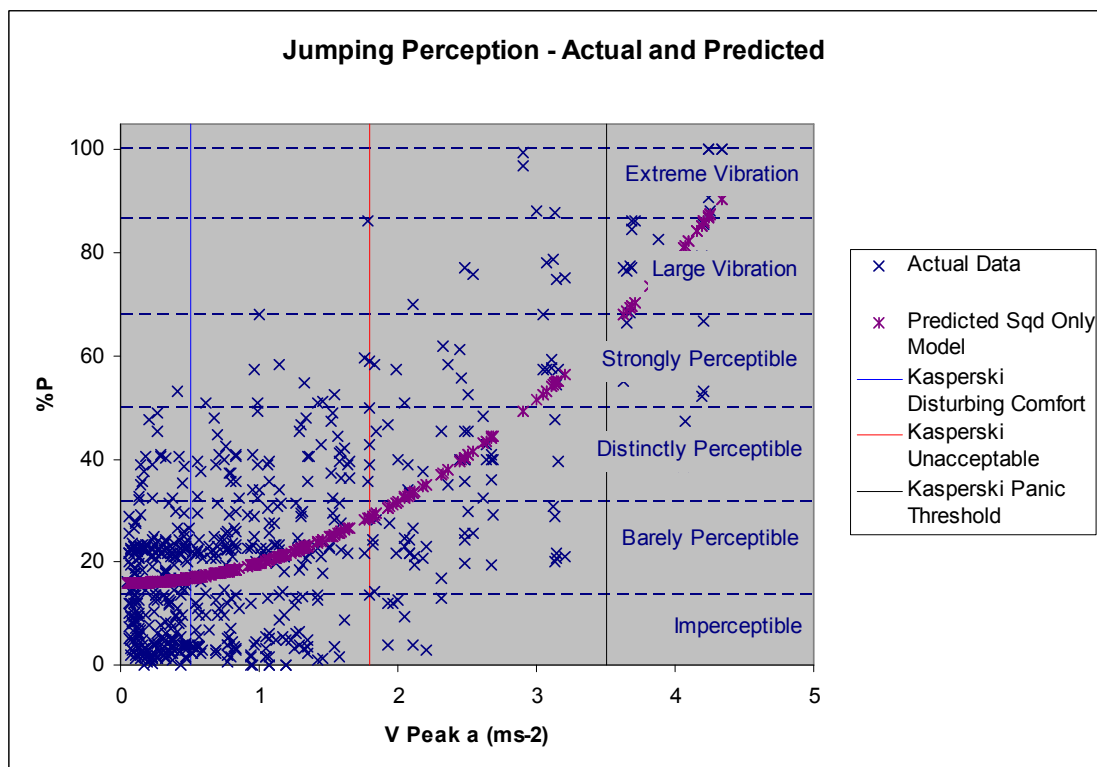


Figure 5.52 Jumping Perception Data showing Questionnaire Categories

From the x^2 perception model (Figure 5.52) those jumping categorised vibrations below Kasperski's comfort disturbing and unacceptable thresholds as barely perceptible, and large and extreme vibrations as above Kasperski's proposed panic threshold.

It is difficult to relate the results of the perception tests directly to Kasperski's threshold limits given the difference in the description of the boundaries. However Figures 5.51 and 5.52 seem to indicate a possible agreement particularly, for those seated, at Kasperski's lower unacceptable threshold (strongly perceptible) and higher disturbing comfort threshold (distinctly perceptible) and; for both seated and jumping participants at Kasperski's upper limit panic threshold (strongly perceptible/large vibrations).

5.3.2 Floor Vibrations

The graphs shown so far are for peak accelerations, as this has been the favoured measure of acceptability of vibrations in grandstands (Kasperski 1996 and NBCC 2005). However, other references regarding human perception of vibration use displacements. For example Reiher and Meister 1931, who carried out a series of experiments to determine human sensitivity to steady-state vibrations in floors, used similar categories for describing the vibrations as this research project but used displacement and frequency as a gauge of human perception (see Section 2.4). To enable superposition of results the recorded data points were firstly divided into the 6 categories shown in Figures 5.51 and 5.52. Then for each data point the recorded peak displacement was plotted against the frequency of the vibration. As previously the split between jumping and seated participants was maintained.

Trendlines were plotted for each category of perception (Figures 5.53 to 5.55) to show generally how the frequency of the vibration (calculated from the output of the vertical displacement transducers) varies with the peak displacement for each test. Linear trendlines were used in this case because the range of vibration frequencies recorded was quite limited (1.1 to 2.4Hz) due to the way that the vibration was created by groups of people jumping. This makes it difficult to plot with any accuracy anything other than the mean values which fell close to a linear line (Figure 5.53).

Again due to the vibration characteristics of the rig the largest vibrations occurred at frequencies of 1.7Hz or greater. It is because of this that the trendlines for 'Large' and 'Extreme' vibrations start at 1.7Hz (Figures 5.54 and 5.55)

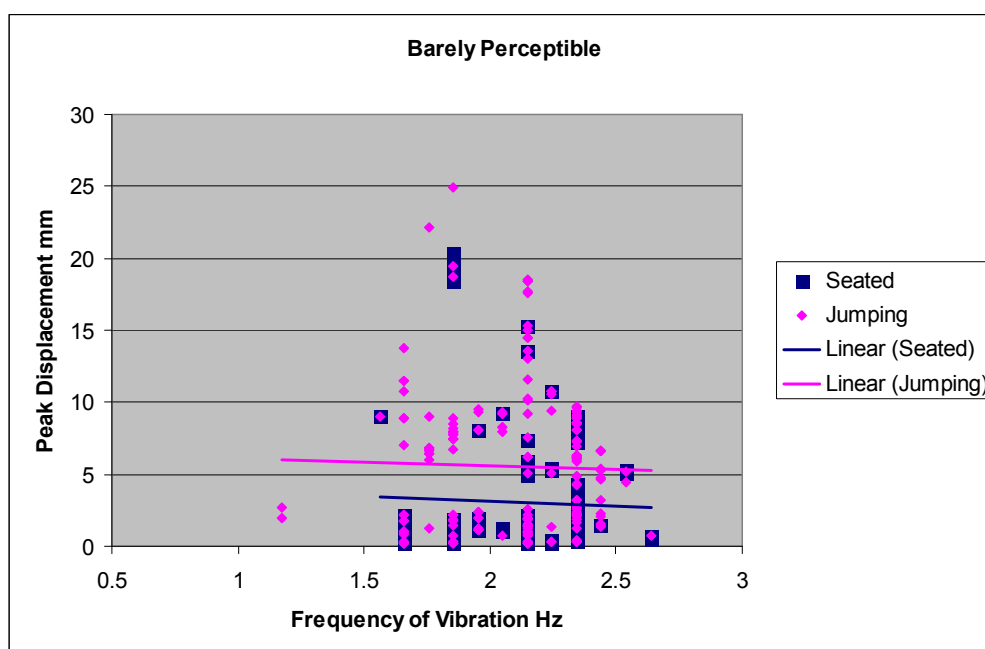


Figure 5.53 Derivation of 'Barely Perceptible' Trendlines

As discussed previously, in Section 5.2, those seated typically perceive a given vibration as being larger than those jumping to create the vibration. Because of this the trendlines in Figure 5.54 for those seated are higher than for those jumping (Figure 5.55). As the seated trendlines are more conservative these were selected to be compared against previous research. Also, although not explicitly set out, past research appears to focus on the response of those stationary, therefore, it is more appropriate to use the data collated from the seated participants in the grandstand tests rather than those jumping.

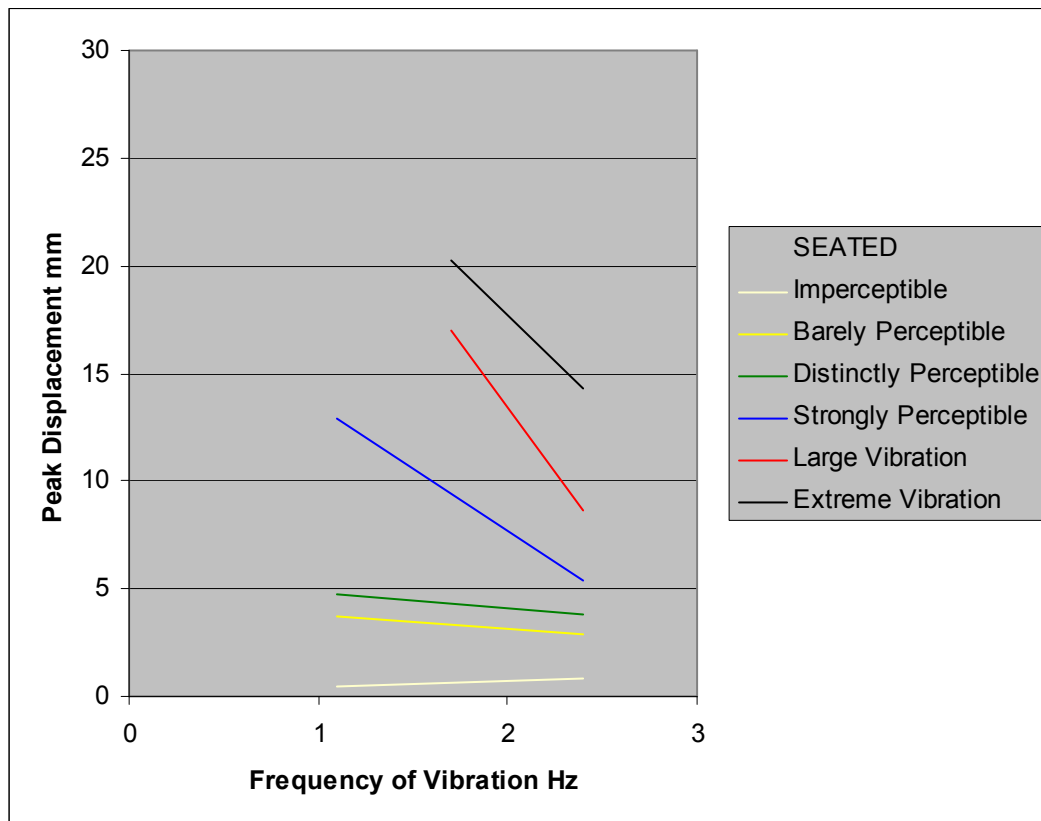


Figure 5.54 Seated Participants' Perception Trendlines

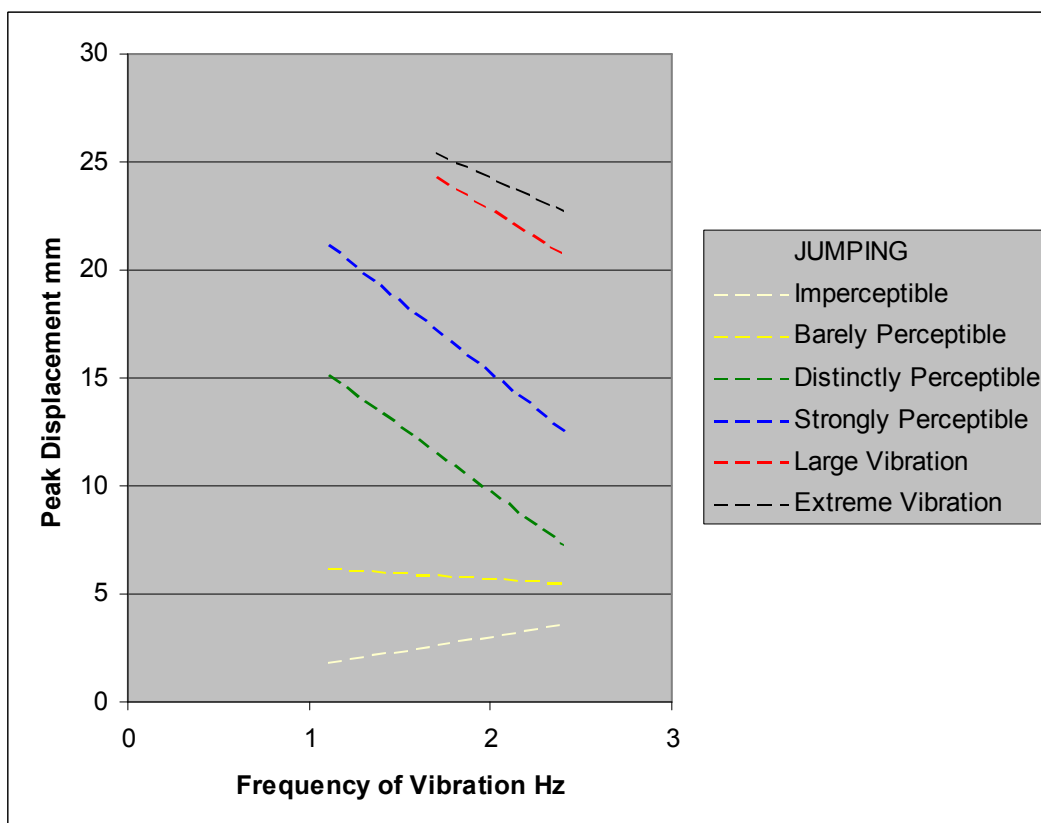


Figure 5.55 Jumping Participants' Perception Trendlines

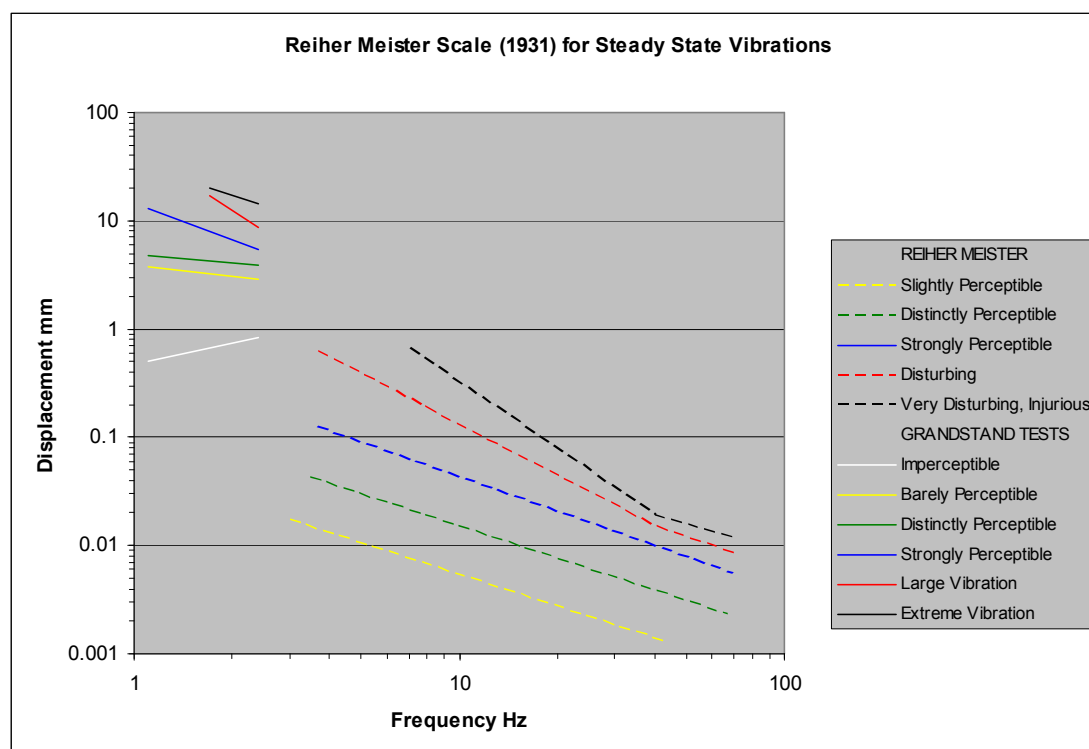


Figure 5.56 Reiher Meister Perception Curves for Steady State Vibrations

The seated trendlines from Figure 5.54 were first superimposed on Reiher and Meister's (1931) results (Figure 5.56). Reiher and Meister's perception curves are shown dashed and the corresponding grandstand trendlines for seated participants solid. It should be noted that Reiher and Mesiter's perception curves do not extend below 3Hz where the grandstand results are located and so the comparisons below have been made on a projection of the Reiher and Mesiter's perception curves. Figure 5.56 shows that, for the grandstand tests, vibrations rated 'barely perceptible' or greater generally fell above Reiher and Meister's disturbing threshold and, 'large' and 'extreme' vibrations above the projection of their very disturbing threshold. There are a number of reasons that could explain this. One obvious one is, perhaps, that in the stadium tests the participants could see the source of the vibration, i.e. the jumpers, and therefore were more tolerant, while Reiher and Meister used a shaker plate beneath the floor. Another explanation is the difference in situation between a tiered grandstand and a horizontal floor. There could also be a generation factor. In the 21st Century we live in a world that constantly moves and with modern machinery and traffic, people experience structural vibrations on a daily basis. In the early 1930s life and expectation was very different and it could be that people then were more sensitive to floor vibrations.

In 1966 Lenzen proposed modifying the Reiher Meister (1931) perception curves, by multiplying by a factor of 10, to make them more applicable for assessing transient vibrations in office floors (Figure 5.57). Even with this modification the seated grandstand test results are much more closely grouped and fall mostly between the curves for strongly perceptible and disturbing for transient vibrations.

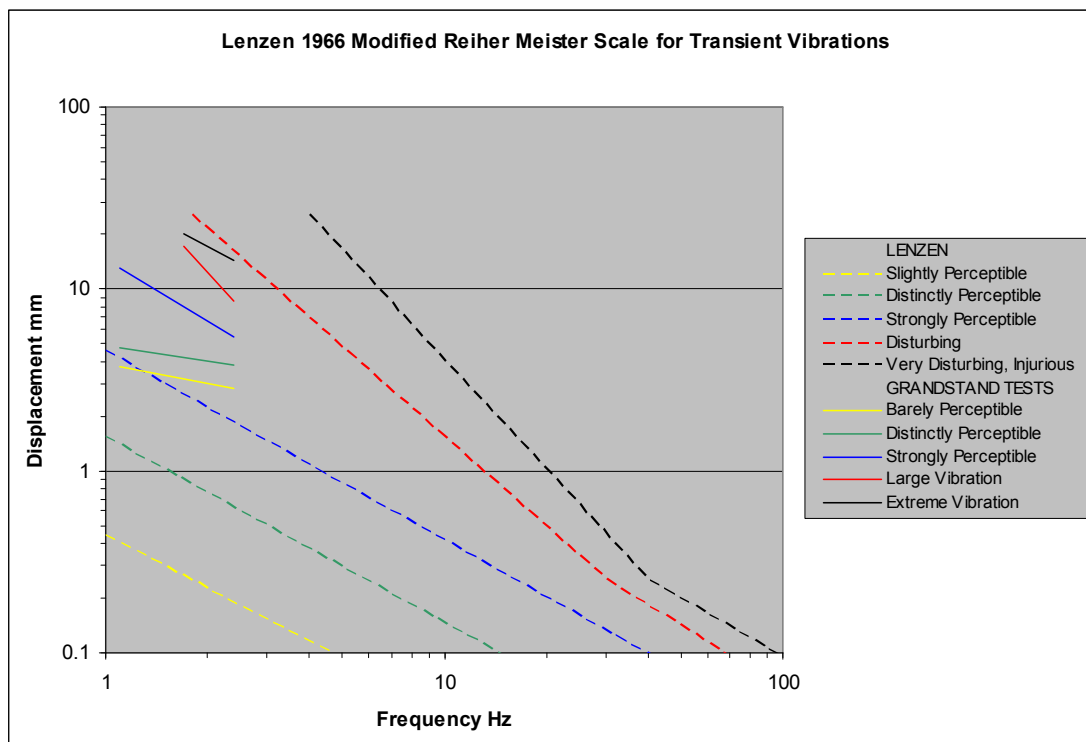


Figure 5.57 Lenzen's Modified Reiher Meister Perception Curves for Transient Vibrations

A similar set of perception curves, for office floors, were collated by McCormick and Mason in 1974 based on various previous publications by others (Figure 5.58). Again the grandstand trendlines are generally well above the corresponding curves for transient vibrations. It appears that vibration limits are clearly situation dependent, with those relevant to office floors being inappropriate for grandstands as the vibrations from the grandstand tests would be deemed much larger in magnitude by those in an office environment.

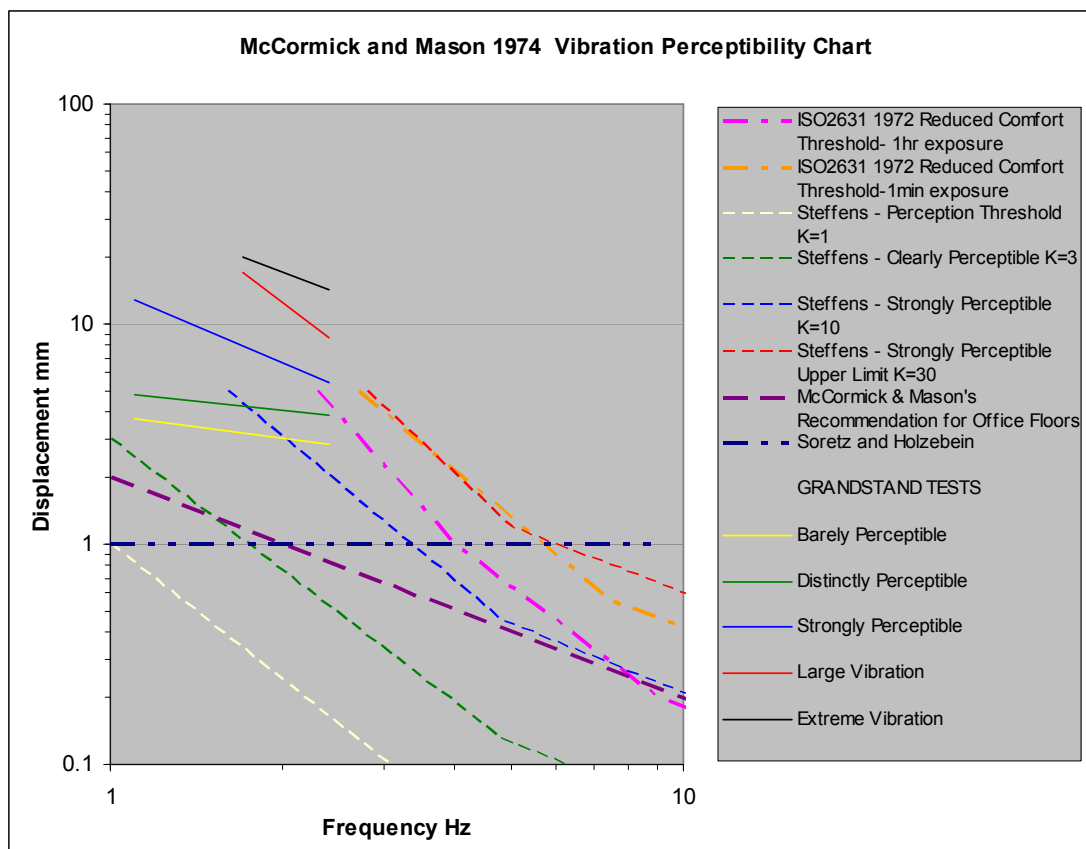


Figure 5.58 McCormick and Mason's Perception Curves for Transient Vibrations

5.3.3 Design Standards

The next step was to compare the grandstand results against acceleration limits given in International Standard ISO2631 'Mechanical vibration and shock- Evaluation of human exposure to whole-body vibration' and so the grandstand frequency trendlines for those seated, in terms of RMS accelerations, were plotted alongside the ISO 2631-2 1989 (from Bachmann et al 1994) vibration limits (for buildings) for comfort, fatigue and exposure (Figure 5.59). [The reduced comfort boundary is the threshold beyond which activities such as eating, reading or writing are disturbed. Fatigue, in this case, is defined as the level at which recurrent vibrations cause fatigue resulting in a loss of efficiency while the exposure limit is the maximum tolerable vibration with respect to health and safety.]

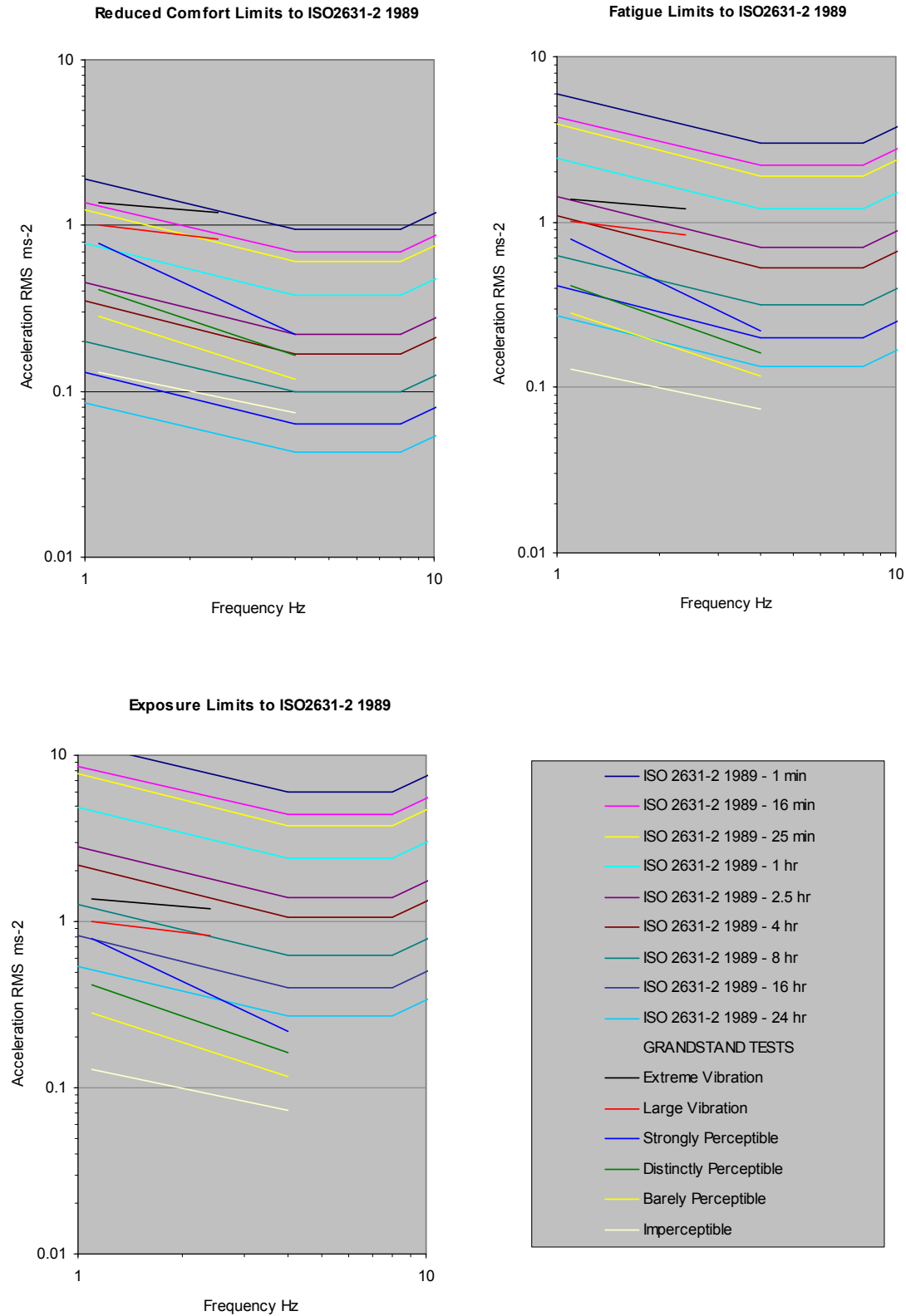


Figure 5.59 Vibration limits to ISO 2631-2 1989

From Figure 5.59, an 'extreme vibration' as defined by those seated at the grandstand tests at a typical excitation frequency of 2Hz could, according to ISO 2631-2 1989, be sustained for approximately 3 minutes before crossing the comfort boundary, which seems quite a long time for such a large vibration. This level of 'extreme vibration' is equivalent to an exposure limit of roughly 5 hours and a fatigue limit of 1.5 hours for vibration frequencies between 1.5 and 2.5 Hz. This shows that even if a crowd could physically jump in a manner to induce such a response, the vibration levels would induce additional fatigue causing the jumping to stop long before it became hazardous to the participants' health.

The informative Annex C of ISO2631-1:1997 gives 'approximate indications of likely reactions to various magnitudes of overall vibration in public transport' in terms of comfort limits as RMS accelerations. As the grandstand results appear generally to be greater than those previously suggested for buildings, the grandstand trendlines were overlaid on the comfort limits to ISO 2631-1:1997 to see if recommendations for public transport were more comparable (Figure 5.60). This shows clearly that within the range of 1-3Hz the grandstand trendlines fit surprisingly well with the ISO 2631-1:1997 comfort bands. 'Extreme vibrations' are at the lower end of the 'very uncomfortable' range and 'large vibrations' are classed as 'uncomfortable'. 'Imperceptible' and 'barely perceptible' vibrations fall below the 'not uncomfortable' boundary whilst 'distinctly' and 'strongly perceptible' vibrations cross the bottom of the 'little' and 'fairly uncomfortable' boundaries respectively.

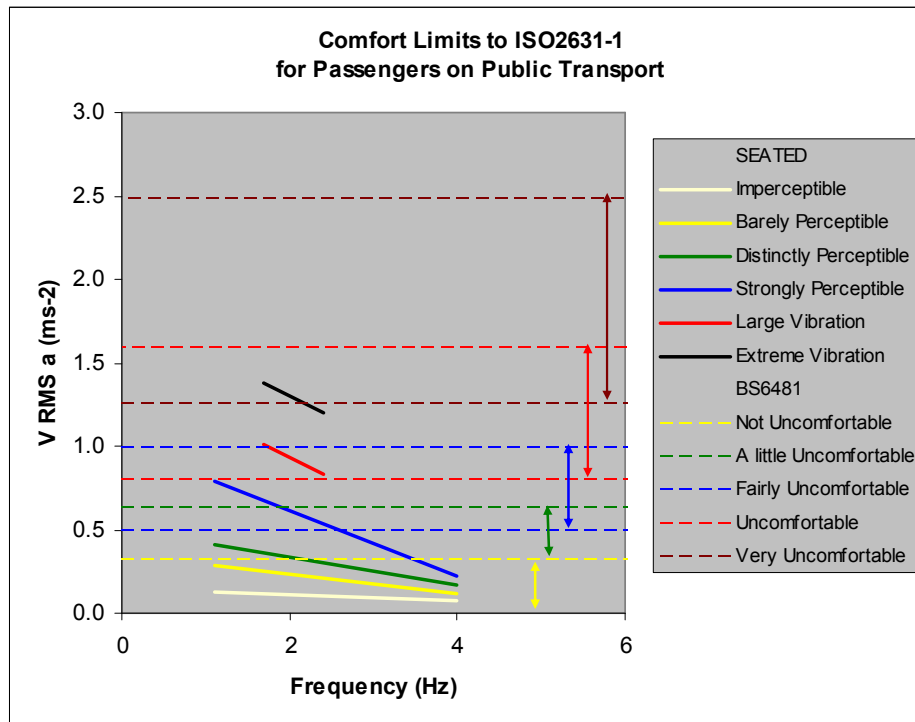


Figure 5.60 Comfort limits to ISO 2631-1:1997 for Passengers on Public Transport

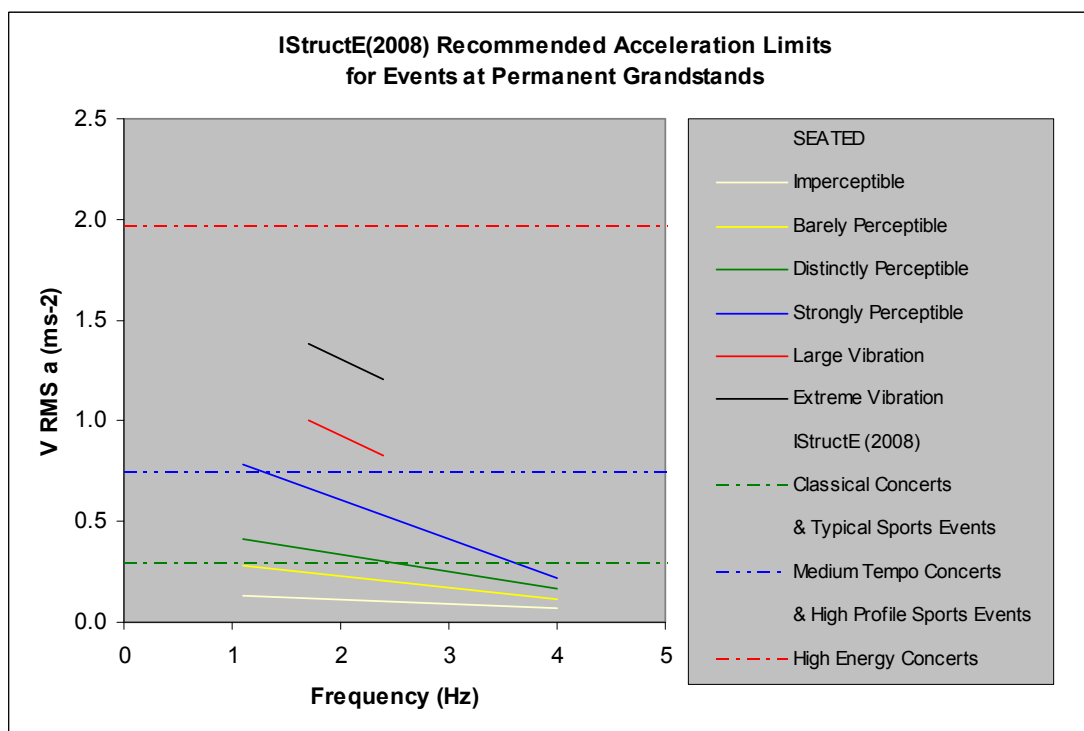


Figure 5.61 IStructE (2008) Recommended Acceleration Limits for Events at Permanent Grandstands

Finally the IStructE's (2008) recommended acceptability limits for events at permanent grandstands were superimposed on the grandstand trendlines. From this 'large and extreme vibrations' are well below the suggested limit for 'high energy concerts' while 'distinctly and strongly perceptible' vibrations would generally be considered satisfactory for 'medium tempo concerts and high profile sporting events' using the IStructE limits (Figure 5.61). Lastly the generated grandstand trendlines for 'imperceptible and barely perceptible' vibrations lie beneath the recommended acceleration limit for 'classical concerts and typical sporting events'. Although the IStructE's lowest limit for 'classical concerts and typical sporting events' appears to tie in with the experimental results it is unexpected that the upper limit for 'high energy concerts' is notably greater than the 'extreme vibration' trendline as the largest vibrations experienced during the tests were above Kasperski's panic threshold (1996).

5.3.4 Summary of Comparison of Perception Tests with other Research

The findings of the grandstand testing show that human perception of vibrations is very situation dependent. When compared with previously published perception curves for steady-state and transient vibrations in floors, vibrations of similar magnitude were rated consistently less perceptible by those in the grandstand tests. When compared against references relating to comfort levels on public transport, where expectation is of perceivable vibrations, the grandstand results fitted remarkably well. Less surprisingly the trendlines derived from the testing fitted well with stadium specific guidelines albeit somewhat lower in cases.

Another observation from comparison of the results with the results of the previous perception testing carried out by Reiher and Meister (1931) is that perception of vibrations due to synchronised crowd loading is influenced by that fact that, even if people are not participating in the dynamic activity, they can see the source of the vibration and may therefore tolerate higher levels of vibration.

[Blank]

6 Acceptability

6.1 Statistical Analysis

6.1.1 Statistical Analysis - Procedure

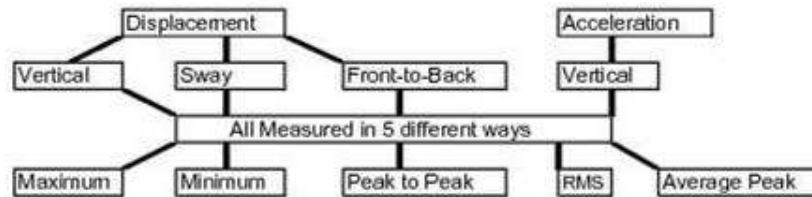
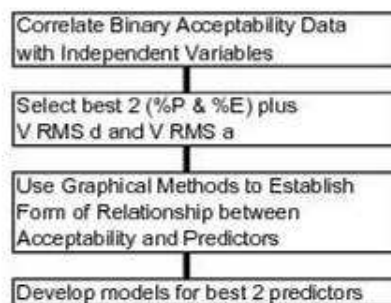
The natural progression of the development of the models to predict the human response to crowd induced vibrations in grandstands was to attempt to link the predictors to acceptability. As part of the second set of tests carried out in October 2007 all participants were asked to record whether they felt the vibration they had just experienced would be unacceptable in a real grandstand situation. For this the definition of 'unacceptable' was defined as 'a vibration which, if experienced in a real stand, would cause the participant to; leave immediately or complain to the management or think twice about returning to that venue' (Figure 4.9). If the participant thought that the vibration was acceptable they were asked to estimate how long that vibration would have to persist for before it became unacceptable.

This data was first converted to binary form using 5 minutes as the cut off between acceptable and unacceptable. Five minutes was chosen as the time threshold as it is roughly equivalent to two songs at a pop concert. Previous recordings at pop concerts (Caprioli et al 2007) show that higher levels of vibration can be tolerated for a single song but songs producing such levels of excitation are usually spaced throughout the programme and interspersed with ones producing more average levels of vibration. Thus a time period equivalent to two adjacent songs (5 minutes) was chosen with the aim of evening out these highest peaks that can be tolerated for a short period. This was backed up by the collected data with the virtually all respondents selecting either 'less than 3 minutes' (i.e. a single song) or 'greater than 5 minutes' (i.e. more than two adjacent songs) as the limit of unacceptability.

The acceptability results were split into jumping and seated participants and then correlated with all the corresponding first and second order (linear, squared, log and exponential) Group 1 and 2 predictors (Table 5.3 and Figure 6.1) as well as the recorded perception and emotion ratings. These correlations showed that the best predictor of acceptability, for both those jumping and seated, was the participant's emotion rating which gave correlations of 68% and 72% respectively. For the seated participants their perception ratings were the next best indicator of

acceptability at 67% correlation while the Group 1 predictors and VIndVDV performed similarly at around 45% increasing to 50% for their logarithms. The rest of the Group 2 predictors gave lower results. For those jumping the square of either vertical displacement, vertical acceleration or individual VDV was the second best gauge of acceptability at around 62% correlation followed by the perception ratings at 59%. The linear correlation of vertical displacement, acceleration or Ind VDV and acceptability for jumpers was approximately 56% with all other predictors producing a maximum of 50% or less.

Figures 6.2 and 6.3 show the distribution of the seated participants' acceptability results when plotted against perception and emotion ratings and the logarithm of vertical RMS acceleration. These graphs illustrate the gradual progression from vibrations that are acceptable to all, at the lower end of the spectrum, to vibrations that are totally unacceptable at the upper end of the recorded range of movements.

DATA DIVISION**Dependent Variables - those being Predicted****Independent Variables (IV) - Predictors****GROUP 1 (20 Independent Variables)****GROUP 2 (5 Independent Variables)****Human Response (2 Independent Variables)****MODEL DEVELOPMENT****Figure 6.1 Flow Chart of Development of Acceptability Model**

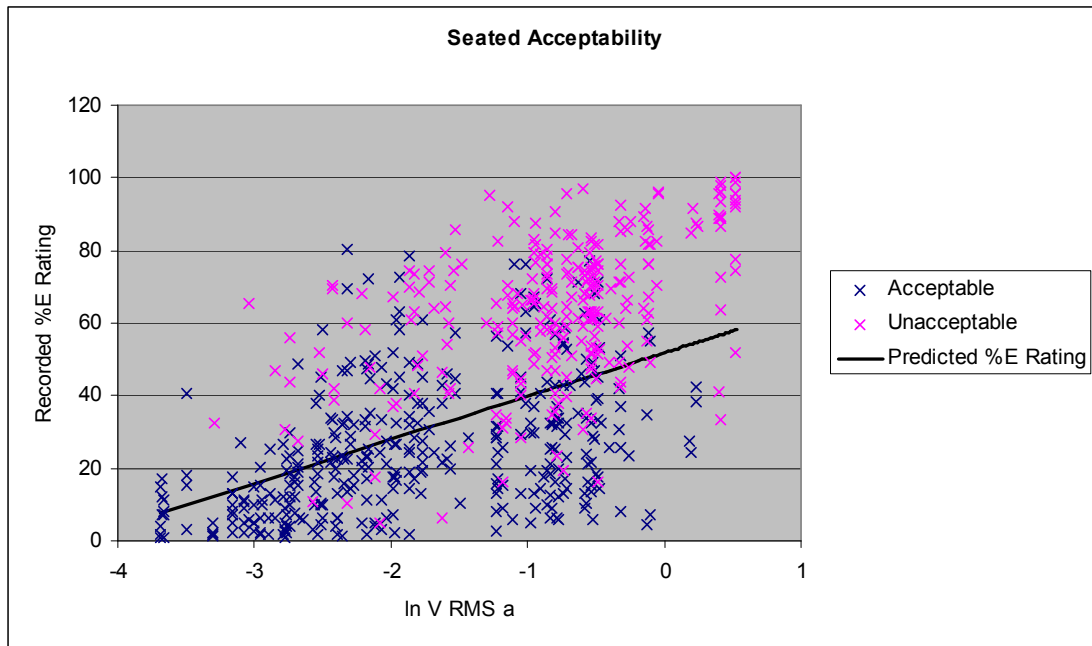


Figure 6.2 Scatter Plot of Recorded %E Rating against log Vertical RMS Acceleration showing Acceptability Results

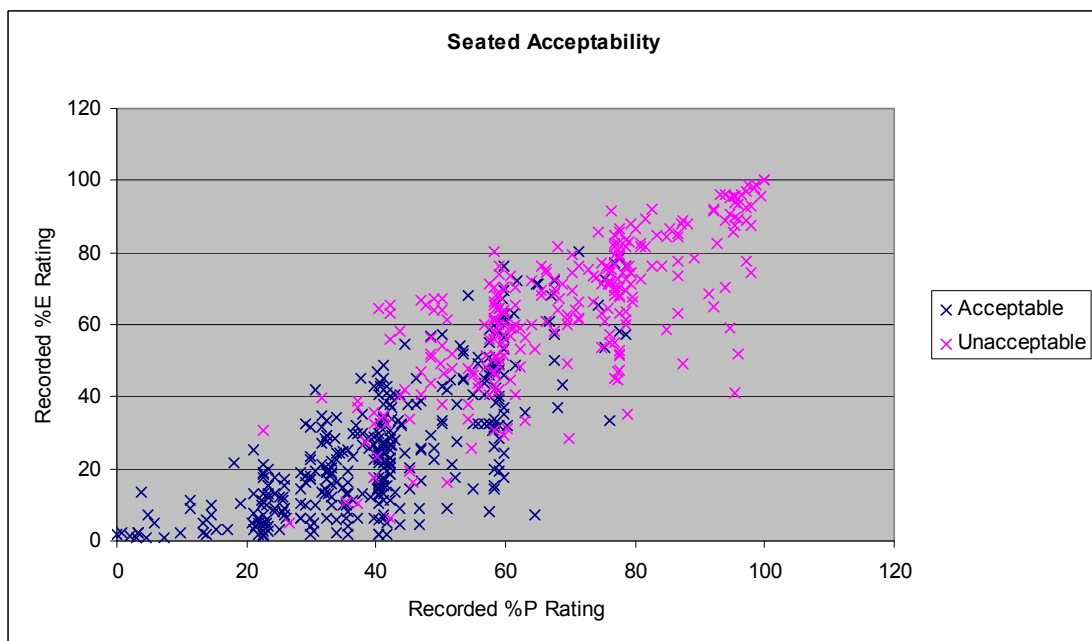


Figure 6.3 Scatter Plot of Recorded %E Ratings against Recorded %P Ratings showing Acceptability Results

Using the results of the correlation analysis as a starting point, frequency distribution histograms were produced to investigate how the percentage of people who found the vibration acceptable varied across the range of the best predictors. This was done first using quite coarse banding by dividing the range of the predictor into 10 equal bands and calculating the percentage of participants (in that band) who found the vibration acceptable. The percentage acceptable/unacceptable for each band of each predictor was plotted on a bar chart as illustrated in Figure 6.4. These charts were produced for recorded emotion and perception ratings, and vertical RMS displacement and acceleration for both jumping and seated participants. Histograms were also drawn for the logarithm of vertical RMS displacement and acceleration for those seated and the squares of vertical RMS displacement and acceleration for those jumping.

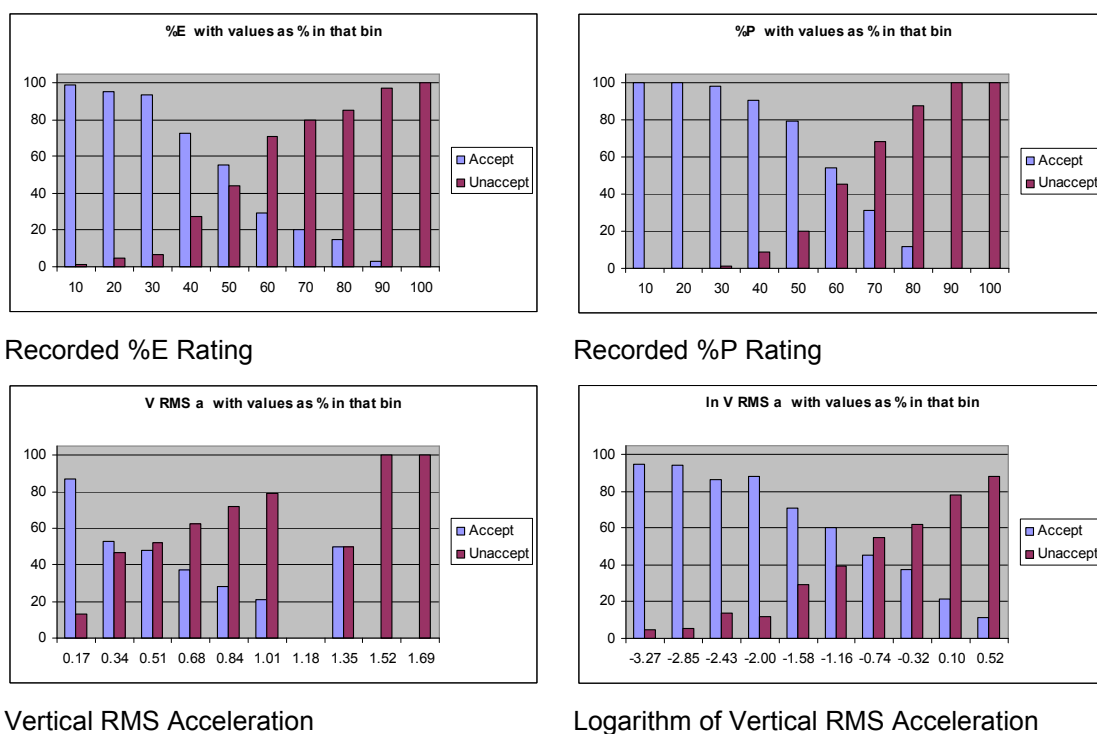


Figure 6.4 Histograms showing Distribution of Acceptability for Seated Participants

The histograms were then assessed visually for goodness of fit to a logistic curve of

the form $f(z) = a \left(\frac{e^{bz}}{1 + e^{bz}} \right) = a \left(\frac{1}{1 + e^{-bz}} \right)$ (shown graphically in Figure 6.5).

(This logistic function is a simple generalised linear model used for binomial regression i.e. fitting a linear relationship between dependent and independent variables where the dependent variable is in binary form. The values of a and b determine the slope and the location of the cross-over point of the curve). A logistic curve of this form was selected as it is a close representation of the transition from 100% acceptable to 100% unacceptable identified by the histograms (Figure 6.4).

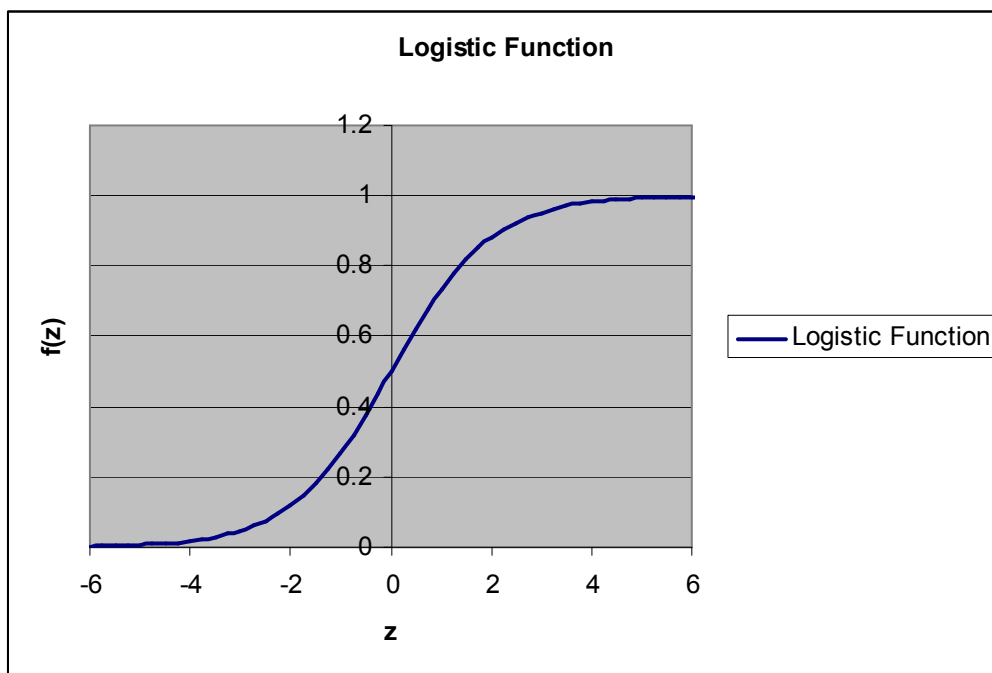


Figure 6.5 **Logistic Function**

Those predictors which produced the closest approximation to a logistic function with the coarse banding were then re-banded using 100 equal divisions rather than 10. The percentage of participants in each band that found the vibration acceptable was recalculated and the bar charts of acceptability versus predictor redrawn. A logistic acceptability curve was then fitted to the results using the Solver function in Excel and by minimising the standard error between the curve and the results (Figures 6.6 to 6.15)

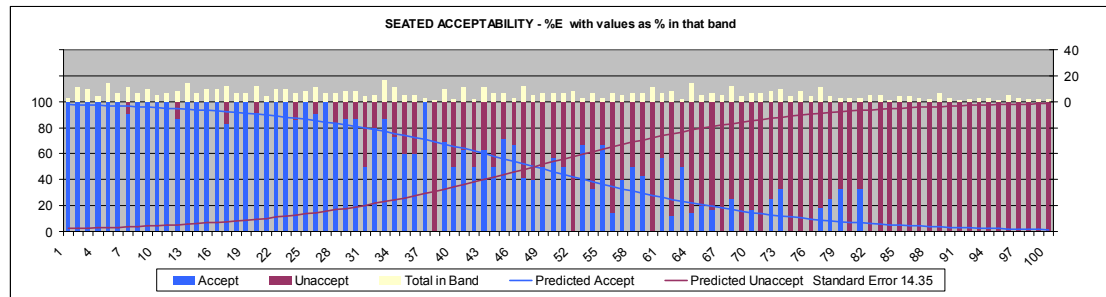


Figure 6.6 Acceptability for Seated Participants using Emotion Rating as the Predictor

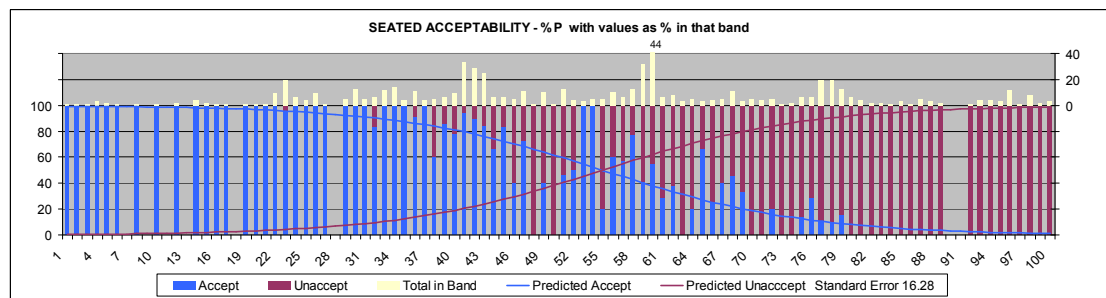


Figure 6.7 Acceptability for Seated Participants using Perception Rating as the Predictor

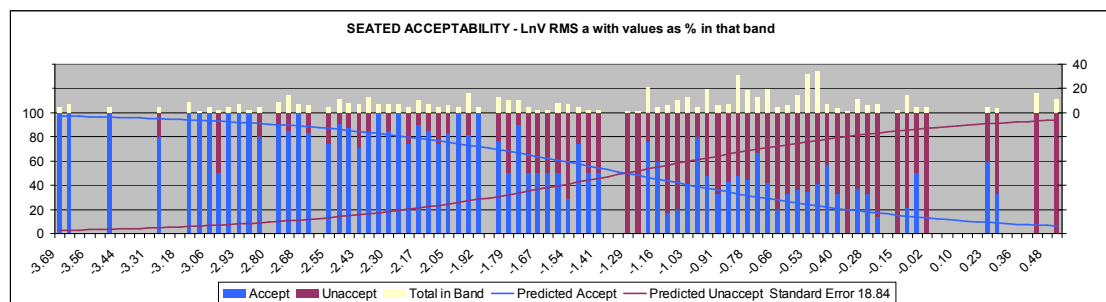


Figure 6.8 Acceptability for Seated Participants using the logarithm of Vertical RMS acceleration as the Predictor

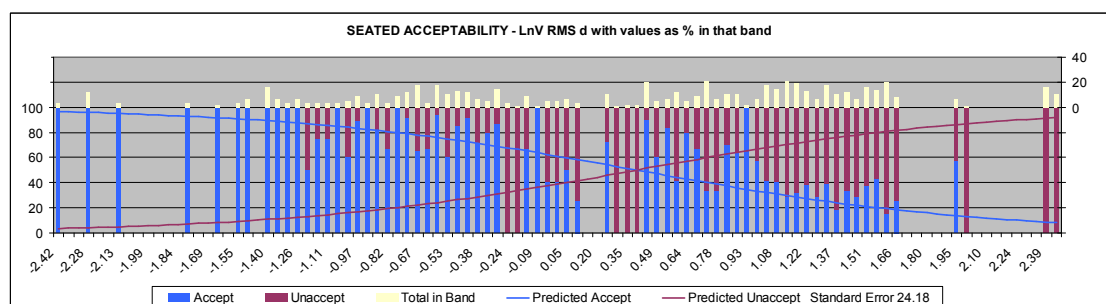


Figure 6.9 Acceptability for Seated Participants using the logarithm of Vertical RMS displacement as the Predictor

6.1.2 Statistical Analysis – Results

The accuracy of the acceptability curve depends on a number of factors including the distribution of the data across the range of the predictor and the deviation between the predicted and actual values. Ideally the spread of the recorded data would be such that each band included the same number of data points but in reality the data is bunched with some bands incorporating a large number of points and others none.

6.1.2.1 Acceptability for Seated Participants

For the seated participants the data is fairly well distributed across the range of the selected predictors. For the recorded emotion ratings there is data in each of the bands and the number of points in each band is fairly uniform (Figure 6.6). When using the recorded perception ratings as the predictor of acceptability, there are a few bands without data points but these are generally in areas where all the seated participants deem the vibration either acceptable or unacceptable i.e. outside the critical cross over region (Figure 6.7). The data is less well distributed along the range compared to the emotion ratings with fewer points at the extremes and two distinct peaks of information in the centre (Figure 6.7). Because of the vibration characteristics of the test rig the models using a form of the vertical movement of the rig as the predictor do not have data points in every band, particularly at the extremes of the recorded movement (Figures 6.8 and 6.9). However the number of responses in each band containing data is reasonably consistent, with a slight concentration of results two-thirds of the way along the range (Figures 6.8 and 6.9).

The next check is to examine the difference between the actual and predicted percentage acceptability by calculating the standard error between the fitted logistic curve and the recorded results. Of the four predictors considered for seated participants (recorded emotion and perception ratings, the logarithm of vertical RMS acceleration and the logarithm of vertical RMS displacement) the logarithm of vertical RMS displacement gives the greatest standard error, approximately 50% larger than the rest, and can therefore be discounted. The emotion ratings give the best balance of distribution of data (with points in every band) and a low standard

error of the fitted curve. The standard error of the curve based on the recorded perception ratings is slightly higher and has 8 of the 101 bands empty (Table 6.1). The logarithm of vertical RMS acceleration gives a standard error which is slightly higher again plus approximately a quarter of the bands are empty.

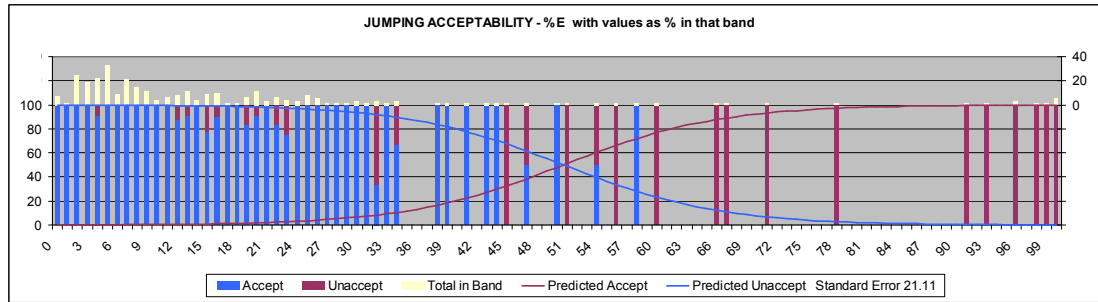


Figure 6.10 Acceptability for Jumping Participants using Emotion Rating as the Predictor

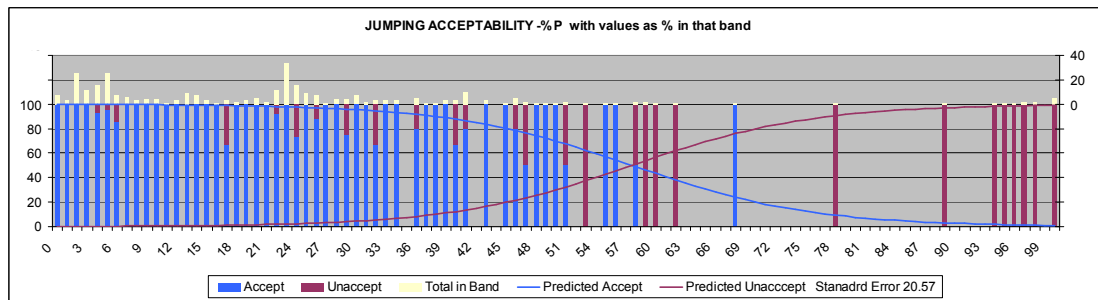


Figure 6.11 Acceptability for Jumping Participants using Perception Rating as the Predictor

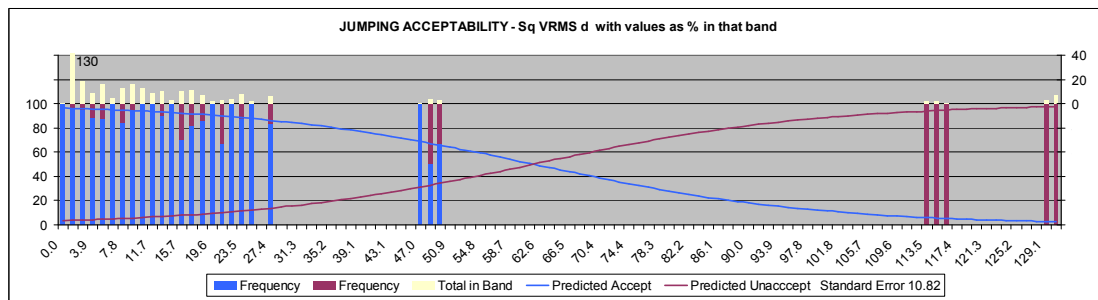


Figure 6.12 Acceptability for Jumping Participants using the square of Vertical RMS Displacement as the Predictor

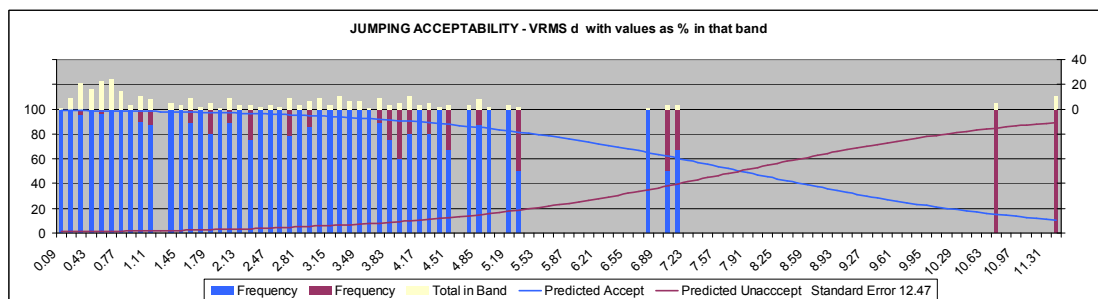


Figure 6.13 Acceptability for Jumping Participants using Vertical RMS Displacement as the Predictor

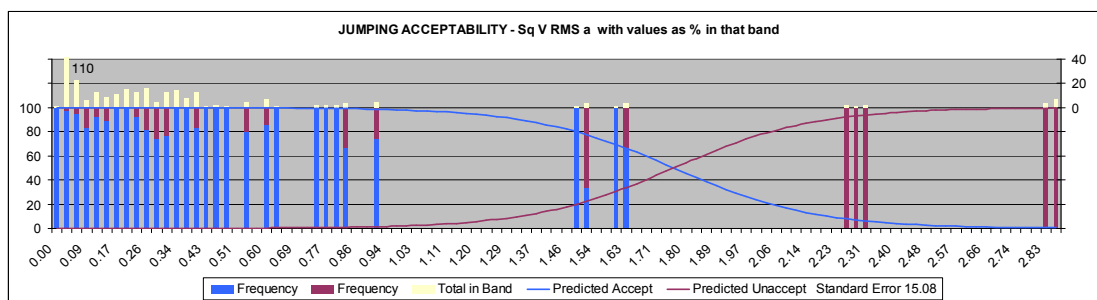


Figure 6.14 Acceptability for Jumping Participants using the square of Vertical RMS Acceleration as the Predictor

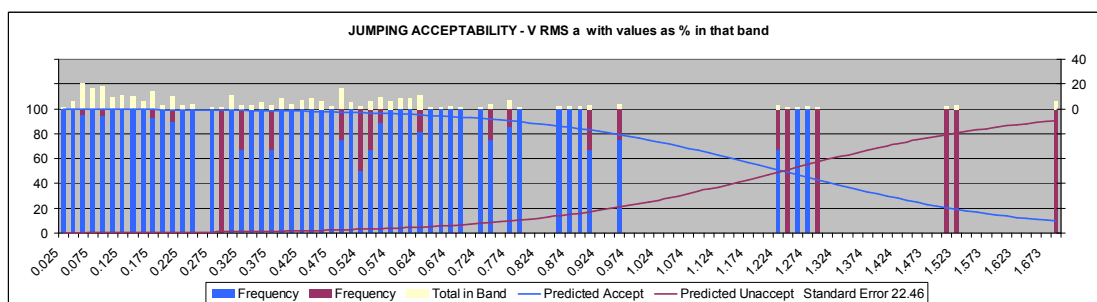


Figure 6.15 Acceptability for Jumping Participants using Vertical RMS Acceleration as the Predictor

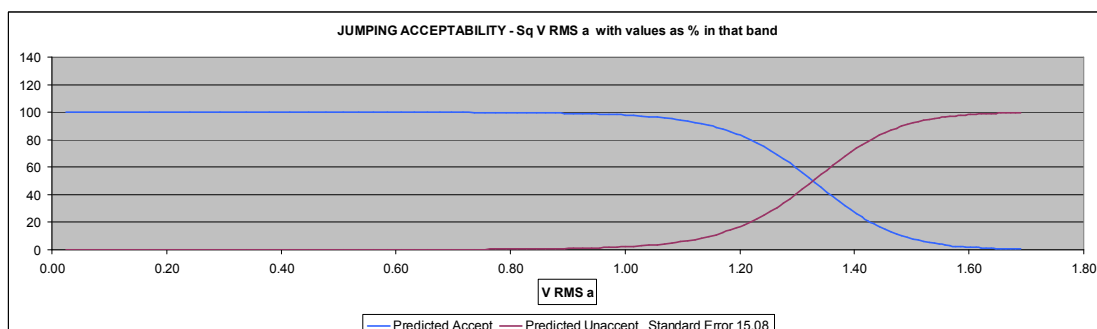


Figure 6.16 Acceptability for Jumping Participants using the square of Vertical RMS Acceleration as the Predictor plotted in terms of Vertical RMS Acceleration

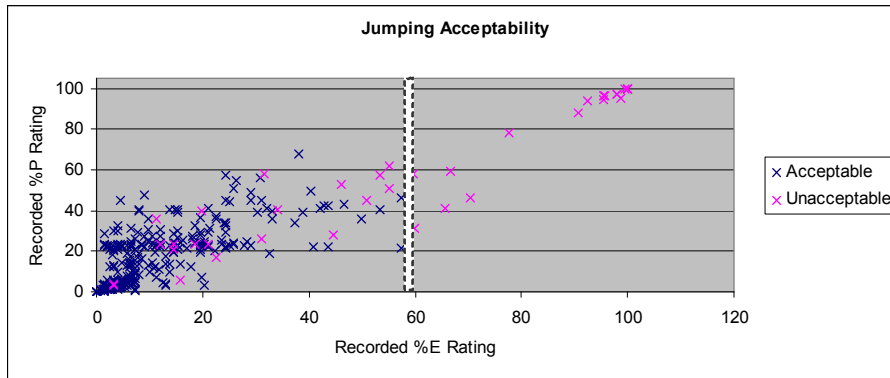
6.1.2.2 Acceptability for Jumping Participants

For all the tests there were fewer participants jumping than seated therefore all the conclusions reached with regard to those jumping are based on a smaller data set. For the previous Chapter concerning the jumping participants' perception and emotional response to the vibration this was not an issue as the results were still based on 653 observations (1400 for those seated). However for the acceptability tests only 320 responses were from jumpers and 634 from seated participants. This means that when the responses are banded for the acceptability histograms it is much less likely that there will be responses in every one of the bands. Despite this, the spread of the results across the bands for emotion and perception ratings is reasonable, as can be seen in Figures 6.10 and 6.11. Because of the jumpers' lower recorded perception and emotion ratings for most of the tests (Chapter 5) there is skew (towards the lower end of the scale) in the banding for these two predictors. Out of the six predictors considered for the jumping participants (emotion and perception ratings and, vertical RMS acceleration and displacement in both linear and squared format) the perception and emotion ratings gave two of the highest standard errors between the predicted acceptability curve and the recorded data due to having the most bands containing data (Table 6.1). Of the two, the perception ratings perform slightly better giving a lower standard error despite the logistic curve being fitted to a greater number of bands.

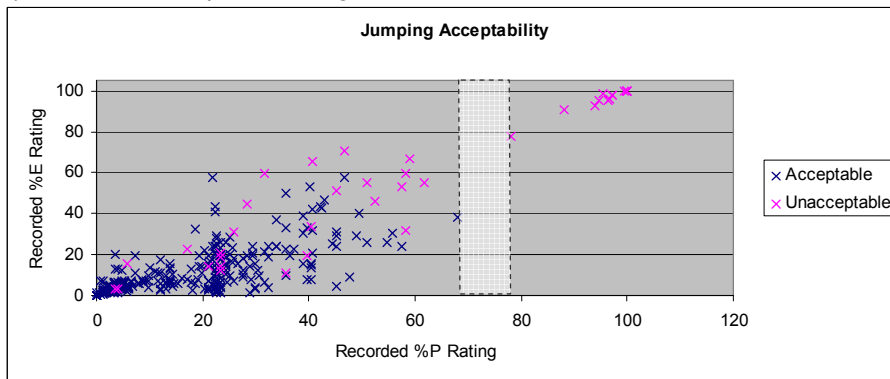
From the initial correlation analysis the best predictor of acceptability for those jumping is likely to be emotion rating, with the next highest correlation being the square of vertical RMS displacement. However squaring the predictor amplifies the distance between recordings and thus increases the number of bands with no data (Figure 6.12). By reverting back to a linear relationship with vertical RMS displacement the spread of the data and the number of empty bands is improved (Figure 6.13). As is to be expected, the standard error between the recorded data and the predicted acceptability curve increases with the number of bands containing data (Table 6.1). The two models result in similar curves with the same vertical RMS displacement value for the 50% acceptability/unacceptability crossover point but the squared model goes closer to 100% at the upper end of the measured vibration scale and is further from 0% at the lowest extreme.

A similar comparison was done for vertical RMS acceleration (Figures 6.14 and 6.15). In this case, also, the change to the linear form (from the squared) helps unify the spread of the data and reduces the number of empty bands. The standard error for the linear model is also higher. When the standard errors for fitting the acceptability curves based on vertical RMS displacement and acceleration are compared, those based on the acceleration values are significantly higher than the equivalent displacement based models (Table 6.1). The linear acceleration model has a similar number of bands of data and standard fitting error to the perception and emotion models but like the linear displacement model only reaches 90% unacceptability at the upper extreme of the recorded range.

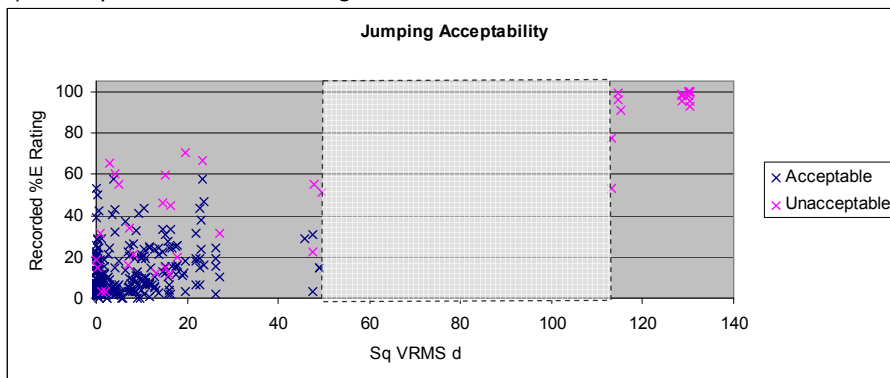
The squared vertical RMS acceleration model has a very short transfer from acceptable to unacceptable (Figure 6.16). This suggests an even simpler relationship for acceptability of those jumping. It implies that over a very short range of vibrations the acceptability for jumpers switches from universally acceptable to universally unacceptable. This theory is borne out by the recorded data where a vertical zone can be plotted on graphs of acceptability versus predictor indicating the change from approximately 95% acceptable on the left to 100% unacceptable to the right (Figure 6.17). A logistic curve with a steeper cross over can be fitted to the data, for each of the predictors, but does not improve on the standard error for any of the predictors. An investigation into how the best fit logistic curve is derived, for those jumping, indicates that the shape of the curve is very dependent on the spacing of the result bands while the crossover point is very sensitive to a few results in the centre of measured range. For those seated the transition between acceptable and unacceptable is more gradual as can be seen by comparing the slopes of the predicted acceptability lines (Figures 6.6 - 6.9 against Figures 6.10 - 6.16). The increased number of filled bands makes the predicted acceptability lines much less sensitive to change.



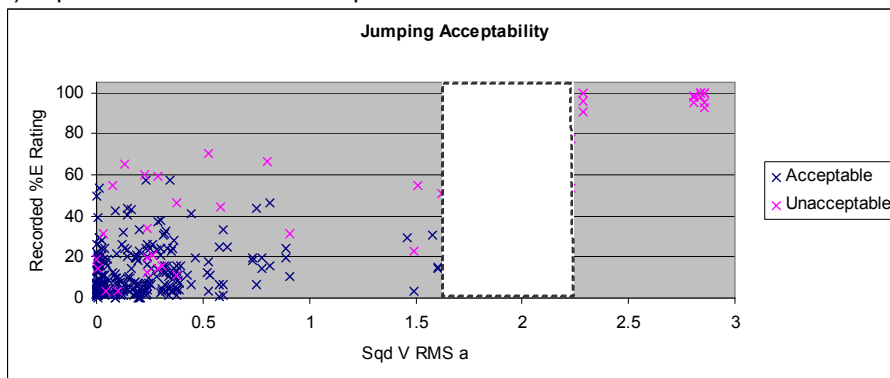
a) Emotion/Perception Ratings



b) Perception/Emotion Ratings



c) Square of Vertical RMS Displacement



d) Square of Vertical RMS Acceleration

Figure 6.17 Acceptability Test Results for Jumping Participants plotted as Recorded Emotion Ratings against Proposed Predictors

6.1.3 Statistical Analysis – Conclusions

For the models generated to predict the acceptability of crowd induced vibrations in grandstands to spectators, those based on emotion ratings prove most accurate for the seated participants while for those creating the vibration (the jumpers) their perception rating provides the best model. This assessment takes into account how well the predicted models fit the collected data as well as the distribution of the data across the range of recorded vibrations (Table 6.1).

Table 6.1 Assessment of Accuracy of Acceptability Models

	Standard Error in Fitting Curve	Full Bands	Empty Bands	Average Number of Data Points in Band	% of Total No. Data Points in Each Band (average)	Standard Deviation in No. of Data Points	Rank
<u>SEATED</u>							
%E	14.35	100	1	6.32	1.00	3.45	1
%P	16.28	93	8	6.80	1.08	7.65	2
Ln V RMS a	18.84	77	24	8.21	1.30	6.82	3
Ln V RMS d	24.18	73	28	8.66	1.37	6.15	4
<u>JUMPING</u>							
%E	21.11	58	43	5.52	1.72	5.78	2
%P	20.57	65	36	4.92	1.54	5.55	1
Sq V RMS a	15.08	35	66	9.14	2.86	11.59	6
Sq V RMS d	10.82	29	72	11.03	3.45	13.38	3
V RMS a	22.46*	57	44	5.54	1.75	4.52	5
V RMS d	12.47*	49	52	6.53	2.04	4.99	4

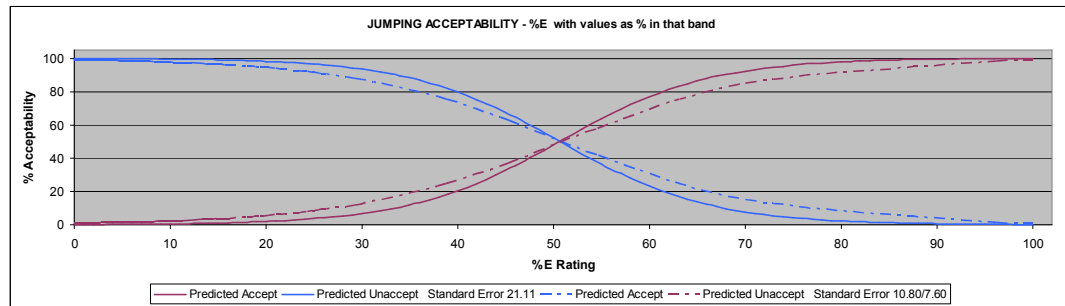
* Acceptability Curve does not reach 100% Unacceptable within Recorded Range of Vibrations

The second best model for those seated is the one based on their perception ratings closely followed by the model using the logarithm of vertical RMS a. Similarly for those jumping it is the other human response predictor, i.e. emotion rating, which gives the second most accurate model. For the jumpers it is difficult to differentiate between the accuracy of the models based on the predictors using the basic recorded vibration data (i.e. vertical RMS displacement and acceleration). This is because the models are based on widely different numbers of data sets and produce varying standard error values. In order to try and reach a conclusion the 320 jumping acceptability responses were divided into bands each containing 4 data points and

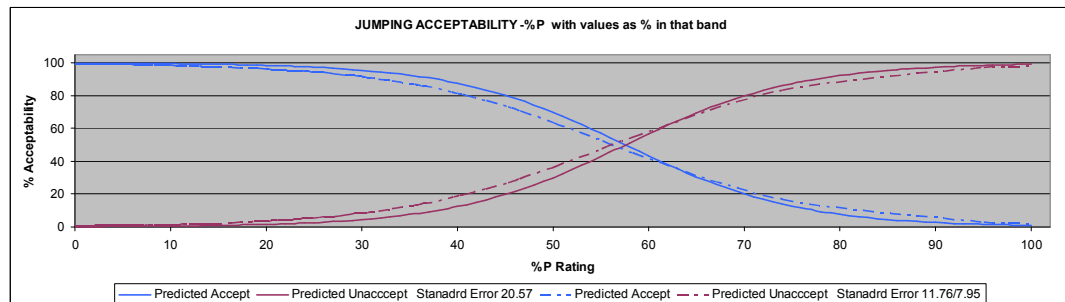
the percentage of acceptable responses in each band was recalculated and plotted against the mean predictor value for each band. A logistic acceptability curve was then fitted to the results using the same procedure as before. This process was repeated again for equal bands containing 7 data points. These new models were overlaid on the ones created using even bandwidths and the results compared (Figure 6.18). Note, the equal 4 and 7 data point banding produced very similar results and so the result is shown only once (dashed line) however both standard errors are given, the higher being for the banding with 4 data points per band.

For the jumping models based on the recorded perception and emotion ratings the equal data point bands produced curves with very similar crossover and extreme values compared to the even bandwidth models (Figure 6.18 a and b). This was taken as validation of these models. The greatest impact of the change in banding was on the models based on the square of vertical RMS acceleration (Figure 6.18 d) where the equal data bands gave a predicted shallower curve, similar to all the other predictors (Figures 6.10 to 6.13), and reduced the crossover and upper extreme values. For the square of vertical RMS displacement (Figure 6.18 c) the cross over point was also reduced slightly, due to the rebanding, but the upper and lower extreme values remained fairly constant.

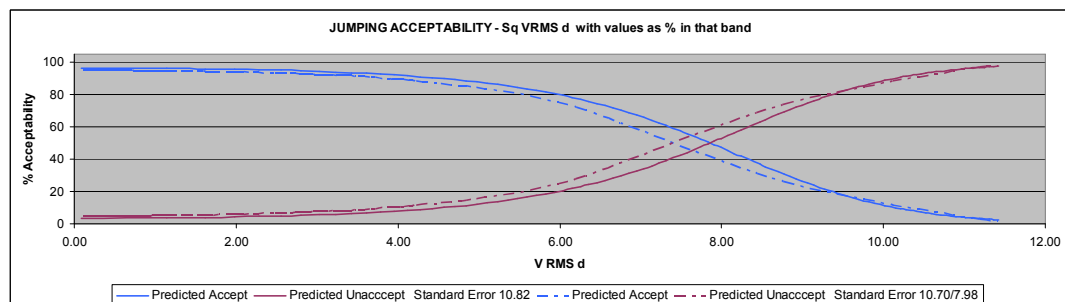
Based on all these results it was decided that of the models developed to predict the acceptability for those jumping, based on the vibration size, those using the square of vertical RMS displacement were most appropriate.



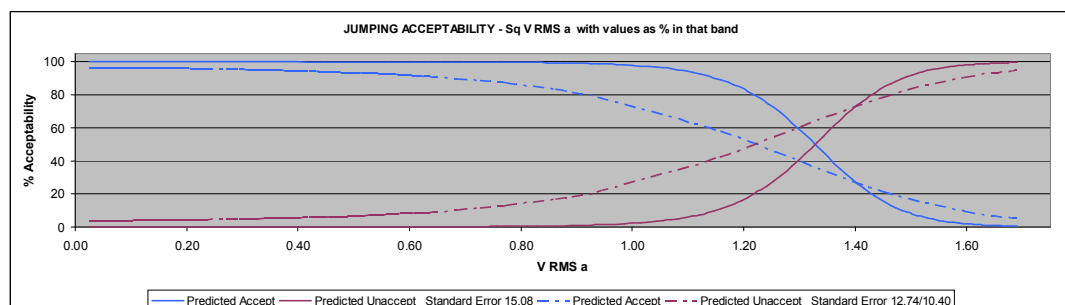
a) Emotion Ratings



b) Perception Ratings



c) Square of Vertical RMS Displacement



d) Square of Vertical RMS Acceleration

Figure 6.18 Comparison of Acceptability Curves for Jumping Participants Calculated using Different Banding Methods [Even Bandwidths shown Solid and Equal Bands (4 or 7 data points) shown Dashed]

The models created in Chapter 5 to predict the human response to grandstand vibrations estimate the mean value for the population. Because these response models do not predict the spread of the ratings about the mean they cannot be used to convert the acceptability models using the human response predictors back to vibration size. This is shown diagrammatically in Figure 6.19 and 6.20 with the predicted emotion rating being calculated from the mean value of %E for a given vertical RMS acceleration (i.e. horizontal slices from Figure 6.19) and the percentage acceptability curves being derived from the average acceptability of participants responses whose %E ratings fall into a certain band e.g. 10-11% (i.e. vertical slices from Figure 6.20).

Because of this if we are to propose a model that can be used to predict spectator response to vibrations in actual grandstands it has to be based on the measured vibration magnitude. The most suitable models for this purpose are the logarithmic vertical RMS acceleration model for seated spectators (Figures 6.21 and 6.22) and the squared vertical RMS displacement model for jumping spectators (Figure 6.23).

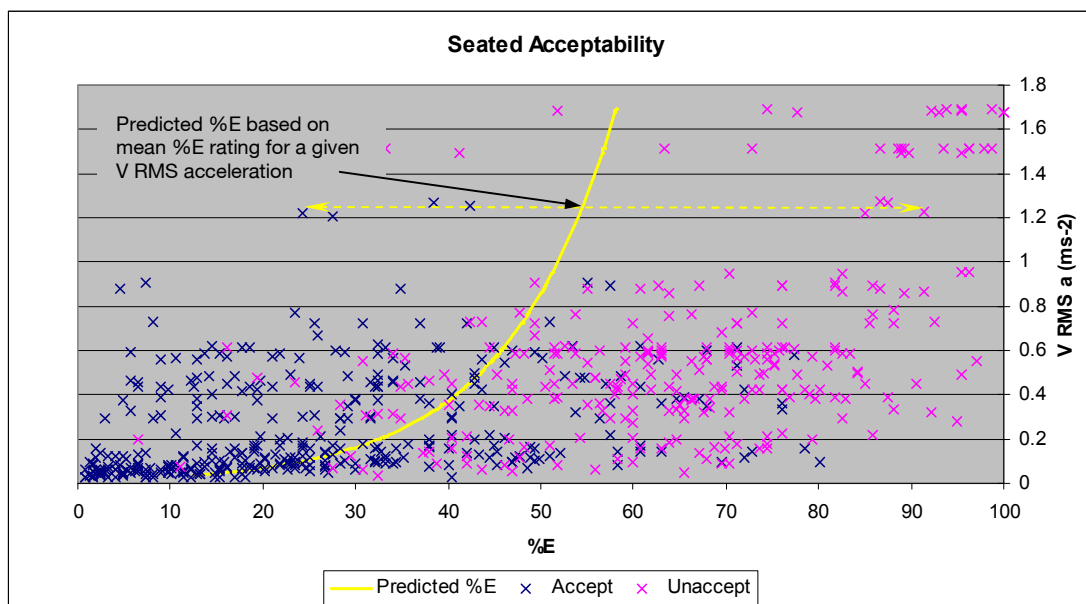


Figure 6.19 Seated Acceptability Data overlaid with estimated %E Rating based on the logarithm of Vertical RMS Acceleration (Chapter 5)

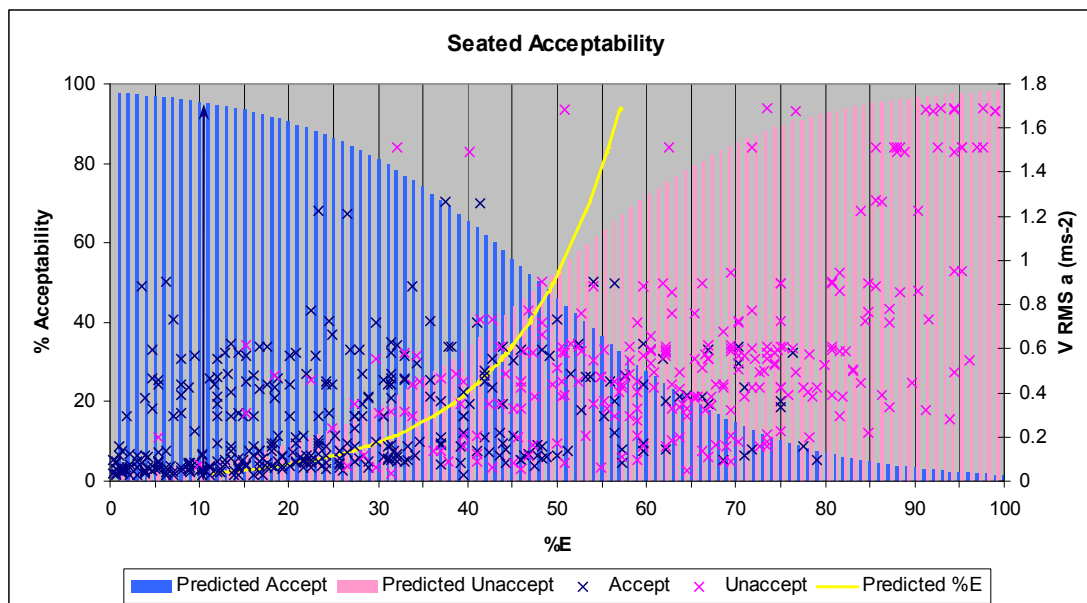


Figure 6.20 Seated Acceptability Graph based on Emotion Ratings

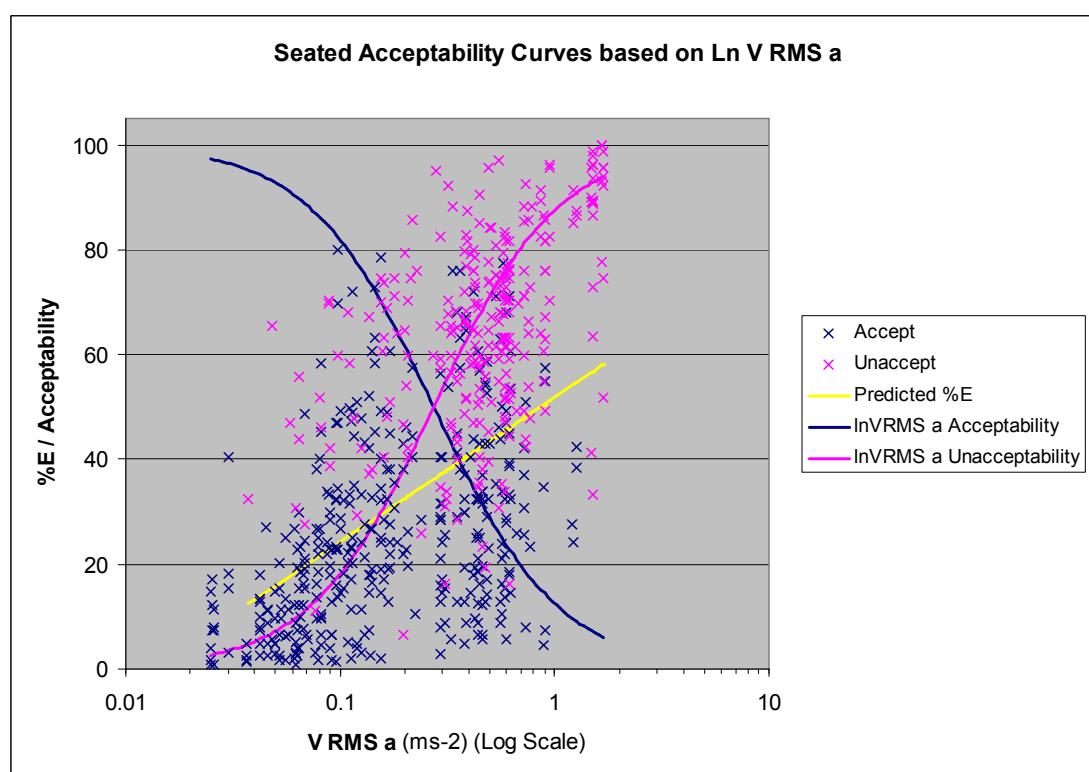


Figure 6.21 Seated Acceptability Graph based on the Logarithm of Vertical RMS Acceleration (Log Scale)

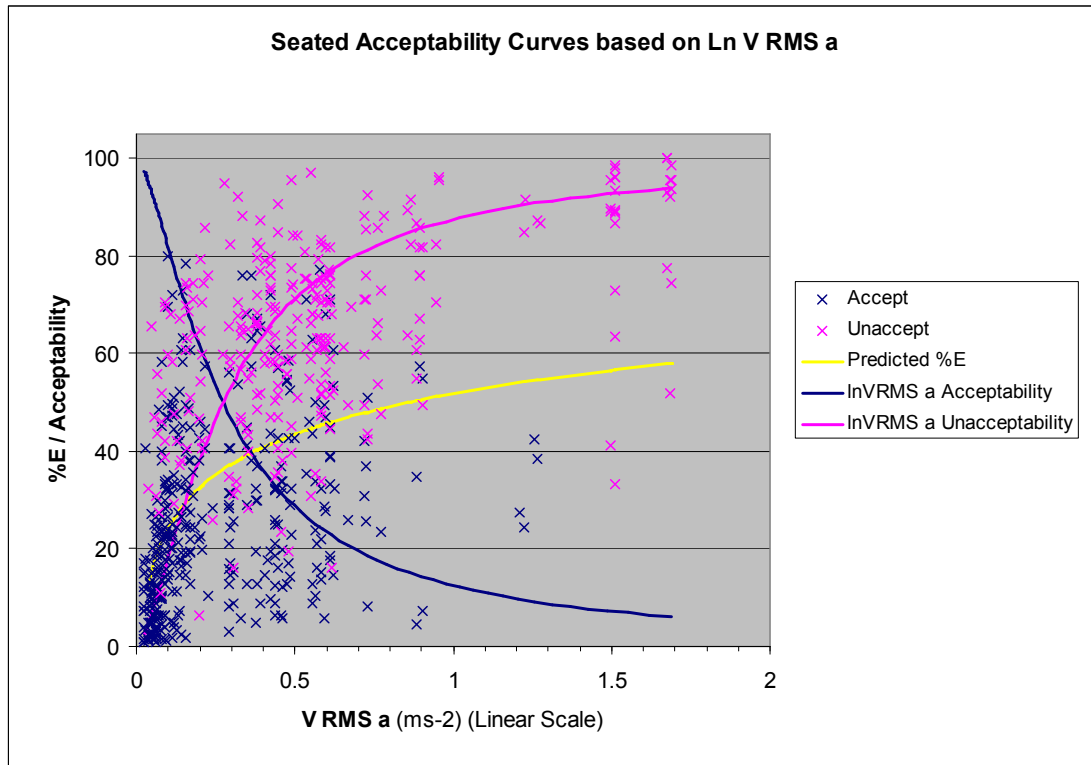


Figure 6.22 Seated Acceptability Graph based on the Logarithm of Vertical RMS Acceleration (Linear Scale)

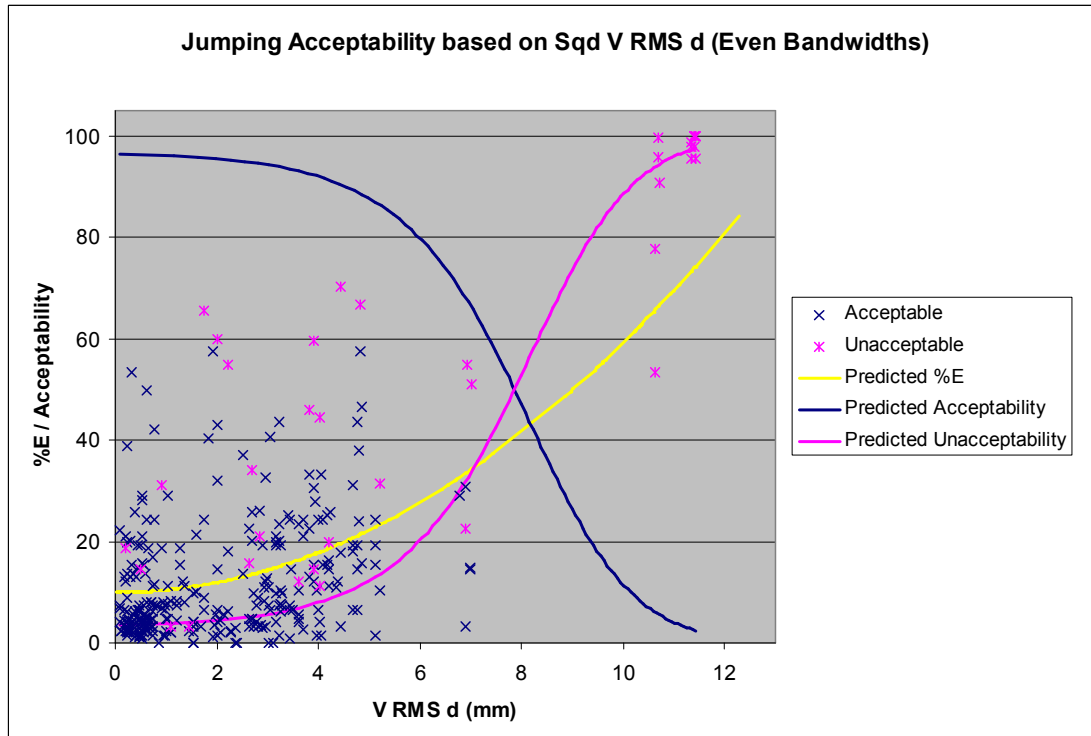


Figure 6.23 Jumping Acceptability Graph based on the Square of Vertical RMS Displacement

The selected acceptability curves for both seated and jumping participants are based on the same form and format of predictor as the selected single variable models for those participants' perception and emotion ratings (Chapter 5, Table 5.20). The selected single variable models for the mean emotion rating are also shown in Figures 6.22 and 6.23, for comparison.

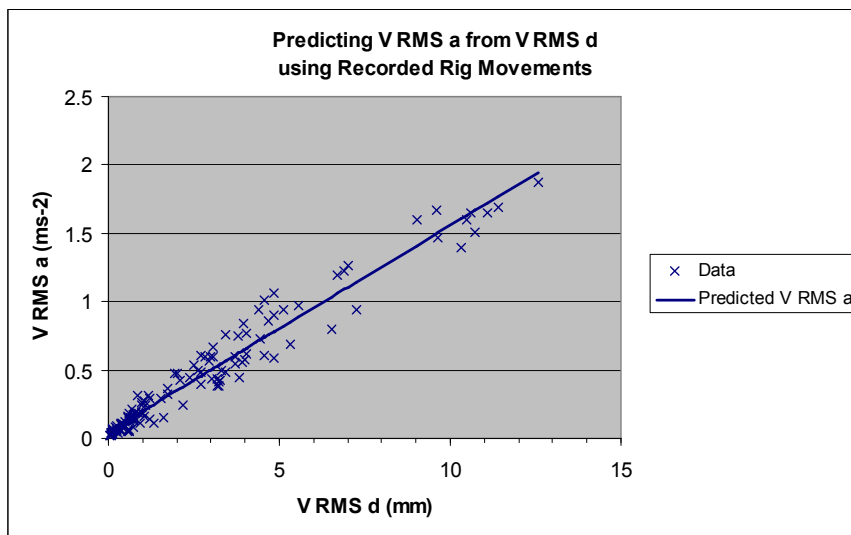
The seated acceptability curve (Figure 6.22) starts with 2.9% of seated participants finding the vibration unacceptable at 0.025ms^{-2} vertical RMS acceleration rising sharply to 20% unacceptable at around 0.1ms^{-2} vertical RMS acceleration. At the upper extreme of the recorded range the curve predicts 94% unacceptability for seated spectators at 1.7ms^{-2} vertical RMS acceleration. The shape of the acceptability curve is very similar to that of the selected model predicting emotional response, increasing steeply for vibrations below approximately 0.5ms^{-2} then plateauing.

Likewise for those jumping the acceptability curve is similar in shape to the models predicting perception and emotion (Chapter 5), with the percentage of jumpers finding the vibrations unacceptable remaining low until the jumpers can feel the vibration and then the unacceptability levels increase. For those jumping the predicted acceptability curve (Figure 6.23) begins with 3.6% of those jumping perceiving the vibration as unacceptable at a RMS vertical displacement of 0.09mm. The level of unacceptability remains below 8% until a RMS vertical displacement of around 4.0mm. The slope of the curve then starts to increase and by 6mm vertical RMS displacement 20% of the jumpers deem the vibration unacceptable rising to 97.5% at 11.4mm vertical RMS displacement at the top end of the recorded range.

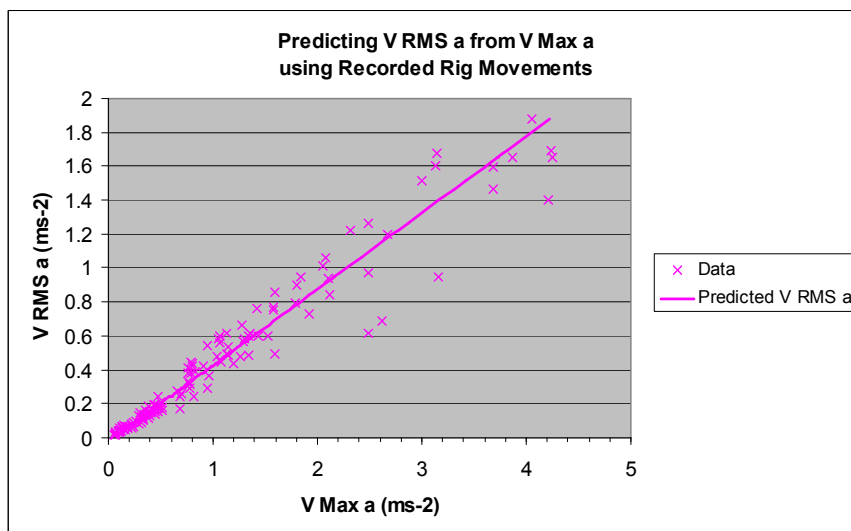
From these results it can be seen that, for the range of vibrations tested, there will typically be around 5% of people who disagree with the general consensus i.e. will find a very small vibration unacceptable or a very large vibration acceptable. This is a normal finding for psychological testing of this nature. Using this knowledge and the graphs shown in Figures 6.22 and 6.23 one can predict the percentage of people that would deem a given crowd induced grandstand vibration unacceptable depending on whether they were jumping to create the vibration or seated. This is covered in greater detail in Section 6.3

6.2 Comparison of Acceptability Results with Published Guidelines

The acceptability curves generated in Section 6.1 were then compared against the current United Kingdom guidelines for acceptable vibrations in grandstands for various events (IStructE 2008). [As these guidelines are in terms of RMS acceleration a formula was determined based on the recorded rig movements to convert the vertical RMS displacements (on which the jumpers' acceptability is based) to the equivalent vertical RMS acceleration experienced during the experiments (Figure 6.24 a). This had a minimal (<2%) impact on the accuracy of the jumping acceptability model.]



a Conversion of Vertical RMS Displacement to Vertical RMS Acceleration



b Conversion of Vertical Peak Acceleration to Vertical RMS Acceleration

Figure 6.24 Conversion to RMS Acceleration using Recorded Rig Movements

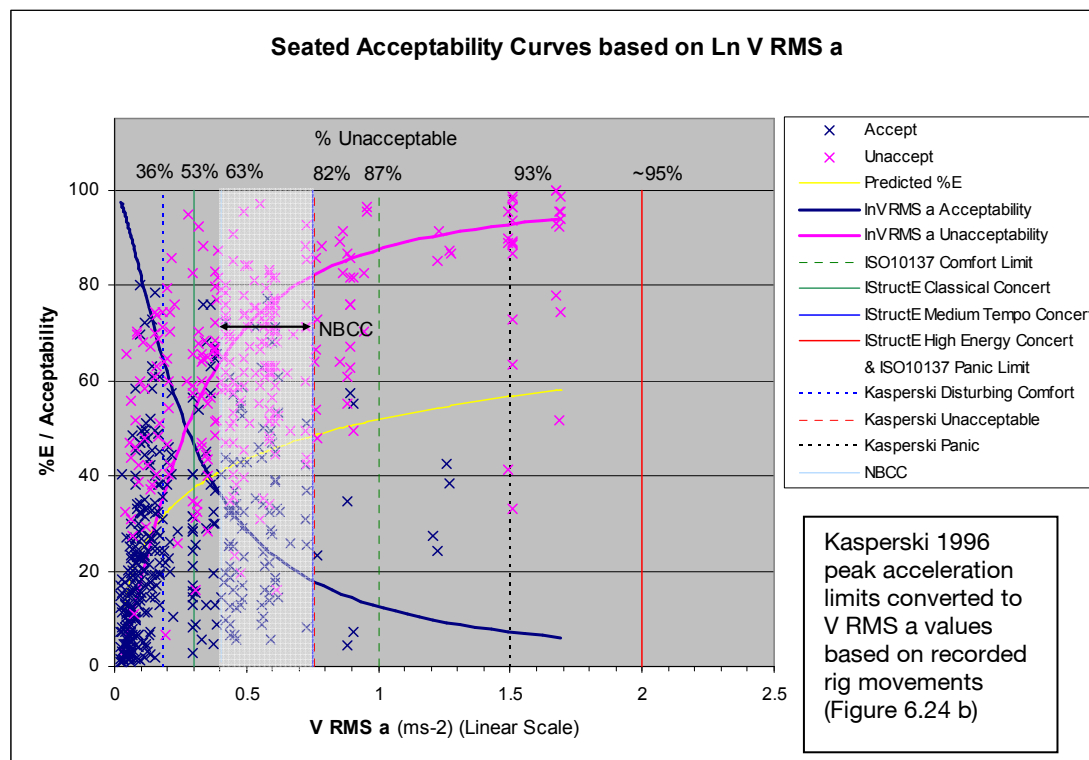


Figure 6.25 Seated Acceptability Curves based on the logarithm of Vertical RMS Acceleration

The guideline limit for classical concerts and well attended sporting events is $3\%g$ (0.29ms^{-2}) RMS acceleration. At this vibration the acceptability curves derived from the experimental work predict that 53% of those seated and 4% of those jumping would find the vibration unacceptable (Figures 6.25 and 6.26). At the guideline limit of $7.5\%g$ (0.74ms^{-2}) for high profile sporting events and concerts with medium tempo music 82% of those seated and 10% of those jumping would find the movement unacceptable based on the experimental acceptability curves. For extreme events including high energy concerts a maximum of $20\%g$ (1.96ms^{-2}) is recommended by the guidelines. This magnitude of RMS acceleration was not achieved during the tests but based on the acceptability curves and the test data a vibration of this size would probably be universally unacceptable to all spectators.

Relating the acceptability curves back to the original Kasperski 1996 peak acceleration limits for uncomfortable ('comfort disturbing'), unacceptable and panic inducing vibrations provides greater insight into published grandstand vibrations guidance.

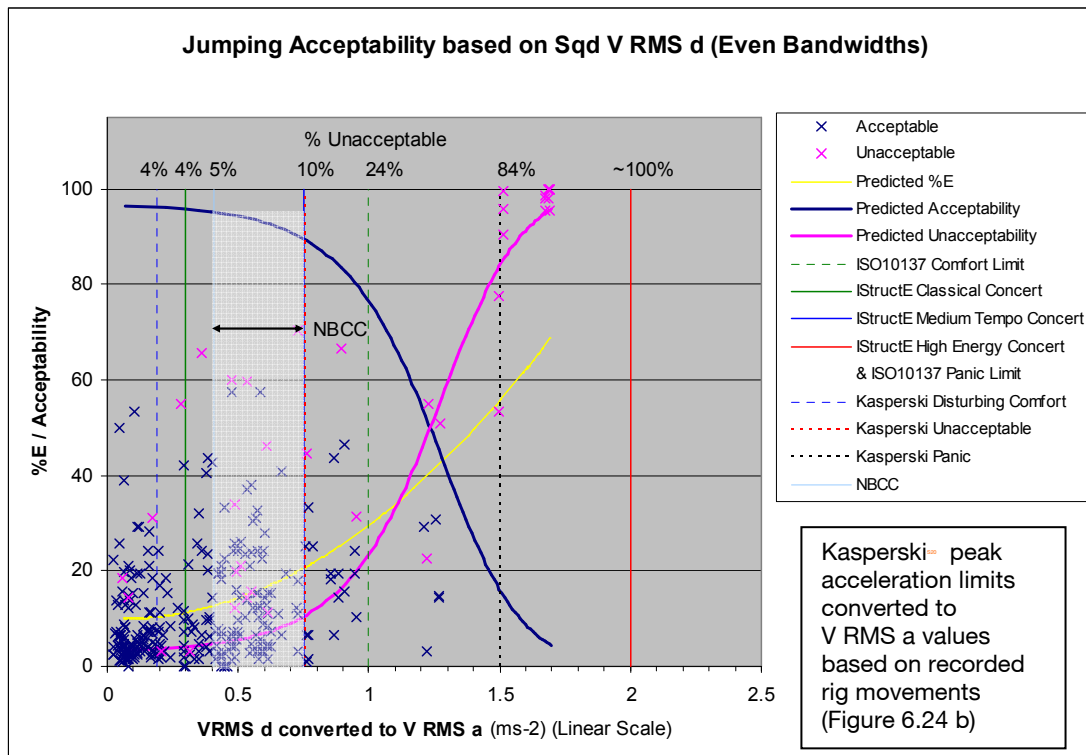


Figure 6.26 Jumping Acceptability Graph based on the square of Vertical RMS Displacement

Kasperski's 1996 peak acceleration values were converted to 'test rig specific' RMS values using the relationship derived from the experimental data (Figure 6.24 b) and then plotted on the acceptability curves (Figures 6.25 and 6.26). The most striking observation is that Kasperski's panic limit of $0.35g$ (peak) lies almost exactly at the point where all recorded responses, both seated and jumping, become 100% unacceptable ($1.5ms^{-2}$ vertical RMS acceleration). On the acceptability curves this translates to a predicted unacceptability of 93% for seated spectators and 84% for jumping spectators. An unacceptable threshold value of $0.18g$ peak acceleration was proposed by Kasperski (1996) and incorporated in the National Building Code of Canada 2005 Structural Commentaries (Part 4 of Division B) (NBCC 2005) as the upper limit for acceptability of vibrations in grandstands and arenas. Overlaid on the experimentally derived acceptability curves $0.18g$ peak acceleration ($0.75ms^{-2}$ vertical RMS acceleration) corresponds to 82% and 10% unacceptability for seated and jumping participants respectively. The lower end of the range of maximum acceptable accelerations proposed by the NBCC is $0.1g$ peak acceleration ($0.4ms^{-2}$ vertical RMS acceleration), which corresponds to an unacceptability level of 63% for seated spectators and 5% for active spectators based the experimentally derived curves.

Finally Kasperski's (1996) limit for vibrations becoming uncomfortable ('comfort disturbing') is $0.05g$ peak acceleration (0.19ms^{-2} vertical RMS acceleration), this reads off the acceptability curves as being unacceptable to 36% of the seated and 4% of the jumping participants.

It is believed that the IStructE (2008) RMS acceleration acceptability criteria were derived from Kasperski's original peak acceleration values and the NBCC Guidelines using a conversion factor of $\sqrt{2}$ as; Kasperski's disturbing comfort threshold of $0.05g/\sqrt{2} = 0.035g$ similar to IStructE limit for classical concerts, the NBCC lower limit for stadium accelerations $0.10g/\sqrt{2} = 0.07g$ comparable to the IStructE guidelines for medium tempo concerts and Kasperski's panic threshold of $0.35g/\sqrt{2} = 0.25g$ slightly greater than the maximum acceptable acceleration recommended by the IStructE (2008). From the testing carried out the conversion factor of peak acceleration to RMS acceleration was in the order of 0.45 (Figure 6.24 b) rather than 0.707 which could possibly explain why the test results tie in slightly better with the Kasperski/NBCC peak values than the IStructE guidelines. Refer to Section 6.3.1 for further discussion on the determination of RMS values.

An additional condition of the Institution of Structural Engineers dynamic performance requirements for permanent grandstands (2008) is that the maximum dynamic component of displacement due to crowd loading should not exceed 7mm RMS. This is derived from Kasperski's (2001) recommendation to restrict visual vibrations in cantilevered stands to avoid anxiety of those situated beneath the stand. A 7mm vertical RMS dynamic displacement corresponds to approximately 1.1ms^{-2} RMS vertical acceleration experienced during the tests (Figure 6.24 a) which from the acceptability curves is predicted to be unacceptable to 89% of those seated on the stand. However as the tests focussed on acceptability of those located on a grandstand, not underneath, it is impossible to comment further on the validity of the IStructE's (2008) dynamic displacement guideline limit.

Most of the current published stadium guidance relates directly back to Kasperski 1996 and is independent of frequency. ISO10137:2007 takes a slightly different approach, magnifying a standard frequency dependent base perception curve by multiplication factors dependent on the situation being assessed. Although forced vibrations due to synchronised crowd loading are generally at the forcing frequency,

the frequency of the acceleration response is dependent on; the natural frequencies of the structure and the periodic loading, as well as the strength of the various harmonic components of the forcing function. Therefore, even though the approximate range of forcing frequencies for grandstands is 1.5 to 2.5Hz it is more prudent to use the section of the base curve between 4 to 8Hz where the acceleration limits are at their lowest. From this the ISO10137 criterion for the comfort of the passive part of the audience in a grandstand is a maximum RMS acceleration of 1ms^{-2} while the safety criterion for the avoidance of panic is twice this limit at 2ms^{-2} RMS acceleration. Compared to the experimentally derived curves the ISO10137 comfort limit of 1ms^{-2} would be unacceptable for 94.5% of seated spectators and 74% of those jumping. The ISO10137 panic safety limit is similar to the IStructE recommended limit for high energy concerts.

6.3 Calculation of Predicted Accelerations

It is apparent that the experimentally determined acceptability curves do not sit easily with the current IStructE guidelines (2008). In addition to the issue regarding RMS values discussed above, this could be due to a discrepancy between the actual recorded RMS accelerations and the method recommended in the guidelines for calculating crowd induced vibrations in grandstands.

6.3.1 Modelling using British Guidelines

The IStructE (2008) proposes 3 load cases relating to different types of crowd loading (Scenarios 2-4). Scenario 2 assumes the crowd to be 'predominantly seated with occasional coordinated rhythmic movement from standing people' and is used to represent the loading at a 'classical concert and typical well attended sports event'. For 'commonly occurring events including high profile sporting events and concerts with medium tempo music' Scenario 3 loading considers the whole crowd to be active and the loading is specified as being as 75% of Parkhouse and Ewins (2006) derived loading for 50 people bobbing. (However an attempt to recreate IStructE (2008) Scenario 3 loading from the data given in Parkhouse and Ewins (2006) suggests that it is in fact a smaller percentage than this. See Section 6.3.2 for a comparison of the StructE (2008) and Parkhouse and Ewins (2006) loadings.)

The most extreme case considered, Scenario 4, is 'an excited crowd, mostly standing and bobbing with some jumping' with loading double that of Scenario 3. These load cases take the form of a Fourier series with 3 harmonics at multiples of the excitation frequency (Table 6.2). The harmonic load factors given for each 'scenario' are independent of frequency but a 'crowd effectiveness factor' is applied to the total load to take account of synchronised crowd loading being more effective at certain frequencies. As Scenario 4 relates to high energy events the IStructE's key consideration is the avoidance of panic and so 'an unrestricted frequency range of possible excitation' is considered 'but with some allowance for reduced effectiveness of the loading at high and low excitation frequencies'. Thus for Scenario 4 the defined effectiveness factor peaks at an excitation frequency of around 2Hz with a value of 1 and does not drop below approximately 0.3 for activities between 0 and 4Hz. As Scenarios 2 and 3 deal with less energetic events the IStructE rules out occurrence of panic due to crowd induced vibrations and instead focuses on spectator comfort. The shared effectiveness factor for Scenarios 2 and 3 is much more focussed and uses data collated by Littler (2003) on the probability of certain song frequencies being played at pop concerts to produce a normally distributed effectiveness curve, peaking at 1 for an activity frequency of 1.8Hz and dropping to 0.0015 at 0 and 3.6Hz.

The model advocated by the IStructE (2008) guidelines represents the crowd and grandstand in the form of a damped 2 degree of freedom system with the periodic loading described above applied as a pair of equal internal forces (as shown in Figure 6.27). This model and its characteristics are described in more detail by Dougill et al (2006).

Table 6.2 Summary of IStructE (2008) Dynamic Crowd Loading

Event Type	IStructE Scenario	Dynamic Load Factor ($m G_i$) in terms of total mass of the crowd m			Crowd Effectiveness Factor ρ
		1st Harmonic	2nd Harmonic	3rd Harmonic	
High Energy Concert	Scenario 4	0.375 m	0.095 m	0.026 m	Scenario 4 EF
Medium Tempo Concert or High Profile Sporting Event	Scenario 3	0.188 m	0.047 m	0.013 m	Scenario 2 & 3 EF
Classical Concerts or Typical Sporting Events	Scenario 2	0.120 m	0.015 m	-	Scenario 2 & 3 EF

where load function $P(t) = \rho mg \sum_{i=1}^{i=3} G_i \cos(2\pi i f t + \theta_i)$ (see Figure 6.27)

with ρ = Crowd Effectiveness Factor
 m = Mass of the crowd (based on 80kg per person)
 g = Acceleration due to gravity, 9.81 ms^{-2}
 i = Harmonic number
 G_i = The i th Dynamic Load Factor
 f = Fundamental Frequency of the crowd activity
 t = Time in seconds
 θ_i = Phase angle of the i th harmonic

and $k_c = 4\pi^2 n^2 m$
 n = Natural frequency of the active crowd
= 2.3Hz for Scenarios 3 & 4
= 5.0Hz for Scenario 2

with c_c = Damping of the Crowd
= 25% critical for Scenarios 3 & 4
= 40% critical for Scenario 2

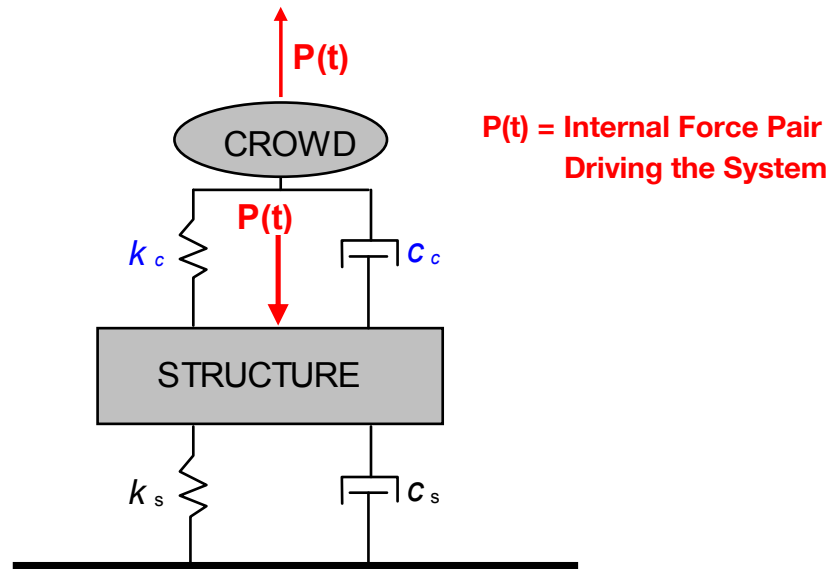


Figure 6.27 IStructE (2008) Body Unit model

To model the crowd component of this system, recommended properties of the crowd ‘body unit’ are given for each of the three loading cases in the guidelines (IStructE 2008). For the active loading of Scenarios 3 and 4, where the crowd is assumed to be mostly standing, the ‘body unit’ is assigned a natural frequency of 2.3Hz and damping of 25% of critical. Scenario 2 is based on a largely seated audience and so the ‘body unit’ is taken as having a much higher damping of 40% critical and a natural frequency of 5Hz. For all load cases each person in the crowd ‘body unit’ is assumed to have a mass of 80kg and it is assumed that every member of the crowd contributes to the dynamic loading of the structure.

In order to confirm whether or not accelerations calculated using the method proposed by the IStructE are compatible with the derived acceptability curves, ‘body unit’ models were set up for each of the test rig set ups and the output of each of the loading scenarios compared to the actual results. Because the design of the test rig resulted in a single clear dominant vertical mode (with the maximum movement under the middle of the centre precast unit) the rig structure was modelled as a very simple mass/spring/damper system as Figure 6.27 rather than a more complex alternative. The results used for the comparison were those recorded under the central precast unit. As a starting point the damping of the rig was taken as 2% of critical for all three rig set ups, similar to the pretesting computational modelling described in Section 3.2. The effect of varying the structural damping of

the rig investigated and was shown not to significantly alter the fit of the results to the model. This was because the test results typically lie at the base of the harmonic peaks and while increasing the structural damping reduces the peak acceleration values it does little to those close to the base.

It is worth mentioning that one of the reasons it was decided to use a simple mass/spring/damper system to represent the test rig is that standard structural engineering software does not typically have the capability to analyse these models due to the vast difference in damping between the crowd and structure. This is because the equations of motion describing the system are coupled meaning that the Rayleigh damping method cannot be used. Therefore a spreadsheet was written in Excel solving the coupled equations of motion using the complex frequency response in order to determine the response of the system.

In the analysis carried out, the input/output were in the form of a Fourier series

$$y(t) = A \sin(\omega t + \theta) + B \sin(2\omega t + \phi) + C \sin(3\omega t + \psi)$$

In order to rationalise the calculations the following approximations were made (as recommended in the IStructE (2008) guidance).

$$y_{PEAK} = A + B + C$$

$$y_{RMS} = \sqrt{A_{RMS}^2 + B_{RMS}^2 + C_{RMS}^2}$$

An important point to note is that although the RMS value of a pure sine wave is

$\frac{y_{PEAK}}{\sqrt{2}}$ the RMS value of a periodic wave made up of a series of sine waves is

approximately the square root of sum of the squares of the peak values of the individual components. This means it is unlikely, given the harmonic loading used in the models, that the RMS acceleration will be 70.7% of the peak acceleration. As an example the peak value of Scenario 4 loading is $0.496 \mu g$ while the corresponding RMS value is $0.274 \mu g$ i.e. 55% of the peak value.

Of the three load cases Scenario 4 produced results in excess of those recorded, while the RMS accelerations calculated using Scenario 2 were typically lower than the test rig results. Scenario 3 gave the closest results (Figure 6.28)

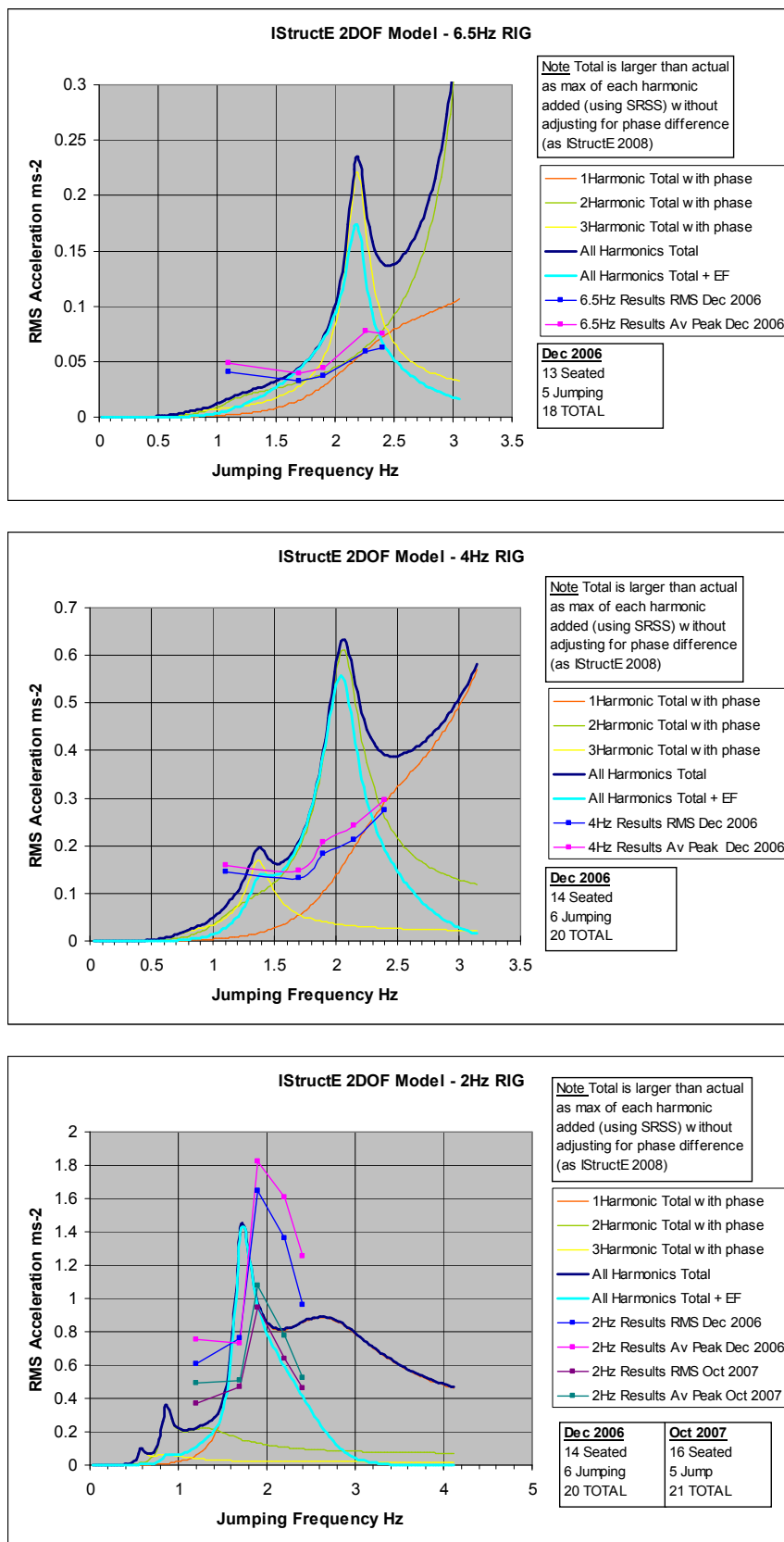


Figure 6.28 Results of IStructE (2008) Scenario 3 Model for each Rig Set-up

6.3.2 Alternative Models Considered

Because the tests carried out had varying percentages of the crowd jumping it was felt that the IStructE model could possibly be improved by adapting the crowd ‘body unit’ to take into consideration the number of people actually creating the dynamic loading. Four different models were developed and are shown schematically in Figure 6.29. These included 2 variations on the 2 degree-of-freedom model (Figure 6.29 a and c) plus a simpler single degree-of-freedom model (Figure 6.29 b) and a more complex 3 degree-of-freedom model (Figure 6.29 d) similar to that proposed by Pavic and Reynolds 2008.

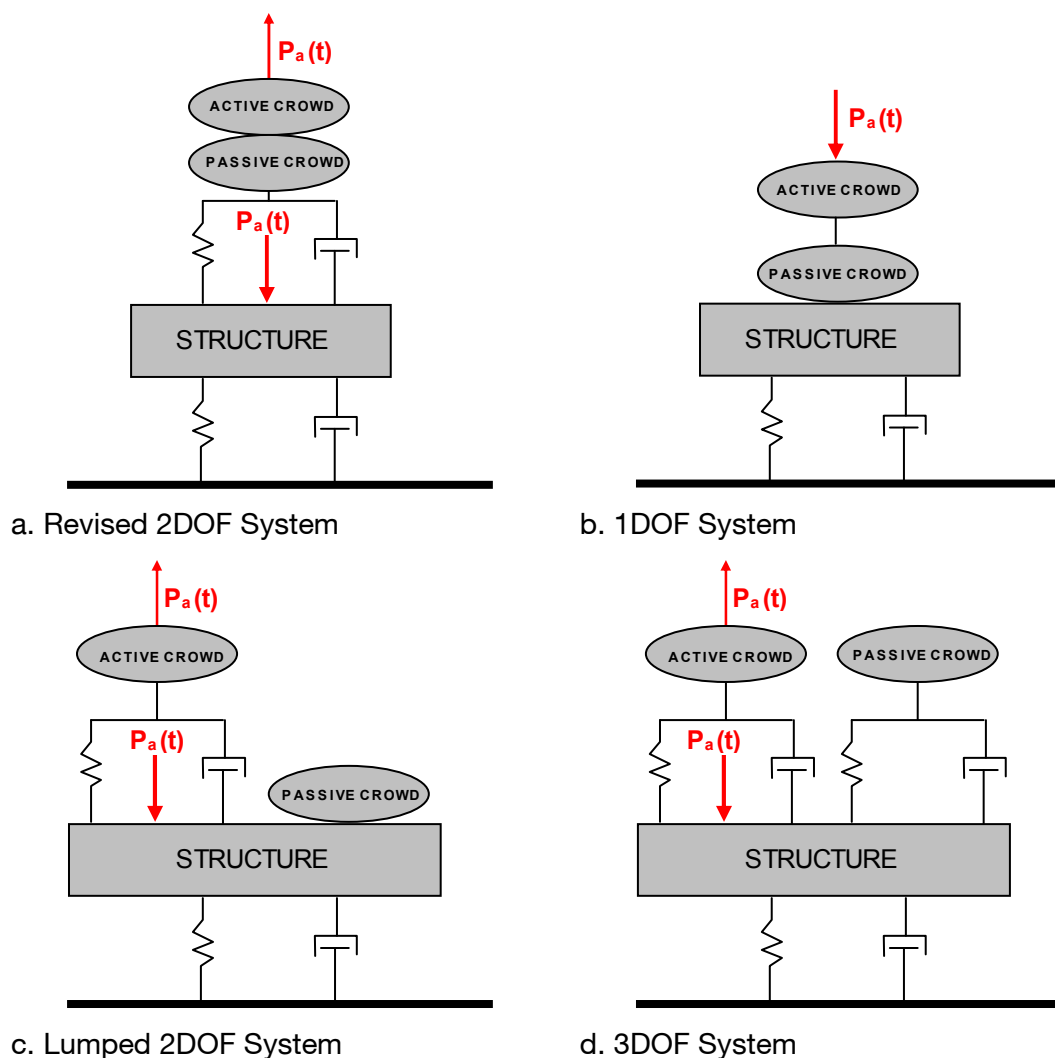


Figure 6.29 Alternative Analysis Models Considered

In order to obtain a realistic loading function that could be related back to actual people jumping or bobbing the various IStructE Scenario loadings were compared with the synthesised crowd loadings produced by Parkhouse and Ewins (2006) and on which Scenarios 3 and 4 are supposedly based. Parkhouse and Ewins generated dynamic load factors for various sizes of crowds (ranging from 5 to 200 people) either jumping or bobbing on the spot at 1.5 Hz, 2 Hz, 2.67Hz and 3.5Hz. These values were based on results of tests of 100 people who were asked individually to jump and bob, in time to a metronome, on a force plate fixed flush and rigidly with the test room floor. The force-time history outputs were then collated to generate synthesised crowd loadings.

The first observation is that the Parkhouse and Ewins' dynamic load factor (DLF) values vary with frequency while the IStructE values are independent of frequency but an effectiveness factor (EF) is applied which is frequency dependent. As mentioned previously there are two IStructE effectiveness factors. The first used with the high energy loading of Scenario 4 accounts for the amount of force people can impart jumping at various frequencies and therefore is more appropriate to compare to Parkhouse and Ewins' results. The second effectiveness factor, for the lower energy Scenarios 2 and 3, is a risk probability factor peaking at the most common frequency for pop songs of 1.8Hz.

The Scenario 4 effectiveness factor is a symmetric normalised *sech* ($\text{sech}(x) = \frac{1}{\cosh(x)}$) curve peaking at 2Hz. Although the peak dynamic load factors

(DLFs) for jumping recorded by Parkhouse and Ewins (2006) were also at 2Hz, plotting the average total DLF for each jump frequency shows that the distribution is non-symmetric and the actual peak value is likely to occur closer to 2.1Hz. Because of the asymmetry of the average total DLF for each of the 4 jump frequencies it is fitting a symmetric curve to all 4 points is difficult. However by selecting the three higher frequency values (2Hz, 2.67Hz and 3.5Hz) a symmetric curve of the form

$$DLF = \frac{a}{[\cosh(f - b)]} - c$$
 can be fitted to the points (where f is the fundamental

frequency of the crowd activity in Hz). As can be seen from Figure 6.30 this jumping effectiveness factor curve is very similar to the Scenario 4 effectiveness factor curve. For bobbing the Parkhouse and Ewins' average total DLFs peak at around 2.6Hz,

higher than for jumping however, they are distributed more symmetrically, similar to the Scenario 4 effectiveness factor and all 4 points can be fitted to an equation of the form $DLF = \frac{a}{[\cosh(f - b)]} - c$ where f is the fundamental frequency of the crowd activity in Hz (Figure 6.30). [The average total DLFs were calculated by summing the individual harmonic DLFs for each separate case and then calculating the average of these totals over all the group sizes whilst maintaining the jump frequency categories.]

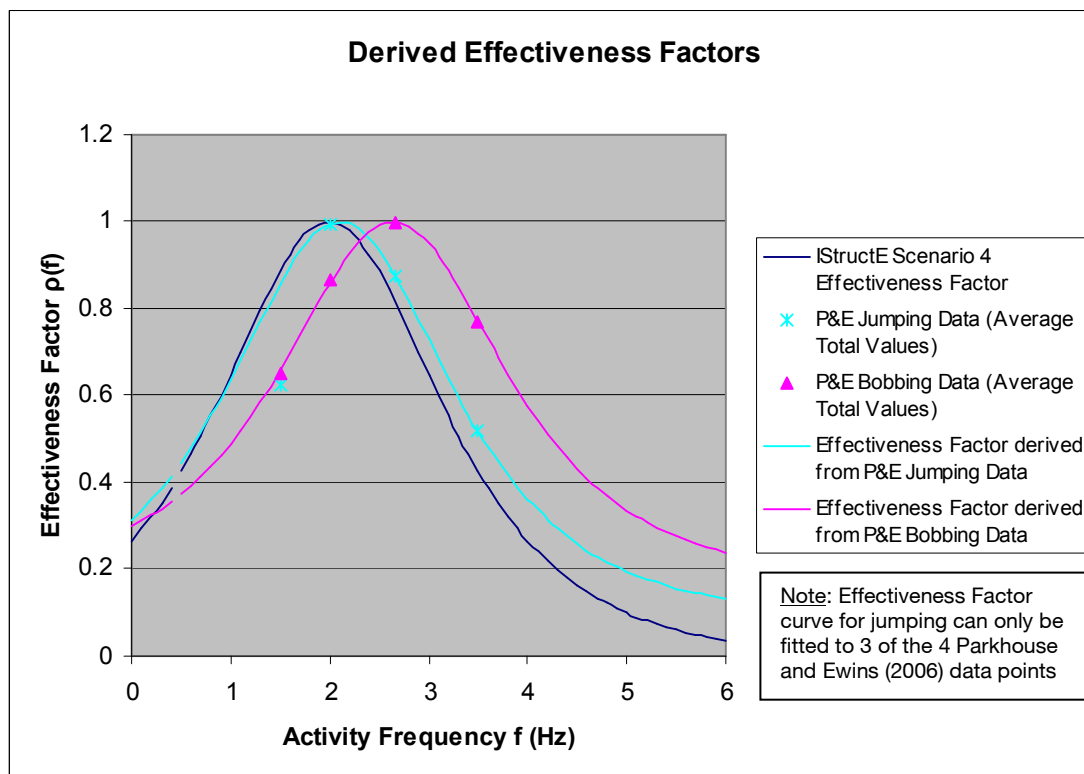


Figure 6.30 Equivalent Effectiveness Factors derived from Parkhouse and Ewins (2006)

Despite the fact that an equivalent effectiveness factor, similar to that given in the IStructE guidance, can be derived from the Parkhouse and Ewins' (2006) data it still does not overcome the issue that the harmonic DLFs produced by Parkhouse and Ewins vary depending on the frequency of the activity. That is, although the total DLF for each case can be divided by the effectiveness factor to give the same total DLF irrespective of frequency (for that group size) the proportions of the various harmonic components that make up the total DLF still vary with frequency (see Table 6.3).

Table 6.3 Dynamic Load Factors (DLFs) from Parkhouse and Ewins (2006)

DLFs from Parkhouse and Ewins for 50 People Bobbing					
Frequency (Hz)	1st Harm	2nd Harm	3rd Harm	4th Harm	Total DLF
1.5	0.193	0.096	0.025	0.01	0.324
2.0	0.322	0.084	0.015	0.009	0.430
2.67	0.408	0.067	0.014	0.008	0.497
3.5	0.294	0.034	0.014	0.01	0.352
Average of all 4 frequencies	0.304	0.070	0.017	0.009	0.401
DLFs from above divided by Effectiveness Factor derived from P&E Data (Figure 6.30)					
Frequency (Hz)	1st Harm	2nd Harm	3rd Harm	4th Harm	Total DLF
1.5	0.296	0.147	0.038	0.015	0.496
2.0	0.372	0.097	0.017	0.010	0.496
2.67	0.408	0.067	0.014	0.008	0.497
3.5	0.382	0.044	0.018	0.013	0.458
Average of all 4 frequencies	0.364	0.089	0.022	0.012	0.487
Scenario 3 DLFs from IStructE 2008					
Frequency (Hz)	1st Harm	2nd Harm	3rd Harm	4th Harm	Total DLF
All	0.188	0.047	0.013	-	0.248
All - divided by 0.75	0.250	0.063	0.017	-	0.330

Therefore, if a single dynamic load function is to be proposed, to cover all frequencies (similar to the IStructE guidance), then average values need to be considered. Scenario 3 loading is described in the IStructE as being ‘moderate bobbing at three quarters Parkhouse and Ewins’ 50 person level’. However as can be seen from Table 6.3 this is neither 75% of the DLFs taken directly from Parkhouse and Ewins nor 75% of the Parkhouse and Ewins’ DLFs amended to allow for an effectiveness factor. Scrutinising the Parkhouse and Ewins’ data shows that the Scenario 3 DLFs are in fact closest to 50% of the average amended DLFs for groups of 10-200 people i.e. the DLFs for groups of 10, 20, 50, 100 and 200 people bobbing firstly divided by the relevant bobbing effectiveness factor for the activity frequency and then averaged (Table 6.4). Similarly Scenario 3 DLFs are approximately equal to 18% of the average amended DLFs for groups of 10-200 people jumping. As Scenario 4 is defined as twice Scenario 3, Scenario 4 can be estimated as equal to the average amended DLFs for groups of 10-200 people

bobbing or 36% of the average amended DLFs for groups of 10-200 people jumping (Table 6.4).

Table 6.4 Average Dynamic Load Factors (DLFs) from Parkhouse and Ewins (2006)

Average amended DLFs from Parkhouse and Ewins for groups of 10 to 200 people i.e. divided by the relevant Effectiveness Factors derived from P&E Data (Figure 6.30) prior to being averaged					
Activity	1st Harm	2nd Harm	3rd Harm	4th Harm	Total DLF
Jumping	1.042	0.265	0.056	0.026	1.389
Bobbing	0.373	0.095	0.025	0.014	0.507
Comparison with IStructE (2008) DLFs					
	1st Harm	2nd Harm	3rd Harm	4th Harm	Total DLF
Scenario 3	0.188	0.047	0.013	-	0.248
18% of P&E Jumping	0.188	0.047	0.010	0.005	0.250
50% of P&E Bobbing	0.187	0.048	0.013	0.007	0.253
Scenario 4	0.375	0.095	0.026	-	0.496
36% of P&E Jumping	0.375	0.095	0.020	0.009	0.500
100% of P&E Bobbing	0.373	0.095	0.025	0.014	0.507

Parkhouse and Ewins' (2006) tests were conducted on a flat laboratory floor while the experimental works detailed in this thesis and the proposed end use of this research relate to raked grandstands. Thus Scenario 4 loading, where each crowd member jumping on a tiered stand is equivalent to the same person bobbing on a level floor or jumping with approximately $\frac{1}{3}$ of the force in a level floor does not seem unrealistic. Because of this and the fact that the effectiveness factor derived from the Parkhouse and Ewins' jumping data was similar to the IStructE's Scenario 4 effectiveness factor, it was decided to proceed with the analysis using the IStructE's Scenario 4 dynamic load factors, in conjunction with the IStructE's Scenario 4 effectiveness factor, to represent the dynamic load induced by the active portion of the crowd.

For each of the models shown in Figure 6.29 the IStructE (2008) pair of internal forces used previously (Section 6.3.1, Figure 6.27) was modified to represent *just* those jumping and was calculated using the Scenario 4 dynamic load and

effectiveness factors combined with the mass of the active section of the crowd. The spring stiffness and damping of the crowd 'body units' was also altered (based on the values given by the IStructE (2008)); taking the active participants as having a natural frequency of 2.3Hz and 25% critical damping and those seated taken as passive with a natural frequency of 5Hz and 40% critical damping. These were used together with the masses of each component of the crowd to calculate the combined frequencies of the models and the response of the each system.

The four models in Figure 6.29 were used to predict the RMS vertical acceleration for each of the crowd/rig combinations tested during the experimental works and then compared against the recorded results together with the output of the IStructE Scenario 3 model (see Section 6.3.1).

The revised 2 degree of freedom system (Figure 6.29 a) produced a reasonable fit for the 6.5Hz rig results but for the remainder of the tests the scale of the predicted accelerations was much lower than those recorded. The very simple single degree of freedom system (Figure 6.29 b) produced surprisingly good results for such a basic model, although the scale of the predictions was typically lower than the actual results. The lumped 2 degree of freedom model (Figure 6.29 c) improved slightly on the fit of the results but the 3 degree of freedom model (Figure 6.29 d) produced by far the closest predicted RMS accelerations to the recorded results for all the tests (Figure 6.31). Unexpectedly the IStructE Scenario 3 model produced better results than the revised 2 degree-of-freedom model using more detailed crowd information.

For all three test rig set ups the results from the 1.1Hz tests produced accelerations in excess of those predicted by any of the models. This could be explained by the fact that in these tests the structure typically vibrated at twice the forcing frequency (i.e. 2.2Hz) and therefore produced a response more similar to that predicted by the models at 2.2Hz.

For all the models the fit of the results was improved by changing the natural frequency of the 4Hz rig to 4.5Hz and the 2Hz rig to 2.1Hz in the models. Increasing the damping of the rig from 2% critical up to 7% critical typically did not improve how well the models related to the recorded results.

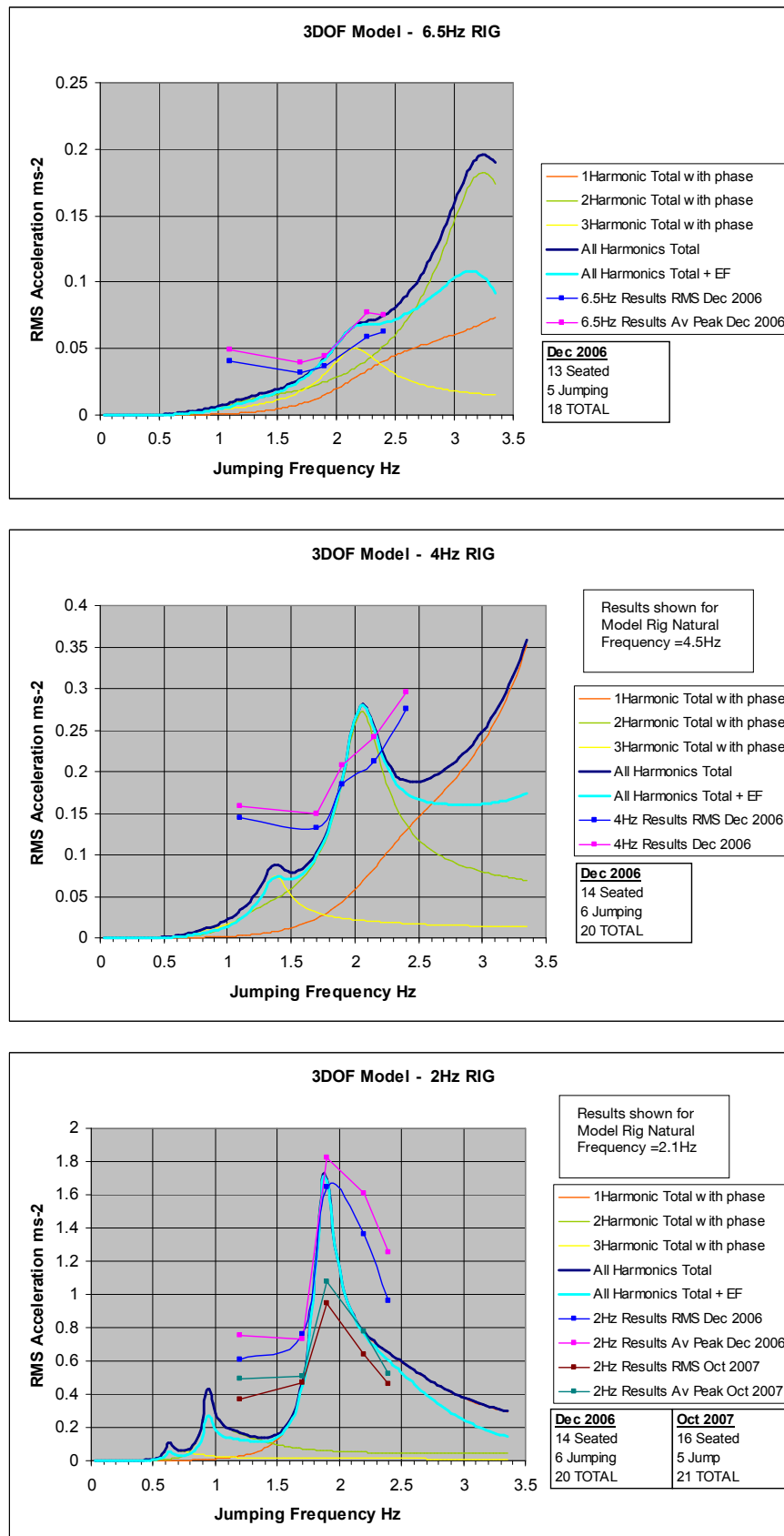


Figure 6.31 Results of 3 DOF Model for each Rig Set-up

Finally the original models (described in Section 3.2) were rerun for the crowd makeup experienced during the tests and compared against the test results. These basic models took the crowd simply as an additional mass without adding any additional damping to the system. Of the two periodic loadings considered; the 'maximum' load case predicted values higher than recorded while the 'realistic' load case produced RMS accelerations generally lower than those logged during the tests. Although the fit of the original models to the results can be improved by modifying the applied forcing function to approximately halfway between the 'maximum' and 'realistic' load cases, it is very difficult to specify a single loading that works for all the cases tested.

With the models considered there are numerous variables than can be altered to seemingly improve their accuracy. However in order to select a single model to proceed with it was decided that the loading and crowd characteristics should be maintained as specified in the IStructE (2008) guidelines. Based on the accuracy of predicting the recorded RMS accelerations and the flexibility to vary the crowd make up for different events, the 3 degree of freedom model using Scenario 4 loading (to represent the active participants jumping on the grandstand) together with the active/crowd system, shown in Figure 6.31 d, is the preferred model for use with the derived acceptability curves.

6.4 Proposed Acceptability and Loading Criteria

For well attended events at permanent grandstands the IStructE (2008) guidelines propose 3 Scenarios covering sporting events and various types of concert, as described in Section 6.3.1. Using the acceptability curves derived from the experimental results each of these Scenarios was interpreted together with the 3 degree-of-freedom analysis model (Figure 6.29 d and reproduced below in Figure 6.32) to develop recommendations for alternative acceptability criteria.

[It must be stressed that the loading and acceptability models described in the following Sections (6.4.1 to 6.4.3) are the author's interpretation of the results of the experimental research carried out on this project, together with currently published guidelines, and show examples of how the experimentally derived acceptance curves could be applied to real and design situations.]

For all cases an absolute maximum excitation frequency of 3.2Hz is considered appropriate when calculating the response of a grandstand to synchronised crowd load, based on the findings of Littler (2003).

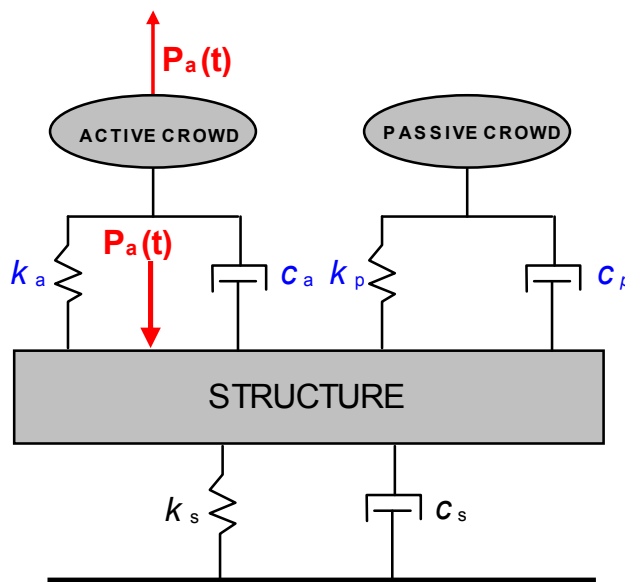


Figure 6.32 3 Degree-of-Freedom Model Recommended for use with the Author's Proposed Loadings and Acceptability Limits

6.4.1 Proposed Acceptability and Loading Criteria - High Energy Concerts

The IStructE's (2008) Scenario 4 covers the 'more extreme events [held at grandstands] including high energy concerts with periods of high intensity music' attended by a 'mainly young and active [crowd] with vigorous participation'. This 'excited crowd' is described as 'mostly standing and bobbing with some jumping' who anticipate structural 'motion but with an expectation of personal safety'.

For this most severe case it was considered appropriate to propose two separate limits to describe acceptability. The first of these being an upper limit based on the whole crowd jumping and with the aim of avoiding panic under this most extreme dynamic loading. While this scenario is very unlikely it seems prudent to check that if such a situation should occur that the consequences are not disastrous and this is possibly a check that should be carried out on all stands irrespective of their intended use.

As described in Section 6.3.2 the Scenario 4 dynamic load and effectiveness factors, proposed by the IStructE, approximate to the dynamic load of spectators jumping on a grandstand. Therefore the recommended loading to be used calculate the predicted RMS acceleration of a grandstand subject to the most extreme dynamic loading described above is 100% of the crowd being considered active (i.e. $m_a =$ the total mass of the crowd and $m_p = 0$) and jumping with the Scenario 4 dynamic load and effectiveness factors (Table 6.5). This is directly equivalent to IStructE's Scenario 4 loading as can be seen by comparing Tables 6.2 and 6.8.

For the corresponding acceptability limit for maximum load case it was decided that the RMS acceleration at which all those participating in the tests both seated and jumping deemed the vibration to be unacceptable was a suitable limit. The clear change in the participants' responses between a mix of acceptable and unacceptable to universally unacceptable is shown in the graphs in Figure 6.33. Due to the vibration response of the test rig this change corresponds to a gap in the recorded accelerations and therefore it was decided to select the lower edge of this range when selecting the recommended absolute maximum acceleration for the avoidance of panic. This uppermost acceptability limit is a RMS acceleration of 1.3ms^{-2} (Table 6.5 and Figure 6.34).

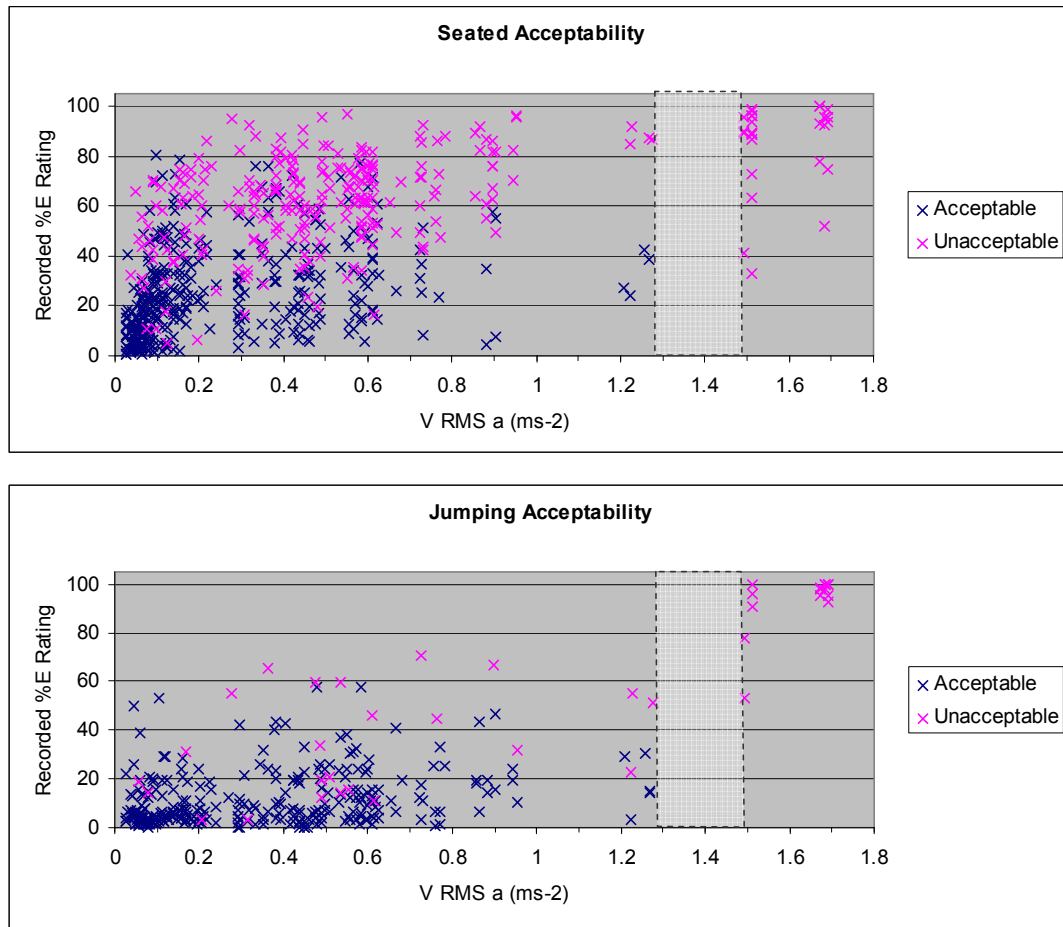


Figure 6.33 Recorded Acceptability Results from Experimental Testing

The IStructE's guidance is based on experience of events in the United Kingdom and highlights that some European football crowds rehearse creating a dynamic load in time to a prompted beat and as such can produce loads in excess of that anticipated for Scenario 4. Their recommendation is that events, where such abnormal loads could occur, be identified and appropriate operational measures and strategies be adopted by the management of the venue. An alternative approach would be to investigate the magnitude of the load imparted by such coordinated jumping and then recalculate the predicted RMS acceleration based on this loading. For example, using the Parkhouse and Ewins' data (2006) for small groups of 5 to 20 people, the loading from very synchronised groups could be in the region of three times greater than the Scenario 4 load factors.

Table 6.5 Proposed Loading and Acceptability Limits for High Energy Concerts

Loading

	Crowd Loading	κ	G_i	ρ	Ratio Active to Passive Crowd $m_a : m_p$
Extreme Limit	100% jumping	1.00	IStructE Scenario 4 DLFs	IStructE Scenario 4 EF	100:0
High Energy Concert	50% jumping 50% bobbing	0.75	IStructE Scenario 4 DLFs	IStructE Scenario 4 EF	100:0
<p>where load function $P_a(t) = \kappa p m_a g \sum_{i=1}^{i=3} G_i \cos(2\pi i f t + \theta_i)$ (see Figure 6.32)</p> <p>with κ = Proportion of IStructE G_i Dynamic Load Factors ρ = Crowd Effectiveness Factor m_a = Mass of the active portion of the crowd (based on 80kg per person) g = Acceleration due to gravity, 9.81 ms^{-2} i = Harmonic number G_i = The i th Dynamic Load Factor f = Fundamental Frequency of the crowd activity t = Time in seconds θ_i = Phase angle of the i th harmonic</p> <p>and $k_a = 4\pi^2 n_a^2 m_a$ n_a = Natural frequency of the active crowd = 2.3Hz as IStructE (2008)</p> <p>with $c_a = 25\%$ critical as IStructE (2008)</p> <p>and $k_p = 4\pi^2 n_p^2 m_p$ n_p = Natural frequency of the passive crowd = 5.0Hz as IStructE (2008) m_p = Mass of the passive portion of the crowd (based on 80kg per person)</p> <p>with $c_p = 40\%$ critical as IStructE (2008)</p>					

Acceptability Limits

	Acceptability Limits as RMS Accelerations			
	5% Unacceptable	10% Unacceptable	15% Unacceptable	20% Unacceptable
Extreme Limit ⁺	1.3 ms^{-2}	1.3 ms^{-2}	1.3 ms^{-2}	1.3 ms^{-2}
High Energy Concert ^{**}	0.44 ms^{-2}	0.74 ms^{-2}	0.87 ms^{-2}	0.95 ms^{-2}
<p>⁺ Acceptability limit based on change in recorded acceptability responses from a mix of acceptable and unacceptable to 100% unacceptable for all participants (Figure 6.33).</p> <p>^{**} Acceptability limits based on jumping acceptability curve (Figure 6.26).</p>				

The second suggested limit is more representative of the situation at such a 'high energy concert'. The author's recommended loading based on the IStructE's description of the 'young active' crowd who participate vigorously, 'mostly standing and bobbing with some jumping' is 50% of the crowd jumping while the remaining 50% bob (i.e. move up and down vertically in time to the music whilst remaining in contact with the floor). This is seen as a slightly conservative interpretation of the IStructE's loading description. For a value for this loading to be determined reference was made to Parkhouse and Ewins 2006 where the average dynamic load factors for people bobbing was approximately 36% of that of the same people jumping (Table 6.4). As these comparisons were for individuals jumping and bobbing on a level laboratory floor not for a tiered grandstand, it was decided to take the ratio of bobbing to jumping as 50% when determining the 'high energy concert' loading as this hopefully slightly overestimates the bobbing component of the grandstand load. Thus the recommended loading for the 'high energy concert' case was calculated at 75% of Scenario 4 Dynamic Load Factors (DLFs) [= 50% Jumping at Scenario 4 DLFs (G_j) + 50% Bobbing at 50% of Scenario 4 DLFs (G_j)], (Table 6.5 and also Tables 6.2 and 6.8). This loading is recommended to be used in conjunction with the 3 degree-of-freedom system model shown in Figure 6.32 with 100% of the crowd being considered as active i.e. the mass used to calculate $P_a(t)$ and k_a should be the whole mass of the crowd and the mass of passive crowd taken as zero.

In deriving the recommended acceptability limits given in this Section it was decided that a range of values corresponding to a range of percentages of the crowd who deemed the vibration unacceptable was most appropriate. This was because it allows those managing the venue to weigh up the risks and decide what level of acceptability is suitable for a particular event. From observation of the experimentally generated acceptability curves (Section 6.1) there will generally be around 5% the crowd who will find a vibration unacceptable no matter how small. This should be born in mind when deciding on the appropriate level of acceptability for a given event. The crowd percentage unacceptable values chosen to be calculated are 10%, 15% and 20% i.e. overall 10%, 15% or 20% of the crowd would find a vibration of that magnitude unacceptable. This can alternatively be thought of as (5+5)%, (10+5)% and (15+5)%, indicating the percentage of the crowd over the baseline 5% who will find any vibration unacceptable. The 5% crowd

percentage unacceptable value has also been calculated to give context to the higher percentage values. Below this vibration magnitude the percentage of the crowd who will find the vibration unacceptable remains at approximately 5%.

When deciding on a crowd percentage unacceptable value to be used for an event several factors need to be considered. The first is the definition of unacceptable. As described in Section 4.2.2, the definition of unacceptable used during the experimental tests, and hence that of the acceptability curves, was 'a vibration which, if experienced in a real stand, would cause the participant to; leave immediately or complain to the management or think twice about returning to that venue' (Figure 4.9). The implication of this is that although, for example, 20% of the crowd may find a vibration unacceptable only a fraction of them will actually complain to those organising the event and others will leave and/or be discouraged from returning to events at that venue in the future. Secondly the loading functions proposed are purposely specified as being upper-bound for the given type of event based on the IStructE description. Therefore in selecting an appropriate crowd percentage unacceptable value the probability of the loading function being achieved, and hence the predicted RMS acceleration against which the acceptability criterion is compared, needs to be calculated. Thus if the chances of the loading function being achieved are low then a higher crowd percentage unacceptable value may be tolerable. Alternatively, because the recommended acceptability levels are specified as curves the designer can define his own loading or testing to calculate the predicted RMS acceleration for an event and then predict the likely percentage acceptability based on his interpretation of the make-up of the crowd (i.e. the ratio of those jumping to those seated).

For the 'high energy concert' scenario the whole crowd is assumed to be actively and energetically involved in creating the dynamic movement of the grandstand therefore, the suggested acceptance criteria for the 'high energy concert' are based solely on the jumping acceptability curves (Figure 6.26). The RMS acceleration values at which 5%, 10%, 15% and 20% of an excited vigorously participating crowd would deem the vibration to be unacceptable have thus been read off Figure 6.26 as 0.44 ms^{-2} , 0.74 ms^{-2} , 0.87 ms^{-2} and 0.95 ms^{-2} and added to Table 6.5 (and Figure 6.34).

6.4.2 Proposed Acceptability and Loading Criteria - Medium Tempo Concerts and High Profile Sporting Events

In the IStructE (2008) guidelines Scenario 3 covers ‘commonly occurring events including, inter alia, high profile sporting events and concerts with medium tempo music and revival pop-concerts with cross generational appeal’. For this case the crowd is assumed to be ‘potentially excitable’ and ‘all be standing and participating during some part of the programme’. This type of loading results in the most onerous situation considered, as although, at times, significant movements can be generated by the crowd there could still be a notable section of the audience seated. This is partly acknowledged by the IStructE (2008) who define the crowd expectation as ‘a few individuals may complain at lack of comfort but most will tolerate the motion’

In order to define an appropriate loading for this Scenario reference was made to Pavic and Reynolds’ 2008 analysis of video footage of a full capacity crowd on a raked cantilevered grandstand during a pop concert. Pavic and Reynolds observed that during the period where the highest structural vibrations were recorded, the ratio of active to passive members of the crowd was approximately 40:60 and both groups were distributed evenly over the stand. From the video footage Pavic and Reynolds concluded that ‘the active crowd were predominantly engaged in bobbing, i.e. maintaining continuous contact with the structure, with very few people jumping’. The published still from the analysed video shows that while the majority of the crowd are on their feet, a proportion remain seated. As discussed above, the loading functions defined in this section are selected so as to be at the upper limit of for the given type of event (or Scenario) while remaining as realistic as possible. Therefore the dynamic loading decided upon for ‘medium tempo concerts and high profile sporting events’ is based on 100% of the crowd bobbing, where as explained in Section 6.4.1, the loading induced by bobbing is taken as half that for jumping on a tiered stand i.e. 50% of the IStructE’s Scenario 4 loading (Table 6.6). This loading ties in with the IStructE’s definition of this Scenario of a crowd that is ‘all standing and participating during some part of the programme’ and is indeed equivalent to the Scenario 3 loading given in IStructE (2008) (Tables 6.2 and 6.8).

Table 6.6 Proposed Loading and Acceptability Limits for Medium Tempo Concerts and High Profile Sporting events

Loading

	Crowd Loading	κ	G_i	ρ	Ratio Active to Passive Crowd $m_a : m_p$
Medium Tempo Concert or High Profile Sporting Event	100% bobbing	0.50	IStructE Scenario 4 DLFs	IStructE Scenario 4 EF	100:0
<p>where load function $P_a(t) = \kappa \rho m_a g \sum_{i=1}^{i=3} G_i \cos(2\pi i f t + \theta_i)$ (see Figure 6.32)</p> <p>with κ = Proportion of IStructE G_i Dynamic Load Factors ρ = Crowd Effectiveness Factor m_a = Mass of the active portion of the crowd (based on 80kg per person) g = Acceleration due to gravity, 9.81 ms^{-2} i = Harmonic number G_i = The i th Dynamic Load Factor f = Fundamental Frequency of the crowd activity t = Time in seconds θ_i = Phase angle of the i th harmonic</p> <p>and $k_a = 4\pi^2 n_a^2 m_a$ n_a = Natural frequency of the active crowd = 2.3Hz as IStructE (2008)</p> <p>with $c_a = 25\%$ critical as IStructE (2008)</p> <p>and $k_p = 4\pi^2 n_p^2 m_p$ n_p = Natural frequency of the passive crowd = 5.0Hz as IStructE (2008) m_p = Mass of the passive portion of the crowd (based on 80kg per person)</p> <p>with $c_p = 40\%$ critical as IStructE (2008)</p>					

Acceptability Limits

	Acceptability Limits as RMS Accelerations			
	5% Unacceptable	10% Unacceptable	15% Unacceptable	20% Unacceptable
Medium Tempo Concert or High Profile Sporting Event*	0.06 ms^{-2}	0.15 ms^{-2}	0.26 ms^{-2}	0.42 ms^{-2}
<p>* Acceptability limits based on the overall acceptability of a crowd with 75% jumping and 25% seated using the seated and jumping acceptability curves shown in Figures 6.25 and 6.26.</p>				

The proposed loading is also greater than that observed by Pavic and Reynolds (2008) at a real grandstand concert event, where if, say, a quarter of the 40% of the crowd who were actively bobbing were in fact jumping and the remaining 60% of the crowd were standing the total dynamic load factor would be 25% of the IStructE's Scenario 4 loading.

Similar to the loading proposed for 'high energy concerts' the whole crowd is assumed to be active and participating in creating the vibration therefore when calculating the dynamic load the mass of the passive portion of the crowd is taken as zero. However for 'medium tempo concerts and high profile sporting events' there is a high likelihood that while a large portion of the audience could be standing, bobbing or jumping, a proportion are likely to remain seated. Because the recommended 'medium tempo concert' loading of 100% bobbing is at the upper bound of what is to be expected at this type of event, the acceptability criteria to be used in conjunction with this loading has to be compatible. Thus the initial reaction is to set the acceptance criteria based on only a small percentage of the crowd being seated e.g. 10%. However the concern is that with a slightly different crowd make up where a smaller proportion of the crowd are more vigorously active similar vibrations could be achieved to the suggested 100% bobbing whilst larger numbers remain seated. Therefore for the definition of the acceptance criteria it was decided to view the crowd build up as 25% jumping, 50% bobbing and 25% seated. This breakdown produces a similar load to 100% of the crowd bobbing while allowing for a quarter of the crowd to remain seated. (This crowd split was not used in the definition of the loading as the 25% of the crowd who are seated would have acted as passive crowd in the model, damping and hence reducing the maximum response of the system (Figure 6.32)). The decision to base the acceptability criteria on a crowd who were jumping, bobbing and seated raised the question - What acceptance criteria should be used for people bobbing? The experimental tests only looked at the perception and emotional response of jumping and seated participants therefore the derived predicted acceptability curves are only directly applicable to these two groups of spectators. Because the IStructE's definition of this loading Scenario is clear that the entire crowd will stand and participate during some part of the programme and will mostly tolerate the motion, the key is the few people who potentially may remain seated during short periods of high crowd activity. Therefore when setting recommended acceptance criteria for 'medium

tempo concerts and high profile sporting events' it was decided that the overall crowd acceptance should be based on 75% of the crowd using the jumping acceptance curves and 25% using the seated acceptance curves. Thus, as an example, the limit at which 20% of the crowd will find the vibration is unacceptable is based on a RMS acceleration of 0.42ms^{-2} at which 4.8% of those creating the vibration (using the jumping acceptance curves Figure 6.26) and 65.5% of those seated (using the seated acceptance curves Figure 6.25) find the vibration unacceptable, giving an overall total of 20% unacceptability (4.8% of 75% plus 65.5% of 25% = 20%). The suggested acceptability limits, calculated in this manner, for 'medium tempo concerts and high profile sporting events' are given in Table 6.6 and Figure 6.34.

The IStructE (2008) defines two effectiveness factors to be used in conjunction with their dynamic loadings. One is to be used with the extreme loading of Scenario 4 'High Energy Concerts' which proportions the dynamic load dependent on the dominant activity frequency based on the amount of force human jumping can impart at various frequencies. The second effectiveness factor, proposed for use with Scenario 3 'Medium Tempo Concerts and High Profile Sporting Events' and Scenario 2 'Classical Concerts and Typical Well-attended Sporting Events', takes the Scenario 4 effectiveness factor and moderates it dependent on the probability of music of a certain frequency being played at a pop concert. The author's recommended loading for 'medium tempo concerts and high profile sporting events' uses the IStructE Scenario 4 effectiveness factor. This could possibly be replaced by the IStructE Scenario 2 & 3 effectiveness factor which would generally reduce the magnitude of the load.

6.4.3 Proposed Acceptability and Loading Criteria - Classical Concerts and Typical Sporting Events

The final dynamic loading case, Scenario 2, given by the IStructE covers 'classical concert[s] and typical well attended sporting event[s]' where the 'audience is considered seated with only [a] few exceptions - minor excitation'. The IStructE treats these two events using the same loading and serviceability criteria however the real dynamic loading of a grandstand at classical concerts and typical sports events is quite different. Although the audiences at classical concerts are

predominantly seated, sections of the crowd may occasionally participate in stamping or gentle bobbing in time to the music during a performance. Crowds at sporting events remain seated until an event occurs on the field of play. At this time the crowd may simultaneously rise to their feet resulting in an impulse rather than a periodic vibration. Other sports crowd induced vibrations may occur but will be largely uncoordinated and short lived. Because of these differences it was decided to introduce two separate cases in place of the single IStructE Scenario 2.

To represent the dynamic loading at classical concerts a loading with 10% of the crowd jumping at IStructE Scenario 4 level while 90% are seated was chosen (Table 6.7). Although the actual loading is unlikely to be applied in this ratio it was felt that the magnitude of 10% jumping was an appropriate upper bound for a larger number of the audience acting less intensely e.g. 20% bobbing, fairly intensely, at 50% of the IStructE Scenario 4 loading or even a greater percentage bobbing more gently. This proposed loading is roughly a third of the IStructE's Scenario 2 loading (Tables 6.2 and 6.8). The IStructE also proposes the use of the Scenario 2 & 3 effectiveness factor for use with this class of loading. However this is a probability weighting, as described above, based on the likelihood of various frequencies of songs being played at pop concerts therefore its relevance to classical concerts is unclear. For this reason the IStructE Scenario 4 effectiveness factor is suggested for use with the loading recommended in Table 6.7 for classical concerts as this factor is based simply on how much force people can impart while jumping at various frequencies.

For classical concerts the vast majority of the audience are seated for the duration of the performance. The crowd make up and expectation of stand vibrations are also very different from that of a pop concert or sports event crowd. Generally the classical concert audience will be older and expect less movement of the grandstand. Therefore it was considered appropriate to base the recommended acceptance criteria for this category of event on the more onerous seated acceptability curve only (Figure 6.25) i.e. assume for acceptability that 100% of the crowd were seated. The overall crowd acceptability levels calculated thus are shown in Table 6.7 and Figure 6.34.

The loading for typical sports events was harder to specify. In the IStructE's Interim Guidance (2001) a distinction was made between 'events where crowd activity would

not be stimulated by music or otherwise synchronised' and those where 'incidental music' and 'music in the form of chants and club songs' 'can stimulate a crowd to develop dynamic loading sufficient to excite grandstands with relatively low natural frequencies so causing possible discomfort to seated spectators'. For the first of these situations a minimum vertical natural frequency of the grandstand of 3.5Hz was recommended to avoid the chance of significant resonance due to first harmonic component of any deliberate synchronised 'vandal' loading. For the second case, where some synchronised crowd loading was expected, the IStructE's guidance was that monitoring and management of incidental music could be used to minimise the risk of unacceptable vibrations and if the minimum vertical natural frequency of the grandstand was greater than 5Hz then the risk could probably be ignored. It is unclear what the IStructE's guidance is for avoiding issues due to vibrations induced by dynamic crowd loading coordinated by chanting or unaccompanied singing but by being described under the 'Incidental Music' heading the implication is that the 5Hz frequency limit is appropriate.

The current IStructE (2008) recommendation for 'Scenario 2- classical concert[s] and typical well attended sporting event[s]' is a minimum vertical stand frequency of 3.5Hz, when using the Route 1 frequency limit approach. Neither incidental music nor self coordinated dynamic crowd loading is mentioned in relation to any specific Scenario. Emphasis is put on the designer to select the appropriate Scenario based on records of past events at the venue and a prediction of the likely crowd behaviour.

Therefore in order to determine the magnitude of load suggested by the IStructE for 'typical well attended sporting events' the dynamic load factors (DLFs) for Scenario 2 were compared with those for Scenario 4 which as described in Section 6.3.2 have been calibrated against the experimental test results and shown to be approximately equal to people jumping on a tiered grandstand. The 1st harmonic DLF for Scenario 2 is 32% of the equivalent DLF for Scenario 4 while the same ratio for the 2nd harmonic component is only 16%. The IStructE does not specify a 3rd harmonic DLF for Scenario 2. Perhaps the reason for the low higher harmonics to the Scenario 2 loading is so as tie in with the minimum 3.5Hz frequency limit that is given for the frequency limit design for this Scenario as a grandstand with a frequency around 3 to 4Hz will be most susceptible to resonance due to the 2nd harmonic component of the loading function. Alternatively the IStructE may have based the Scenario 2 DLFs on

research of the actual loading that occurs at these events but as no specific references are given this cannot be verified. Because of this lack of information on the derivation of the loading it makes sense to recommend a loading that can be related back to actual crowd activity as described in Section 6.3.2. Thus the suggested upper bound loading for 'typical well attended sporting events' given in Table 6.7 is based on a third of the crowd jumping while the rest remain seated. This proposed load is slightly greater than the IStructE's Scenario 2 loading, with the majority of the increase being in the 2nd and 3rd harmonic DLFs (Tables 6.2 and 6.8). Due to the 3 degree-of-freedom model (Figure 6.32) to be used with the proposed load the calculated magnitude of the vibration will be reduced due to the damping effect of the passive portion of the crowd compared to that calculated using the IStructE's model (Figure 6.27). Despite this a maximum load based on 33% of the crowd jumping and 67% of the crowd seems appropriate for this classification of event, where the IStructE description is of an audience who are predominantly seated, as it is two-thirds of that recommended for 'medium tempo concerts and high profile sporting events' (Table 6.8) and Scenario 3 (Table 6.2). As for the other suggested load cases the use of the IStructE's Scenario 4 effectiveness factor is recommended as the exact nature and stimulus of the dynamic crowd loading for 'typical well attended sporting events' is unclear and therefore the use of the lower risk based, probability weighted, Scenario 2 & 3 effectiveness factor is inappropriate.

The recommended acceptability limits for use with the suggested loading for 'typical well attended sporting events' (Table 6.7) are based on the same proportion of spectators jumping to seated used to calculate the load i.e. 33% of the crowd jumping while the rest remain seated. For example to calculate the overall crowd unacceptability of 20% shown in Table 6.7 for 'typical sporting events' the RMS acceleration was found where, with 33% of the crowd's acceptability based on the jumping acceptability curves (Figure 6.26) and 67% of the crowd's acceptability based on the seated acceptability curves (Figure 6.25), the total unacceptability was 20%. In this case at the RMS acceleration of 0.15ms^{-2} the acceptability curves predict that 3.6% of the 33% jumping (i.e. 1.2% of the total crowd) and 28% of the 67% seated (i.e. 18.8% of the total crowd) resulting in a predicted overall crowd unacceptability of 20%. The RMS accelerations, calculated as described above, at which 5%, 10%, 15% and 20% of the crowd overall are predicted to find the magnitude of the vibration unacceptable are given in Table 6.7 and Figure 6.34.

It must be noted that the suggested RMS acceleration limits given in Table 6.7 for both 'Classical Concerts' and 'Typical Sporting Events' should not be compared on a like for like basis with those recommended by the IStructE's (2008) guidelines due to differences in the load models (Figures 6.32 and 6.27). The additional degree-of-freedom, representing the passive seated crowd, in the 3 degree-of-freedom model (advocated for use with the loading and acceptability limits in Table 6.7) acts to damp the peak accelerations of the system and therefore, lower magnitude vibrations are predicted by this model compared to the IStructE's 2 degree-of-freedom model when using the same input loading $P(t)$. This is only applicable where the mass of the seated crowd is taken as greater than zero such as for 'classical concerts and typical well attending sporting events'. For the other load cases described for 'high energy concerts', 'medium tempo concerts and high profile sporting events' the proposed loading (Tables 6.5, 6.6 and 6.8) assumes that the entire crowd is actively involved in creating the vibration and so the 3 degree-of-freedom model (Figure 6.32) becomes the 2 degree-of-freedom model (Figure 6.27) as there is no passive crowd element.

Table 6.7 Proposed Loading and Acceptability Limits for Classical Concerts and Typical Sporting Events

Loading

	Crowd Loading	κ	G_i	ρ	Ratio Active to Passive Crowd $m_a : m_p$
Classical Concerts	10% jumping	1.00	IStructE Scenario 4 DLFs	IStructE Scenario 4 EF	10:90
Typical Sporting Events	33% jumping	1.00	IStructE Scenario 4 DLFs	IStructE Scenario 4 EF	33:67

where load function $P_a(t) = \kappa \rho m_a g \sum_{i=1}^{i=3} G_i \cos(2\pi i f t + \theta_i)$ (see Figure 6.32)

with κ = Proportion of IStructE G_i Dynamic Load Factors
 ρ = Crowd Effectiveness Factor
 m_a = Mass of the active portion of the crowd (based on 80kg per person)
 g = Acceleration due to gravity, 9.81ms^{-2}
 i = Harmonic number
 G_i = The i th Dynamic Load Factor
 f = Fundamental Frequency of the crowd activity
 t = Time in seconds
 θ_i = Phase angle of the i th harmonic

and $k_a = 4\pi^2 n_a^2 m_a$
 n_a = Natural frequency of the active crowd = 2.3Hz as IStructE (2008)

with $c_a = 25\%$ critical as IStructE (2008)

and $k_p = 4\pi^2 n_p^2 m_p$
 n_p = Natural frequency of the passive crowd = 5.0Hz as IStructE (2008)
 m_p = Mass of the passive portion of the crowd (based on 80kg per person)

with $c_p = 40\%$ critical as IStructE (2008)

Acceptability Limits

	Acceptability Limits as RMS Accelerations			
	5% Unacceptable	10% Unacceptable	15% Unacceptable	20% Unacceptable
Classical Concerts ⁺	0.04 ms^{-2}	0.06 ms^{-2}	0.09 ms^{-2}	0.11 ms^{-2}
Typical Sporting Events ^{**}	0.04 ms^{-2}	0.08 ms^{-2}	0.11 ms^{-2}	0.15 ms^{-2}

⁺ Acceptability limit based on seated acceptability curve (Figure 6.25)
^{**} Acceptability limits based on the overall acceptability of a crowd with 33% jumping and 67% seated using the seated and jumping acceptability curves shown in Figures 6.25 and 6.26.

Table 6.8 Summary of Proposed Loading to be used with Recommended Acceptability Limits

	Crowd Loading	(κ m _a G _i) in terms of total mass of the crowd m			Ratio Active to Passive Crowd m _a : m _p
		1st Harmonic	2nd Harmonic	3rd Harmonic	
Extreme Limit	100% jumping	0.375m	0.095 m	0.026 m	100:0
High Energy Concert	50% jumping 50% bobbing	0.281 m	0.071 m	0.020 m	100:0
Medium Tempo Concert or High Profile Sporting Event	100% bobbing	0.188 m	0.047 m	0.013 m	100:0
Typical Sporting Events	33% jumping	0.125 m	0.032 m	0.009 m	33:67
Classical Concerts	10% jumping	0.038 m	0.010 m	0.003 m	10:90

where load function $P_a(t) = \kappa \rho m_a g \sum_{i=1}^{i=3} G_i \cos(2\pi i f t + \theta_i)$ (see Figure 6.32)

with κ = Proportion of IStructE G_i Dynamic Load Factors

ρ = Crowd Effectiveness Factor

m_a = Mass of the active portion of the crowd (based on 80kg per person)

g = Acceleration due to gravity, 9.81ms⁻²

i = Harmonic number

G_i = The i th Dynamic Load Factor

f = Fundamental Frequency of the crowd activity

t = Time in seconds

θ_i = Phase angle of the i th harmonic

and $k_a = 4\pi^2 n_a^2 m_a$

n_a = Natural frequency of the active crowd = 2.3Hz as IStructE (2008)

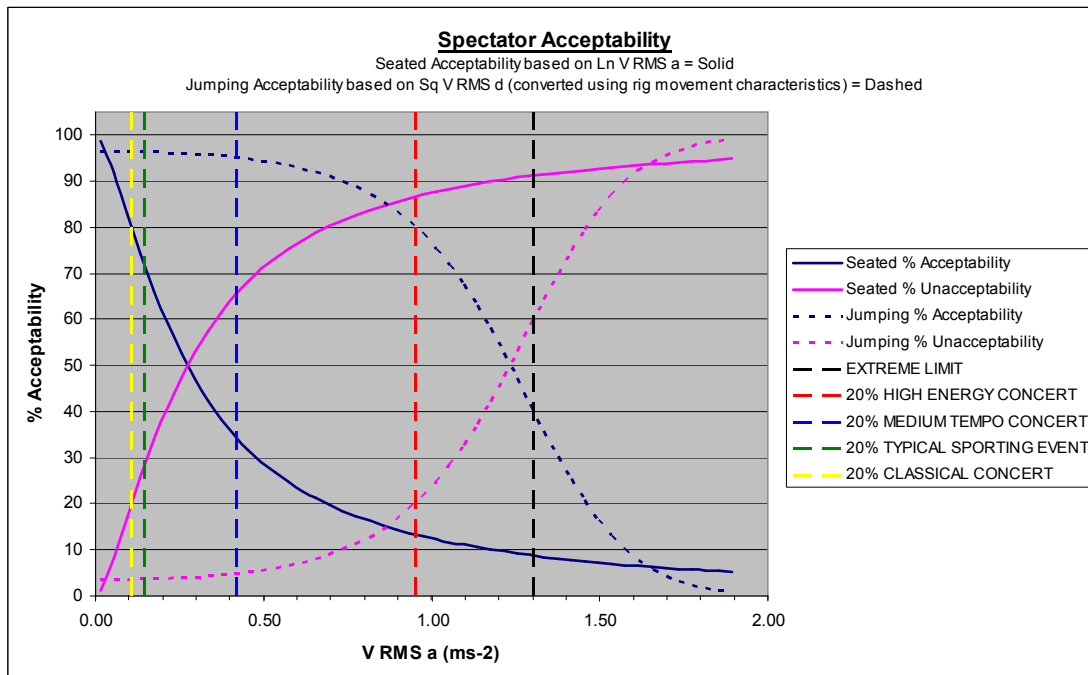
with c_a = 25% critical as IStructE (2008)

and $k_p = 4\pi^2 n_p^2 m_p$

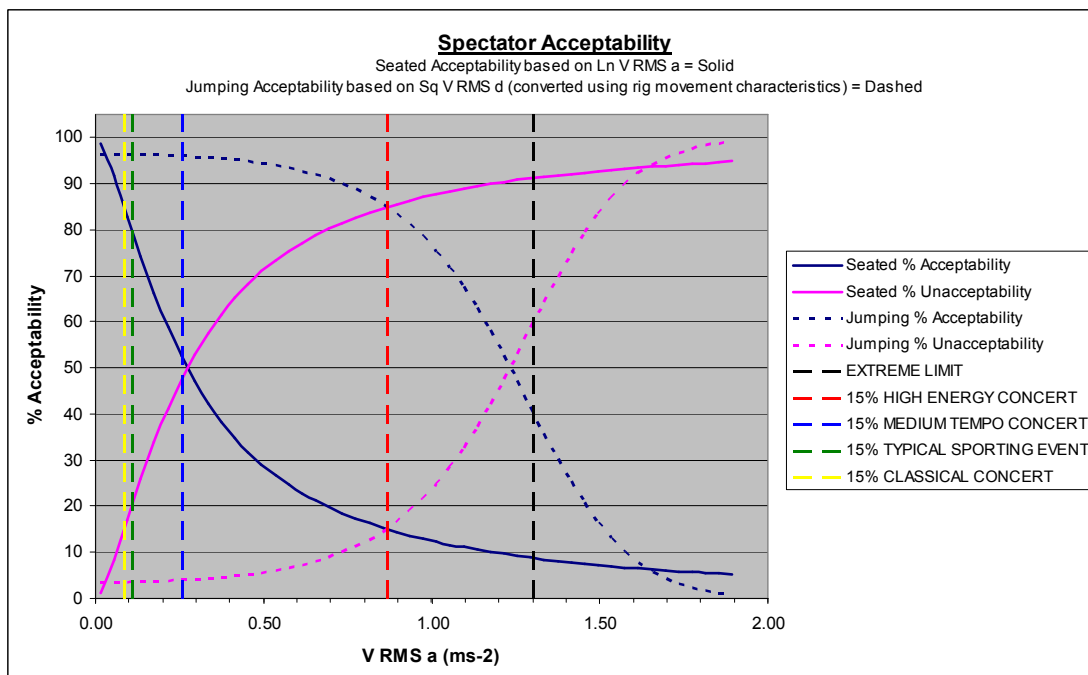
n_p = Natural frequency of the passive crowd = 5.0Hz as IStructE (2008)

m_p = Mass of the passive portion of the crowd (based on 80kg per person)

with c_p = 40% critical as IStructE (2008)

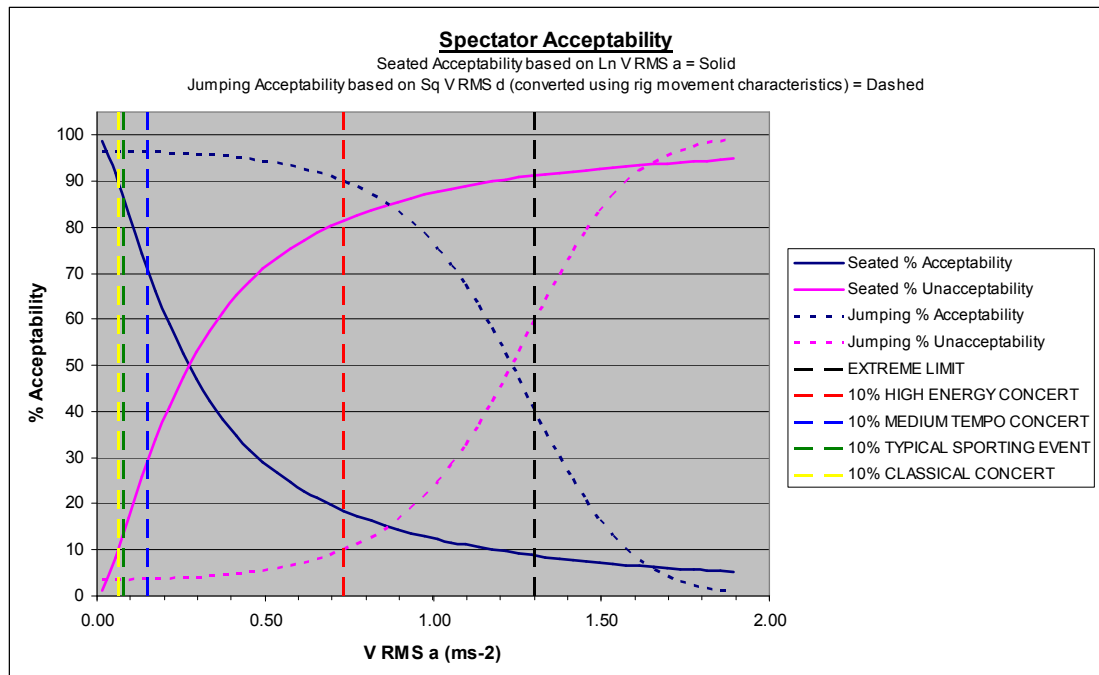


a) 20% Overall Crowd Unacceptability

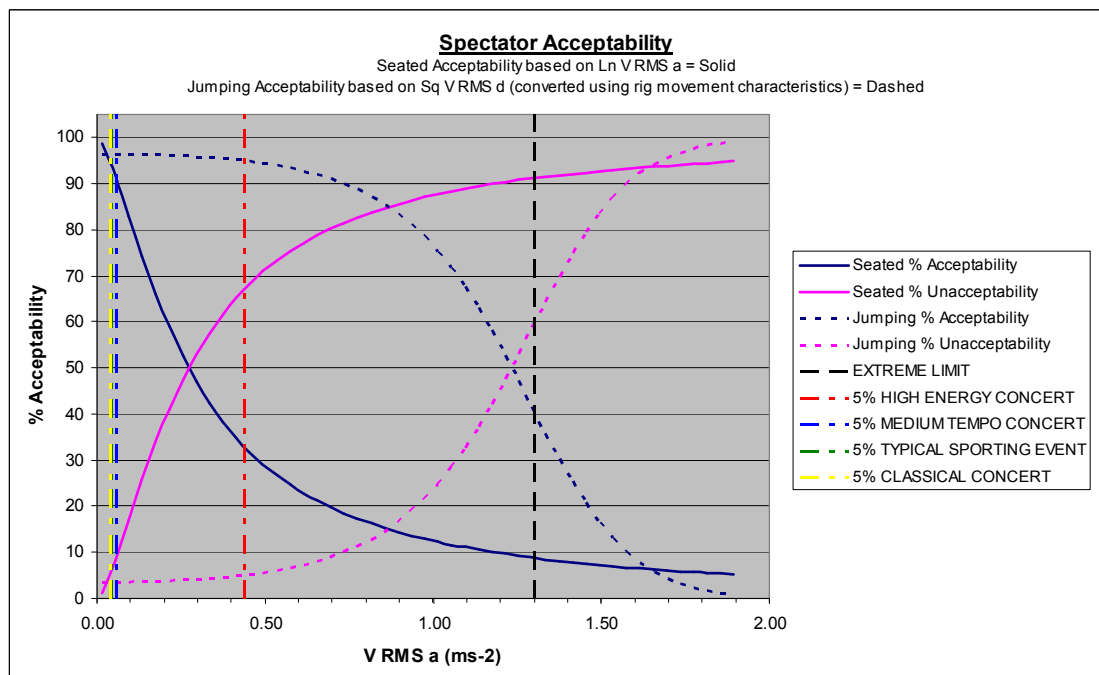


b) 15% Overall Crowd Unacceptability

Figure 6.34 Recommended Acceptability Criteria (Continued over)



c) 10% Overall Crowd Unacceptability



d) 5% Overall Crowd Unacceptability

Figure 6.34 (Continued) Recommended Acceptability Criteria

6.5 Comparison of Proposed Acceptability Criteria with Published Guidelines

In order to set the recommended acceleration limits described above against previously published guidelines Figure 6.34 was overlaid with the values given by Kasperski (1996), the National Building Code of Canada (NBCC 2005), the IStructE (2008) and ISO10137:2007 (Figure 6.35).

6.5.1 Comparison of Proposed Acceptability Criteria - High Energy Concerts

From Figure 6.35 a) showing the recommended RMS acceleration limits for 'high energy concerts' it can be seen that the extreme limit of 1.3ms^{-2} is much less than the IStructE value for high energy concerts and ISO10137 panic limit but only slightly lower than Kasperski's panic threshold. (As previously, the peak accelerations published by Kasperski and the NBCC have been converted to an equivalent RMS value using the relationship derived from the results of the experimental tests (Figure 6.24 b). Although the ISO10137 panic limit is given as an RMS acceleration it has to be calculated over a 1s period rather than 10s for IStructE and ISO10137 comfort limit. This means that it will be closer to a peak value than the other RMS accelerations discussed and as such shouldn't be compared on a like-for-like basis).

As described in Section 6.4.1 the recommended acceptability limits for 'high energy concerts' are based on the jumping acceptability curve (Figure 6.26) assuming that the entire crowd is actively and energetically jumping or bobbing. The suggested 20% overall crowd unacceptability limit for 'high energy concerts' of 0.95ms^{-2} is very similar to ISO10137 comfort limit (Figure 6.35 a). Both the 15% and 20% overall crowd unacceptability limit for 'high energy concerts' are slightly greater than the upper bound value for stadiums and arenas given in the NBCC which is equal to Kasperski's threshold for vibrations becoming unacceptable. The IStructE limit for 'medium tempo concerts and high profile sporting events' is less than the 15% and 20% overall crowd unacceptability limit for 'high energy concerts' and equal to the 10% overall crowd unacceptability limit for 'high energy concerts'.

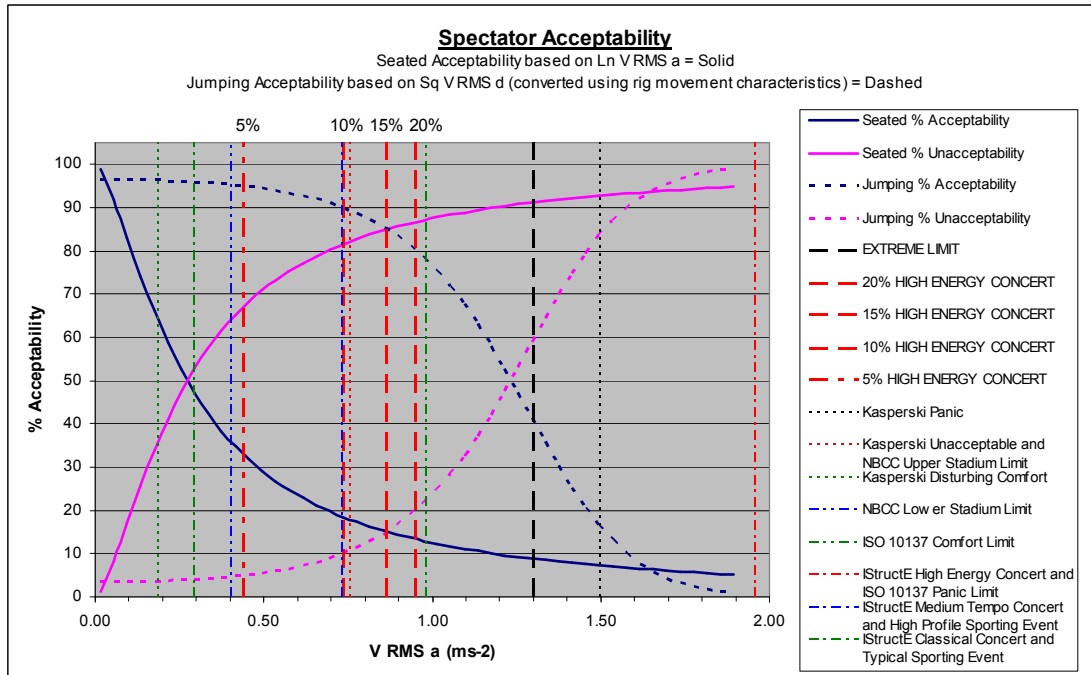
Although the 5% overall crowd unacceptability limits were calculated for each of the event categories in Section 6.4 these were only included for information rather than as a suggested acceptability limit. This is because the 5% overall crowd unacceptability level is a lower bound value below which the percentage of the crowd who deem the vibration unacceptable remains fairly constant at approximately 5%.

For 'high energy concerts' the 5% overall crowd unacceptability limit lies just above the NBCC's lower bound value of their recommended range of acceptable vibrations for stadiums and arenas.

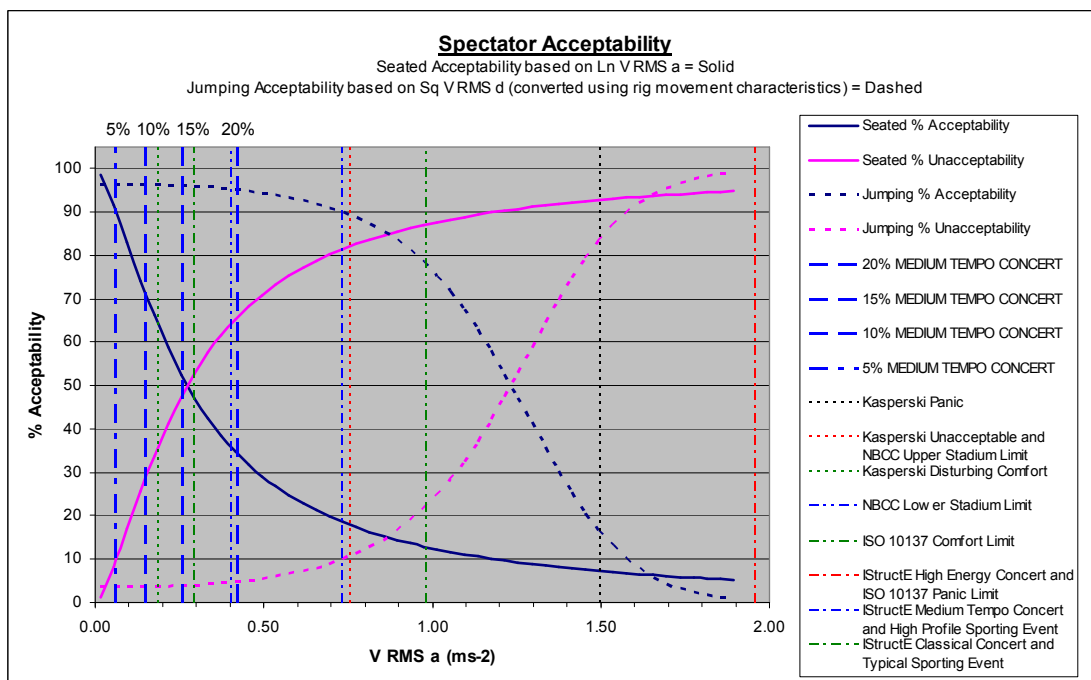
6.5.2 Comparison of Proposed Acceptability Criteria - Medium Tempo Concerts and High Profile Sporting Events

The proposed acceptability limits for 'medium tempo concerts and high profile sporting events' are based on 25% of the crowd remaining seated while the rest participate in creating the dynamic movement of the stand (Section 6.4.2). Because the suggested limits have been calculated using the seated acceptability curves (Figure 6.25) as well as the jumping acceptability curves (Figure 6.26) the acceptability values are significantly lower than the corresponding values for 'high energy concerts' which just use the jumping acceptability curves. This is because those seated are considerably more sensitive to vibrations than those jumping (Section 6.1).

The recommended 20% overall crowd unacceptability limit for 'medium tempo concerts and high profile sporting events' is similar to the 5% overall crowd unacceptability limit for 'high energy concerts' and so lies close to the lower end of the range of acceptable accelerations suggested by the NBCC for stadiums and arenas (Figure 6.35 b). As such it is almost half the IStructE's acceleration limit for the same type of event and is well below Kasperski's unacceptable threshold. The suggested 15% overall crowd unacceptability limit for 'medium tempo concerts and high profile sporting events' is slightly less than the IStructE's guideline acceptability limit for 'classical concerts and typical sporting events'. Both the 5% and 10% overall crowd unacceptability limit for 'medium tempo concerts and high profile sporting events' fall below Kasperski's disturbing comfort threshold.

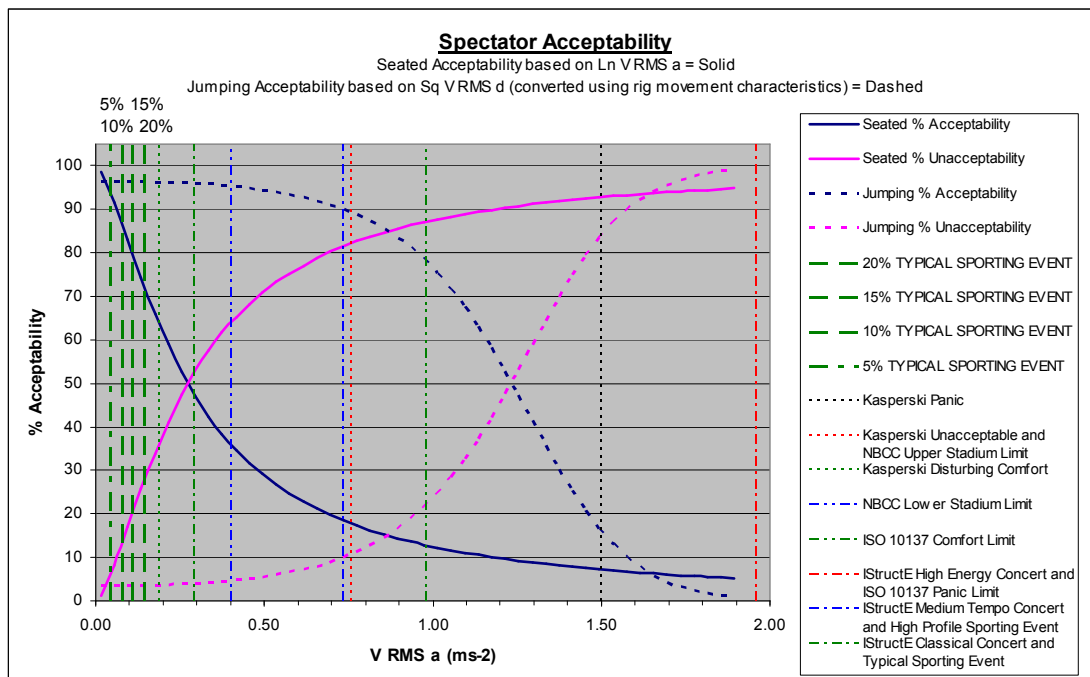


a) High Energy Concerts

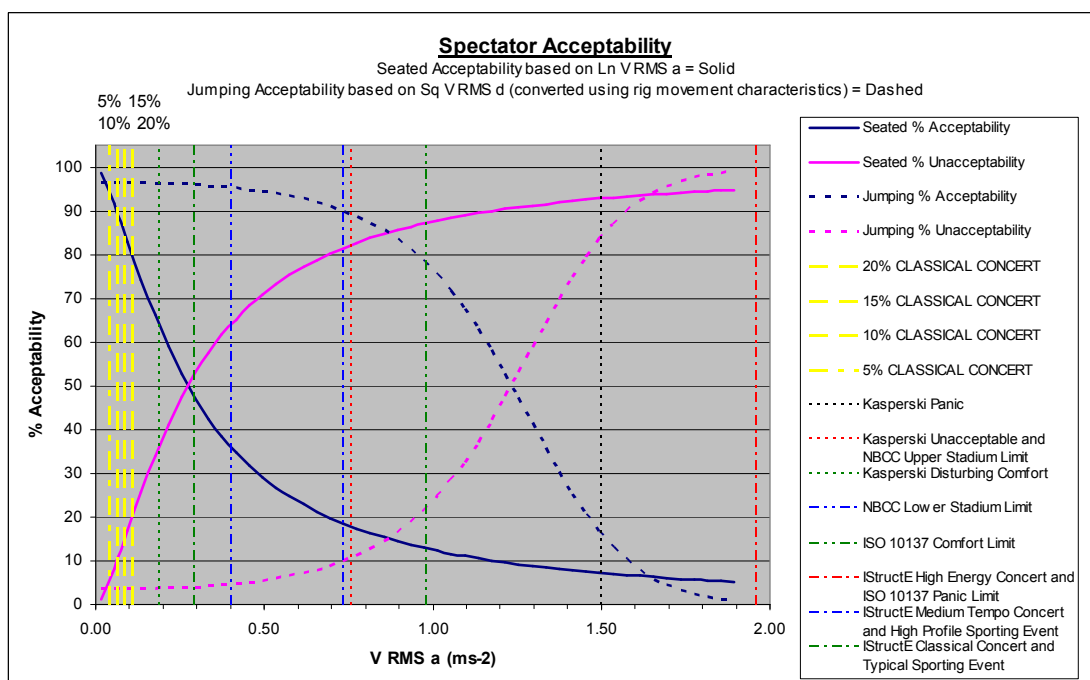


b) Medium Tempo Concerts and High Profile Sporting Events

Figure 6.35 Recommended Acceptability Criteria together with Previously Published Guidelines (Continued over)



c) Typical Well Attended Sporting Events



d) Classical Concerts

Figure 6.35 (Continued) Recommended Acceptability Criteria together with Previously Published Guidelines

6.5.3 Comparison of Proposed Acceptability Criteria - Typical Well Attended Sporting Events

For 'typical well attended sporting events' the crowd build up decided upon for the calculation of the recommended acceptability limits was 33% jumping and 67% seated (Section 6.4.3). Due to the large portion of the crowd who are seated the suggested acceptable RMS accelerations are low, with all four defined percentage overall crowd unacceptability levels (5%, 10%, 15% and 20%) falling below Kasperski's disturbing comfort threshold (Figure 6.35 c). Similar to the situation for 'medium tempo concerts and high profile sporting events' the recommended 20% overall crowd unacceptability limit for 'typical well attended sporting events' is approximately half that proposed by the IStructE for the same type of event.

6.5.4 Comparison of Proposed Acceptability Criteria - Classical Concerts

Because of the nature of the event the acceptability criteria recommended for 'classical concerts' have been based on the entire crowd being seated (Section 6.4.3) and as such produce the lowest acceptable RMS acceleration. Surprisingly, these values are only slightly less than the ones suggested for 'typical well attended sporting events' where only 67% of the crowd are assumed to be seated (Figure 6.35 c & d).

6.5.5 Further Comparisons of Proposed Acceptability Criteria

Although it appears from an initial comparison with previously published acceptability limits that the proposed vibration limits derived from the acceptability curves appear to sit well with the previously published guidelines of Kasperski and the NBCC it is misleading to compare just the acceleration limits as the recommended methods of calculation vary significantly. Therefore in order to compare on a like-for-like basis a test case was set up. This was a grandstand with a mass ratio (crowd to stand) of 0.28 and damping of 2% of critical (similar to that of the test rig). The models and loadings were taken directly from the publications and are summarised in Figure 6.36 and Table 6.9 below. For each case the minimum

stand frequency required to meet the given acceleration limit (Table 6.9) was calculated (to the nearest 0.5Hz) and the results are summarised in Table 6.10.

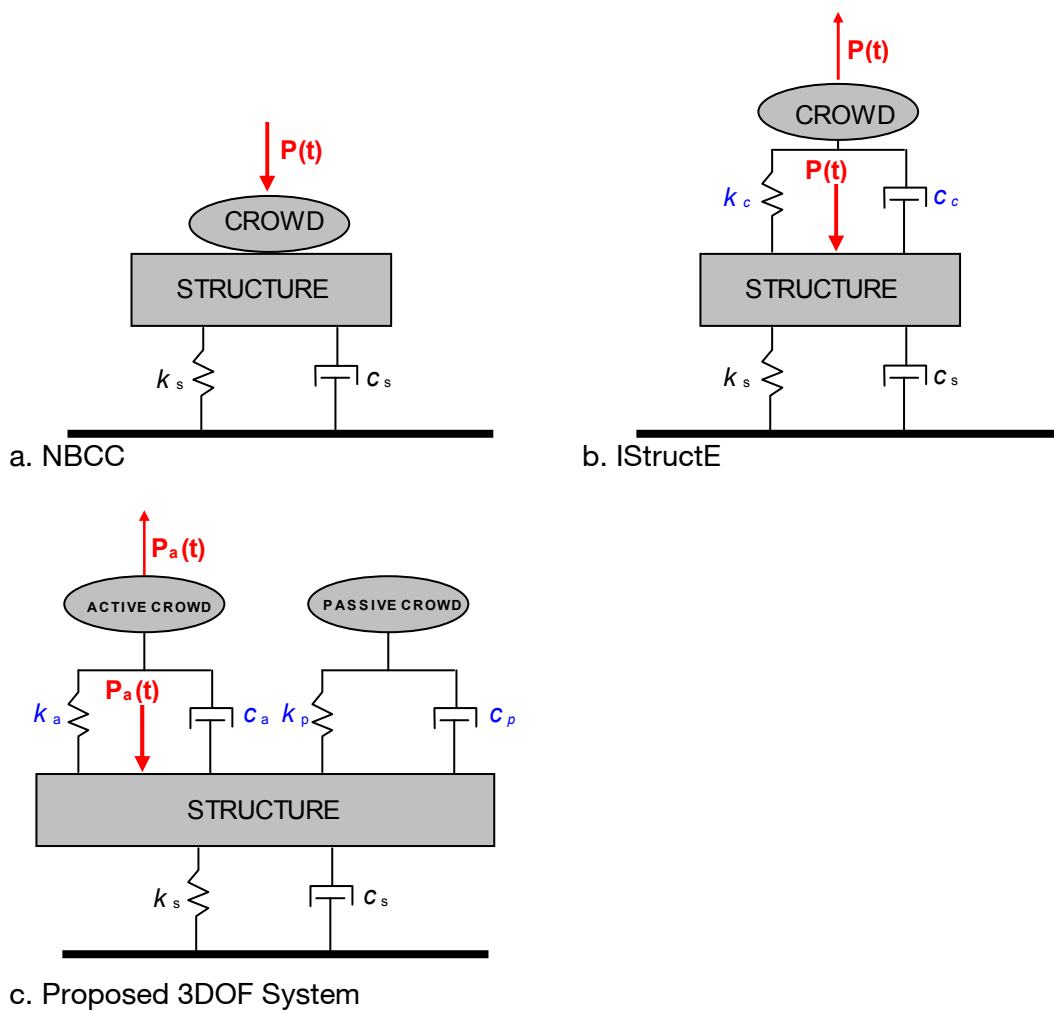


Figure 6.36 Load Models for Calculating Acceptability

Table 6.9 Loadings and Acceptability Limits used with the Load Models shown in Figure 6.36

	Dynamic Load Format	Weight of Participants
NBCC Lively Concert or Sports Event	$P(t) = w_p \sum_{i=1}^{i=3} \alpha_i \sin(2\pi i f t)$	$w_p = 1.5 \text{ kN/m}^2 (0.5 \text{ m}^2 / \text{person})$ or $w_p = mg = 76.5 \text{ kg/person} \times 9.81 \text{ ms}^{-2}$
IStructE All Scenarios	$P(t) = \rho m g \sum_{i=1}^{i=3} G_i \cos(2\pi i f t + \theta_i)$	$mg = 80 \text{ kg/person} \times 9.81 \text{ ms}^{-2}$
Proposed	$P_a(t) = \kappa \rho m_a g \sum_{i=1}^{i=3} G_i \cos(2\pi i f t + \theta_i)$	$m_a g = 80 \text{ kg/active.person} \times 9.81 \text{ ms}^{-2}$ $m_p g = 80 \text{ kg/passive.person} \times 9.81 \text{ ms}^{-2}$
High Energy Concert		Extreme Limit $m_a : m_p = 100:0$ High Energy Concert $m_a : m_p = 100:0$
Medium Tempo Concert or High Profile Sporting Event		$m_a : m_p = 100:0$
Typical Sporting Event		$m_a : m_p = 33:67$
Classical Concert		$m_a : m_p = 10:90$
<p>with κ = Proportion of IStructE G_i Dynamic Load Factors ρ = Crowd Effectiveness Factor m_a = Mass of the active portion of the crowd m_p = Mass of the passive portion of the crowd m = Total mass of the crowd g = Acceleration due to gravity, 9.81 ms^{-2} i = Harmonic number G_i = The i th Dynamic Load Factor f = Fundamental frequency of the crowd activity t = Time in seconds θ_i = Phase angle of the i th harmonic</p> <p>and $k_c = 4\pi^2 n^2 m$ n = Natural frequency of the crowd</p> <p>where $n = 2.3 \text{ Hz}$ for IStructE (2008) Scenarios 3 & 4 $n = 5 \text{ Hz}$ for IStructE (2008) Scenario 2</p> <p>with $c_c = 25\%$ critical for IStructE (2008) Scenarios 3 & 4 $c_c = 40\%$ critical for IStructE (2008) Scenario 2</p> <p>and $k_a = 4\pi^2 n_a^2 m_a$ n_a = Natural frequency of the active crowd = 2.3 Hz as IStructE (2008)</p> <p>with $c_a = 25\%$ critical as IStructE (2008)</p> <p>and $k_p = 4\pi^2 n_p^2 m_p$ n_p = Natural frequency of the passive crowd = 5.0 Hz as IStructE (2008)</p> <p>with $c_p = 40\%$ critical as IStructE (2008)</p>		

Table 6.9 Continued Loadings and Acceptability Limits used with the Load Models shown in Figure 6.36

	Load Components (in terms of total mass of the crowd $m = m_a + m_p$)			Effectiveness Factor
	1st Harmonic	2nd Harmonic	3rd Harmonic	ρ
NBCC	$m\alpha_1=0.25 \text{ m}$	$m\alpha_2=0.05 \text{ m}$	$m\alpha_3=0 \text{ m}$	-
IStructE Scenario 4	$mG_1=0.375 \text{ m}$	$mG_2=0.095 \text{ m}$	$mG_3=0.026 \text{ m}$	$\rho(f) = \text{sech}(f - 2)$
IStructE Scenario 3	$mG_1=0.188 \text{ m}$	$mG_2=0.047 \text{ m}$	$mG_3=0.013 \text{ m}$	$\rho(f) = e^{-2(f-1.8)^2}$
IStructE Scenario 2	$mG_1=0.120 \text{ m}$	$mG_2=0.015 \text{ m}$	$mG_3=0 \text{ m}$	$\rho(f) = e^{-2(f-1.8)^2}$
Proposed Extreme Limit	$\kappa mG_1=0.375 \text{ m}$	$\kappa mG_2=0.095 \text{ m}$	$\kappa mG_3=0.026 \text{ m}$	For all cases use IStructE Scen. 4 EF $\rho(f) = \text{sech}(f - 2)$ Although could potentially use IStructE Scen. 2 & 3 EF $\rho(f) = e^{-2(f-1.8)^2}$ for Medium Tempo Concerts and, High Profile and Typical Sporting Events
High Energy Concert	$\kappa mG_1=0.281 \text{ m}$	$\kappa mG_2=0.071 \text{ m}$	$\kappa mG_3=0.020 \text{ m}$	
Medium Tempo Concert or High Profile Sporting Event	$\kappa mG_1=0.188 \text{ m}$	$\kappa mG_2=0.047 \text{ m}$	$\kappa mG_3=0.013 \text{ m}$	
Typical Sporting Event	$\kappa mG_1=0.125 \text{ m}$	$\kappa mG_2=0.032 \text{ m}$	$\kappa mG_3=0.009 \text{ m}$	
Classical Concert	$\kappa mG_1=0.038 \text{ m}$	$\kappa mG_2=0.010 \text{ m}$	$\kappa mG_3=0.003 \text{ m}$	

	Acceleration Limits
NBCC	
Upper Limit	1.77 ms^{-2} peak acceleration
Lower Limit	0.98 ms^{-2} peak acceleration
IStructE	
Scenario 4	1.96 ms^{-2} RMS acceleration
Scenario 3	0.74 ms^{-2} RMS acceleration
Scenario 2	0.29 ms^{-2} RMS acceleration
Proposed	(Range for 20% to 5% overall crowd unacceptability given)
Extreme Limit	1.30 ms^{-2} RMS acceleration
High Energy Concert	0.44 ms^{-2} to 0.95 ms^{-2} RMS acceleration
Medium Tempo Concert or High Profile Sporting Event	0.06 ms^{-2} to 0.42 ms^{-2} RMS acceleration
Typical Sporting Event	0.04 ms^{-2} to 0.15 ms^{-2} RMS acceleration
Classical Concert	0.04 ms^{-2} to 0.11 ms^{-2} RMS acceleration

Table 6.10 Minimum Vertical Natural Frequency at which Acceleration Limit is met when calculated for a Stand with a Crowd to Mass Ratio of 0.28 and 2% Critical Damping and a Maximum Fundamental Frequency of the Crowd Activity of 3.2Hz

	NBCC 2005*	IStructE 2008	Proposed (Range for 20% to 5% overall crowd unacceptability given)
Lively Concert or Sports Event	5.75Hz for upper limit 5.5Hz for lower limit		
High Energy Concert		Scenario 4 3.25Hz	5.85Hz driven by Extreme Limit (5.9Hz to 7.6Hz for High Energy Concert limit)
Medium Tempo Concert and High Profile Sporting Event		Scenario 3 2.95Hz	6.6Hz to 11.0Hz using IStructE Scenario 4 effectiveness factor (4.7Hz to 8.35Hz if use IStructE Scenario 2 & 3 effectiveness factor)
Typical Sporting Event		Scenario 2 3.35Hz	6.85Hz to 10.9Hz using IStructE Scenario 4 effectiveness factor (5.55Hz to 8.3Hz if use IStructE Scenario 2 & 3 effectiveness factor)
Classical Concert		Scenario 2 3.35Hz	4.7Hz to 8.05Hz

*NBCC results based on original peak acceleration limits not RMS conversion

From Table 6.10 it can be seen that, for the test case considered, the upper extreme limit for high energy concerts requires a similar natural frequency of stand (5.85Hz) to that calculated using the NBCC's upper bound requirements, of 18%g peak acceleration, for lively concerts and sports events 5.75Hz. For 'high energy concerts' the proposed extreme limit rather than the 'high energy concert' limit governed. Interestingly, despite having different loading and acceptability criteria, the proposals for 'medium tempo concerts and high profile sporting events' and 'typical well attended sporting events' produced very similar results for the test case with frequency ranges of 6.6Hz (20% overall crowd unacceptability) to 11.0Hz (5% overall crowd unacceptability) and 6.85Hz (20% overall crowd unacceptability) to 10.9Hz (5% overall crowd unacceptability) respectively. This is largely due to the proportion of the crowd that was deemed to be seated when deriving the acceptance criteria. The dynamic crowd loading for 'medium tempo concerts and high profile sporting events' (Table 6.9) is 50% greater than that for 'typical well

attended sporting events'. However, because the acceptability limits for 'typical well attended sporting events' are based on a much larger portion of the crowd being seated, two-thirds compared to a quarter for 'medium tempo concerts and high profile sporting events', the acceptance criteria for 'typical well attended sporting events' are potentially more onerous due to the sensitivity of seated spectators to vibrations. For both these event scenarios it is possible to reduce the required minimum vertical natural frequency of the stand in order to meet the acceptance criteria by applying the IStructE's Scenario 2 & 3 effectiveness factor in place of the Scenario 4 effectiveness factor (Table 6.10). The applicability of the Scenario 2 & 3 effectiveness factor is dependent on the probability of the beat exciting the dynamic crowd action fitting the music profile used in the derivation of the effectiveness factor (see Sections 6.3 and 6.4). The calculated minimum vertical stand frequencies required for 'classical concerts' ranging from 4.7Hz (20% overall crowd unacceptability) to 8.05Hz (5% overall crowd unacceptability) are the lowest of the test case stand frequencies calculated using the proposed limits.

For the IStructE loading and guideline RMS acceleration limits the results of the test case are surprising. Scenario 2 for 'typical sporting events and classical concerts' produced the highest required stand frequency at 3.35Hz (Table 6.10). The required stand frequency to meet the Scenario 4 loading and acceleration limit for 'high energy concerts' was slightly lower at 3.25Hz. The lowest stand frequency calculated was to meet the IStructE guidelines for 'medium tempo concerts and high profile sporting events' at 2.95Hz. All these values are significantly lower than the comparable stand frequencies calculated using the proposed limits and the NBCC guidelines.

The acceptability thresholds proposed by Kasperski in 1996, upon which most current stadium acceptance criteria are based, were related to recorded peak accelerations. In order to tie these values back to current guidelines the test case was rerun using peak accelerations for the three IStructE load cases (Table 6.9) and the minimum stand frequency at which the Kasperski threshold limits were reached recorded (Table 6.11). Concurrently the IStructE guideline RMS acceleration limits were converted to peak values and the minimum natural frequency required for the test case stand to meet these peak limits calculated (Table 6.11). The conversion of the IStructE guidelines from RMS to peak accelerations was carried out simply by

multiplying the limits by $\sqrt{2}$, as this is how it is believed the IStructE RMS values were originally derived from Kasperski's original peak acceleration thresholds and the NBCC guidelines (Section 6.2).

The results show that, when using the same loading, the Kasperski thresholds produce lower minimum stand frequencies than the IStructE peak acceleration limits. This is not surprising as the Kasperski threshold values (excluding that for 'disturbing comfort') are considerably higher than the comparable IStructE peak accelerations. The results for the Kasperski tests are more similar to those using the IStructE RMS acceleration limits (Table 6.10) although the Kasperski frequencies are still slightly lower. The most interesting outcome is that the frequencies calculated using the IStructE peak acceleration limits are more comparable with those using the proposed experimentally derived limits and loading for 20% overall crowd acceptability (Table 6.10).

Table 6.11 Frequency at which Peak Acceleration Limit is met when calculated for a Stand with a Crowd to Mass Ratio of 0.28 and 2% Critical Damping and a Maximum Fundamental Frequency of the Crowd Activity of 3.2Hz

Loading Used	Kasperski**	IStructE***
High Energy Concert (Scenario 4 loads & EF)	Panic – 3.43ms^{-2} 2.95Hz	Scenario 4 – 2.77ms^{-2} 5.1Hz
Medium Tempo Concert and High Profile Sports Event (Scenario 3 loads & EF)	Unacceptable – 1.77ms^{-2} 2.65Hz	Scenario 3 – 1.04ms^{-2} 4.35Hz
Classical Concert and Typical Sports Event (Scenario 2 loads & EF)	Disturbing Comfort – 0.49ms^{-2} 3.0Hz	Scenario 2 – 0.42ms^{-2} 3.05Hz

**Results based on original peak acceleration limits not RMS conversion

*** IStructE limits converted to peak accelerations by multiplying by $\sqrt{2}$

To investigate whether this potential relationship between the proposed limits and the IStructE peak acceleration limits holds for other stands two further combinations were tested. The first with a crowd to structure mass ratio of 0.19 (similar to that of the December 2006 tests) and the second, representing a lightweight structure, with a crowd to stand mass ratio of 1.0. In both cases the structural damping was taken

as 2% of critical and the maximum fundamental frequency of the crowd activity as 3.2Hz as previously. The results for these additional test cases are given in Table 6.12.

Table 6.12 Frequency at which Peak Acceleration Limit is met when calculated for a Stand with varying Mass Ratio μ and 2% Critical Damping and a Maximum Fundamental Frequency of the Crowd Activity of 3.2Hz

	Proposed* $\mu=0.19$	IStructE** $\mu=0.19$	Proposed* $\mu=0.28$	IStructE** $\mu=0.28$	Proposed* $\mu=1.0$	IStructE** $\mu=1.0$
High Energy Concert	3.15 Hz from both limits	Scenario 4 3.25Hz	4.75Hz driven by Concert Limit	Scenario 4 5.1Hz	6.85Hz driven by Extreme Limit	Scenario 4 7.3Hz
Medium Tempo Concert and High Profile Sporting Event	6.55Hz using IStructE Scen. 4 EF (3.95Hz if use IStructE Scen. 2 & 3 EF)	Scenario 3 2.8Hz	6.2Hz using IStructE Scen. 4 EF (4.4Hz if use IStructE Scen. 2 & 3 EF)	Scenario 3 4.35Hz	8.8Hz using IStructE Scen. 4 EF (6.6Hz if use IStructE Scen. 2 & 3 EF)	Scenario 3 6.55Hz
Typical Sporting Event	5.6Hz using IStructE Scen. 4 EF (4.8Hz if use IStructE Scen. 2 & 3 EF)	Scenario 2 2.8Hz	6.25Hz using IStructE Scen. 4 EF (5.25Hz if use IStructE Scen. 2 & 3 EF)	Scenario 2 3.05Hz	9.85Hz using IStructE Scen. 4 EF (8.0Hz if use IStructE Scen. 2 & 3 EF)	Scenario 2 4.25Hz
Classical Concert	3.8Hz	Scenario 2 2.8Hz	4.1Hz	Scenario 2 3.05Hz	6.05Hz	Scenario 2 4.25Hz
<p>* Frequencies calculated using RMS limits previously described for 20% overall crowd unacceptability converted to peak accelerations using formula based on recorded rig movements during testing (Figure 6.24 b)</p> <p>** Frequencies calculated using RMS limits converted to Peak values by multiplying by $\sqrt{2}$</p>						

From these three test cases it appears that for the cases where the loading and effectiveness factor are the same (Scenario 4 'High energy concert' and Scenario 3 'Medium tempo concert and high profile sporting event') the limiting frequencies are generally very similar. This is because the peak acceleration acceptability limits for

IStructE and the proposed 20% overall crowd acceptability for these cases are also comparable (Table 6.13).

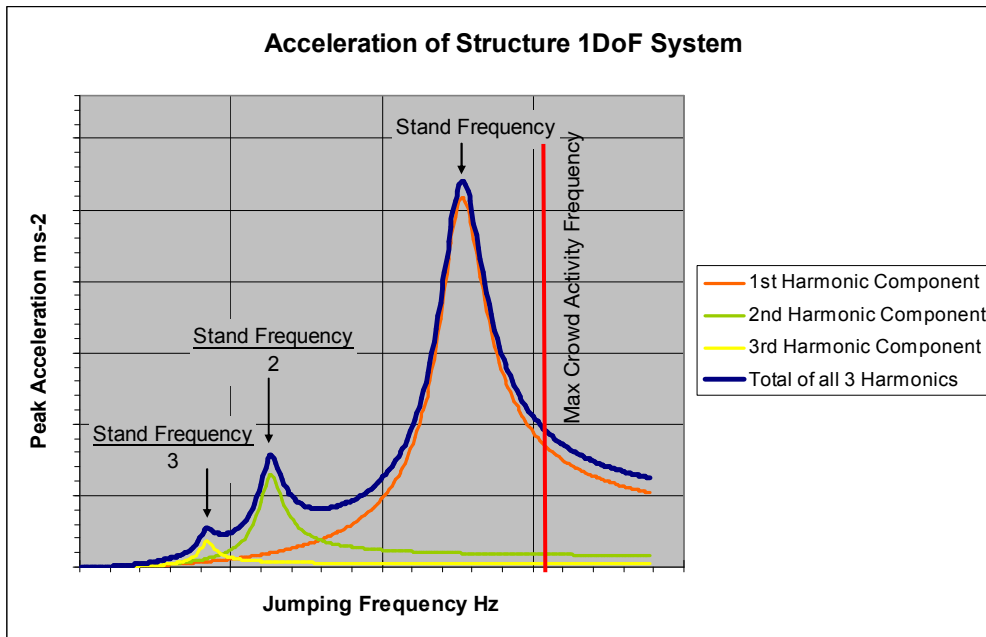
Table 6.13 Acceptability Limits based on Peak Accelerations

	Proposed* 20% Overall Crowd Acceptability Limit	IStructE** Acceptability Limit
High Energy Concert	2.98 ms ⁻² Upper Limit 2.20 ms ⁻² Standard Limit	2.77 ms ⁻²
Medium Tempo Concert and High Profile Sports Event	1.01 ms ⁻²	1.04 ms ⁻²
Typical Sports Event	0.40 ms ⁻²	0.42 ms ⁻²
Classical Concert	0.32 ms ⁻²	0.42 ms ⁻²
* RMS limits converted to Peak values using experimental data from tests (Figure 6.24 b)		
** RMS limits converted to Peak values by multiplying by $\sqrt{2}$		

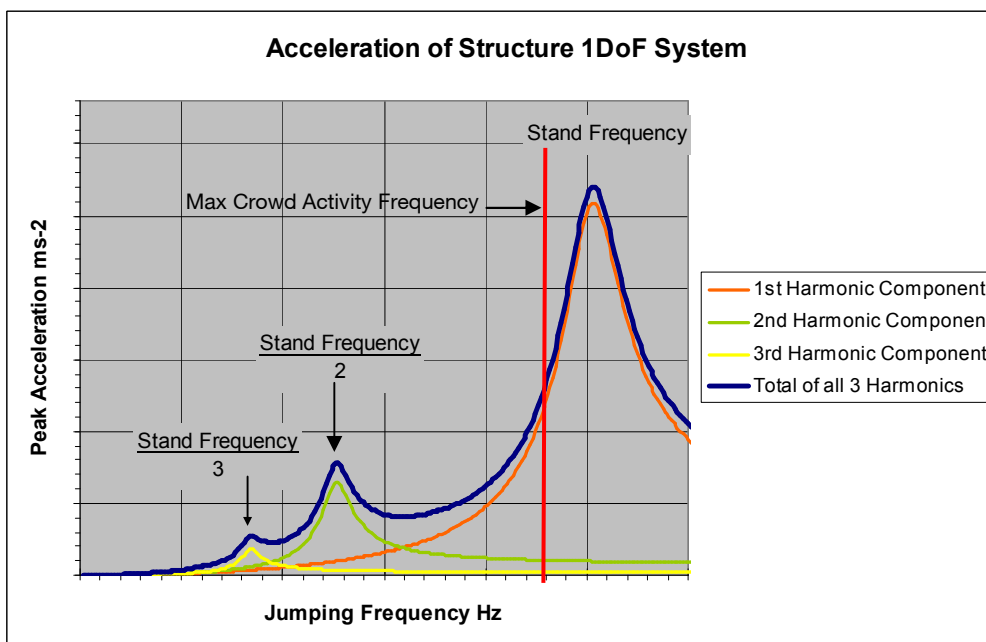
Unlike the other Scenario 3 and Scenario 4 cases, the test case for ‘Medium tempo concerts and high profile sporting events’ with a mass ratio $\mu=0.19$ produced noticeably different limiting frequencies for the same loading and very similar acceptability criteria, 3.95Hz proposed compared to 2.8Hz for the IStructE guidelines. Because the passive crowd element of the proposed 3 degree-of-freedom model (Figure 6.36 c) is taken as zero for both the ‘High energy concert’ and ‘Medium tempo concert and high profile sporting event’ load cases the model becomes the same as the IStructE 2 degree-of-freedom model (Figure 6.36 b). Thus if the loads, effectiveness factors and models are the same the only explanation for the discrepancy in the frequency limits is down to the slight 0.03ms⁻² difference in acceptability criteria.

Taking the response of a simple single degree-of-freedom system (similar to Figure 6.36 a) as an example, the impact of slight changes in the acceptability limit can be explained. In order to determine the likely peak acceleration of the system the relationship between the maximum crowd activity frequency and the stand frequency needs to be examined (Figure 6.37). If the maximum crowd activity frequency is greater than that of the stand then the peak acceleration response will occur when the crowd jump at a frequency equal to that of the stand, shown by the tallest peak on the graph in Figure 6.37 a. This is a resonant response due the 1st

harmonic component of the forcing function. If the maximum crowd activity frequency falls between the stand frequency and half the stand frequency then one of two situations occurs. The first (Option 1, Figure 6.37 b) being that the predicted acceleration at the maximum crowd activity frequency is greater than that if the crowd jump at half the natural frequency of the stand i.e. the resonant response due to the 2nd harmonic component of the forcing function indicated by the second largest peak in Figure 6.37. The second option (Figure 6.37 c) is that the predicted acceleration at the maximum crowd activity frequency is less than the 2nd harmonic resonant peak and therefore the peak acceleration response in this case is at this peak corresponding to half the stand frequency. A similar situation occurs when the maximum crowd activity frequency falls between half and a third of the natural frequency of the stand (Figure 6.37 d).

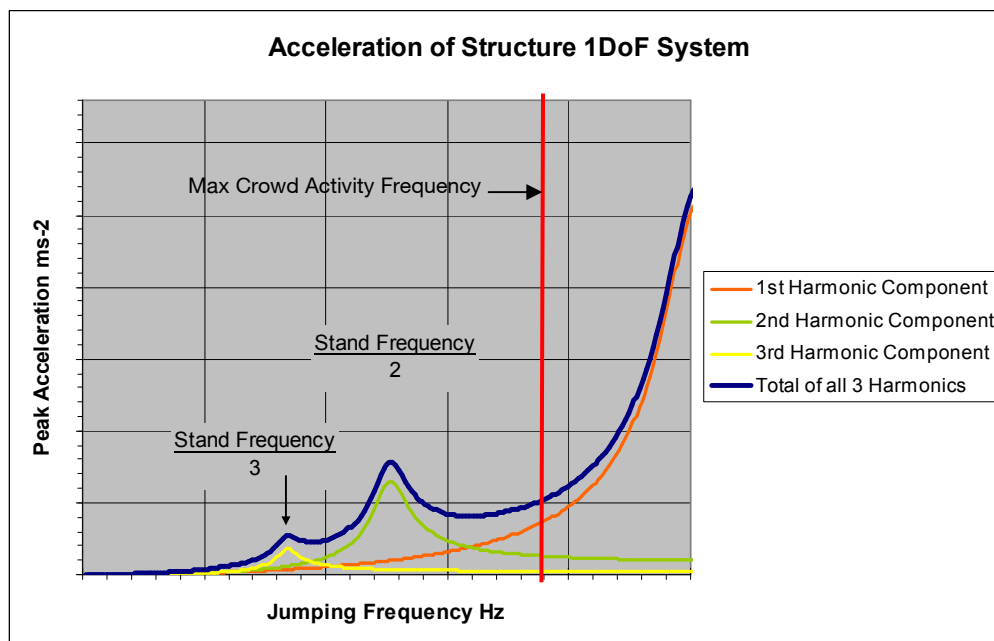


- a) Maximum Crowd Activity Frequency greater than Natural Frequency of the Stand

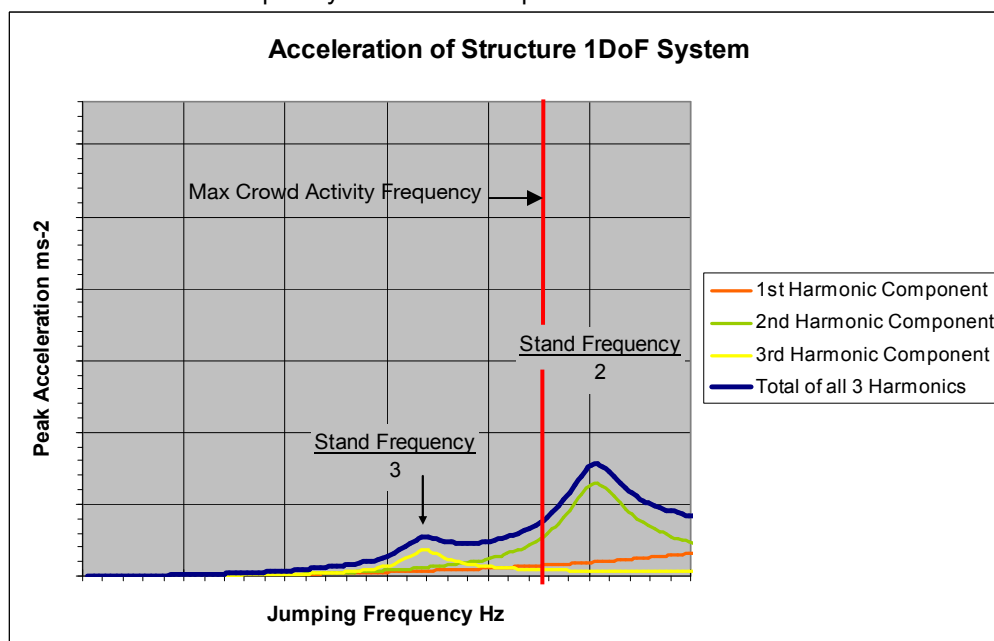


- b) Maximum Crowd Activity Frequency between Natural Frequency of the Stand and Half Natural Frequency of the Stand Option 1

Figure 6.37 Acceleration Response of a Single Degree-of-freedom System (Continued over)



- c) Maximum Crowd Activity Frequency between Natural Frequency of the Stand and Half Natural Frequency of the Stand Option 2



- d) Maximum Crowd Activity Frequency between a Half and a Third of the Natural Frequency of the Stand

Figure 6.37 (Continued) Acceleration Response of a Single Degree-of-freedom System

However this is a slight simplification as the use of an effectiveness factor, which prioritises certain frequencies of vibration, can change the magnitude and location of the predicted peak acceleration shown in Figures 6.37 a to d. The IStructE Scenario 4 and Scenario 2 & 3 effectiveness factors, used in calculating the peak accelerations described above, leave vibrations generated by crowd activity in the region of 2Hz as the predicted peak acceleration (shown in Figures 6.37) but significantly reduce the accelerations either side of this. This modification can have a large or a small effect on the calculated maximum acceleration dependent on the relative frequencies of the crowd activity and the natural frequency of the grandstand. This is shown clearly in Figures 6.38 a and b, where relatively small changes in the natural frequency of the stand can be seen to shift the predicted maximum acceleration from the 1st to the 2nd harmonic peaks and also reduce the magnitude of the peaks themselves. A similar shift happens between the 2nd and 3rd harmonic peaks as the stand frequency increases relative to the crowd activity frequency (Figures 6.38 b and c).

When determining the minimum stand frequency required to meet the specified acceleration limit, one starts by checking whether the 3rd harmonic peak (Figure 6.38 c(iii)) is less than the required limit and then gradually reduces the natural frequency of the stand until the predicted peak acceleration reaches the specified limit, i.e. one works through the Figures 6.38 a to c in reverse order.

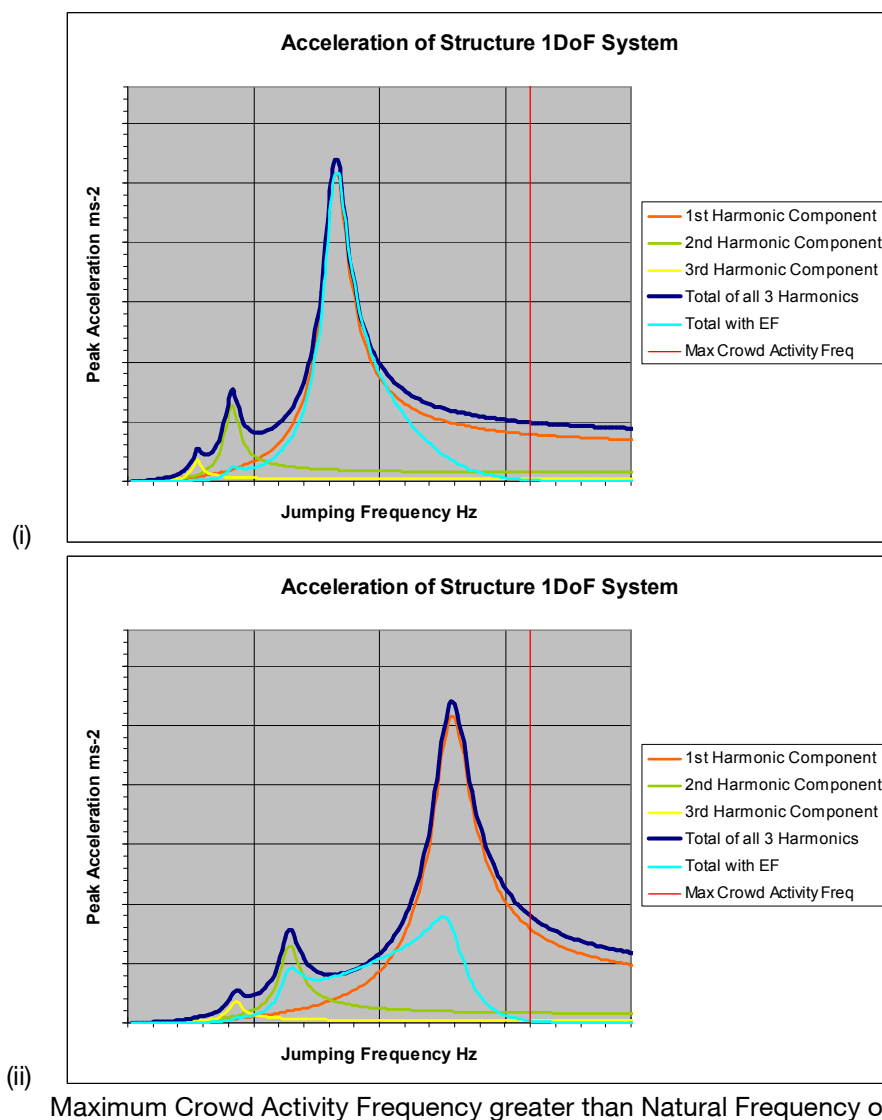


Figure 6.38 Acceleration Response of a Single Degree-of-freedom System showing the Effect of the IStructE Scenario 3 Effectiveness Factor (Continued over)

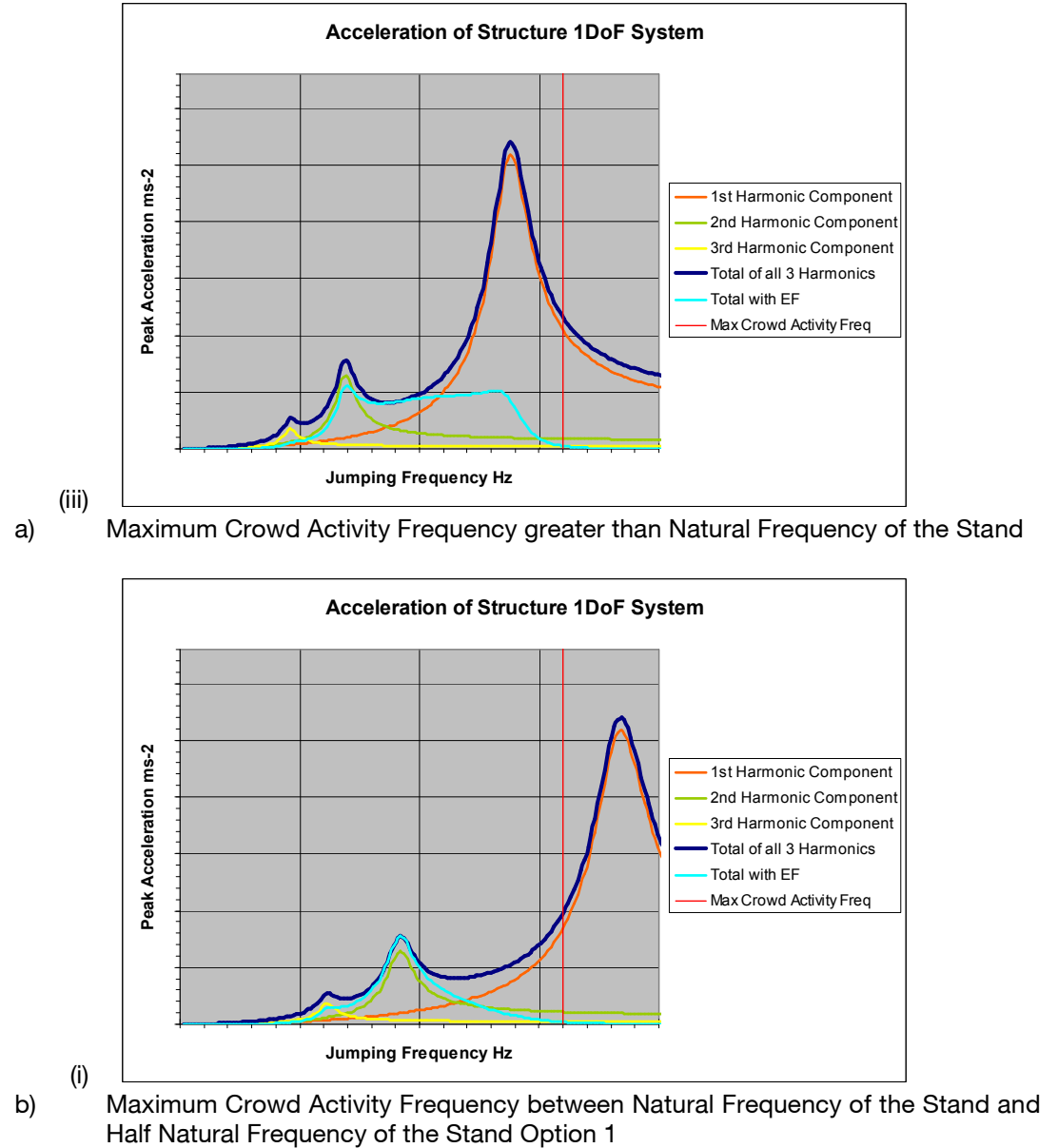
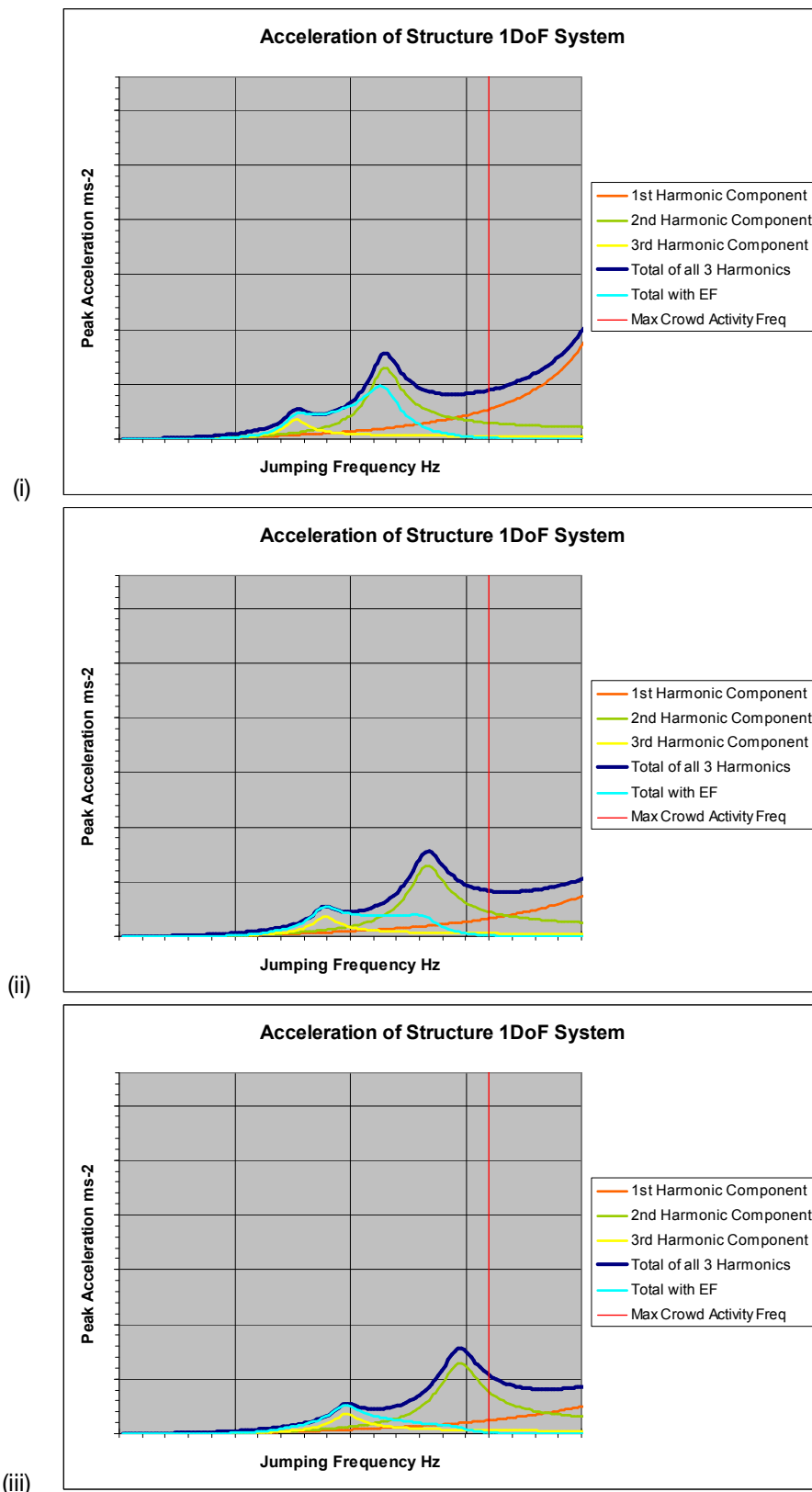


Figure 6.38 (Cont.) Acceleration Response of a Single Degree-of-freedom System showing the Effect of the IStructE Scenario 3 Effectiveness Factor



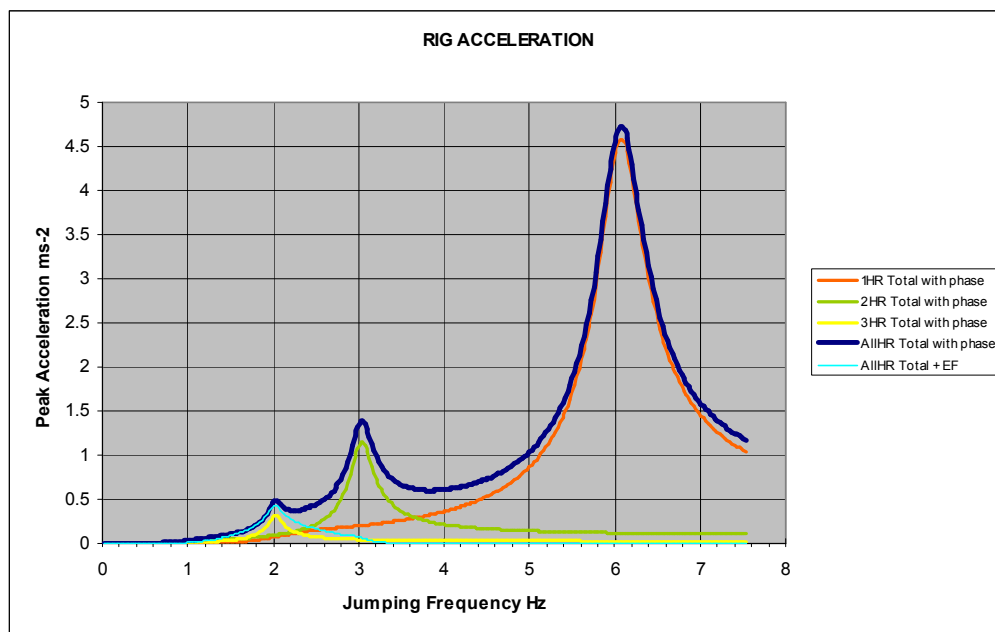
c) Maximum Crowd Activity Frequency between Natural Frequency of the Stand and Half Natural Frequency of the Stand Option 2

Figure 6.38 (Cont.) Acceleration Response of a Single Degree-of-freedom System showing the Effect of the IStructE Scenario 3 Effectiveness Factor

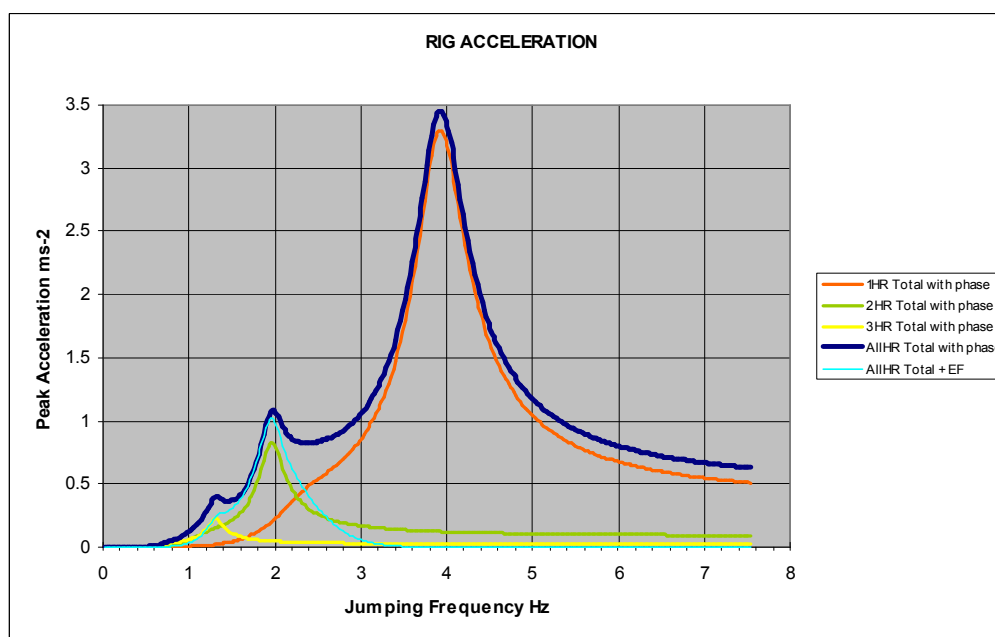
For the IStructE Scenario 3 test case with $\mu=0.19$ the 3rd harmonic peak (Figures 6.38 c(iii) and 6.39 a) is significantly lower than the guideline peak acceleration limit of 1.04ms^{-2} (Table 6.13) while the 2nd harmonic peak (Figures 6.38 b(i) and 6.39 b) is only marginally lower at 1.02ms^{-2} . Therefore the minimum frequency limit in this case is set by a proportion of the 1st harmonic peak with the 1.04ms^{-2} peak acceleration being reached when the stand frequency is 2.8Hz just below the maximum crowd activity frequency of 3.2Hz and the graph (Figure 6.39 c) lies somewhere between Figures 6.38 a(i) and a(ii). The comparable proposed limit for this test case is slightly lower than the IStructE value at 1.01ms^{-2} (Table 6.13) and therefore is achieved by the 2nd harmonic peak (Figure 6.39 b) at a frequency of 3.95Hz. Thus it can be seen how a very slight difference in the acceptance criteria can have a marked influence in the calculated minimum required stand frequency and hence stiffness (and more than likely cost).

While Figures 6.37 and 6.38 used a simple single degree-of-freedom model to explain the calculation of grandstand accelerations due to a Fourier forcing function containing 3 harmonic components the IStructE and proposed models (Figures 6.36 b and c) contain 2 and 3 degrees-of-freedom respectively. In fact, as described above, because the proposed model assumes that there is no passive crowd for 'High energy concerts' and 'Medium tempo concerts and high profile sporting events' load cases the 3 degree-of-freedom model becomes a 2 degree-of-freedom model as per the IStructE model (Figure 6.36 b). Therefore the test case reviewed in the paragraph above is modelled using a 2 degree-of-freedom model which explains the differences between the Figure 6.38 and 6.39 graphs which are most noticeable for Figures 6.38 a(i) & (ii) and Figure 6.39 c.

A 2 degree-of-freedom system, as shown in Figure 6.36 b, has two fundamental vertical frequencies based on the relative mass and stiffness of the crowd and the structure. When the individual frequencies of the crowd and the structure are similar the damping effect of the crowd is most marked, as can be seen by the truncated peak around 2.3Hz in Figure 6.39 d where the empty stand frequency = crowd frequency = 2.3Hz. As the difference between the individual frequencies of the crowd and the structure become greater the damping effect of the crowd reduces, Figures 6.37 c to a. This is similar to the action of tuned mass dampers.

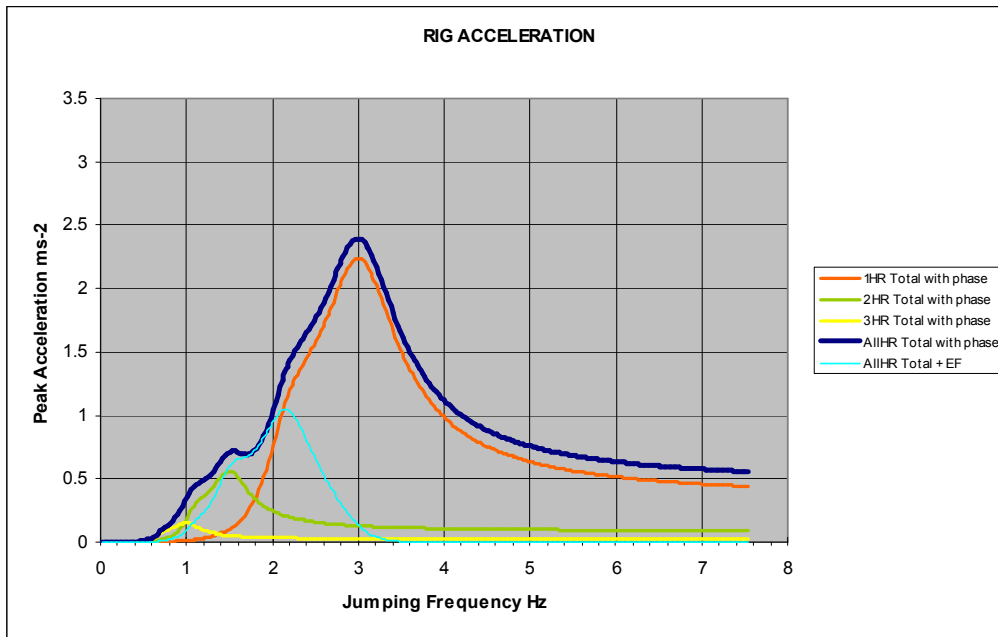


a) Natural Frequency of Stand = 6.0 Hz

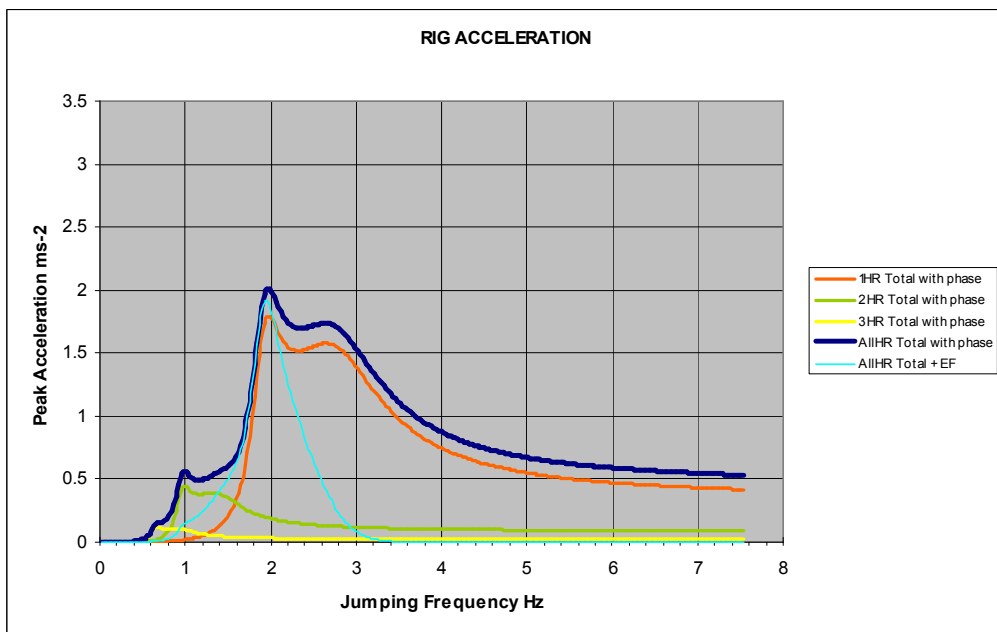


b) Natural Frequency of Stand = 3.8 Hz

Figure 6.39 Graphs showing calculation of Peak Accelerations for a Stand with Mass Ratio $\mu=0.19$ and 2% Damping using IStructE Scenario 3 Loading and Effectiveness Factor and 2 Degree-of-freedom Model (shown in Figure 6.36 b) (Figure 6.39 continued over)



c) Natural Frequency of Stand = 2.8 Hz



d) Natural Frequency of Stand = 2.3 Hz

Figure 6.39 (Continued) Graphs showing calculation of Peak Accelerations for a Stand with Mass Ratio $\mu=0.19$ and 2% Damping using IStructE Scenario 3 Loading and Effectiveness Factor and 2 Degree-of-freedom Model (shown in Figure 6.36 b)

The differences between the calculated IStructE and proposed minimum stand frequencies for 'typical sporting events' in Table 6.13 are more complex. This is because although the peak acceleration limits for 'typical sporting events' (Table 6.13) and the loadings (Table 6.9 (IStructE Scenario 2)) are similar the load models are different. The IStructE uses a 2 degree-of-freedom model and the proposed, a 3 degree-of-freedom model. Although the proposed limits are slightly lower and the loading slightly higher than the IStructE, the calculated minimum grandstand frequencies are significantly higher despite the 3 degree-of-freedom model providing a damped response due to the passive component of crowd (67% of the total crowd are assumed seated). This is because the IStructE scenario for 'typical sporting events' (Scenario 2) assumes even greater damping, with the whole crowd being taken as having the damping characteristics of 'predominantly seated' spectators (i.e. a natural frequency of 5Hz and critical damping of 40%). This compares to the 'active and mostly standing crowd (with a natural frequency of 2.3Hz and critical damping of 5%) assumed for IStructE Scenarios 3 and 4.

For 'classical concerts' the proposed acceptability criteria (and associated loading) are different from those for typical sporting events' unlike the IStructE 2008 guidance which groups them together under Scenario 2. The proposed 20% overall crowd acceptability (peak) acceleration limit is approximately 25% lower than the equivalent IStructE Scenario 2 limit (Table 6.13). Therefore despite the differences in modelling and the fact that the proposed loading is less than that for IStructE Scenario 2 (Table 6.9), it is not surprising that the minimum stand frequencies required to meet the proposed acceptance criteria for 'classical concerts' are higher than to meet the equivalent IStructE limits (Table 6.12).

Calculating the minimum vertical natural frequencies required for a grandstand to meet the serviceability criteria fulfilled two objectives. Firstly it identified the impact small changes in modelling and target acceleration limits can have on the design of the structure, with stiffer (and potentially more costly) structures required to achieve higher natural frequencies. Secondly it highlights the contrast between the two routes proposed by the IStructE (2008) for determining the acceptability of a grandstand subject to synchronised crowd loading. Route 1 uses minimum natural frequency requirements (3.5Hz for Scenario 2 events and 6Hz for Scenarios 3 and 4) while Route 2 uses acceleration limits. Table 6.12 shows that the two routes only

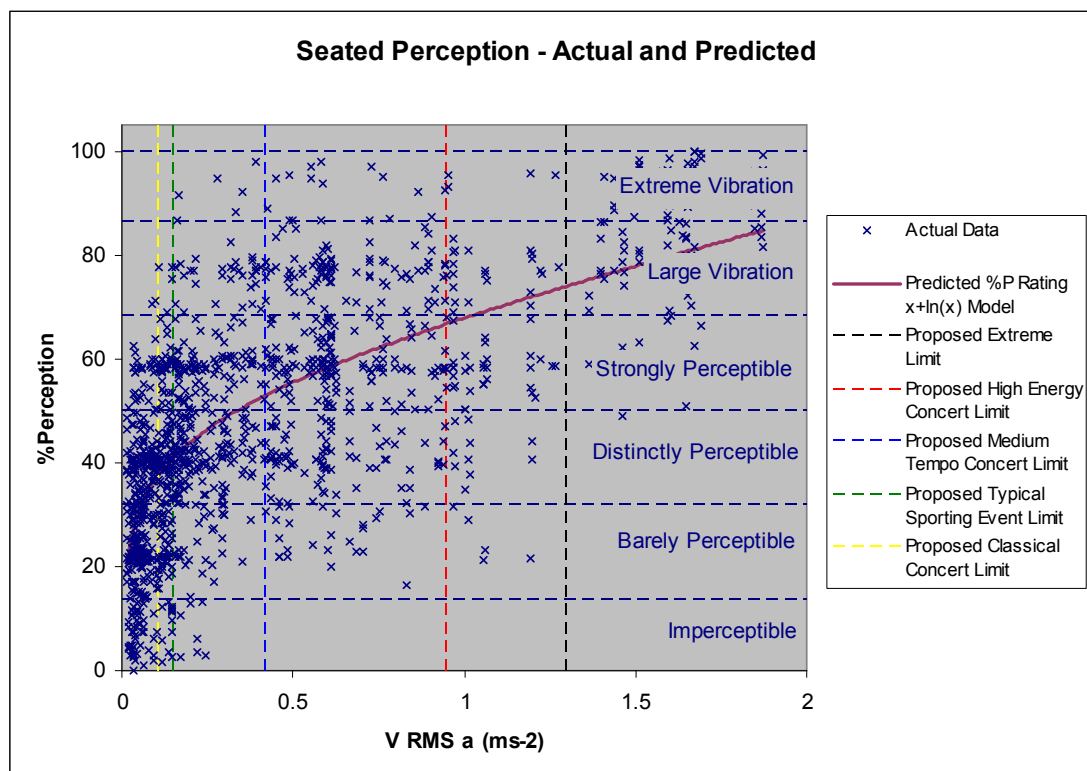
produce similar results for relatively heavy stands (crowd to stand mass ratio $\mu \sim 0.28$) e.g. concrete terracing supported on a steel frame. For lighter structures (e.g. $\mu = 1.0$) the frequency limit Route 1 is less onerous whilst for heavier structures (e.g. $\mu = 0.19$) the acceleration driven Route 2 is more beneficial. This emphasises the simplistic nature of frequency limit design.

6.6 Comparison of Proposed Acceptability Criteria with Recorded Perception Ratings

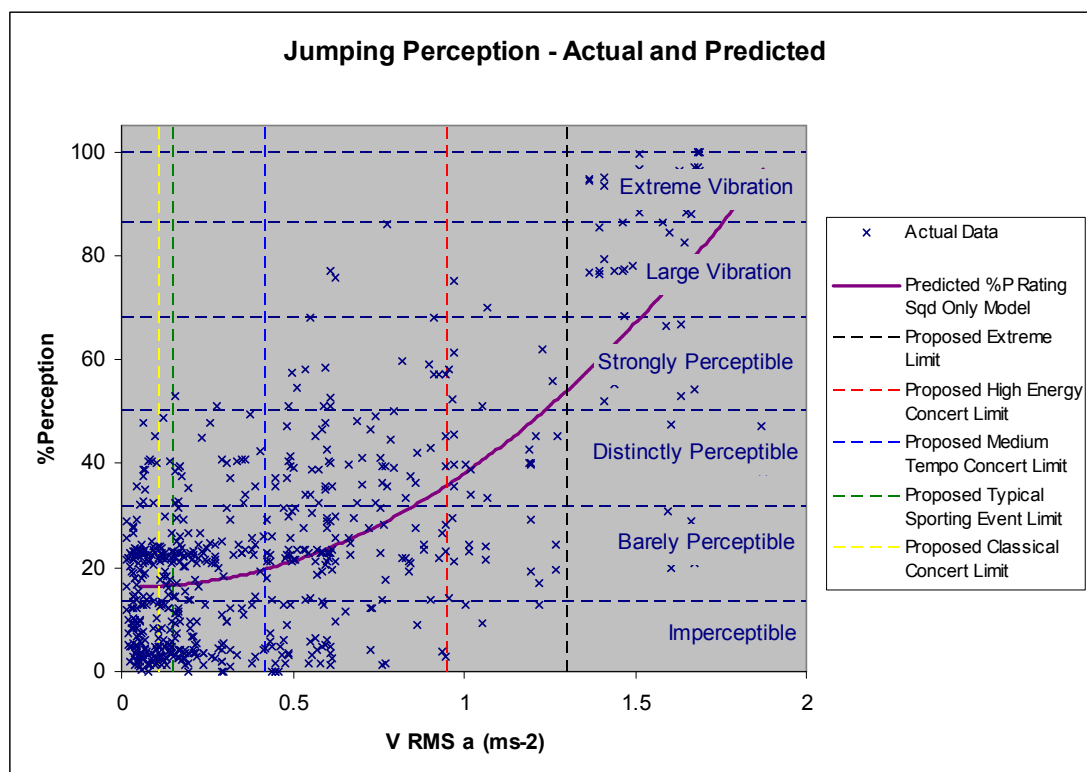
In order to compare the proposed acceptability limits with the experimentally recorded data regarding human perception of vibration magnitude graphs similar to those used in Section 5.3.1 were utilised. As described previously the six perception bands given in the participants' questionnaires (0-Imperceptible to 5-Extreme Vibration) were overlaid on the recorded data and the recommended perception models from Chapter 5 (Figure 6.40). As the recommended acceptability limits are defined in terms of RMS acceleration this was the predictor used for the graphs, with the model for predicting the jumpers perception ratings converted from RMS displacement to RMS acceleration using the vibration characteristics of the test rig.

For all the comparisons described in this section the suggested acceleration limits based on an overall crowd acceptability of 20% has been used as these proved most similar to previously published guidelines (Section 6.5).

The recommended acceleration limits for all but the most extreme 'high energy concert' events are derived primarily from the seated acceptability curves (Figure 6.25). Therefore it is against the seated participants perception ratings that the limits for 'Medium tempo concerts and high profile sporting events', 'Typical sporting events' and 'Classical concerts' should be compared.



a) Seated Participants



b) Jumping Participants

Figure 6.40 Recorded Experimental Perception Data showing Recommended Acceleration Limits based on 20% Overall Crowd Acceptability

The lower two limits, 'Typical sporting events' and 'Classical concerts', are very similar in acceleration magnitude. However they fall on the portion of the curve, predicting the mean seated % perception rating, where the slope is changing most rapidly. Therefore although the recommended limit for 'Typical sporting events' is roughly midway across the 'distinctly perceptible' band, the 'Classical concert' limit is only a third of the way across and consequently closer to the upper boundary of 'barely perceptible'. The recommended acceleration limit for 'Medium tempo concerts and high profile sporting events' lies very close to the point where the model predicting the mean perception rating of those seated changes from 'distinctly perceptible' to 'strongly perceptible'. These comparisons seem to fit well with the levels of vibration that might be expected by spectators attending these various types of event.

For the 'High energy concerts' it was assumed that all the crowd were actively participating in the event and therefore the acceptability curves based on jumping participants (Figure 6.26) were used to define the acceleration limits. From Figure 6.40 the suggested 'High energy concert limit' falls approximately where those seated generally deem the vibration as just becoming a large vibration and those jumping are typically starting to find it 'distinctly perceptible'. The recommended upper-most 'extreme limit' for a vigorously active crowd was based on the vibration level at which all the participants during the testing unanimously deemed the vibration to be unacceptable irrespective of whether they were jumping or seated. Based on the models predicting the mean response this level of vibration would be regarded as a 'large vibration' for those seated and 'strongly perceptible' for those jumping. While the comparisons using the jumping participants data do not provide as clear an agreement as those using the seated data for the lower categories, the recommended 'High energy concert' and 'extreme' limits do not conflict with the experimental perception bands. Again the model predicting the mean perception response of those seated ties in well with the suggested upper two grandstand limits.

All the suggested limits are well below the level at which the experimentally derived models would predict the mean perception of the crowd to be an 'extreme vibration'.

As a less prescriptive sliding scale was used for recording the human emotion responses during the testing, with only the extremes defined, the proposed acceptability limits could not be compared in any detail against the percentage emotion ratings except as covered briefly in Section 6.1.

6.7 Comparison of Proposed Acceptability Criteria with Published Recorded Vibrations

Finally the acceleration acceptability levels derived through this research were compared against accelerations recorded during actual events (Section 2.2 and summarised in Table 6.14). Due to previous guidance (Kasperski 1996 and NBCC 2005) being based on peak accelerations, the published values are typically in this format and so need to be compared against peak acceleration guidelines, therefore the converted proposed 20% overall crowd acceptability limits shown in Table 6.13 were used.

Table 6.14 Acceleration Levels recorded by others during live events

Event Type	Peak Recorded Acceleration	Stand Frequency	Country	Ref
Concert	0.804ms^{-2}	4.69Hz	UK	Little (2000c)
Concert	0.9ms^{-2}	3.8Hz	UK	Pavic and Reynolds (2008)
Concert	1ms^{-2} fairly consistently maximum peaks at 1.25ms^{-2}	4-5Hz	UK	Caprioli et al (2007)
Concert	0.3ms^{-2} for global artist 1.25ms^{-2} for local artist	4-5Hz	Italy	Caprioli et al (2007)
Concert	2.7ms^{-2} for <4s $2 - 2.5\text{ms}^{-2}$ for 20s > 0.5ms^{-2} for most of the time during energetic songs	2.73Hz	Canada	Pernica (1983)
Sport	0.949ms^{-2}	2.66Hz	UK	Little (2000c)
Incidental music at American Football Match	0.8ms^{-2} for <12s 0.4ms^{-2} for >30s <u>Note</u> Coordinated jumping to music was prompted using the scoreboards at this event	2.7Hz	USA	Salyards and Hansen (2007)
Football	2.6ms^{-2}	4.6Hz	Brazil	Batista et al (2008)

What the comparison showed was that for standard concerts the measured acceleration levels typically fell around or below the 1.0ms^{-2} recommended limit for Medium Tempo Concerts. Peak accelerations of 1.25ms^{-2} were recorded at concerts in the UK and Italy but this value is well below the suggested limit of 2.2ms^{-2} for High Energy Concerts. The concert that produced the most extreme vibrations was recorded at a grandstand in Canada. The vibrations measured during the most energetic song at the Canadian concert (Pernica 1983) slightly exceeded the proposed standard limit for High Energy Concerts but only a short period of time (<20 seconds) and the upper limit of 2.98ms^{-2} peak acceleration was not exceeded.

For the sporting events, on permanent grandstands in the UK (Littler 2000c), the maximum recorded peak acceleration was just below 1ms^{-2} , this ties in well with the suggested acceptability limit of 1.0ms^{-2} proposed for High Profile Sporting Events. The acceleration levels recorded during an American Football match where the crowd was actively encouraged to jump in a coordinated fashion to a musical beat (Salyards and Hansen 2007) also did not exceed this limit and only exceeded the proposed lower limit for Typical Sporting Events of 0.40ms^{-2} for a very short period of time despite the low natural frequency of the stand at 2.7Hz.

The final published acceleration level considered was one recorded in Brazil during a football match. The Brazilians are renowned for their highly energetic and extremely coordinated celebrations following a goal event and the peak acceleration of 2.6ms^{-2} recorded at the Maracana Stadium (Batista et al 2008) is similar to the most extreme vibration measured at the Canadian pop concert (Pernica 1983). This highlights the importance of understanding local crowd behaviour as there are some nations, e.g. Germany, Brazil and some Scandinavian countries, where groups of supporters purposefully sit together in blocks and perform vigorous synchronised movements in time to a beat. In designing a stadium for such crowds not only are the dynamic loads considerably higher than in the UK but the acceptability limits must be different as it is possible that highly active crowds are more tolerant of larger vibrations.

The recorded vibration data also identifies that for crowd induced vibrations very high peak accelerations can be generated but these only last for a few seconds and

therefore it is crucial that a time period is specified over which any acceptance criteria is applied.

6.8 Acceptability - Conclusion

To date very little research has been published in the field of human perception of vibrations due to synchronised crowd loading in relation to acceptability levels in grandstands. The experimentally derived acceptability curves and proposed limits fit well with the peak acceleration thresholds and range specified by Kasperski (1996) and the NBCC (2005) and, tie in well with previously published acceleration recorded during events at permanent UK grandstands.

The current IStructE (2008) British guidance for the 'dynamic performance requirements for permanent grandstands subject to crowd action' gives recommendations for calculating the magnitude of vibrations likely to be experienced during different types of events and gives corresponding acceptable RMS accelerations. While the method of calculating the acceleration of the stand seems adequate, if somewhat simplified, the acceptability criteria in RMS form are significantly higher than those proposed by this research. It is believed that the IStructE RMS acceptability limits are based on the original Kasperski (1996) peak acceleration thresholds and when the IStructE recommended RMS values are converted back to peak accelerations they are much more compatible with the proposed limits (Table 6.13).

What has been made clear by this analysis is that any published acceptability limits should be left in the format they were originally calculated unless the full vibration data upon which the limits were based is available to aid conversion. Comparison of the proposed acceptability criteria against vibration magnitudes recorded at actual events has also highlighted the important difference between specifying peak or RMS acceleration limits. During real concerts extreme peak accelerations can occur but only for very short periods of time (< 5 seconds). Therefore specifying acceptance criteria in terms of RMS acceleration over 10s (as suggested by the IStructE guidelines) removes the question of how long a peak acceleration has to last before it is unacceptable and also uses the format of specifying a vibration

magnitude that proved most accurate in determining human perception and emotional response to a crowd generated grandstand vibration.

7 Conclusions and Further Research

7.1 Conclusions

7.1.1 Current Design Limitations and Aims of Research Project

Until relatively recently the design of structures, in the UK, subject to dynamic crowd loading has been based on a frequency limit approach i.e. minimising serviceability issues by specifying a minimum fundamental frequency of the structure which avoids a resonant response due to the key harmonic components of the loading from an active crowd. This approach can at times be conservative with structures below the guideline frequency performing adequately in service.

Therefore more recent research in the field of grandstand design has focussed on defining the loading due to synchronised crowds at various types of event, ranging from football matches to high energy pop concerts, as well as defining the most appropriate method to represent the complex human-structure interaction that occurs when large numbers of people load a structure. The culmination of this research was the publication of the IStructE's 'Dynamic Performance Requirements for Permanent Grandstands subject to Crowd Action' in December 2008. This provides an alternative method in addition to the traditional frequency limit approach. Loadings are provided for various event scenarios covering classical and pop concerts and, sporting events. These are to be used with the recommended 2 degree-of-freedom system model, representing the crowd and the structure, to predict the accelerations likely to be experienced during a specific type of event. Despite all the new research that went into this publication, the human acceptance criteria to be used in conjunction with the calculated accelerations are based on extremely limited published research, namely Kasperski (1996). This much referenced paper is the basis for the acceptability limits for grandstand design from Europe to North America. However even Kasperski (1996) relies on acceleration limits suggested by others whose derivation are unclear and not grandstand specific. Due to the major influence of human acceptance criteria on the design and management of grandstand venues, relevant stadium specific guidelines are vital. Therefore, based on the significant lack of research based acceptability limits for permanent grandstands, this research project set out to understand human perception of vibrations due to synchronised crowd loading of tiered seating, using experimental

testing, with the aim of defining explicit acceptance criteria for permanent grandstands.

7.1.2 Experimental Testing

Because human perception is highly situation dependent the testing needed to represent as closely as possible an actual grandstand event. In order for key factors to be controlled, such as the rig frequency and the magnitude of the vibration, the testing was carried out in the laboratory. Therefore the critical factor was constructing a test rig that resembled a genuine permanent grandstand. To this end, three precast terrace units (designed for a real stand) were supported on a stiff triangular steel frame to create a solid feeling rig 5.6m long by 3.5m high. The elevation and rake of the units gave the impression to the participants of being on an elevated cantilevered tier rather than on a more gently sloping terrace close to the ground. To ensure that the vibrations experienced were as realistic as possible they were entirely generated by small groups of the participants jumping in unison, to a metronome beat, while the remainder of the crowd remained seated. Those jumping were spread uniformly over the stand in order to produce a symmetric load which was critical for the cases when the rig was supported on springs (see below).

The fundamental vertical natural frequency of the unloaded test rig was designed to be greater than 6Hz (as recommended by IStructE (2002 and 2008)) for grandstands subject to the most onerous scenario of 'high energy concerts'. The reason for this was to provide a stand that responded, during the testing, as one designed to the current frequency limit design approach, where a resonant response could only be excited by the 3rd or 4th harmonic component of the dynamic crowd loading. Two sets of springs were then designed to allow the vertical natural frequency of the stand to be reduced to around 2Hz and 4Hz. Through varying the jump frequency of the participants this enabled a wide range of vibration sizes to be generated by the test crowds, from 0.1mm to 30mm peak displacement and from 0.05ms^{-2} to 4.34ms^{-2} peak acceleration, easily covering Kasperski's lowest threshold of 0.49ms^{-2} for 'disturbing comfort' and his highest 'panic' threshold of 3.43ms^{-2} peak acceleration. The spring set-ups also allowed resonance of the rig due to both the 1st and 2nd harmonic components of the crowd loading to be investigated.

The testing took place in two main sessions. The first in December 2006 used a test group of 20 people of whom 6 jumped at a time to produce the vibrations. During a single afternoon these participants tested each of the 3 rig set-ups over a predetermined range of 5 jump frequencies chosen to induce both resonant and non-resonant responses. Following each test the participants noted whether they were jumping or seated together with their perception rating of how large the vibration was and how they felt emotionally about the vibration. Their perception and emotional responses were recorded on a sliding scale ranging from 'Imperceptible' to 'Extreme Vibration' for perception and from 'Does not bother me at all' to 'Very Disturbing' for emotion. A similar format was followed for the second set of tests in October 2007. This time the testing was split into 4 sessions spread over 4 days with various sized groups of 8, 15 and 21 people, using 4 or 5 of the crowd jumping to create the vibrations. Based on the results of the December 2006 tests it was decided to focus on the 2Hz and 4Hz rigs as the vibrations generated by these rigs were in the region where perception levels start to change and the possibility of unacceptability arises. The same jump frequencies as for the December 2006 tests were used. The perception and emotion questionnaires also remained largely unchanged save for the addition of an unacceptability column where participants were asked to decide whether the vibration just experienced would have been unacceptable if experienced during an event at a real grandstand. Clear guidance was provided on the definition of unacceptable in this case.

7.1.3 Human Perception and Emotional Response to Crowd Induced Vibrations

Following the testing the collected data was collated, with the results from the participants' questionnaires converted to numeric form and linked to the recorded magnitude of the experienced vibration. Preliminary analysis of the results was carried out graphically to obtain an initial understanding of how the seated and jumping participants' perception and emotion ratings varied with vibration magnitude. This was followed up by more detailed analysis using statistical methods to ascertain the most accurate model of predicting human perception and emotional response to a grandstand vibration generated by synchronised crowd loading. The purpose of this was to use a scientific method to determine the key factors influencing human response to crowd vibrations in grandstands e.g.;

- is there a difference in perception/emotion response of those experiencing the vibration whilst seated and those jumping to create the vibration
- is human perception/emotion linked more closely to displacement, acceleration, vibration dose values (incorporating both RMS acceleration and vibration duration) or frequency of vibration,
- what form does the relationship between human perception/emotion and vibration magnitude take, i.e. is it best described by a linear, logarithmic, exponential, polynomial or power function,
- are average forms for describing a vibration (RMS, average peak) more accurate than peak (maximum, minimum, peak to peak) forms when modelling human perception or emotion,
- although the vibrations recorded have a dominant vertical component, do generally much smaller horizontal components have a significant influence on human perception/emotion,
- does including terms describing the displacement of the structure in three dimensions plus the vertical acceleration and vibration duration significantly improve the accuracy of the models or can a much simpler model based on a single variable be just as accurate.

The results of the statistical modelling showed that;

- There is a clear difference between how those jumping and those seated perceive crowd induced grandstand vibrations. Those seated are much more sensitive and can perceive the relative magnitude of even very small vibrations. Indeed if anything they are more sensitive to smaller vibrations applying the same increase in rating to a small change in a small vibration as a larger change to a larger vibration, shown by the near linear trend of the data when plotted on a logarithmic scale. Therefore it is not surprising that a logarithmic function was found to be the best way to represent the perception ratings of those seated (Table 7.1 and Figure 7.1).
- The jumping participants found it much harder to distinguish between the sizes of the smaller vibrations but once the magnitude reached a certain size they were as able to perceive the size of the vibration as those seated. This was shown by the recorded data points remaining fairly constant up to a certain vibration magnitude and then rapidly increasing with the increase in

vibration size. Thus for those jumping a squared function proved the most accurate way to model perception (Table 7.1 and Figure 7.2).

- However those jumping typically rated their perception of the vibration lower than those seated.
- Generally the trend for the emotion ratings, for both the seated and jumping groups followed that of the concurrent perception rating but with the percentage ratings being approximately 10-20% lower (Figures 7.1 and 7.2). And so the best variables and model formats for predicting the participants' emotional response proved to be the same as for their perception rating (Table 7.1 and Figures 7.1 and 7.2).
- For all participants, jumping and seated, it was found that models using the RMS form of displacement or acceleration generally equalled or outperformed those using a peak form to describe the vibration.
- The nature of the human response to vibrations whilst seated is complex and requires a greater number of predictors, describing the vibration, in order to achieve a similar level of accuracy to that achieved with fewer variables for the jumping models. For those jumping the relationship is much simpler with a single variable model (based on vertical displacement) obtaining results of over 90% of the accuracy of the most complex model.
- For those seated, predictors describing the vertical acceleration in conjunction with front-to-back displacement give a good balance of accuracy combined with a restricted number of variables in the models, for both perception and emotion. Given the inclined nature of the stand although the primary displacement is vertical there is always a front-to-back horizontal component which, for some of the tests was relatively large due to the positioning of the crowd together with a near resonant response. As such it is not surprising that this front-to-back displacement influences the seated human response to the vibration although the vertical component still dominates the perception and emotion models for those seated.
- Of all the models selected and statistically checked those with fewer variables performed almost as well as the saturated models which used considerably more predictors. Therefore despite a second variable improving the accuracy of the seated perception and emotion models the additional complexity was not deemed justifiable for the relatively small increase in accuracy and so the best single variable models for the seated and jumping groups were the ones

recommended for predicting the human perception and emotion response (Table 7.1).

- Factors such as the jump frequency and the frequency of the resulting vibration were found to have little impact on the accuracy of the models. From the results of the analysis the key factors in determining the perception and emotion response appear to be vertical displacement or acceleration followed by front-to-back displacement and then sway displacement. This, unsurprisingly, is typically the order of magnitude of these components (from large to small) of the recorded results taken from the test rig. The inclusion of a time component in the form of VDV improves the accuracy of the models marginally but the additional complexity this adds to the model does not generally justify its use.

Table 7.1 Recommended Perception and Emotion Models

Perception	Variable and Constants	R² value
$\%P_{SEAT} = \alpha x + \beta \ln x + \phi$	$x = VRMSa$ $\alpha = 13.46, \beta = 8.15, \phi = 54.35$	0.496
$\%P_{JUMP} = \alpha x^2 + \phi$	$x = VRMSd$ $\alpha = 0.54, \phi = 16.44$	0.625
Emotion	Variable and Constants	R² value
$\%E_{SEAT} = \alpha \ln x + \phi$	$x = VRMSa$ $\alpha = 6.51, \beta = 9.75, \phi = 45.72$	0.318
$\%E_{JUMP} = \alpha x^2 + \phi$	$x = VRMSd$ $\alpha = 0.49, \phi = 9.98$	0.544

When compared against results of similar perception tests and vibration guidelines, those in the grandstand tests perceived the vibrations as smaller than those rating vibrations in floors showing how situation dependent human responses are. The fact that the participants were expecting some level of vibration and could see the source of the vibration, i.e. the people jumping, may well have increased their tolerance thresholds.

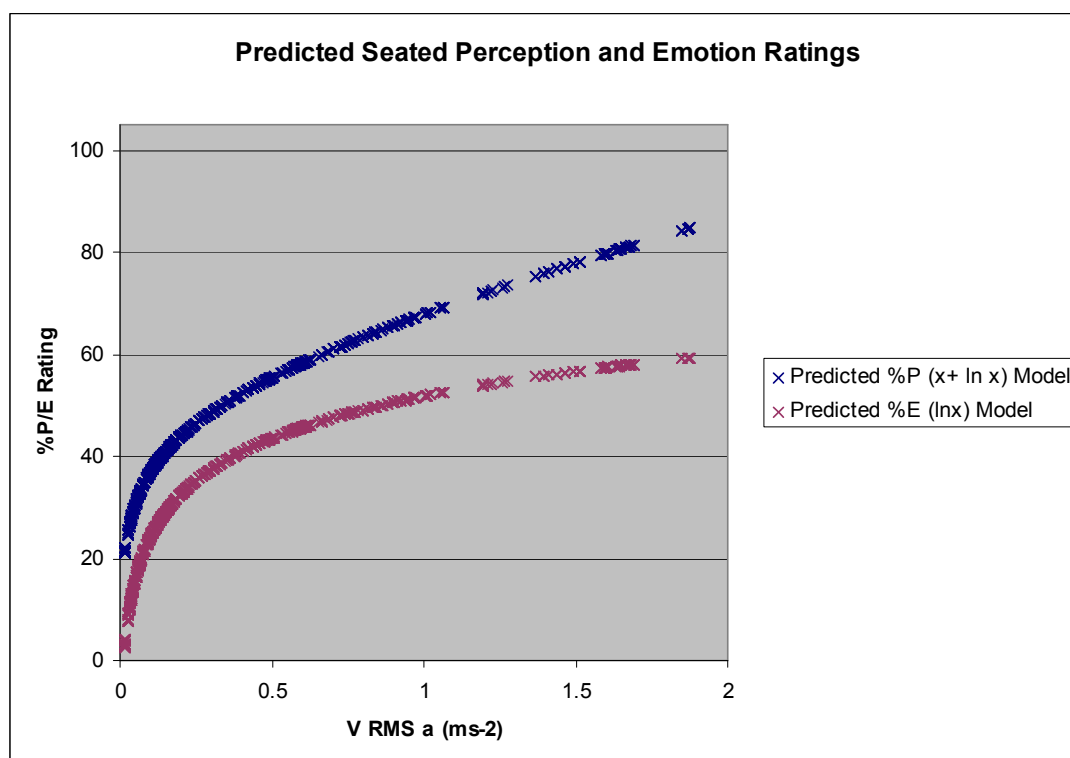


Figure 7.1 Recommended Seated Perception and Emotion Models

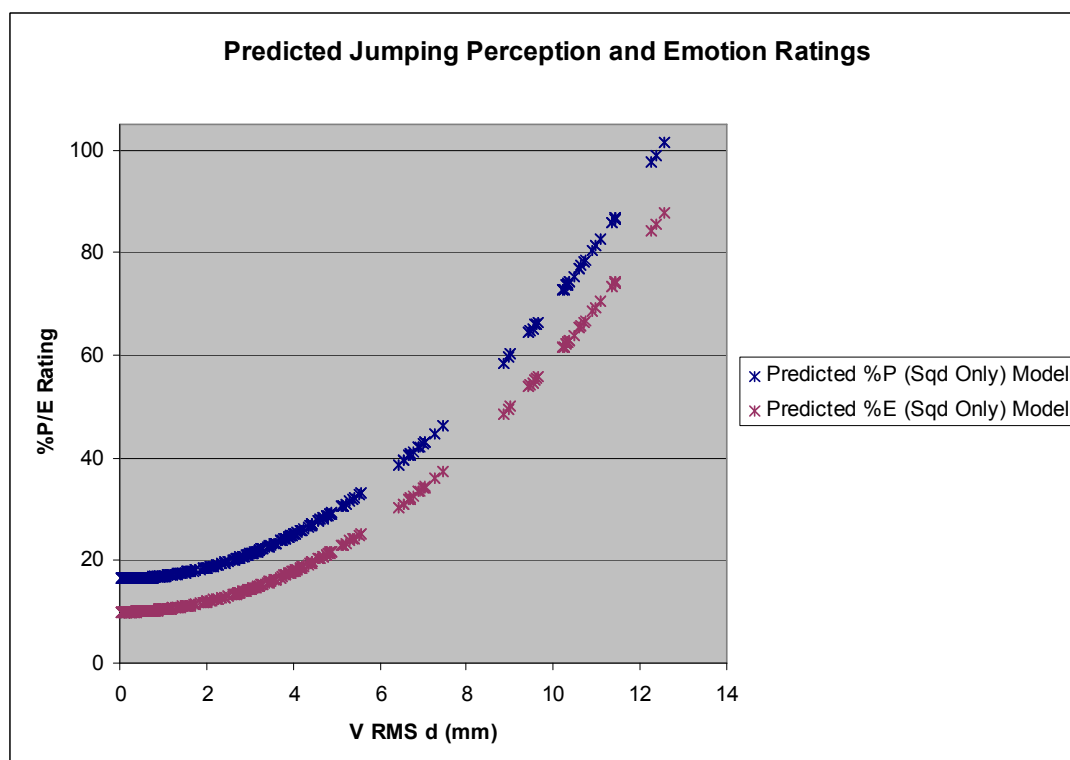


Figure 7.2 Recommended Jumping Perception and Emotion Models

7.1.4 Acceptability

Once a better understanding had been obtained of how those seated and jumping on a grandstand perceive crowd induced vibrations and what the key factors are influencing their emotional response, the next step was to investigate the link to acceptability. As previously, graphical methods were used to explore the relationship between the participants' acceptability responses and potential predictors, first using scatter plots and then frequency distribution histograms. These identified the possibility of using a logistics curve to model the transition from acceptable to unacceptable. The histograms were developed for the predictors that correlated most closely with the acceptability test results, which were % perception and emotion ratings and the RMS format of vertical displacement and acceleration. As for the previous statistical analysis the seated and jumping groups were treated separately. Acceptability logistic curves were derived for each of the variables and their accuracy assessed. For both groups the human response in the form of % perception or emotion rating proved the best indicator of acceptability. However due to complexity of predicting these ratings, given the large scatter of the recorded values about the modelled mean, the acceptability curves based on these variables were not deemed suitable for application in the wider field. Therefore the focus was on developing the curves based on vertical RMS displacement and acceleration.

It was found that the best indicators of acceptability were the same format and form of the predictors used in the selected perception and emotion models (Table 7.1) i.e. logarithm of vertical RMS acceleration for those seated and the square of vertical RMS displacement for those jumping. Similar to the perception and emotion responses those jumping are more tolerant of vibrations and do not deem the motion to be unacceptable until a much higher acceleration than those seated (Figure 7.3). At the lower end of vibrations tested the number of seated participants finding the vibration unacceptable steadily grew as the vibration increased in size while the number jumping unacceptable responses remained fairly constant until the magnitude reached around 0.5ms^{-2} RMS. At the upper end of the test range of vibrations all the participants agreed that the vibration was unacceptable. For both groups the acceptability curves show that on average, for the vibration magnitudes tested, there will always be approximately 5% of the population who disagree with the general opinion, indicated by the graphs failing to reach 0% and 100% at the

extremes of the graphs. (Note for comparison purposes the jumping acceptability curves have been converted to vertical RMS acceleration format using a formula generated from the vibration characteristics of the test rig Figure 6.24 a)

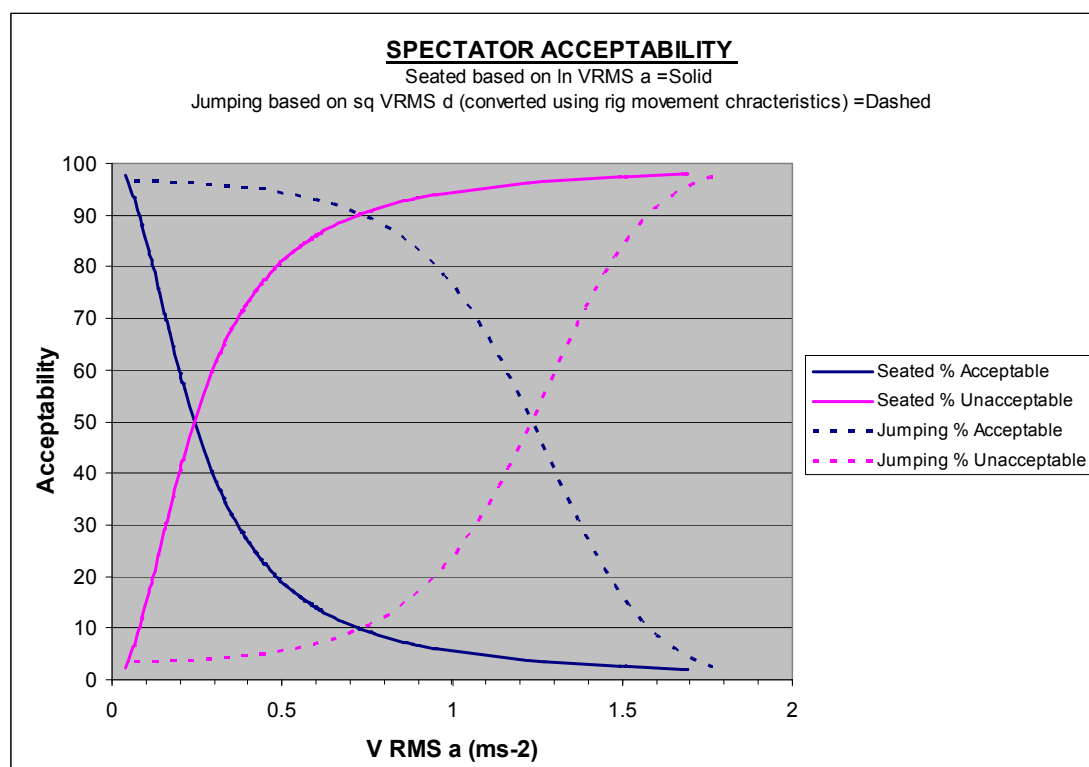


Figure 7.3 Acceptability Curves for Seated and Jumping Spectators

The selected acceptability curves shown in Figure 7.3 were compared against previously published acceptability criteria for grandstands namely Kasperski (1996), NBCC (2005) and IStructE (2008). It was found that the curves corresponded reasonably well to the limits set by the NBCC (2005) and to Kasperski's (1996) thresholds. However the IStructE limits seemed potentially on the high side relative to the percentage acceptabilities given by the curves. Therefore further investigation into the differences between the experimentally derived curves and the IStructE guidelines was instigated, starting with the load model used to predict the likely grandstand accelerations. The IStructE two degree-of-freedom load model was firstly compared against the results from the grandstand tests. The IStructE loading for 'medium tempo concerts and high profile sporting events' proved closest to the experimental results but the lack of ability to change the proportion of active to passive members of the crowd was seen as a drawback. Alternative load models were then considered which allowed for different numbers of the crowd to be taken

as jumping and compared against the recorded test accelerations. It was found that a 3 degree-of-freedom model best represented the human-structure interaction of the test rig when the IStructE loading function for 'high energy concerts' was used to represent the jumping members of the crowd. The second stage was to develop more specific recommendations for acceptable vibration levels for various types of grandstand events based on the acceptability curves (Figure 7.3). This allowed the IStructE event 'scenarios' to be viewed on a comparable basis with the experimentally derived acceptance criteria and for a method to be detailed on how the acceptability curves can be utilised within the design process for a grandstand. The difficulty in deriving the recommended acceptability levels was deciding on the level of crowd activity for each type of event as there is limited available research on the crowd make-up at different grandstand events. Therefore the IStructE (2008) crowd descriptions and loadings had to be used as guidelines. As a result the proposed loadings for all but 'classical concerts' were very similar to the IStructE loadings. Therefore the main differences were the balance of active to passive crowd in the recommended 3 degree-of-freedom model and the acceptance criteria. Suggested acceptability limits were calculated based on the experimentally derived acceptance curves and the active to passive crowd ratio for 5%, 10%, 15% and 20% overall crowd acceptability. It was found that while the 20% overall crowd acceptability levels fitted well with the NBCC acceleration limits the IStructE values were still considerably higher.

However further investigation found that if both the suggested and IStructE RMS acceleration limits were converted to peak values then they were remarkably similar. The key here was the factor used to convert RMS accelerations to peak accelerations. For the suggested limits a formula derived from the characteristic movements of the test rig was used, with a value of approximately 2.2 (Figure 6.24 b). The value used to convert the IStructE RMS limits to peak accelerations was $\sqrt{2}$ (i.e. 1.41) based on the belief that the criteria were derived from Kasperski's thresholds and the NBCC limits, as when multiplied by $\sqrt{2}$ the IStructE limits tie in with these guidelines.

Although the RMS value of a pure sine wave is $\sqrt{2}$ times the peak value, dynamic crowd loading produces a forcing function which can be simplified to a Fourier series consisting of harmonic sine waves and so the structural response is also in the form of a Fourier series with various harmonics. Thus if the acceleration response of the structure is in the form

$$y(t) = A\sin(\omega t + \theta) + B\sin(2\omega t + \phi) + C\sin(3\omega t + \psi)$$

then $y_{PEAK} = A + B + C$ assuming that at some point all the peaks are coincident

$$\text{and so } y_{RMS} = \sqrt{\frac{A^2}{2} + \frac{B^2}{2} + \frac{C^2}{2}} \text{ or } y_{RMS} = \frac{1}{\sqrt{2}} \times \sqrt{A^2 + B^2 + C^2}$$

Consequently it is incorrect to convert any peak value of a periodic acceleration response to an RMS value simply by dividing by $\sqrt{2}$. Therefore it is crucial that any acceptability criteria remain in the format in which they were originally specified (unless the full details of the response upon which the limits are based are available to aid the conversion).

In conclusion, the results of the experimental grandstand perception tests show that those seated are much more sensitive to crowd generated vibrations than those jumping. Consequently when specifying acceptability limits the critical factor is understanding the proportion of the crowd that are likely to be seated as it is likely to be their response that governs the overall acceptability level of the crowd. Thus although the preferred basis for determining acceptability of those jumping is vertical displacement, as the best predictor for those seated is vertical acceleration, this is the recommended measure of vibration acceptability in grandstands. The statistical analysis showed that RMS values were generally better than peak values for predicting the human reaction to a grandstand vibration although the margins were relatively small. Therefore the suggested format of grandstand acceptability criteria is RMS vertical acceleration.

7.2 Further Research

The research carried out during this project has provided a valuable insight into the factors affecting human perception and emotional response to crowd generated vibrations in grandstands. It has also given an initial understanding of the limitations of the current acceptability criteria for the design of permanent grandstands for vibrations and a proposed method for improving on these. However the data on which the recommendations are based is limited to that collected during the experimental testing and therefore can be greatly improved by building the knowledge bank of information regarding human perception and acceptance of vibrations in grandstands. Additional research that would greatly aid this includes;

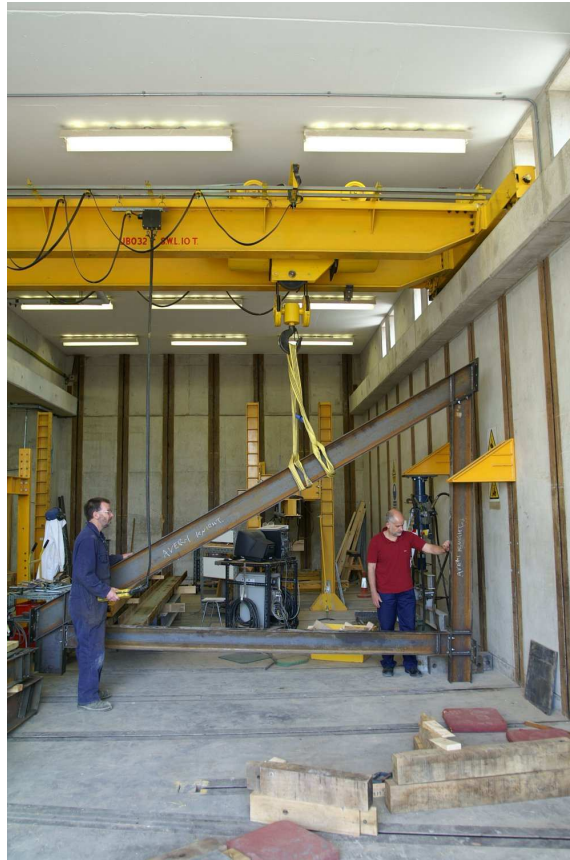
- Correlating the test results with similar tests carried out on an actual grandstand preferably during a real event.
- Carrying out spectator acceptability surveys following different types of event at actual grandstands, for which the experienced vibrations had been recorded, to allow a database linking recorded vibrations with real crowd acceptability to be collated. Alternatively use real-time data collection for the human response (e.g. using clickers) so that it can be directly overlaid on the vibration recording. This would also allow an investigation into the use of Vibration Dose Values (VDVs) to gauge human acceptability over the duration of an entire event. This information becomes even more valuable if numerous types of events can be surveyed for a particular venue.
- Data collection on actual vibrations on grandstands combined with information on the crowd make-up and level of activity throughout the event to give a better understanding of the range of vibrations experienced during events and the loading generating these vibrations.
- Further investigation on what the differences in perception, emotion and acceptability responses are for those standing or bobbing on a grandstand compared to those seated or jumping. This would hopefully allow more accurate serviceability criteria to be developed based on a realistic crowd make-up with a combination of people seated, standing, bobbing and jumping.
- Surveying the expectation of those attending different grandstand events. How are they feeling about the event itself e.g. excited, keen to participate or want to sit and soak in the atmosphere? What are their expectations of the

venue and vibrations and is this influenced by where they are seated e.g. lower terracing, front of cantilevered tier, at very back of upper tier. Investigating whether a warning of possible crowd induced vibrations printed on the ticket affects their expectation and their response if the stand does vibrate.

- Further research using data from this project not used so far e.g. how does the jumpers' ability effect the magnitude of the vibration generated?, how does a resonant response of the stand affect the coordination of those jumping on it?, does the age, sex, height, weight etc of the participant affect their perception?
- Investigating how the period over which RMS acceleration/displacement is calculated (e.g. 1s or 10s rolling RMS) affects the accuracy of predicting perception, emotion and acceptability using the collected experimental data. And then possibly carrying out similar tests but with the crowd jumping for longer, with periods of very intense crowd action, to allow further comparison on the relative merits of using peak or RMS values or even Vibration Dose Values (VDVs) to gauge acceptability. The potential use of frequency weighting of the acceleration response, similar to BS6481:1987 and BS6472:2008, could also be investigated with a view to possibly improving the accuracy of the acceptance criteria.

[Blank]

Appendix A Photographs of Experimental Work



1. Installing the first raker end frame



2. Raker end frames linked by 5m long PFC sections



3. Precast terrace unit after being cut to correct length



4. Installation of the front two precast terrace units



5. Installing the third precast unit



6. Connection of a precast terrace unit to the steel raker



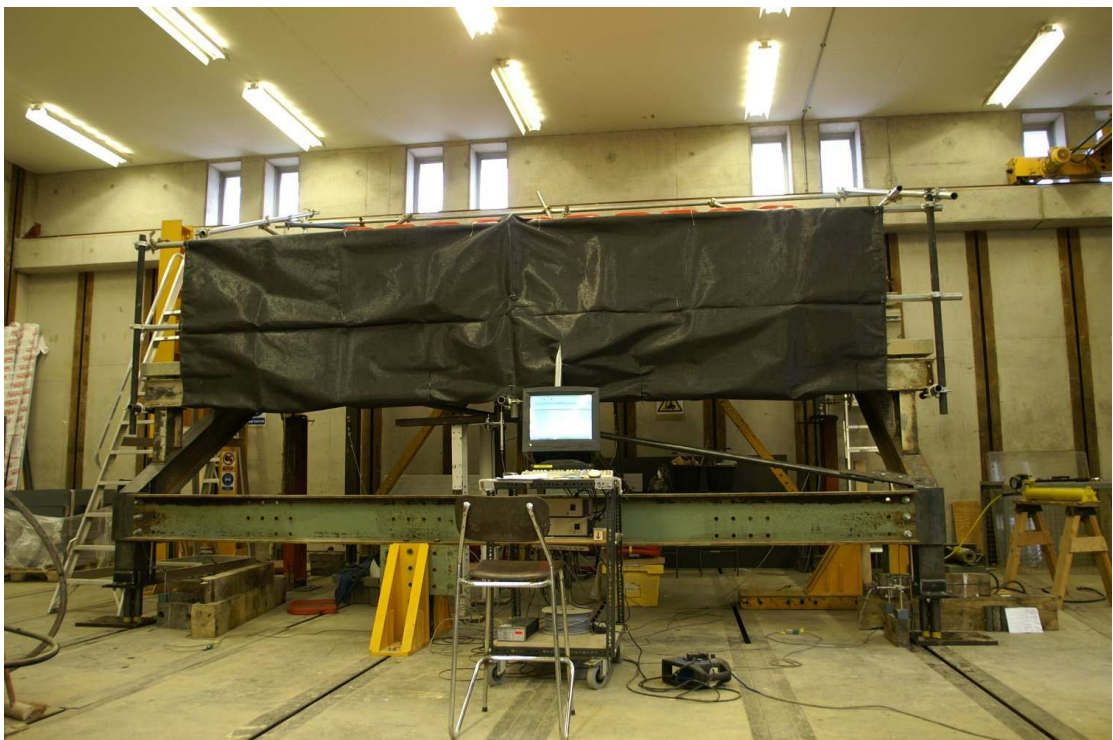
7. Installation of the stadium seating



8. Installed stadium seating



9. Completed test rig



10. Test rig with clad front barrier



11. Completed test rig prior to testing



12. View of the laboratory from the test rig



13. Bracing to rakers showing one of the raker transducers



14. Lateral bracing to the rear of the rig



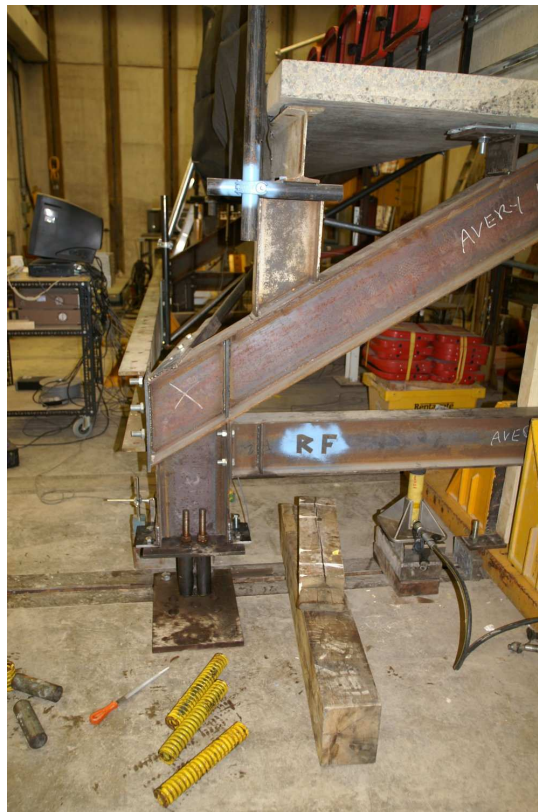
15. Bracing and instrumentation to the underside of the test rig



16. Transducers and accelerometer to the underside of a precast terrace unit

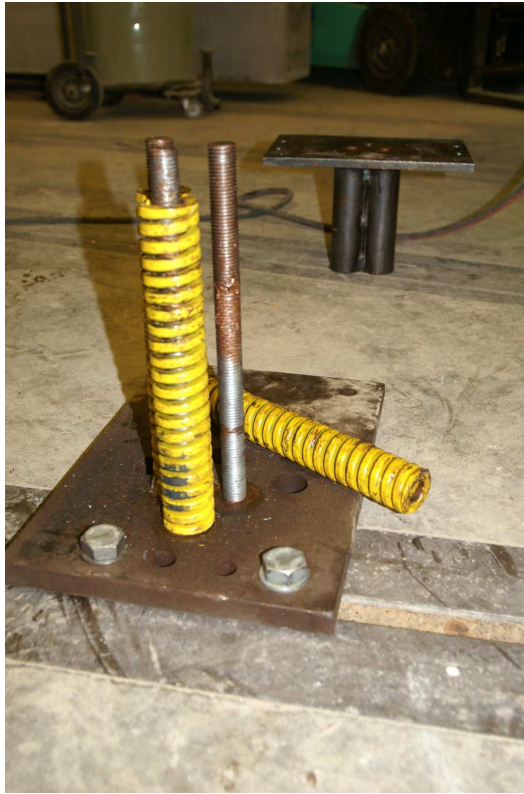


17. Transducers clamped to the laboratory strong wall



18. Sprung support detail (6.5Hz set-up) showing packing and jacks used to change over springs

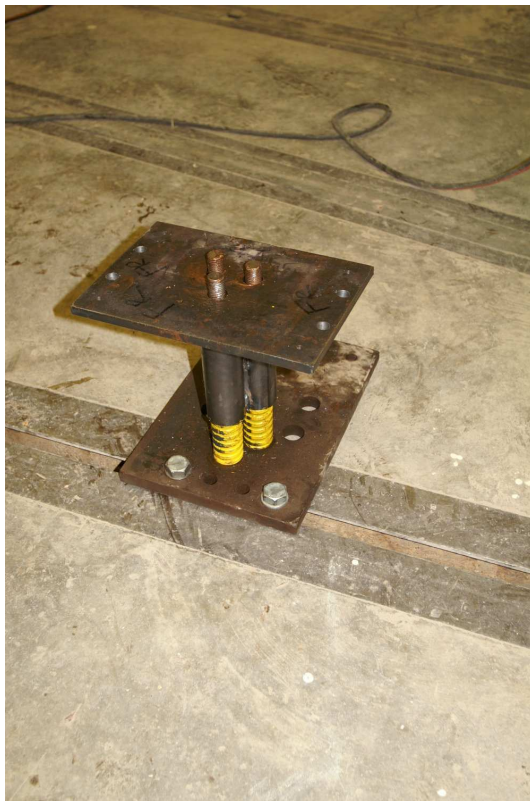
19. Components of the sprung supports to the test rig



a. 2Hz springs and baseplate



b. 4Hz springs with extension CHS and top-plate with spring restraint tubes



c. Sprung support prior to installation



d. Installed support with transducers



20. Testing December 2006



21. Testing October 2007

References

- Allen, D.E. 1990b. Vibrations from Human Activities. *Concrete International- Design and Construction*, June 1990 Vol 12 No 6, pp.66-73. American Concrete Institute.
- Allen, D.E., 1990a. Floor Vibrations from Aerobics. *Canadian Journal of Civil Engineering*, 1990 Vol 17 Part 5, pp.771-779.
- Allen, D.E., Rainer, J.H. and Pernica, G., 1985. Vibration Criteria for Assembly Occupancies, *Canadian Journal of Civil Engineering*, Vol 12 Part 3, pp.716-623.
- Bachmann, H., et al, 1994. *Vibration Problems in Structures*. Berlin: Birkhauser.
- Bastista, R.C. and Magluta, C., 1993. Spectator Induced Vibrations of Maracana Football Stadium, *Proceedings of the 2nd European Conference on Structural Dynamics: EURODYN '93*, 21-23 June 1993, Trondheim, Norway. Rotterdam: Balkema, pp.985-992.
- Bastista, R.C., Varela, W., Dos Santos, E. and Correa, W., 2008. Measurements and Control of People Induced Vibration in Stadium Grandstands. In: M.J. Brennan, ed. *Proceedings of the 7th European Conference on Structural Dynamics: EURODYN 2008*, 7-9 July 2008, Southampton, United Kingdom. Southampton: ISVR, E229.
- Braun, D., Kennedy, S.J., Kennedy, D.J.L. and Allen, D.E., 2002. Sandwich Plate System Risers for Stadia. *SSRC 2002 Annual Stability Conference*, Seattle, Washington, USA, 24-27 April 2002. Available from <http://www.ie-sps.com/Resource.html?sku=19> [Accessed 1 March 2011].
- BRE Digest 426, *The Response of Structures to Dynamic Crowd Loads*, 1997. Garston: BRE.
- BRE Digest 426, *The Response of Structures to Dynamic Crowd Loads*, 2004. 2nd Edn. (Ellis, B. R. and Ji, T.) Garston: BRE.
- BS 5228-2:2009, *Code of Practice for Noise and Vibration Control on Construction and Open Sites - Part 2 : Vibration*. London: BSI.
- BS 5400-2:2006, *Steel, Concrete and Composite Bridges - Part 2 Specification for Loads*. London: BSI.
- BS 5950-1:2000 Incorporating Corrigendum No. 1, *Structural use of Steelwork in Building - Part 1: Code of Practice for Design - Rolled and Welded Sections*. London: BSI.
- BS 6399:Part 1:1984 with details of 1985,1988 and 1989 Amendments, *Loading for Buildings - Part 1:Code of Practice for Dead and Imposed Loads*. London: BSI.
- BS 6399:Part 1:1996 with 2002 amendment, *Loading for buildings - Part 1: Code of Practice for Dead and Imposed Loads*. London: BSI.
- BS 6399:Part 1:1996, *Loading for buildings - Part 1:Code of Practice for Dead and Imposed Loads*. London: BSI.
- BS 6472:1992, *Guide to Evaluation of Human Exposure to Vibration in Buildings (1Hz to 80Hz)*, London: BSI.
- BS 6472-1:2008, *Guide to Evaluation of Human Exposure to Vibration in Buildings - Part 1: Vibration Sources other than Blasting*: London: BSI.

- BS 6611:1985, *Guide to Evaluation of the Response of Occupants of Fixed Structures, especially Buildings and Off-shore Structures, to Low Frequency Horizontal Motion (0.063Hz to 1Hz)*, London: BSI.
- BS 6841:1987, *Guide to Measurement and Evaluation of Human Exposure to Whole Body Mechanical Vibration and Repeated Shock*, London: BSI.
- BS 7385-1:1990 (ISO 4866:1990), *Evaluation and Measurement for Vibrations in Buildings - Part 1: Guide for Measurement of Vibrations and Evaluation of their Effects on Buildings*, London: BSI.
- BS 7385-2:1993, *Evaluation and Measurement for Vibrations in Buildings - Part 2: Guide to Damage Levels from Groundbourne Vibration*, London: BSI.
- BS 8110-1:1997 Incorporating Amendments Nos 1 and 2, *Structural use of Concrete - Part 1: Code of Practice for Design and Construction*, London :BSI.
- BS 8110-2:1985 Reprinted, incorporating Amendments Nos. 1, 2 and 3, *Structural use of Concrete - Part 2: Code of Practice for Special Circumstances*, London: BSI.
- BS ISO 4866:2010, *Mechanical Vibration and Shock - Vibration of Fixed Structures - Guidelines for the Measurement of Vibrations and Evaluation of their Effects on Structures*, London: BSI.
- Caprioli A., Reynolds P., Vanali M., 2007, Evaluation of Serviceability Assessment Measures for Different Stadia and Different Live Concert Events, 25th International Modal Analysis Conference: *IMAC-XXV, Orlando, Florida, 19-22 February 2007*.
- Chen, P. and Robertson, I.L., 1972. Human Perception Thresholds of Horizontal Motion. *Journal of the Structural Division, Proceedings of the American Society of Civil Engineers*, Vol 98 No ST8 August 1972, pp.1681-1695.
- Cohen, J., 1992. A Power Primer. *Psychological Bulletin, American Psychological Association*, Vol 112, No. 1, pp.155-159.
- CP3: Chapter V: Part 1: 1968, British Standard Code of Practice. *Code of Basic Data for the Design of Buildings, Chapter V Loading, Part 1 Dead and Imposed Loads*, London: BSI.
- Dickie, J.F., 1983. Demountable Grandstands. *The Structural Engineer*, Vol 61A (3), pp.81-86.
- Dickson, M.G.T., 1991. Towards Safer Stadia. *The Structural Engineer*, Vol 69 (19), pp.348.
- DIN 4150:1999, *Structural Vibration Part 3: Effects of Vibration on Structures*, Berlin: DIN.
- DIN 4150-2:1999, *Structural Vibration Part 2: Human Exposure to Vibration in Buildings*, Berlin: DIN.
- Dougill, J.W., Wright, J.R., Parkhouse, J.G., Harrison, R.E., 2006. Human Structure Interaction during Rhythmic Bobbing. *The Structural Engineer*, Vol 84 (22), pp.32-39.
- Ebrahimpour, A. and Sack, R., 1992. Design Live Loads for Coherent Crowd Harmonic Movements. *Journal of Structural Engineering (American Society of Civil Engineers)*, Vol 118 No 4, April 1992, pp.1121-1136.

- Ellis, B.R. and Ji, T., 1996. The Effects of Human Structure Interaction on Structural Vibrations, *Proceedings of the 3rd European Conference on Structural Dynamics: EURODYN '96*, 5-8 June 1996, Florence, Italy. Rotterdam: Balkema, Vol 1, pp.447-453.
- Ellis, B.R. and Ji, T., 1997. Human Structure Interaction in Vertical Vibrations. *Proceedings of ICE, Structures and Buildings*, Vol 122, February 1997, pp.1-9.
- Ellis, B.R. and Ji, T., 2002. Loads Generated by Jumping Crowds: Experimental Assessment, *BRE Information Paper IP4/02*. Garston: BRE.
- Ellis, B.R. and Littler, J., 2004. The Response of Cantilever Grandstands to Crowd Loads. Part 1 Servicability Evaluation. *Proceedings of ICE, Structures and Buildings*, Vol 157, August 2004, pp.235-241.
- Ellis, B.R. and Littler, J., 2004. The Response of Cantilever Grandstands to Crowd Loads. Part 2 Load Evaluation. *Proceedings of ICE, Structures and Buildings*, Vol 157, October 2004, pp.297-307.
- Ewins, D.J., 2000. *Modal Testing: Theory Practice and Applications*. 2nd Edn. Baldock: Research Studies Press Ltd.
- Ginty, D., Derwent, J.M. and Ji, T., 2001. The Frequency Ranges of Dance Type Loads. *The Structural Engineer*, Vol 79 (6), pp.27-31.
- Hicks, S.J. and Devine, P.J., 2004. Design Guide on the Vibration of Floors in Hospitals. *SCI Publication P331*. Ascot: Steel Construction Institute.
- HMSO Green Guide, 1997. *Guide to Safety at Sports Grounds*. 4th Edn. London: HMSO.
- Institution of Structural Engineers, 1989. *Safety Considerations for the Design and Erection of Demountable Grandstands*. London: IStructE.
- Institution of Structural Engineers, 1991. *Appraisal of Sports Grounds*. London: IStructE.
- Institution of Structural Engineers, 1995. *Temporary Demountable Structures: Guidance on Procurement Design and Use*. 1st Edn. London: IStructE.
- Institution of Structural Engineers, 1999. *Temporary Demountable Structures: Guidance on Procurement Design and Use*. 2nd Edn. London: IStructE.
- Institution of Structural Engineers, 2001. *Dynamic Performance Requirements for Permanent Grandstands Subject to Crowd Action: Interim Guidance on Assessment and Design*. London: IStructE.
- Institution of Structural Engineers, 2002. *Dynamic Testing of Grandstands and Seating Decks*. London: IStructE.
- Institution of Structural Engineers, 2003. Advisory Note on Calculation of Natural Frequencies of Grandstand Seating Decks. *The Structural Engineer*, Vol 81 (22), pp.20-21.
- Institution of Structural Engineers, 2007. *Temporary Demountable Structures: Guidance on Procurement Design and Use*. 3rd Edn. London: IStructE.
- Institution of Structural Engineers, 2008. *Dynamic Performance Requirements for Permanent Grandstands Subject to Crowd Action: Recommendations for Management, Design and Assessment*. London: IStructE.

- Institution of Structural Engineers/Department of the Environment, 1994. Interim Guidance on Temporary Grandstands. *The Structural Engineer*, Vol 72 (15), pp.249-250.
- ISO 10137:1992(E). *Bases for Design of Structures - Serviceability of Buildings Against Vibration*. Geneva: ISO.
- ISO 10137:2008. *Bases for Design of Structures - Serviceability of Buildings Against Vibration*. Geneva: ISO.
- ISO 2631-1 1997. *Mechanical Vibration and Shock - Evaluation of Human Exposure to Whole Body Vibration - Part 1: General Requirements*. Geneva: ISO.
- ISO 2631-2 2004. *Mechanical vibration and shock - Evaluation of Human Exposure to Whole Body Vibration - Part 2: Vibration in Buildings (1Hz to 80 Hz)*. Geneva: ISO.
- Ji, T. and Ellis, B.R., 1994a. Floor Vibration Induced by Dance Type Loads: Theory. *The Structural Engineer*, Vol 72 (3), pp.37-44.
- Ji, T. and Ellis, B.R., 1994b. Floor Vibration Induced by Dance Type Loads: Verification. *The Structural Engineer*, Vol 72 (3), pp.45-50.
- Ji, T., 2003a. *Human-structure Interaction - Applying Body Biodynamics into Structural Dynamics*. Manchester: UMIST - University of Manchester. <http://personalpages.manchester.ac.uk/staff/tianjian.ji/research/hulme/human.htm> [Accessed 1 March 2011].
- Ji, T., 2003b. Understanding the Interactions between People and Structures. *The Structural Engineer*, Vol 81 (14), pp.12-13.
- Kasperski M. and Niemann H.J., 1993. Man Induced Vibrations of a Stand Structure, *Proceedings of the 2nd European Conference on Structural Dynamics: EURODYN '93*, 21-23 June 1993 Trondheim, Norway. Rotterdam: Balkema, pp.977-983.
- Kasperski M., 1996. Actual Problems with Stand Structures due to Spectator Induced Vibrations, *Proceedings of the 3rd European Conference on Structural Dynamics: EURODYN '96*, 5-8 June 1996, Florence, Italy. Rotterdam: Balkema, Vol 1, pp.455-461.
- Kasperski M., 2001. Safety Assessment of Stadia in Regard to Human Induced Vibrations, *One Day Institution Of Civil Engineers Conference : Safer Solutions in Sport and Leisure*, 5 April 2001, Manchester, United Kingdom.
- Kasperski M., 2002. Men Induced Dynamic Excitation of Stand Structures. *15th American Society of Civil Engineers - Engineering Mechanics Conference*, June 2002, New York, USA.
- Khan, F. and Parmelee, R., 1971. Service Criteria for Tall Buildings for Wind Loading. *Proceedings of the 3rd International Conference on Wind Effects on Buildings and Structures*. September 1971, Tokyo, Japan. Tokyo: Saikon.
- Lenzen, K.H., 1966. Vibration of Steel Joist Floor Concrete Floor Slabs. *American Institute of Steel Construction Engineering Journal*, 1966 Vol 3, pp.133-136.
- Littler, J. D., 2003. Frequencies of Synchronised Human Loading from Jumping and Stamping. *The Structural Engineer*, Vol 81 (22), pp.27-35.

- Littler, J., 2000a. Temporary Demountable Grandstands: Dynamic Response, *BRE Information Paper IP3/00*. Garston: BRE.
- Littler, J., 2000b. Retractable Grandstands: Dynamic Response, *BRE Information Paper IP4/00*. Garston: BRE.
- Littler, J., 2000c. Permanent Cantilever Grandstands: Dynamic Response, *BRE Information Paper IP5/00*. Garston: BRE.
- McCormick, M. and Mason, D., 1974. Office Floor Vibrations - Design Criteria and Tests. *Noise and Shock Vibration Conference*, Melbourne, Australia, May 1974, pp.198-207.
- NA to BS EN 1991-1-1:2003. *UK National Annex to Eurocode 1: Actions on Structures - Part 1-1: General Actions - Densities, Self-weight, Imposed Loads for Buildings*. London: BSI.
- National Building Code of Canada (NBCC), 1995. *User's Guide - NBC 1995 Structural Commentaries (Part 4)*. Canada: IRC.
- National Building Code of Canada (NBCC), 2005. *User's Guide - NBC 2005, Structural Commentaries (Part 4 of Division B) Commentary D*. Canada: IRC.
- New Civil Engineer, 1981. Double Design Load Needed for London Concert Venues. *New Civil Engineer*, 9 April 1981, pp.6.
- Parkhouse, J.G. and Ewins, D.J., 2006. Crowd-induced Rhythmic Loading. *Proceedings of ICE, Structures and Buildings*, Vol 159 (SB5), October 2006, pp.247-259.
- Parsons, K.C. and Griffin, M.J., 1988. Whole-body Vibration Perception Thresholds. *Journal of Sound and Vibration*, Vol 121 No 2, pp.237-258.
- Pavic, A. and Reynolds, P., 2008. Experimental Verification of Novel 3DOF Model for Grandstand Crowd Structure Dynamic Interaction. *26th International Modal Analysis Conference: IMAC-XXVI*, Orlando, Florida, USA, 4-7 February 2007, Paper 257.
- Pernica, G., 1983. Dynamic Live Loads at a Rock Concert. *Canadian Journal of Civil Engineering*, 1983 Vol 10 Part 2, pp.185-191.
- Pernica, G., 1990. Dynamic Load Factors for Pedestrian Movements and Rhythmic Exercises. *Canadian Acoustics*, 1990 Vol 18 Part 2, pp.3-18.
- Reiher, H. and Meister, F.J., 1931. Die Empfindlichkeit des Menschen gegen Erschütterungen (The Effect of Vibrations on People). *Forschung auf dem Gebiete des Ingenieurwesens 2. Jahrgang der Zeitschrift Technische Mechanik und Thermodynamik*, (Research in the Areas of Engineering 2nd Year of the Journal of Applied Mechanics and Thermodynamics) Berlin. Band 2, Nr 11, November 1931, pp.381-386.
- Reynolds, P. and Pavić, A., 2005. The Dynamic Performance of Sports Stadia under Crowd Dynamic Loading at Concert Events. In: Soize, C. and Schuëller, G.I. eds. *Proceedings of the 6th European Conference on Structural Dynamics: EUROLYN 2005*, 4-7 September 2005, Paris, France. Rotterdam: Millpress, pp.473-478.
- Reynolds, P., Pavić, A. and Ibrahim, Z., 2004. Changes of Modal Properties of a Stadium Structure Occupied by a Crowd. *22nd International Modal Analysis Conference: IMAC XXII*, Dearborn, Detroit, USA, January 2004.

- Rogers, D., 2000. Two More Wobbly Stands. *Construction News*, 17 August 2000, pp.4.
- Sachse, R., 2002. Modelling Effects on Human Occupants on Modal Properties of Slender Structures. *The Structural Engineer*, Vol 80 (5), pp.21.
- Sachse, R., 2003. *The Influence of Human Occupants on the Dynamic Properties of Slender Structures*. Thesis (PhD). University of Sheffield.
- Sachse, R., Pavic, A. and Reynolds, P., 2003a. Human Structure Dynamic Interaction in Civil Engineering Dynamics: A Literature Review. *Shock and Vibration Digest*, Vol 35 No 1, January 2003, pp.3-18.
- Sachse, R., Pavic, A. and Reynolds, P., 2003b. Parametric Study of Modal Properties of Damped Two Degree of Freedom Crowd Structure Dynamic Systems. *Journal of Sound and Vibration*, 274 (2004), pp.461-480.
- Salyards, K.A. and Hansen, L.M., 2007, Analysis of Coordinated Crowd Vibration Levels in a Stadium Structure. 25th International Modal Analysis Conference: *IMAC-XXV, Orlando, Florida, 19-22 February 2007*.
- SCOSS, 1986. Structural Safety 1983-85: Review and Recommendations - Incl Safety of Demountable Grandstands. *Sixth Report of SCOSS (The Standing Committee on Structural Safety) published in The Structural Engineer*, Vol 64A (1), January 1986, pp.28-32.
- SCOSS, 1989. Structural Safety 1987-89: 3.9 Safety in Sports Grounds. *Eighth Report of SCOSS (The Standing Committee on Structural Safety)*, pp.24-25.
- SCOSS, 1992. Structural Safety 1989-92: Incl Sports and Concert Stadia. *Ninth Report of SCOSS (The Standing Committee on Structural Safety)* pp.15-17 & pp.26.
- SCOSS, 1994. Structural Safety 1992-94: 3.1 Structures where Large Numbers of People may Congregate. *Tenth Report of SCOSS (The Standing Committee on Structural Safety)*, pp.16.
- SCOSS, 1997. Structural Safety 1994-96: 4.1 Temporary Stands and Stage Structures. *Eleventh Report of SCOSS (The Standing Committee on Structural Safety)*, pp.25.
- SCOSS, 1999. Structural Safety 1997-99: Review and Recommendations - 3.2 Safety of Sports Stadia Structures. *Twelfth Report of SCOSS (The Standing Committee on Structural Safety)*, pp.28-29.
- SCOSS, 2001. Structural Safety 2000-01 - 3 Dynamic Response of Structures. *Thirteenth Report of SCOSS (The Standing Committee on Structural Safety)*, pp.23-26.
- Snelson, R., 1989. Engineering Appraisal of Sports Grounds. *The Structural Engineer*, Vol 67 (24), pp.442.
- Steel Designers' Manual, 1994. 5th Edn. Eds: Owens, G.W. and Knowles, P.R., Oxford: Blackwell Scientific Publications (for The Steel Construction Insitute).
- Van Staalduinen, P. and Courage, W., 1994. Dynamic Loading of Feyenoord Stadium During Pop Concerts. *IABSE (International Association for Bridge and Structural Engineering) Symposium Report Vol 71: Places of Assembly and Long-span Buildings Structures*, Birmingham 1994. pp.283-288.
- Wade, S., 1981. Pop Concert Shock for Loading Code. *New Civil Engineer International*, May 1981, pp.18.

- Willford, M., 2001. An Investigation into Crowd Induced Vertical Dynamic Loads. *The Structural Engineer*, Vol 79 (12), pp.21-28.
- Willford, M., 2005. Chapter 8 - Dynamic Performance of Stands. *In*: Culley, P. and Pascoe, J. eds. *Stadium Engineering*. London: Thomas Telford, pp.46-53.
- Wiss, J.F. and Parmelee, M., 1974. Human Perception of Transient Vibrations. *Journal of the Structural Division, Proceedings of the American Society of Civil Engineers*, Vol 100 No ST4, pp.773-787.
- Wyatt, T.A., 1989. Design Guide on the Vibration of Floors. *SCI Publication 076*. Ascot: Steel Construction Institute.
- Yao, S., Wright, J., Reynolds, P., Pavic, A. and Satche, R., 2003. The Effect of People Jumping on a Flexible Structure. *21st International Modal Analysis Conference: IMAC XXI*, Florida, USA, February 2003.